SPR-742 AUGUST 2019

Evaluation of MSCR Testing for Adoption in ADOT Asphalt Binder Specifications

Arizona Department of Transportation Research Center

ADOT

Evaluation of MSCR Testing for Adoption in ADOT Asphalt Binder Specifications

SPR-742

August 2019

Published by:
Arizona Department of Transportation
206 South 17th Avenue
Phoenix, Arizona 85007
In cooperation with
U.S. Department of Transportation
Federal Highway Administration

This report was funded in part through grants from the Federal Highway Administration, US Department of Transportation. The contents of this report reflect the views of the authors, who are responsible for the facts and the accuracy of the data, and for the use or adaptation of previously published material, presented herein. The contents do not necessarily reflect the official views or policies of the Arizona Department of Transportation or the Federal Highway Administration, US Department of Transportation. This report does not constitute a standard, specification, or regulation. Trade or manufacturers' names that may appear herein are cited only because they are considered essential to the objectives of the report. The US government and the State of Arizona do not endorse products or manufacturers.

This report is subject to the provisions of 23 USC § 409. Any intentional or inadvertent release of this material, or any data derived from its use, does not constitute a waiver of privilege pursuant to 23 USC § 409, which reads as follows:

23 USC § 409 — Discovery and admission as evidence of certain reports and surveys

Notwithstanding any other provision of law, reports, surveys, schedules, lists, or data compiled or collected for the purpose of identifying, evaluating, or planning the safety enhancement of potential accident sites, hazardous roadway conditions, or railway-highway crossings, pursuant to sections 130, 144, and 148 of this title or for the purpose of developing any highway safety construction improvement project which may be implemented utilizing Federal-aid highway funds shall not be subject to discovery or admitted into evidence in a Federal or State court proceeding or considered for other purposes in any action for damages arising from any occurrence at a location mentioned or addressed in such reports, surveys, schedules, lists, or data.

1. Report No. FHWA-AZ-19-742	2. Government Accession No.	3. Recipient's Catalog No.
4. Title and Subtitle Evaluation of MSCR Testing for Adoption in ADOT Asphalt Binder Specifications		**5. Report Date** August 2019
		6. Performing Organization Code
7. Author(s) Kamil E. Kaloush, B. Shane Underwood, Ramadan Salim, and Akshay Gundla		**8. Performing Organization Report No.**
9. Performing Organization Name and Address Arizona State University Office for Research and Sponsored Projects Administration Tempe, Arizona 85287-5303		**10. Work Unit No.**
		11. Contract or Grant No. SPR -PL-1(189) 742
12. Sponsoring Agency Name and Address Arizona Department of Transportation 206 S. 17th Avenue Phoenix, Arizona 85007		**13. Type of Report and Period** FINAL
		14. Sponsoring Agency Code

15. Supplementary Notes
Prepared in cooperation with the US Department of Transportation, Federal Highway Administration

16. Abstract
The purpose of this study is to recommend whether ADOT should consider adopting AASHTO T 350, *Standard Method of Test for Multiple Stress Creep Recovery (MSCR) Test of Asphalt Binder Using a Dynamic Shear Rheometer (DSR),* and AASHTO M 332,*Standard Specification for Performance-Graded Asphalt Binder Using Multiple Stress Creep Recovery (MSCR) Test*. The methods used in this study include a survey of the literature, interviews with personnel from other state DOTs, and laboratory experiments on asphalt binder and asphalt mixtures used by ADOT. The asphalt binder experiments include those currently called for by ADOT specifications and by AASHTO T 350. Asphalt mixture experiments include tests for the dynamic modulus as well as for fatigue and rutting resistance. The results of these experiments are compared to determine whether the AASTHO T 350 test is a better predictor of asphalt mixture performance than the tests currently used. The study finds that the AASHTO T 350 test parameter, nonrecoverable creep compliance, J_{nr}, is a better indicator of rutting than $|G^*|/\sin\delta$. ($|G^*|$ is the dynamic shear modulus and δ is the material phase angle, both of which are measured as part of current ADOT specifications.) The study also finds that the recovery value, *%R*, from the AASHTO T 350 test can discern between asphalt binder with and without polymer-modification. Finally, the study finds that polymer-modified asphalt mixtures exhibit substantially better fatigue performance than do non-polymer-modified mixtures, and that the *%R* can also capture this increased performance. The primary conclusions from this study are that (1) the J_{nr} value is a better indicator of rutting performance for ADOT materials than $|G^*|/\sin\delta$; (2) polymer-modified binders provide a greater fatigue life for ADOT materials than do non-polymer-modified binders; and (3) the *%R* parameter is not an indicator of rutting resistance, but it can distinguish between materials with better or worse fatigue performance.

17. Key Words	18. Distribution Statement		23. Registrant's Seal
Asphalt binder, multiple stress creep and recovery test, axial fatigue, specifications, Hamburg wheel tracking test	Document is available to the US public through the National Technical Information Service, Springfield, VA 22161.		
19. Security Classification Unclassified	**20. Security Classification** Unclassified	**21. No. of Pages** 318	**22. Price**

SI* (MODERN METRIC) CONVERSION FACTORS

APPROXIMATE CONVERSIONS TO SI UNITS

Symbol	When You Know	Multiply By	To Find	Symbol
		LENGTH		
in	inches	25.4	millimeters	mm
ft	feet	0.305	meters	m
yd	yards	0.914	meters	m
mi	miles	1.61	kilometers	km
		AREA		
in^2	square inches	645.2	square millimeters	mm^2
ft^2	square feet	0.093	square meters	m^2
yd^2	square yard	0.836	square meters	m^2
ac	acres	0.405	hectares	ha
mi^2	square miles	2.59	square kilometers	km^2
		VOLUME		
fl oz	fluid ounces	29.57	milliliters	mL
gal	gallons	3.785	liters	L
ft^3	cubic feet	0.028	cubic meters	m^3
yd^3	cubic yards	0.765	cubic meters	m^3
		NOTE: volumes greater than 1000 L shall be shown in m^3		
		MASS		
oz	ounces	28.35	grams	g
lb	pounds	0.454	kilograms	kg
T	short tons (2000 lb)	0.907	megagrams (or "metric ton")	Mg (or "t")
		TEMPERATURE (exact degrees)		
^oF	Fahrenheit	5 (F-32)/9 or (F-32)/1.8	Celsius	^oC
		ILLUMINATION		
fc	foot-candles	10.76	lux	lx
fl	foot-Lamberts	3.426	$candela/m^2$	cd/m^2
		FORCE and PRESSURE or STRESS		
lbf	poundforce	4.45	newtons	N
lbf/in^2	poundforce per square inch	6.89	kilopascals	kPa

APPROXIMATE CONVERSIONS FROM SI UNITS

Symbol	When You Know	Multiply By	To Find	Symbol
		LENGTH		
mm	millimeters	0.039	inches	in
m	meters	3.28	feet	ft
m	meters	1.09	yards	yd
km	kilometers	0.621	miles	mi
		AREA		
mm^2	square millimeters	0.0016	square inches	in^2
m^2	square meters	10.764	square feet	ft^2
m^2	square meters	1.195	square yards	yd^2
ha	hectares	2.47	acres	ac
km^2	square kilometers	0.386	square miles	mi^2
		VOLUME		
mL	milliliters	0.034	fluid ounces	fl oz
L	liters	0.264	gallons	gal
m^3	cubic meters	35.314	cubic feet	ft^3
m^3	cubic meters	1.307	cubic yards	yd^3
		MASS		
g	grams	0.035	ounces	oz
kg	kilograms	2.202	pounds	lb
Mg (or "t")	megagrams (or "metric ton")	1.103	short tons (2000 lb)	T
		TEMPERATURE (exact degrees)		
^oC	Celsius	1.8C+32	Fahrenheit	^oF
		ILLUMINATION		
lx	lux	0.0929	foot-candles	fc
cd/m^2	$candela/m^2$	0.2919	foot-Lamberts	fl
		FORCE and PRESSURE or STRESS		
N	newtons	0.225	poundforce	lbf
kPa	kilopascals	0.145	poundforce per square inch	lbf/in^2

*SI is the symbol for the International System of Units. Appropriate rounding should be made to comply with Section 4 of ASTM E380.
(Revised March 2003)

Contents

List of Figures

List of Tables

List of Abbreviations, Acronyms, and Symbols

AADT	annual average daily traffic
AASHTO	American Association of State Highway and Transportation Officials
ADOT	Arizona Department of Transportation
AI	Asphalt Institute
ALF	accelerated loading facility
AMRL	AASHTO Materials Reference Library
AR	aging ratio
ASTM	ASTM International (formerly American Society for Testing and Materials)
ASU	Arizona State University
ATR	attenuated total reflectance
BBR	bending beam rheometer
CA	carbonyl area
CA+SA	carbonyl plus sulfoxide area
DOT	department of transportation
DSR	dynamic shear rheometer
ESAL	equivalent single axle load
FHWA	Federal Highway Administration
ER	elastic recovery
FT-IR	Fourier transform infrared spectroscopy
HD	historical database
HMA	hot-mix asphalt
HSB	high-stiffness binder
HWTT	Hamburg wheel tracking test
ILS	interlaboratory studies
LTPP	Long-Term Pavement Performance
MSCR	multiple stress creep and recovery
NCAT	National Center for Asphalt Technology
NCHRP	National Cooperative Highway Research Program
NCSC	North Central Superpave Center
NEAUPG	North East Asphalt User/Producer Group
NHPN	National Highway Performance Network
PAV	pressure aging vessel
PCCAS	Pacific Coast Conference on Asphalt Specifications
PG	performance grade
PMB	polymer-modified binder
PPA	polyphosphoric acid
PSP	proficiency sample program
RAP	recycled asphalt pavement
RAS	recycled asphalt shingles

RTFO	rolling thin-film oven
SA	sulfoxide area
SBR	styrene-butadiene-rubber
SBS	styrene-butadiene-styrene
SEAUPG	Southeastern Asphalt User/Producer Group
SHRP	Strategic Highway Research Program
S-VECD	simplified viscoelastic continuum damage
TFO	thin-film oven
T_{LF}	truck load factor
TTC	Truck Traffic Classification
TRID	Transportation Research International Documentation
VFA	voids filled with asphalt
VMA	voids in mineral aggregate

SYMBOLS AND VARIABLES

C	material integrity
d2s%	acceptable range of two test results as a percentage
|E*|	dynamic modulus (mixture)
|G^*|	complex shear modulus
|G^*|sin δ	Superpave binder fatigue parameter
|G^*|/sin δ	Superpave binder rutting parameter (ratio of dynamic modulus to the sine of the phase angle)
J_{nr}	average nonrecoverable creep compliance
$J_{nr3.2}$	average nonrecoverable creep compliance at 3.2 kPa
$J_{nr0.1}$	average nonrecoverable creep compliance at 0.1 kPa
J_{nrdiff}	percent difference in nonrecoverable creep compliance at 3.2 and 0.1 kPa
m	slope
%R	percent recovery
R^2	correlation coefficient
$R_{3.2}$	average percent recovery at 3.2 kPa
$R_{0.1}$	average percent recovery at 0.1 kPa
R_{diff}	percent difference in average percent recovery at 3.2 and 0.1 kPa
S	damage; creep stiffness
δ	phase angle
με	microstrain
S, H, V, E	designations for Standard, High, Very high, and Extremely high traffic loading, respectively

EXECUTIVE SUMMARY

BACKGROUND AND PURPOSE

When engineers need to build, rehabilitate, or maintain asphalt pavements, one of the first decisions they must make is which asphalt binder to use. The asphalt binder must be carefully selected because binders that are too stiff for the climate and traffic are likely to crack, and those that are too soft will likely experience rutting. The purpose of this study is to recommend, based on experimental study, whether the Arizona Department of Transportation (ADOT) should consider adopting the new standards from the American Association of State Highway and Transportation Officials (AASHTO) for testing and specification of asphalt binders. The specific standards evaluated include AASHTO T 350, *Standard Method of Test for Multiple Stress Creep Recovery (MSCR) Test of Asphalt Binder Using a Dynamic Shear Rheometer (DSR)* (AASHTO 2014c), and AASHTO M 332, *Standard Specification for Performance-Graded Asphalt Binder Using Multiple Stress Creep Recovery (MSCR) Test* (AASHTO 2014d). This study is needed because much of the substantial development work that has been done by other organizations across the country is not applicable to Arizona. There are several reasons for this:

1. The majority of the test method and grading evaluations have been limited to the East Coast, where binder supplies, the number of binders used, and mixture designs are drastically different from those in Arizona.
2. The climate in Arizona is substantially more extreme both in heat (in the southern and central sections of the state) and in cold (in the northern sections of the state).
3. The validation efforts presented in the literature include only a limited number of the types of materials regularly used in Arizona.

The methods adopted in this study include a survey of the literature, interviews with other state agencies, and laboratory experiments on asphalt binder and asphalt mixtures used by ADOT. The experiments on the asphalt binder include those tests currently used in ADOT specifications and in the AASHTO T 350 test standard. Asphalt mixture experiments include tests for dynamic modulus as well as fatigue and rutting resistance. Finally, results from the asphalt binder and asphalt mixture experiments are compared to determine whether the AASHTO T 350 test result is a better predictor of asphalt mixture performance than the tests currently used by ADOT.

RECOMMENDATIONS

The research concluded:

- The study findings demonstrated that the AASHTO T 350 test parameter is a better indicator of rutting than the currently used parameter of $|G^*|/\sin\delta$.
    - The recovery value, *%R*, from the AASHTO T 350 test can discern between asphalt binders with and without polymer modification.
    - The polymer-modified asphalt mixtures exhibited substantially better fatigue performance than the non-polymer-modified mixtures, and the study results showed that *%R* can also capture this increased performance.
- If ADOT is expecting to increase the use of polymer-modified binders, it is recommended that it adopt the AASHTO M 332 specification.
    - It is recommended that ADOT follow the specification's testing-temperature guidelines, which means testing binders at the intended temperatures in which they will be used.
    - ADOT may consider modifying the standards as follows:
        - Change the PAV aging temperature for PG 64 H, V, and E grades to 110°C.
        - Eliminate the J_{nrdiff} parameter for H-, V-, and E-grade binders.
        - This study showed no definitive evidence that S-graded binders with J_{nrdiff} greater than 75 percent will fail in their performance. More study of S-graded binders with high J_{nrdiff} will be necessary to provide a more specific recommendation.
        - Eliminate the 10°C elastic recovery and other plus-tests for polymer-modified binders, and adopt the modified J_{nr} versus *%R* relationship given below.

$$\%R_{3.2} = \begin{cases} 75 & J_{nr3.2} \le 0.1 \text{ kPa}^{-1} \\ 33.133\left(J_{nr3.2}\right)^{-0.35} & J_{nr3.2} > 0.1 \text{ kPa}^{-1} \end{cases}$$

CHAPTER 1. INTRODUCTION

PROJECT OVERVIEW

Pavements surfaced with asphalt mixtures represent nearly 98 percent of the roadways under the control of the Arizona Department of Transportation (ADOT 2013). When engineers need to build, rehabilitate, or maintain one of these pavements, one of the first decisions they must make is to decide on the asphalt cement to use. Asphalt cement is the binding agent in asphalt mixtures (the actual paving material) and is often colloquially referred to as asphalt binder or simply binder. The binder used in any given application has to be carefully selected because binders that are too stiff for the climate and traffic are likely to crack, and those that are too soft will likely experience rutting. Cracking can negatively impact the load-carrying capacity of a pavement as well as accelerate losses in ride quality and, ultimately, longevity (Huang 2004). Rutting, defined as surface depressions in the wheel path, can severely impact ride quality and can also negatively affect safety, since the depressions can allow water accumulation that may result in vehicle hydroplaning (Huang 2004). To deliver the best-performing, longest-lasting, and lowest-cost pavement infrastructure for Arizona, ADOT engineers must carefully select designs and materials so as to balance cracking and rutting risks. The specification used to determine, select, and ultimately purchase binder is a critically important mechanism for achieving this goal. The current research study focuses on binder specification in Arizona. It specifically examines technological advances that have occurred since the initial deployment of the current ADOT specification, the application of such advances in Arizona, and the potential impacts to ADOT from adopting new specifications.

CURRENT ADOT PRACTICE

Current ADOT binder purchase specifications are based largely on an American Association of State Highway and Transportation Officials (AASHTO) standard—AASHTO M 320, *Standard Specification for Performance-Graded Asphalt Binder* (AASHTO 2010)—developed in the early to mid-1990s during the Strategic Highway Research Program (SHRP). SHRP was authorized by the U.S. Congress in 1987 to improve the performance, durability, and safety of the nation's highway system. The term "Superpave" is used to encompass the results of SHRP's asphalt research segment, which investigated asphalt binder specifications, design methods for hot-mix asphalt (HMA), and HMA tests and models for predicting performance.

The M 320 specification that emerged from SHRP assigns a performance grade (PG) describing the high and low pavement temperatures appropriate for each binder. For example, a binder graded PG 76-16 is appropriate for a location where the high pavement temperature is 76°C and the low pavement temperature is no lower than –16°C. To produce a manageable system, grades are standardized in 6°C increments. The grades are assigned to binders based on a suite of standardized laboratory tests (AASHTO T 315, AASHTO T 313, and AASHTO T 316) conducted at different temperatures. The individual tests relate to specific performance measures (rutting, cracking, construction, etc.).

When choosing a PG binder for a given application, ADOT engineers use prior experience and/or a series of maps that are based on the historical climate conditions across the state. For high-volume roads, ADOT also follows the convention of increasing the required high-temperature binder grade by a single increment. Many agencies specify only two or three binders for the entirety of their state, but because of the range of climates in Arizona, ADOT currently has specifications for more than eight binder grades. The need for so many binder grades places unique pressures on ADOT to develop specifications and on material suppliers to produce, store, and supply binders.

LIMITATIONS OF CURRENT ADOT SPECIFICATIONS

The AASHTO M 320 specification was developed using experimental data for binders that were common in the late 1980s to early 1990s. These binders did not incorporate many modern technological developments such as chemical and polymer modification (Anderson et al. 1994). Agencies have begun to make extensive use of these modern binders because they lead to better-performing and thus less-costly pavements (Buncher and Rosenberger 2005). Since modified binders have become more prevalent, practitioners have identified certain limitations with the AASHTO M 320 parameters. AASHTO T 350, *Standard Method of Test for Multiple Stress Creep Recovery (MSCR) Test of Asphalt Binder Using a Dynamic Shear Rheometer (DSR)* (AASHTO 2014c), and AASHTO M 332, *Standard Specification for Performance-Graded Asphalt Binder Using Multiple Stress Creep Recovery (MSCR) Test* (AASHTO 2014d), are two recent advances that address the shortcomings in AASHTO M 320. ADOT does not currently use these two newer standards in its operational efforts.

Although substantial development work on these recent advances has been carried out by the Asphalt Institute, user/producer organizations, and other researchers across the country, a large amount of the work is not immediately applicable to Arizona. There are several reasons:

1. The majority of the test method and grading evaluations have been limited to the East Coast, where binder supplies, the number of binders used, and mixture designs are drastically different from those in Arizona.
2. The climate in Arizona is substantially more extreme both in heat (in the southern and central sections of the state) and in cold (in the northern sections of the state) than in many other parts of the country.
3. The validation efforts presented in the literature include only a limited number of the types of materials regularly used in Arizona.

In addition, there exists a high level of interest in the test and grading standards used by surrounding DOTs that share common sources of binder, and whose decisions ultimately affect the materials available in Arizona. The research documented in this report addresses the three shortcomings listed above so that ADOT can make better-informed decisions about implementing the AASHTO M 332 specification. To accomplish this goal, the researchers pursued the following specific objectives:

1. Determine if the MSCR test parameter is a better indicator of the rutting performance of Arizona asphalt pavements than is the currently used AASHTO M 320 parameter.

2. Determine whether there are other undesirable performance impacts associated with using the MSCR test parameter. Specifically, does adopting the MSCR test parameter correlate to undesirable results in aging and/or cracking resistance?
3. Confirm the applicability of the MSCR test to Arizona binders and conditions.
4. Determine if key industry representatives anticipate possible economic effects on Arizona binder suppliers if ADOT chooses to adopt AASHTO M 332.

To understand the need for and importance of this study to improve the performance of asphalt pavements in Arizona, it is important to know more about the MSCR test and the AASHTO M 332 specification.

Multiple Stress Creep and Recovery (MSCR) Test

The MSCR test is standardized by AASHTO in AASHTO T 350, and by ASTM International (ASTM) in ASTM D7405, *Standard Test Method for Multiple Stress Creep and Recovery (MSCR) of Asphalt Binder Using a Dynamic Shear Rheometer* (ASTM 2015). The main motivation behind the development of the MSCR test was to identify a parameter that is a better indicator of rutting. The current parameter used to ensure rutting resistance is a stiffness quantity ($|G^*|/\sin \delta$) measured through oscillatory loading experiments—AASHTO T 315 (AASHTO 2012b). However, research has suggested that this parameter has limited applicability to polymer-modified binders (D'Angelo and Dongre 2002, Dongre and D'Angelo 2003). Polymer-modified binders are becoming increasingly important tools for DOTs since they can often yield substantial improvements in pavement performance and, therefore, reductions in long-term cost (Sargand and Kim 2001). The MSCR test subjects binders to larger deformations than the AASHTO T 315 experiment. These deformations are more similar to those observed with in-service pavements and thus better reflect the material's behavior.

The test parameter resulting from both the AASHTO and the ASTM experiments is nonrecoverable creep compliance, J_{nr}, which relates the strain response of the sample to the applied stress. That is, nonrecoverable creep compliance is a measure of the resistance of an asphalt binder to permanent deformation. A material that deforms by a large amount under a prescribed load has a high J_{nr}, while one that deforms very little has a low J_{nr}. Low-J_{nr} binders would be used for high-value applications (interstates, US routes, etc.); higher-J_{nr} binders would be used for less-critical and lower-traffic-volume applications; and very-high-J_{nr} binders would be avoided altogether. While standards exist to objectively quantify the meaning of "low," "high," and "very high," the underlying developmental work has been largely based on experiments with materials that are not representative of those used across the range of temperatures and traffic levels that exist in Arizona.

The MSCR test traces its beginnings to the research of Bahia et al. (2001) and D'Angelo et al. (2007), but the test itself has evolved as more materials and conditions have been encountered. In the case of AASHTO T 350, the method began as an AASHTO provisional standard (TP70) in 2009, was refined in 2010, 2012, and 2013, and achieved full standard status in 2014. At ASTM, the first version of D7405 appeared in 2008, and the standard was refined in 2010 and 2015. The changes that occurred in each

iteration mean that the literature must be carefully reviewed to ensure that the findings are relevant to the overall study objectives.

AASHTO M 332—Performance-Graded Asphalt Binder Using MSCR Test

In the binder specification process, consideration is always given to the material's response at different life stages: unaged, short-term-aged, and long-term-aged. In AASHTO M 332, the MSCR test replaces AASHTO T 315 as the key grading experiment for the short-term-aged binders. It also assigns binder grades with two designations, one for temperature and the other for traffic. Aside from these changes, the two specifications are essentially the same (see Appendix A for the grading tables from both standards). For the short-term-aged binders, a traffic-level-dependent J_{nr} limit is used instead of a single stiffness measure. There are four different Equivalent Single Axle Load (ESAL) based traffic levels included in the specification; (S)tandard (less than 10 million ESALs), (H)eavy (between 10 and 30 million ESALs), (V)ery Heavy (greater than 30 million ESALs), and (E)xtreme (greater than 30 million ESALs plus standing traffic). This additional grading parameter allows objective and performance-based specifications for both climate and traffic conditions. As described earlier, the current ADOT specification requires an empirical adjustment to the specified grade based on traffic. Limits on the J_{nr} value decrease with each successively higher traffic level; thus, more rut-resistant binders are deployed in higher-value applications.

Another contribution from AASHTO M 332 is a function that distinguishes between (a) polymer-modified binders that have achieved sufficient microstructural cross-linking to see performance benefits, and (b) non-polymer-modified and polymer-modified binders without sufficient cross-linking. The function as given in the AASHTO specification is shown in Figure 1. The figure also shows (as a dashed line) a modification recommended by the Asphalt Institute (AI) wherein the function is truncated for very-low-J_{nr} values (Anderson 2016).

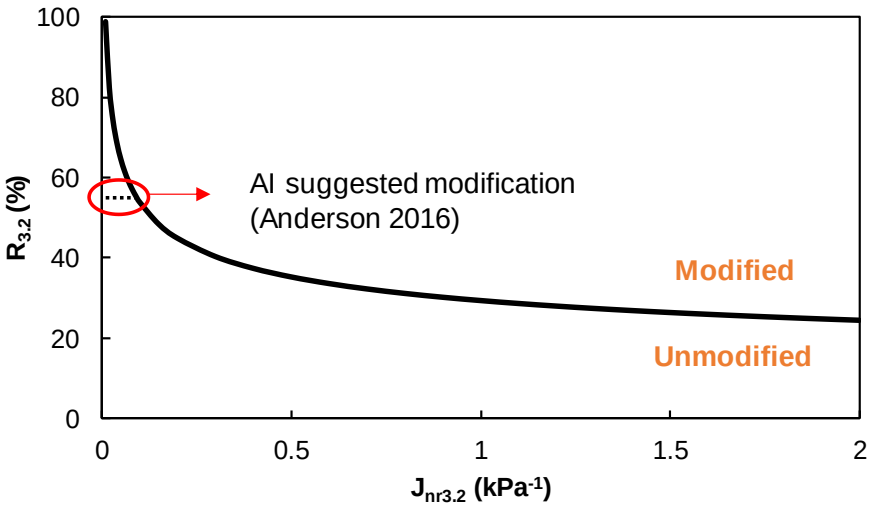

Figure 1. Relationship Specified in AASHTO M 332 for Detecting Cross-Linked Polymer Modification

As stated earlier, the goal of any experiment and specification is to ensure that the grading system accurately reflects the likely performance of the material. For new binder technologies, AASHTO M 320 may not adequately capture the potential performance enhancements those technologies provide; moreover, strict adherence to the specification may present a major challenge to the reliable incorporation of those binders into projects. Many DOTs, Arizona's included, have recognized this shortcoming with AASHTO M 320, and have developed supplementary specifications for use with newer binders. These tests are generally referred to as PG+ tests and exist outside the AASHTO M 320 framework.

Since the PG+ tests exist outside the AASHTO M 320 framework, agencies have adopted their own experiments, which have led to inconsistencies across the nation and even between neighboring DOTs (Asphalt Institute 2016). For example, ADOT uses the elastic recovery test for unaged binders, whereas Nevada, New Mexico, and Utah have adopted different tests (toughness and tenacity for unaged binders and elastic recovery for aged binders). The technical criticism associated with many of these tests is that they can detect the presence of the polymer/modifier but do not directly relate it to any particular performance behavior (i.e., just because the polymer/modifier is present does not mean it is actively improving performance). The AASHTO M 332 standard is meant, in part, to provide a specification that eliminates the need for additional PG+ tests and thus delivers a more consistent, national grading system. Unfortunately, since much of the basic development work with the MSCR test has been conducted with materials that are not like those in Arizona, the applicability of the AASHTO M 332 specification to Arizona conditions is in question.

STATUS OF ADOT EFFORTS AT PROJECT OUTSET

Recognizing that Arizona conditions are unique, especially in the number of required grades, ADOT has been proactive in investigating the MSCR test and AASHTO M 332 grading standard. Since 2008, ADOT's Construction and Materials Group has conducted experiments on more than 340 mostly unmodified binder samples. In addition, ADOT has reviewed its projects and used FHWA's LTPPBind V2 software to determine appropriate binder grades across the state (Figure 2). LTPPBind analyzes climatic data to determine the binder type needed for a given location. It should be noted that LTPPBind V2 is not the most recent version of this software, but was used for this analysis because LTPPBind V3 (the newest version) yields unrealistically high grades for many locations in central and southern Arizona.

The fact that LTPPBind V3 yields unrealistic values is evidence that conditions and materials in Arizona are substantially different from those in many other parts of the country. Mohseni et al. (2005) developed the algorithms underlying the LTPPBind V3 software by using rutting models calibrated from national performance databases. Recent recalibration of these models specifically for Arizona conditions revealed that the models overestimate rutting for Arizona pavements by approximately 1.4 times (Darter et al. 2014). Additionally, discussions with experts confirm that the LTPPBind V2 grades yield positive results in Arizona, but the higher grades recommended by LTPPBind V3 would likely result in constructability issues (McGennis 2005).

Stevens et al. (2015) analyzed the ADOT MSCR database and compared the measured J_{nr} values against the AASHTO M 332 grading criteria. The analysis showed that at the existing grading temperatures used by ADOT, the majority of binders (74 percent) would grade as "S" according to AASHTO M 332 (Figure 3). Another 14 percent would grade as "H", 9 percent would be "V" or "E," and the remaining 3 percent would fail the specification. (In Figure 3, the dashed red lines indicate the divisions between S, H, V, and E grades; I, J, K, L, and M represent different suppliers.) The study further examined how these binders would grade at different high temperature values. Despite some variation, it was generally found that reducing the high temperature grade by one increment resulted in an increase in traffic-level grade by one level. The study also examined the ability of the standard to detect polymer modification for binders currently in use in Arizona. As shown in Figure 4, it was found that the standardized curve did distinguish between modified and non-modified binders. Note in these figures that the suppliers are anonymous.

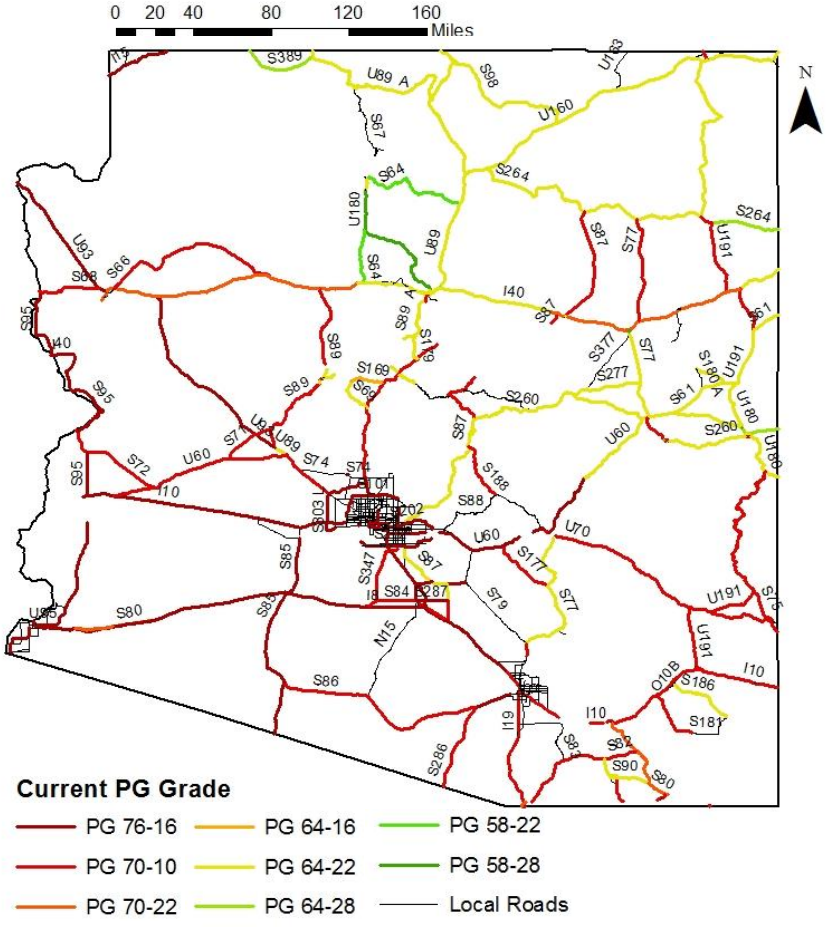

Figure 2. Distribution of Current Asphalt Binder Grades Across Arizona

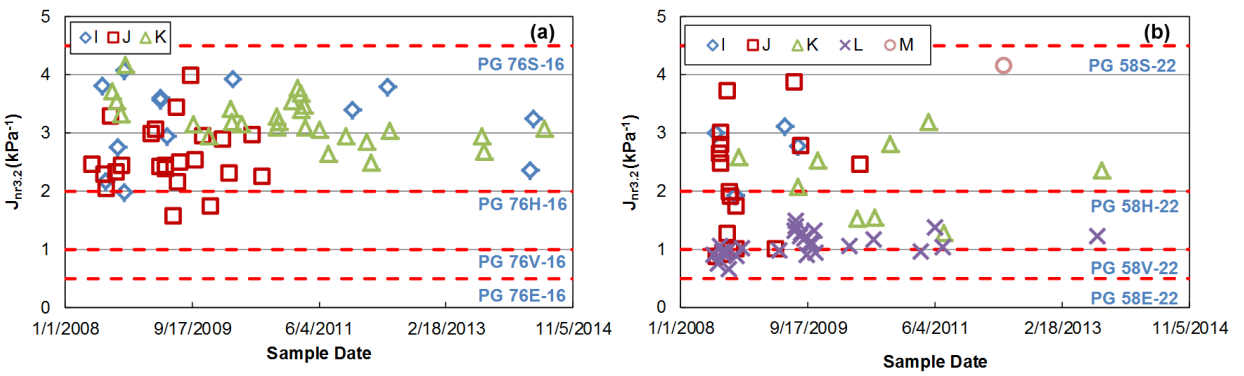

Figure 3. Asphalt Binder (a) PG 76-16 and (b) PG 58-22 Grouped by Supplier

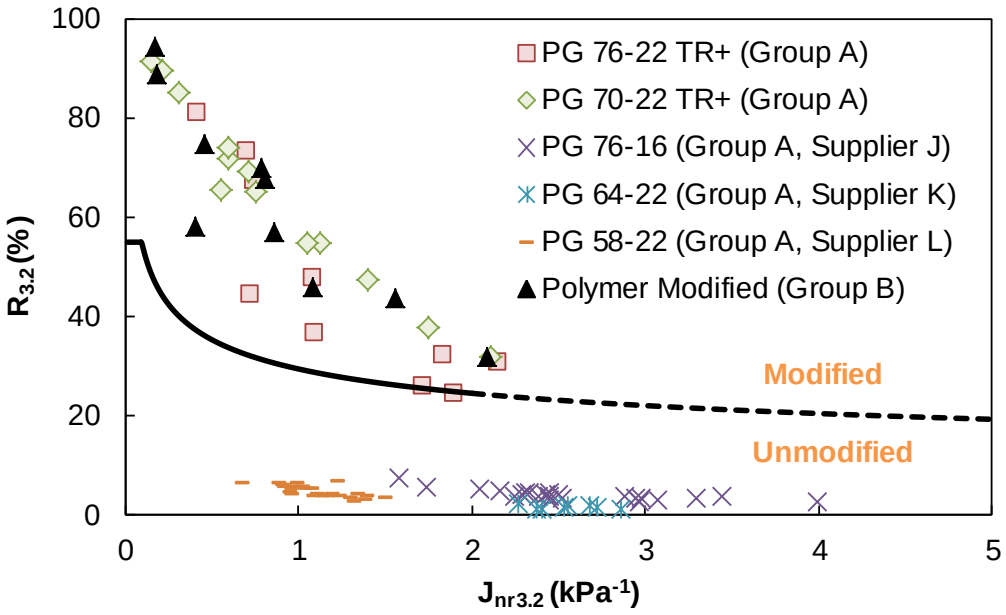

Figure 4. Presence of Modifiers in Arizona Binders

Stevens et al. (2015) laid the groundwork for the current investigation by demonstrating in principle the benefits of the MSCR test (delineation of behaviors and performance of polymer-modified binders in Arizona) and the AASHTO M 332 specification (recognition and separation of Arizona binders by expected traffic applications). Both tests also have other practical considerations, such as consistency in results across time. However, confirming that the two standards result in better and more reliably performing pavements in Arizona.

SUMMARY

ADOT makes extensive use of asphalt mixtures across its pavement network. To design and construct these pavements, ADOT currently uses a binder specification that is rooted in studies conducted more than 20 years ago. While ADOT has successfully used this grading standard for many years, studies and experience have shown potential shortcomings in the standard's ability to capture the benefits of newer binder technologies. Technological advancements in testing and specification have provided tools to overcome these shortcomings. However, much of this developmental work is based on investigations from locations that have drastically different conditions (in climate and materials) than Arizona, and thus direct transfer of those investigations' findings to Arizona cannot be reliably performed. The present research investigates the applicability of the AASHTO T 350 testing protocol and the associated AASHTO M 332 purchase specification to Arizona conditions and will answer the question of whether adopting the AASHTO M 332 specification will lead to better-performing pavements in Arizona.

CHAPTER 2. LITERATURE REVIEW

To conduct the literature review for this project, the research team adopted a multimethod approach. First, it conducted searches of databases that contain relevant contents (the Transportation Research Board's Transportation Research International Documentation [TRID] database, Google Scholar, and Scopus). For relevant sources not always cited in these databases (such as the *Journal of the Association of Asphalt Paving Technologists* and the Federal Highway Administration's technical bulletins), the team conducted a manual review of publications in the last 15 years. Second, the research team reviewed presentations and (if available) reports given by key researchers and industry members at local, regional, and national professional meetings. Third, the team carried out Internet surveys and telephone interviews with DOTs to ensure that the most up-to-date practice information was obtained. The research team had also received substantial background from key ADOT personnel prior to the start of the research project, and the team incorporated these findings into the review as well. Using these methods, the team examined the following topics:

- Studies showing the correlation between nonrecoverable creep compliance (Jnr) and rutting, and between the Superpave parameter ($|G^*|/\sin\delta$) and rutting.
- Experiences of neighboring DOTs, which either have incorporated the MSCR test parameters into their binder specifications or are currently testing and evaluating the scope of MSCR implementation.
- Interlaboratory studies ascertaining the variability of the different MSCR test parameters, which have been conducted with the support of the Asphalt Institute and professional bodies such as the Northeast Asphalt User-Producer Group, the Southeast Asphalt User-Producer Group, and the Pacific Coast Conference on Asphalt Specifications (PCCAS).
- Practices followed by DOTs in incorporating recycled asphalt pavement (RAP) under the AASHTO M 332 specification.
- DOT concerns, if any, regarding use of RAP in polymer-modified asphalt mixtures.

CORRELATIONS BETWEEN J_{NR} AND MIXTURE RUTTING

The key technical shortcoming of the Superpave rutting parameter is its poor correlation with asphalt mixture rutting (Minnesota DOT 2015). Studies have been performed to evaluate the correlation between rutting and the J_{nr} value. Of relevance to this research, and Arizona, is the evaluation of binders that have high stiffness. In the evaluations cited below, when high-stiffness binders are used, they have been polymer-modified. In Arizona, by contrast, high-stiffness binders are commonly used and are non-polymer-modified. Nevertheless, the correlations given are strong and hence they are reported here.

D'Angelo et al. (2007) compared the correlation between rutting and the J_{nr} parameter, as well as between rutting and the Superpave parameter ($|G^*|/\sin\delta$), in tests conducted on pavement sections using the Federal Highway Administration's transportable Accelerated Loading Facility (ALF). The binder under evaluation was PG 64-40, and hence the MSCR test and the measurement of $|G^*|/\sin\delta$ were performed at 64°C. The correlation between the mixture and the rutting parameter was found to be substantially higher when the parameter used was J_{nr} than when it was $|G^*|/\sin\delta$ (Figure 5).

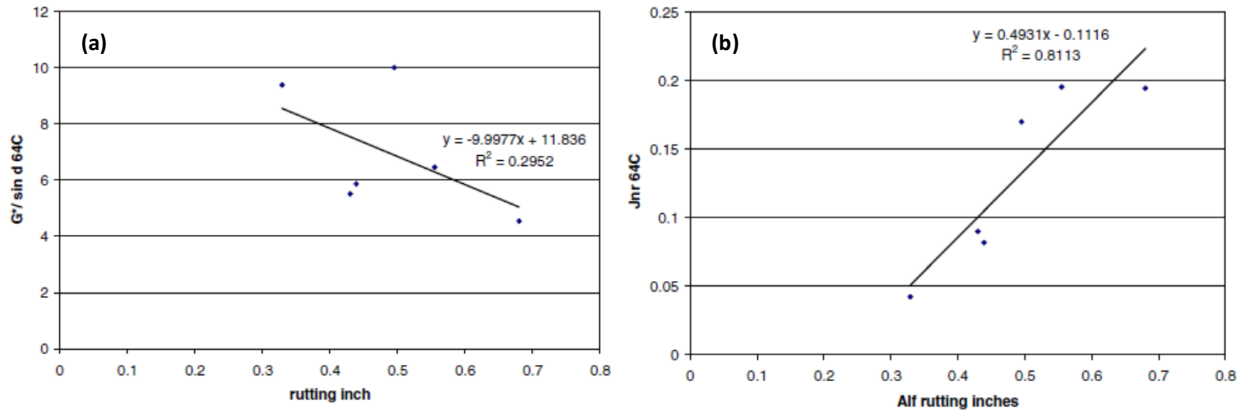

Figure 5. Relationship Between Rutting at the ALF Sections and (a) $|G^*|/\sin\delta$ or (b) J_{nr} of the Binders at 64°C (D'Angelo et al. 2007)

D'Angelo et al. (2007) also included a field investigation of pavement sections on Interstate 55 in Mississippi. The study compared the rutting after six years of service to J_{nr} values and obtained an R^2 value of about 0.75. The binder grades in the study included cryo-rubber-modified binders, polymer-modified binders, and unmodified binders. Continuous PG grades ranged from PG 70-24 to PG 82-27. Rutting was estimated using the Hamburg wheel tracking test (HWTT), and the rut depth was correlated to the J_{nr} at 12.8 kilopascals (kPa) ($R^2 > 0.9$). Similar observations were made in a Minnesota study, which evaluated binder grades of PG 58-28, PG 58-34, and PG 58-40 (Minnesota DOT 2015). Zhang et al. (2015) measured rutting of Texas asphalt mixtures using HWTT and compared it to the J_{nr} at 0.1 and 3.2 kPa. The continuous grade of the binders used in this study ranged from PG 70 to PG 87, and the low-temperature grade was either –22 or –28. It has to be noted that the evaluations were performed on plant mixtures, so the binder tests were performed after extracting the binder from these mixtures. Zhang et al. (2015) reported a good correlation between J_{nr} and rutting, with R^2 in excess of 0.75 and 0.85 in most of the cases. Laukkanen et al. (2015) measured the rutting of Finland asphalt mixtures using the Laboratoire Central des Ponts et Chaussées wheel tracking test, and related the rutting parameters to both $J_{nr3.2}$ and $|G^*|/\sin\delta$. The first parameter was rate of rutting, which was measured as the relationship between linear slope of the rut depth and number of cycles between 10,000 and 50,000 cycles. The second rutting parameter was based on the functional fit of the relationship between rut depth and number of cycles. The authors fitted the data to a power law function with the functional form as shown in Equation 1:

$$RD = aN^b \qquad \text{(Eq. 1)}$$

Where RD = rut depth
N = number of cycles
a and b = fitting coefficients

The authors observed an R^2 value of 0.976 with rate of rutting and 0.982 with b value, indicating that the rutting parameters are strongly correlated to $J_{nr3.2}$.

CORRELATIONS BETWEEN $|G^*|/\sin\delta$ AND MIXTURE RUTTING

The majority of the binders in the ALF, Minnesota, and Mississippi studies were polymer-modified, and good correlation was reported between J_{nr} and rutting relative to the correlation of $|G^*|/\sin\delta$ and rutting. It should be noted that in the ALF and Mississippi studies, the correlations were based on field rutting, whereas in the current project the rut depths are to be measured from the HWTT, an approach similar to that used in the Minnesota and Texas studies. Under its current specifications, ADOT does not currently use large quantities of polymer-modified binders; therefore, the improved correlations to rutting may have little impact on current ADOT practice.

The most immediate way to assess the applicability of the $|G^*|/\sin\delta$ parameter to Arizona conditions is to isolate the unmodified binders in the above studies and then check the $|G^*|/\sin\delta$ vs. rutting relationship. However, in the aforementioned studies, only one or two non-polymer-modified binders are included, a number that is insufficient to carry out any reliable correlation comparisons. Conversely, the research by Leahy et al. (1994) evaluated a factorial combination of 16 binders (all unmodified), two aggregate sources (high- and low-absorption limestone and greywacke), and two air void levels (4 and 7 percent). Of the binders tested in this study, seven were PG 64, eight were PG 58, and one was PG 52. The wheel tracking test was employed to measure the rut depth after 5000 passes. Both the binder and the wheel tracking tests were conducted at 40°C. The correlation between rut depth and $|G^*|/\sin\delta$ was poor, with a correlation coefficient of 0.30 (Figure 6a). $|G^*|/\sin\delta$ was also correlated to the normalized rut rate, which was the rate of increase in rut depth between 2000 and 4000 passes divided by the contact stress of the wheel (Figure 6b). The correlation coefficient achieved in that case was even lower, 0.18. Leahy et al. (1994) attributed this low correlation to three factors:

1. The size of the wheel tracking equipment used and the surface area of the mix specimen were relatively small, considering that the aggregates size was typical of that used in a conventional pavement.
2. The variability obtained in the wheel tracking tests was high.
3. The binder and wheel tracking tests were conducted at 40°C, which may not have been sufficiently high to allow the viscous characteristics of the binders to affect mixture performance.

Bouldin et al. (1994) reported data from four modified and two unmodified binders to support the relationship between $|G^*|/\sin\delta$ and rutting (Figure 7). These researchers compared $|G^*|/\sin\delta$ with the rut rate and with the rate of strain accumulation. Both relationships had a very good correlation coefficient of 0.96 and 0.98, respectively. The test temperature for both the binder tests and the wheel tracking tests was 60°C with a test frequency of 1 radian/second. The maximum contact pressure was 29 pounds per square inch (psi), which is much lower than the 105 psi used by Leahy et al. (1994).

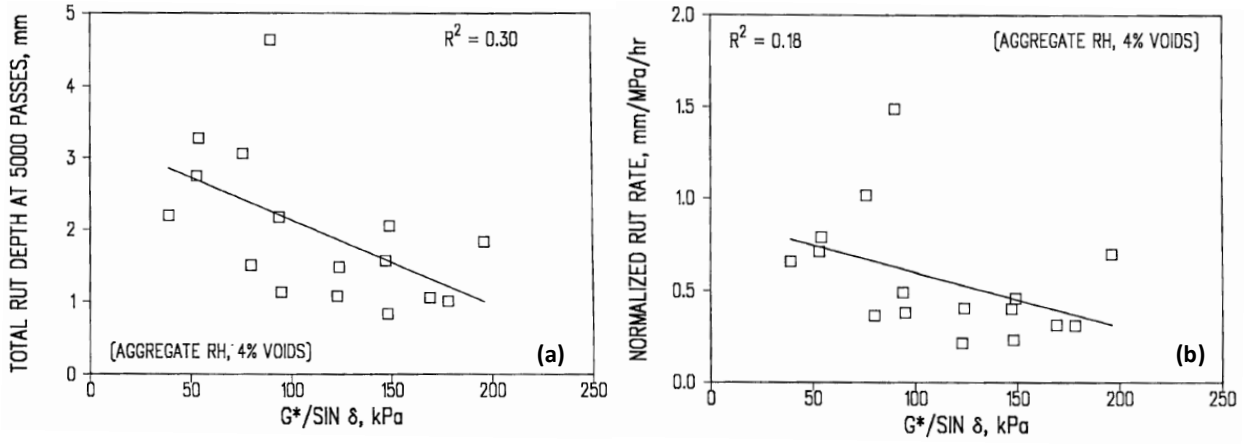

Figure 6. Relationship Between $|G^*|/\sin\delta$ and (a) Total Rut Depth and (b) Normalized Rut Rate (Leahy et al. 1994)

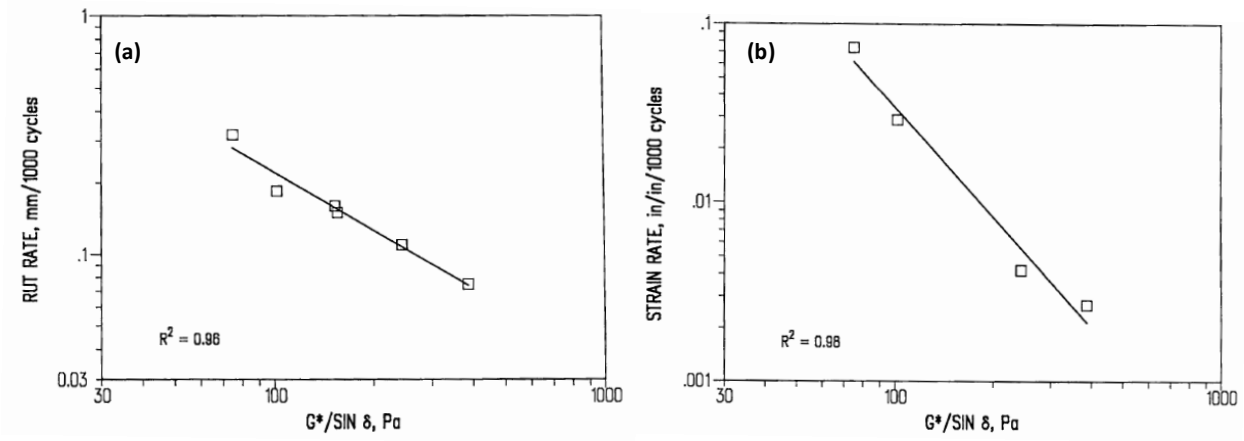

Figure 7. Relationship Between $|G^*|/\sin\delta$ and (a) Rut Rate and (b) Strain Rate (Bouldin et al. 1994)

Apart from the wheel tracking tests, Leahy et al. (1994) also conducted repeated simple shear tests at constant height. Figure 8 shows the resultant correlations between mixture performance and the binder parameter. The correlation parameters in this case were for $|G^*|/\sin\delta$ and both the number of load cycles at 2 percent permanent strain and the cumulative shear strain after 5000 cycles. The correlation coefficients were higher (at 0.52 and 0.58, respectively) than those obtained for the wheel tracking tests (0.30 and 0.18).

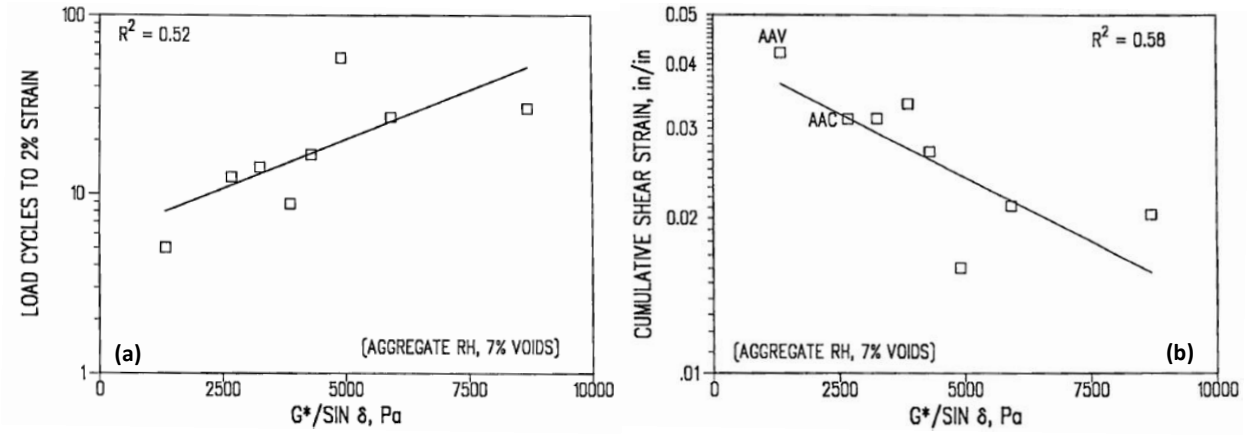

Figure 8. Relationship Between $|G^*|/\sin\delta$ and (a) Load Cycles at 2% Strain and (b) Cumulative Shear Strain (Leahy et al. 1994)

The significance of this review is that the binders used for $|G^*|/\sin\delta$ validation, although unmodified, may not represent those used currently in Arizona, both with respect to the binder grades themselves (the validation consisted of PG 64-XX, PG 58-XX, and PG 52-XX binders) and also with respect to changes that may have occurred in processing and formulating since the advent of Superpave.

As mentioned in the previous section, Laukkanen et al. (2015), related the rutting parameters to both $J_{nr3.2}$ and $|G^*|/\sin\delta$ to rutting. Laukkanen et al. (2015) found that the rate of rutting and the "b" value both related poorly to $|G^*|/\sin\delta$, with R^2 values of 0.401 and 0.502, respectively, when the data were fitted to a linear function. However, if the data were fitted to a power law function, then the R^2 values improved to 0.758 and 0.741, respectively. These were still lower than the R^2 values observed in the relationship with $J_{nr3.2}$.

EXPERIENCE OF NEIGHBORING DEPARTMENTS OF TRANSPORTATION

As part of the literature review, the research team reached out to neighboring departments of transportation (DOTs) to document their experiences and plans with respect to MSCR and AASHTO M 332 implementation. DOT personnel in 12 states were contacted and asked to either respond to a questionnaire about their experiences (see Appendix B) or participate in a brief phone interview. The DOTs were divided into two groups based on proximity to Arizona (Figure 9). The DOTs in Group 1 are color-coded purple and those in Group 2 are color-coded green. The only agency that did not respond was the Idaho Transportation Department, and for this reason the state is colored in a lighter shade. The survey and interview results are discussed below, while Table 1 and

Table 2 summarize the most important findings.

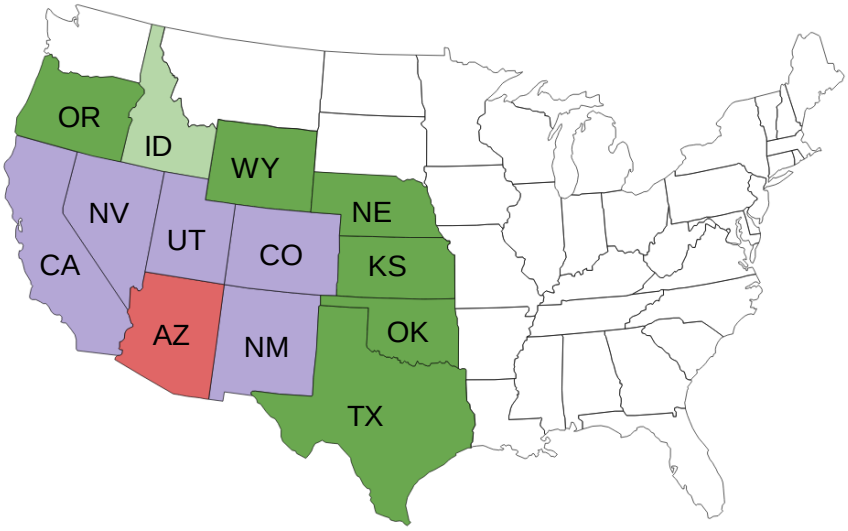

Figure 9. Neighboring DOTs Contacted During Experience Survey

Group 1

California

The California Department of Transportation (Caltrans) currently uses five unmodified binder grades (PG 58-34, PG 64-10, PG 64-16, PG 70-10, and PG 64-28) and two modified binders (PG 64-22[M] and PG 76-22[M]). Caltrans indicated that PG 76 is used for chip seal spray applications only. The PG 70 grade is warranted in some regions because of climate, and in other regions, it is used when a bump in grade is warranted because of traffic volume. Caltrans personnel believe that the agency does possess the capability to run the MSCR test, but the agency has neither adopted it nor evaluated the scope of implementing MSCR. At this time, Caltrans has no plans to implement MSCR since the agency is satisfied with the current binders and their performance. However, Caltrans has indicated that if binders specified using AASHTO M 332 can be proven to perform better than those specified by AASHTO M 320, the agency would be willing to reconsider implementation (Kee Foo, telephone interview, May 11, 2016).

Colorado

Colorado DOT currently uses PG 58-28, 58-34, 64-22, 64-28, 70-28, and 76-28 binders. The majority of the binders are modified, with PG 64-28 or PG 76-28 as the more common binder grade for the top lift. The DOT does not specify the type of modifier used in the binder, but reportedly sees a lot of styrene-butadiene-styrene (SBS) and styrene-butadiene-rubber (SBR) modification. The DOT also points out that it does not allow polyphosphoric acid (PPA) modification of the binder. The PG 76 binder grade is mainly used as a bumped grade because of traffic, but it also is necessary because of climate in a few areas of the state. The DOT indicates that it is monitoring the research on the benefits of the MSCR test and

corresponding AASHTO M 332 specifications, but it does not have immediate plans for implementation. The agency's main concern is that adopting MSCR as a replacement for its current PG+ tests (elastic recovery, AASHTO T 301; ductility, AASHTO T 51; and toughness and tenacity, ASTM D5801) will result in a lower-quality or significantly different binder than the agency is currently using. The DOT also points out that it has heard from its binder suppliers that adopting less-DOT-specific testing requirements would decrease cost and encourage competition with suppliers outside Colorado. The DOT may pursue MSCR testing only as a replacement for the time-consuming elastic recovery procedure (Vincent Battista, email interview, March 28, 2016).

Nevada

Nevada DOT uses two main binder grades, PG 64-28NV and PG 76-22NV. The DOT also has the same specifications with the addition of tire rubber, but these are optional and rarely used. Both specifications have plus-tests added, and the PG 76-22NV has a 1.3 minimum original dynamic shear rheometer (DSR) value and minimum polymer content of 3 percent. The DOT has been using PG 64-28NV in northern Nevada for years and is happy with its performance. Both cold ductility testing and toughness-and-tenacity testing are done on the original binder and on the residue from the rolling thin-film oven (RTFO) procedure. The DOT believes that this combination of tests guarantees high-quality crude binders, polymer types, minimum polymer content, and good compatibility. The DOT notes that the cold ductility test looks at the base binder, cold temperature elasticity, polymer type, and percentage, while the toughness-and-tenacity test looks at polymer type and percentage, rutting resistance, flexibility, workability, adhesiveness, and polymer compatibility. Also, both cold ductility and toughness-and-tenacity place limitations on binder aging.

The DOT has been collecting data for J_{nr} and creep recovery in the PG 64-28NV grade for several years. However, the agency does not feel that J_{nr} and creep recovery would be an adequate replacement for the cold ductility and toughness-and-tenacity tests that are currently specified. One concern is that because J_{nr} and creep recovery increase with aging of the material over time, J_{nr} and creep recovery can be improved simply through binder aging, rather than by adjusting polymer content, polymer type, cross-linking, etc. The parameter appears to the DOT to be more of an indicator of stiffness than of elasticity. The DOT also feels that the elastic response curve is not indicative of good SBS-modified binder. The agency has seen recovery on its current products to be significantly higher than what is recommended by AASHTO. It is concerned that adopting the AASHTO specification could actually reduce the current recovery that the agency now obtains. It should be noted that the research team requested and received J_{nr} test records from Nevada DOT for more than 623 samples. A review of those data shows that the recovery on some samples is much higher, similar to what was found in the ADOT preliminary study. Nevada DOT is concerned that dropping cold ductility and toughness-and-tenacity testing and adopting the MSCR specifications could result in a significant change in binder properties. The DOT believes that it could see inferior crude sources, different polymer types, lower polymer percentages, and less compatibility.

For the PG 76-22NV grade, the DOT added J_{nr} and creep recovery into its specifications in 2015. Prior to 2015, the DOT used the cold ductility test on original binder and RTFO residue. The toughness-and-

tenacity test could not be used with this binder because the binder was too stiff and could damage the test apparatus. The current J_{nr} specification is consistent with the H-grade traffic recommendations. The new specification still includes the cold ductility test on the unaged binder to try to ensure the use of an SBS polymer. The reason for replacing cold ductility of RTFO residue with J_{nr} was that over time, the material that the DOT received kept getting softer. The DOT reports that the change to incorporate the MSCR specification into PG 76-22NV has been successful, and the agency is getting a product more to its liking (Wayne Brinkmeyer, email and telephone interview, April 22, 2016).

New Mexico

New Mexico DOT uses a wide range of binders owing to the stark climatic difference from north to south (similar to the climatic variation in Arizona). The commonly used binders are PG 70-22 (polymer-modified binder, PMB), PG 64-28, and PG 64-22 with recycled asphalt pavement (RAP). The DOT also uses PG 58-28, PG 76-28 (PMB), and PG 76-22 (PMB). The DOT specifies rubberized binder for open-grade friction courses, and notes that a PG 76 grade is warranted because of climate considerations and not because of adjustment for increased traffic. The DOT has neither partially implemented MSCR nor done any MSCR evaluation. Its current specification for polymer-modified binder includes a 65 percent elastic recovery obtained from the PG+ test. The DOT does not have any immediate plans to evaluate MSCR parameters for incorporation into binder specifications but might do so in two to three years, subject to budget allocation. The DOT did say that if AASHTO recommends the MSCR protocol, the DOT may accelerate its plans for evaluating MSCR (Parveez Anwar, telephone interview, March 28, 2016).

Utah

Except for temporary pavement and maintenance materials, all binders specified by Utah DOT are polymer-modified; however, local governments still use unmodified binders. Currently, the DOT predominantly uses PG 64-34, PG 64-28, PG 70-28, and PG 58-28. The DOT is currently conducting research to evaluate the use of PG 76-34 as a highly modified binder to allow for lower-mix air void design and higher binder contents. The highest standard grade, PG 70-28, is used in the St. George area owing to the climate; it is also used as the standard binder for stone mastic asphalt mixtures. The DOT evaluates rut resistance using the HWTT and does not bump binder grades for traffic. The agency noted that all mixes are very rut-resistant. The DOT currently performs the MSCR test for information purposes only; it has not adopted the MSCR specification because it is having very good success with its current specifications (Howard Anderson, email interview, April 21, 2016).

Group 2

Kansas

Kansas DOT uses PG 76-28, PG 70-28, PG 70-22, PG 64-34, PG 64-28, PG 64-22, PG 58-34, PG 58-28, and PG 52-34 binders. The binders are generally SBS-modified. The DOT rarely uses the PG 76 grade, but when it does, it is because of traffic. The agency is currently evaluating the implementation of MSCR guidelines. According to DOT personnel, there are currently no systemic issues with rutting, which would be their primary motivation for transitioning to MSCR. Other concerns include replacing recovery in

ductility-bath testing with MSCR percent recovery. The DOT has not seen a strong correlation with the recovery in the ductility bath, and worries that using AASHTO M 332 could lead to reduced polymer content. In short, DOT personnel believe that there might be issues with characterizing the presence of an elastomer in some of their PG 58-34 and PG 64-28 binders ($J_{nr3.2} > 2$ kPa^{-1}) and issues with "grade dumping." Grade dumping is a nonstandard term that the DOT uses to convey a mismatch between climate temperature and test temperature that is the opposite of what occurs in a grade-bumping scenario. In a grade-bumping scenario, the climate temperature is lower than the PG high temperature (under AASHTO's M 320 system), and the binder can be graded as a high-traffic grade. Grade dumping occurs because the DOT has decided to run MSCR at 64°C regardless of climate, and in Kansas the predominant temperature grade is PG 58 (Blair Heptig, email interview, March 28, 2016).

Nebraska

Nebraska DOT uses three basic grades, PG 52-34, PG 58-34 (PMB), and PG 64-34 (PMB) and a fourth, less common PG 70-34 (PMB) grade that are all created from a base binder grade with a continuous grade of approximately PG 49-34. The DOT uses a very low temperature grade because of the high proportion of RAP (greater than 40 percent) in its mixtures. The DOT plans to implement MSCR in two phases. The first phase began in July 2015 and included replacing the AASHTO T 301 elastic recovery specification with the MSCR percent recovery and completely eliminating other PG+ specifications. The DOT currently specifies a minimum MSCR percent recovery of 25 percent for PG 58-34, 45 percent for PG 64-34, and 75 percent for PG 70-34. These recoveries are determined at the binder-grade high temperature. The DOT indicates that it is currently working on analyzing correlations between rutting data and the J_{nr} parameter. It notes that there have been no issues with Phase 1 implementation thus far and that the binder suppliers are happy. The implementation of Phase 2, which involves adoption of the AASHTO M 332 specification, might be difficult, and the DOT plans to discuss it with the binder suppliers in April 2016 (Robert Rea, email interview, March 25, 2016).

Oklahoma

Oklahoma DOT uses four basic grades: PG 58-28, PG 64-22, PG 70-28 (PMB), and PG 76-28 (PMB). The agency also specifies one AASHTO M 332–based binder, PG 76E-28, which has a high polymer content and, according to the DOT, showed good fatigue and rutting performance at the National Center for Asphalt Technology test track. The DOT has partially implemented AASHTO M 332 for its other grades by adopting MSCR percent recovery but not J_{nr}. The DOT specifies a minimum MSCR percent recovery of 50 percent for PG 70-28 (PMB) and 80 percent for PG 76-28 (PMB). It has also indicated that it is still using some PG+ tests, such as the high-temperature flash point test, for some modifiers. The University of Oklahoma, with support from Oklahoma DOT, performed a comprehensive study to develop guidelines for MSCR testing for the local conditions in Oklahoma (Hossain et al. 2015). At the time of our interview, the DOT was scoping the full implementation for the remaining two binders (PG 64-22 and PG 76E-28) and planned to initiate it in 2017. The agency pointed out that local agencies were not involved in any of the decision making; however, the process did involve personnel from academia, Oklahoma DOT, binder suppliers, and mixture suppliers (Kenneth Hobson, phone interview, March 25, 2016).

Oregon

In general, Oregon DOT uses four binders, PG 64-22 and PG 64-28 (unmodified) and PG 70-22 and PG 70-28 (polymer-modified). The RTFO residues of the modified binders are tested in accordance with AASHTO T 301 to ensure a minimum elastic recovery of 50 percent. The DOT indicated that the PG 70 grade is primarily used because of traffic bumping. The agency has done very minimal evaluation of MSCR and does not have any immediate plans to incorporate MSCR into its specifications. Agency personnel indicated that it may be five or more years before MSCR is adopted. An important concern with adopting AASHTO M 332 is that personnel are trained to formulate binders and mix designs for the current specifications, and it would be challenging to familiarize them with the new grading system. The DOT is also concerned about the impact adoption would have on the current binder grades and on suppliers. However, the biggest concern is about how RAP and recycled asphalt shingles (RAS) are incorporated into AASHTO M 332. Also, DOT personnel said that it is unclear at this point how a multistate supplier would manage different grades for each state, in case one DOT follows AASHTO M 320 and another follows AASHTO M 332 (Larry Ilg, phone interview, May 12, 2016).

Texas

The majority of Texas DOT projects use PG 64-22, but polymer-modified binders (primarily SBS-based) are also common on its surface courses. The DOT does use PG 76 grade, but only because of high traffic volumes. The DOT is planning partial implementation (MSCR percent recovery) soon. Its decision is based on a study conducted by the University of Texas at Austin and the DOT that evaluated over 100 binders for MSCR-based specifications (Arega et al. 2017). According to the new specifications, the DOT will require MSCR percent recovery to be reported only if the difference between the high and low temperature grades is greater than 92°C. The DOT is also planning to do J_{nr} and rutting correlation testing; however, the DOT has no plans to pursue full implementation at this point, as it sees no evidence for adoption. The main concern envisioned by the DOT is that its mixture personnel are trained to formulate binders and mix designs for the current specifications, and that it will be a challenge to teach them to adapt to the new specifications (Gerald D. Peterson, phone interview, March 24, 2016).

Wyoming

Wyoming DOT uses PG 58-34, PG 64-28, PG 70-28, and PG 76-28. However, PG 58-34 is used infrequently since it is restricted to very-high-elevation regions. PG 64-28, PG 70-28, and PG 76-28 are modified binders and are used on Interstates 25, 80, and 90. The PG 76 grade is used on I-80 because of traffic volume and frequent steep grades. The DOT has been collecting data on MSCR testing for the past five years and is still in the data-collection phase. The agency is currently specifying modified binders based on AASHTO T 301. For binders with a high- and low-temperature difference greater than 90°C, a minimum elastic recovery of 60 percent is required. Some of the concerns reported by DOT personnel included the challenge of getting everyone familiar with the AASHTO M 332 specification, reluctance to change, the issue of tankage for the suppliers, and fears over getting a lower quality product that has a higher J_{nr} (Bruce Morgenstern and Michael Farrar, phone interview, June 8, 2016).

Table 1. Group 1 Experience with MSCR Test

DOT	Binders	PMBs[a]	HSB[b] Issues	Modification	Grade Bumping	Adopted MSCR?	% Recovery Limits	Reason for Not Considering MSCR	Any Concerns in Adoption?
CA	PG 58-34, PG 64-10, PG 64-16, PG 70-10, PG 64-28, PG 64-22(M), PG 76-22(M)	PG 64-22(M), PG 76-22(M)	None	SBS	Climate and traffic	No	–	Satisfied with current specs	–
CO	PG 58-28, 58-34, 64-22, 64-28, 70-28, 76-28	Yes	No	SBS, SBR (no PPA)	Climate and Traffic	No	–	No noted problems with current specs	Lower quality or significantly different binder
NV	PG 64-28NV PG 76-22NV	Both	None	SBS, SBR	Climate	Yes for PG 76-22NV	Min. 30%	Happy with current PG 64-28NV specs	Inferior crudes; lower polymer percentages; unknown polymers
NM	PG 58-28, PG 76-28, PG 76-22, PG 70-22, PG 64-28, PG 64-22+RAP	All PG 76 & PG 70 binders	No	SBS	Climate	No	65% from PG+ spec	Might evaluate if AASHTO recommends	–
UT	PG 64-34, PG 64-28, PG 70-28, PG 58-28	All	Not a lot of HSB	SBS	Climate	No	–	Success with current specs	–

[a] PMB = polymer-modified binder
[b] HSB = high-stiffness binder

Table 2. Group 2 Experience with MSCR Test

DOT	Binders	PMBs[a]	HSB[b] Issues	Modification	Grade Bumping	Adopted MSCR?	% Recovery Limits	Reason for Not Considering MSCR	Any Concerns in Adoption?
KS	PG 76-28, PG 70-28, PG 70-22, PG 64-34, PG 64-28, PG 64-22, PG 58-34, PG 58-28, PG 52-34	Yes	None	SBS	Traffic	Evaluating	–	Concerns about reduction in polymer content; no current issues with rutting	Do not see a strong correlation with ER in the ductility bath
NE	PG 52-34, PG 58-34, PG 64-34	Yes (58, 64)	No HSB	SBS	Climate	Partial (% recovery)	Min. 25% for PG 58-34; 45% for PG 64-34; 75% for PG 70-34	–	None with phase 1 (% recovery)
OK	PG 58-28, PG 64-22, PG 70-28, PG 76-28, PG 76E-28	Yes	None	SBS	Traffic	Partial (% recovery)	Min. 50% for PG 70-28; 80% for PG 76-28	–	–
OR	PG 64-22, PG 64-28, PG 70-22, PG 70-28, PG 70-28 ER[c], PG 70-22 ER	PG 70-28 ER, PG 70-22 ER	Issues were due to higher RAP	SBS	Traffic	Minimal evaluation	-	Might have impact on current grades	How supplier will manage multiple grades
TX	PG 64-22 predominant	Yes, a lot	Not a lot of HSB	SBS	Traffic	Partial - May/June16	If T_{diff} >92°C, then do ER (PG+)	–	Training personnel to get familiar with M 332
WY	PG 58-34, PG 64-28, PG 70-28, PG 76-28	PG 64-28, PG 70-28, PG 76-28	None	SBS	Traffic	Evaluating	If T_{diff} > 90°C, then ER (PG+) should be ≥60%	Familiarity with AASHTO M 320; desire to simplify; tankage issues	Fear of getting a lower-quality product which has a higher J_{nr}

[a] PMB = polymer-modified binder
[b] HSB = high-stiffness binder
[c] ER = elastic recovery

INTERLABORATORY PRECISION STUDIES

NEAUPG, SEAUPG, and PCCAS, with support from the Asphalt Institute, have initiated interlaboratory studies (ILS) to assess the repeatability and reproducibility of the MSCR test. The research team has reviewed the NEAUPG ILS studies from 2010 and 2012, the SEAUPG ILS study from 2011, and the PCCAS ILS studies from 2013 and 2014. Additionally, the team has reviewed AASHTO proficiency test results for 2011 through 2015. Summaries of these studies appear below.

NEAUPG

In 2010, NEAUPG conducted an ILS study by sending each of the 21 participating laboratories four unaged binders (PG 52-28, PG 64-22, PG 70-28, and PG 76-22) and one RTFO-aged binder (PG 76-22) (NEAUPG 2011). The labs were instructed to conduct RTFO aging for the unaged binders at their respective facilities. Precision limits for single-operator and multilaboratory tests were developed for percent recovery at 0.1 and 3.2 kPa, and for J_{nr} at 0.1 and 3.2 kPa. The data indicated that a tiered precision statement was unwarranted for J_{nr} because the precision for J_{nr} did not vary from binder to binder. The data also indicated that individual-laboratory RTFO aging had an insignificant effect on the results (NEAUPG 2011).

NEAUPG conducted a follow-up study in 2012 that involved 28 laboratories (NEAUPG 2013). Five binders, PG 58-28, PG 64-22, PG 64-28, PG 70-28, and PG 76-22, were provided to the participating laboratories along with the required testing temperatures and conditioning protocols. In addition to percent recovery at 0.1 and 3.2 kPa, and J_{nr} at 0.1 and 3.2 kPa, precision limits were developed for J_{nr} difference, J_{nrdiff}. It should be noted that the precision limits for percent recovery in both NEAUPG studies were determined using only the results obtained from modified binders. The results from the follow-up study (NEAUPG 2013) showed that (1) the precision limits for J_{nr} were similar to those in NEAUPG 2011, and (2) the precision estimates for recovery were lower than those in NEAUPG 2011 . The results were framed in the context of two factors. First, the improvement may have been related to the range of recovery values obtained in 2012, which were higher than those obtained in 2010. Second, it was possible that the participants had become more familiar with the test, and increased familiarity resulted in lower precision values since there was no change in specification from 2010 to 2012 (NEAUPG 2013). The precision estimates for J_{nr} difference were higher than the calculated estimates for both recovery and J_{nr}. Table 3 presents the repeatability and reproducibility estimates resulting from the two NEAUPG studies.

SEAUPG

SEAUPG conducted an ILS study in 2011 using 23 laboratories (SEAUPG 2012). As in the NEAUPG studies, participating laboratories were provided with three binders (PG 64-22, PG 76-22, and a lab blend similar to PG 70-22) and asked to conduct RTFO aging at their respective facilities. All binders were tested at 0.1 kPa and 3.2 kPa stress levels at a temperature of 64°C. Precision limits for single-operator and multi-laboratory were developed for percent recovery at 0.1 kPa and 3.2 kPa, and for J_{nr} at 0.1 kPa and 3.2 kPa. The study concluded that the repeatability and reproducibility values were similar for J_{nr} for all

binders, a finding that was in agreement with that of NEAUPG 2011. Table 3 shows the repeatability and reproducibility estimates resulting from this study.

PCCAS

The ILS initiated by PCCAS in 2013 sought to evaluate the repeatability and reproducibility of the AASHTO TP 70 MSCR test (currently AASHTO T 350) (PCCAS 2013). The study also compared the results and the variability from the MSCR test with those from the PG+ tests that are commonly used in PCCAS DOTs. Sixteen laboratories participated in the study, and each was supplied with unaged PG 76-28, PG 70-22ER, PG 64-28NV, PG 64-28PM, and PG 58-34PM and with RTFO-aged PG 76-28 and PG 58-34. All binder samples, except PG 76-28 and PG 58-34, were tested at the PG-grade high temperature and at one grade lower. For PG 76-28 and PG 58-34, the test was performed only at the high-temperature PG grade. Precision limits for single-operator and multi-laboratory were developed for percent recovery at 0.1 kPa and 3.2 kPa, for J_{nr} at 0.1 kPa and 3.2 kPa, and for J_{nr} difference (PCCAS 2013). The repeatability and reproducibility estimates appear in Table 3.

Table 3. Comparison of Estimated Repeatability and Reproducibility for NEAUPG, SEAUPG, and PCCAS MSCR ILS Studies

	Acceptable Range of Two Test Results (d2s%) from ILS Studies			
	2010 NEAUPG	**2012 NEAUPG**	**2011 SEAUPG**	**2013 PCCAS**
Single-Operator Precision:				
Rec-0.1 (%Recovery at 0.1 kPa)	9.7	2.0	3.2	4.9
Rec-3.2 (%Recovery at 3.2 kPa)	7.7	2.3	3.9	8.0
Multi-laboratory Precision:				
Rec-0.1 (%Recovery at 0.1 kPa)	14.0	6.2	6.8	10.5
Rec-3.2 (%Recovery at 3.2 kPa)	18.7	7.6	9.8	17.3
Single-Operator Precision:				
J_{nr}-0.1 (J_{nr} at 0.1 kPa)	14.5	12.9	13.3	16.7
J_{nr}-3.2 (J_{nr} at 3.2 kPa)	15.5	11.6	13.0	17.6
Multi-laboratory Precision:				
J_{nr}-0.1 (J_{nr} at 0.1 kPa)	25.6	35.5	26.1	34.1
J_{nr}-3.2 (J_{nr} at 3.2 kPa)	33.7	33.0	28.0	36.0
Single-Operator Precision:				
J_{nr}-Diff	n/a	23.80	n/a	34.3
Multi-laboratory Precision:				
J_{nr}-Diff	n/a	41.50	n/a	55.3

AASHTO

The AASHTO Materials Reference Laboratory (AMRL) has been evaluating the laboratory performance of MSCR testing through its proficiency sample program (PSP) over the past five to six years. The results of the proficiency samples are published online along with relevant statistics (AASHTO 2016). The latest round of available testing data, at the time of this writing, is from May 2018. For the PSP, two identical samples (with unique identification codes) are sent to the participating laboratories in each testing cycle along with instructions for tests to be performed. In each of these rounds, the samples consist of the same binder. Table 4 shows the precision estimates and number of participating labs from each round of testing. The single-operator precision limits obtained from the AMRL studies are similar to those identified from other studies (NEAUPG 2011, NEAUPG 2013, SEAUPG 2012, PCCAS 2013). The multi-laboratory precision limits of AMRL, which were higher in the first few rounds of AMRL testing (lower-numbered cycles), are now comparable to those obtained from the NEAUPG, SEAUPG, and PCCAS studies.

One important observation that can be made regarding the $J_{nr3.2}$ parameter is that the single-operator and multi-laboratory precision values have been decreasing over time, except in the case of the 241/242, 245/246, and 249/250 sample testing cycles. This decrease may have a twofold cause: increased familiarity with the test, and a change in standard during the period between PSP samples 217/218 and 241/242. The test cycle 217/218 was conducted around the fall of 2011, when the MSCR test was still a provisional standard (AASHTO TP 70-11). One major change made in the standard during the period from AASHTO TP 70-11 to AASHTO TP 70-13—and retained when the test was adopted as a full standard (in AASHTO T 350)—was that in AASHTO TP 70-13, 10 additional cycles at 0.1 kPa were added as conditioning cycles. Informal discussions with researchers, AASHTO, and FHWA personnel, as well as anecdotal evidence gathered by the research team during this phase of the study, support the conclusion that the addition of the 10 conditioning cycles helped to reduce variability.

Variability Comparison of the Parameters $J_{nr3.2}$ and $|G^*|/\sin\delta$

One concern that has persisted in the literature and among practitioners regarding the $J_{nr3.2}$ parameter is its high variability compared to $|G^*|/\sin\delta$. To verify this concern, the precision estimates (d2s%) in Table 5 for $|G^*|/\sin\delta$ for RTFO-aged binders as reported in PSPs 217/218 through 251/252 were compared with the precision estimates (d2s%) for $J_{nr3.2}$ in Table 4. The results suggest a different conclusion than the common belief that the variability in J_{nr} is higher. Overall, the single-operator and multi-laboratory precision values for $J_{nr3.2}$ have been decreasing over time and are very comparable to the $|G^*|/\sin\delta$ values. The single-operator and multi-laboratory precision values for $|G^*|/\sin\delta$ and $J_{nr3.2}$ in PSPs 229/230 through 251/252 (except for the testing cycles mentioned above) only differ by about 2 percent.

Table 4. Estimated Repeatability and Reproducibility for MSCR Test Parameters from AMRL Proficiency Sample Program (PSP)

Acceptable Range of Two Test Results (d2s%) from AMRL PSP for Each Sample																
Test Cycle	239	240	237	238	235	236	233	234	229	230	225	226	221	222	217	218
No. of Labs	191		182		173		165		156		137		113		101	
Single-Operator Precision:																
Rec-0.1 (%Recovery at 0.1 kPa)	22.7	22.2	17.9	17.9	12.6	12.7	2.36	2.37	1.53	1.53	8.87	8.75	n/a	n/a	n/a	n/a
Rec-3.2 (%Recovery at 3.2 kPa)	16.0	15.7	22.7	22.5	17.1	17.1	7.68	7.59	3.25	3.25	16.3	15.9	2.75	2.75	5.43	5.42
Multi-laboratory Precision:																
Rec-0.1 (%Recovery at 0.1 kPa)	43.1	44.4	38.3	38.1	27.1	26.3	7.99	8.04	4.15	4.38	21	22.2	n/a	n/a	n/a	n/a
Rec-3.2 (%Recovery at 3.2 kPa)	85.1	83.2	111	109	47	43.1	20.4	20.6	7.96	8.37	51.4	51.7	10.8	11.1	19.5	18.5
Single-Operator Precision:																
J_{nr}-0.1 (J_{nr} at 0.1 kPa)	7.30	7.39	9.18	9.25	9.87	9.83	9.64	9.65	8.92	8.91	14	14.3	n/a	n/a	n/a	n/a
J_{nr}-3.2 (J_{nr} at 3.2 kPa)	7.06	7.15	8.3	8.38	9.12	9.1	13	13.2	10.6	10.6	14.1	14.3	11	11	16.6	16.8
Multi-laboratory Precision:																
J_{nr}-0.1 (J_{nr} at 0.1 kPa)	18.9	18.2	23.3	22.9	20.5	20.7	27.7	27	20.7	22.4	36.9	39.2	n/a	n/a	n/a	n/a
J_{nr}-3.2 (J_{nr} at 3.2 kPa)	18.7	17.4	21.7	21.9	20.5	19.7	34.3	34.4	25	25.8	37.5	39.5	51.1	52.1	43.6	43.3
Single-Operator Precision:																
J_{nr}-Diff	16.1	16	13	13	10.4	10.4	13.9	14.1	8.82	8.85	10.4	10.3	38.2	38.6	21	21.1
Multi-laboratory Precision:																
J_{nr}-Diff	33	36.6	25.2	24.4	17.5	17.4	70.1	70.5	32.6	32.6	31.3	32.8	169	175	111	111

Table 4 (Continued). Estimated Repeatability and Reproducibility for MSCR Test Parameters from AMRL Proficiency Sample Program (PSP)

Acceptable Range of Two Test Results (d2s%) from AMRL PSP for Each Sample										
Test Cycle	251	252	249	250	247	248	245	246	241	242
No. of Labs	238		240		230		238		212	
Single-Operator Precision:										
Rec-0.1 (%Recovery at 0.1 kPa)	n/a	n/a	2.83	2.83	15.59	15.4	7.56	7.56	6.36	6.34
Rec-3.2 (%Recovery at 3.2 kPa)	n/a	n/a	4.53	4.53	20.43	19.95	14.97	14.86	11.2	11.1
Multi-laboratory Precision:										
Rec-0.1 (%Recovery at 0.1 kPa)	n/a	n/a	11.86	11.8	29.15	27.28	20.69	21.39	20.8	20.8
Rec-3.2 (%Recovery at 3.2 kPa)	n/a	n/a	9.57	10.19	55.75	56.88	30.00	32.26	22.2	22.7
Single-Operator Precision:										
J_{nr}-0.1 (J_{nr} at 0.1 kPa)	8.07	8.09	14.32	14.38	9.62	9.76	14.51	14.69	16.7	17.2
J_{nr}-3.2 (J_{nr} at 3.2 kPa)	7.92	7.95	14.11	14.83	9.99	10.13	13.61	13.78	15.3	15.8
Multi-laboratory Precision:										
J_{nr}-0.1 (J_{nr} at 0.1 kPa)	21.17	19.87	37.07	38.21	21.31	22.05	34.24	35.65	47	48.5
J_{nr}-3.2 (J_{nr} at 3.2 kPa)	20.21	19.33	29.43	31.13	21.14	22.19	31.7	31.13	30	33.2
Single-Operator Precision:										
J_{nr}-Diff	11.29	11.35	11.63	11.57	13.41	13.5	13.41	13.56	15	15.2
Multi-laboratory Precision:										
J_{nr}-Diff	41.04	40.47	88.3	87.16	35.09	34.53	49.52	49.52	92.3	92.7

Table 5. Estimated Repeatability and Reproducibility for $|G^*|/\sin\delta$ from AMRL Proficiency Sample Program (PSP)

Acceptable Range of Two Test Results (d2s%) from AMRL PSP for Each Sample																
Test Cycle	239	240	237	238	235	236	233	234	229	230	225	226	221	222	217	218
No. of Labs	255		249		244		243		242		235		235		216	
Single-Operator Precision:																
$\|G^*\|/\sin\delta$ (RTFO-Aged)	5.87	5.83	7.53	7.46	7.14	7.17	6.65	6.63	7.46	7.44	9.08	9.02	6.5	6.47	7.88	7.85
Multi-laboratory Precision:																
$\|G^*\|/\sin\delta$ (RTFO-Aged)	17.4	16.8	19	18.5	16.2	16	17.3	16.8	16.3	16.8	23.5	23.8	14.7	15.3	22.6	22.6

Table 5 (Continued). Estimated Repeatability and Reproducibility for $|G^*|/\sin\delta$ from AMRL Proficiency Sample Program (PSP)

Acceptable Range of Two Test Results (d2s%) from AMRL PSP for Each Sample										
Test Cycle	251	252	249	250	247	248	245	246	241	242
No. of Labs	274		270		273		252		255	
Single-Operator Precision:										
$\|G^*\|/\sin\delta$ (RTFO-Aged)	5.89	5.89	6.4	6.34	7.98	7.9	6.57	6.51	7.45	7.33
Multi-laboratory Precision:										
$\|G^*\|/\sin\delta$ (RTFO-Aged)	17.94	16.9	16.02	17.4	17.8	19.02	15.31	16.1	15.6	16.4

INCORPORATING RAP WHEN USING AASHTO M 332 SPECIFICATION

National Guidance and Practice

Throughout the data collection effort, the research team faced the reoccurring issue of how AASHTO M 332 could be adapted to consider recycled asphalt pavement (RAP). In the early 1990s, the U.S Environmental Protection Agency in partnership with the Federal Highway Administration (FHWA) estimated that more than 90 million tons of asphalt pavement was reclaimed every year, of which 80 percent (or 72 million tons) was used in construction-related activities, including pavement construction. The remaining 20 percent (or 18 million tons) was simply disposed of by traditional means (e.g., landfilling, stockpiling) (FHWA 1993). As of 2007, the total yearly RAP usage was estimated to be around 100 million tons, which makes asphalt mixture the most frequently recycled material (Copeland 2011). Of the 100 million tons used every year, about 40percent go into pavement-related applications (Copeland 2011). Others have evaluated aged-binder properties and high-PG binder grades, confirming the high stiffness of RAP binder (Huang et al. 2014, McDaniel et al. 2000, Li and Gibson 2013, Basueny et al. 2014). Higher-percent RAP mixes are more brittle, thus raising concerns about their adequacy in resisting thermal and fatigue cracking (Loria et al. 2011). The allowable amount of RAP in asphalt mixes has always been debated. Before 2012, the percent RAP was limited to 10–15 percent owing to the high stiffness of the aged binder (Copeland 2011). As of 2012, the national average RAP content was 19 percent, which was 7 percentage points higher than the national average of 12 percent in 2007 (Copeland 2011, Hansen and Copeland 2013).

Guidance for incorporating RAP was initially established in National Cooperative Highway Research Program (NCHRP) Project 9-12 (McDaniel et al. 2000). This study concluded that for RAP contents below approximately 10–20 percent, and depending on the low-temperature binder grade, the impact of RAP content was not significant enough to noticeably affect the overall binder rheology. For RAP contents of 10–20 percent, mix designs could include binder that would normally be used for similar non-RAP mixes. Table 6 shows the NCHRP study recommendations. Many agencies currently use substantially higher RAP contents, and in these cases, the selection of the mix design binder involves a process of blending the RAP and the binder and evaluating the blended residue (Hansen and Copeland 2013).

Table 6. Virgin Binder Selection Criteria for RAP Mixes (McDaniel et al. 2000)

	Recovered RAP Grade[a]		
Recommended Asphalt Binder Grade	**PG XX-22 or lower**	**PG XX-16**	**PG XX-10 or higher**
No change in binder selection	<20%	<15%	<10%
Select virgin binder one grade softer than normal (e.g., use PG 58-28 if a PG 64-22 would be normal)	20–30%	15–25%	10–15%
Follow recommendations from blending charts	>30%	>25%	>15%

[a] Percentages indicate RAP content.

One of the most significant contributions of NCHRP Project 9-12 was the development of blend charts, which permitted reliable inclusion of higher percentages of RAP. The primary purpose of the blend

charts was to arrive at a relationship between the PG grade of virgin binder and the percent of RAP to be used in the mixture. McDaniel et al. (2000) proposed two methods for the development of blend charts:

- Method A: Blending at a known RAP percent (virgin binder grade unknown)
- Method B: Blending with a known virgin binder (RAP percent unknown)

Both methods require an assumption as to the required blended binder grade. Method A requires determination of the properties of recovered RAP binder at high, intermediate, and low critical temperatures. High, intermediate, and low temperatures refer to the SHRP binder performance-grading protocol. Since the percent of RAP is known, the critical temperature of the virgin binder at all three temperatures can be calculated with Equation 2. Table 10 presents an example of the blend chart using method A.

$$T_{critical} = \frac{T_{Blend} - (\%RAP \times T_{RAP})}{(1 - \%RAP)} \qquad \text{(Eq. 2)}$$

Where $T_{critical}$ = critical high temperature grade of virgin binder
T_{Blend} = high temperature grade of blended binder
T_{RAP} = high temperature grade of RAP binder
$\%RAP$ = RAP binder content by total mass of binder

In the example shown in Figure 10, 30 percent RAP is used, and the desired blended binder grade is PG 64-22. The critical high temperature of RAP binder is 86.6°C. Based on these values, the blend chart is constructed and extrapolated to 0 percent to find the virgin binder grade. The $T_{critical}$ value at 0 percent is 54.4°C, so the virgin binder to be used should have a high-temperature grade of 58. A similar analysis would be carried out at critical low temperature to find the low-temperature grade of the virgin binder.

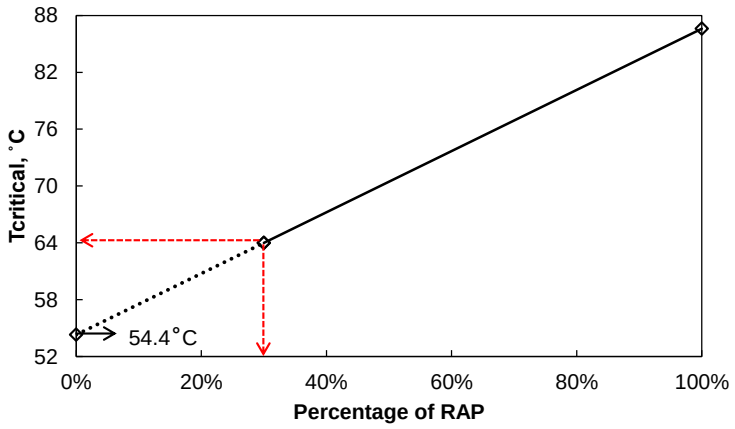

Figure 10. Schematic of a Blending Chart Using Method A (McDaniel et al. 2000)

Method B requires determination of the properties of both virgin binder and recovered RAP binder at high, intermediate, and low temperatures. The amount of RAP to be added can be calculated using Equation 3. It should be remembered that the RAP percent obtained is the minimum percent of RAP that can be used based on the assumption of the blended binder grade. To arrive at the maximum percent of RAP that satisfies the assumed blended binder grade, the RAP percent at one PG grade higher than the assumed blended PG grade is found. This step now gives the range for the percent of RAP to be incorporated into the mix. Figure 11 presents an example of this process. In this method, the critical high temperatures for the virgin and RAP binder are known to be 60.5°C and 86.6°C, respectively. It is desired to have blended binder which is PG 64-XX (i.e., $T_{critical}$ between 64°C and 70°C). With this information, the range of RAP binder to be used to achieve a blend which is PG 64-XX is estimated as 14–36 percent.

$$\%RAP = \frac{T_{Blend} - T_{Virgin}}{T_{RAP} - T_{Virgin}} \quad \text{(Eq. 3)}$$

Where the variables are the same as those defined in Equation 2.

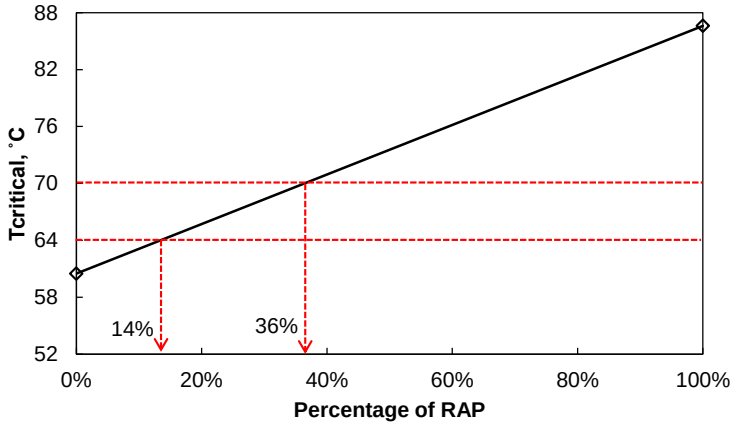

Figure 11. Schematic of a Blending Chart Using Method B (McDaniel et al. 2000)

DOT Experiences

Binders designed under the AASHTO M 320 specification were used to develop the blending charts, the current guidance on RAP limits, and the guidelines for binder grade selection in the AASHTO M 323 specification. However, there may be a need to revisit the specifications since binders specified in AASHTO M 320 may be different from those specified in AASHTO M 332. Such investigation is beyond the scope of the current study, but it is important to understand that these issues exist and thereby understand the implementation challenges. During the literature review, the research team identified

four DOTs that have fully implemented MSCR parameters (Connecticut, Maryland, New York, and Virginia). The practices of these four DOTs are summarized below.

Connecticut

Connecticut DOT specifies two binder grades, PG 64S-22 (neat binder) and PG 64E-22 (which is solely modified with SBS polymer). For mixtures containing RAP, up to 15 percent RAP can be used with no binder grade modification. For RAP amounts between 15 percent and 20 percent, the engineer must submit a new job mix formula, which must be accompanied by a blending chart and supporting test results in accordance with AASHTO M 323, Appendix X1. The engineer/supplier also has the option to submit test results proving that the combined binder (recovered binder from the RAP, virgin binder at the mix design proportions, warm mix asphalt additive, and any other modifier, if used) meets the requirements of the specified binder grade (i.e., PG 64S-22 if unmodified binder is used or PG 64E-22 if modified binder is used) (Connecticut DOT 2016).

Maryland

Maryland DOT requires that PG binders for mixes containing all virgin materials, RAP materials, or roofing shingles from manufacturing waste meet AASHTO M 332 for the specified performance grade. If the maximum allowable binder replacement is 30 percent, no binder grade change is required; however, if the maximum allowable binder replacement is greater than 30 percent, the AASHTO M 323 blending charts are to be followed (Maryland DOT 2015).

New York

New York State DOT specifies a maximum of 20 percent RAP for most of its mixtures except for those with a nominal maximum aggregate size of 37.5 mm, where up to 30 percent RAP is allowed. The standard PG grades specified are PG 64S-22 for upstate New York and PG 64H-22 for other areas when the calculated equivalent single axle loads (ESALs) are 10 million or less. The polymer-modified PG grades, PG 64V-22 and PG 64E-22, are used on all controlled-access highways and roadway segments where the calculated ESALs are greater than 10 million (New York State DOT 2014). The DOT also specifies that no adjustment be made to the PG binder grade to account for the hardness of the RAP binder (New York State DOT 2012).

Virginia

Virginia DOT recommends that the binder grade be based on the layer type (surface, intermediate, base), aggregate gradation, and traffic level (Table 7). The DOT does not allow RAP in certain mixes, and it specifies the use of a softer binder (PG 64S-22) when high RAP is used in mixtures for lower-volume traffic, and a stiffer binder (PG 64H-22) when high RAP is used in mixtures for higher-volume traffic (Virginia DOT 2016).

Table 7. Recommended Asphalt Binder for RAP Mixes (Virginia DOT 2016)

Mix Type[a,b,c]	Percentage of Reclaimed Asphalt Pavement (RAP) in Mix		
	%RAP ≤ 25.0%	25.0% < %RAP ≤ 30.0%	25.0% < %RAP ≤ 35.0%
SM-4.75A, SM-9.0A, SM-9.5A, SM-12.5A	PG 64S-22	PG 64S-22	
SM-4.75D, SM-9.0D, SM-9.5D, SM-12.5D	PG 64H-22	PG 64S-22	
IM-19.0A	PG 64S-22	PG 64S-22	
IM[a]-19.0D	PG 64H-22		
BM[a]-25.0A	PG 64S-22		PG 64S-22
BM-25.0D	PG 64H-22		PG 64S-22

[a] SM = Surface Mixture, IM = Intermediate Mixture, BM = Base Mixture

[b] Number designates nominal maximum aggregate size

[c] A, D refers to the volume of traffic, with D being high traffic and A, low traffic

Use of RAP in Polymer-Modified Mixtures

Developing guidelines for polymer-modified or AASHTO M 332–specified asphalt mixes with RAP is beyond the scope of this study. However, it is relevant to understand the use of RAP since, as the literature review suggests, MSCR testing is most relevant in polymer-modified binders. The basic issue is that when polymer-modified binder is used in a RAP mixture, the total polymer content of the binding medium is reduced from that specified for the virgin binder (unless the RAP supply also contains intact polymer modification). If a polymer-modified binder specification includes a compositional requirement (e.g., a minimum polymer loading value), then effectively, the binding material that exists in a polymer-modified RAP mixture does not have sufficient polymer content. If the specification is developed based on a supposition that polymer content is a key contributor to performance, then it stands to reason that the potential exists for RAP mixes containing polymer-modified binder to have lower quality than what is typically expected for a non-RAP mixture with polymer-modified binder. A review of the literature on this issue revealed that there is no current national effort to address this question. Instead, the research team obtained information from six DOTs (Nebraska, Nevada, New Mexico, Texas, Virginia, and Oklahoma) to assess those agencies' practices. The team also contacted the North Central Superpave Center (NCSC) to assess the practice in Indiana; NCSC also provided perspective on several other states as well. All the states recognize that the issue is relevant and important but deal with it differently.

Indiana

Indiana DOT is not concerned with the level of polymer in the binder, as long as the blend meets the specification. The DOT allows up to 40 percent binder replacement in its surface mixtures. According to NCSC, with low RAP content, there isn't enough to worry about lowering of effective polymer content, and with higher RAP content, the virgin binder grade drops to a lower unmodified grade (Rebecca McDaniel, email interview, August 5, 2016).

Nebraska

Nebraska DOT uses large quantities of both polymer-modified binder and RAP (often exceeding 40 percent). The DOT realizes that use of polymer-modified binder and RAP raises questions related to long-term performance, but the agency believes that the performance benefit of lower RAP content is minimal compared with the cost savings from using higher RAP content. Though it provided no technical reference, the DOT reported that it had saved approximately $43 million by using higher RAP content. As for performance, the DOT has been using RAP for almost eight years, and though it has conducted no formal comparative analysis, its engineers report that the performance is similar to if not better than what they had observed before (Robert Rea, phone interview, July 29, 2016).

Nevada

As previously discussed, Nevada DOT specifies PG 76-22NV and PG 64-28NV, both of which are polymer-modified binders. The DOT recognizes the issue with polymer-modified binder, but believes the impact would be minimal since the RAP content is limited to 5–15 percent. The DOT specifications only consider the properties of the binder that is added to the mixture. There are no provisions requiring extraction/recovery and characterization of binder properties after mixing, whether RAP is included or not (Wayne Brinkmeyer, email and telephone interview, August 1, 2016).

New Mexico

New Mexico DOT allows up to 35 percent RAP in its mixtures. The DOT recently released a special provision in which it outlined guidelines for using RAP in conjunction with polymer-modified binder. In this provision, if more than 15 percent RAP is used, the recovered binder has to be evaluated using the elastic recovery test (AASHTO T 301). The recovery should be a minimum of 65 percent, and if the binder fails to meet this specification, the RAP dosage should be limited to 15 percent (Parveez Anwar, telephone interview, July 29, 2016).

Oklahoma

Oklahoma does not place limitations on RAP for polymer modified specifically; however, it has, until recently, not allowed RAP in surface mixtures. Oklahoma DOT currently limits RAP content to 12 percent of recycled binder in the total binder. According to the DOT, this dosage would be about 10 percent RAP by weight. The DOT also realizes that the effective polymer content can be an issue, but believes that at such a low RAP content, it would not be a major issue (Kenneth Hobson, phone interview, August 4, 2016).

Texas

Texas DOT limits the RAP content to 20 percent in surface mixtures and also places limitations on the percent of recycled binder in the total binder (20 percent or 30 percent depending on the type of binder being used). The DOT realizes that lowering of total polymer content is an issue, but bases its decision about mix quality on performance characteristics (based on HWTT). Irrespective of modification or the presence of RAP, the mixtures must meet the agency's HWTT specifications. As long as mixtures meet

those criteria, lowering of effective polymer is not a concern (Gerald D. Peterson, phone interview, August 1, 2016).

Virginia

Virginia DOT limits the RAP content to 15 percent and the RAS content to 3 percent by weight in polymer-modified asphalt mixtures. The DOT understands that lowering the effective polymer content is an issue, and has an ongoing study that is investigating the issue in more detail (Harikrishnan Nair, email and phone interview, August 3, 2016).

NCSC

Many northeastern and mid-Atlantic DOTs (Connecticut, Delaware, District of Columbia, Maine, Maryland, Massachusetts, New Hampshire, New Jersey, New York, Pennsylvania, Rhode Island, and Vermont) are lowering binder grades at both the high and the low temperatures when using more than 15–20 percent RAP (depending on the DOT). So, if they would normally use a PG 64S-22, mixes with RAP percentages above 15–20 percent would require a PG 58S-28. There was a discussion in the region about developing a "recycle," or "R," grade—the binder would be tested at the environmental temperature of interest but the J_{nr} value would be raised to a maximum of 9 kPa. However, this idea was not well received or accepted by the DOTs in this region. Also, there was a brief discussion of lowering only the low temperature grade when using higher amounts of RAP (e.g., in the previous example, using a PG 64S-28 instead of a PG 64S-22). The motivation for this recommendation was the belief that with polymer-modified grades, such a change would ensure that the overall polymer concentration would not be diluted when RAP was used (Greg Harder, email interview, August 30, 2016).

Binder Formulations Post–AASHTO M 332 Implementation: DOT Experience

One technical concern with transitioning to AASHTO M 332 has been the unintended consequences that may emerge from potential formulation changes. To address this question, the research team contacted DOTs that have implemented or plan to implement AASHTO M 332 guidelines. The Asphalt Institute's MSCR implementation database (last updated in 2015) was used as the reference for identifying the DOTs to contact. A total of 12 DOTs were selected (Connecticut, Delaware, District of Columbia, Florida, Maine, Maryland, New Hampshire, New Jersey, New York, Pennsylvania, Rhode Island, and Wisconsin). Five DOTs responded (Delaware, District of Columbia, Florida, New Hampshire, and Wisconsin). The experiences of these agencies are summarized below.

Delaware

For the binders specified by Delaware DOT, there have been very minimal changes to the formulations other than those normally made when the crude sources are changed. Not all DOTs in the region adopted AASHTO M 332, so the suppliers provide dual grades (i.e., meeting both AASHTO M 320 and AASHTO M 332). Delaware DOT noted that the biggest change was an increase in the elasticity of the PG 76-22 (PG 64E-22) binder.

District of Columbia

The binder suppliers for the District DOT combine the AASHTO M 320 grades with the AASHTO M 332 grades in the bill of lading. The PG 64-22 binder is PG 64S-22, PG 70-22 binder is PG 64H-22, and PG 76-22 binder is PG 64E-22. The DOT uses 64°C as its designated high temperature and performs MSCR at that temperature. According to DOT personnel, no change in formulations was observed in this transition. The only minor change was in the warm mix product which was specified as PG 70-22 and was expected to be PG 64H-22, but became PG 64V-22 because of the addition of Evotherm.

Florida

Florida DOT has seen very few significant changes with the transition to the AASHTO M 332 specification. According to DOT personnel, trade secrets laws restrict requests for supplier formulations. The DOT acts more as a regulatory entity to keep the products and materials qualified for meeting the needs of Florida roadways. The DOT does recognize that adoption of AASHTO M 332 will place tighter regulations on the binder formulations; however, the supplier is solely responsible for delivering a qualifying product.

New Hampshire

New Hampshire DOT's use of MSCR graded binders was very limited, since it was restricted to polymer-modified binders only. In 2015, the DOT allowed either PG 76-28 or PG 64E-28 for its high-stiffness polymer-modified binders. At the time, both binders were very similar, and the manufacturer could use the same material to satisfy both grades. However, the DOT was concerned about failing the J_{nr} difference criteria (75 percent upper limit) and elected to go back to using only PG 76-28.

Wisconsin

Wisconsin DOT adopted AASHTO M 332 in 2015. According to one of the suppliers, binder formulations had to be changed to meet the new specification. This supplier noted that Wisconsin DOT was completely aware of this possibility and was satisfied with the binders that were being produced under the new specification; the supplier said that the DOT had not voiced any concerns.

SUMMARY

The literature review identified the following issues as relevant to the current study:

- The main motivation for DOTs to adopt AASHTO M 332 is the higher correlation between rutting and the MSCR parameter (J_{nr}) for modern binders.
- No studies have evaluated AASHTO T 350 or AASHTO M 332 with high-modulus and unmodified binders like those used in central and southern Arizona.
- Most neighboring DOTs either are evaluating the implementation of AASHTO M 332 or do not plan to implement it for at least 2 to 3 years. Nebraska, Oklahoma, Nevada, and Texas DOTs plan to complete partial implementation soon or are currently implementing some of the standard.

- The repeatability of the AASHTO T 350 test is improving with time, and the precision limits for the MSCR parameter are comparable to those for the $|G^*|/\sin \delta$ parameter.
- National guidelines exist with respect to AASHTO M 332 and RAP, but the DOTs that have fully implemented the standard have their own procedures in place for using RAP.
- Of the five agencies that presented their responses on formulation changes, four have seen no changes. Among those four, the most notable is Florida DOT, which possesses high-temperature grade requirements similar to those for the majority of Arizona binders. It was noted that formulation changes were made in Wisconsin, but without any apparent adverse effects.

Since no data exist for the particular types of high-modulus binders used in Arizona, experiments are needed to correlate the performance of Arizona asphalt mixtures and the AASHTO T 350 test. This information is critical to establishing the potential benefits of AASHTO M 332. The review also demonstrates the importance of consensus building and validates the concerns that ADOT has about supplier support.

CHAPTER 3. MATERIALS AND EXPERIMENTS

MATERIALS

The research team acquired 15 binder samples and four aggregate sources for the experimental phase of this study. These materials were obtained from Arizona suppliers to ensure that the study results would be directly applicable to materials used in the state. The following sections provide details about the specific materials used.

Asphalt Binder

Three suppliers in Arizona (Alon Asphalt Company, Holly Frontier, and Western Refining) provided the binders. Ten of the 15 binders are non-polymer-modified (referred to as the Group 1 binders), and five are polymer-modified (referred to as the Group 2 binders). Group 1 binders reflect current and likely future binder usage and give equal representation, to the extent possible, to each supplier. Group 2 binders represent those that would likely be supplied under a future specification like AASHTO M 332. This allowance has been made since current ADOT specifications list only one type of polymer-modified binder (PG 76-22TR+). Other modified binders may be used, but this decision is left to the discretion of the contractor/supplier.

Besides these 15 binders, the study included a third group (the Group 3 binders) to identify the effects of percent recovery on the performance of the asphalt mixture. These binders were lab-blended in order to more accurately control the recovery and compliance values.

Group 1 Binders

The Group 1 binders are listed in Table 8. The research team—prior to this project and in collaboration with the ADOT materials group—identified the most prevalent grades specified in ADOT projects (Figure 12). The three most prevalent grades in Arizona (PG 64-22, PG 70-10, and PG 76-16) constitute approximately 89 percent of asphalt mixtures (by lane mileage). Of these, PG 76-16 is the singularly most used binder grade. For this study, PG 76-16 has been sampled from each of the three suppliers, and PG 70-10 and PG 64-22 have each been sampled from two of the three suppliers. PG 70-22 and PG 70-16 have been sampled based on the suppliers' current usage.

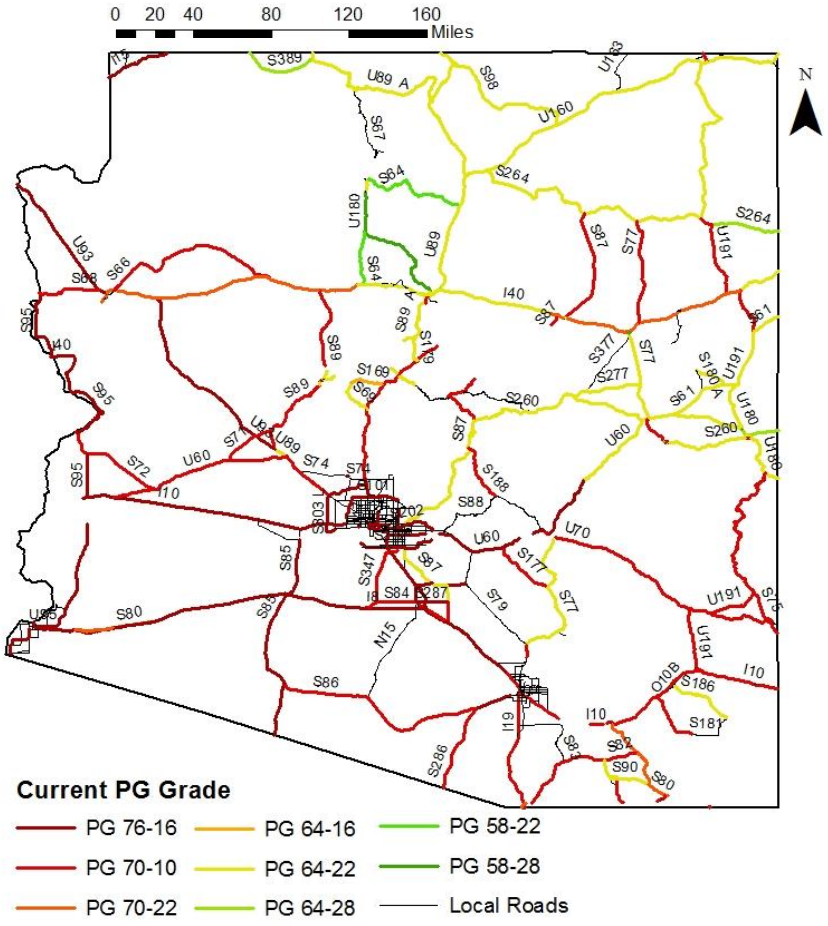

Figure 12. Distribution of Current Asphalt Binder Grades Across Arizona

Table 8. Asphalt Binder Grades and Notations

Group	Supplier	Notation	Grade	Group	Supplier	Notation	Grade
1	X	X1	PG 70-10	2	X	X3	PG 64H-22
		X2	PG 76-16			X4	PG 64V-22
	Y	Y1	PG 64-22			X5	PG 76-22TR+
		Y2	PG 70-22		Y	Y5	PG 70H-16
		Y3	PG 70-16			Y6	PG 70V-16
		Y4	PG 76-16	3	-	A3	PG 64H-22
	Z	Z1	PG 64-22			A2-B	PG 64H-22
		Z2	PG 70-22			A4	PG 70S-28
		Z3	PG 70-10			A3-B	PG 70S-28
		Z4	PG 76-16			B2	PG 70H-28
						D0.5	PG 70H-28
						B5	PG 76V-28

Group 2 Binders

One of the primary areas of focus for the current study is to determine the potential impacts on ADOT from adopting AASHTO M 332. One such impact could be the increased usage of different types of polymer-modified binders. Currently, polymer-modified binders are not widely used in Arizona, with PG 76-22TR+ being the only such material specified. Thus, it was essential that polymer-modified binders be included in the study. As shown in Table 8, five different polymer-modified binders were selected: the PG 76-22TR+ binder that is currently specified, and four other polymer-modified binders that meet the AASHTO M 332 specification and could likely be supplied in Arizona under a similar specification. Suppliers X and Y said they were capable of supplying PG 64(H,V)-22 and PG 70(H,V)-16, respectively.

Group 3 Asphalts

Asphalt binders with varying levels of polymer modification were also part of this study. The goal for testing these materials was to evaluate the sensitivity of rutting performance to changes in the elastic recovery (*R3.2*) measured in the MSCR experiment. Binders in this group have varying recovery levels, but were grouped according to similar $J_{nr3.2}$. A total of nine binders were split into one of four groups based on the similarity of their $J_{nr3.2}$ values at 64°C. The ranges of $J_{nr3.2}$ for the four groups were (J) $J_{nr3.2} < 0.1$; (K) $0.1 < J_{nr3.2} < 0.5$; (L) $0.5 < J_{nr3.2} < 1.5$; and (M) $1.5 < J_{nr3.2} < 2$. Two of these binders (PG 70V-16, and PG 64H-22) were also Group 2 binders. The remaining seven polymer-modified binders were prepared in the Arizona State University (ASU) laboratory using a high-shear mixer. The base for all these binders was PG 58-28; the polymer used was an SBS linear polymer, Kraton D1192. Cross-linking agents such as sulfur and PPA were used where required. Appendix C provides the dosages of SBS, sulfur, and PPA for the seven binders along with the detailed laboratory procedure used for the preparation of those binders.

Aggregates

The aggregates were sourced from three suppliers in Arizona: Hanson Aggregates in Globe, Brimhall-Sand and Rock in Snowflake, and Granite Construction in Tucson. The sections that follow briefly describe the aggregates and their corresponding characteristics.

Globe

The aggregate sourced from Globe consisted of four stockpiles—washed sand, crusher fines (CF), 3/8-inch aggregate, and 3/4-inch aggregate—plus a portland cement admixture. Table 9 provides the characteristics of these stockpiles; Table 10, the gradations of the individual stockpiles; and Table 11, the aggregate gradations used for preparing the asphalt mixture samples. The mixtures consisted of 15 percent sand, 17 percent CF, 32 percent 3/8-inch aggregate, and 36 percent 3/4-inch aggregate. Finally, 1 percent portland cement by total aggregate mass was added. (Percentages do not add to 100 because of rounding.)

Table 9. Characteristics of Aggregates Sourced from Globe

Aggregate Properties	Coarse Aggregate	Fine Aggregate	Spec. Limits	Admixture (portland cement)
Bulk Specific Gravity	2.57	2.556	2.350–2.850	3.14
SSD Specific Gravity	2.605	2.592		
Apparent Specific Gravity	2.664	2.651		
Water Absorption (%)	1.37%	1.399%	0–2.5%	–
Sand Equivalent	85		Min. 55	
1 Fracture Face (%)	94%		Min. 92%	
2 Fracture Face (%)	90%		Min. 85%	
Uncompacted Voids	46.50%		Min. 45%	
Flat and Elongated Aggregate	1%		Max. 10%	
Carbonates	–		Max. 20%	
L.A. Abrasion, 100 rev., % loss	6%		Max. 9%	
L.A. Abrasion, 500 rev., % loss	24%		Max. 40%	

Table 10. Gradation of Aggregate Stockpiles Sourced from Globe

Standard	Metric (mm)	Washed Sand	Crusher Fines	3/8" Aggregate	3/4" Aggregate	Cement
2"	50.0	100	100	100	100	100
1.25"	31.5	100	100	100	100	100
1"	25.0	100	100	100	100	100
3/4"	19.0	100	100	100	98	100
1/2"	12.5	100	100	100	42	100
3/8"	9.50	100	100	100	11	100
1/4"	6.30	100	100	87	1	100
No. 4	4.75	100	99	57	1	100
No. 8	2.36	88	80	2	1	100
No. 10	2.00	82	73	2	1	100
No. 16	1.18	62	53	1	1	100
No. 30	0.600	40	36	1	1	100
No. 40	0.425	29	30	1	1	100
No. 50	0.300	20	25	1	1	100
No. 100	0.150	7	16	1	1	100
No. 200	0.075	1.5	10.5	1.0	0.7	100

Table 11. Asphalt Mixture Aggregate Gradation for Aggregates Procured from Globe

Standard	Metric (mm)	% Passing (Without Cement)	% Passing (With Cement)
1"	25.0	100	100
3/4"	19.0	98	98
1/2"	12.5	89	89
3/8"	9.50	76	76
No. 4	4.75	54	54
No. 8	2.36	30	31
No. 16	1.18	23	24
No. 30	0.600	16	17
No. 50	0.300	10	11
No. 100	0.150	6	7
No. 200	0.075	3.5	4.5
Pan	<0.075	–	–

Snowflake

The aggregate sourced from Snowflake consisted of four stockpiles—washed crusher fines (WCF), crusher fines (CF), 3/8-inch SHRP chips, and 7/8-inch rock—plus a portland cement admixture. Tables 12, 13, and 14 show the characteristics of these stockpiles, the gradations of the individual stockpiles, and the gradations of the aggregates used for preparing the asphalt mixture samples, respectively. The mixtures consisted of 15 percent WCF, 25 percent CF, 27 percent 3/8-inch aggregate, and 33 percent 7/8-inch aggregate. Finally, 1 percent portland cement by total aggregate mass was added.

Table 12. Characteristics of Aggregates Sourced from Snowflake

Aggregate Properties	Coarse Aggregate	Fine Aggregate	Spec. Limits	Admixture (portland cement)
Bulk Specific Gravity	2.562	2.589	2.350–2.850	3.14
SSD Specific Gravity	2.59	2.619		
Apparent Specific Gravity	2.635	2.67		
Water Absorption (%)	1.08	1.17	0–2.5%	–
Sand Equivalent	79		Min. 55	
1 Fracture Face (%)	95%		Min. 92%	
2 Fracture Face (%)	92%		Min. 85%	
Uncompacted Voids	46.20%		Min. 45%	
Flat and Elongated Aggregate	0%		Max. 10%	
Carbonates	2%		Max. 20%	
L.A. Abrasion, 100 rev., % loss	5%		Max. 9%	
L.A. Abrasion, 500 rev., % loss	24%		Max. 40%	

Table 13. Gradation of Aggregate Stockpiles Sourced from Snowflake

Standard	Metric (mm)	Washed Crusher Fines	Crusher Fines	3/8" SHRP Chips	7/8" Rock	Cement
2"	50.0	100	100	100	100	100
1.5"	31.5	100	100	100	100	100
1"	25.0	100	100	100	100	100
3/4"	19.0	100	100	100	92	100
1/2"	12.5	100	100	100	31	100
3/8"	9.50	100	100	100	12	100
1/4"	6.30	100	100	79	2	100
No. 4	4.75	100	100	37	1	100
No. 8	2.36	79	67	5	1	100
No. 10	2.00	74	60	4	1	100
No. 16	1.18	61	45	4	1	100
No. 30	0.600	44	34	3	1	100
No. 40	0.425	35	30	3	1	100
No. 50	0.300	22	24	2	1	100
No. 100	0.150	5	16	2	1	100
No. 200	0.075	1.1	11.0	1.0	0.2	100.0

Table 14. Asphalt Mixture Aggregate Gradation for Aggregates Procured from Snowflake

Standard	Metric (mm)	% Passing (without cement)	% Passing (with cement)
1"	25.0	100	100
3/4"	19.0	98	98
1/2"	12.5	80	80
3/8"	9.50	72	72
No. 4	4.75	51	51
No. 8	2.36	30	31
No. 16	1.18	21	22
No. 30	0.600	16	17
No. 50	0.300	10	11
No. 100	0.150	5	6
No. 200	0.075	3.1	4.1
Pan	<0.075	–	–

Tucson

The aggregate sourced from Tucson consisted of five stockpiles—crusher fines (CF), washed crusher fines (WCF), 3/8-inch mineral aggregate (MA), 1/2-inch MA, and 3/4-inch MA—plus a portland cement admixture. Tables 15 and 16 provide the characteristics of these stockpiles and their gradations. Table 17 shows the gradations of the aggregates used in preparing the asphalt mixture samples. The mixtures

consisted of 40 percent WCF, 15 percent CF, 10 percent 3/8" aggregate, 10 percent 1/2" aggregate, and 25 percent 3/4" aggregate. Finally, 1 percent portland cement by total aggregate mass was added.

Table 15. Characteristics of Aggregates Sourced from Tucson

Aggregate Properties	Coarse Aggregate	Fine Aggregate	Spec. Limits	Admixture (portland cement)
Bulk Specific Gravity	2.587	2.581	2.350–2.850	3.14
SSD Specific Gravity	2.614	2.610		
Apparent Specific Gravity	2.657	2.657		
Water Absorption (%)	1.02	1.11	0–2.5%	–
Sand Equivalent	84		Min. 55	
1 Fracture Face (%)	99%		Min. 92%	
2 Fracture Face (%)	92%		Min. 85%	
Uncompacted Voids	47.9%		Min. 45%	
Flat and Elongated Aggregate	–		Max. 10%	
Carbonates	0.2%		Max. 20%	
L.A. Abrasion, 100 rev., % loss	3%		Max. 9%	
L.A. Abrasion, 500 rev., % loss	18%		Max. 40%	

Table 16. Gradation of Aggregate Stockpiles Sourced from Tucson

Standard	Metric (mm)	Crushed Fines	Washed Crushed Fines	3/8" Mineral Aggregate	1/2" Mineral Aggregate	3/4" Mineral Aggregate	Cement
2"	50.0	100	100	100	100	100	100
1.25"	31.5	100	100	100	100	100	100
1"	25.0	100	100	100	100	100	100
3/4"	19.0	100	100	100	100	83	100
1/2"	12.5	100	100	100	60	12	100
3/8"	9.50	100	100	100	29	8	100
1/4"	6.30	100	100	68	10	6	100
No. 4	4.75	100	100	33	8	4	100
No. 8	2.36	78	75	6	6	2	100
No. 10	2.00	71	67	6	6	2	100
No. 16	1.18	54	48	4	5	2	100
No. 30	0.600	39	30	4	4	1	100
No. 40	0.425	32	22	3	4	1	100
No. 50	0.300	26	16	3	3	1	100
No. 100	0.150	17	6	3	3	1	100
No. 200	0.075	11.5	1.3	2.1	2.2	0.8	100.0

Table 17. Asphalt Mixture Aggregate Gradation for Aggregates Procured from Tucson

Standard	Metric (mm)	% Passing (without cement)	% Passing (with cement)
1"	25.0	100	100
3/4"	19.0	96	96
1/2"	12.5	75	76
3/8"	9.50	69	69
No. 4	4.75	58	59
No. 8	2.36	44	44
No. 16	1.18	29	30
No. 30	0.600	19	20
No. 50	0.300	11	12
No. 100	0.150	6	7
No. 200	0.075	2.8	3.7
Pan	<0.075	–	–

Mix Design

All of the asphalt mixtures evaluated are in line with the current ADOT Superpave mix design criteria. Table 18 details the mix design parameters of interest for all of the asphalt mixtures used. The limits for the parameters shown in the table are for ADOT's 417 Superpave mixture. The prefixes "T," "S," and "G" indicate the source of the aggregate, which is Tucson, Snowflake, and Globe, respectively.

Table 18. Mix Design Properties of Arizona Asphalt Mixtures Used in the Study

Group	Mixture	Mix Design Property						
		Asphalt Binder Content (%)	Absorbed Asphalt (%)	% VMA[a]	% VFA[b]	%G_{mm}[c] @ $N_{initial}$[d]	%G_{mm} @ N_{max}[e]	Dust Proportion (%)
1	GY3	5.3	1.09	14.4	65.3	80.9	90.4	0.85
	GY4	5.3	0.99	14.6	65.8	80.7	90.4	0.83
	GZ2	5.3	1.05	14.4	65.3	80.9	90.6	0.86
	SY1	5.5	0.59	17.3	63	84.2	93.5	0.96
	SZ1	5.3	0.09	17.8	64.1	84.9	94.7	0.91
	TX1	5.8	0.71	17.5	63.5	85.5	93.6	0.73
	TZ4	5.8	0.74	17.5	63.5	85.5	93.6	0.74
2	GX4	5.2	0.88	14.6	65.9	81.5	91.4	0.84
	GX5	5.4	0.96	14.8	66.2	80.7	90.3	0.82
	GY6	5.3	0.96	14.6	65.7	80.8	90.5	0.84
	SX3	5.6	0.43	17.8	64.1	82.1	92.2	0.91
	TY5	5.5	0.49	17.6	63.6	84.9	93.6	0.75

[a] VMA = Voids in Mineral Aggregate

[b] VFA = Voids Filled with Asphalt

[c] %Gmm = Theoretical Maximum Specific Gravity

[d] $N_{initial}$ = Initial Number of Gyrations

[e] N_{max} = Maximum Number of Gyrations

EXPERIMENTS

The experimental program, summarized in Figures 13 and 14, consisted of tests on binders as well as on asphalt mixtures. The binder tests were used to measure the properties of the binders and characterize their performance grade in both AASHTO M 320 and AASHTO M 332. The asphalt mixture tests were conducted to establish how changes in binder properties would affect asphalt mixture performance. Summaries appear below of the most relevant aspects of the test methods as they apply to this study, but more details of the tests are provided in Appendix C.

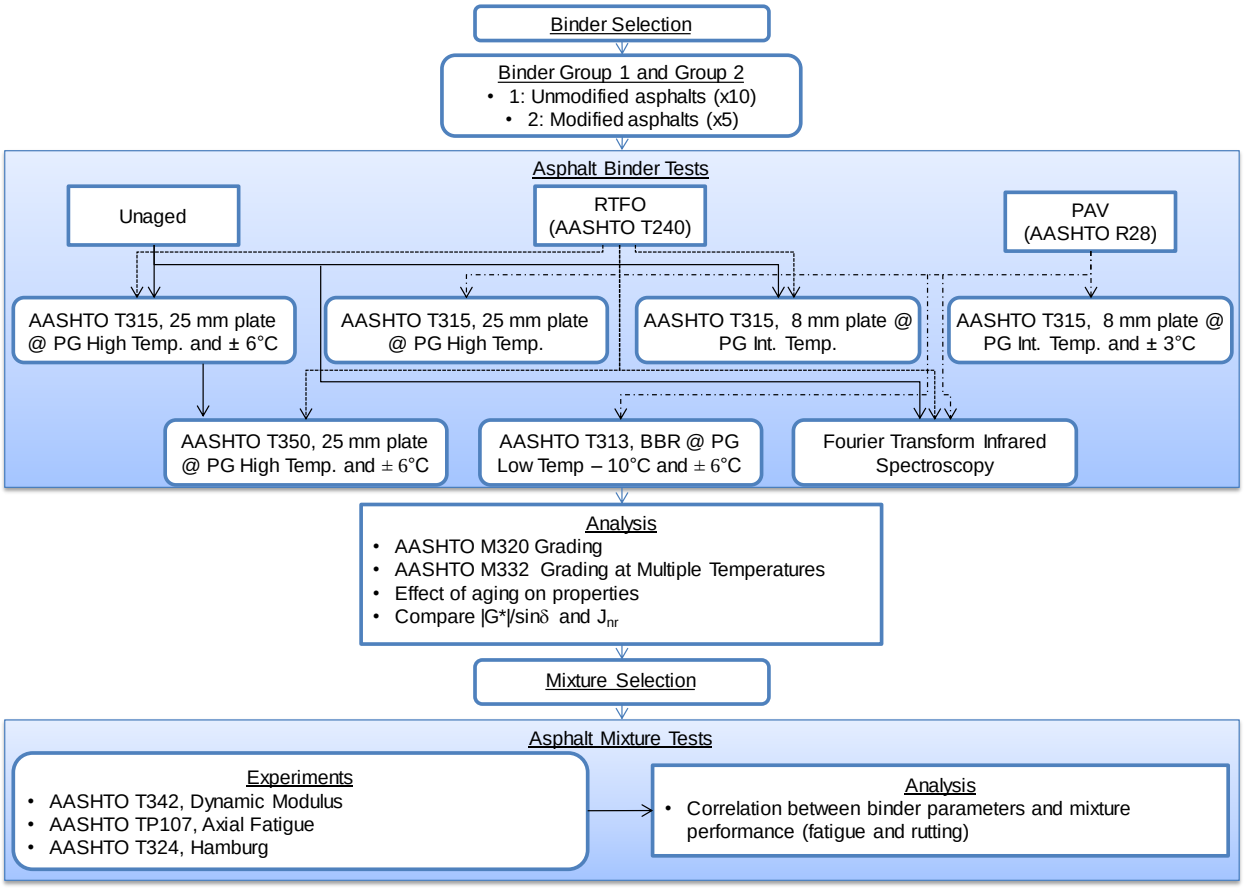

Figure 13. Flowchart of the Experimental Program for Group 1 and 2 Binders

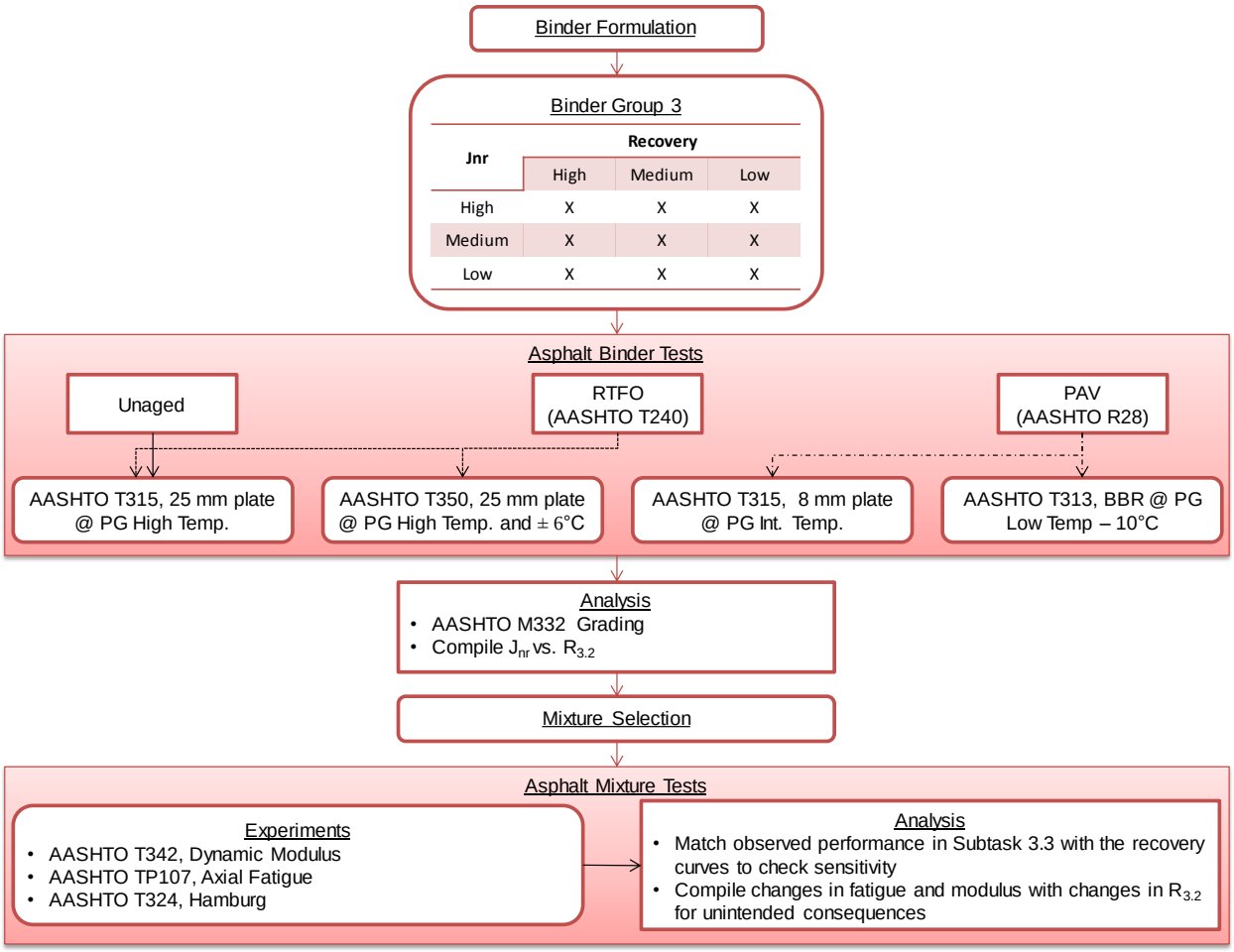

Figure 14. Flowchart of the Experimental Program for Group 3 Binders

Asphalt Binder Experiments

As Figures 13 and 14 demonstrate, the binder experiments used the dynamic shear rheometer (DSR) for determining the intermediate- and high-temperature linear and nonlinear viscoelastic properties of the binders, and used the bending beam rheometer (BBR) for determining the low-temperature properties. These figures also show that testing was conducted on the binders after different age conditioning.

Conditioning Protocols

The experiments were conducted on binder samples that had been conditioned to three different oxidative states: unaged, short-term-aged, and long-term-aged. Other than initial heating to separate the binder from the as-delivered 5-gallon pails into test quantities, unaged binders were not subjected to any specialized process. They represented the binder as it existed at the time of mixing. Short-term aging was in accordance with AASHTO T 240 (Rolling Thin-Film Oven, RTFO) (AASHTO 2013a), and long-term aging was in accordance with AASHTO R 28 (Pressure Aging Vessel, PAV) (AASHTO 2012c). The

conditioning temperature for PAV was chosen based on the current ADOT guidelines, which means that PAV aging was conducted at 100°C for PG 64 and at 110°C for PG 70 and PG 76. As per AASHTO R 28, all PAV-aged binders were subjected to the RTFO procedure prior to being aged in the PAV. In the interest of brevity, these samples are referred to simply as PAV-aged instead of RTFO+PAV-aged.

Shear Modulus and Phase Angle

Oscillatory, parallel plate testing was conducted in accordance with AASHTO T 315 to determine the shear modulus, $|G^*|$, and phase angle, δ, of the binders. Tests were performed using either a 25-mm parallel plate geometry (for temperatures greater than 58°C) or an 8-mm parallel plate geometry (for temperatures between 22°C and 37°C). All tests were carried out at a 10 radians/second frequency. Table 19 summarizes the strain levels and test temperatures used in the experiments for both test geometries.

Table 19. Summary of AASHTO T 315 Testing Conditions

Geometry	Aging Level	Test Temperatures	Strain Level (%)
25 mm	Unaged	AASHTO M 320 high-temperature grade and ±6°C	12[a]
	RTFO	AASHTO M 320 high-temperature grade and ±6°C	10[a]
	PAV	AASHTO M 320 high-temperature grade	0.5[b]
8 mm	Unaged	AASHTO M 320 intermediate-temperature grade	1.0
	RTFO	AASHTO M 320 intermediate-temperature grade	1.0
	PAV	AASHTO M 320 intermediate-temperature grade and ±3°C	1.0[a]

[a] Strain levels chosen from guidelines in AASHTO T 315

[b] Strain level chosen from strain sweep experiment

Flexural Creep Stiffness

The BBR test (AASHTO T 313) is used to measure the flexural creep stiffness (S) and the logarithmic change in the creep stiffness at 60 s (*m value*) (AASHTO 2012a). In this study, the BBR test was conducted at the standard temperature for the given grade (10°C higher than the low-temperature grade of the binder) and at ±6°C of this value. For example, with a PG 64-22 binder, the test temperatures would be –6°C, –12°C, and –18°C.

Percent Recovery and Nonrecoverable Creep Compliance

MSCR testing was conducted according to AASHTO T 350. The four parameters extracted from this test were the nonrecoverable creep compliance at both 3.2 kPa and 0.1 kPa stress levels, $J_{nr3.2}$ and $J_{nr0.1}$, respectively; the percentage of difference between these two quantities (J_{nrdiff}); and the percentage of strain recovery during the 3.2 kPa loading, $R_{3.2}$. Appendix C presents details of the calculations. The tests were conducted at the AASHTO M 320 high-temperature binder grade and at ±6°C, except for the PG 76 binders, which were tested at 76°, 70°, and 64°C.

Elastic Recovery Test

The elastic recovery test was conducted on all the polymer-modified binders (i.e., Group 2 and Group 3 binders). The test was performed on binders in the original, unaged condition, and in accordance with AASHTO T 301 at 10°C (AASHTO 2013b). The binder samples were placed in a ductility bath and pulled until the elongation reached 20 cm. After a wait of five minutes, the elongated sample was cut in the middle and the recovery was measured.

Fourier Transform Infrared Spectroscopy (FT-IR Spectroscopy)

Attenuated Total Reflectance Fourier Transform Infrared Spectroscopy (ATR-FT-IR) was used for measuring changes in binder chemical properties caused by oxidation. The test measures the infrared spectrum of energy absorption of the aged and unaged binder at multiple wavelengths. The spectra resulting from the ATR-FT-IR method contain peaks at wave numbers that correspond to different types of bonds within the binder. Oxidation results in an increase in the number of double bonds between hydrocarbons and oxygen, which can be detected with the ATR-FT-IR test. The two specific functional groups examined in this study were the carbonyl and sulfoxide groups. Studies have linked the increase in absorbances at these groups to binder oxidation. The metrics adopted are the areas under the carbonyl and sulfoxide peaks (Jemison et al. 1992, Petersen and Glaser 2011), referred to as CA and CA+S, respectively. The effect of oxidation is quantified by examining the changes in these quantities with RTFO and PAV aging.

Proficiency Study

A proficiency study was conducted to confirm that the ASU experiments yielded results consistent with current ADOT practice. Three laboratories participated in the study: the ASU laboratory, the ADOT Materials Group Central Laboratory in Phoenix, and the ADOT Materials Group Regional Laboratory in Prescott. The study included two binders, PG 64-16 (a non-polymer-modified binder) and PG 76-22TR+ (a polymer-modified binder). The standard tests and reporting parameters are summarized in Table 20. For this study, each laboratory was provided with original binder, which had to be aged at its own facility.

Table 20. Summary of Proficiency Study Tests and Parameters

Test	Aging	Temperature (°C)		Parameters
		PG 64-16	PG 76-22TR+	
AASHTO T 315—DSR (25 mm plate)	Unaged and RTFO	64	76	$\|G^*\|$, δ, and $\|G^*\|/\sin\delta$
AASHTO T 315—DSR (8 mm plate)	PAV[a]	28	31	$\|G^*\|$, δ, and $\|G^*\|\sin\delta$
AASHTO T 350—MSCR	RTFO	64	76	$J_{nr0.1}$, $J_{nr3.2}$, $R_{0.1}$, $R_{3.2}$, J_{nrdiff}, and R_{diff}
AASHTO T 313—BBR	PAV[a]	–6	–12	S and m

[a] PG 64-16 aged at 100°C and PG 76-22TR+ aged at 110°C

The results from the three labs were analyzed based on the d2s% statistical parameter (acceptable range of two test results conducted in different laboratories on the same sample), which is calculated in accordance with ASTM C670. This parameter is then compared to the multilaboratory d2s% limits specified in AASHTO T 315 and AASHTO T 313. Since there are no such limits in the AASHTO T 350 standard, the d2s% limits listed for the MSCR test are the ASTM D7405 d2s% limits and the limits determined from the last four AMRL PSP cycles. Table 21 summarizes the d2s% limits for each of these tests.

Table 21. Limits on d2s% for AASHTO T 315, T 313, and T 350 as Obtained from ASTM D7405 and AMRL PSP Studies

Parameters	**Specification Limits (d2s%)**					
$\|G^*\|/\sin\delta$ (kPa)	17.0					
$\|G^*\|/\sin\delta$ (kPa)	22.2					
$\|G^*\|\sin\delta$ (kPa)	40.2					
S (MPa)	17.8					
m	6.8					
	ASTM D7405		**AMRL PSP**			
	PG 64-16	**PG 76-22TR+**	**(241/242)**	**(239/240)**	**(237/238)**	**(235/236)**
$R_{0.1}$ (%)	15.0	15.0	20.8	43.8	38.2	26.7
$R_{3.2}$ (%)	18.1	18.1	22.5	84.2	110.0	45.1
R_{diff} (%)			57.9	24.0	20.5	11.8
$J_{nr0.1}$ (1/kPa)[1]	25.6	46.8	47.8	18.6	23.1	20.6
$J_{nr3.2}$ (1/kPa)[1]	22.0	39.0	31.6	18.1	21.8	20.1
J_{nrdiff} (%)[1]			92.5	34.8	24.8	17.5

[1]ASTM specifies four different d2s% limits for J_{nr} based on the J_{nr} values: (i) >1.00; (ii) 0.26-1.00; (iii) 0.1-0.25; and (iv) <0.1.

Table 22 shows the results and the computed test statistics for PG 64-16, and Table 23 shows the results for PG 76-22TR+. In these tables, the cells highlighted in green indicate that the d2s% values across all labs are within the AASHTO specification limits. The tables show that the tests conducted in accordance with AASHTO T 315 and AASHTO T 313 yield results that are within the specification limits for both binders. Moreover, for both binders, the AASHTO T 315 results are well within the specification limits. (The d2s% limits for MSCR test parameters as obtained from ASTM D7405 and the AMRL PSP studies are shown in Table 21.) The cells highlighted in yellow indicate that the computed MSCR d2s% values meet the ASTM specification limit and also the highest d2s% limit of the listed AMRL studies for that parameter. The cells in orange indicate that the MSCR d2s% values fail the ASTM limit but pass the highest limit of the listed AMRL studies. The cells in red indicate that the d2s% values fail both the ASTM limit and the highest limit of the listed AMRL studies for that parameter. For PG 64-16, the variability in percent recovery is higher than the ASTM or AMRL limits. However, the values of the recoveries themselves are very low (<1 percent at 3.2 kPa) and will not affect the resultant grade. The d2s% values for J_{nr} at both 0.1 and 3.2 kPa and J_{nrdiff} are within the ASTM and AMRL limits. For PG 76-22TR+ binder, the high variability in $R_{3.2}$, $J_{nr0.1}$, and $J_{nr3.2}$ can be attributed to the noticeably different values obtained by

the ADOT's central lab in comparison to the ASU and ADOT Prescott labs. However, d2s% values calculated based on the results obtained by ASU and ADOT Prescott are within the ASTM and AMRL specification limits. The PG 76-22TR+ binder is not a straight-run polymer-modified sample, so the differences were expected and deemed acceptable by the ADOT Technical Advisory Committee.

Table 22. Results and Computed Statistical Parameters for PG 64-16

Parameter	Laboratory			Mean	Std. Dev.	d2s% (Comparison Laboratories)		
	ASU	Central	Prescott			ASU and Central	Prescott and Central	Prescott and ASU
AASHTO T 315 (Unaged)								
$\|G^*\|$ (kPa)	1.34	1.38	1.36	1.36	0.02	-2.94	-1.46	1.48
δ (degree)	88.1	88.2	88.2	88.2	0.06	-0.11	0.00	0.11
$\|G^*\|/\sin\delta$ (kPa)	1.34	1.38	1.36	1.36	0.02	-2.94	-1.46	1.48
AASHTO T 315 (RTFO)								
$\|G^*\|$	3.35	3.47	3.16	3.33	0.16	-3.52	-9.35	-5.84
δ (degree)	85.7	85.8	86.1	85.9	0.21	-0.12	0.35	0.47
$\|G^*\|/\sin\delta$	3.36	3.48	3.17	3.34	0.16	-3.51	-9.32	-5.82
AASHTO T 315 (PAV)								
$\|G^*\|$ (kPa)	6434	6370	6160	6321	143	1.00	-3.35	-4.35
δ (degree)	41.2	42.1	41.4	41.6	0.47	-2.16	-1.68	0.48
$\|G^*\|\sin\delta$ (kPa)	4237	4280	4070	4196	111	-1.01	-5.03	-4.02
AASHTO T 313								
S (MPa)	117	121	124	121	3.51	-3.36	2.45	5.81
m	0.307	0.302	0.299	0.303	0.004	1.64	-1.00	-2.64
AASHTO T 350								
$R_{0.1}$ (%)	3.46	2.70	1.82	2.66	0.82	24.68	-38.94	-62.12
$R_{3.2}$ (%)	0.90	-0.07	-0.20	0.21	0.60	233.73	96.30	-314.29
R_{diff} (%)[1]	74.0	102.5	111.0	95.8	19.4	-32.36	7.93	40.03
$J_{nr0.1}$ (1/kPa)	2.7	2.7	3.1	2.8	0.25	2.27	15.72	13.46
$J_{nr3.2}$ (1/kPa)	2.9	2.8	3.3	3.0	0.25	1.90	14.99	13.10
J_{nrdiff} (%)[1]	5.5	5.9	5.2	5.6	0.38	-6.97	-13.67	-6.72

[1]There are no d2s% ASTM limits for R_{diff} and J_{nrdiff}.
Green: d2s% values across all labs are within the AASHTO specification limits.
Yellow: MSCR d2s% values meet the ASTM specification limit and the highest d2s% limit of the listed AMRL studies for that parameter.
Orange: MSCR d2s% values fail the ASTM limit but pass the highest limit of the listed AMRL studies.
Red: d2s% values fail both the ASTM limit and the highest limit of the listed AMRL studies for that parameter.

Table 23. Results and Computed Statistical Parameters for PG 76-22TR+

Parameters	Laboratory			Mean	Std. Dev.	d2s% (Comparison Laboratories)		
	ASU	Central	Prescott			ASU and Central	Prescott and Central	Prescott and ASU
AASHTO T 315 (Unaged)								
$\|G^*\|$ (kPa)	1.52	1.38	1.40	1.43	0.08	9.66	1.44	-8.22
δ (degree)	64.0	66.4	64.9	65.1	1.21	-3.68	-2.28	1.40
$\|G^*\|/\sin\delta$ (kPa)	1.69	1.50	1.54	1.58	0.10	11.91	2.63	-9.29
AASHTO T 315 (RTFO)								
$\|G^*\|$	2.38	2.34	2.25	2.32	0.07	1.69	-3.92	-5.62
δ (degree)	63.3	64.2	63.9	63.8	0.46	-1.41	-0.47	0.94
$\|G^*\|/\sin\delta$	2.67	2.60	2.50	2.59	0.09	2.66	-3.92	-6.58
AASHTO T 315 (PAV)								
$\|G^*\|$ (kPa)	2384	2200	2490	2358	147	8.03	12.37	4.35
δ (degree)	52.1	54.7	52.3	53.0	1.5	-4.87	-4.49	0.38
$\|G^*\|\sin\delta$ (kPa)	1881	1790	1970	1880	90	4.96	9.57	4.62
AASHTO T 313								
S (MPa)	184	169	198	184	14.5	8.50	15.80	7.33
m	0.338	0.341	0.326	0.335	0.01	-0.88	-4.50	-3.61
AASHTO T 350								
$R_{0.1}$ (%)	92.1	87.7	93.1	91.0	2.85	4.79	5.96	1.17
$R_{3.2}$ (%)	77.9	62.1	76.5	72.2	8.76	22.63	20.78	-1.87
R_{diff} (%)[1]	15.3	29.3	17.9	20.8	7.42	-62.42	-48.33	15.24
$J_{nr0.1}$ (1/kPa)	0.18	0.27	0.16	0.20	0.06	-42.51	-52.09	-10.15
$J_{nr3.2}$ (1/kPa)	0.49	0.88	0.54	0.63	0.21	-57.08	-47.98	9.77
J_{nrdiff} (%)[1]	176.4	223.0	237.4	212.3	31.9	-23.37	6.23	29.49

[1]There are no d2s% ASTM limits for R_{diff} and J_{nrdiff}
Green: d2s% values across all labs are within the AASHTO specification limits.
Yellow: MSCR d2s% values meet the ASTM specification limit and the highest d2s% limit of the listed AMRL studies for that parameter.
Orange: MSCR d2s% values fail the ASTM limit but pass the highest limit of the listed AMRL studies.
Red: d2s% values fail both the ATM limit and the highest limit of the listed AMRL studies for that parameter.

Asphalt Mixture Experiments

Figures 13 and 14 show that the asphalt mixture tests included the dynamic modulus test, the axial fatigue test, and the Hamburg wheel tracking test (HWTT). These tests are used, respectively, to identify the ability of the mixtures to resist deformation, resist fatigue, and resist rutting. The sections below highlight the specific details of each test most relevant to the current study, but for a fuller description of the experimental setup and analytical methods used for each experiment, see Appendix C.

Dynamic Modulus

The test for axial dynamic modulus, $|E^*|$, is performed using a servohydraulic testing machine and involves repeated sinusoidal loading of a cylindrical specimen along its symmetrical axis. Standardized in

AASHTO T 342, the test involves subjecting test specimens to cyclical compression loading at frequencies of 25, 10, 5, 1, 0.5, and 0.1 Hz and at temperatures of –10°, 4.4°, 21.1°, 37.8°, and 54°C (AASHTO 2015). Tests are conducted in an increasing order of temperature and in a decreasing order of loading frequency. The load is varied with temperature and frequency so that the on-specimen strains remain in the range of 40–80 microstrains. In accordance with the standard, $|E^*|$ is calculated by sinusoidal regression of the stress and strain responses of the last five cycles of each temperature and frequency combination.

Axial Fatigue

The uniaxial fatigue test is conducted in accordance with AASHTO TP 107, and involves the repeated sinusoidal displacement of a cylindrical sample until it fails (AASHTO 2014a). The cylindrical specimen is 150 mm tall and 75 mm in diameter. The test temperature is selected based on the 98-percent-reliability performance grade of the binder used in the mixture. The testing temperature should be determined as the average of high- and low-temperature PG grades minus 3°C. For example, the test temperature for PG 64-22 binder is 18°C. If the calculated test temperature exceeds 21°C, then 21°C is used as the testing temperature. The uniaxial fatigue test is run until a sudden decrease in phase angle is observed, which indicates that a crack has localized and failure has occurred.

Hamburg Wheel Tracking Test

The HWTT (standardized in AASHTO T 324) evaluates the rutting and moisture susceptibility of asphalt mixtures (AASHTO 2014b). The equipment consists of a reciprocating wheel, which simulates a moving concentrated load. Test specimens are compacted in the Superpave gyratory compactor and have a diameter of 150 mm. Following ADOT and AASHTO protocols, all tests are performed at a loading frequency of 52 ± 2 passes per minute and for a maximum of 20,000 passes. Tests are conducted at temperatures based on the S-grade of the binder in question (Table 24). It is worth noting that ADOT has been conducting HWTT at 50°C, irrespective of the binder grade. So, in line with ADOT practice, mixtures with PG 76S binder are tested at 50°C in addition to 56° and 62°C.

Table 24. HWTT Temperatures by Asphalt Binder Grade

Asphalt Binder Grade	Test Temperatures (°C)
PG 76S	62 and 56
PG 70S	56 and 50
PG 64S	50 and 44

Specimen Fabrication

All test specimens are compacted in a Servopac Superpave gyratory compactor. The ram pressure, gyration angle, and gyration speed are 600 kPa, 1.16°, and 30 gyrations per minute, respectively. All specimens are compacted with a diameter of 150 mm. Specimens for dynamic modulus and axial fatigue testing are first compacted to a height of 180 mm, while those for HWTT are compacted to a height of 100 mm. HWTT is conducted on the as-compacted samples, but dynamic modulus and fatigue specimens are cored from the compacted samples (100 mm core for dynamic modulus and 75 mm core for axial fatigue) and cut to a final test height of 150 mm. This process is followed to ensure as uniform an air void distribution as possible throughout the test specimen.

Once specimens of the appropriate dimensions are obtained, air void measurements are taken via the AASHTO T 166 method, and the specimens are stored until testing. The air voids for the dynamic modulus and axial fatigue specimens in this study are between 6 and 7 percent, while those for HWTT are between 6 and 8 percent. During storage, specimens are sealed in bags and placed in an unlit cabinet to reduce aging effects. Furthermore, no test specimens are stored for longer than two weeks before testing.

CHAPTER 4. PROPERTIES OF ARIZONA BINDERS

EXPERIMENTAL PROGRAM

The experimental program outlined in Figures 13 and 14 forms the basis for the results, discussion, and analysis presented in this chapter. As shown in those figures, the experimental program involved testing of Arizona binders. The binder experiments used the DSR for determining the intermediate- and high-temperature linear and nonlinear viscoelastic properties of the binders, and used the BBR for determining the low-temperature properties. The tests were used to measure the properties of the binders and characterize their performance grade in accordance with both AASHTO M 320 and AASHTO M 332. The tests performed, and the test methodology used, have been summarized in Chapter 3 and presented in detail in Appendix C. The overall goal of the experiments and analysis presented here was to characterize the J_{nr} of the study binders and understand how it is related to other grading parameters so that the likely performance improvements and unintentional consequences from moving toward the AASHTO M 332 grading system can be estimated.

RESULTS, DISCUSSION, AND ANALYSIS

High-Temperature Properties

Two sets of experiments, one under AASHTO T 315 (DSR) and the other under AASHTO T 350 (MSCR), were performed to determine the high-temperature properties of Arizona binders.

AASHTO T 315

The results from AASHTO T 315 testing indicate that all the binders tested passed the original and the RTFO high-temperature criterion in AASHTO M 320 at their specified PG high temperatures and also at 6°C lower than their PG high temperatures. Thus, if a binder was graded as PG 64-22 by the supplier, the binder met the original and the RTFO $|G^*|/\sin\delta$ criteria at 64°C and 58°C. It should be recalled that the testing was also performed at 6°C higher than the specified PG high temperature. At this temperature, none of the binders, except for binder Y6, passed both the original and the RTFO $|G^*|/\sin\delta$ criterion. Figure 15 shows the variation of the $|G^*|/\sin\delta$ parameter with temperature and aging level for binder Y1 for both the original and the RTFO conditions, and Figure 16 shows the variation for binder X3. Similar graphs for all the binders can be found in Appendix D, Figures D-1 through D-13.

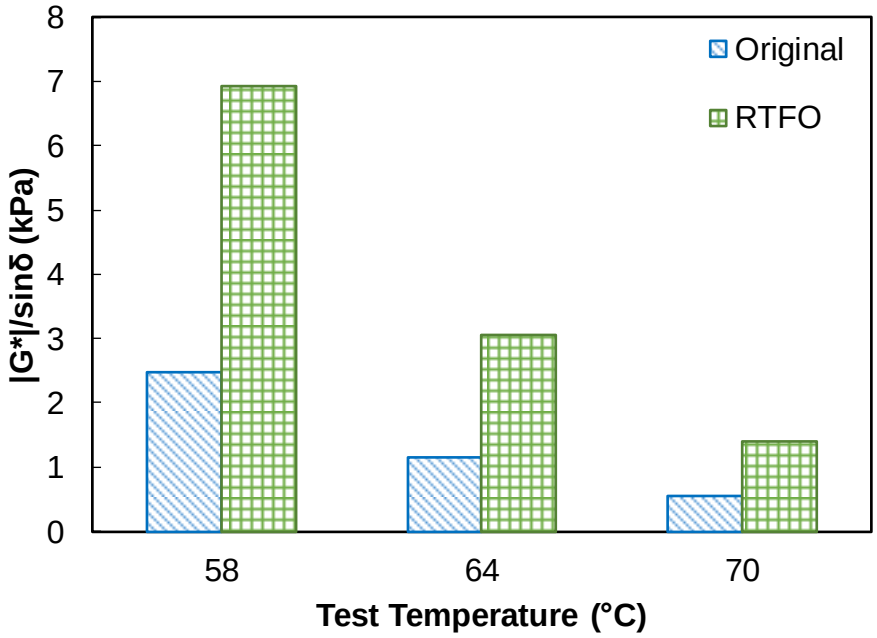

Figure 15. Variation of $|G^*|/\sin\delta$ Parameter with Temperature and Aging Level for Binder Y1

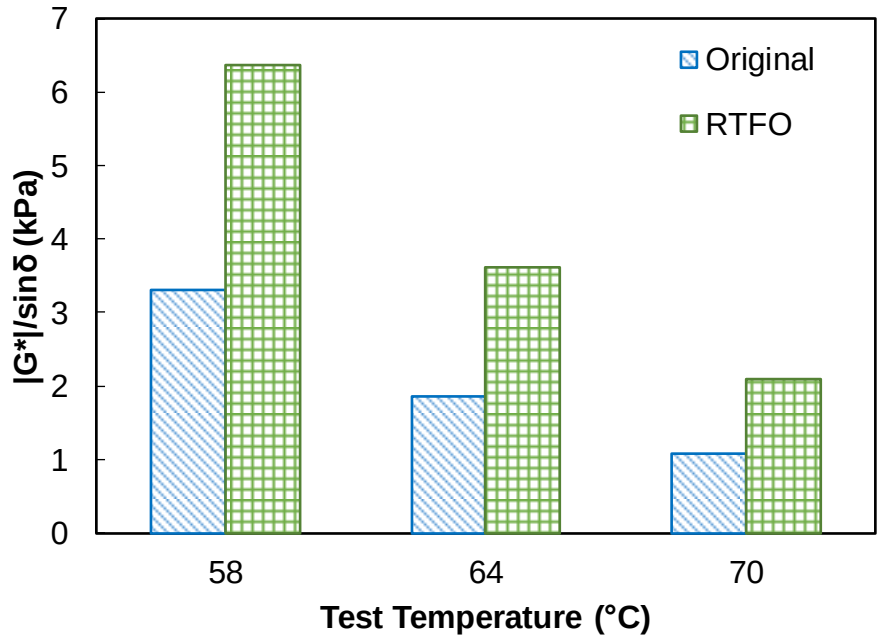

Figure 16. Variation of $|G^*|/\sin\delta$ Parameter with Temperature and Aging Level for Binder X3

AASHTO T 350

The MSCR test was performed on all the RTFO-aged study binders at three temperatures: the high-temperature PG grade (as designated by the supplier) and that temperature plus 6°C and minus 6°C. For PG 76 binders, + 6°C would result in a test temperature of 82°C, which was unreasonable for Arizona conditions, as none of the binders were PG 82. Hence, the decision was made to test PG 76 binders at –6°C and –12°C. The test results showed that all the unmodified binders have an AASHTO M 332 traffic grade of "S" at the temperature they are currently specified under AASHTO M 320. For example, unmodified binders currently specified as PG 70-10 under AASHTO M 320 have a designation of PG 70S-10 under AASHTO M 332. The polymer-modified binders X3 and X4 are true to their designated grade as provided by the supplier (64H-22 in the case of X3 and 64V-22 in the case of X4). The polymer-modified binder X5 (a PG 76-22TR+ binder) grades as an "H" at 76°C and as an "E" at 70°C and 64°C. The binders Y5 and Y6, which were based on Oklahoma DOT specifications, exceeded the designated PG grade. These two binders, which the supplier had graded as PG 70H-16 and PG 70V-16, respectively, were also found to be satisfactory for PG 70E-16 and for PG 76E-22. Table 25 summarizes the grades of each binder at the different temperatures. Although the limits of the intermediate temperature $|G^*|\sin\delta$ parameter have not yet been described, these binder grades fall within those limits.

Table 25. Classification of Study Binders According to AASHTO M 332 Binder Grades

Modified or Unmodified Binder	Binder PG Grade (per Supplier)	Study Binder Designation	Binder Grade According to AASHTO M 332															
			PG 58				PG 64				PG 70				PG 76			
			S	H	V	E	S	H	V	E	S	H	V	E	S	H	V	E
Unmodified	PG 64-22 (Y)	Y1		X			X											
	PG 64-22 (Z)	Z1			X		X											
	PG 70-22 (Y)	Y2						X			X							
	PG 70-22 (Z)	Z2						X			X							
	PG 70-10 (X)	X1						X			X							
	PG 70-10 (Z)	Z3							X		X							
	PG 76-16 (Y)	Y4							X			X			X			
	PG 76-16 (Z)	Z4								X		X			X			
	PG 76-16 (X)	X2								X		X			X			
	PG 70-16 (Y)	Y3						X			X							
Polymer Modified	PG 76-22TR (X)	X5								X				X		X		
	PG 64V-22 (X)	X4				X			X		X							
	PG 64H-22 (X)	X3				X		X			X							
	PG 70H-16 (Y)	Y5								X				X				X
	PG 70V-16 (Y)	Y6								X				X				X

The MSCR test also measures the recovery of the strains at 3.2 kPa as a check for the presence of polymer and, as reported by others, the action of polymer to cross-link the binder (D'Angelo 2010). It should be noted that cross-linking is only inferred from rheological testing and morphological study of modified binders by fluorescence microscopy. Cross-linking is not objectively measured, and the use of the term "cross-linking" is an indication of a different morphology and an accompanying correlation to binder rheology (D'Angelo 2010). As revealed in Figure 17, which shows the behavior of the study binders at their current PG high-temperature grade, all the polymer-modified binders lie above the $J_{nr3.2}$ vs. $R_{3.2}$ curve, while all non-polymer-modified binders lie below the curve. Based on the D'Angelo 2010, and on personal communication (John D'Angelo, personal communication, 2015), the location above the line indicates the presence of polymer and confirms a more uniform morphological structure of the polymer in the binder. The line shown in Figure 17 is the one depicted in AASHTO M 332. The Asphalt Institute has recently suggested a modification to the line in which the minimum recovery for all binders having $J_{nr3.2} < 0.1$ is set at 55 percent (Figure 18) (Anderson 2016). The main motivation behind this modification was that the original line represented an extrapolation of real observations. Based on our conversations with experts, some suppliers had also reported difficulty achieving level of recovery dictated by the original line with binders known to perform well.

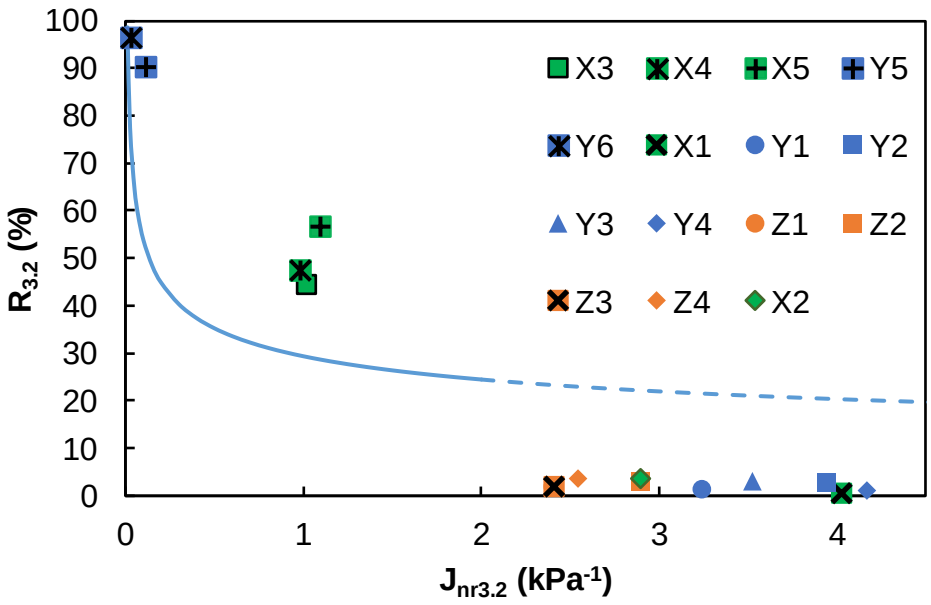

Figure 17. $J_{nr3.2}$ vs. $R_{3.2}$ (%) Relationship for the Study Binders Using the Delineation in AASHTO M 332

It should be noted that the AASHTO M 332 grades were based only on $J_{nr3.2}$. The J_{nrdiff} criterion was not considered as part of the grading considerations because there is currently substantial debate on whether the parameter relates to performance. Many DOTs have seen that even though their polymer-modified binders do not meet the J_{nrdiff} criterion, the performance of their asphalt mixtures has not been

hampered. All the unmodified binders have $J_{nrdiff} \leq 75$ percent, whereas three of the five polymer-modified binders (X3, X4, and X5) have $J_{nrdiff} > 75$ percent (X3 = 409 percent, X4 = 250 percent, and X5 = 344 percent at their M 320 high-temperature grade).

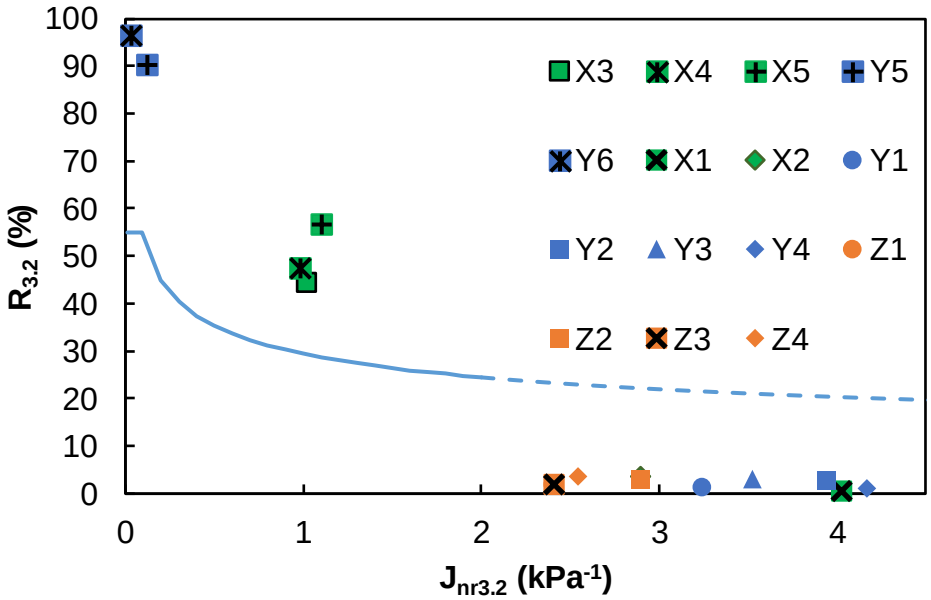

Figure 18. $J_{nr3.2}$ vs. $R_{3.2}$ (%) Relationship for the Study Binders Using the Delineation Suggested by the Asphalt Institute

Elastic Recovery Test

Currently, there are two widely accepted tests to measure the degree of elasticity of binders. The first test is the MSCR test, whose results are presented above, and the second test is the elastic recovery test. The elastic recovery test is included in the test plan for two reasons. The first reason is to verify the similarities/dissimilarities with MSCR percent recovery, and the second is that ADOT over the years has had experience with the elastic recovery test. And the only polymer-modified binder currently specified by ADOT, PG 76-22TR, has an elastic recovery specification associated with it. In the present study, the test was conducted per AASHTO T 301 at 10°C and was performed only on polymer-modified binders. Table 26 presents the elastic recovery results for these binders.

Table 26. Percent Elastic Recovery of the Polymer-Modified Binders Used in the Study

Binder	Elastic Recovery (%) at 10°C
X3	84.00
X4	88.00
X5	83.75
Y5	72.50
Y6	88.00

The comparisons between elastic recovery and MSCR percent recovery were made at two MSCR temperatures, 64°C and 70°C. Figure 19, which charts the results, shows that there is no correlation between the two parameters. There may be two reasons for this finding: (1) the comparison is being made between two parameters which are measured using two very different temperature ranges, and (2) the conditions of the binders are different (i.e., MSCR recovery was measured using RTFO-aged binder, and ER was performed using original binder). While the AASHTO T 350 standard mandates that the testing be conducted on RTFO-aged binder, in the current study MSCR was also conducted on original binders. Figure 20 presents the results of the correlation between MSCR recovery and elastic recovery using original binder. Overall, there is still no correlation, but if the data sets are divided—X3 and X4 into one group and X5, Y5, and Y6 into another group—then there seems to be a good agreement between the MSCR recovery and elastic recovery tests.

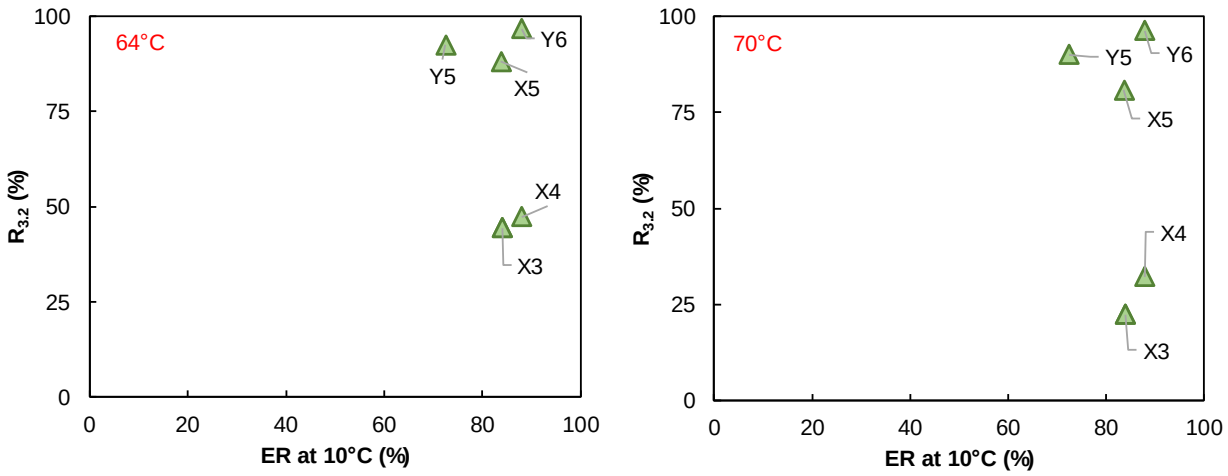

Figure 19. Relationship Between MSCR %$R_{3.2}$ (Using RTFO-Aged Asphalt) and ER at 10°C (Using Original Asphalt)

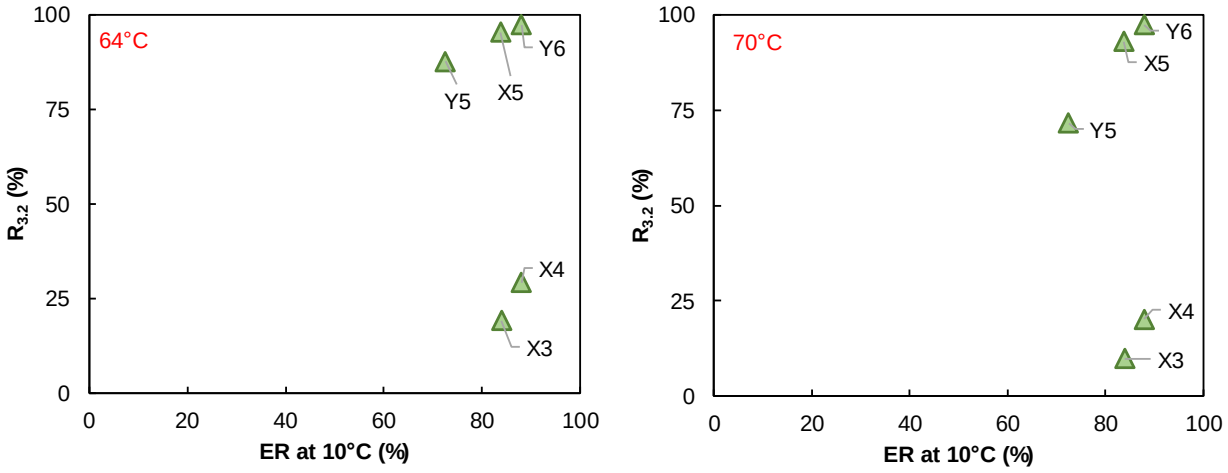

Figure 20. Relationship Between MSCR %$R_{3.2}$ and ER at 10°C Using Original Asphalt

Intermediate-Temperature Properties

The intermediate-temperature properties were measured for the original binder and for the RTFO- and PAV-aged binder. The main objectives of performing intermediate-temperature testing for the latter two cases were to (1) identify how the properties of Arizona binders change with the level of aging, and (2) assess whether any unintended effects on in-service binder oxidation behaviors might result from a change to AASHTO M 332. The testing was performed at three temperatures: the critical temperature, and the critical temperature + 3°C and – 3°C. For the PAV-aging condition, all study binders passed the AASHTO M 320 intermediate temperature criterion of $|G^*|\sin\delta < 5000$ kPa at their current grade temperature. All results are tabulated in test memoranda attached with Appendix D. Figure 21 shows the $|G^*|\sin\delta$ values for the study binders at their critical intermediate temperatures. It can be seen from the figure that the polymer-modified binders in part (d) of the figure have the lowest stiffness value. The $|G^*|\sin\delta$ values presented in Figure 21 are at their respective "S" grade critical intermediate temperatures. However, with the implementation of AASHTO M 332, there is a potential for multigrading of binders. This means that the same binder can be used in multiple climatic locations provided it meets high-, intermediate-, and low-temperature criteria of the PG grading system for that climatic location. For example, a PG 70S-22 binder may also be graded as PG 64H-22 if it meets the J_{nr} and $|G^*|\sin\delta$ criteria at the appropriate temperatures. To accommodate this, the $|G^*|\sin\delta$ limit in AASHTO M 332 has been increased to 6000 kPa for H, V, and E grades. The potential for multigrading with respect to H, V, and E grades was checked for the study binders by performing the intermediate-temperature testing at 3°C lower than the critical intermediate temperature. Figure 22 shows the results. As the figure indicates, even at 3°C lower, only one of the binders, Y4, exceeds 5000 kPa and all of the binders are lower than 6000 kPa, which is the maximum limit under AASHTO M 332.

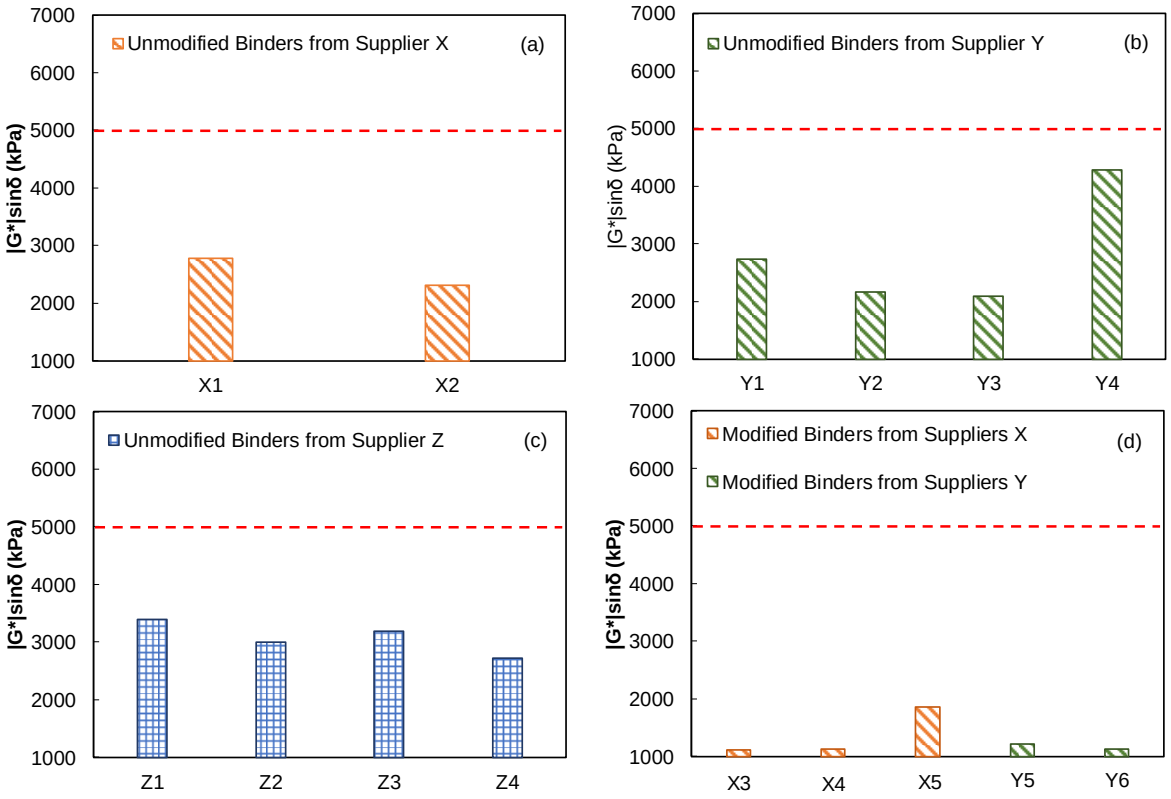

Figure 21. $|G^*|\sin\delta$ Values at the Critical Intermediate Temperature Corresponding to the "S" Grade of Unmodified Binders from (a) Supplier X, (b) Supplier Y, (c) Supplier Z, and (d) Modified Binders from Suppliers X and Y

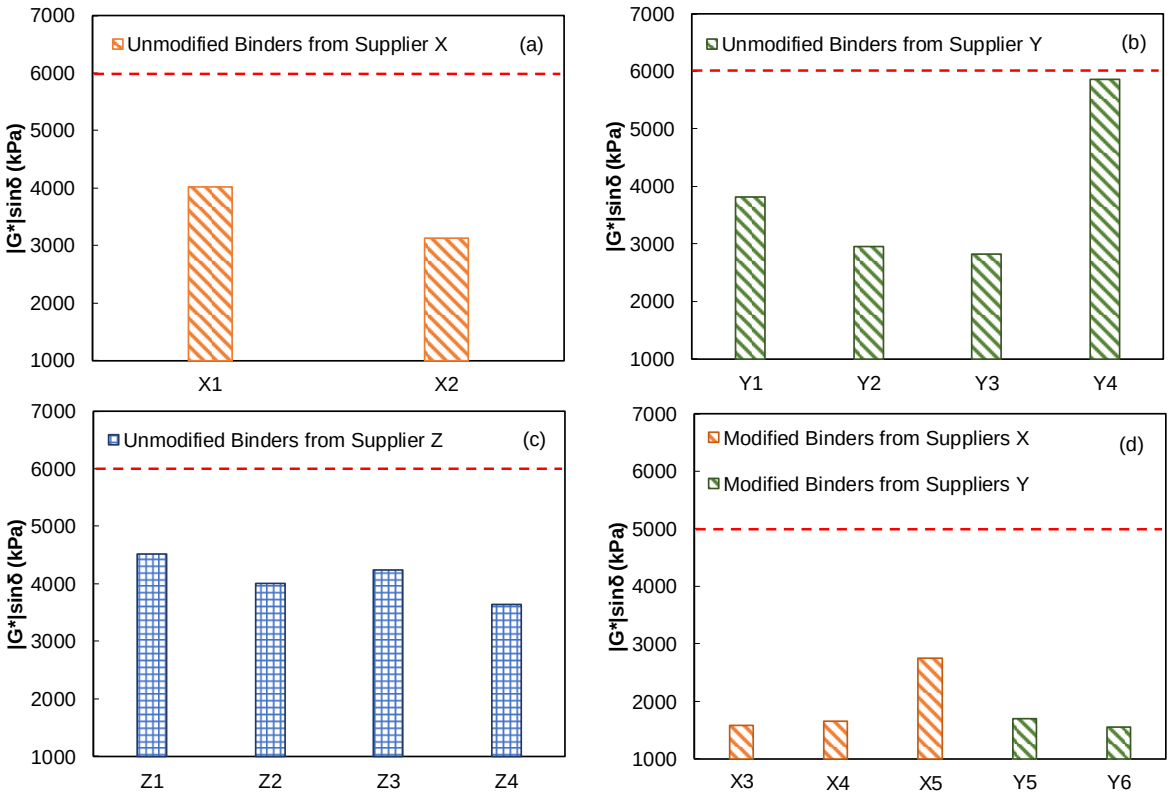

Figure 22. $|G^*|\sin\delta$ Values at 3°C Lower Than Intermediate Temperature Corresponding to the "S" Grade of Unmodified Binders from (a) Supplier X, (b) Supplier Y, (c) Supplier Z, and (d) Modified Binders from Suppliers X and Y

Low-Temperature Properties

The low-temperature properties were measured by testing the PAV-aged binder in the BBR. The test was performed at three temperatures: the critical temperature for that PG grade and the critical temperature + 6°C and – 6°C. All study binders at their current specified PG grade were found to pass the AASHTO M 320 low-temperature grading criteria. The binders X3 and X4 (PG 64H-22 and PG 64V-22, respectively) were too soft to test at – 6°C, and instead were tested only at – 12°C and – 18°C. The creep stiffness, *S*, and slope of the creep stiffness curve, *m,* for the study binders have been tabulated in test memoranda in Appendix D and are shown in Figure 23 at the critical low temperatures.

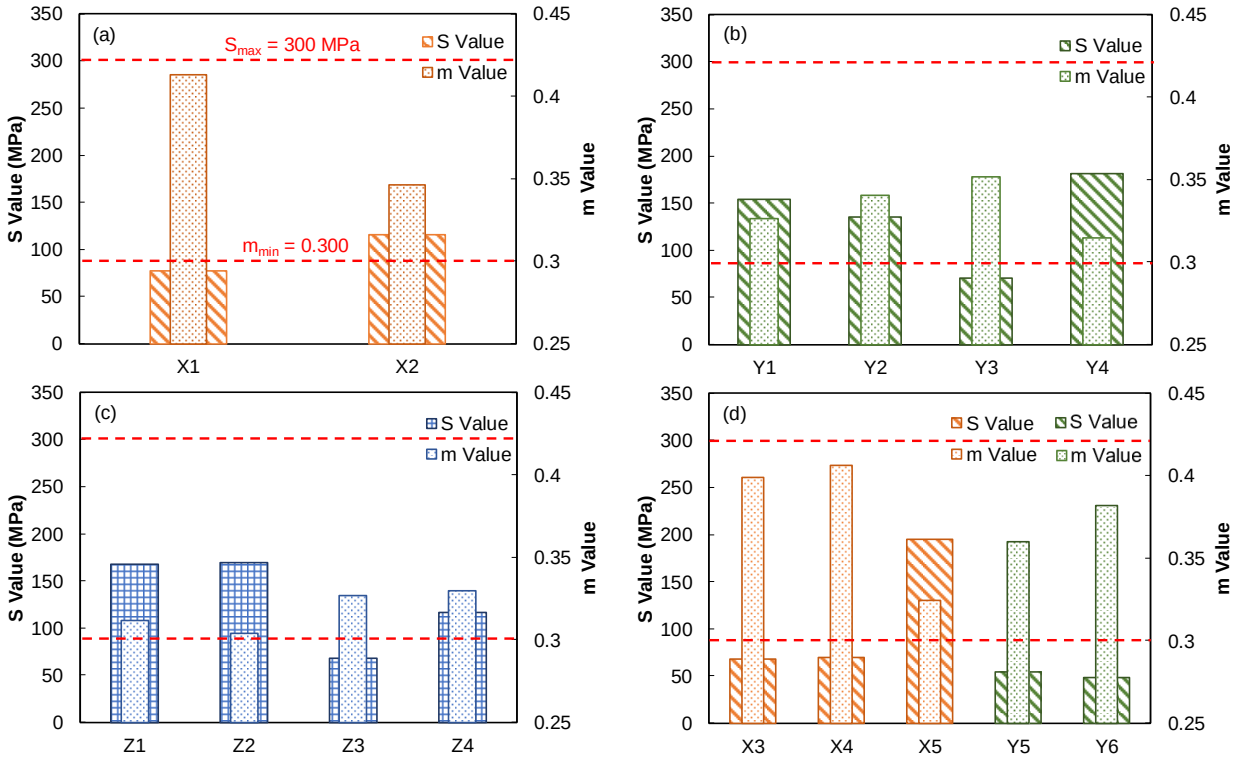

Figure 23. Values for Creep Stiffness, *S*, and slope, *m*, at the Critical Low Temperatures for (1) Unmodified Binders from Suppliers X, Y, and Z, and (2) Modified Binders from Suppliers X and Y

Propensity to Oxidation

An important characteristic of a binder is its resistance to oxidation. The propensity to oxidize is measured by calculating the aging ratio, which is the ratio of aged shear modulus to unaged shear modulus at a fixed temperature and frequency, as shown in Equation 4. This parameter is examined to determine whether there may be some unintended effects on in-service aging performance from transitioning to AASHTO M 332. This potential exists because when grade bumping is carried out, AASHTO M 332 allows a larger difference in stiffness between the original and the RTFO specification limits. The potential for unintended effects, and the resultant impact on aging, if any, are explained in detail in the later sections of this report.

Figure 24 and Figure 25 show the aging ratios for binders Y1 (PG 64-22) and Y6 (PG 70V-16), respectively, at intermediate and high temperatures. It is clearly evident that the aging ratio increases with aging level and varies with temperature. Different binders have different aging behaviors based on their grades and inherent formulations. Aging ratio provides one methodology for gauging these propensities. Table 27 presents the aging ratios for all the study binders at three different temperatures.

$$AR = \left(\frac{|G^*|(\omega_i, T_j)_{after\ aging}}{|G^*|(\omega_i, T_j)_{Original}} \right) \quad \text{(Eq. 4)}$$

Where $|G^*|\ (\omega_i, T_j)_{after\ aging}$ = dynamic shear modulus at frequency ω_i and temperature T_j after aging

$|G^*|\ (\omega_i, T_j)_{Original}$ = dynamic shear modulus at frequency ω_i and temperature T_j before aging

AR = aging ratio

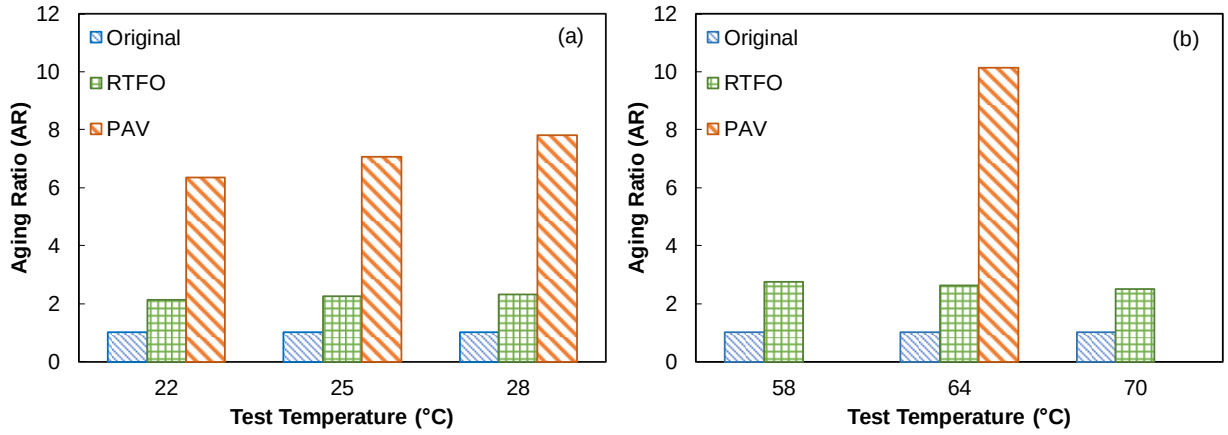

Figure 24. Variation in Aging Ratio for Binder Y1 at (a) Intermediate Temperatures and (b) High Temperatures

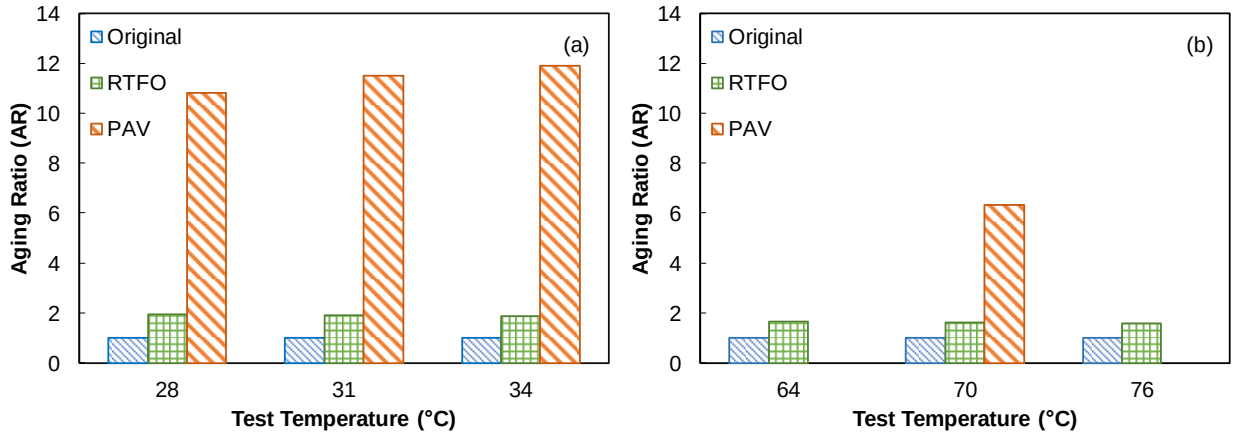

Figure 25. Variation in Aging Ratio for Binder Y6 at (a) Intermediate Temperatures and (b) High Temperatures

Table 27 shows that the *AR* varies with temperature and that, in general, the *AR*s at intermediate temperatures are lower than the *AR*s at high temperatures. However, much more interesting observations can be made by comparing the *AR*s of binders of the same grade. Table 27 tabulates the aging ratios of all the study binders at intermediate and high temperatures. Comparisons can be made between binders Y1 and Z1 for PG 64-22; Y2 and Z2 for PG 70-22; X1 and Z3 for PG 70-10; and Y4, Z4, and X2 for PG 76-16. For PG 64-22, the table shows that binder Y1 has lower *AR*s at all test temperatures. For PG 70-22, binder Y2 has lower *AR*s at all the test temperatures. For PG 70-10, binder X1 has lower *AR*s at all test temperatures. Among the PG 76-16 binders, Y4 and X2 have very similar aging ratios at both intermediate and high temperatures and have lower ratios than those of Z4 binder. The main conclusion to be drawn from this comparison of aging ratios for binders of same grade is that the binders' oxidative properties are source- and formulation-dependent. The differing *AR* values indicate that similar PG grade doesn't necessarily equate to similar oxidative properties.

A secondary objective of performing the *AR*-based analysis was to evaluate the effect of polymer modification on binder oxidation. This was done by comparing binders Y1 and Z1, which are PG 64-22 unmodified binders, with X3 (PG 64H-22) and X4 (PG 64V-22), which are polymer-modified binders. The X3 and X4 data are also shown in Table 27. At intermediate temperatures, the polymer-modified binders have aging ratios that are lower than, though still similar to, those of the neat binders. At 25°C for PAV-aged condition, the maximum difference in *AR* between the two sets of binders is between X4 and Z1, where the difference is 1.66 (a 27 percent difference). At 64°C, there is a greater difference in *AR*—7.26—between the same two binders, with the polymer-modified binders showing lower aging ratios. The percentage difference between the *AR* values at the PAV-aged condition is approximately 150 percent, which shows that the polymer-modified binders have a clearly lower oxidation potential. One other comparison that was possible was between binder Y3, which is unmodified PG 70-16 binder, and binders Y5 (PG 70H-16) and Y6 (PG 70V-16), which are polymer-modified binders. Even in this case, the aging ratios of the unmodified and polymer-modified binders at PAV conditions are very similar at intermediate temperatures, with the latter having a lower aging ratio. However, at higher temperature of 64°C the polymer-modified binders, X3 and X4, have noticeably lower aging ratios than the neat binder, Y1 and Z1 (4.91 on average versus 11.1 at 64°C). The difference at 70°C between the *AR* values for Y3 and Y5 at the PAV-aged condition was 101 percent, and between Y3 and Y6 was 240 percent. The *AR*-based analysis clearly shows that the polymer-modified binders have a lower propensity to aging.

Table 27. Aging Ratios for the Study Binders at Intermediate and High Temperatures

Temperature (°C)	Aging Condition	PG Grade														
		PG 64-22	PG 64-22	PG 70-22	PG 70-22	PG 70-10	PG 70-10	PG 76-16	PG 76-16	PG 76-16	PG 70-16	PG 76-22TR	PG 64V-22	PG 64H-22	PG 70H-16	PG 70V-16
		Y1	Z1	Y2	Z2	X1	Z3	Y4	Z4	X2	Y3	X5	X4	X3	Y5	Y6
Intermediate-Temperature Results																
22	Original	1.00	1.00						1.00	1.00	1.00	1.00	1.00	1.00	1.00	1.00
	RTFO	2.14	2.64										2.07	2.04		
	PAV	6.36	6.83										6.01	6.21		
25	Original	1.00	1.00	1.00	1.00				1.00	1.00	1.00	1.00	1.00	1.00	1.00	1.00
	RTFO	2.25	2.77	1.54	2.30								2.03	2.04		
	PAV	7.06	7.80	5.82	8.44								6.14	6.60		
28	Original	1.00	1.00	1.00	1.00				1.00	1.00	1.00	1.00	1.00	1.00	1.00	1.00
	RTFO	2.32	2.90	1.57	2.37						1.82	1.66	2.02	2.07	1.95	1.92
	PAV	7.81	8.72	6.51	9.63						8.48	5.74	6.28	6.94	9.51	10.82
31	Original			1.00	1.00	1.00	1.00	1.00	1.00	1.00	1.00	1.00	1.00	1.00	1.00	1.00
	RTFO			1.62	2.46	2.24	2.30	1.82	2.26	1.73	1.88	1.65			1.94	1.91
	PAV			7.24	10.91	8.30	9.32	5.76	8.00	6.26	9.64	6.08			10.45	11.50
34	Original					1.00	1.00	1.00	1.00	1.00	1.00	1.00	1.00	1.00	1.00	1.00
	RTFO					2.31	2.41	1.89	2.33	1.77	2.16	1.62			1.92	1.88
	PAV					9.32	10.85	6.61	9.00	6.93	10.79	6.25			11.15	11.90
37	Original							1.00	1.00	1.00	1.00	1.00	1.00	1.00	1.00	1.00
	RTFO							1.95	2.41	1.83						
	PAV							7.51	10.07	7.62						
High-Temperature Results																
58	Original	1.00	1.00					1.00	1.00	1.00	1.00	1.00	1.00	1.00	1.00	1.00
	RTFO	2.76	3.10										1.87	1.86		
	PAV															
64	Original	1.00	1.00	1.00	1.00	1.00	1.00	1.00	1.00	1.00	1.00	1.00	1.00	1.00	1.00	1.00
	RTFO	2.64	2.99	1.90	3.12	2.15	2.95	2.18	3.11	2.27	2.33	1.28	1.85	1.87	1.85	1.63
	PAV	10.13	12.08										4.82	5.00		
70	Original	1.00	1.00	1.00	1.00	1.00	1.00	1.00	1.00	1.00	1.00	1.00	1.00	1.00	1.00	1.00
	RTFO	2.50	2.78	1.93	3.09	2.06	2.83	2.20	3.07	2.31	2.36	1.43	1.81	1.88	1.83	1.61
	PAV			15.36	25.77	10.75	25.75				21.43				10.65	6.31
76	Original			1.00	1.00	1.00	1.00	1.00	1.00	1.00	1.00	1.00	1.00	1.00	1.00	1.00
	RTFO			1.92	3.01	1.96	2.66	2.16	3.11	2.38	2.37	1.33			1.83	1.58
	PAV							15.83	21.87	15.27		3.56				
82	Original							1.00	1.00	1.00	1.00	1.00	1.00	1.00	1.00	1.00
	RTFO							2.10	3.04	2.38		1.22				
	PAV															

Blank cells indicate that experiments were not conducted on the relevant binder at the relevant temperature and so no *AR* is calculated.

The changes in the binders due to oxidation were also gauged based on the chemical formation of oxidation products, which was assessed using Attenuated Total Reflectance Fourier Transform Infrared Spectroscopy (ATR-FT-IR) test. (Chapter 3 and Appendix C explain this test in detail.) Oxidation causes an increase in the number of double bonds between hydrocarbons and oxygen, which can be detected with the ATR-FT-IR test. Figure 26 shows the ATR-FT-IR spectra for the study binder PG 70-10(Z). The two specific functional groups examined in this study are the carbonyl and sulfoxide groups. Studies have shown that the area of the spectra encompassed by these functional groups has a direct correlation with the level of oxidation in the binders (Jemison et al. 1992, Petersen and Glaser 2011). This relationship can be seen in Figure 27, which displays the carbonyl and sulfoxide regions for different aging levels of PG 70-10(Z).

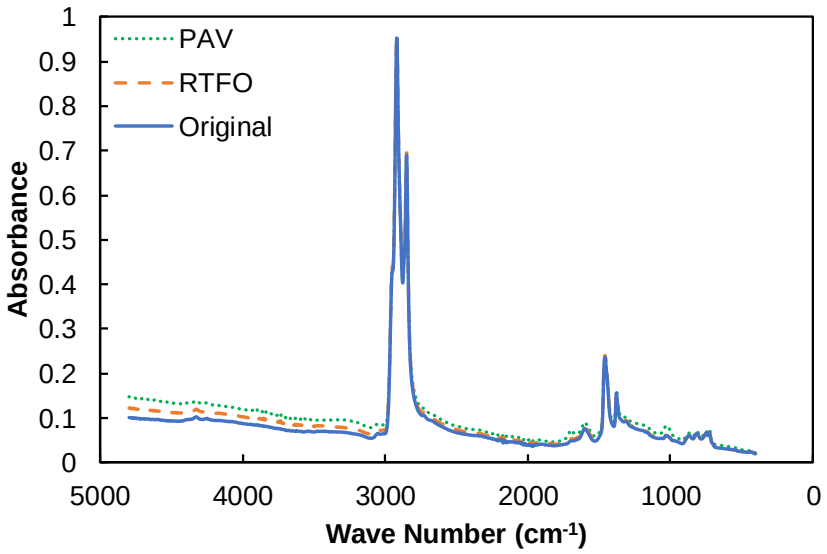

Figure 26. ATR-FT-IR Spectra for Original, RTFO-, and PAV-Aged Conditions for PG 70-10(Z)

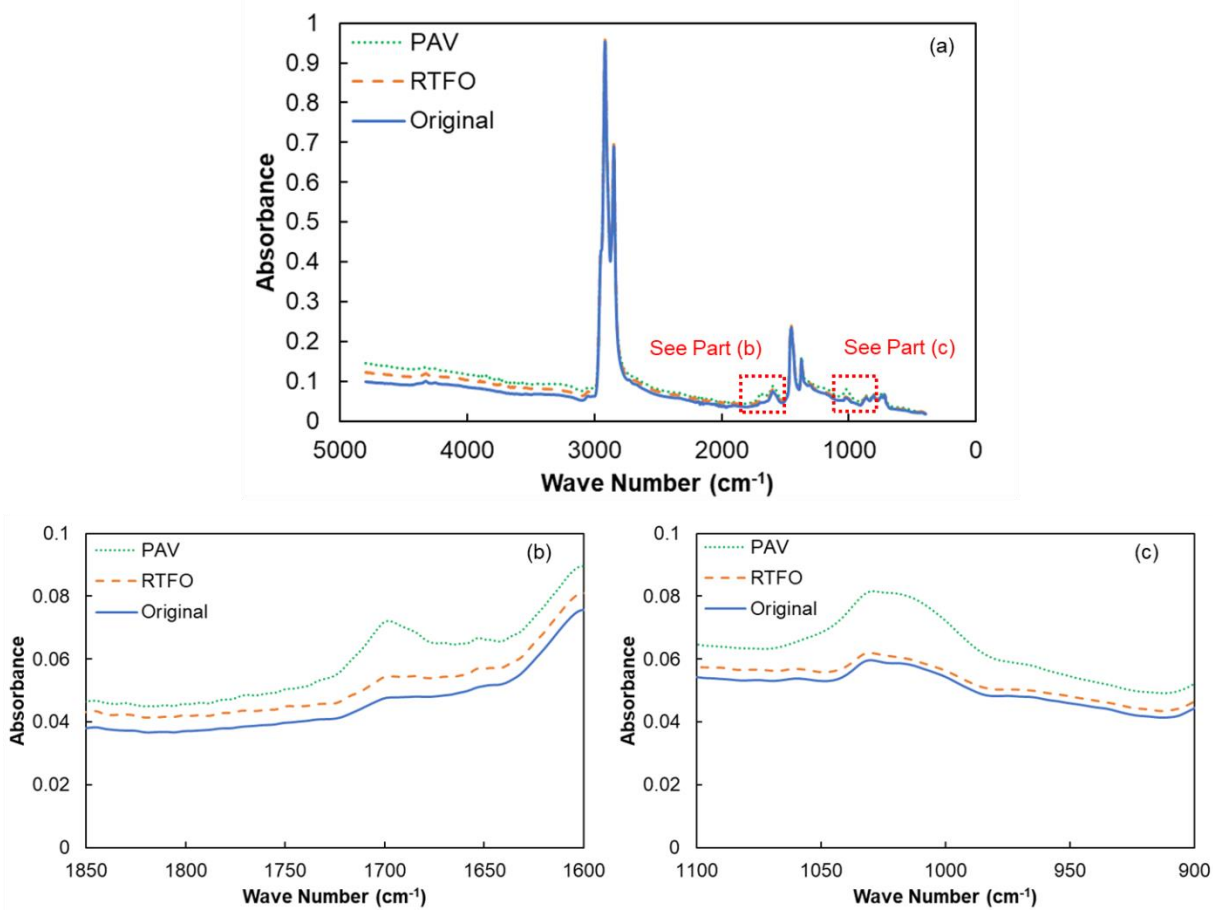

Figure 27. ATR-FT-IR Spectra for PG 70-10(Z) at Original, RTFO, and PAV Aging Levels: (a) Overall Spectra, (b) Carbonyl Region, and (c) Sulfoxide Region

The main objective of the ATR-FT-IR testing was to obtain the chemical signatures of the binders and to confirm the changes in $|G^*|$ and J_{nr} as a result of oxidation. The carbonyl and sulfoxide areas were calculated as described in Appendix C. As can be seen from Figure 28, which shows the sum of carbonyl and sulfoxide areas (*CA*+*SA*) for all the study binders, *CA*+*SA* rises with the increase in aging level. The higher *CA*+*SA* of the polymer-modified binders X3, X4, and X5 can be attributed to increased sulfoxide presence in these binders. Polymer-modified binders when blended are infused with sulfur, which purportedly acts as a cross-linking agent, leading to higher overall *CA*+*SA*. Although *CA*+*SA* provides information regarding the chemical signatures of these binders, what is more important is the relative increase in *CA*+*SA* with aging. The ratio of post-aging *CA*+*SA* to *CA*+*SA* of the original condition, as shown in Equation 5, is used as the parameter for calculating the relative increase. This parameter is termed $AR_{FT\text{-}IR}$. The values of $AR_{FT\text{-}IR}$ for all study binders are summarized in Figure 29. It can be seen from the figure that values of $AR_{FT\text{-}IR}$ increase with aging level. It also can be seen that X3, X4, and X5, which are polymer-modified binders, have the lowest aging ratios among the study binders. This supports the

observations from the rheological testing that also show that polymer-modified binders have lower aging ratios.

$$AR_{FTIR} = \frac{(CA + SA)_{Aged}}{(CA + SA)_{Original}} \qquad \text{(Eq. 5)}$$

Where CA = carbonyl area from ATR-FT-IR spectra
SA = sulfoxide area from ATR-FT-IR spectra
$Aged$ = refers to the summation of CA and SA after aging
$Original$ = refers to the summation of CA and SA before aging
AR_{FTIR} = aging ratio from ATR-FT-IR

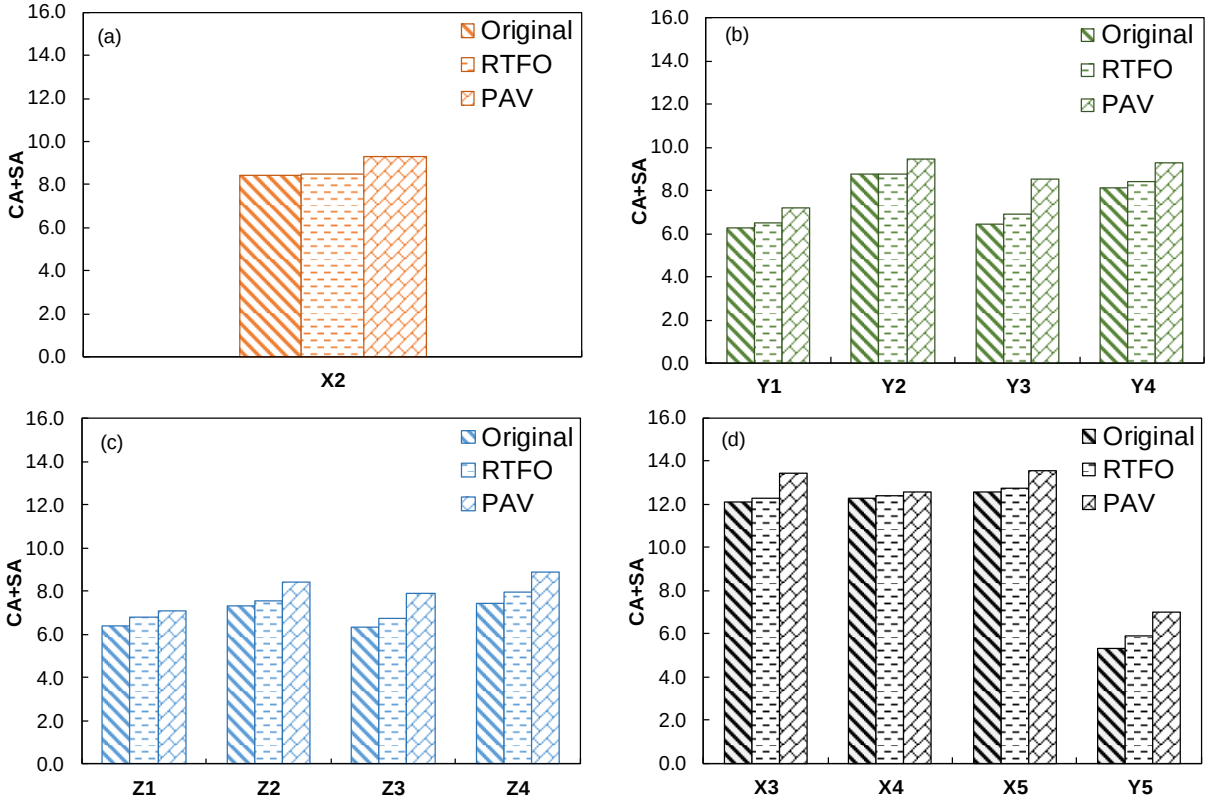

Figure 28. The Sum of Carbonyl and Sulfoxide Areas at Original, RTFO-, and PAV-Aged Condition for Unmodified Binders from (a) Supplier X, (b) Supplier Y, and (c) Supplier Z, and for (d) Modified Binders from Suppliers X and Y

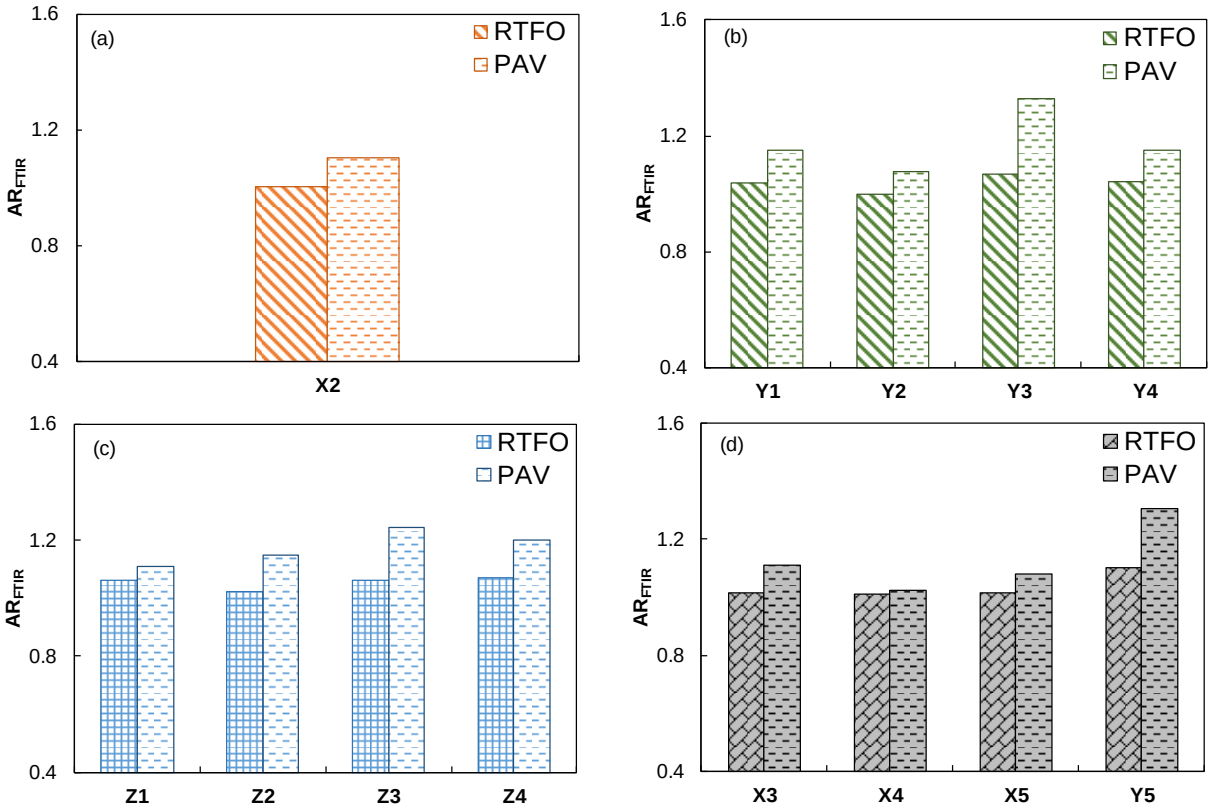

Figure 29. ATR-FT-IR–Based Aging Ratios for Unmodified Asphalt Binders from (a) Supplier X, (b) Supplier Y, and (c) Supplier Z, and for (d) Modified Binders from Suppliers X and Y

Translating AASHTO T 350 Traffic Grades to Equivalent $|G^*|/\sin\delta$ Values

As mentioned previously, one important reason for moving to an AASHTO M 332–based grading parameter is the explicit separation of climate and traffic levels. One of the major findings of the current research relating to this advantage is the existence of a well-defined relationship between the SHRP rutting parameter ($|G^*|/\sin\delta$) and the $J_{nr3.2}$ for unmodified binders. In Figure 30, each binder is shown at three points representing the three temperatures at which the MSCR test was performed (see Chapter 3 for details on these temperatures). Using the relationship from unmodified binders, one can equate the J_{nr} specification limits to equivalent $|G^*|/\sin\delta$ values for the traffic grades S, H, V, and E. The values are tabulated in Table 28. The significance of the findings is that at least for the unmodified binders, additional specification parameter $J_{nr3.2}$ may not be required since the traffic grades can be specified based on $|G^*|/\sin\delta$. However, the same cannot be said about the modified binders, for which this relationship breaks down, as is shown in Figure 31. The binders used in Arizona are predominantly non-polymer-modified; however, ADOT may use more polymer-modified binders in the future. This prospect coupled with the need to have a uniform grading system for both unmodified and polymer-modified binders necessitates the use of $J_{nr3.2}$ as a specification parameter.

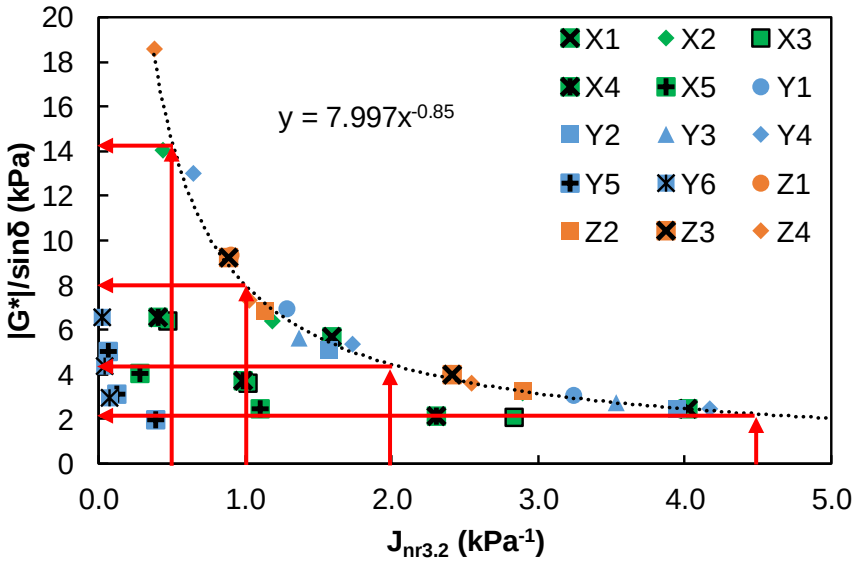

Figure 30. Relationship Between $|G^*|/\sin\delta$ and $J_{nr3.2}$

Table 28. Range of $|G^*|/\sin\delta$ for AASHTO T 350 Traffic Grades for Current Arizona Unmodified Binders

Parameter	Traffic Levels			
	S	H	V	E
$\lvert G^*\rvert/\sin\delta_{RTFO}$ (kPa)	2.2 – 4.4	4.4 – 8.0	8.0 – 14.4	> 14.4

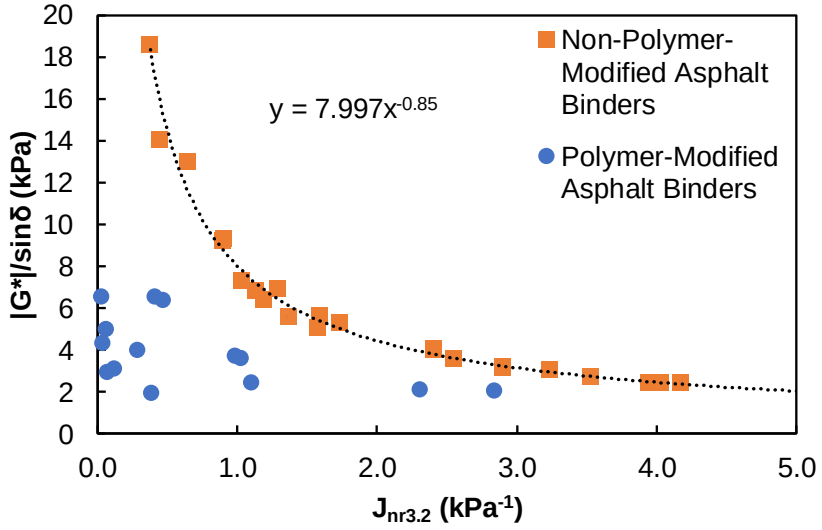

Figure 31. Relationship Between $|G^*|/\sin\delta$ and $J_{nr3.2}$ with Distinction Between Polymer-Modified and Non-Polymer-Modified Asphalt Binders

Finding the Dictating AASHTO M 320 Specification Parameter

To consider the potential implications of a change to AASHTO M 332, it is necessary to know which AASHTO M 320 grading parameters dictated the current grading of the binders (in their current formulations). For this purpose, two terms have been introduced, "critical parameter" and "noncritical parameter." Critical parameters are assumed to be the ones for which the measured property was closest to the specification limit. Noncritical parameters are assumed to be the ones for which the measured property was farthest from the specification limit. Since the limits have different magnitudes and units, the percentage difference from the specification limit was computed. Table 29 shows the results.

Equation 6 shows the equation used to calculate the percentage difference for $|G^*|/\sin\delta$ at the original and RTFO-aged conditions. The specification limit for $|G^*|/\sin\delta$ at the original condition is 1.00 kPa, whereas for the RTFO-aged condition, it is 2.20 kPa. The $|G^*|/\sin\delta$ value for the binder here is at the high temperature corresponding to its current-as-supplied PG grade. Table 29 shows the percentage differences calculated for the study binders.

$$Percentage\ Difference_{|G^*|/\sin\delta} = \frac{|G^*|/\sin\delta_{Binder} - |G^*|/\sin\delta_{Specification\ Limit}}{|G^*|/\sin\delta_{Specification\ Limit}} \times 100 \quad \text{(Eq. 6)}$$

The equation used to calculate the percentage difference for the PAV-aged condition is shown in Equation 7. The specification limit for $|G^*|\sin\delta$ at the PAV-aged condition is 5000 kPa. The $|G^*|\sin\delta$ value for the binder in the equation is at the intermediate temperature corresponding to the binder's current-as-supplied PG grade.

$$Percentage\ Difference_{|G^*|\sin\delta} = \frac{5000 - |G^*|\sin\delta_{Binder}}{5000} \times 100 \quad \text{(Eq. 7)}$$

The equations used to calculate the percentage difference for the creep stiffness (*S*) and *m* values at the PAV-aged condition are shown in Equations 8 and 9, respectively. The specification limit for the *S* value at the PAV-aged condition is 300 MPa, and for the *m* value it is 0.300. The *m* and *S* values in these two equations are at the low temperature corresponding to a binder's current-as-supplied PG grade.

$$Percentage\ Difference_{S\ Value} = \frac{300 - S_{Binder}}{300} \times 100 \quad \text{(Eq. 8)}$$

$$Percentage\ Difference_{m\ Value} = \frac{m_{Binder} - 0.3}{0.3} \times 100 \quad \text{(Eq. 9)}$$

The parameter with the highest difference from the specification limit is termed the noncritical parameter (or parameters, if two have percentage differences that are close), and the one with the lowest difference from the specification limit is termed the most critical parameter (or critical parameters, if two or more are close). Others are not given descriptive names. The cells have been color-coded to indicate the range of percentage difference. For example, in the case of PG 64-22 (Y) in

Table 29, the parameters under consideration are Original $|G^*|/\sin\delta$ and RTFO $|G^*|/\sin\delta$ at 64°C; PAV $|G^*|\sin\delta$ at 25°C; and BBR *S* and *m* values at –12°C. The most critical specification parameter is the BBR *m* value, whose percentage difference is 8.8%; and the noncritical specification parameter is the BBR *S* value, whose percentage difference is 48.7 percent. Overall, for most of the unmodified binders, the *m* value from the BBR test is the most critical parameter, and the *S* value from the BBR test along with the RTFO $|G^*|/\sin\delta$ are the noncritical parameters. Even for the polymer-modified binders, the *m* value from the BBR test is the most critical parameter; however, except in one case, the magnitude of the values is noticeably higher than it is for the unmodified binders. For four of the five modified binders, the noncritical parameter is the original $|G^*|/\sin\delta$. It should be noted that polymer-modified binders do not possess the same ability to roll around the RTFO bottle as freely as neat binders. This might also be one of the reasons why polymer-modified binders at RTFO condition might not age as much as neat binders. Thus, for the polymer-modified binders, the designation of original $|G^*|/\sin\delta$—and not RTFO $|G^*|/\sin\delta$—as the noncritical parameter can be an artifact of the above-mentioned phenomenon.

Table 29. Percentage Difference Between Computed Parameters of the Study Binders and the Limits for Those Parameters Specified by AASHTO M 320

Binder PG Grade (Supplier)		Percentage Difference from the Specification Criteria									
		Notation	$\|G^*\|/\sin\delta$		$\|G^*\|\sin\delta$	BBR *S* value	BBR *m* value	Most Critical Specification Parameter		Noncritical Specification Parameter	
			Orig.	RTFO	PAV	PAV	PAV				
Unmodified	PG 64-22 (Y)	Y1	14.8	38.6	45.2	48.7	8.8	8.8	BBR, *m*	48.7	BBR, *S*
	PG 64-22 (Z)	Z1	35.0	84.8	32.1	44.2	3.8	3.8	BBR, *m*	84.8	RTFO
	PG 70-22 (Y)	Y2	26.3	12.7	56.9	54.8	13.5	12.7	RTFO	56.9	PAV
	PG 70-22 (Z)	Z2	3.0	48.0	40.0	43.5	1.3	1.3	BBR, *m*	48.0	RTFO
	PG 70-10 (X)	X1	20.2	12.8	19.6	74.4	37.7	12.8	RTFO	74.4	BBR, *S*
	PG 70-10 (Z)	Z3	41.1	82.7	36.3	77.3	9.0	9.0	BBR, *m*	82.7	RTFO
	PG 76-16 (Y)	Y4	13.3	11.8	14.3	39.5	4.8	4.8	BBR, *m*	39.5	BBR, *S*
	PG 76-16 (Z)	Z4	13.6	64.3	45.5	61.2	9.8	9.8	BBR, *m*	64.3	RTFO
	PG 76-16 (X)	X2	31.5	45.5	53.8	61.5	15.5	15.5	BBR, *m*	61.5	BBR, *S*
	PG 70-16 (Y)	Y3	14.0	24.5	58.3	76.5	17.2	14.0	Orig.	76.5	BBR, *S*
Modified	PG 76-22TR (X)	X5	94.6	11.7	62.8	35.0	8.2	8.2	BBR, *m*	94.6	Orig.
	PG 64V-22 (X)	X4	96.4	68.6	77.5	76.7	35.3	35.3	BBR, *m*	96.4	Orig.
	PG 64H-22 (X)	X3	85.6	64.3	77.8	77.3	33.0	33.0	BBR, m	85.6	Orig.
	PG 70H-16 (Y)	Y5	62.4	42.3	75.8	82.0	20.0	20.0	BBR, *m*	82.0	BBR, S
	PG 70V-16 (Y)	Y6	162.4	98.2	77.4	83.9	27.3	27.3	BBR, *m*	162.4	Orig.

= 0–10% Difference; = 10.1–20% Difference; = 20.1–30% Difference; = 30.1–40% Difference; = 40.1–50% Difference; = > 50.1% Difference

Some interesting correlations can be made between the aging propensity of the study binders and the noncritical specification parameter. Aging propensity is gauged by the aging ratio, *AR*. It is seen that the

polymer-modified binders with the lowest *AR*s have the noncritical parameter as their original specification, because of their higher original $|G^*|/\sin\delta$. Conversely, the non-polymer-modified binders which have higher *AR*s, which mostly are low-stiffness binders, are controlled by RTFO $|G^*|/\sin\delta$, which is their noncritical parameter. Low-stiffness binders tend to exhibit greater oxidation and thus show a larger difference between original and RTFO $|G^*|/\sin\delta$. This is one possible reason why low-stiffness binders have the RTFO parameter as their noncritical parameter.

Effect of Adoption of AASHTO M 332 on Long-Term Aging

One of the main advantages of the AASHTO M 332 specification is that it enables multigrade binder use provided such use meets all the specification criteria. For example, a PG 64S-22 binder can also be used where a PG 58H-22 binder is needed, provided it passes the intermediate-temperature criterion at the appropriate temperature. However, when this approach is viewed from the perspective of AASHTO M 320 and current practice, a clear and potentially important difference is observed. Currently, ADOT follows a practice of grade bumping in which the high-temperature grade is increased by a single, standard increment above the one actually required. This practice means that when the climate requires a PG 64-10 but traffic is high, ADOT will use a PG 70-10. Under AASHTO M 320, ADOT would specify a PG 64H-10. Based on the findings presented in Table 28, for a binder to be "H" grade or above, the |G*|/sin δ for the RTFO-aged binder (at the given test temperature) should be more than 4.40 kPa. However, irrespective of traffic grade used, the original criteria remain the same (i.e., $|G^*|/\sin\delta$ greater than 1.00 kPa). The issue is illustrated in Table 30 below, which considers a situation where a binder is used in a location where the climate warrants a PG 58-22, but the traffic warrants PG 64-22 (which is the grade called for under the current AASHTO M 320 + grade bump system). The current specification for PG 64-22 binders dictates that at 64°C, $|G^*|/\sin\delta$ for original and RTFO-aged binder should be greater than 1.00 and 2.20 kPa, respectively. If AASHTO M 332 is adopted, then the testing must be conducted at 58°C, and the specification limits for an H-grade binder dictate that $|G^*|/\sin\delta$ for RTFO-aged binder should be greater than 4.4 kPa (Table 28) and $|G^*|/\sin\delta$ for original binder should be greater than 1 kPa. An investigation of the PG 64-22 binders from suppliers Y and Z that were tested at 58°C showed that these limits currently were easily met (2.5 and 3 kPa for original binder, and 6.9 and 9.3 kPa for RTFO-aged binder, respectively). However, it should be recalled that the suppliers formulate the binders to meet the specification at 64°C, and whatever values are achieved at 58°C are a consequence of those formulations. So now, if the specification is to be met at 58°C, there may be changes in the formulations, especially when the stiffness of the original binder need not be as high as 2.5 or 3 kPa since the limit is just greater than 1 kPa. This can lead to binders which are softer than those currently produced. However, a greater concern is that AASHTO M 332 allows a greater difference between original and RTFO specification limits than the AASHTO M 320 + grade bump system. The consequences of this change, especially if the change has any bearing on long-term aging, are unknown. So the question to be answered is, If a binder specification allows for greater difference between original and RTFO specification limits, what is the effect on the kinetics of aging/long-term aging?

Table 30. Limits for Original and RTFO $|G^*|/\sin\delta$ Values for PG 64-22 Binders Based on Current AASHTO M 320 and Future AASHTO M 332

Condition	Current (PG 64-22)	Future (58H-22)
	M 320 + Grade Bump	M 332
Original $|G^*|/\sin\delta$ (kPa)	At 64°C > 1.00; At 58°C > 2.00	At 58°C > 1.00
RTFO $|G^*|/\sin\delta$ (kPa)	At 64°C > 2.20; At 58°C > 4.40	At 58°C > 4.40

This question is answered with the help of three sets of analyses. Analysis 1, shown in Figure 32, shows the relationship between the increase in $|G^*|$ when going from original to RTFO condition and the increase which occurs when going from RTFO to PAV condition. The data shown in this figure are for all PG 70 binders tested at 70°C. If the resultant relationship is positive, then it can be concluded that oxidation occurring between original and RTFO condition directly correlates with the aging that will occur from RTFO to PAV aging condition. Allowing for a greater difference between original and RTFO specification limits will result in binders which will be more prone to long-term aging. Figure 32 shows that there exists a generally positive correlation between the level of stiffening from original to RTFO and the level of stiffening from RTFO to PAV. This general correlation suggests that binders with a larger difference between original and RTFO conditions may also have a larger increase in modulus between RTFO and PAV conditions. However, the relationship is weak, as indicated by an R^2 value of 0.57. If only the non-polymer-modified binders are considered, then the relationship is weakened even further, as indicated by an R^2 value of 0.27.

The second analysis, presented in Figure 33, shows the increase in dynamic viscosity, μ, of SHRP binders with aging time (Branthaver et al. 1993). Long-term (i.e., PAV) aging ratios were extracted from the data for the SHRP binders and were used to construct a plot like the one constructed for the study binders in Figure 32. For the SHRP binders, two long-term aging times, 48 hours and 144 hours, were used. The resultant plots are shown in Figure 34(a) and (b), where the x-axis shows the ratio of μ for the TFO and tank condition and the y-axis shows the ratio of μ from the TFO condition and different PAV aging durations . It is clear from the plots that no correlation exists, at either 48 hours or 144 hours, between the magnitudes of aging for tank to thin film oven aged (TFO) and the magnitudes for TFO to PAV. The correlation as gauged by the R^2 value shown in Figure 34 is close to zero for both 48 and 144 hours, which means there is no correlation. This finding suggests that the aging that occurs from original to RTFO state does not necessarily affect the aging that occurs from RTFO to PAV aging condition. However, some caution should be used in directly applying these findings to current binders, since the experiments were performed on binders that were common in the late 1980s and early 1990s.

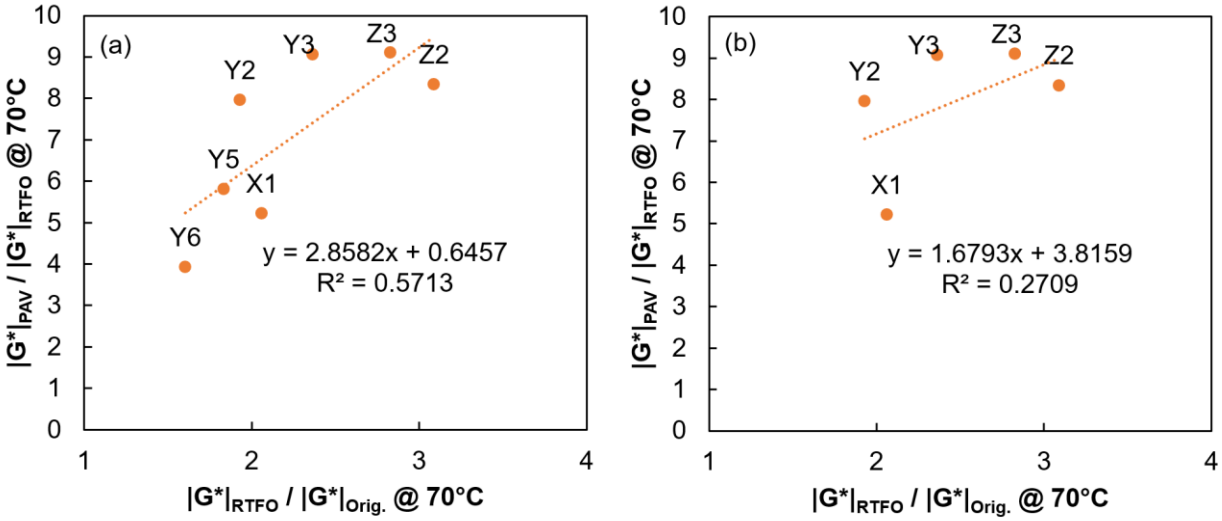

Figure 32. Relationship Between Aging Ratios at RTFO and PAV Conditions for (a) All PG 70 Binders Used in the Study, and (b) All Non-Polymer-Modified PG 70 Binders Used in the Study

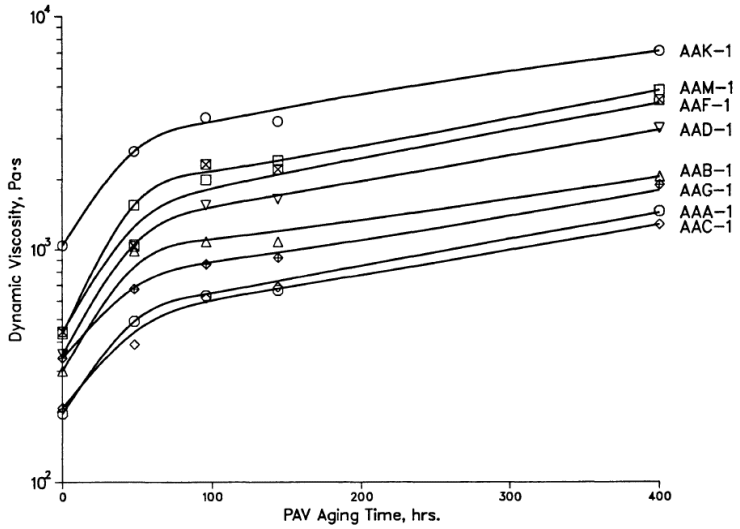

Figure 33. Variation of Dynamic Viscosity with Aging Times Depicted in SHRP-A-368 (Branthaver et al. 1993)

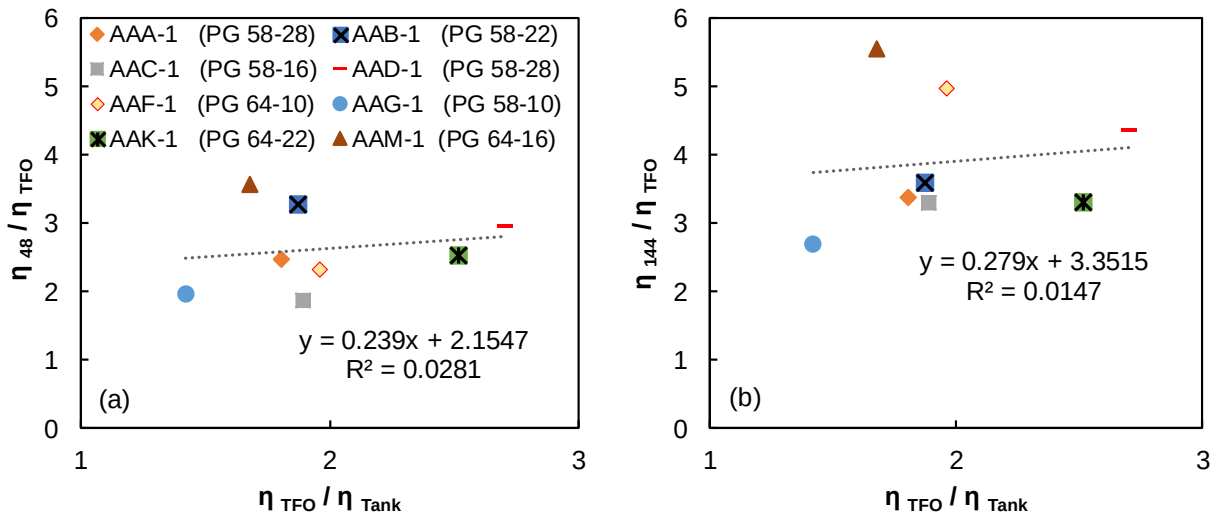

Figure 34. Relationship Between Aging Ratios at TFO and PAV Conditions for Two Long-Term Aging Times: (a) 48 hours and (b) 144 hours (Branthaver et al. 1993)

The third analysis is based on the work of Jin et al. (2011), who developed a fast-rate/constant-rate kinetics model for oxidation in binders. Researchers have found that oxidation in binders occurs in two distinct phases: a so-called fast-rate oxidation reaction that occurs relatively early in the life of the binder (at approximately years 1 to 2), and a so-called slow-rate oxidation reaction that occurs over a longer time span. The mathematical model articulated around this concept by Jin et al. (2011) is shown in Equations 10–12.

$$CA = CA_{tank} + M(1 - e^{-k_f t}) + k_c t \quad \text{(Eq. 10)}$$

$$k_f = A_f e^{\frac{-E_{af}}{RT}} \quad \text{(Eq. 11)}$$

$$k_c = A_c e^{\frac{-E_{ac}}{RT}} \quad \text{(Eq. 12)}$$

Where CA = Total carbonyl area growth after time "t" days
CA_{tank} = Carbonyl area of unaged tank binder
M = CA_0 - CA_{tank} (CA_0 is the intercept of constant rate line)
k_f = Fast-rate reaction constant, Eq. 11
k_c = Constant-rate reaction constant, Eq. 12
A_f = Fast-reaction frequency factor
A_c = Constant-reaction frequency factor
E_{af} = Activation energy for fast-rate reaction
E_{ac} = Activation energy for constant-rate reaction

To allow for comparisons similar to those in analyses 1 and 2, it was required to find the carbonyl area at the end of the fast-rate reaction period and the carbonyl area at the end of constant-rate reaction period. The data from Jin et al. (2011) were used for that analysis. It should be recalled that carbonyl area as calculated from the ATR-FT-IR test (see Chapter 3) has a direct correlation with the level of oxidation in the binder:

- Carbonyl area of unaged binder in tank (A) = CA_{tank}
- Carbonyl area at the end of the fast-rate reaction period (B) = $CA_{tank} + M(1 - e^{-k_f t})$
- Carbonyl area at the end of the constant-rate reaction period (C) = $CA_{tank} + M(1 - e^{-k_f t}) + k_c t$

Under the hypothesis presented in analyses 1 and 2, if there does not exist a positive relationship between the carbonyl at the end of the fast-rate reaction period and the carbonyl of the unaged binder (growth factor B/A), and between the carbonyl at the end of the constant-rate reaction period and the carbonyl at the end of the fast-rate oxidation period (growth factor C/B), then the aging that occurs from original to RTFO state does not necessarily affect the aging that occurs from RTFO to PAV state. The relationships are plotted below in Figure 35 for time values of 2, 20, 45, and 90 days of oxidation. The plots show that as the B/A value increases, the C/B value actually decreases. This can be interpreted as follows: If a binder has higher carbonyl growth after short-term aging (i.e., after the fast-reaction period), then after this period, the rate of carbonyl growth will slow. This finding is worth noting in that it suggests that a stiffer binder at short-term aging condition might actually be beneficial, since it would be less susceptible to long-term aging.

The objective of the three analyses presented above was to investigate whether a larger difference between binder stiffness at original condition and binder stiffness at RTFO condition will have any bearing on long-term aging. The first analysis, which was based on the data produced through the current study, suggests (albeit with a weak correlation) that increased aging at the RTFO condition may result in greater long-term oxidation of the binder. The second analysis, carried out using the SHRP-A-368 data, suggests that aging occurring in the RTFO condition has no bearing on long-term aging as evidenced by an R^2 value of near 0. However, the third analysis, which was based on the data presented in Jin et al. (2011), suggests that increased aging at the RTFO condition, as gauged by increased carbonyl area, might be beneficial. This last suggestion is based on the fact that the increase in carbonyl area at long-term aging condition slows down as the increase in carbonyl area at RTFO condition speeds up. It should be noted that the third analysis was a kinetics-based approach, whereas the other two analyses were modulus- and dynamic-viscosity-based, respectively. The other—and probably the most striking—difference between the three analyses is that the long-term aging procedures are different. For the data generated from the current project, the standard PAV aging protocol, AASHTO R 28, was employed in accordance with ADOT's practice. The binders in the SHRP project were aged in a PAV at 2.07 MPa at 60°C for 48 and 144 hours. (Also, binders in the SHRP project were those in use before the PG grading system was adopted, so caution should be exercised when drawing conclusions from those data, since binder formulations have changed since the adoption of the PG system.) For the third analysis, the binders were aged in a pressurized oxygen vessel, at a film thickness of 0.8 mm at 373 K, which is 100°C.

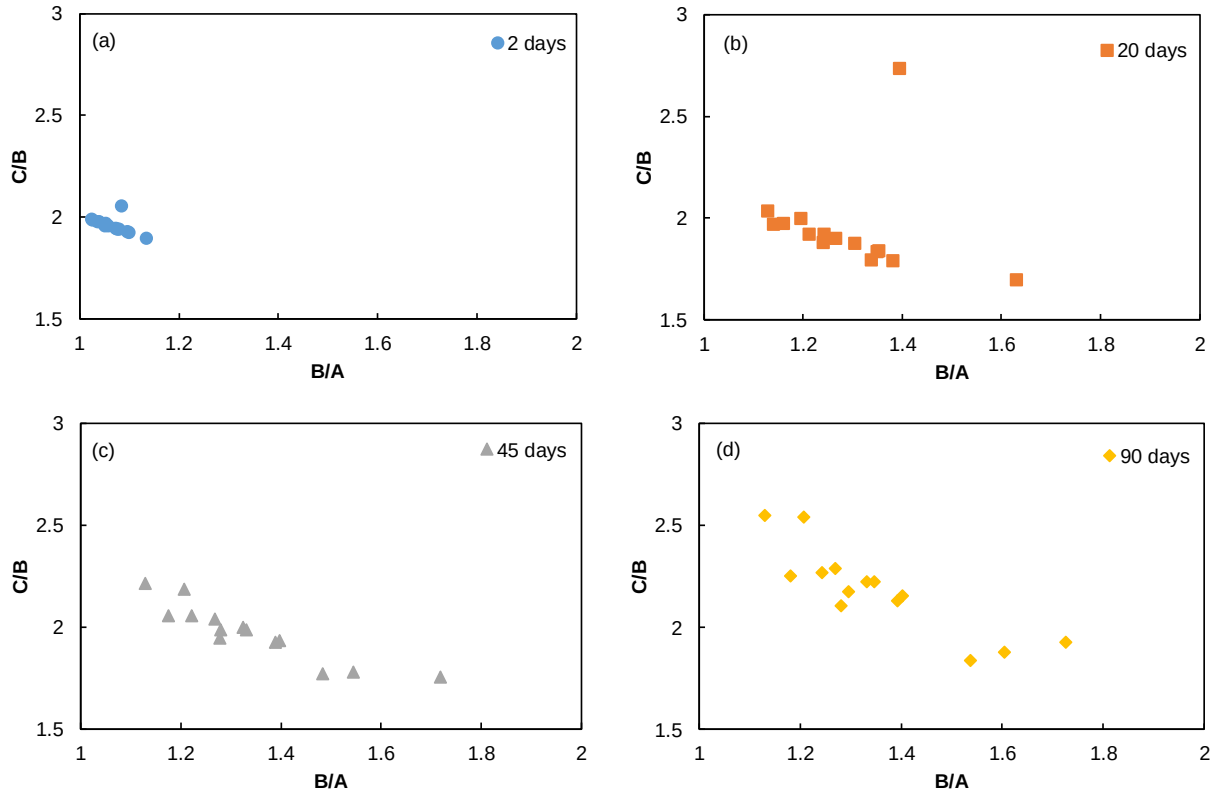

Figure 35. Relationship Between Carbonyl Area Growth Factors B/A and C/B for Four Aging Times: (a) 2 days; (b) 20 days; (c) 45 days; and (d) 90 days

While there is a potential for impacts in locations that are currently selecting the binder grade after empirically adjusting for traffic, overall, the data generated in this study and available through studies elsewhere are inconclusive. However, since many of these binders are currently controlled by the BBR test parameter, the impacts are expected to be minimal.

SUMMARY

This chapter has presented results and analyses pertaining to the binder testing phase of the project. Rheological experiments were performed at high and intermediate temperatures on the study binders at original, RTFO-aged, and PAV-aged conditions. The low-temperature characteristics were measured using the bending beam rheometer. Based on the results from the those experiments, traffic grades based on AASHTO M 332 were assigned to each binder. These grades were based on their $J_{nr3.2}$ value as obtained from the AASHTO T 350 MSCR test. The chemical signature of the binders was obtained using ATR-FT-IR, and carbonyl and sulfoxide areas were used to determine the extent of aging in each binder. Using the data generated, the researchers sought to investigate the impact of adoption of AASHTO M 332 on long-term aging. The data suggest that based on the current binder formulations, adoption of AASHTO M 332 could potentially lead to increased aging potential above current levels for locations that

are adjusting the PG grades for traffic considerations. The precise level of impact may be small and cannot be quantified in the current study. This chapter has also presented an analysis to determine the parameters which are critical/noncritical under the current AASHTO M 320 specification. For most of the binders, the *m* value as obtained from the BBR test was the critical parameter. For the majority of the low-stiffness binders, the RTFO specification parameter was the noncritical parameter. For polymer-modified binders, the original specification parameter was the noncritical parameter.

CHAPTER 5. PERFORMANCE EVALUATION OF ARIZONA ASPHALT MIXTURES

INTRODUCTION

This chapter discusses performance-related aspects of asphalt mixtures used in the study. Performance measures include dynamic modulus for stiffness evaluation, and resistance to fatigue cracking and rutting. While this chapter provides a brief description of the tests conducted, Chapter 3 and Appendix C covers them in detail. The main goal of the performance testing was to see if there is a relationship between binder rutting parameters and asphalt mixture rutting. A secondary goal was to evaluate whether mixture formulation may have impacts on dynamic modulus and fatigue.

Of the 15 binders in the study, 12 were selected for performance testing. The selected binders were used to prepare asphalt mixture samples for gyratory compaction; those samples were subsequently cored and cut to prepare specimens for the performance testing. Of the 12 mixtures on which testing was performed, eight were binders currently used by ADOT. The remaining four binders were polymer-modified binders not currently included in ADOT specifications. As discussed in Chapter 3, three performance tests were conducted: the dynamic modulus test to measure stiffness; the Hamburg Wheel Tracking Test (HWTT) to measure rutting resistance; and the axial fatigue test to measure fatigue resistance. The conditions under which tests were performed are also described in Chapter 3.

MATERIALS

Binders

Twelve binders (five polymer-modified and seven non-polymer-modified) were selected for asphalt mixture testing. The seven unmodified binders were selected based on three criteria: (a) that there be a maximum spread of grades; (b) that at least three of the binders be of grades PG 70T-16 or PG 64T-22 (T denotes a traffic grade, such as H); and (c) that all three suppliers be represented. This ensured that all PG grades procured for the study were represented in the mixture testing. Table 31 lists the binders selected for mixture testing.

Table 31. Group 1 (Unmodified) and Group 2 (Polymer-Modified) Asphalt Binders Selected for Asphalt Mixture Testing

Group	Supplier	Notation	Grade	Group	Supplier	Notation	Grade
1	X	X1	PG 70-10	2	X	X3	PG 64H-22
	Y	Y1	PG 64-22			X4	PG 64V-22
		Y3	PG 70-16			X5	PG 76-22TR+
		Y4	PG 76-16		Y	Y5	PG 70H-16
	Z	Z1	PG 64-22			Y6	PG 70V-16
		Z2	PG 70-22				
		Z4	PG 76-16				

Mixtures

The asphalt mixtures were prepared using aggregates from three locations in Arizona: Snowflake, Globe, and Tucson. (In the tables and figures below, the asphalt mixtures corresponding to these locations are denoted by an "S," "G," or "T" preceding the binder notation.) The selection of binders for an aggregate location was based on the typical PG grade that would be used in that location. Figure 36 shows the binders used for the aggregates procured from the three locations. The properties of the aggregates and the gradations of the individual stockpiles were detailed in Chapter 3. The gradation of the final blends from the three locations—along with other mix design details such as binder content, VFA, and VMA—were also provided in Chapter 3.

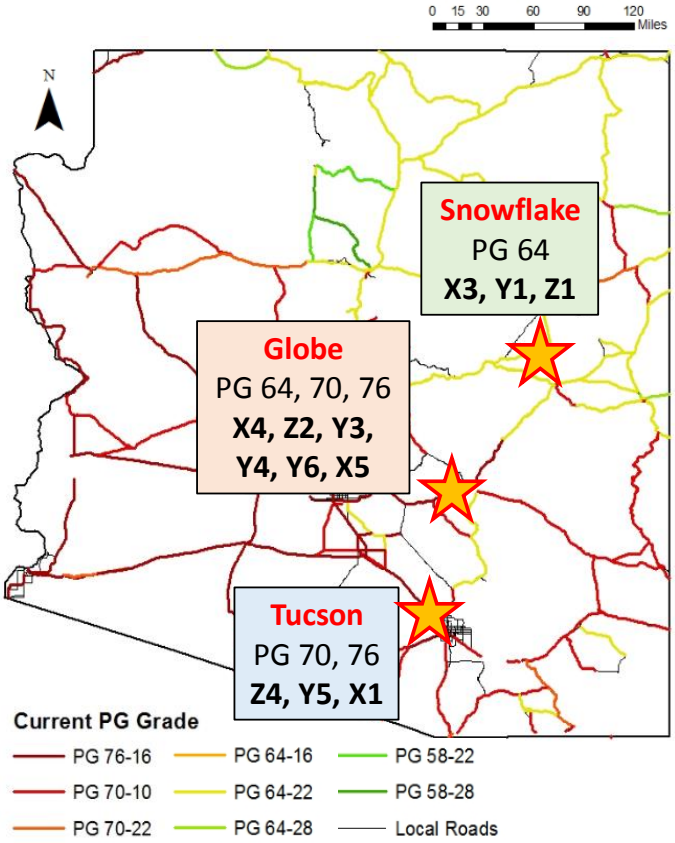

Figure 36. Asphalt Binders Used for Each Aggregate Location

RESULTS AND ANALYSIS

Dynamic Modulus Test

The dynamic modulus test is performed to measure asphalt mixture stiffness at a range of temperatures and loading frequencies. Appendix E shows the test results for all 12 mixtures, but the results are best displayed using master curves as shown in Figure 37. (Detailed master curves with the individual data

points at multiple temperatures and frequencies are also presented in Appendix E.) As Figure 37 shows, GY4 has the highest modulus, followed by TX1, and GX5. For ease of observation, the results in Figure 37 have been separated by aggregate type and are shown in Figures 38 to 40. The Figure 38 grouping consists of three mixtures prepared with aggregates procured from Snowflake, binder X3 (a polymer-modified binder) and binders Y1 and Z1 (unmodified binders). As the figure shows, the polymer-modified mixture has a lower modulus than do SY1 and SZ1 (the unmodified mixtures), which have similar moduli.

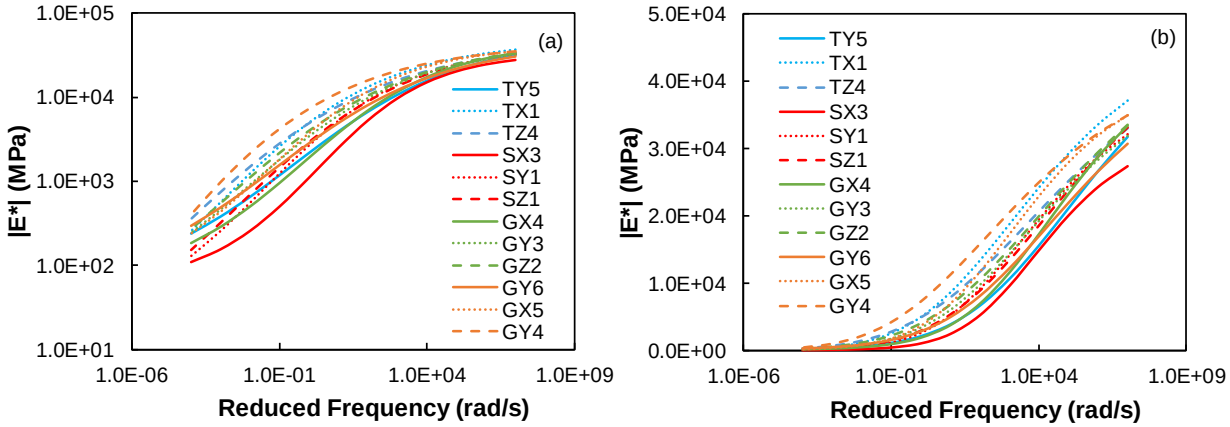

Figure 37. Dynamic Modulus Results for All Asphalt Mixtures in (a) Log-Log Space and (b) Semilog Space

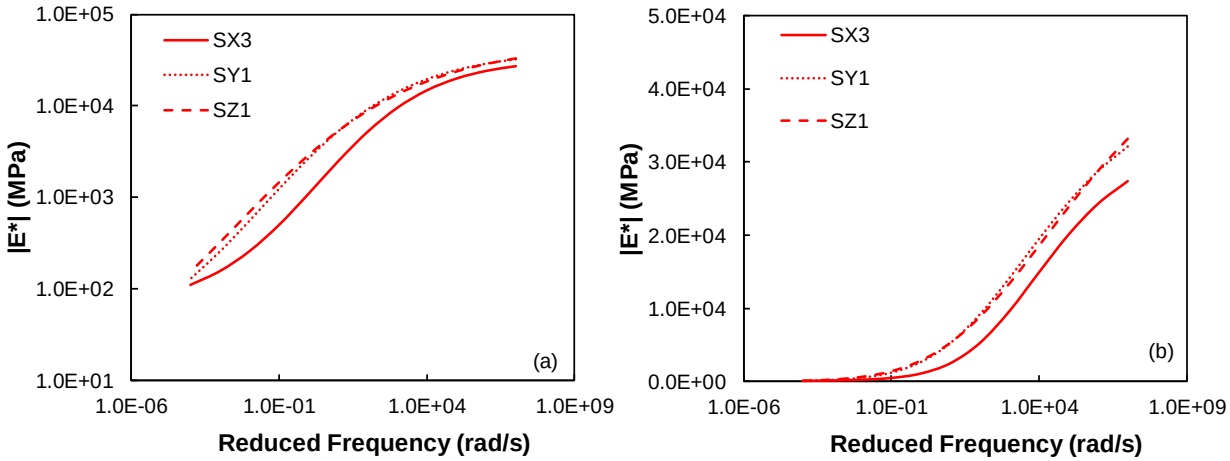

Figure 38. Dynamic Modulus Results for Asphalt Mixtures Prepared with Aggregate Procured from Snowflake in (a) Log-Log Space and (b) Semi-log Space

The second group (Figure 39) consists of mixtures prepared with aggregate procured from Tucson, binder Y5 (a polymer-modified binder) and binders X1 and Z4 (unmodified binders). Again, for this group, the polymer-modified mixture TY5 has a lower modulus than the other two mixtures. TX1 has the highest modulus at lower temperatures, but at higher temperatures TZ4 (using PG 76-16) has a higher modulus.

The final group consists of mixtures prepared with aggregate from Globe (Figure 40). This group includes a total of six mixtures, three polymer-modified (X4, X5, and Y6) and three non-polymer-modified (Y3, Y4, and Z2). The mixture GY4 (using PG 76-16) has the highest modulus. The mixture GX5 (using PG 76-22TR+) ranks second at low and intermediate temperatures; however, at high temperatures the modulus is lower than other non-polymer-modified mixtures (GZ2 and GY3). The remaining two polymer-modified mixtures rank lowest in modulus, with the GX4 mixture having the least modulus. Overall, the mixture modulus results rank and go hand-in-hand with the binder modulus results. That is, polymer-modified mixtures predominantly have lower moduli than do non-polymer-modified mixtures.

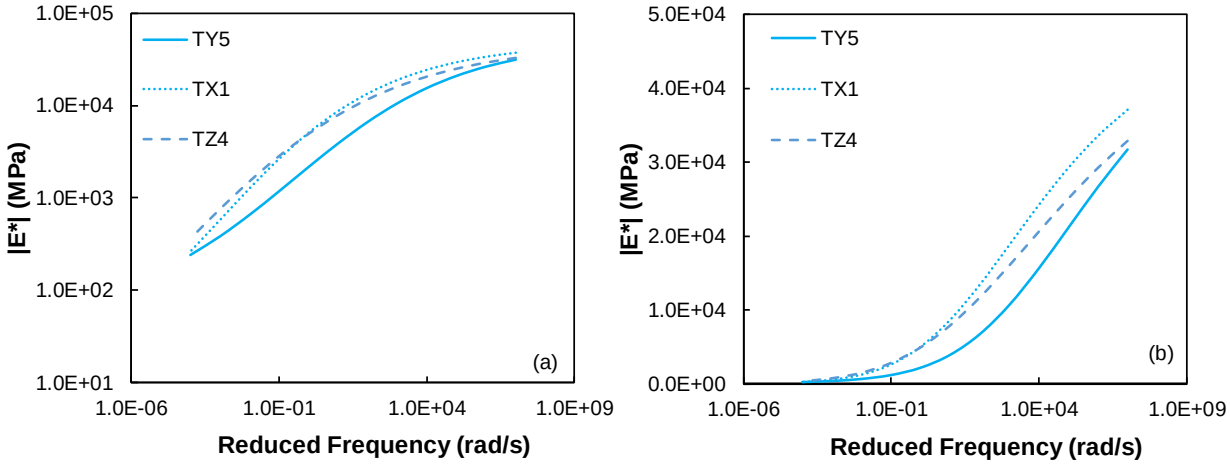

Figure 39. Dynamic Modulus Results for Asphalt Mixtures Prepared with Aggregate Procured from Tucson in (a) Log-Log Space and (b) Semi-log Space

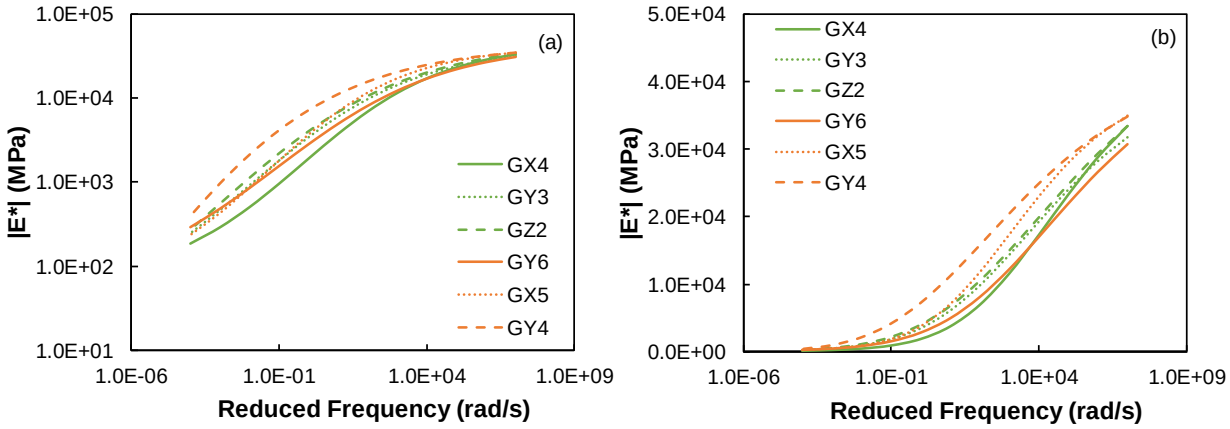

Figure 40. Dynamic Modulus Results for Asphalt Mixtures Prepared with Aggregate Procured from Globe in (a) Log-Log Space and (b) Semi-log Space

Hamburg Wheel Tracking Test

The HWTT evaluates the rutting and moisture susceptibility of asphalt mixtures. The sample preparation methods for the HWTT were carried out in accordance with AASHTO T 324. Each asphalt mixture was tested at two temperatures, based on its PG S-grade. These temperatures were compared to the effective temperatures proposed as part of the NCHRP 9-22 study by El-Basyouny and Jeong (2009). The effective temperatures for various cities in Arizona were calculated using the equation proposed by El-Basyouny and Jeong (2009) and shown in Equation 13.

$$T_{eff} = 14.62 - 3.361\ln(freq) - 10.94(z) + 1.121(MAAT) + 1.718(\sigma_{MAAT}) - 0.431(wind) + 0.333(sunshine) + 0.08(rain) \quad \text{(Eq. 13)}$$

Where $freq$ = loading frequency (Hz)
z = depth (inches)
$MAAT$ = Mean Annual Air Temperature (°F)
σ_{MAAT} = standard deviation of MAAT
$wind$ = annual average wind speed (mph)
$sunshine$ = annual average percent sunshine (%)
$rain$ = annual average depth of rain (inches)

All variable values were obtained from the AASHTOWare climatic database. A frequency of 10 Hz was used for the calculation of effective temperatures. Based on the calculations performed, this frequency was seen to correspond to a vehicle traveling at a speed of 50 mph and having a 14-inch tire radius.

The effective temperatures calculated for 14 cities in Arizona are shown in Table 32 and graphically represented on a map in Figure 41. Also presented in the table are the representative HWTT

temperatures from those evaluated in this study that most closely correspond to the T_{eff} value. For example, if the T_{eff} value is between 38° and 44°C, then 44°C is chosen as the corresponding temperature at which to run the HWTT. Similarly, if the T_{eff} values are between 44° and 50°C, between 50° and 56°C, and between 56° and 62°C, then the corresponding HWTT temperatures are 50°C, 56°C, and 62°C, respectively.

Table 32. Effective Temperature and Prospective HWTT Temperature

Location	PG Grade	T_{eff} (°C)	T_{eff}-Based HWTT Temp. (°C)
Flagstaff	PG 58/64	41.4	44
Grand Canyon	PG 58	43.0	44
Window Rock	PG 58	44.7	50
Prescott	PG 64/70	47.5	50
St. Johns	PG 64	48.3	50
Winslow	PG 70	49.5	50
Page	PG 64	51.8	56
Nogales	PG 70	52.5	56
Bisbee	PG 70	52.9	56
Kingman	PG 70	53.3	56
Tucson	PG 70/76	55.8	56
Safford	PG 70	56.7	62
Phoenix	PG 76	59.3	62
Scottsdale	PG 76	60.0	62

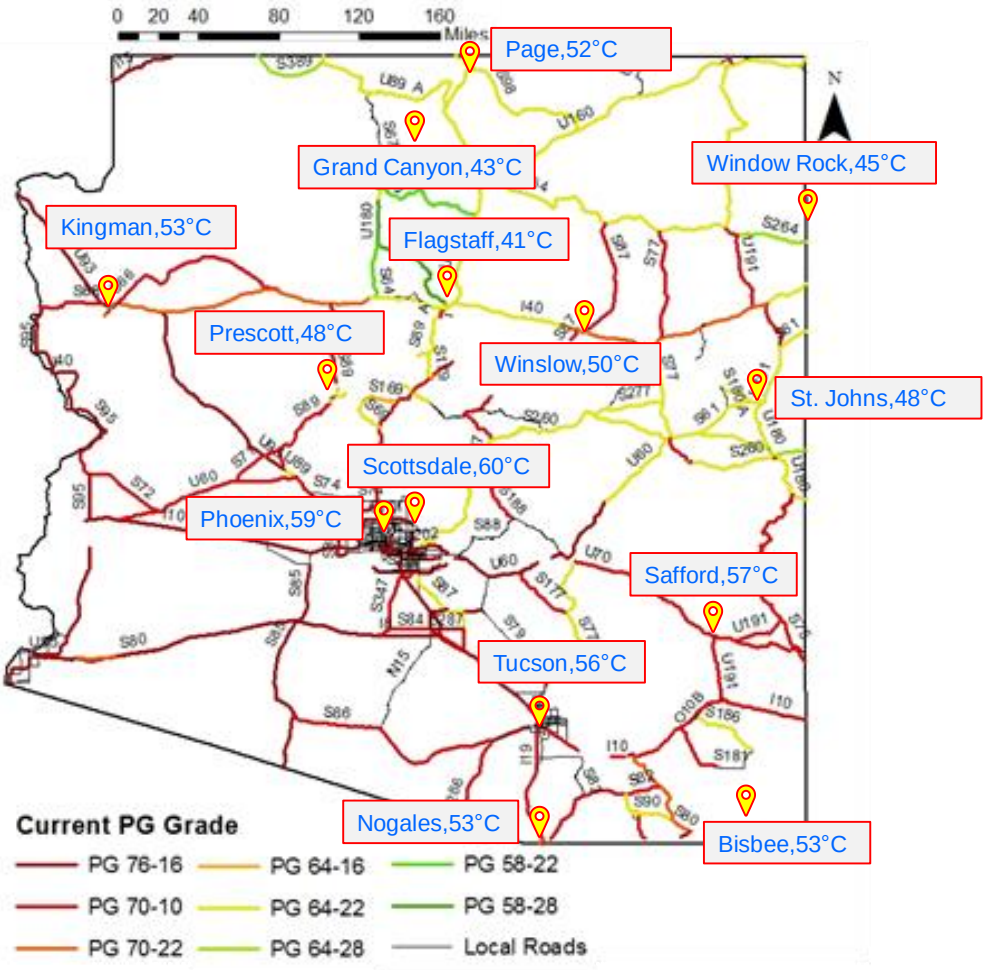

Figure 41. Effective Temperatures for Various Locations in Arizona

Table 33 presents the results from the HWTT for all 12 mixtures at their corresponding temperatures. ADOT's current acceptance criteria for rutting resistance are based on HWTT performed at 50°C, in which the rutting should be less than 20 mm. It can be seen from Table 33 that all the mixtures used in the study yield rut depths below the 20 mm permissible at 50°C.

The rut depths reported in Table 33 are also in compliance with current ADOT practice and the methodology proposed in AASHTO T 324, under both of which only the maximum rut depth across all sensors is reported. The values in Table 33 are the average of these maximum rut depths obtained under the left and right wheels. Currently, the AASHTO T 324 specification contains no precision and bias statement, so the variability measure used for this study is simply the difference between the specimens in the right and left wheel paths. This difference is presented in the form of error bars in Figures 42 to 44. Also, while the rut depths are shown at multiple temperatures, the appropriate rut depth to be considered for a particular mixture would be the one at the effective temperature. These values are highlighted in red in Figures 43 and 44 and in bold in Table 33. It should be noted that while

Table 33 and the three figures present only the maximum rut depth, Appendix E presents the rut depths using the averaging methods specified by various DOTs.

Table 33. Rut Depths for Asphalt Mixtures Tested at Different Temperatures

Group	Mixture Notation	Impression (mm)			
		44°C	50°C	56°C	62°C
1	TX1	–	3.77	**13.39**	19.71
	SY1	2.75	**8.88**	–	–
	GY3	–	3.45	**3.71**	–
	GY4	–	2.61	–	**6.52**
	SZ1	3.11	**12.37**	–	–
	GZ2	–	3.21	**4.87**	–
	TZ4	–	3.16	2.43	**3.34**
2	SX3	3.49	**5.67**	–	–
	GX4	–	**4.60**	6.93	–
	GX5	–	2.54	–	**8.80**
	TY5	–	3.27	**3.92**	11.90
	GY6	–	2.10	–	5.17

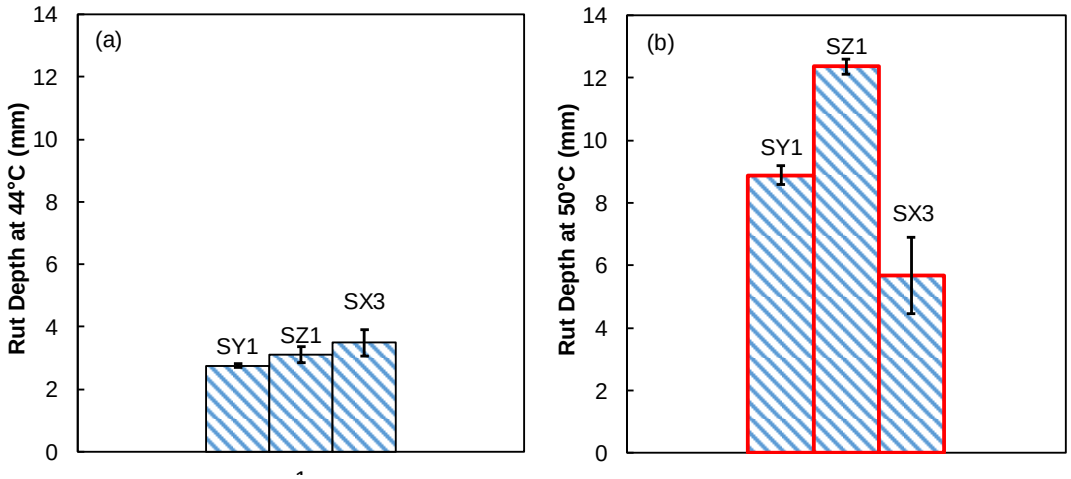

Figure 42. Rut Depths for Asphalt Mixtures Prepared at (a) 44°C and (b) 50°C with Aggregate Procured from Snowflake

In total, 27 HWTTs were conducted across mixtures and temperatures. For 14 of these tests, the difference between the left and right wheels was less than 10 percent of the mean rut depth. For eight

of the tests, this difference was between 10 percent and 20 percent. For one test, it was between 20 percent and 25 percent; and for four tests, it was greater than 25 percent. The mixtures for which the difference was greater than 25 percent were TX1 at 56°C, and GX5, GY6, and TY5 at 62°C. In all four tests in which the variability exceeded 25 percent, stripping was observed under one of the wheels. The stripped sample produced larger deformation than the sample that did not experience stripping, and therefore may have been the cause of higher variability.

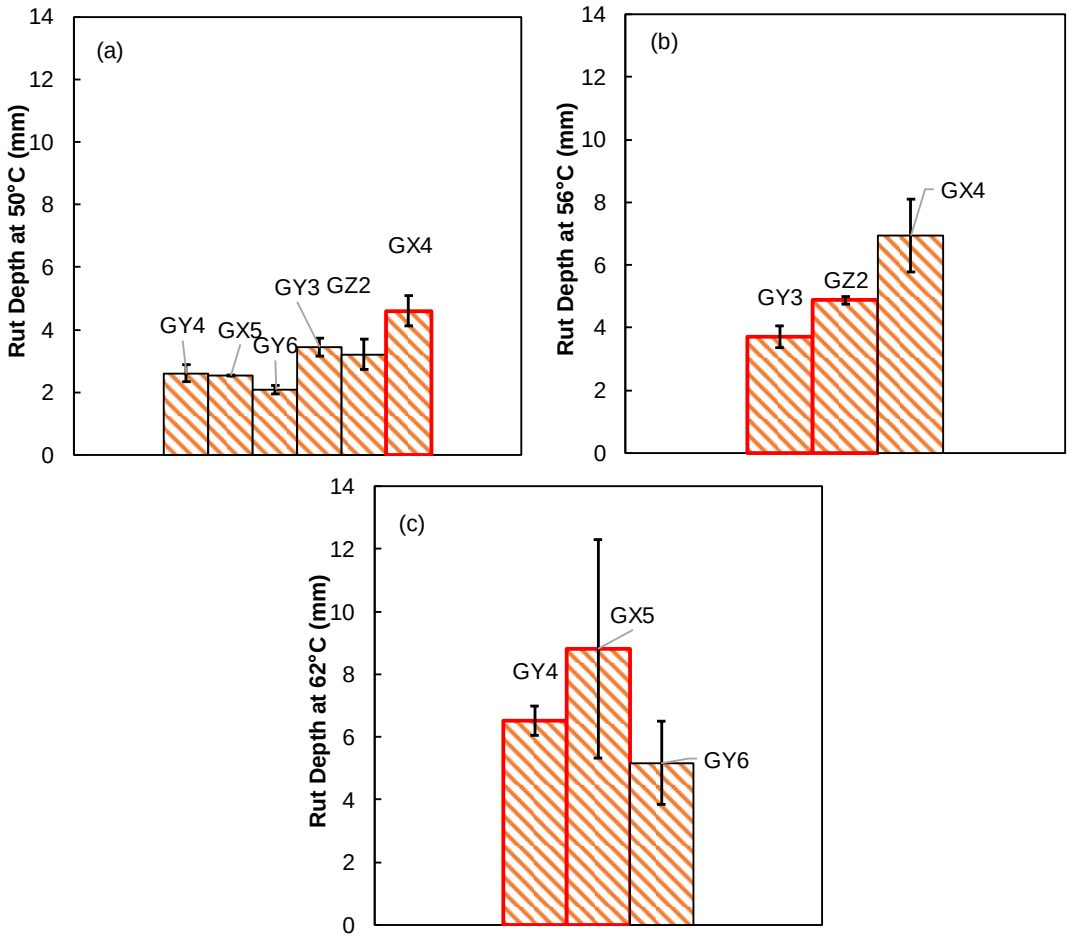

Figure 43. Rut Depths for Asphalt Mixtures Prepared at (a) 50°C, (b) 56°C, and (c) 62°C with Aggregate Procured from Globe

One of the main goals of this chapter is to compare mixture rutting to the binder rutting parameters $|G^*|/\sin\delta$ and $J_{nr3.2}$. In the literature review presented in Chapter 2, this relationship was shown by first plotting the two rutting parameters against rut depth; then fitting the relationship to a linear function; and inferring the suitability of one parameter over the other from the goodness of fit or the R^2 value. Figure 45 shows the application of this type of analysis to the test data in this study, using the binder

property data at 64°C and mixture rut depth at 50°C. If a linear regression function is used to fit the data presented in Figure 45, mixture rutting is found to better correlate with $J_{nr3.2}$ than with $|G^*|/\sin\delta$ (R^2 of 0.65 versus 0.19, respectively). An improved linear fit is ideal because it would be easier to quickly interpret what a change in binder rutting parameter would mean for mixture rutting. However, a low R^2 value based on a linear fit is not a guarantee than one parameter is "better" than another. In this case, it might not be a good representation of the true potential of $|G^*|/\sin\delta$ in relation to mixture rutting, since nonlinear functional relationships may also be acceptable for a specification parameter. Thus, using a linear regression fit may unfairly penalize the $|G^*|/\sin\delta$, since the relationship in Figure 45(b) appears closer to a power law fit than a linear fit. Therefore, to have a better understanding of these relationships and to make an informed decision about which parameter is better to use, the research team also performed additional comparisons to assess the suitable binder rutting parameter.

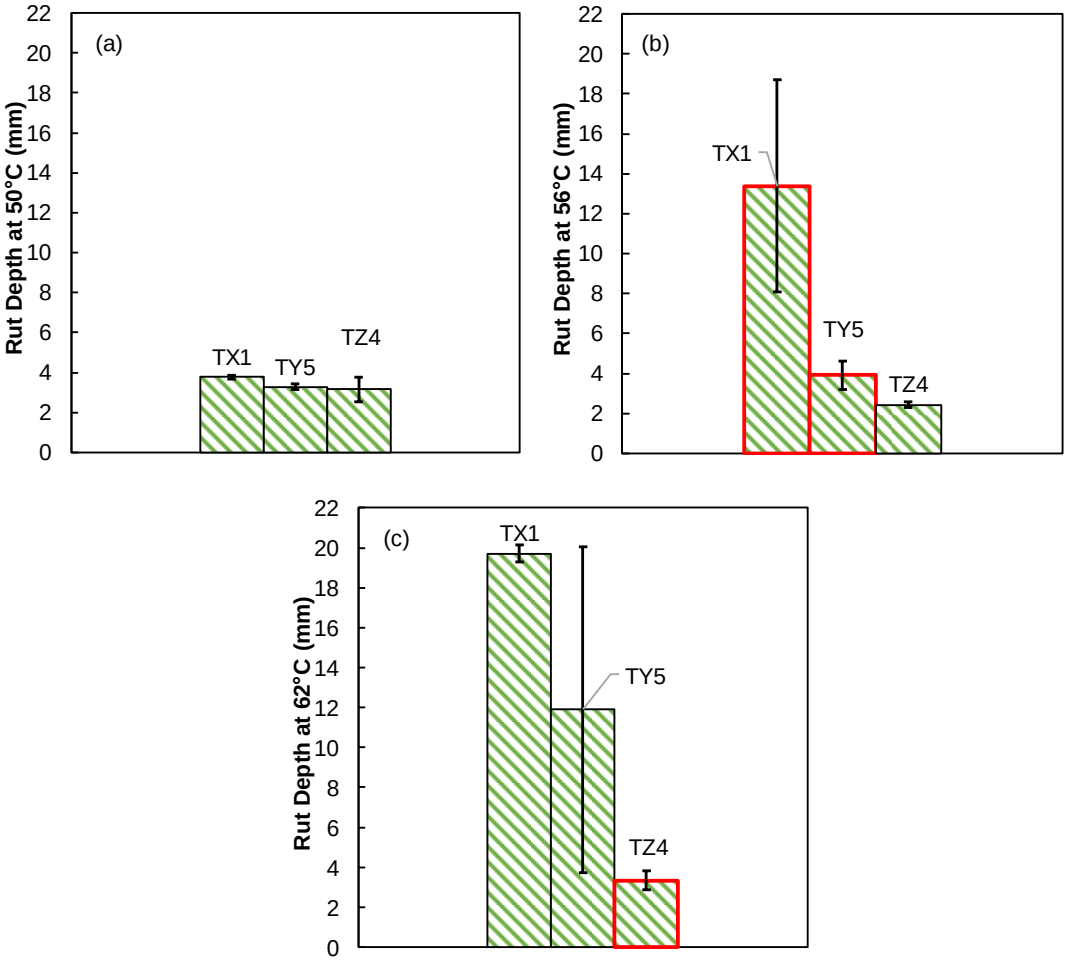

Figure 44. Rut Depths for Asphalt Mixtures Prepared at (a) 50°C, (b) 56°C, and (c) 62°C with Aggregate Procured from Tucson

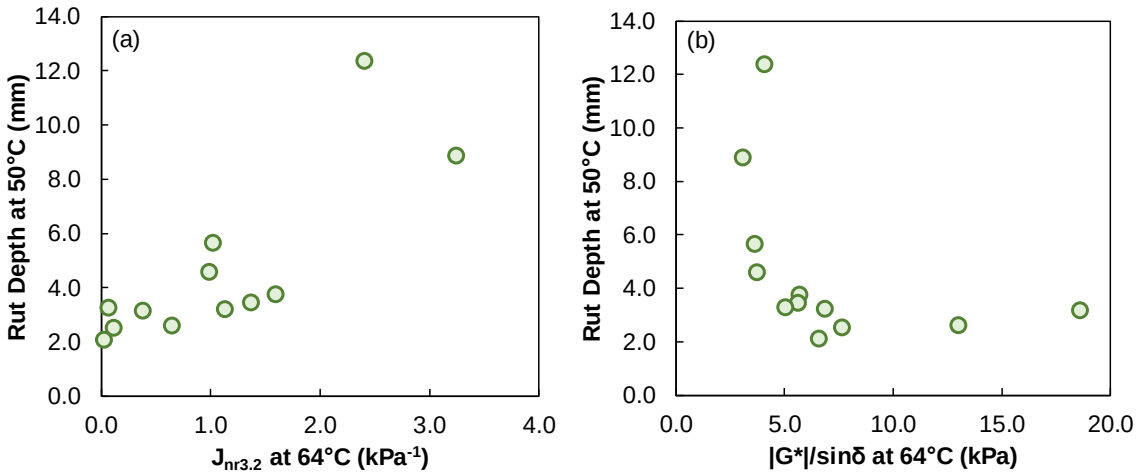

Figure 45. Comparison of Binder Rutting Parameters at 64°C and Mixture Rutting at 50°C, for Binder Parameters (a) $J_{nr3.2}$ and (b) $|G^*|/\sin\delta$

The approach to this assessment was to identify mixtures with binders of similar and different $J_{nr3.2}$ and $|G^*|/\sin\delta$, and then compare the individual changes in rut depth for these mixtures. Only the temperatures corresponding to in-use conditions (see Table 32) were used for these comparisons. The first step in performing the assessment was to cluster the binders into groups that possessed similar $J_{nr3.2}$ and different $|G^*|/\sin\delta$ and vice versa at 64°C and 70°C. A statistical segregation technique called *k*th moment clustering was used to cluster and identify the binders. The basic principle of the technique is to segregate the data into different clusters or groups based on the proximity to a mean value. The process is completed in multiple steps (two are used for this study) wherein arbitrary cluster mean values are first assumed to represent the mean and the 25th and 75th quartiles of the data. The data are then clustered to the closest value based on their proximity (calculated based on the minimum squared distance from the given observation to each assumed mean value). Once the initial clustering is completed, the mean values for each cluster are calculated, the proximity of each observation to the new means are determined, and the results are re-clustered. If the initial step eliminates a group altogether, then in the second iteration the mean of that cluster is assumed equal to the average of the other two. This process is repeated until convergence occurs, which for this study required two iterations.

As Table 34 shows, the output from the clustering operation were binders with the same $J_{nr3.2}$ and different $|G^*|/\sin\delta$ and vice versa at 64°C and 70°C . Based on the clusters obtained, mixtures prepared with these binders were then organized into pairs along with their corresponding rut depths, as shown in Table 35. If the similarities in $J_{nr3.2}$ or $|G^*|/\sin\delta$ existed at 64°C, the rut depth considered was at 50°C. For binder similarities or differences at 70°C, the rut depth at 56°C was considered. To check if similarities existed in rut depths as well, a t-test was conducted at the 95 percent confidence interval on the rut depths of mixtures produced using the clustered binders. Samples that experienced stripping during the HWTT were excluded from the t-test analysis.

Table 34. Output from *k*th Moment Clustering Operation for $J_{nr3.2}$ and $|G^*|/\sin\delta$ at 64°C and 70°C

64°C						70°C					
Same $J_{nr3.2}$ and Different $\|G^*\|/\sin\delta$			Same $\|G^*\|/\sin\delta$ and Different $J_{nr3.2}$			Same $J_{nr3.2}$ and Different $\|G^*\|/\sin\delta$			Same $\|G^*\|/\sin\delta$ and Different $J_{nr3.2}$		
Cluster	**Binder**	**Mixture**	**Cluster**	**Binder**	**Mixture**	**Cluster**	**Binder**	**Mixture**	**Cluster**	**Binder**	**Mixture**
1	Y6	GY6	1	Y6	GY6	1	Y6	GY6	1	X4	GX4
	Y5	TY5		Z2	GZ2		Y5	TY5		X3	SX3
2	X4	GX4		Y3	GY3	2	X4	GX4		X1	TX1
	X3	SX3		X1	TX1		Z2	GZ2	2	Z2	GZ2
	Z2	GZ2	2	Z1	SZ1	3	Y3	GY3		Y3	GY3
	Y3	GY3		Y1	SY1		X1	TX1		Y5	TY5
3	X1	TX1		X4	GX4				3	Y6	GY6
	Z1	SZ1		X3	SX3						
4	Y1	SY1	3	Y5	TY5						

The results from the t-tests are shown in Tables 35 to 38. Mixture pairs sharing the same aggregate type are highlighted in bold in the tables. The inferences based on such mixture pairs can be considered to have a higher degree of accuracy, given that they share the same aggregate.

To understand the outcomes of this analysis and their significance, consider the second pair in Table 35, which is GX4 and GZ2. The binders of these two mixtures have similar $J_{nr3.2}$ and different $|G^*|/\sin\delta$ at 64°C. The check to be made now is to see if their rut depths are also similar. The t-test results at the 95 percent confidence level reveal that there is no statistically significant difference in rutting between the two mixtures, as indicated in the table by the abbreviation "NS." Thus, it can be inferred that the rut depths are also similar. This means that for the pair under consideration, $J_{nr3.2}$ is a good indicator of rutting. If there is a statistically significant difference in rutting between the two mixtures, then the abbreviation "S" is used. This means that for the mixture pair under consideration, binder $J_{nr3.2}$ is not a good indicator of rutting (since in this table $J_{nr3.2}$ is considered to be the same for each pair). Such checks were repeated for all pairings in Tables 35 to 38.

Table 35. Results from t-Tests for Rutting Parameter Evaluation Using Mixtures Whose Binders Have the Same $J_{nr3.2}$ and Different $|G^*|/\sin\delta$ at 64°C

Comparison Pair	Same $J_{nr3.2}$ and Different $\|G^*\|/\sin\delta$ (Temperature at 64°C)						
	Mix.	Temp. (°C)	$\|G^*\|/\sin\delta$ (kPa)	$J_{nr3.2}$ (kPa^{-1})	Rut Depth (mm)	p-value	Sig.
1	GY6	64	6.56	0.02	2.10	0.01	S
	TY5	64	5.02	0.06	3.27		
2	**GX4**	**64**	**3.71**	**0.98**	**4.60**	**0.18**	**NS**
	GZ2	**64**	**6.83**	**1.13**	**3.21**		
3	**GX4**	**64**	**3.71**	**0.98**	**4.60**	**0.18**	**NS**
	GY3	**64**	**5.61**	**1.36**	**3.45**		
4	SX3	64	3.61	1.02	5.67	0.20	NS
	GZ2	64	6.83	1.13	3.21		
5	SX3	64	3.61	1.02	5.67	0.22	NS
	GY3	64	5.61	1.36	3.45		

Table 36. Results from t-Tests for Rutting Parameter Evaluation Using Mixtures Whose Binders Have the Same $|G^*|/\sin\delta$ and Different $J_{nr3.2}$ at 64°C

Comparison Pair	Same $\|G^*\|/\sin\delta$ and Different $J_{nr3.2}$ (Temperature at 64°C)						
	Mix.	Temp. (°C)	$\|G^*\|/\sin\delta$ (kPa)	$J_{nr3.2}$ (kPa^{-1})	Rut Depth (mm)	p-value	Sig.
1	TX1	64	5.68	1.59	3.77	0.39	NS
	GZ2	64	6.83	1.13	3.21		
2	TX1	64	5.68	1.59	3.77	0.41	NS
	GY3	64	5.61	1.36	3.45		
3	**GY6**	**64**	**6.56**	**0.02**	**2.10**	**0.04**	**S**
	GY3	**64**	**5.61**	**1.36**	**3.45**		
4	**GY6**	**64**	**6.56**	**0.02**	**2.10**	**0.15**	**NS**
	GZ2	**64**	**6.83**	**1.13**	**3.21**		
5	GY6	64	6.56	0.02	2.10	0.00	S
	TX1	64	5.68	1.59	3.77		
6	GX4	64	3.71	0.98	4.60	0.00	S
	SZ1	64	4.06	2.40	12.37		
7	**SX3**	**64**	**3.61**	**1.02**	**5.67**	**0.03**	**S**
	SZ1	**64**	**4.06**	**2.40**	**12.37**		

Of the six pairings across 64°C and 70°C that have similar $J_{nr3.2}$ and different $|G^*|/\sin\delta$, the rut depths measured in five of these pairs were found to be statistically similar. More importantly, of these six pairs, three pairs shared the same aggregate type, and all three reported similarities in rut depth. Of the 10 pairings across 64°C and 70°C that have similar $|G^*|/\sin\delta$ and different $J_{nr3.2}$, six were found to have

statistically similar rutting. Of the 10 pairs, four shared the same aggregate type, and of those four, two pairs reported significant differences in rut depth.

Based on the above comparisons, a higher percentage (83 percent) of mixture pairs that possessed binders with similar $J_{nr3.2}$ were found to have similar rut depths. In contrast, only 60 percent of mixture pairs that possessed binders with similar $|G^*|/\sin\delta$ were found to have similar rut depths. It is believed that the above assessment, taken in combination with the general improvement in the linear functional fit with respect to rut depth and $J_{nr3.2}$, supports the conclusion that $J_{nr3.2}$ is a better indicator of rutting than is $|G^*|/\sin\delta$ for Arizona asphalt mixtures.

Table 37. Results from t-Tests for Rutting Parameter Evaluation Using Mixtures Whose Binders Have the Same $J_{nr3.2}$ and Different $|G^*|/\sin\delta$ at 70°C

Comparison Pair	Same $J_{nr3.2}$ and Different $\|G^*\|/\sin\delta$ (Temperature at 70°C)						
	Mix.	Temp. (°C)	$\|G^*\|/\sin\delta$ (kPa)	$J_{nr3.2}$ (kPa^{-1})	Rut Depth (mm)	p-value	Sig.
1	**GX4**	**70**	**2.1425**	**2.31**	**6.93**	**0.22**	**NS**
	GZ2	**70**	**3.25595**	**2.89**	**4.87**		

Table 38. Results from t-Tests for Rutting Parameter Evaluation Using Mixtures Whose Binders Have the Same $|G^*|/\sin\delta$ and Different $J_{nr3.2}$ at 70°C

Comparison Pair	Same $\|G^*\|/\sin\delta$ and Different $J_{nr3.2}$ (Temperature at 70°C)						
	Mix.	Temp. (°C)	$\|G^*\|/\sin\delta$ (kPa)	$J_{nr3.2}$ (kPa^{-1})	Rut Depth (mm)	p-value	Sig.
1	TY5	70	3.13	0.12	3.92	0.32	NS
	GZ2	70	3.26	2.89	4.87		
2	TY5	70	3.13	0.12	3.92	0.82	NS
	GY3	70	2.74	3.53	3.71		
3	**GZ2**	**70**	**3.26**	**2.89**	**4.87**	**0.08**	**NS**
	GY3	**70**	**2.74**	**3.53**	**3.71**		

Axial Fatigue Test

The axial fatigue test was performed to assess the resistance of the current Arizona asphalt mixtures to fatigue damage. The test was performed at an intermediate temperature of 18°C and was run at four strain levels. The strain levels were estimated using an expectation that the material would fail in less than 10,000 cycles, between 10,000 and 50,000 cycles, between 50,000 and 100,000 cycles, and after more than 100,000 cycles. The fatigue test data were analyzed using simplified viscoelastic continuum damage (S-VECD) theory, as explained in Appendix C. The first step in the S-VECD approach is to establish the damage characteristic (*C* vs. *S*) curve. *C* represents the integrity of the material, which

decreases as the material is repeatedly loaded, and *S* represents the damage accumulated by the material during the test. The *C* vs. *S* curve has a unique relationship to a given asphalt mixture and is independent of test conditions. These test conditions include strain levels, temperatures, mode of loading, and loading history. The *C* vs. *S* curves for the study mixtures are shown in Figure 46. The *C* vs. *S* curves for each individual mixture at different strain levels, along with on-specimen strain at cycle 80, are summarized in Appendix E.

The interpretation of the figure can be explained using an example. Consider two mixtures, SX3 and SY1. At failure, SY1 suffered a loss in material integrity that dropped to around 0.5 (50 percent), and it accumulated a damage of around 7×10^4. In comparison, SX3 could resist failure until its material integrity dropped to around 0.15 (15 percent), and in the process it accumulated damage of more than 1.5×10^5. While SX3 accumulates more damage, it resists failure until its material integrity drops to 15 percent. If all other factors are the same, then this characteristic would make SX3 superior to SY1 in fatigue resistance.

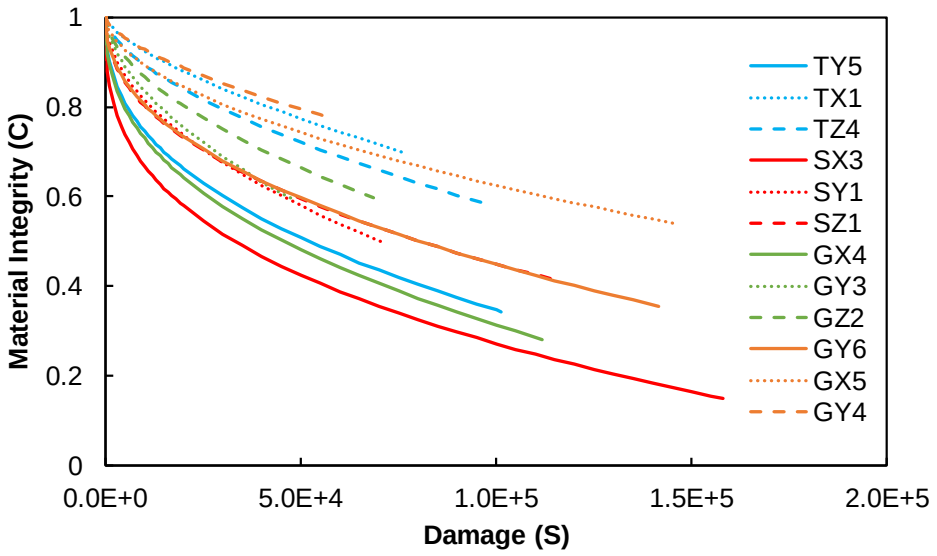

Figure 46. *C* (Material Integrity) vs. *S* (Damage) Curves for the Study Asphalt Mixtures

While the *C* vs. *S* damage curves are good indicators of performance, they cannot be considered alone in assessing the fatigue performance of the asphalt mixtures. Simulations were carried out using Equation 42 of Appendix C to estimate the strain level that the sample would need to be tested at to fail in 10,000, 100,000, and 1,000,000 cycles. The result of these simulations, known as fatigue failure envelopes, are shown in Figure 47. In simple terms, the vertical positioning of a mixture's line indicates the performance of the mixture in fatigue. The higher the vertical position, the better the fatigue resistance. So, in the example used above, SX3 has a higher vertical position than SY1 and thus has better fatigue resistance than SY1.

Among all the mixtures used in the study, the mixture prepared with the X3 binder provided the greatest amount of fatigue resistance. As Figure 47 shows, five of the top six best-performing mixtures are polymer-modified. For ease of observation, Figures 48 to 50 show the *C* vs. *S* curves in Figure 46 and the fatigue failure envelopes in Figure 47 separated by aggregate type. This presentation illustrates clearly that the best-performing mixtures in each aggregate type are polymer-modified mixtures.

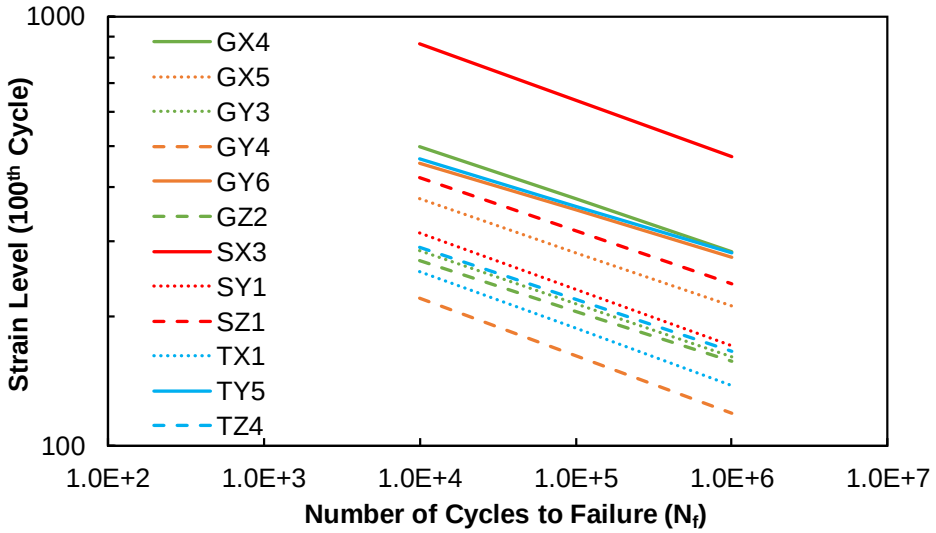

Figure 47. Simulated Fatigue Failure Envelopes for the Study Asphalt Mixtures

To quantify and compare the differences observed in fatigue behavior of the asphalt mixtures, the fatigue life for all 12 mixtures was estimated at 400 με using the failure envelopes shown in Figure 47. Table 39 presents the results, which reaffirm the trends seen in Figure 47. Overall, irrespective of the source of the aggregate, polymer-modified mixtures are more fatigue-resistant. To put the statement into perspective, the average N_f value for the five polymer-modified mixtures across three aggregate sources is 728,166, which compares with an average value of 2,702 for the seven non-polymer-modified mixtures. The increase in average fatigue life from polymer-modified mixtures is 26,853 percent. The large average N_f value of the polymer-modified mixtures is due to the high fatigue resistance offered by SX3. Even without SX3, if only the other four polymer-modified binders are averaged, the average N_f is 34,428, which is 1174 percent higher than the average N_f value for the non-polymer-modified mixtures.

Table 39. Simulated Fatigue Life for Study Asphalt Mixtures at 400 με

Mixture	N_f
GX4	59,512
GX5	6,073
GY3	631
GY4	116
GY6	32,186
GZ2	360
SX3	3,503,118
SY1	1,537
SZ1	15,234
TX1	334
TY5	39,941
TZ4	699

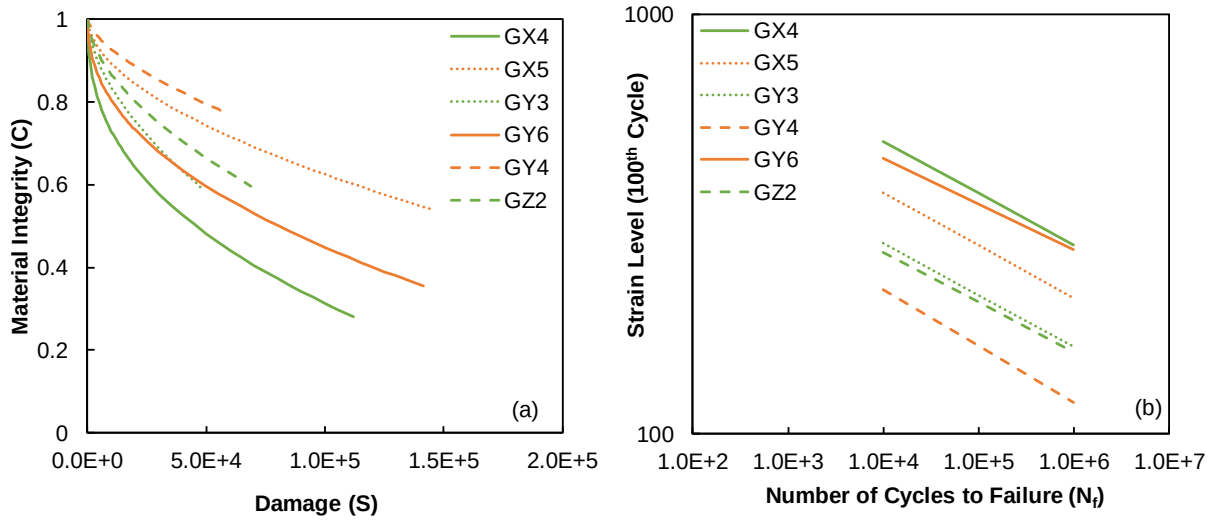

Figure 48. (a) *C* vs. *S* Damage Curves and (b) Simulated Fatigue Failure Envelopes for Asphalt Mixtures Prepared with Globe Aggregate

The mixtures prepared with Globe aggregate contain three polymer-modified binders, X4, X5, and Y6. As Figure 48 shows, the mixtures prepared with these binders rank 1, 3, and 2, respectively, in fatigue resistance. Based on Table 39, GX4, which is the best-performing mixture, delivers an improvement of 9337 percent over the best-performing non-polymer-modified mixture, GY3, and an improvement of 85 percent over the next-best-performing polymer-modified binder, GY6.

The mixtures prepared with Snowflake aggregate contain one polymer-modified binder, X3. The mixture prepared with X3 ranks best in fatigue resistance not only among the Snowflake mixtures but among all

12 mixtures tested in this study. The mixture SX3 provides an improvement of 22,895 percent over SZ1. The mixtures prepared with Tucson aggregate contain one polymer-modified binder, Y5. The mixture prepared with Y5 ranks best in fatigue resistance among the Tucson mixtures and third best overall. In Table 39, the mixture TY5 provides an improvement of 5614 percent over TZ4.

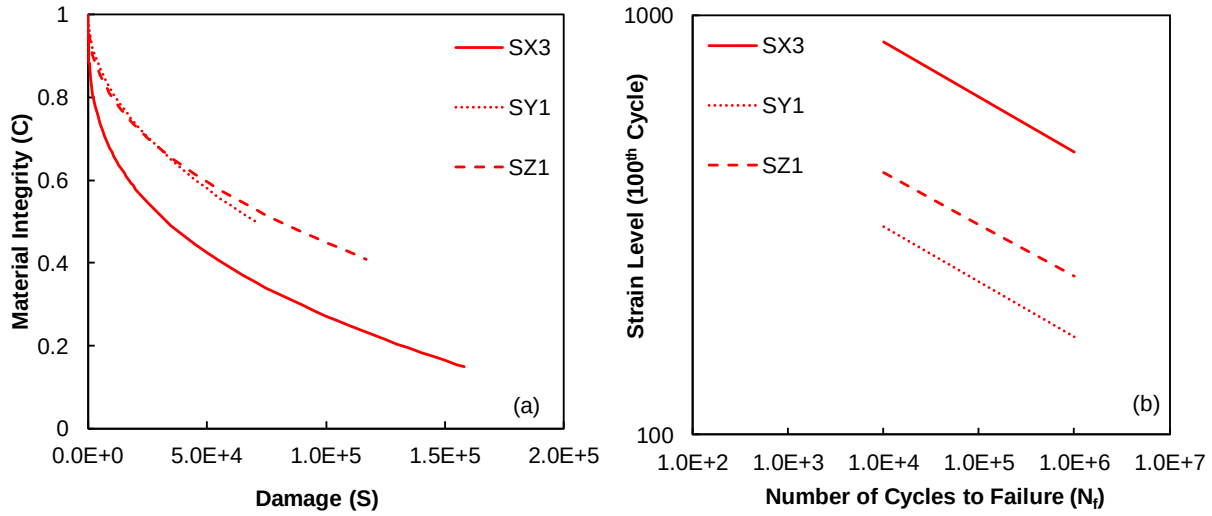

Figure 49. (a) *C* vs. *S* Damage Curves and (b) Simulated Fatigue Failure Envelopes for Asphalt Mixtures Prepared with Snowflake Aggregate

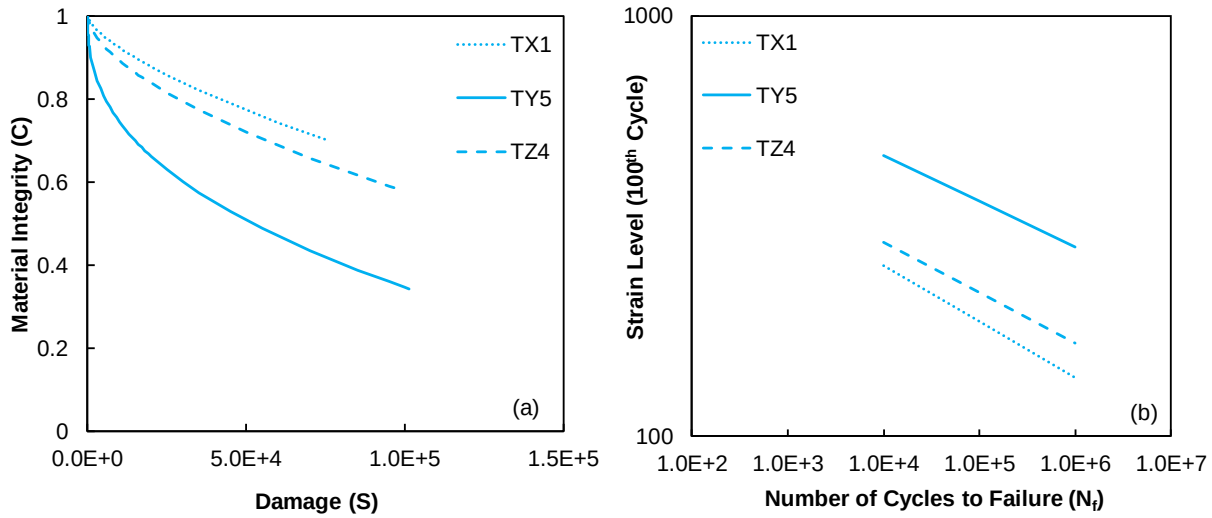

Figure 50. (a) *C* vs. *S* Damage Curves and (b) Simulated Fatigue Failure Envelopes for Asphalt Mixtures Prepared with Tucson Aggregate

Three main observations can be made regarding the fatigue performance of the asphalt mixtures:

1. Polymer modification has a profound impact on fatigue performance. Within each aggregate type, the best-performing polymer-modified mixture had an average improvement of 12,615 percent over the best non-polymer-modified mixture, with the improvements ranging from 5614 percent to 22,895 percent. These differences are significant and warrant further investigation, which is unfortunately outside the scope of the current work. One key factor believed to be responsible for these differences is related to the observed failure mechanisms in the polymer- versus non-polymer-modified mixtures. Among the polymer-modified mixtures, failure was consistently cohesive (i.e., in the asphalt film), as evidenced by the fact that the failure surface was black in color. Among the non-polymer-modified binders, there was a consistent showing of mixed adhesion/cohesion failure, which was evidenced by the presence of thinly coated aggregate particles on the failure surface.
2. Of the binders currently in the ADOT specifications, Z1 (PG 64-22) and X5 (PG 76-22TR) perform the best. PG 76-22TR is the only polymer-modified binder that is currently specified by ADOT and included in these experiments.
3. The original purpose of performing the axial fatigue test was to see if there may be any unintended effects on fatigue performance if ADOT adopts AASHTO M 332. It can be concluded that there are no negative consequences for fatigue performance, but it also can be stated that polymer-modified mixtures have higher fatigue resistance than non-polymer-modified mixtures.

SUMMARY

This chapter has presented the results and corresponding analyses for performance tests conducted on 12 asphalt mixtures. Three tests—dynamic modulus, HWTT, and axial fatigue—were performed on all 12 mixtures at the prescribed test conditions. In the dynamic modulus tests, mixtures prepared with non-polymer-modified binders had higher moduli than mixtures prepared with polymer-modified binders. The data from the HWTT showed that the rut depths for all mixtures were below the acceptance limit currently used by ADOT. The rut depths were then related to the binder rutting parameters J_{nr} at 3.2 kPa and $|G^*|/\sin\delta$. It was concluded that $J_{nr3.2}$ relates better to mixture rutting than does $|G^*|/\sin\delta$. The fatigue performance of the asphalt mixtures showed that the polymer-modified asphalt mixtures possess greater fatigue resistance than non-polymer-modified asphalt mixtures. ADOT currently follows AASHTO M 320 for its binder specifications, and AASHTO M 320 calls for $|G^*|/\sin\delta$ to be used as the binder rutting parameter. Given the results in this chapter, it is recommended that $J_{nr3.2}$ be included in ADOT's binder specifications.

CHAPTER 6. EVALUATION OF IMPACTS OF CHANGES IN PERCENT RECOVERY CRITERIA

INTRODUCTION

Chapter 4 showed that polymer-modified binders exhibit a superior percent recovery in the MSCR test. And Chapter 5 showed that asphalt mixtures using polymer-modified binders exhibited greater resistance to fatigue. While it is known that polymer-modified binders provide superior resistance to rutting, the effect that percent recovery measured during the MSCR test has on mixture performance is largely unknown. Percent recovery is not itself a specification parameter within AASHTO M 332, but it is suggested as a parameter to be used in screening for the presence of polymer (see Chapter 1). As shown in Figure 51, Arizona binders, and more specifically PG 76-22TR binders (the only polymer-modified binders Arizona specifies), have historically been above the demarcation line specified in AASHTO M 332 (identified by the black line in the figure). This indicates that the line does differentiate to at least some degree between polymer-modified and non-polymer-modified binders (as discussed in Chapter 3). Figure 51 also shows that many other Arizona binders are positioned well above the demarcation line, which raises the question whether the achieved performance of these binders is related to the high amount of recovery. Since the literature is incomplete regarding the impact of percent recovery itself on performance, it is not known whether the benefits are due to the large vertical distance from the line or whether they can be solely attributed to the low J_{nr} of the binder.

The objective of the experiments and analyses reported in this chapter is to identify whether the percent recovery affects performance (or, more specifically, captures a performance-related behavior) and whether the demarcation line identified in AASHTO M 332 needs to be modified to ensure Arizona binders perform as expected. The first step in the experiments conducted to meet this objective was to create laboratory-blended binders with nearly identical J_{nr} but differing percent recovery. Then, these samples were mixed with aggregate, compacted, and tested for fatigue, rutting, and modulus.

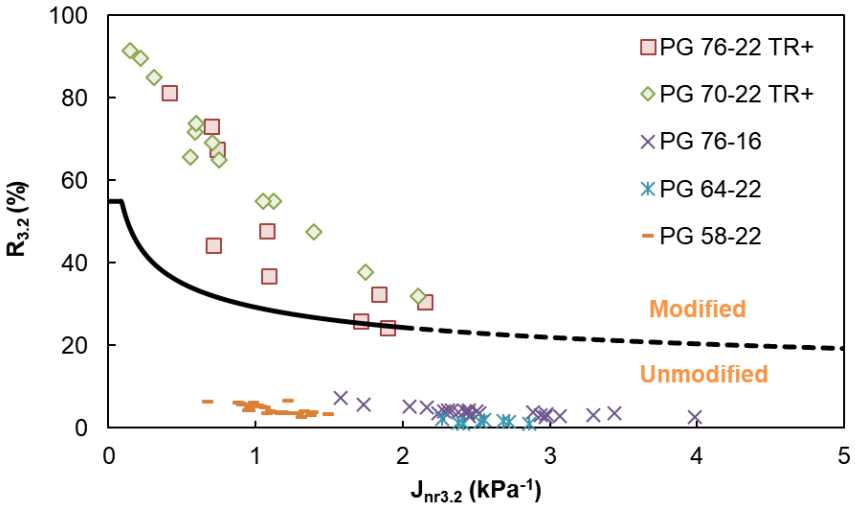

Figure 51. $J_{nr3.2}$ vs. $R_{3.2}$ (%) Relationship as a Means for Distinguishing Polymer-Modified Binders from Unmodified Binders, Using a Sample of Historical ADOT Binder Data

MATERIALS

Asphalt Binders

All nine binders used in the experiment were polymer-modified. For seven of the nine binders, the polymer modification was carried out at ASU by blending a base binder, PG 58-28, with various dosages of SBS polymer, sulfur, and PPA. Linear SBS, commercially named D1192 and supplied by Kraton Polymers, was used for the study. The sulfur and PPA were used as cross-linking agents. PPA was obtained from ICL Food Specialties. Initial trials of these seven showed that it was impossible to create materials with precisely the same $J_{nr3.2}$ and varying recovery, so the binders were divided into four groups—J, K, L, and M—based on the similarity of their $J_{nr3.2}$ value at 64°C. The seven binders were supplemented with two others (PG 70H-16 and PG 64H-22) selected from the Group 2 polymer-modified binders discussed in Chapter 3. The detailed procedure for specimen preparation is presented in Appendix C. Table 40 shows the nine binders along with their composition.

Table 40. Polymer-Modified Binder Designations and Compositions

Group	Sample	Weight Percentage (%)			
		Asphalt	SBS	Sulfur	PPA
J	Y5	Provided by Supplier			
	B5	94.417	5.0	0.083	0.5
K	D0.5	97.983	0.5	0.017	1.5
	B2	97.433	2.0	0.067	0.5
L	A3-B	96.925	3.0	0.075	0
	A4	96.000	4.0	0.000	0
	X3	Provided by Supplier			
M	A2-B	97.933	2.0	0.067	0
	A3	97.000	3.0	0.000	0

Mixtures

Tucson aggregate was used for the preparation of the asphalt mixtures. The aggregate gradations are shown in Table 41. The mixtures were prepared using ADOT's Superpave mix design criteria. The estimated binder content for all mixtures was in the range of 5.7 to 5.8 percent. The samples for dynamic modulus and axial fatigue testing were compacted to an air void content of 6 ± 0.5 percent, and the samples prepared for the HWTT were compacted to one of 7 ± 1 percent. These air void contents are in line with those used for the tests described in Chapter 5.

Table 41. Asphalt Mixture Aggregate Gradation for Aggregates Procured from Tucson

Sieve No.	Sieve Size (mm)	% Passing	% Mineral Admixture
1"	25.0	100	1
3/4"	19.0	96	–
1/2"	12.5	76	–
3/8"	9.50	69	–
No. 4	4.75	59	–
No. 8	2.36	44	–
No. 16	1.18	30	–
No. 30	0.600	20	–
No. 50	0.300	12	–
No. 100	0.150	7	–
No. 200	0.075	4	–
Pan	<0.075	0	–

RESULTS AND ANALYSIS

Binders

The same binder characterization tests used elsewhere in this study—AASHTO T 315, AASHTO T 313, and AASHTO T 350—were performed. The PG binder grades were determined using the data obtained from the above-mentioned tests. Table 42 lists the binder grades and their corresponding $J_{nr3.2}$ and $R_{3.2}$ values, and Figure 52 presents these results graphically. All test data from the binder characterization tests are summarized in test memos attached as Appendix F. As noted above, the binders are divided into Groups J, K, L, and M based on the similarity of their $J_{nr3.2}$ values at 64°C.

Table 42. AASHTO M 320 and AASHTO M 332 PG Grades of Asphalt Binders Used for the Percent Recovery Study

Group	Sample	PG Grade		J_{nr} at 3.2 kPa at 64°C	% Percent Recovery at 3.2 kPa at 64°C
		AASHTO M 320	AASHTO M 332		
J	Y5	PG 70-16	PG 70H-16	0.06	92.46
	B5	PG 82-28	PG 76V-28	0.08	73.83
K	B2	PG 70-28	PG 70H-28	0.50	51.60
	D0.5	PG 70-28	PG 70H-28	0.41	41.60
L	X3	PG 64-22	PG 64H-22	1.03	47.00
	A3-B	PG 70-28	PG 70S-28	0.84	35.50
	A4	PG 70-28	PG 70S-28	0.86	21.40
M	A2-B	PG 64-22	PG 64H-22	1.70	23.40
	A3	PG 64-22	PG 64H-22	1.90	6.80

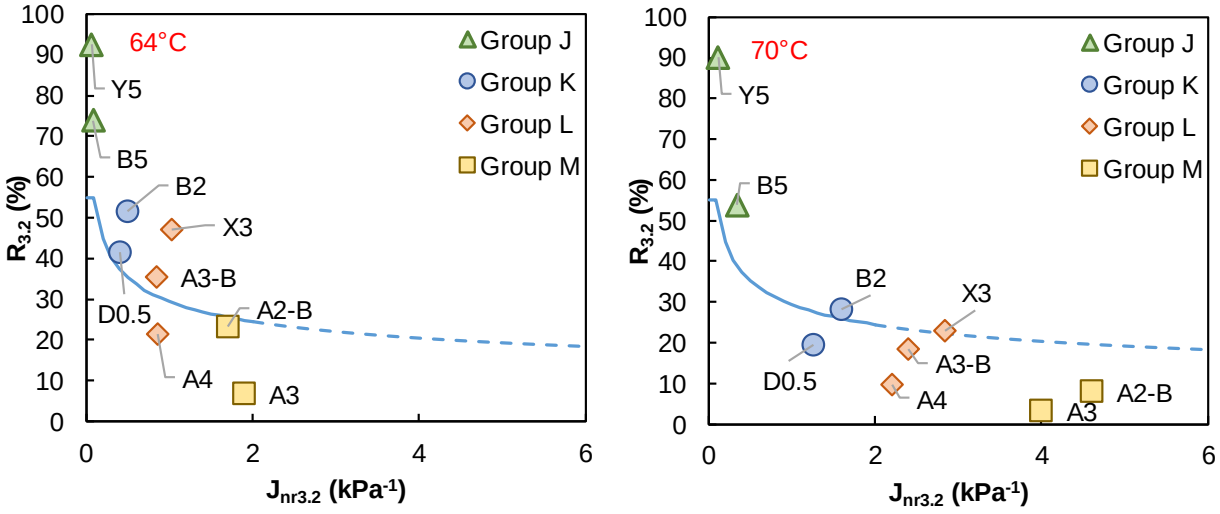

Figure 52. $J_{nr3.2}$ vs. $R_{3.2}$(%) Relationship for the Study Binders at 64°C and 70°C

Mixtures

The selected binders were prepared in bulk, to manufacture asphalt mixture specimens for performance testing. The dynamic modulus test, HWTT, and axial fatigue test were conducted to gauge the impact of MSCR recovery on the performance of the asphalt mixtures.

Dynamic Modulus Test

The dynamic modulus was performed under the test conditions presented in Chapter 3. Figure 53 presents the dynamic modulus results for all Group 3 binders. The figure shows that TD0.5 is has the highest modulus and TX3 has the lowest modulus. The prefix "T" in the binder notation indicates the source of the aggregate, which is Tucson in this case. To understand the effect of MSCR percent recovery on the dynamic modulus of these asphalt mixtures, the analysis that follows will focus in turn on Groups J, K, L, and M. The binders are color-coded to reflect the group they belong to, and the change in the series from solid to dotted line indicates the decreasing level of MSCR percent recovery.

Binders in Group J. This group consists of two binders, Y5 and B5. Based on the binder $|G^*|$ values at 64°C, B5 has the highest dynamic modulus. A similar trend is seen in the dynamic modulus of the mixtures, as shown in Figure 54. TB5 also has higher modulus than TY5 at all other temperatures and frequencies. The differences between the two mixtures were checked for statistical significance by performing a two-tailed t-test at the 95 percent significance level at all five test temperatures at the test frequency of 10 Hz. It was found that the moduli of the two mixtures were statistically different only at intermediate and high temperatures but not at the low temperatures (4.4°C and –10°C). As for the influence of MSCR percent recovery, it was found that increased binder elasticity as gauged by the MSCR percent recovery parameter led to mixtures with lower stiffness, as seen with binder Y5 and its

corresponding mixture. The influence of both binder |*G**| and the MSCR percent recovery can be inferred from the observed dynamic modulus values for group J binders.

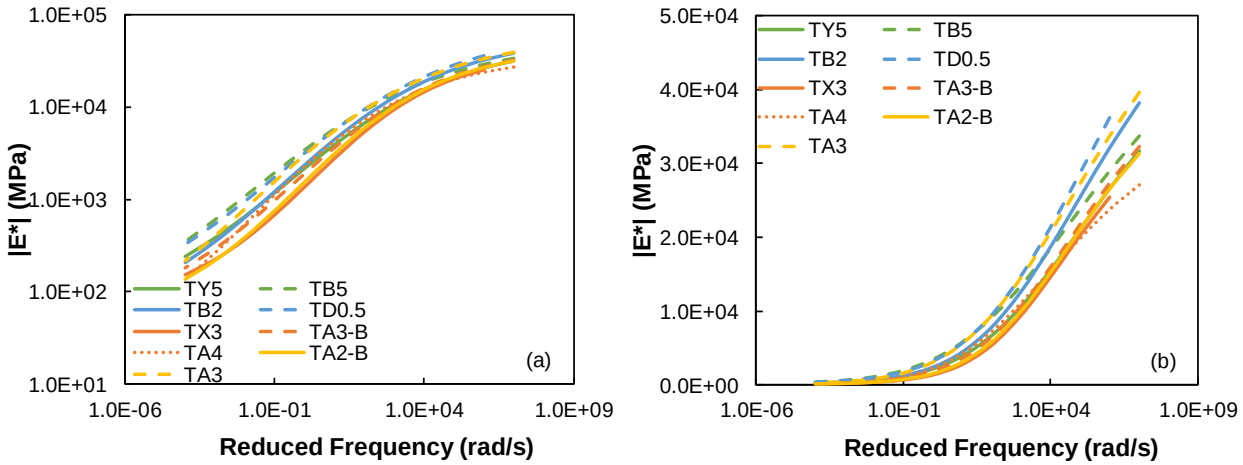

Figure 53. Dynamic Modulus Results for Mixtures Prepared with Group 3 Asphalt Binders in (a) Log-Log Space and (b) Semilog Space

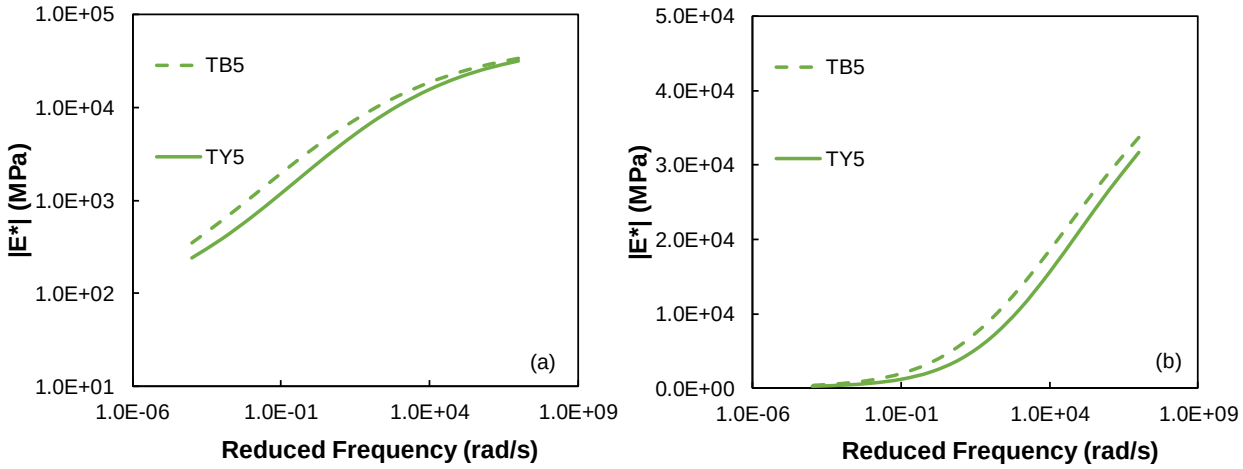

Figure 54. Dynamic Modulus Results for Mixtures Prepared with Group J Asphalt Binders in (a) Log-Log Space and (b) Semilog Space

Binders in Group K. This group consists of two binders, B2 and D0.5. With regard to binder modulus at 64°C, D0.5 has a higher |*G**| than B2 does. A similar trend appears in the results for the mixture dynamic modulus (see Figure 55). As in the previous comparison, the differences between the moduli of mixtures TD0.5 and TB2 are significant only at intermediate and high temperatures. Regarding

the effect of percent recovery, the binder with higher recovery is seen to possess lower mixture modulus.

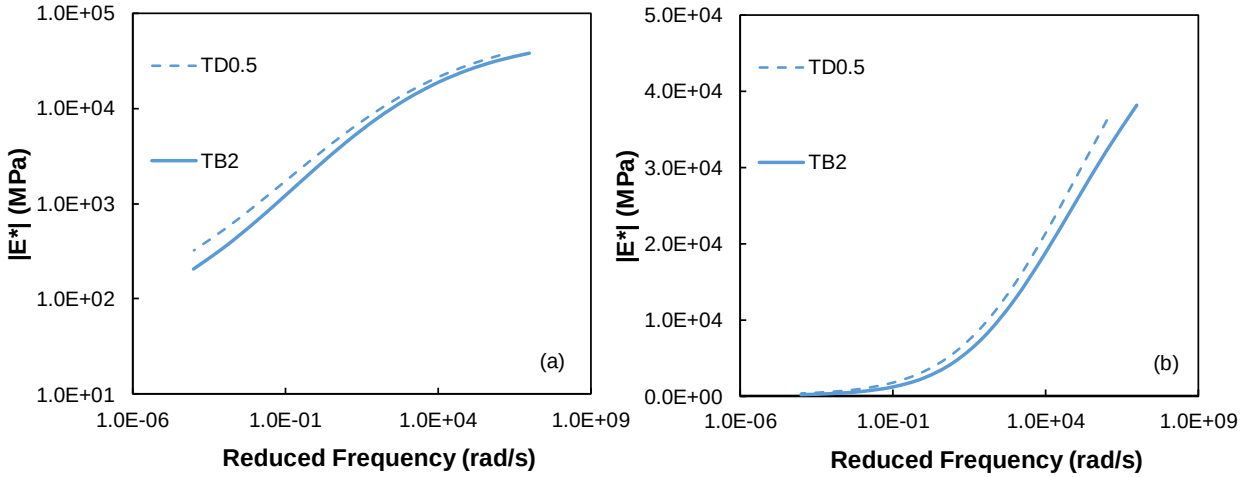

Figure 55. Dynamic Modulus Results for Mixtures Prepared with Group K Asphalt Binders in (a) Log-Log Space and (b) Semi-log Space

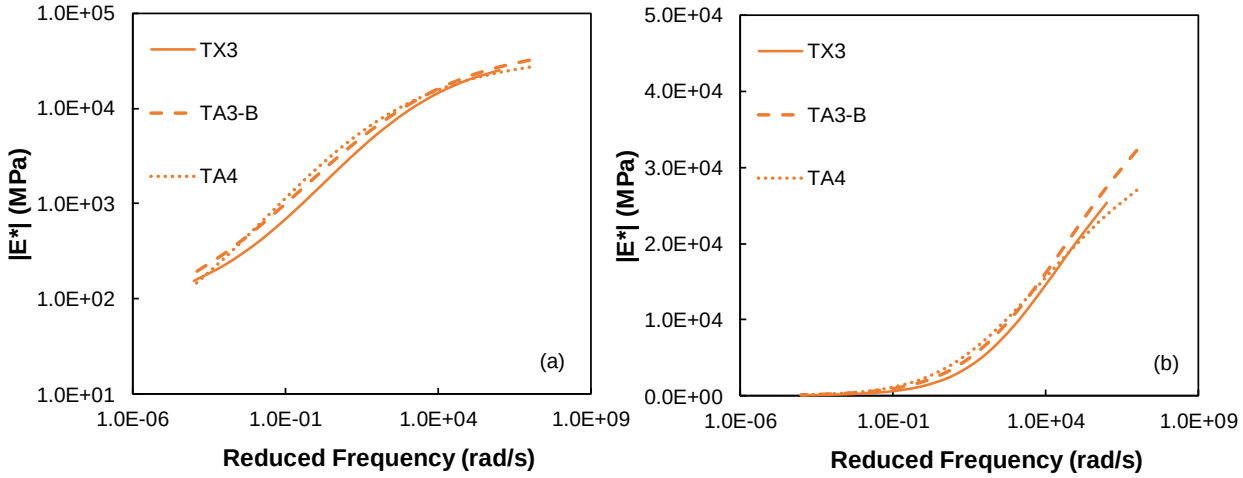

Figure 56. Dynamic Modulus Results for Mixtures Prepared with Group L Asphalt Binders in (a) Log-Log Space and (b) Semi-log Space

Binders in Group L. This group consists of three binders, X3, A3-B, and A4. Based on the $|G^*|$ values of the three binders at 64°C, A4 has the highest modulus, followed by A3-B and X3. A similar trend appears in the mixture modulus results, as seen in Figure 56. However, a statistically significant difference is seen only between TA4 and TX3 at intermediate and high temperatures. All other combinations of comparisons (i.e., TA4 vs. TA3-B, and TA3-B vs. TX3) are found to be statistically

insignificant at the 95 percent significance level). In this group, as well, binders with the highest MSCR recovery are seen to produce an asphalt mixture which has the lowest modulus.

Binders in Group M. This group consists of two binders, A2-B and A3. A3 has a higher binder $|G^*|$ than A2-B, and a similar trend is observed in the results for mixture dynamic modulus as shown in Figure 57. Also, statistically significant differences were seen between the two mixtures at all temperatures except –10°C. As with the other groups, the binder with the highest recovery is seen to produce a mixture with a lower modulus.

Overall, the conclusions from the dynamic modulus test are as follows:

1. Within each group, the mixture dynamic modulus follows the same trend as the binder $|G^*|$.
2. Mixture $|E^*|$ is inversely proportional to the MSCR percent recovery at 3.2 kPa (i.e., binders with higher MSCR recovery will produce asphalt mixtures which have lower modulus, provided the binders have similar $J_{nr3.2}$).

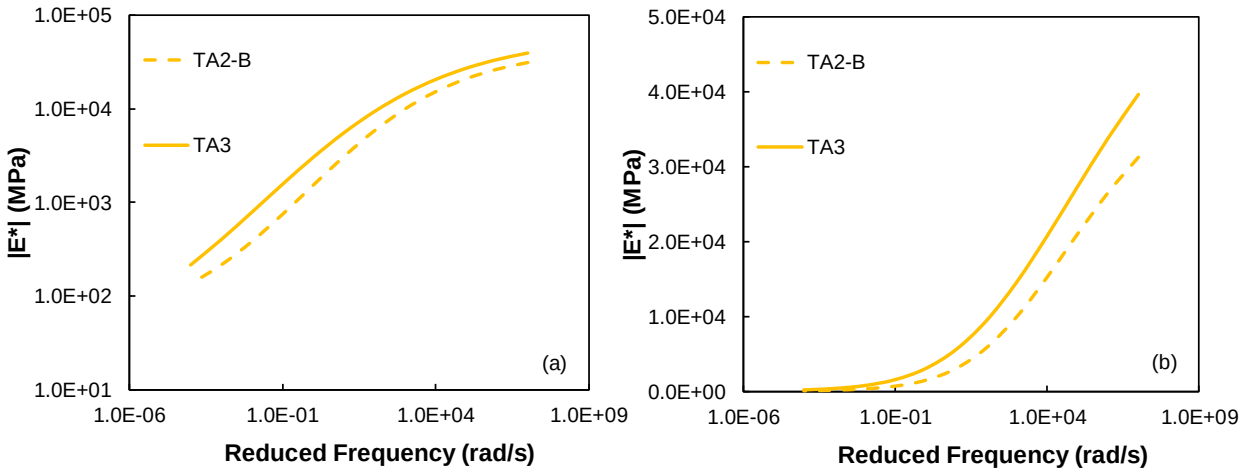

Figure 57. Dynamic Modulus Results for Mixtures Prepared with Group M Asphalt Binders in (a) Log-Log Space and (b) Semi-log Space

Hamburg Wheel Tracking Test

For all mixtures except TB5, the HWTT was performed under the conditions described in Chapter 3. For TB5, the HWTT was performed only at 56° and 62°C. The main reason for this inconsistency is that when TB5 was tested at 62°C, it did not produce any significant rutting, and so 50°C was eliminated from the testing matrix to conserve materials. Table 43 presents the rut depths for all nine binders at their corresponding test temperatures. These rut depths are reported in the same way as in Chapter 5; results for other calculation methods are given in Appendix F. As in the dynamic modulus analysis, discussions are presented group-wise to aid understanding of the effect of MSCR recovery on rutting.

Table 43. Rut Depths for Mixtures Prepared with Group 3 Asphalt Binders at Their Corresponding Test Temperatures

Group	Notation	Rut Depth (mm)			
		44°C	50°C	56°C	62°C
Group J	TY5	–	3.27	3.92	11.90
	TB5	–	–	2.16	2.97
Group K	TD0.5	–	3.16	3.31	–
	TB2	–	3.08	4.03	–
Group L	TA3-B	2.25	3.60	–	–
	TA4	–	2.57	13.02	–
	TX3	3.56	6.81	–	–
Group M	TA2-B	2.29	7.82	–	–
	TA3	2.51	4.99	–	–

Binders in Group J. This group consisted of two binders, Y5 and B5. The rut depths at 50°C and 56°C for these binders are presented in Figure 58. The error bars shown in the figure correspond to the rut depths achieved at the left wheel and the right wheel, and the marker shows the average of these two values. For these high-stiffness binders, it is seen that the percent recovery has little impact on the rut depth that is achieved. This observation is based on the data at 56°C; however, it holds true for data at 50°C also. As the recovery changes from 92 percent for Y5 to 74 percent for B5, the rut depth changes from 3.92 mm to 2.16 mm. This result was a bit surprising, since binders with lower recovery are thought to be more susceptible to rutting, but what is seen here is the opposite. A two-tailed t-test was performed to check for statistical significance, and it was found that there was no statistically significant difference between the rut depths for the two mixtures. As stated earlier, testing at 50°C was not conducted for B5 binder. But it can be estimated that the rutting will be lower than the rutting observed at 56°C. So, the observations made at 56°C will hold for 50°C also, and the trend will remain the same at 50°C and 56°C. Two main conclusions can be drawn based on the rut depths for this group of binders: (a) for these high-stiffness binders, the rutting resistance is driven more by the stiffness than by the percent recovery, and (b) there is no statistically significant difference in rutting between the two mixtures at 56°C.

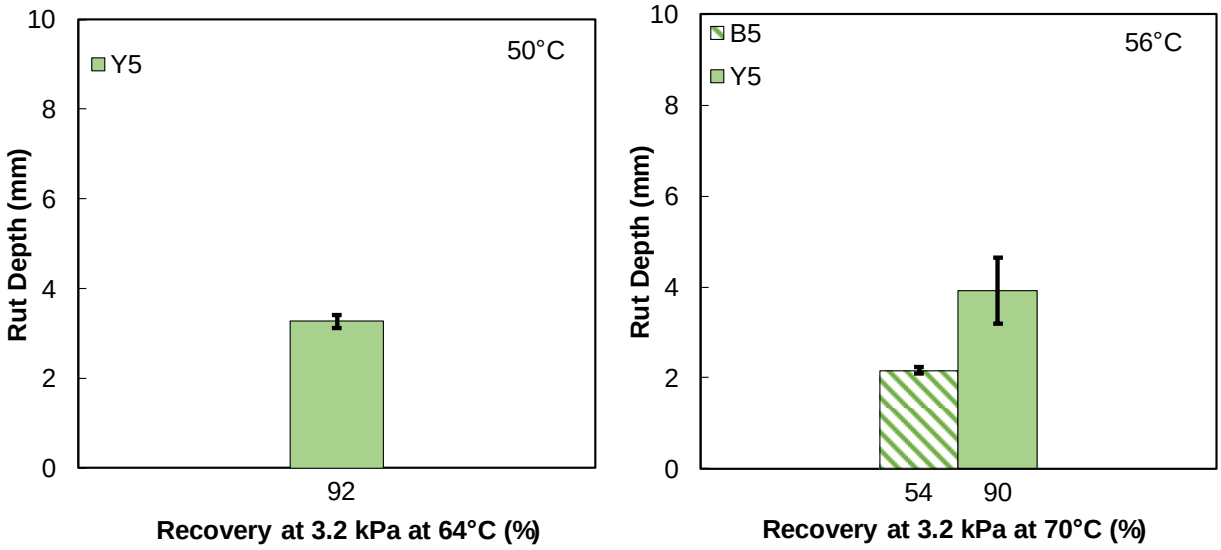

Figure 58. Rut Depth for Asphalt Mixtures Prepared with Group J Binders

Binders in Group K. This group consists of two binders, B2 and D0.5. Even though B2 has higher recovery than D0.5, the rut depths for mixtures TB2 and TD0.5 are very similar at both 50°C and 56°C, as seen in Figure 59. Statistically, there is no significant difference between the two rut depths. Recovery is seen to have minimal effect on rut depths in this set of binders.

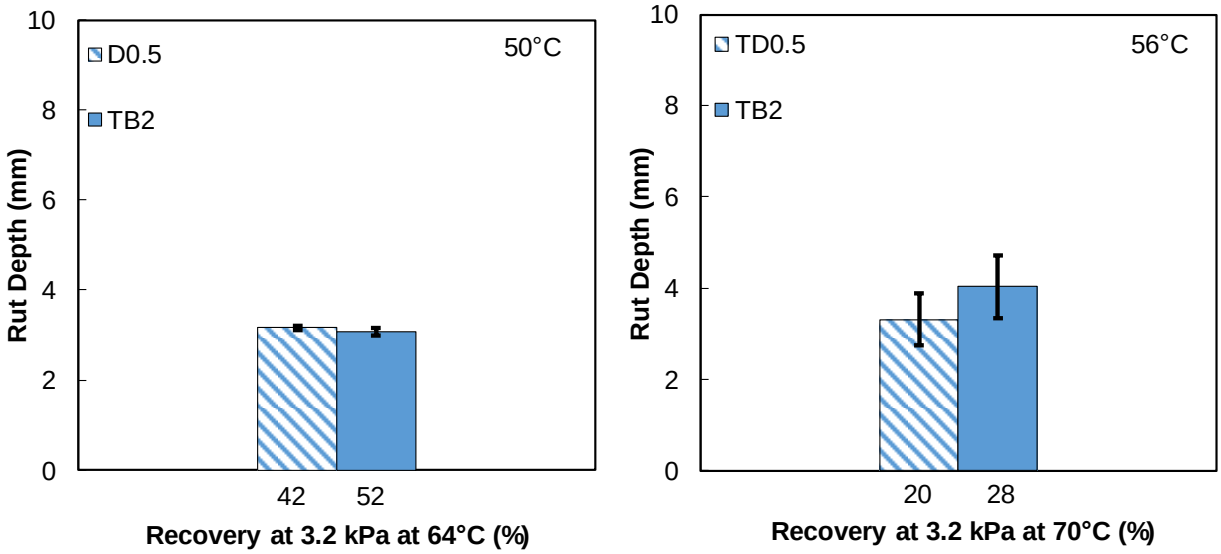

Figure 59. Rut Depth for Asphalt Mixtures Prepared with Group K Binders

Binders in Group L. This group consists of three binders, X3, A3-B, and A4. The rut depths for these binders were calculated at 44°C and 50°C. Binder A4 was also tested at 56°C while X3 and A3-B were tested at 44°C. In this group of binders, it is seen that rutting increases as the recovery increases, as shown in Figure 60. However, in this set of mixtures, there is no statistically significant difference between the mixtures. It is worth noting here that though the difference between TX3 and TA4 is high, the inherent variability of TX3 is causing the difference to be statistically insignificant. A better repeatability in TX3 will make the difference statistically significant.

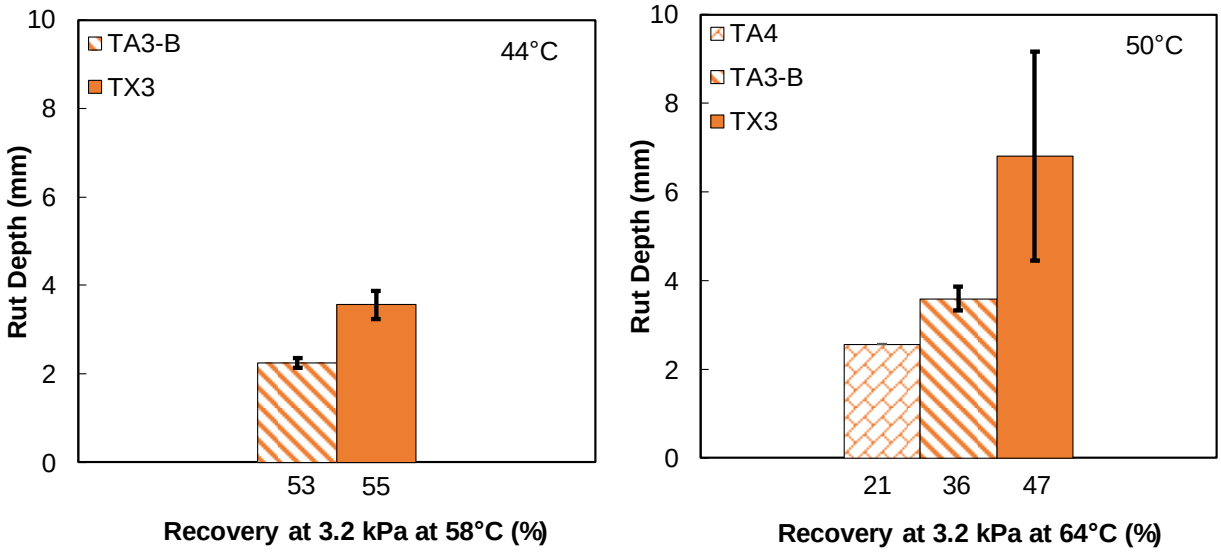

Figure 60. Rut Depth for Asphalt Mixtures Prepared with Group L Binders

Binders in Group M. This group consists of two binders, A2-B and A3. The rut depths for the corresponding mixtures are presented in Figure 61. This set of mixtures, because of their lower modulus, produce higher rut depths. Still, there is no statistically significant difference between the rut depths of the two mixtures. Also, as in the previous sets of mixtures, there is no positive effect of recovery on rut depths.

The main observations from the rutting analysis are as follows:

1. For the gradation used in the present study, very little rutting is seen in the asphalt mixtures. These rutting values are far from the widely accepted limit of 20 mm, and so are believed to represent realistic mixtures for Arizona.
2. There is no statistically significant difference to suggest that recovery has an effect on rutting performance.
3. The rutting resistance of the above mixtures depends more on the modulus of the binder and of its corresponding mixture than on the recovery of the binders.

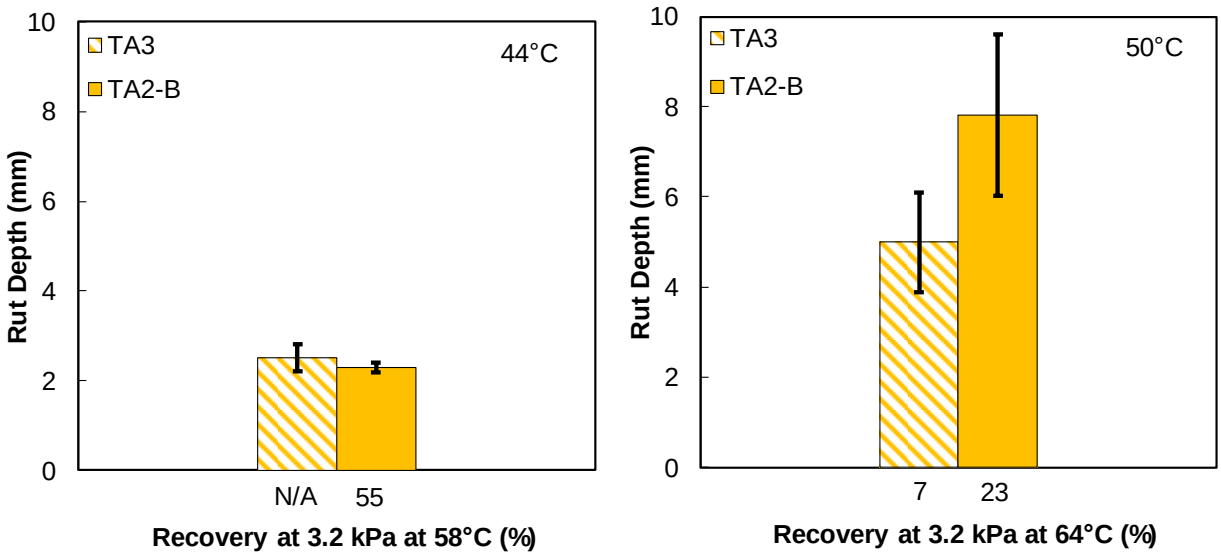

Figure 61. Rut Depth for Asphalt Mixtures Prepared with Group M Binders

Axial Fatigue Test

Similar to the HWTT, the purpose of the axial fatigue test was to ascertain the impact of MSCR percent recovery on the fatigue performance of binders listed in Table 40. The fatigue tests were conducted at an intermediate temperature of 18°C and were run at four strain levels, which were estimated using an expectation that the material would fail in less than 10,000 cycles, between 10,000 and 50,000 cycles, between 50,000 and 100,000 cycles, and after more than 100,000 cycles. The fatigue test data were analyzed using simplified viscoelastic continuum damage (S-VECD) theory as explained in Appendix C. The result of the S-VECD model is the damage characteristic curve, or *C* vs. *S* curve. *C* represents the integrity of the material, which decreases as the material is repeatedly loaded, and *S* represents the damage accumulated by the material during the test. The curves were fitted to the power function shown in Equation 14. Figure 62 shows the *C* vs. *S* curves that were developed for all nine binders listed in Table 40.

$$C = 1 - aS^b \qquad \text{(Eq. 14)}$$

The interpretation of the figure can be explained using an example. Consider two mixtures, TA3 and TA3-B. At its failure, TA3 has suffered a loss that brings its material integrity down to around 0.4 (40 percent), and has accumulated damage of around 1.0E+5. In contrast, TA3-B resists failure until its material integrity drops to around 0.2 (20 percent), and in the process it accumulates damage of more than 1.5E+5. While TA3-B accumulates more damage, it resists failure until its material integrity drops to 20 percent. This makes TA3-B superior to TA3 in fatigue resistance; TA3 accumulates less damage but fails at a higher material integrity level (40 percent).

While the *C* vs. *S* damage curves are good indicators of performance, they cannot be considered alone in assessing the fatigue performance of the asphalt mixtures. Simulations were carried out to estimate the strain level that the sample would need to be tested at to fail in 10,000, 100,000, and 1,000,000 cycles. The results of these simulations, called fatigue failure envelopes, are shown in Figure 63. The binders are color-coded to reflect the group they belong to, and the change from solid to dotted line indicates a decreasing level of MSCR percent recovery. In simpler terms, the vertical positioning of the line indicates the performance of the mixture in fatigue. The higher the vertical position, the better the fatigue resistance. So, for the example in the previous paragraph, TA3-B has a higher vertical position than TA3, and thus has better fatigue resistance. More specifically, at a fixed strain level, asphalt mixture prepared with binder A3-B can go through more cycles before failing than can A3. Among all binders prepared for the study, A3-B has the best resistance to fatigue, and A4 has the worst resistance.

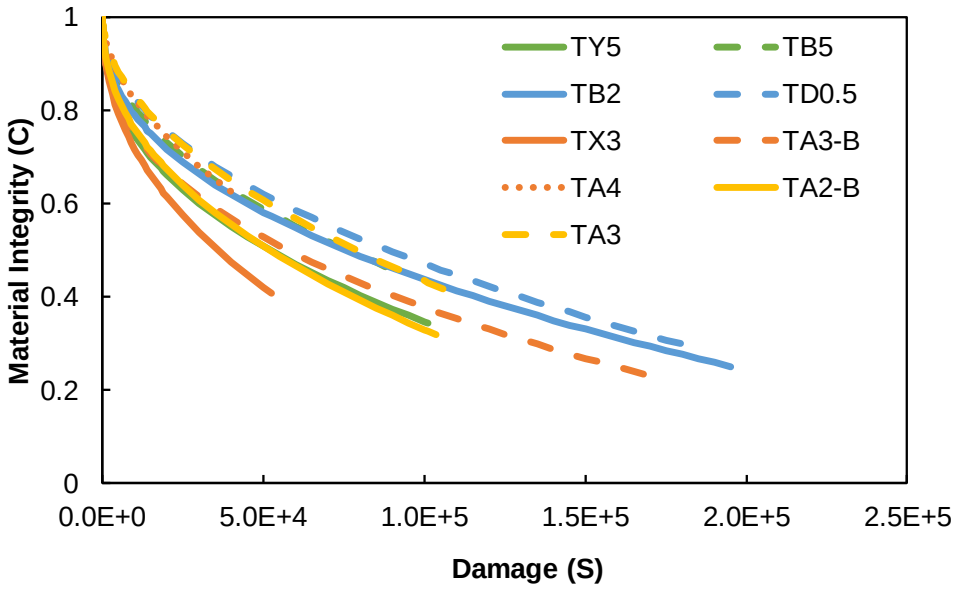

Figure 62. *C* (Material Integrity) vs. *S* (Damage) Curves Developed Using Data from Axial Fatigue Test

To aid understanding of the effect of MSCR recovery on the asphalt mixtures' fatigue resistance, analysis will proceed group-wise for the groups listed in Table 42.

Binders in Group J. This group consists of two binders, Y5 and B5. The *C* vs. *S* damage curves and the fatigue failure envelopes for this group are presented in Figure 64. It can be seen that Y5, which has the highest MSCR recovery in Table 42, has better fatigue resistance than B5. One of the main reasons for the poor performance of TB5 is that TB5 is an extremely stiff binder, PG 82-28, and it might have been too brittle at intermediate temperature, leading to early failure.

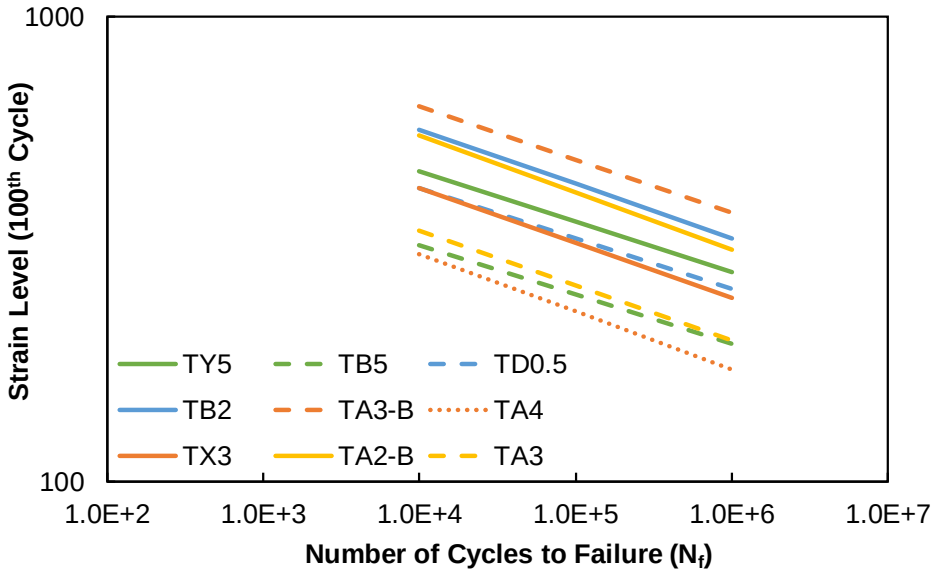

Figure 63. Simulated Fatigue Failure Envelopes for the Study Mixtures

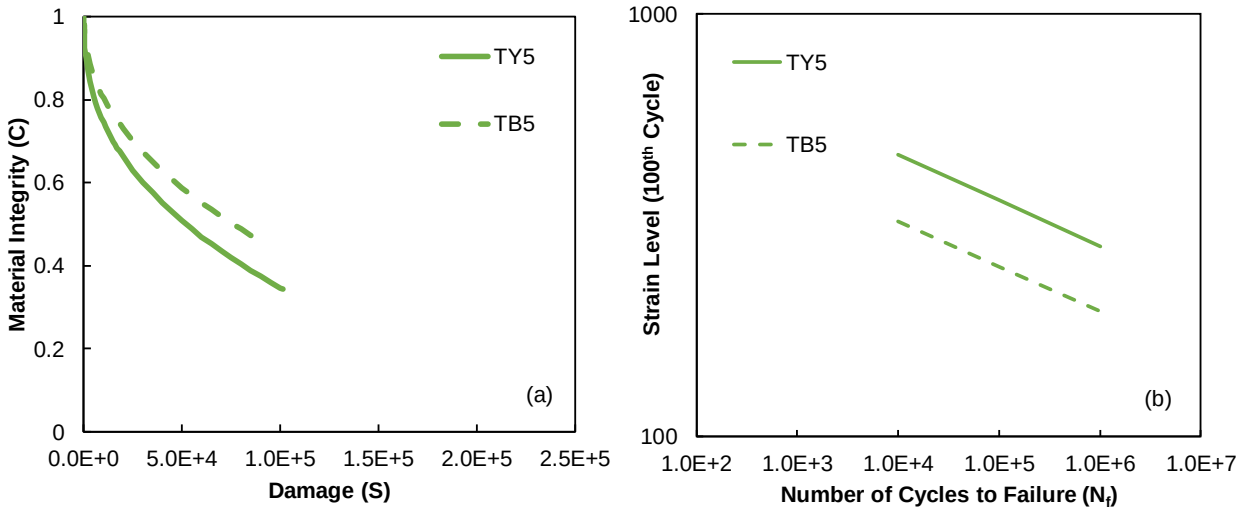

Figure 64. (a) *C* vs. *S* Damage Curves and (b) Simulated Fatigue Failure Envelopes for Asphalt Mixtures Prepared with Group J Binders

Binders in Group K. This group consists of binders B2 and D0.5. The *C* vs. *S* damage curves and the fatigue failure envelopes for these binders are presented in Figure 65. It can be seen that TB2, which has a higher MSCR recovery in Table 42 than does D0.5, possesses higher fatigue resistance. Overall, for this set of binders, higher MSCR recovery leads to better fatigue performance.

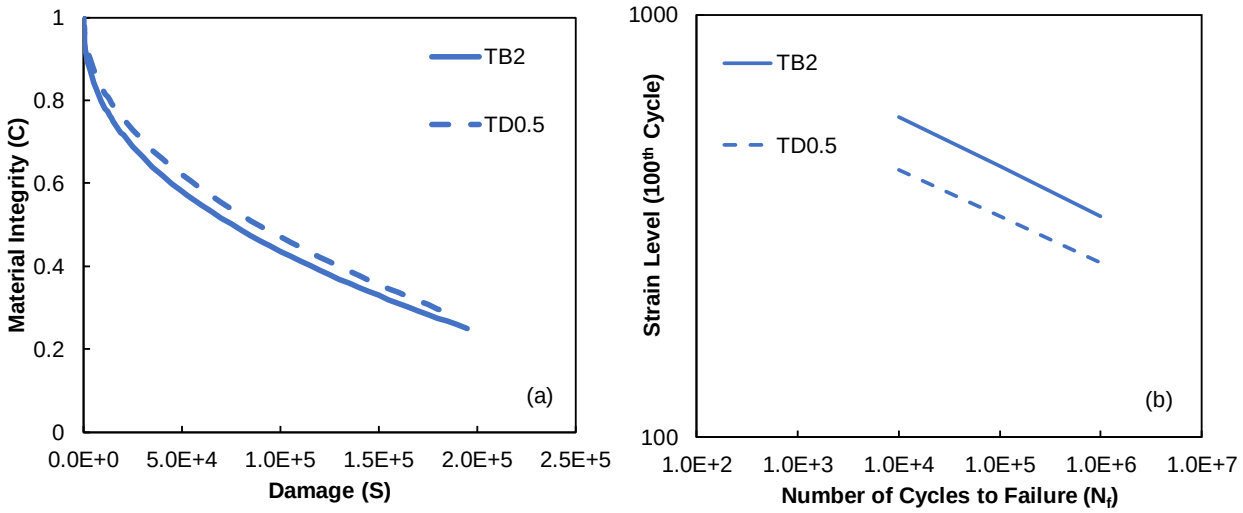

Figure 65. (a) *C* vs. *S* Damage Curves and (b) Simulated Fatigue Failure Envelopes for Asphalt Mixtures Prepared with Group K Binders

Binders in Group L. This group consists of binders X3, A3-B, and A4. The *C* vs. *S* damage curve, and the fatigue failure envelopes for these binders are presented in Figure 66. The first observation to be made about this figure is the striking difference in fatigue resistance between TA4 and the other two binders. This shows the importance of the cross-linking mechanism. Binder composition is unknown for TX3 but known for the other two: TA4 has 4 percent polymer, and TA3-B has 3 percent. However, TA4 was not modified with any cross-linking agent, whereas TA3-B was modified with sulfur. TX3 is known to contain both sulfur and PPA. It can be seen that both binders with cross-linking agents have better fatigue resistance than does TA4. A4 also has the lowest MSCR recovery in Table 42 among all three binders, so in this group recovery does have a positive effect on fatigue resistance. While X3 has the highest recovery, its fatigue resistance is second to A3-B's. Overall, in this group of binders, MSCR recovery is seen to have a positive effect, and what is even more clearly seen is the effect of polymer cross-linking on the performance of these mixtures.

Binders in Group M. This group consists of two binders, A2-B and A3. The *C* vs. *S* damage curves and the fatigue failure envelopes for the two binders are presented in Figure 67. In this set of binders, the effects of cross-linking are clearly visible, with non-cross-linked binder A3 having lower fatigue resistance than cross-linked A2-B. Overall, the positive effect of MSCR recovery is clearly seen in this set of binders as well.

Three main conclusions can be drawn from the fatigue analysis:

- MSCR recovery does have a positive impact on fatigue resistance of asphalt mixtures.
- Cross-linking mechanism in polymers has a positive effect on fatigue resistance.

- Mixtures with very high modulus, in spite of their binders having high MSCR recovery, will perform poorly in fatigue, as evidenced by the performance of TB5 and TD0.5.

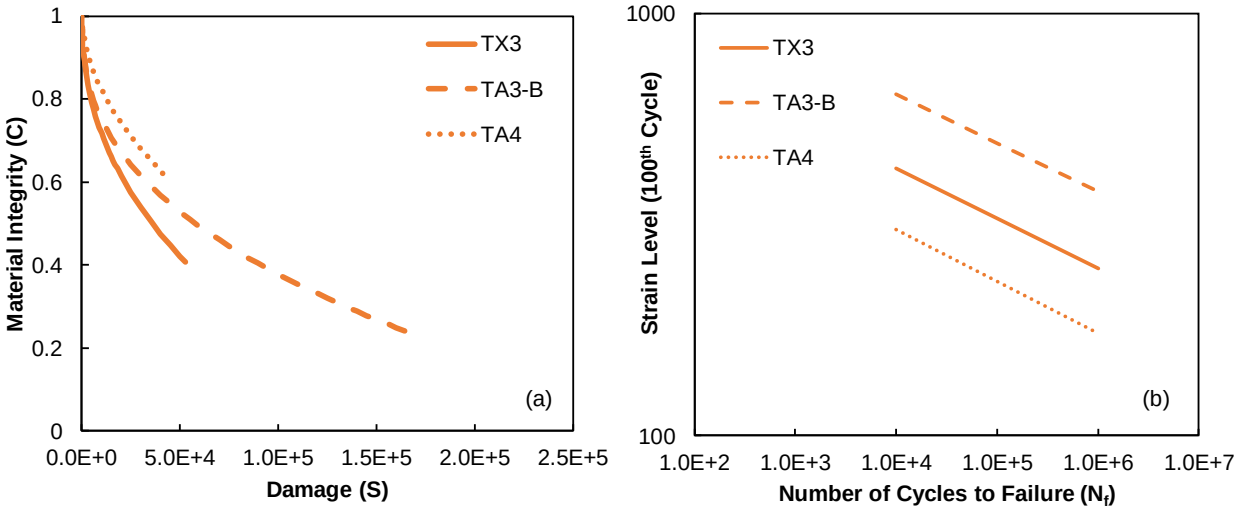

Figure 66. (a) *C* vs. *S* Damage Curves and (b) Simulated Fatigue Failure Envelopes for Asphalt Mixtures Prepared with Group L Binders

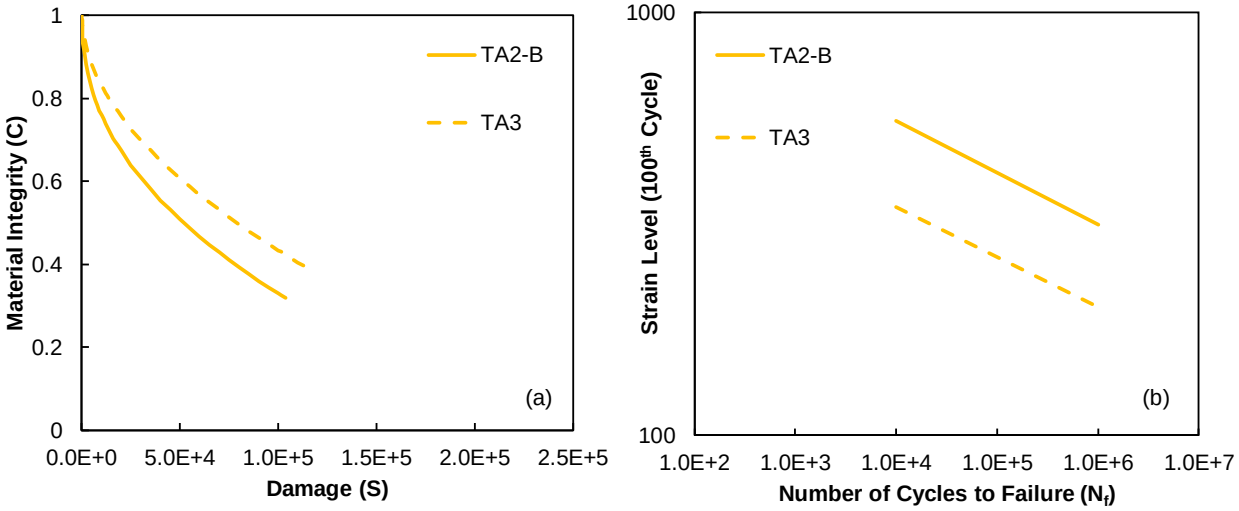

Figure 67. (a) *C* vs. *S* Damage Curves and (b) Simulated Fatigue Failure Envelopes for Asphalt Mixtures Prepared with Group M Binders

Comparison Between MSCR Percent Recovery, Elastic Recovery, and Fatigue Performance

The above section indicates that the improvement in fatigue resistance is captured well using the MSCR percent recovery parameter, in that increased MSCR percent recovery results in increased fatigue resistance. In this project, an elastic recovery test was also performed on all polymer-modified binders at 10°C, since the researchers wanted to see if the improvement in fatigue resistance could also be captured using the percent elastic recovery (%ER) parameter. To make this assessment, the researchers first compared the MSCR recovery with the %ER to see if any relationship exists. As Figure 68 shows, however, there is almost no correlation between MSCR recovery and elastic recovery.

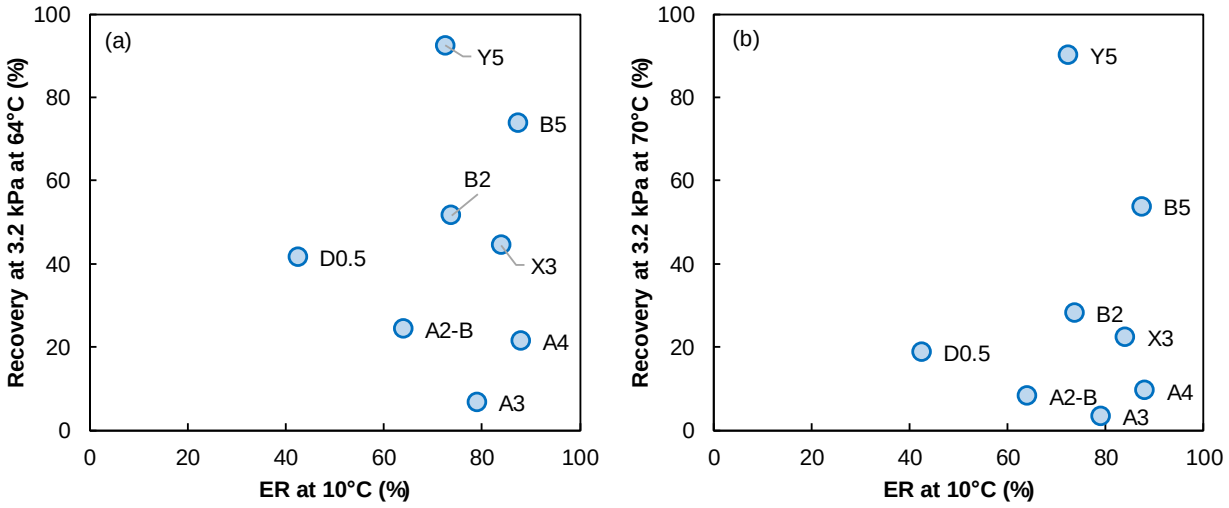

Figure 68. Relationship Between Elastic Recovery at 10°C and MSCR Recovery at (a) 64°C and (b) 70°C

To find the relative effect of MSCR recovery and %ER on fatigue behavior, researchers divided binders into the same groups as shown in Table 42. The fatigue life for all mixtures was first estimated at 400 με. Then, the increase in fatigue life between the binders within each group was calculated. Similarly, the increases in MSCR recovery and elastic recovery were computed. MSCR recovery at 64°C was used for this purpose. These results are tabulated in Table 44. The increase in fatigue life was then compared with the increase in MSCR recovery and the increase in elastic recovery. These comparisons are graphically plotted in Figure 69. There are two main inferences that can be drawn from these comparisons:

1. The increase in MSCR recovery is directly proportional to the increase in fatigue life, whereas for three of the four groups the increase in elastic recovery is inversely proportional to the increase in fatigue life. Also, in three of the four groups, binders with lower ER in their respective groups were seen to have better resistance to fatigue.

2. The elastic recovery relationship in part (b) of Figure 69 has a very steep slope in comparison with the slope of the MSCR recovery relationship in part (a) of the figure. This means that small changes in elastic recovery of the binder will have huge implications for the fatigue behavior of the corresponding mixture. On the other hand, small changes in MSCR recovery will change the fatigue life of the mixture by only a small amount, as the relationship has a relatively steady slope. This observation is important especially if there is a specification that is being formulated around MSCR percent recovery and elastic recovery.

Overall, MSCR percent recovery of a binder provides a better representation of the fatigue performance of the corresponding mixture than does elastic recovery.

Table 44. Relative Comparison Between MSCR Recovery, Elastic Recovery, and Fatigue Life

Group	Binder	Mix Fatigue Life at 400με (cycles)	% Increase in Fatigue Life	% Increase in MSCR Recovery	% Increase in Elastic Recovery
J	Y5	39,941	2842.7	25.2	–17.1
	B5	1,357			
K	B2	212,335	1020.6	24.0	73.5
	D0.5	18,949			
L	X3	18,049	1386.9	107.7	–4.5
	A4	1,214			
M	A2-B	142,093	4775.4	258.8	–19.0
	A3	2,914			

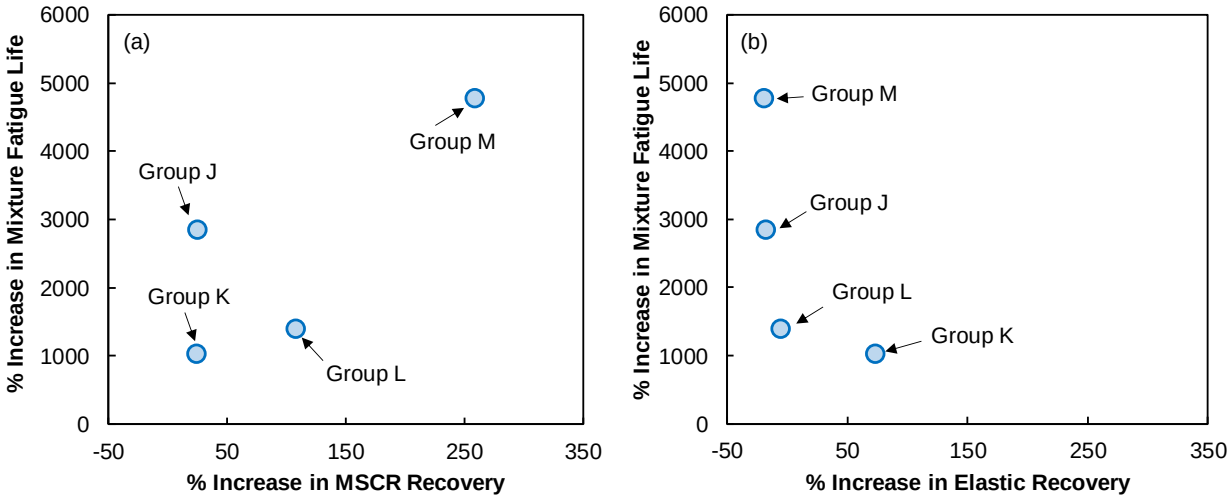

Figure 69. Graphical Representation of Relative Comparison Between MSCR Recovery, Elastic Recovery, and Fatigue Life

SUMMARY

In the portion of the project that this chapter describes, nine asphalt mixtures were tested to evaluate the effect of MSCR percent recovery on the performance of the mixtures. Binders with similar $J_{nr3.2}$ and varying MSCR percent recovery were divided into four groups based on their $J_{nr3.2}$ values. Comparisons were made based on the results obtained from three types of tests: the dynamic modulus test, the HWTT, and the axial fatigue test. Based on the mixture performance results presented above, it can be said that the MSCR percent recovery of binders has a significant effect on the dynamic modulus of asphalt mixtures, especially at intermediate and high temperatures. Binders with lower MSCR recovery will have a higher dynamic modulus. Also, the effect of MSCR recovery on the fatigue performance of the asphalt mixtures can be clearly seen. Binders with high MSCR recovery will have a greater fatigue resistance. However, MSCR percent recovery has little to no effect on the rutting resistance of the asphalt mixtures at the temperatures tested in this study. It can also be said that rut depths and rutting resistance of asphalt mixtures is more a function of the binder and mixture modulus than of the MSCR percent recovery.

CHAPTER 7. ANTICIPATED IMPACTS OF A CHANGE TO AASHTO M 332

INTRODUCTION

This chapter summarizes the current AASHTO M 332 specification and its pertinent parameters, and also presents the recommended specification that the research team has developed based on historical ADOT data and the experimental results in Chapters 5 and 6. The goal of this chapter is to assess the impact of transition to the AASHTO M 332 specification on the suppliers in Arizona. To do this, the research team took a detailed look at various aspects of the M 332 specification and surveyed supplier perspectives on the potential change in specification. The chapter summarizes the results of this assessment.

DEVELOPMENT OF RECOMMENDED SPECIFICATION

Current AASHTO M 332 Specification Table

The AASHTO M 332 specification is similar to the AASHTO M 320 specification. Two areas where these standards differ are in their RTFO high-temperature specification criteria and the PAV intermediate-temperature criteria (see Appendix A for the grading tables from both standards). In the AASHTO M 332 standard, a traffic-level-dependent J_{nr} limit is used for RTFO-aged binder instead of the single stiffness measure used in AASHTO M 320. AASHTO M 332 supplements the AASHTO M 320 temperature grade with one containing four different traffic-level grades ranging from (S)tandard (low-to-moderate-volume roads) to (E)xtreme (high-volume roads plus standing traffic). This additional grading parameter allows for objective and performance-based binder specifications for both climate and traffic conditions. With regard to the PAV intermediate-temperature criteria, AASHTO M 332 increases the specification limit for $|G^*|\sin\delta$ for H, V, and E binders from 5000 kPa to 6000 kPa. In AASHTO M 320, binders that grade as H, V, or E are those that have been grade-bumped to the next-highest temperature grade for traffic considerations. Under AASHTO M 332, the intermediate-temperature testing would occur at 3°C lower than the temperature used in a grade-bumping scenario. The increase of the $|G^*|\sin\delta$ limit to 6000 kPa thus accounts for existing practice and provides enough leeway for existing binders to still pass the specification. The third contribution from AASHTO M 332 is a function to delineate between polymer-modified binders that have sufficient cross-linking and non-polymer-modified or polymer-modified binders without sufficient cross-linking (see Chapter 1, Figure 1).

Investigation of Aspects of AASHTO M 332 Specification Table

To develop the recommendations shown later in this chapter, the research team considered various aspects of the specification table. Each was investigated using information from the literature review, from the experiments reported in Chapters 5 and 6, or both. The sections below detail the findings.

J_{nr} Difference

The parameter J_{nrdiff} is defined as the percent difference between J_{nr} at 0.1 kPa and J_{nr} at 3.2 kPa, as shown in Equation 15. It is included in the AASHTO M 332 specification to control for the stress

sensitivity of the binders. While not explicitly stated or well defined in the literature, the original intent of placing an upper specification limit of 75 percent on the J_{nrdiff} parameter was to set a limit on the change in a binder's nonrecoverable creep compliance (J_{nr}) as a safety factor in case a pavement experiences loading stress or temperatures that are higher than expected (D'Angelo 2009, D'Angelo 2010, Anderson 2011).

$$J_{nrdiff} = \frac{[J_{nr3.2} - J_{nr0.1}]}{J_{nr0.1}} \times 100 \quad \text{(Eq. 15)}$$

While correlations between rutting performance and J_{nr} have been documented for both unmodified and modified binders, relationships between laboratory-measured changes in J_{nr} across the range of applied stress (currently assessed using J_{nrdiff}) and changes in the field performance of asphalt mixtures are nonexistent in the literature. Yet it remains unknown whether J_{nrdiff} has the ability to provide meaningful insight into the relationship between laboratory-measured changes in J_{nr} across the range of applied stress and changes in asphalt mixture field performance caused by increased stresses and higher temperatures. As a result, the inclusion of the J_{nrdiff} parameter in the current AASHTO M 332 specification presents a problem. Agencies and suppliers working with AASHTO T 350 and AASHTO M 332 have reported challenges in meeting the J_{nrdiff} specification especially for modified binders with low J_{nr}. This problem becomes more pronounced for binders with $J_{nr3.2}$ values less than 0.5 kPa^{-1}. Reported J_{nrdiff} values can be more than 400 percent for modified binders that anecdotally perform well in pavements (Dongre 2016). This issue was also seen with some of the polymer-modified binders in this study. In addition, it has become apparent that J_{nrdiff} is extremely variable. Proficiency sampling across the hundreds of laboratories that participate in the AASHTO accreditation process shows that many labs receive very low scores on J_{nrdiff} despite having very good scores on the other AASHTO T 350 parameters (Dongre 2016).

As a potential solution to the specification problem, Dongre (2016) presented a modification of the MSCR method to stabilize the observed variation in the J_{nrdiff} parameter. This modification included testing at 0.32 kPa rather than 0.1 kPa and increasing the loading time from one to three seconds. While the decreased variability results obtained were promising, the fact remains that binders with small $J_{nr3.2}$ can still have very large J_{nrdiff} values. Recent recommendations from the national Asphalt Binder Expert Task Group are similar and essentially suggest testing at 0.8 kPa instead of 0.1 kPa. These methods attempt to overcome the issue by modifying the test procedure to yield higher J_{nr} values at the lower stress level by increasing the load level and/or load time and thus reducing the recoverable strain. While this approach deserves consideration, it does not address the larger challenge of relating laboratory-measured changes in J_{nr} across the range of applied stress to changes in field performance.

A study conducted by Stempihar et al. (2018) identified two main issues with the J_{nrdiff} parameter. The authors found that the parameter inaccurately represents stress sensitivity in the semilogarithmic domain and relates poorly to pavement performance. They evaluated the parameter's relationship to performance by relating the J_{nrdiff} to incremental rut depth. The idea behind using incremental rut depth was that the initial MSCR test data and observed rut depths on the Mississippi I-55 test section indicated that a 50 percent reduction in $J_{nr3.2}$ resulted in an approximate observed field rut depth reduction of 50

percent (D'Angelo 2009, D'Angelo 2010). To support the belief of Stempihar et al. (2018) that stress sensitivity of binders should be assessed in the semilogarithmic domain, the research team in the present Arizona study compared an incremental change in rutting (50 percent in this case) with the resultant J_{nrdiff} values for the Arizona binders. The results are presented in Figure 70. Gundla (2018) showed that the findings of Stempihar et al. (2018), who used historical data from Arizona binder testing, can be extended to study binders used in this project. For this comparison, rut depth was first predicted for $J_{nr3.2}$ using the I-55 relationship and then this resultant rut depth was increased by 50 percent. Next, resultant $J_{nr3.2}$ was back-calculated using the I-55 relationship and the rut depth with the 50 percent increase. Finally, resultant J_{nrdiff} was calculated using the original $J_{nr0.1}$ and resultant $J_{nr3.2}$ value associated with increased rut depth.

It can be seen from Figure 70 that the J_{nrdiff} parameter poorly characterizes the change in nonrecoverable creep compliance (between 0.1 and 3.2 kPa, semilogarithmic domain) and in associated incremental changes in rut depth. Using the laboratory rutting data obtained from the study mixtures, the researchers calculated the incremental rut depth for each mixture by taking the difference between the rut depths at two temperatures. This difference is termed $D_{rutting}$ and is shown in Figure 70. Overall, the data from the study binders and mixtures follow the trend presented using the simulated incremental rut depth data. More importantly, the data confirm that J_{nrdiff} does not show a strong relationship with performance. Note that both polymer-modified and non-polymer-modified binders are included in this analysis, but it is mainly the polymer-modified binders that exhibit high J_{nrdiff}.

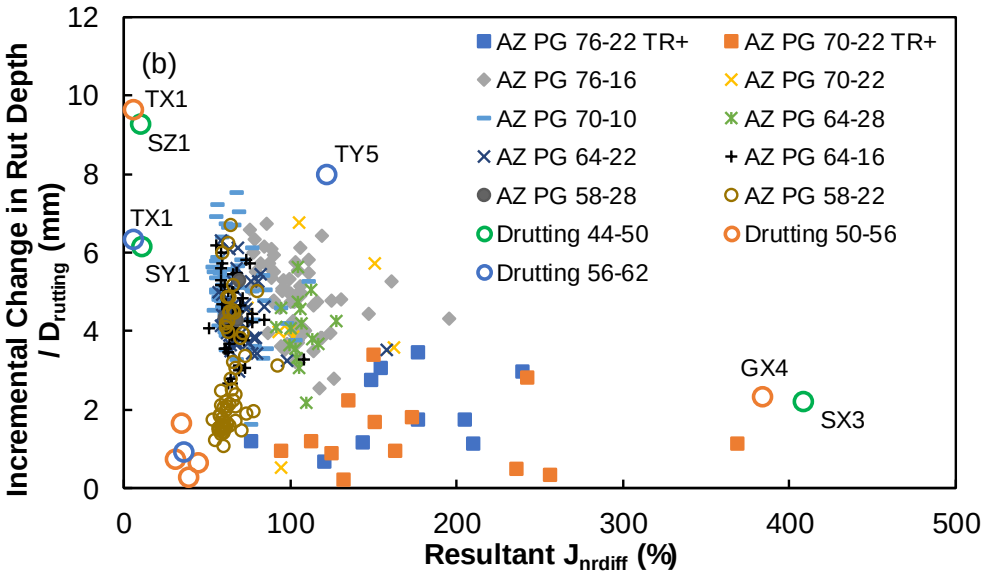

Figure 70. Relationship Between an Incremental Increase in Rut Depth (Including Laboratory Calculated Rut Depths) and Resultant J_{nrdiff}

Besides uncertainty in in-service load levels, the second argument in favor of J_{nrdiff} is that it acts as a surrogate parameter for temperature sensitivity. One original intent of the 75 percent limit on J_{nrdiff} was to ensure that the change in binder nonrecoverable creep compliance would be such that, if the binder were tested at a temperature that was 6°C higher, the new $J_{nr0.1}$ value would be at or below the $J_{nr3.2}$ at the lower temperature. Thus, by limiting the change in J_{nr} between 0.1 kPa and 3.2 kPa, J_{nrdiff} essentially serves to limit the nonrecoverable creep compliance of the binder if in practice the binder is exposed to a temperature 6°C higher than the specified performance-grade temperature. However, Stempihar et al. (2018) demonstrated that this concept may not be applicable across a wide range of binders by comparing J_{nrdiff} and a change in $J_{nr3.2}$ when the same binder is tested at a 6°C higher temperature. The data set was examined by comparing J_{nrdiff} with the percent difference in $J_{nr3.2}$ as defined in Equation 16.

$$\%Difference\ J_{nr3.2} = \frac{\left[J_{nr3.2(T+6)} - J_{nr3.2(T)}\right]}{J_{nr3.2(T)}} \times 100 \qquad \text{(Eq. 16)}$$

Where $\%\ Difference\ J_{nr3.2}$ = percent difference in $J_{nr3.2}$ for a 6°C increase in test temperature

$J_{nr3.2(T)}$ = average nonrecoverable creep compliance at 3.2 kPa (test temperature, T°C)

$J_{nr3.2(T+6)}$ = average nonrecoverable creep compliance at 3.2 kPa (T+6°C)

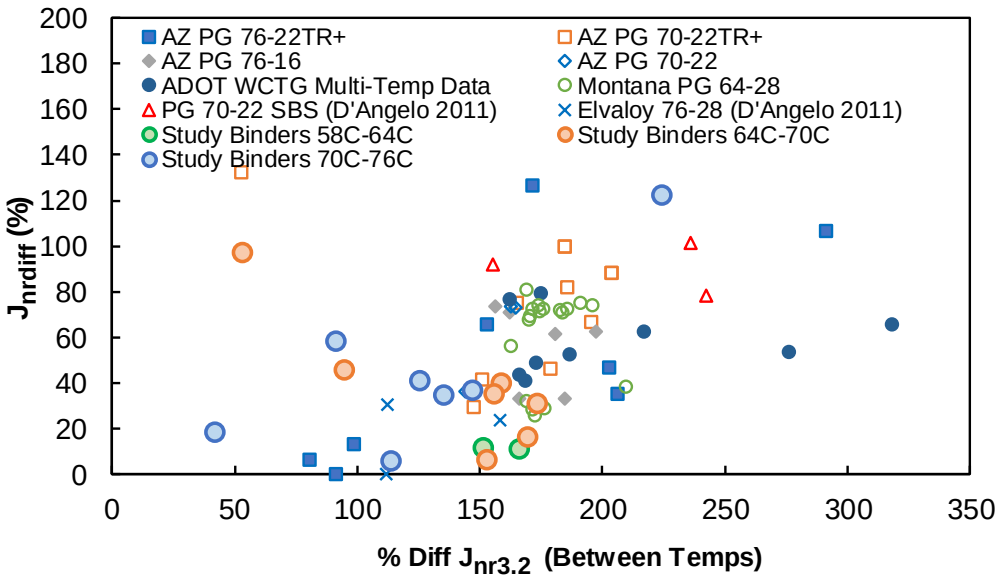

Figure 71. Relationship Between J_{nrdiff} and the Percent Change in $J_{nr3.2}$ with Temperature

Figure 71 presents a graphical summary of the correlations in AASHTO T 350 between J_{nrdiff} and percentage change in $J_{nr3.2}$ for a 6°C incremental temperature increase. Data from Stempihar et al.'s

(2018) original investigation and from the binder tests in the current study are also included in Figure 71. The graph shows that J_{nrdiff} does not demonstrate a correlation with the percent difference in $J_{nr3.2}$ for a 6°C increase in test temperature; therefore, it is not a good indicator of the temperature sensitivity of a binder in AASHTO T 350. J_{nrdiff} currently serves to address the uncertainty between the stress levels applied in the MSCR test and the actual stress levels exerted on asphalt pavements. But equally important is the goal of addressing the uncertain relationship between increased temperature in the MSCR test and the impacts of increased temperature on asphalt pavements. However, the Figure 71 analysis shows that J_{nrdiff} does not provide a promising means to address this uncertainty.

|G|sin δ of PAV-Aged Asphalt Binder*

If the AASHTO M 332 specification is adopted, one major change will be the elimination of grade bumping. The effect of this practice on intermediate-temperature testing has been to increase the test temperature by 3°C above that required by climate alone. For example, currently ADOT may specify PG 76-16 binder for a location in a climate requiring PG 70-16, but for which the traffic condition is severe. Under this scenario, the climate-based intermediate temperature for grading is 31°C, but the temperature that the grade-bumped binder is tested at is 34°C because that is the appropriate intermediate temperature for PG 76-16 binder. The effect of grade bumping is to produce binders with a higher stiffness at the intermediate temperature for a given climatological grade. AASHTO M 332 accounts for this potential by increasing the intermediate-temperature threshold from 5000 kPa to 6000 kPa when H, V, or E traffic grades are specified. Table 45 shows the increase in $|G^*|\sin\delta$ of the study binders for every 3°C decrease in temperature.

Table 45. Increase in $|G^*|\sin\delta$ of the Study Binders for Every 3°C Decrease in Temperature

Binder Designation	Change in |G*|sin δ/3°C (kPa)	$\|G^*\|\sin\delta$ (kPa)		
		At $T_{critical}$	At $T_{critical}$ – 3°C	At $T_{critical}$ – 6°C
X1	1249.0	2772.8	4021.8	5270.8
X2	725.5	2309.3	3125.5	3851.0
X3	417.0	1107.5	1582.5	1999.5
X4	445.1	1123.2	1645.7	2090.8
X5	762.5	1860.5	2749.4	3511.9
Y1	952.7	2737.7	3815.5	4768.2
Y2	698.6	2156.5	2957.3	3655.8
Y3	653.2	2087.4	2824.2	3477.4
Y4	1384.8	4286.3	5867.0	7251.8
Y5	423.5	1210.5	1694.8	2118.3
Y6	388.9	1131.6	1548.7	1937.6
Z1	1040.3	3394.8	4518.1	5558.4
Z2	888.8	2998.8	3999.4	4888.2
Z3	1185.5	3183.2	4242.6	5428.1
Z4	820.6	2725.5	3646.0	4466.6

For non-polymer-modified binders, the increases ranged from 653.2 kPa to 1384.8 kPa, and for polymer-modified binders, the increases ranged from 388.9 kPa to 762.5 kPa, meaning that polymer-modified binders are less sensitive to temperature changes. Also presented in the table is the $|G^*|\sin\delta$ value at the critical intermediate temperature for each binder and at temperatures 3°C and 6°C lower. If the location (climate) warrants that $|G^*|\sin\delta$ be tested at 6°C lower (equivalent to two grade bumps in the current binder specification), all of the study binders meet the intermediate-temperature criteria, provided the threshold is set at 6000 kPa. If the location warrants that $|G^*|\sin\delta$ be tested at 3°C lower, then all the study binders, except Y4, are below the threshold of 6000 kPa. However, binder Y4 is a PG 76-16 binder, and two grade bumps would mean that this binder would be used in a PG 64-16 climate. In that case, there are arguments (discussed in the next section) for possibly reducing the PAV aging temperature, which may compensate for the increase in $|G^*|\sin\delta$.

Impacts of PAV Aging Temperature

The issue of PAV aging temperature is important if ADOT decides to adopt the AASHTO M 332 specification as it currently exists, or the modified version of the specification presented in this chapter. It is most important in locations where PG 64H, PG 64V, or PG 64E would be specified. Currently in these locations, the ADOT specifications require PG 70 or PG 76 binder, which are graded after PAV aging at 110°C. Under the AASHTO M 332 specification, all traffic grades of PG 64 binders are aged at a PAV temperature of 100°C, while all traffic grades of PG 70 binders can be aged at a PAV temperature of 110°C. Thus, there is a disconnect between ADOT's current practice and the AASHTO M 332 specification. For the binders currently specified as a result of grade bumping, the transition to AASHTO M 332–based specification will change the acceptance criteria for the binder at the intermediate temperature. The intermediate temperature for the $|G^*|\sin\delta$ parameter will be lower than under current practice (see the previous section and compare the intermediate temperature for PG 76-16 [Y4] with that for PG 70H-16 [Y5]). This change results in an increase in $|G^*|\sin\delta$ value, provided the binder is aged at the same temperature as before. The AASHTO M 332 specification allows for some leeway in the upper threshold for the $|G^*|\sin\delta$ parameter in that the threshold is increased to 6000 kPa for H, V, and E binders.

Analysis to understand the potential implications of the change in aging temperature was limited in this project based on the project scope set by the ADOT Technical Advisory Committee. However, some limited study suggests that the binders, which grade as PG 58V and E and PG 64H, V, and E, also meet the requirements of PG 70S or PG 76S binders, which are currently aged at 110°C. The study was carried out by using the study binders for four different scenarios specifying PAV aging temperature. The four scenarios are as follows:

1. PAV aging temperature is based on the "S" grade of the binder. This is the current ADOT aging protocol.
2. PAV aging temperature is based on the "S" grade of the binder, but the $|G^*|\sin\delta$ parameter is set to a maximum of 5000 kPa.
3. PAV aging temperature is based on a 98 percent reliability-based climate grade. This would be strict adherence to the AASHTO M 332 guidance.

4. PAV aging temperature is based on a 98 percent reliability-based climate grade but the $|G^*|\sin\delta$ parameter is set to a maximum of 5000 kPa.

Table 46 presents the possible AASHTO M 332 grading for binders from Supplier X for the four different PAV-aging-temperature scenarios. The cells highlighted in green indicate that the grade has been experimentally confirmed. The cells highlighted in yellow indicate that the grade has not been experimentally confirmed. The grades printed in red indicate that the grade fails to meet the specification for that scenario, and the grades printed in bold text are additional grades necessitated by a change in PAV temperature.

Consider the example of X1 binder, which is a PG 70-10 in the current ADOT specification. In Scenario 1, the PAV aging temperature of the binder is 110°C, as the S grade of the binder is PG 70S-10. In ASU testing, this binder will also meet the requirements of PG 70S-16. The various PG grades that can be obtained are listed under Scenario 1. In this scenario, the binder will still meet the requirements of PG 64H-10 and PG 64E-16 even though it was aged at 110°C. However, in Scenario 2, if the $|G^*|\sin\delta$ parameter is restricted to 5000 kPa (i.e., if the grade-bumping-related adjustment explained in the previous section is ignored), then one of the grades, PG 64H-16, will fail to meet the specification.

In Scenario 3, the PAV aging temperature is now based on a 98 percent reliability-based PG grade. Under this scenario, for PG 70 and PG 76 binders to be graded as PG 64 H, V, and E, they have to be aged at 100°C. For X1 and X2 binders, this might result in the addition of one more grade—PG 64H-22 and PG 64E-28, respectively. In the case of PG 64E-28 binder, the critical intermediate temperature for this grade is 22°C, and at the 110°C aging level, the value of $|G^*|\sin\delta$ from Table 45 is estimated to be 5301 kPa. If the binder is aged at 100°C, this value will be even lower. Thus, it appears that the intermediate temperature criteria will be satisfied easily. For low-temperature BBR data, supplier guidance says that reduction in PAV temperature by 10°C increases the lower-temperature PG grade by one increment. Binder X2, aged at 110°C, passes the *S*-value and *m*-value requirements at –12°C, with values of 241 MPa and 0.302, respectively. That means that the binder can be used as PG 64E-22. When the binder aging temperature is reduced to 100°C, PG 64E-28 might be possible, since the binder stiffness will decrease and relaxation will improve at low temperatures. In scenario 4, when $|G^*|\sin\delta$ is restricted to 5000 kPa, the additional grade from X1 fails the specification, but the additional grade from X2, PG 64E-28, might still pass the specification. While Table 46 presents the grades for supplier X only, the grades for supplier Y and Z are presented in Appendix G.

In summary, the PAV aging-temperature decision has the potential to affect binder grading, but for the binders studied, the effects do not appear to be large. If the goal is to maximize the number of AASHTO M 332 grades that can be achieved from the current AASHTO M 320 binders, then Scenario 3 should be adopted, meaning that PG 64H, V, and E binders should be graded based on PAV testing at 100°C. However, the most direct translation of the current ADOT specifications would be to require all PG 64H, V, and E binders to be graded based on PAV testing at 110°C. As shown in the Potential Distribution of Grades section below, these binders may not constitute a large proportion of the binders supplied.

Table 46. AASHTO M 332 Grades for Binders from Supplier X for Four Different PAV-Aging-Temperature Scenarios

Scenario 1					Scenario 2				
Binder	**S Grades**	**H Grades**	**V Grades**	**E Grades**	**Binder**	**S Grades**	**H Grades**	**V Grades**	**E Grades**
X1	70S-10	64H-10	–	–	X1	70S-10	64H-10	–	–
	70S-16	64H-16	–	–		70S-16	64H-16	–	–
X2	76S-16	70H-22	–	64E-16	X2	76S-16	70H-22	–	64E-16
	76S-22	–	–	64E-22		76S-22	–	–	64E-22
X3	–	64H-22	–	58E-22	X3	–	64H-22	–	58E-22
	–	64H-28	–	58E-28		–	64H-28	–	58E-28
X4	–	–	64V-22	58E-22	X4	–	–	64V-22	58E-22
	–	–	64V-28	58E-28		–	–	64V-28	58E-28
X5	–	–	–	70E-22TR	X5	–	–	–	70E-22TR
	–	76H-22TR	–	64E-22TR		–	76H-22TR	–	64E-22TR
Scenario 3					**Scenario 4**				
Binder	**S Grades**	**H Grades**	**V Grades**	**E Grades**	**Binder**	**S Grades**	**H Grades**	**V Grades**	**E Grades**
X1	70S-10	64H-10	–	–	X1	70S-10	64H-10	–	–
	70S-16	64H-16	–	–		70S-16	64H-16	–	–
	–	**64H-22**	–	–		–	64H-22	–	–
X2	76S-16	70H-22	–	64E-16	X2	76S-16	70H-22	–	64E-16
	76S-22	–	–	64E-22		76S-22	–	–	64E-22
	–	–	–	**64E-28**		–	–	–	64E-28
X3	–	64H-22	–	58E-22	X3	–	64H-22	–	58E-22
	–	64H-28	–	58E-28		–	64H-28	–	58E-28
X4	–	–	64V-22	58E-22	X4	–	–	64V-22	58E-22
	–	–	64V-28	58E-28		–	–	64V-28	58E-28
X5	–	–	–	70E-22TR	X5	–	–	–	70E-22TR
	–	76H-22TR	–	64E-22TR		–	76H-22TR	–	64E-22TR
	–	–	–	64E-28TR		–	–	–	64E-28TR
XX	Acceptable grade, and experimental data exist				XX	Experimental data do not exist, and grade is estimated to be acceptable			
XX	Unacceptable grade, and experimental data exist				XX	Experimental data do not exist, and grade is estimated to be unacceptable			
XX	Additional grades added				–				

Percent Recovery for Rutting Performance

AASHTO M 332 does not make percent recovery (*%Recovery*) itself a specification parameter, but it does suggest it as a parameter to screen for the presence of polymer (see Chapter 1 and Chapter 4). Experiments were conducted to identify whether the percent recovery affects rutting performance, and to ensure that Arizona binders perform as expected under AASHTO M 332 (see Chapter 6 for the details). Based on these experiments, the researchers was concluded that the *%Recovery* parameter was not an indicator or predictor of rutting resistance. They found that for two binders with the same J_{nr}, the one with a higher *%Recovery* did not consistently outperform the one with a lower *%Recovery*. Additionally, there was no statistically significant difference identified in the experimental results that suggests *%Recovery* has an effect on rutting performance.

% Recovery as a Plus Specification

The current AASHTO M 332 specifies a functional relationship between J_{nr} and *%Recovery* at 3.2 kPa, which can be used for acceptance or rejection of polymer-modified mixtures. Historically, Arizona polymer-modified binders have lain well above the recovery curve, and some concerns have been expressed that adoption of the relationship as presented in the specification might lead to the acceptance of binders that are inferior to what ADOT is currently procuring. The experimental data presented in Chapter 6 showed that while *%Recovery* is not a good predictor of rutting performance, it is strongly related to the fatigue performance of asphalt mixtures. Thus, it may have value as a screening, or "Plus Specification," parameter. For this reason, the researchers have modified the relationship in AASHTO M 332 from its original form (shown in Chapter 1). The modification is justified by the following factors:

1. In this study and historically, Arizona binders have been found to lie above the published *%Recovery* line.
2. There are concerns that directly adopting the AASHTO M 332 curve may result in binders with lower *%Recovery* and possibly worse performance than the binders currently delivered to ADOT.
3. In this study, higher *%Recovery* correlates with better fatigue resistance. The amount of improved fatigue resistance continuously increases with higher *%Recovery*.
4. This relationship depends on J_{nr} values, meaning that there is no fixed *%Recovery* for all binders at all J_{nr} values. Asphalts with lower J_{nr} values require greater *%Recovery* to show similar fatigue performance benefits.
5. This study has also found that non-polymer-modified binders tested at a temperature resulting in a "low" J_{nr} may have high *%Recovery*. This can occur when testing non-polymer-modified binders at a low temperature in combination with PPA or possibly other modifiers. Thus, the positioning of the *%Recovery* line should be reasonably high to avoid such circumstances.

With these issues in mind, the researchers had the goal, in modifying the AASHTO M 332 curve, of setting the limits so that there would be no obvious likelihood that binder performance would be negatively affected by adoption of the modification. They also sought to create limits that suppliers could meet. The new limits, which are based on the testing and analysis completed in this research, are shown in Figure 72. The tests used are described in Chapter 6. Figure 73 shows the binders used for the development of the proposed relationship, and the location of those binders relative to the curve under both AASHTO M 332 and the proposed modification.

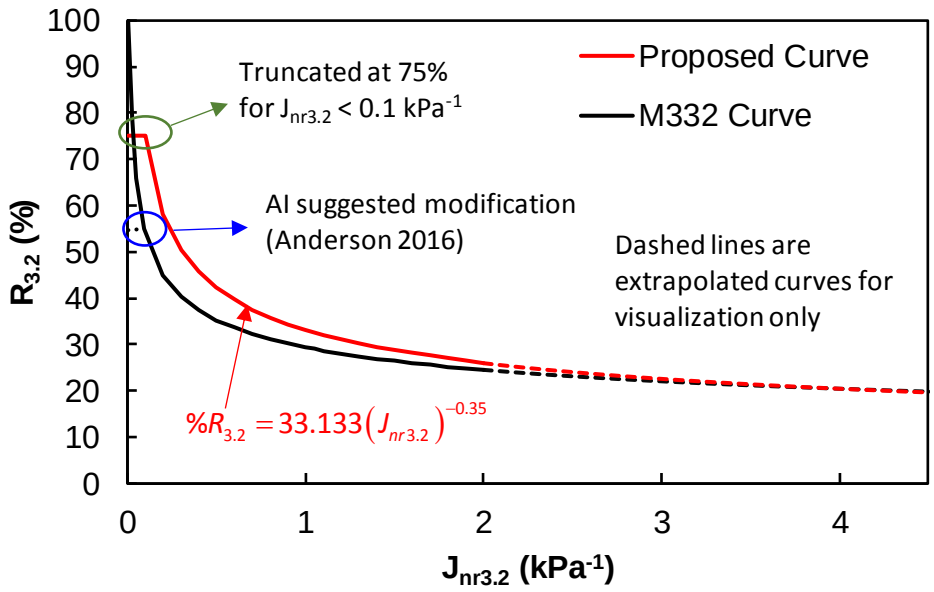

Figure 72. *%Recovery* Curve Under AASHTO M 332 and Under the Proposed Modification

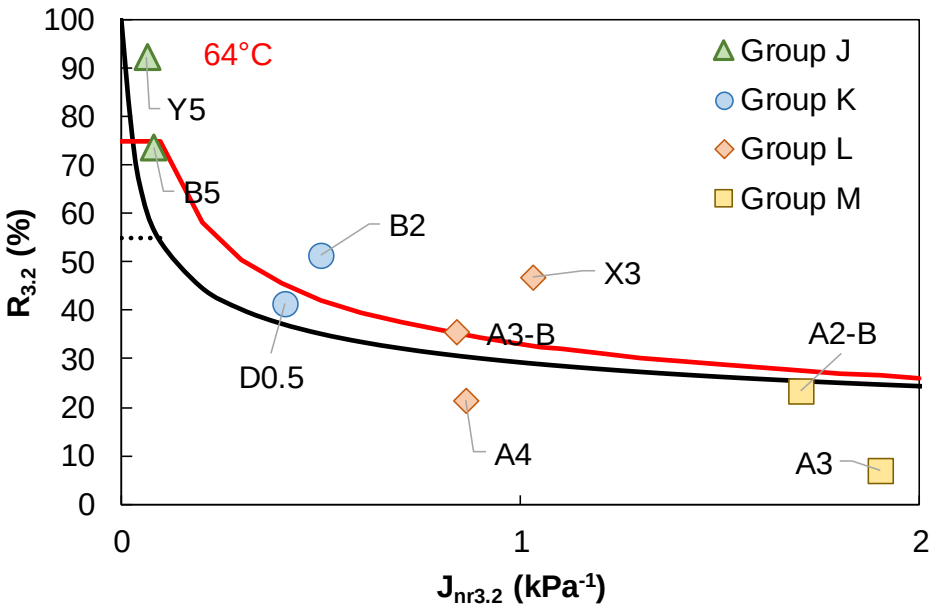

Figure 73. Position of the Laboratory-Prepared Binders in the *%Recovery* Space at 64°C Under AASHTO M 332 and Under the Proposed Modification

In Figure 74, the distance between the observed *%Recovery* curve and the proposed line is plotted against fatigue life. It can be seen that as the *%Recovery* value gets further from the curve, there is a

positive impact on fatigue performance. Therefore, the thresholds were set so that the binder with the lowest recovery within each group would not pass the modified specification. However, two exceptions exist. For group L binders, A3-B is used as the lowest-recovery binder, since A4 is already below the existing specification. For group M binders, since both A2-B and A3 are already below the existing specification, effort was made to match the modified curve to the existing curve for this range of $J_{nr3.2}$ onwards. The proposed curve does not go below the existing function in order to prevent non-polymer-modified binders, which are tested at lower-than-normal temperatures and/or are modified with PPA, from passing the limit. While the curve for low $J_{nr3.2}$ binders can be extended to 100 percent, this would eliminate many well-performing binders. In this study, the lower recovery value for binders with $J_{nr3.2}$ of less than 0.1 was 73 percent. Based on the evidence in Figure 74, it can be confirmed that any binder having recovery higher than 73 percent will see an increase in fatigue performance. Therefore, the curve was truncated at 75 percent. With this adjustment, Figure 73 provides a good visual basis for the selection of the modified curve, and Figure 74 validates the selection of the curve.

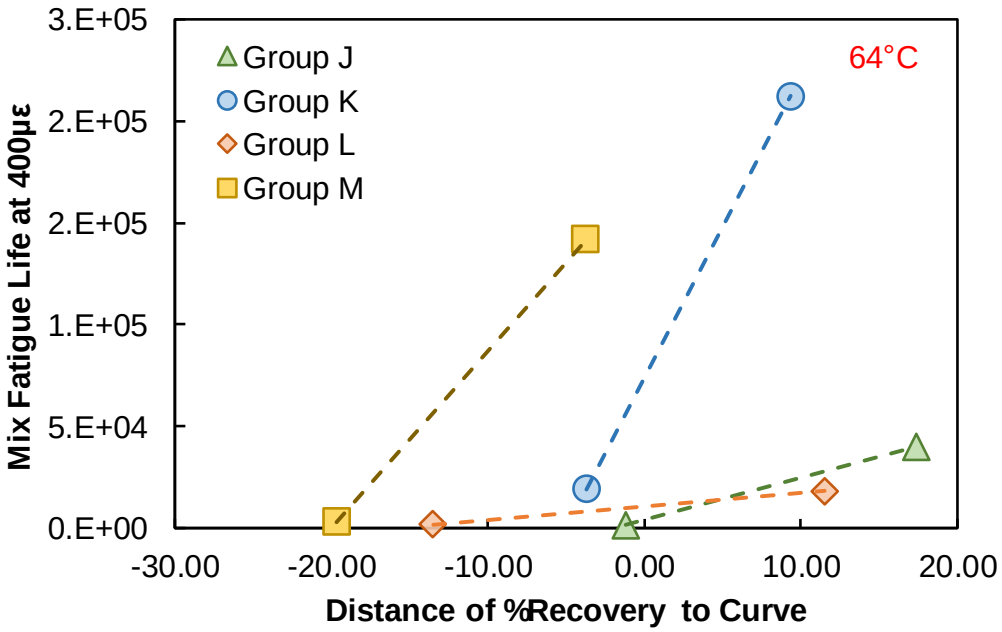

Figure 74. Relationship Between Mixture Fatigue Life and Distance of Binders' *%Recovery* Value from the Modified *%Recovery* Curve

Figures 75 to 77 show the locations of all binders in the current study and the binders from the study by Stevens et al. (2015), noted as historical database (HD). For these binders, the $J_{nr3.2}$ and *%Recovery* are taken at their high-temperature climate grade (e.g., for PG 64H-22 binder, $J_{nr3.2}$ and *%Recovery* are plotted in Figure 75 at 64°C). It can be seen that the polymer-modified binders used in the study and a majority of those in the historical data pass the modified specification. Note from Figure 76 the location of the HD PG 76-16 binder. In this figure, the $J_{nr3.2}$ and *%Recovery* are those measured at 64°C, demonstrating how non-polymer-modified binders can be positioned nearer to the threshold by reducing the test temperature. In this case, the binder would grade as PG 64E-16, but based on the

results of this study, would not perform as well in fatigue as another binder with a similar $J_{nr3.2}$ value but with *%Recovery* greater than 50 percent.

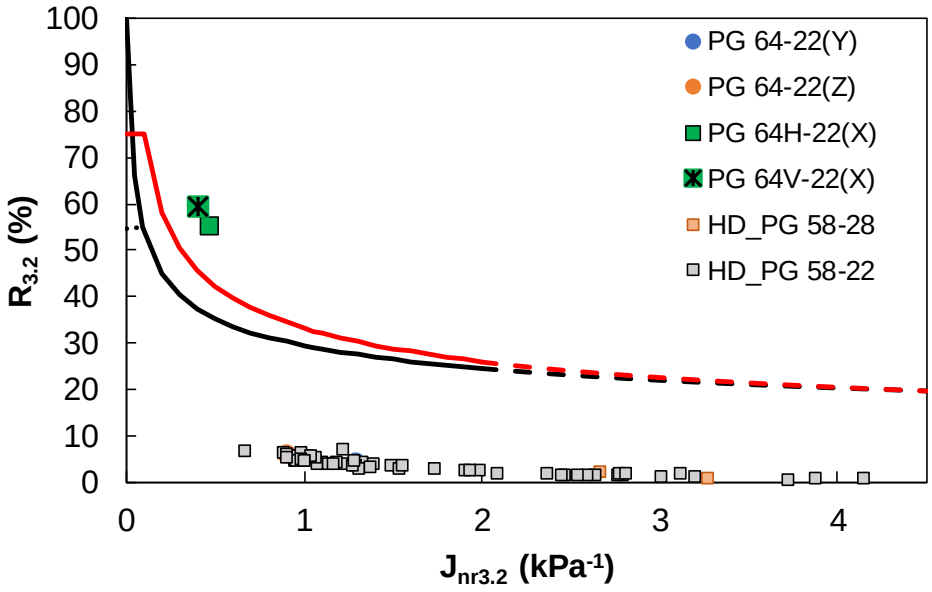

Figure 75. Comparison of Study Binders and Historical-Data Binders at 58°C in the Modified $J_{nr3.2}$ vs. *%Recovery* Space

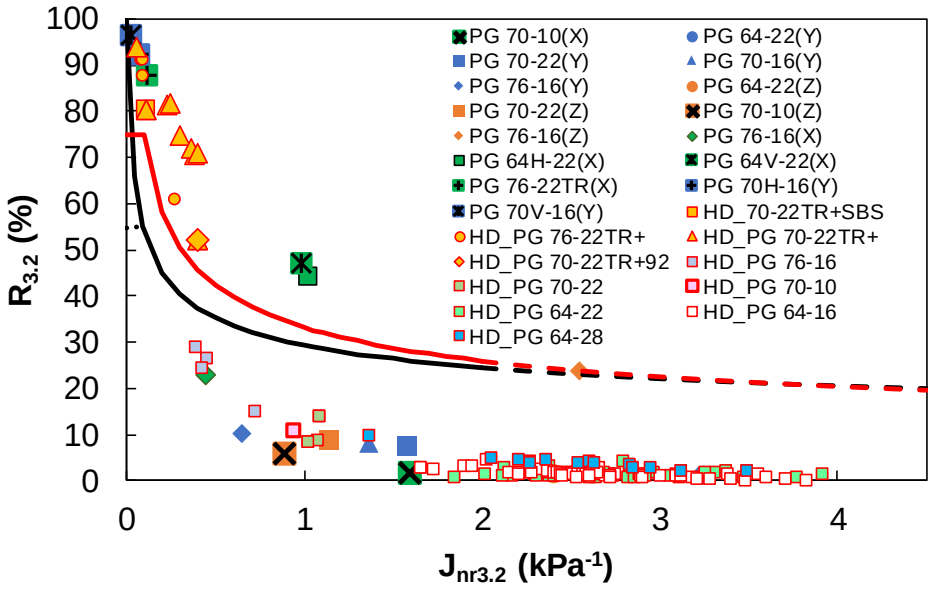

Figure 76. Comparison of Study Binders and Historical-Data Binders at 64°C in the Modified $J_{nr3.2}$ vs. *%Recovery* Space

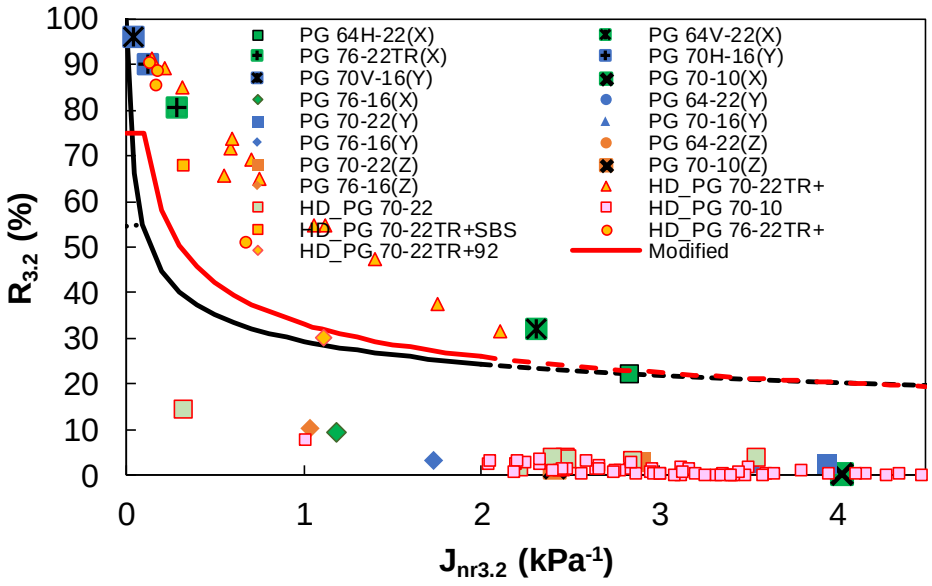

Figure 77. Comparison of Study Binders and Historical-Data Binders at 70°C in the Modified $J_{nr3.2}$ vs. *%Recovery* Space

Recommended Asphalt Grading Table for Arizona

Table 47 presents the recommended specification for PG grading of Arizona binders based on traffic grades. This table is a nearly direct translation of the AASHTO M 332 specification with two exceptions. First, the PAV aging temperatures for PG 64H, V, and E are 110°C, since this study did not investigate in detail the issue of PAV aging temperature but did find that for locations where ADOT is specifying PG 70 after grade bumping, the equivalent grade would be PG 64H binder. Also note that for all H, V, and E binders, the intermediate temperature threshold is kept at 6000 kPa. While most of the binders investigated in the current study would pass a lower threshold specification (e.g., keeping the threshold at 5000 kPa for H, V, and E binders), this would be a deviation from current practice in Arizona.

Table 47. Recommended Specification for Performance-Graded Arizona Asphalt Binders

Performance Grade	PG 58			PG 64			PG 70			PG 76	
	22	28	34	16	22	28	10	16	22	10	16
Average 7-day max. pavement design temp, °C[b]	<58			<64			<70			<76	
Min. pavement design temp, °C[b]	> –22	> –28	> –34	> –16	> –22	> –28	> –10	> –16	> –22	> –10	> –16
	Original Binder										
Flash point temp., T 48, min. °C	230										
Viscosity, T 316:[c] max. 3 Pa•s, test temp., °C	135										
Dynamic shear, T 315:[d] G*/sin δ, min. 1.00 kPa[e] test temp. @ 10 rad/s, °C	58			64			70			76	
	Rolling Thin-Film Oven Residue (T 240)[a]										
Mass change, max., percent[f]	1.00										
MSCR, T 350: Standard Traffic "S," $J_{nr3.2}$, max. 4.5 kPa^{-1}, J_{nrdiff}, max. 75%, test temp, °C	58			64			70			76	
MSCR, T 350: Heavy Traffic "H," $J_{nr3.2}$, max. 2.0 kPa^{-1}, test temp., °C	58			64			70			76	
MSCR, T 350: Very Heavy Traffic "V," $J_{nr3.2}$, max. 1.0 kPa^{-1}, test temp., °C	58			64			70			76	
MSCR, T 350: Extremely Heavy Traffic "E," $J_{nr3.2}$, max. 0.5 kPa^{-1}, test temp., °C	58			64			70			76	
	Pressurized Aging Vessel Residue (R 28)										
PAV aging temp., °C[g]	100			100 for S (110 for H, V, and E)			110			110	
Dynamic shear, T 315: "S," G* sin δ, max. 5000 kPa,[e] test temp. @ 10 rad/s, °C	22	19	16	28	25	22	34	31	28	37	34
Dynamic shear, T 315: "H," "V," "E," G* sin δ, max. 6000 kPa,[e] test temp. @ 10 rad/s, °C	22	19	16	28	25	22	34	31	28	37	34
Creep stiffness, T 313[h]: *S*, max. 300 MPa, *m*-value, min. 0.300, test temp. @ 60 s, °C	–12	–18	–24	–6	–12	–18	0	–6	–12	0	–6

[a] MSCR testing on RTFO residue should be performed at the PG grade based on the environmental high pavement temperature. Grade bumping is accomplished by requiring a lower J_{nr} value while testing at the environmental temperature.

[b] Pavement temperatures are estimated from air temperatures using an algorithm contained in the LTPP Bind program, and may be provided by the specifying agency, or by following the procedures as outlined in M 323 and R 35, excluding the provisions for "grade bumping."

[c] This requirement may be waived at the discretion of the specifying agency if the supplier warrants that the binder can be adequately pumped and mixed at temperatures that meet all applicable safety standards.

[d] For quality control of unmodified binder production, measurement of the viscosity of the original binder may be used to supplement dynamic shear measurements of G*/sin δ at test temperatures where the binder is a Newtonian fluid.

[e] G*/sin δ = high-temperature stiffness and G* sin δ = intermediate-temperature stiffness.

[f] The mass change shall be less than 1.00 percent for either a positive (mass gain) or a negative (mass loss) change.

[g] The PAV aging temperature is based on simulated climatic conditions and is one of three temperatures, 90°C, 100°C, or 110°C. Normally, the PAV aging temperature is 100°C for PG 58 and above. However, in desert climates, the PAV aging temperature for PG 70 and above may be specified as 110°C.

[h] If the creep stiffness is below 300 MPa, the direct tension test is not required. If the creep stiffness is between 300 and 600 MPa, the direct tension failure strain requirement can be used in lieu of the creep stiffness requirement. The *m*-value requirement must be satisfied in both cases.

Second, based on the findings from the literature review and experiments in the current study, it is suggested that the J_{nrdiff} parameter be excluded from the specification for H, V, and E traffic grades but that the current 75 percent limit be maintained for binders with traffic grade S. The study binders for which J_{nrdiff} exceeded 75 percent were polymer-modified binders that were graded H, V, or E at the temperatures they are intended to be used. Evidence from the axial fatigue and HWTT analyses suggested that these binders performed well and, in many cases, exceeded the performance of binders whose J_{nrdiff} was less than 75 percent. Also, the same conclusions can be drawn regarding the Arizona TR+ binders evaluated by Stempihar et al (2018). The J_{nrdiff} values for almost all of the TR+ binders evaluated by Stempihar et al. (2018) exceeded 75 percent, but anecdotal evidence based on current performance and past experience with these binders suggests that they perform well and are rated as premium binders in Arizona. Based on this evidence, the J_{nrdiff} criteria can be excluded for H-, V-, and E-graded binders. However, the experimental data from the current study do not contain any S-graded binders whose J_{nrdiff} is more than 75 percent. Therefore, no conclusive comment can be made regarding performance and, specifically, the effect of high J_{nrdiff} and the impact of data extrapolation to exclude J_{nrdiff} criteria for binders that may be available in the future.

Potential Distribution of Grades Across Arizona

Two methods were used to evaluate the feasibility of an AASHTO M 332 implementation and estimate the binder usage under such a scenario. Method 1 used expert judgment coupled with an analysis of recent binder bid documentation. Method 2 used the binder grade maps developed by ADOT and material suppliers in the early 1990s. Neither method is a perfect representation of the state of practice with respect to binder grades in Arizona. Thus, neither analysis can exactly predict the likely impact of a transition to AASHTO M 332 grading. However, as is shown in the following sections, both analyses suggest that the total number of binders would remain consistent with what currently exists. Scenarios for potentially reducing the number of grades are also evaluated and are meant to demonstrate how grade reduction might occur. Actual reduction and reconciliation of binder grades would require a collaborative effort between ADOT and suppliers.

Method 1: Expert Judgment

In Method 1, ADOT engineers evaluated bid documents for paving projects and used engineering judgment to catalog current grades in Arizona (the cataloging is shown in Chapters 1 and 3). They then combined the current grades with known traffic conditions to estimate the likely AASHTO M 332 grades. This analysis was based on 10-year traffic volumes. The distribution of expected AASHTO M 332 grades across Arizona is shown in Figure 78. Table 48 summarizes the percentage of total ADOT roadway mileage associated with each grade. For comparison purposes, the table also includes the percentages based on the analysis of current grades.

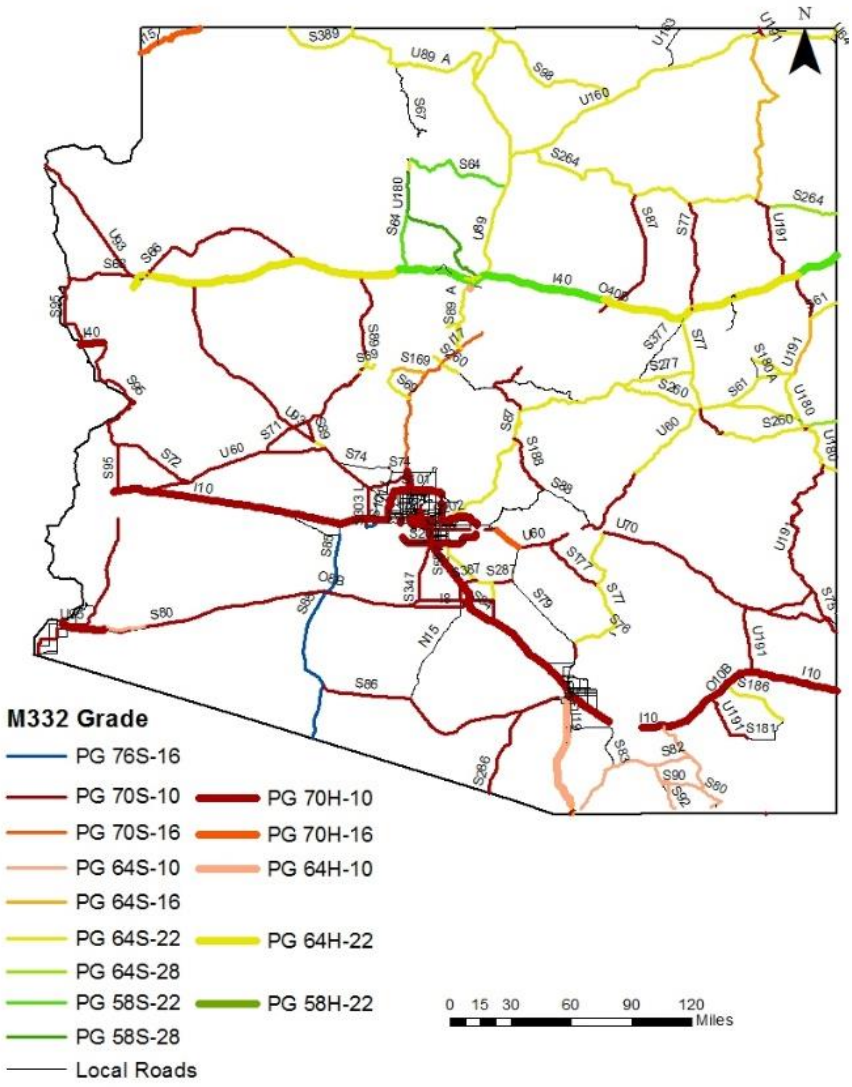

Figure 78. Distribution of Expected AASHTO M 332 Grades Across Arizona Using Method 1

The analysis suggests that a strict adoption of AASHTO M 332 could result in as many as 14 binder grades for ADOT. This estimate does not include binder grades necessary for local agencies, though many use the same grades as ADOT, nor does it include any necessary grade adjustments for crumb-rubber-modified binder or asphalt mixtures containing RAP. Despite the large number of grades, only three make up more than 5 percent of the total roadway mileage. This unequal distribution suggests that grade reduction through engineering judgment, similar to what was done in the early AASHTO M 320 adoption, may be feasible. Such a reduction could include:

- Locations where PG 70S-16 and PG 76S-16 are suggested could be specified at PG 76S-16 grade.
- Locations where PG 70H-10 and PG 70H-16 are suggested could be specified at PG 70H-16.
- For locations requiring PG 64S-10, PG 64S-16, PG 64S-22, and PG 64S-28, these grades could be combined into a single PG 64S-22 grade. Note that based on Method 1, for locations where PG

64S-28 would have been used, the combined grade would still have a reliability of 96 percent at a low temperature of –22°C.

- Locations where PG 64H-22 and PG 64H-10 are suggested could be specified at PG 64H-22.
- Locations where PG 58S-22 and PG 58S-28 are suggested could be specified at PG 58S-28. This combination would serve the additional purpose of providing a PG 64S-22 binder for locations where high RAP applications exist.

These five combinations, in addition to the observation that many PG 58H-22 binders are rheologically identical to PG 64S-22, would reduce the number of grades to six, with three grades (PG 70S-10, PG 64S-22, and PG 70H-10) making up 86.8 percent of the binder grades (according to mileage demand), which is a breakdown similar to what is currently used. In Table 48 these combinations are shown by color with the bold grade being the one specified for the given group.

Table 48. Summary of Binder Grade Distribution as Percentage of Total ADOT Roadway Mileage Under Method 1

AASHTO M 320 Grade		AASHTO M 332 Grade	
Grade	**Percent**	**Grade**	**Percent**
PG 58-28	1.9	PG 58S-28	1.9
PG 58-22	1.6	**PG 58S-22**	1.6
PG 64-28	1.6	PG 58H-22	2.1
PG 64-22	30.9	PG 64S-28	0.9
PG 64-16	0.3	**PG 64S-22**	26.6
PG 70-22	5.7	**PG 64H-22**	4.1
PG 70-10	32.7	PG 64S-16	2.8
PG 76-16	25.3	PG 64S-10	3.8
		PG 64H-10	1.2
		PG 70S-16	1.7
		PG 70H-16	0.6
		PG 70S-10	40.2
		PG 70H-10	9.9
		PG 76S-16	2.7

Method 2: Existing Grade Map Evaluation

Method 2 is based on (1) the original map of ADOT binder grades (Figure 79a) developed during initial implementation of the Strategic Highway Research Program (SHRP) in Arizona, and (2) 98-percent-reliability temperature maps developed under the Long-Term Pavement Performance program (LTPP) using LTPPBind Version 2.1 software (Figures 79b and 79c). Roadways in each binder sector were identified by digitally overlaying the ADOT binder grade map on the data layer for Arizona from the National Highway Performance Network (NHPN). The results of this overlay exercise are shown in Figure 79d.

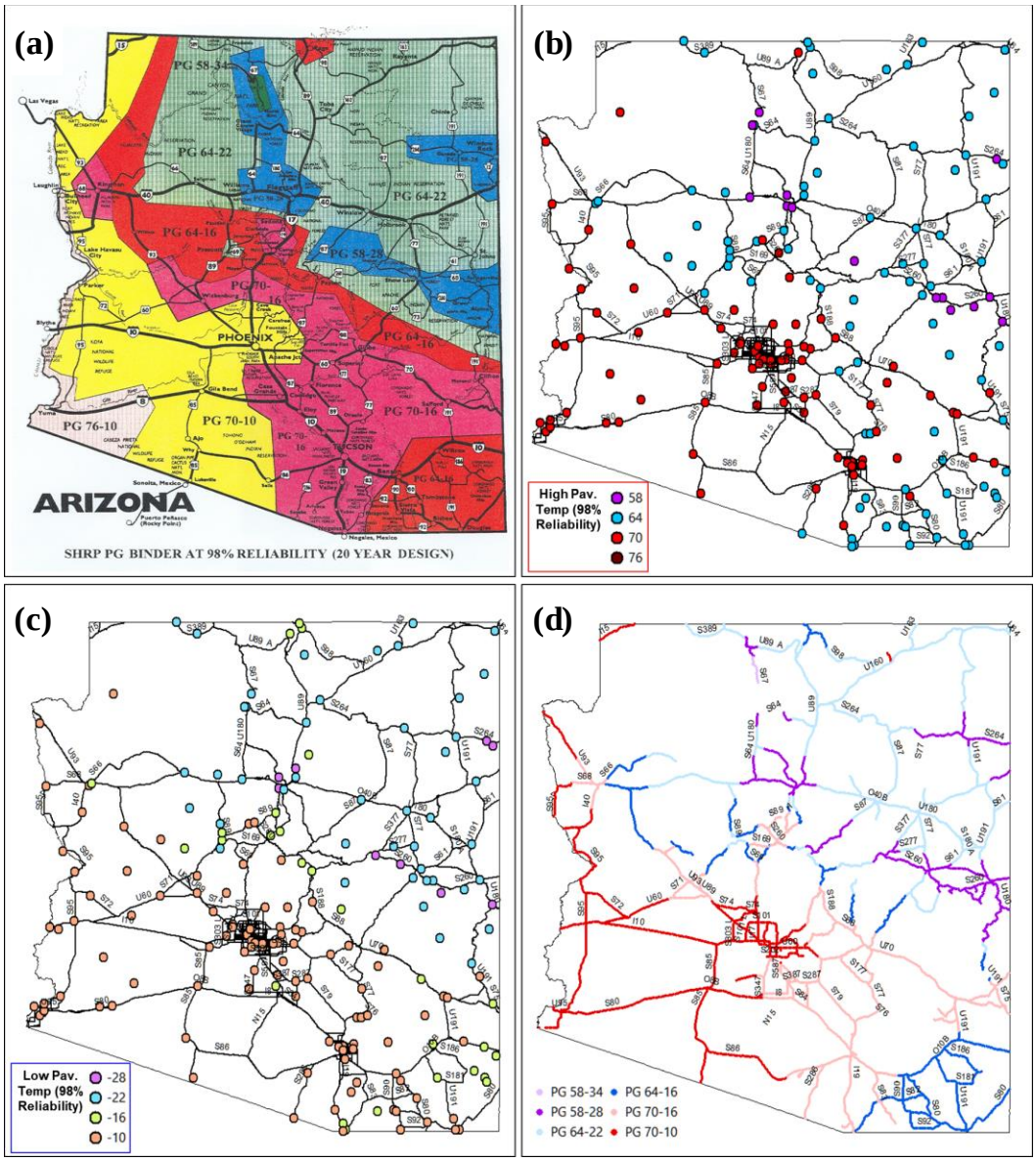

Figure 79. (a) Map of ADOT Binder Grades, (b) LTPP High-Temperature Map, (c) LTPP Low-Temperature Map, and (d) PG Binder Grade for Arizona Roadways According to ADOT Map

To identify potential AASHTO M 332 grades, the ADOT annual average daily traffic (AADT) database for 2016 was downloaded and matched to each roadway segment in the NHPN overlay. Roadways were identified by their Truck Traffic Classification (TTC) and Truck Load Factor (T_{LF}) cluster. These identifications were performed using information in the AADT database along with ADOT data on the total percentage of combination trucks on the roadway. In total, six different TTCs (Table 49) and four T_{LF} clusters (Table 50) were identified. ESAL projections for 10, 20, and 30 years were made using the TTC, T_{LF}, total AADT number, and growth rate given in the database (Equation 17).

Table 49. Summary of Vehicle Class Distribution Based on ADOT TTC Groups

TTC	% Combo Units	% of Trucks by FHWA Truck Classification									
		Class 4	Class 5	Class 6	Class 7	Class 8	Class 9	Class 10	Class 11	Class 12	Class 13
AZ-1	80–100	1.8	6.5	1.9	0.2	10.3	73.2	1	3.1	1.9	0.1
AZ-2	70–79	3.1	14.7	2.9	0.1	9.3	64.4	1.3	1.9	1.5	0.8
AZ-3	51–69	3.7	21.3	5.7	0.4	19	45.6	1.7	1.5	0.7	0.4
AZ-4	43–50	5.3	38.6	6.2	0.2	9	36.9	1.8	1.3	0.3	0.4
AZ-5	23–42	5.3	46.3	5.7	0.7	16.1	24.1	1.1	0.3	0.1	0.3
AZ-6	0–22	7.8	65.8	4.4	0.2	11.7	9.1	0.7	0.2	0	0.1

Table 50. Summary of ADOT T_{LF} Classifications

Cluster	Truck Load Factors by FHWA Vehicle Classification										
	Class 1-3	Class 4	Class 5	Class 6	Class 7	Class 8	Class 9	Class 10	Class 11	Class 12	Class 13
1	0.0008	1.07	0.33	0.64	0.58	0.61	1.62	1.43	1.75	1.31	3.51
2	0.0008	1.06	0.39	0.96	0.61	0.91	1.34	1.53	1.96	1.33	3.50
3	0.0008	1.20	0.13	0.86	0.64	0.52	1.93	1.78	2.25	1.17	2.07
4	0.0008	1.20	0.13	0.86	0.64	0.52	1.93	1.78	2.25	1.17	2.07

$$ESAL = \sum_{i=1}^{13}\left[AADT_c \times T_{LF,c}\right] \times \left(\frac{(1+r)^Y - 1}{r}\right) \times \left(D_L \times D_o \times 365\right) \quad \text{(Eq. 17)}$$

Where D_L = Lane distribution factor (assumed as 100% when 1 lane in design direction, 90% when 2 lanes in design direction, 80% when 3 lanes in design direction, and 70% when 4 or more lanes in the design direction)

D_o = Directional distribution factor (given in ADOT traffic database)

$AADT_c$ = Traffic volume for each vehicle class (calculated from total AADT, percent trucks, and percent non-trucks)

$T_{LF,c}$ = Truck load factor for vehicle class c

r = growth rate expressed as a decimal

Y = design analysis period

Finally, ESAL projections were combined with the climate grade determined from the overlaid NHPN analysis to identify grades required for AASHTO M 332 implementation. The results are shown in Figure 80. As was done in Table 48 for Method 1, the required grades as a percentage of roadway mileage are summarized in Table 51.

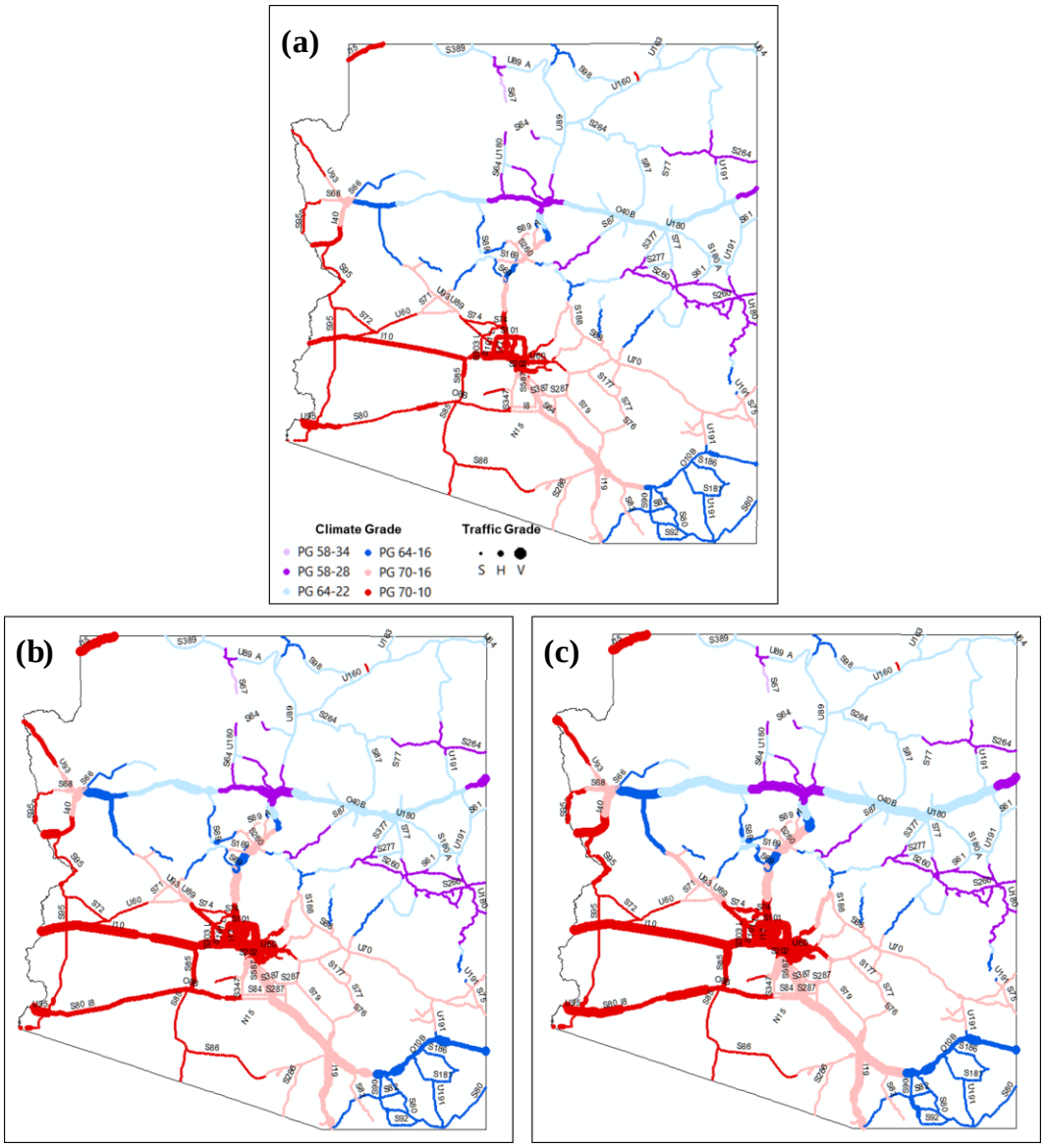

Figure 80. Distribution of Expected AASHTO M 332 Grades Across Arizona Under Method 2: (a) Using 10-Year ESAL Projections, (b) Using 20-Year ESAL Projections, and (c) Using 30-Year ESAL Projections

The Method 2 analysis suggests that a strict adoption of AASHTO M322 could result in as many as 16 binder grades for ADOT. However, most of these apply to less than 5percent of the total mileage, and one, PG 58S-34, is used only for AZ-67 from approximately Jacob Lake to the North Rim of the Grand Canyon (this grade was not included in the expert opinion analysis conducted in Method 1). The experimental results also demonstrated that unmodified binders grading as an S at one temperature often grade as an H at the next-lowest temperature increment (i.e., PG 64S-22 is also PG 58H-22). Together, these considerations suggest that grade reduction would be possible. The following groupings might be considered:

1. Locations where PG 58S-34 and PG 58S-28 are suggested could be specified at PG 58S-28.
2. Locations where PG 58H-28, PG 64S-16, and PG 64S-22 are suggested could be specified at PG 64S-22 (PG 64S-22 would also grade as PG 58H-22).
3. Locations where PG 64H-16, PG64H-22, and PG 70S-16 are suggested could be specified to use a co-graded binder meeting both PG 64H-22 and PG 70S-22.
4. Locations where PG 64V-16 and PG 64V-22 are suggested could be specified at PG 64V-22.
5. Locations where PG 70H-10 or V-10 and PG 70H-16 or V-16 are suggested could be specified at PG 70H-16 or V-16.

These groupings would reduce the total number of grades to six for a 10-year horizon and eight for 20- and 30-year horizons. In all cases, four grades (PG 58S-28, PG 64S-22, PG 64H-22, and PG 70S-10) would make up between 89.5 percent (for a 10-year horizon scenario) and 73.1 percent (for a 30-year horizon) of total roadway mileage. In Table 51 these combinations are shown by color with the bold grade being the one specified for the given group.

Table 51. Summary of Binder Grade Distribution as Percentage of Total ADOT Roadway Mileage Under Method 2

AASHTO M 320 Grade		AASHTO M 332 Grade			
Grade	Percent	Grade	Percent		
			10-Year Project.	20-Year Project.	30-Year Project.
PG 58-34	0.4	PG 58S-34	0.4	0.4	0.4
PG 58-28	11.3	**PG 58S-28**	11.5	11.5	11.3
PG 64-28	1.3	PG 58H-28	1.2	0.6	0.1
PG 64-22	22.2	**PG 58V-28**	0.0	0.6	1.2
PG 64-16	11.5	PG 64S-16	14.2	12.3	11.5
PG 70-22	3.4	PG 64H-16	1.2	2.5	2.8
PG 70-16	20.6	PG 64V-16	0.0	0.7	1.2
PG 70-10	8.4	**PG 64S-22**	22.9	22.4	22.2
PG 76-16	7.2	**PG 64H-22**	2.7	2.5	0.2
PG 76-10	13.7	**PG 64V-22**	0.0	0.7	3.2
		PG 70S-16	20.0	18.4	16.5
		PG 70H-16	3.5	2.4	3.0
		PG 70V-16	0.4	3.1	4.4
		PG 70S-10	15.5	10.5	8.1
		PG 70H-10	6.0	7.0	6.5
		PG 70V-10	0.5	4.5	7.4

ASSESSMENT OF IMPACTS ON PRODUCERS

To assess what impact transitioning to the AASHTO M 332 specification might have on the binder suppliers, it was proposed to conduct an economic impact assessment study. As a first step, the

research team conducted individual conference calls with the three binder suppliers to obtain such information as whether they would need to build additional storage tanks at their facilities. A questionnaire, covering three main topics (production, storage, and operations), was provided to the suppliers several weeks prior to the conference call so they would have enough time to gather the information. The questionnaire is shown in Appendix G. The following three sections below summarize the discussions with the suppliers. In accordance with the suppliers' request, specific details related to their facilities have not been shared.

Production

Most suppliers did not share their current production tonnage because of proprietary concerns. The suppliers divulged that they had provided binders to ADOT, cities, counties, and private entities. According to the client breakdown provided by the suppliers, binder supply to ADOT constituted a significant portion of their production. While two suppliers did not provide a grade-based breakdown, one supplier did indicate that most of the market was more or less equally divided between PG 70-10, PG 76-16, and PG 64-22. Currently, all suppliers were either supplying or planning to supply neighboring DOTs from their Arizona terminals. Two of the suppliers also indicated that their out-of-state terminals catered to ADOT's needs.

Storage

While one supplier, citing proprietary concerns, declined to report the storage at its facilities, the other two suppliers said that the total combined storage at their Arizona facilities was about 745,000 barrels. As indicated earlier, the basic goal of this project task was to determine if the suppliers would require additional tanks at their facilities. One supplier indicated that it had no options for increasing its storage capacity, either because of surrounding properties or other constraints. Another supplier indicated that it was in the process of adding new tanks (which would increase the current storage capacity by about 5 percent), and then would have no additional room for expansion. The third supplier indicated that it would be able to add about three tanks, totaling 55,000 barrels in storage. This was the supplier that regarded its current total storage as proprietary information, and said that it was therefore not possible to estimate what percentage of the total this additional storage would constitute. To summarize, two of the three suppliers indicated an inability to add more tanks. Also, any addition of a tank would only be for profit reasons, as the existing tankage could accommodate the expected grade levels for Arizona.

The suppliers provided approximate costs of adding new tanks. One supplier indicated that a 15,000-barrel tank would cost about $1.2 million, while another supplier indicated it would cost about $500,000 for a 200-ton-capacity tank, which is roughly 1200 barrels. The final supplier provided estimates for three tank sizes: a 5000-barrel tank, which would will cost about $750,000; a 25,000-barrel tank, which would be about $1.5 million; and a 50,000-barrel tank, which would cost about $2.25 million. These estimates suggest that total start-up costs for a tank of any size could be as large as approximately $570,000, with each 1000-barrel addition costing approximately $35,000.

Most of the suppliers indicated that polymer-modified binders require dedicated tanks. Non-polymer-modified tanks are rotated depending upon the demand. As for the associated cleaning and disposal of

tanks, the suppliers said that it was not a significant issue. Cleaning costs anywhere between $20,000 and $250,000, depending on the type of binder in the tank (modified versus nonmodified versus tire rubber), and is not done regularly.

Operations

The questions on the suppliers' current operations focused on such topics as the operational area of the terminals, the suppliers' willingness to expand, costs of acquiring real estate, and existence of any current delivery issues. Regarding the operational area, only one supplier provided the facility acreage, while the other two suppliers said they did not know what it was. However, all suppliers indicated their inability to expand the terminal area, owing to various constraints such as operating from a leased facility, being restricted by the presence of other facilities close by, or being hampered by more technical reasons, such as insufficient boiler/steam capacity. With regard to expansion costs, two out of three suppliers indicated that they had looked at acquisition costs. The third supplier said that its current terminal area would not need to expand to accommodate more tank storage. Finally, regarding delivery, the suppliers said that in Arizona, New Mexico, and the mid-continent region as a whole there was a concern about a limited number of trucks and drivers.

Concerns with a New Specification

At the end of the conference call discussion, the suppliers were asked if they had any other concerns about implementation of the new specification. The issues brought up by the suppliers can be classified broadly in two categories—grade proliferation and change in formulations.

Grade Proliferation

One of the biggest concerns, as pointed out by one of the suppliers, was extreme proliferation of grades, which ties into tank limitations. ADOT currently has 13 grades in its specification, the result of prior implementation of RAP use. For projects requiring asphalt rubber, PG 64-16 is used most of the time, and PG 58-28 some of the time. There are three TR+ products, PG 76-22TR+, PG 70-22TR+, and PG 64-22TR+, and two SBS-based binders, PG 70-22 SBS and PG 70-28 SBS. The remaining six are neat binders. The supplier also mentioned that nonuniform specifications are found across the state, but noted that that is technically not an ADOT issue.

One supplier brought up the issue of in-line blending as one strategy that might address storage limitations. There are many challenges with in-line blending, and it is not currently allowed in Arizona. However, the supplier pointed out that Texas DOT allows samples prepared using in-line blending to be tested. The supplier added that if ADOT would be willing to work with suppliers to implement in-line blending, tank limitations might be fixed, and many grades could be added with current tank capacity.

Change in Formulations

One of the suppliers indicated that formulation changes might occur as a result of AASHTO M 332 implementation. The supplier explained this comment by using PG 70-22 binder as an example. This binder is currently graded by performing PAV aging at 110°C. If AASHTO M 332 is implemented, the

supplier said, the binder might grade as a 64H-22. In that case, it was the supplier's opinion that the PAV temperature should be 100°C, which might potentially affect the formulations.

One of the other suppliers mentioned that it would not have any issues with changing to the AASHTO M 332 specification as long as the number of grades remained manageable. The supplier added that about 10 to 15 binder grades would be optimum, though it is currently producing about 20 to 25 grades per year. The supplier also said that the best-case scenario would be if the products currently being produced can be graded under AASHTO M 332, which would avoid the need to reengineer and reformulate the binders.

In conclusion, two of the three suppliers indicated that they would be unable to add more tanks. All of the suppliers indicated that they would add tanks only to increase their profits, since the existing storage capacity can accommodate the grade levels expected for Arizona. These findings suggest that there would be no apparent economic impact from the adoption of AASHTO M 332, and the suppliers agreed with this outcome.

SUMMARY

This chapter presented analyses of various aspects of the AASHTO M 332 specification. Based on these analyses, the research team recommended a modified binder grading specification for Arizona binders. Two main differences exist between the recommended specification and the AASHTO M 332 specification. In the former, the relationship between $J_{nr3.2}$ and *%Recovery* at 3.2 kPa was modified, and the J_{nrdiff} criterion were eliminated for all H, V, and E binders. However, for S-graded binders, the J_{nrdiff} criterion remain and are the same as those specified in AASHTO M 332 (i.e., maximum of 75 percent). This chapter also analyzed the potential distribution of grades across Arizona if the AASHTO M 332–based specification is implemented. The resulting distribution was based on two approaches: (1) expert judgment and (2) existing grade map evaluation. Based on expert judgment, the binder needs of the entire state can be met by using just six binder grades. The same value is obtained from grade map evaluation when a 10-year forecast is used. If a 20- or 30-year forecast is considered, then the number of grades needed increases to eight. Another important issue the chapter addressed was the potential impact on binder producers resulting from the transition to the AASHTO M 332–based specification. Based on discussions held with the suppliers, the research team concluded that there will be no apparent economic impact.

CHAPTER 8. SUMMARY AND CONCLUSIONS

OVERVIEW

Pavements surfaced with asphalt mixtures constitute the vast majority of ADOT's roadways. To achieve the best-performing, longest-lasting, and lowest-cost pavement infrastructure, ADOT engineers must carefully select the asphalt materials that are used in these pavements. Thus, the specification used to determine, select, and ultimately purchase the optimal binder is a critically important tool for the engineers. This research study has focused on binder specifications in Arizona. It has specifically examined technological advances that have occurred since the initial deployment of the current ADOT specification, the applicability of those advances to Arizona, and the potential impacts on ADOT from adopting new specifications. In particular, the present research has focused on the applicability of the AASHTO T 350 testing protocol and the associated AASHTO M 332 purchase specification. Substantial developmental work on the technological advances has been carried out by the Asphalt Institute, user/producer organizations, and other researchers across the country; however, a large amount of the work is not immediately applicable to Arizona for several reasons:

1. Most of the test and grading evaluations have been limited to the East Coast, where binder supplies, the number of binders used, and mixture designs are drastically different from those in Arizona.
2. There is a large variation in temperatures between northern Arizona and central/southern Arizona.
3. The validation efforts presented in the literature include only a limited number of the types of materials regularly used in Arizona.

The present study utilized multiple research methods: First, the research team conducted a review of the literature and of presentations and reports given by key researchers and industry members at local, regional, and national professional meetings (Chapter 2). This review confirmed the need for this study. Next, the researchers performed a series of tests of binders and asphalt mixtures using Arizona materials (Chapters 3–6). These experiments showed that the material parameters specified by the AASHTO T 350 protocol better correlate with asphalt mixture performance than do the material parameters from AASHTO T 315, which are part of the current ADOT specifications. Finally, the researchers combined the results from the experiments with the findings from the literature review and from the survey of local binder suppliers to develop a recommended binder specification for Arizona that incorporates the AASHTO T 350 material parameters.

CONCLUSIONS FROM THE LITERATURE REVIEW

The literature review resulted in the following findings:

- The main motivation for many other DOTs in adopting the AASHTO M 332 specification is the higher correlation between asphalt mixture rutting and the MSCR parameter for modern and/or modified binder technologies.

- No studies exist that have evaluated the use of AASHTO T 350 or AASHTO M 332 with high-modulus and unmodified binders like those used in central and southern Arizona.
- At the time of the literature review, the majority of neighboring DOTs either are evaluating the implementation of AASHTO M 332 or did not plan to implement it for the next 2 to 3 years. The Nebraska, Oklahoma, Nevada, and Texas DOTs, as well as the District of Columbia DOT, plan to complete partial implementation very soon, or they are currently implementing a part of the standard.
- The repeatability of the AASHTO T 350 test is improving with time, and the precision limits for the MSCR parameter are comparable to those for the $|G^*|/\sin \delta$.
- National guidelines exist for AASHTO M 332–graded binder and RAP, but the DOTs that have fully implemented the standard do have procedures in place for using RAP.
- Limited data exist on changes in binder formulations that may occur after AASHTO M 332 implementation. The responses received from stakeholders in the above-mentioned five DOTs suggest that changes in formulations, if any, have been limited.

CONCLUSIONS FROM THE EXPERIMENTAL STUDY

- Under AASHTO M 332, non-polymer-modified binders in Arizona have an S grade. At one standard temperature increment below the current high-temperature PG grade, most non-polymer-modified binders in Arizona have an H grade under AASHTO M 332. This rule does not apply universally to the polymer-modified binders.
- When binders are specified using grade-bumping practices, the required modulus and phase angle of the unaged binder are based on the bumped temperature value. Under AASHTO M 332, these binders would be tested at the unbumped, or climate-based, temperature instead of at one or two temperature increments above the climate-based temperature. Since the $|G^*|/\sin \delta$ threshold value of the unaged binder would not change for these binders, but the test temperature would change, adoption of AASHTO M 332 could potentially lead to an increase in aging potential for locations that are adjusting the PG grade for traffic considerations. The actual level of impact may be small and cannot be quantified in the current study.
- For most of the binders tested, the *m*-value obtained from the BBR test was the critical parameter. For the low-stiffness binders, the RTFO specification parameter was the noncritical parameter, while for polymer-modified binders, the original specification parameter was the noncritical parameter.
- From the dynamic modulus tests, mixtures prepared with non-polymer-modified binders had higher moduli than mixtures prepared with polymer-modified binders.
- The MSCR percent recovery of binders had a notable effect on the dynamic modulus of asphalt mixtures, especially at intermediate and high temperatures. Binders with lower MSCR recovery were found to have a higher dynamic modulus. This finding was consistent with the mixture fatigue and modulus results (lower mixture moduli favor better fatigue performance; polymer-modified mixtures have lower moduli; and higher MSCR recovery shows lower mixture moduli).
- The data from the HWTT showed that the rut depths for all mixtures were below the acceptance limit currently used by ADOT.

- The rut depths were related to the binder rutting parameters J_{nr} at 3.2 kPa and $|G^*|/\sin\delta$. It was concluded that $J_{nr3.2}$ of the binder related better to mixture rutting than did $|G^*|/\sin\delta$. For mixtures containing polymer-modified binders, the relative improvement in correlation between $J_{nr3.2}$ and $|G^*|/\sin\delta$ was greater than for mixtures with non-polymer-modified binders.
- The relationship between the $J_{nr3.2}$ and $|G^*|/\sin\delta$ parameters for unmodified binders was highly predictable, and current ADOT practices using grade bumping reflect this relationship adequately.
- The fatigue performance of the asphalt mixtures showed that polymer-modified asphalt mixtures possess greater fatigue resistance than non-polymer-modified asphalt mixtures.
- The elastic recovery test at 10°C was able to identify polymer but did not accurately rank the fatigue performance of the polymer-modified binders.
- Asphalt binders with higher MSCR recovery were found to have greater fatigue resistance. This is an important conclusion because it demonstrates that while the primary purpose of the MSCR test is to address rutting performance, the test can capture the improved fatigue performance of polymer-modified binders.
- MSCR percent recovery has little to no effect on the rutting resistance of asphalt mixtures at the temperatures tested in this study. It was seen that rut depths and rutting resistance of asphalt mixtures were more a function of the binder and mixture modulus than of the MSCR percent recovery.
- Evidence from the axial fatigue test and HWTT suggested that H, V, and E grades with high J_{nrdiff} values performed well and, in many cases exceeded the performance of binders whose J_{nrdiff} was less than 75 percent. The experimental data from the current study did not contain any S-graded binders whose J_{nrdiff} was more than 75 percent. Therefore, no conclusive comment could be made regarding performance and, specifically, the effect of high J_{nrdiff} for these binders.

CONCLUSIONS FROM DISCUSSIONS WITH SUPPLIERS

The research team drew the conclusions presented in this section after conducting surveys and interviews with the suppliers regarding their practices. These interviews involved objective questions about production, storage, and operations and subjective questions about concerns with any new specification.

- Suppliers were concerned that a new specification might cause binder grades to proliferate. Most suppliers would be unable to add more storage for additional binders if such binders were required.
- It is likely that any change in the binder specification could result in modification of the binder formulation.
- Based on the discussions held with the suppliers, the research team concluded that there was no basis for an economic analysis tied specifically to a change in specification. However, if suppliers were to add additional tanks at their facilities or be required to provide more binder grades than are currently used, then there would be an expectation that their costs would increase.

RECOMMENDATIONS

This study's recommendations are based on the results of the experiments. The research concluded:

- The study findings demonstrated that the AASHTO T 350 test parameter is a better indicator of rutting than the currently used parameter of $|G^*|/\sin\delta$.
    - The recovery value, *%R*, from the AASHTO T 350 test can indicate whether asphalt binders have or lack polymer modification.
    - The polymer-modified asphalt mixtures exhibited substantially better fatigue performance than the non-polymer-modified mixtures, and the study results showed that *%R* can also capture this increased performance.
- If ADOT is expecting to increase the use of polymer-modified binders, it is recommended that it adopt the AASHTO M 332 specification because the specification would better represent the performance of binders irrespective of modified formulations.
    - It is recommended that ADOT follow the specification's testing temperature guidelines, which means testing binders at the climatic conditions where they will be used. Figure 81 shows the recommended AASHTO M 332 MSCR testing temperatures for Arizona based on the location of intended use.

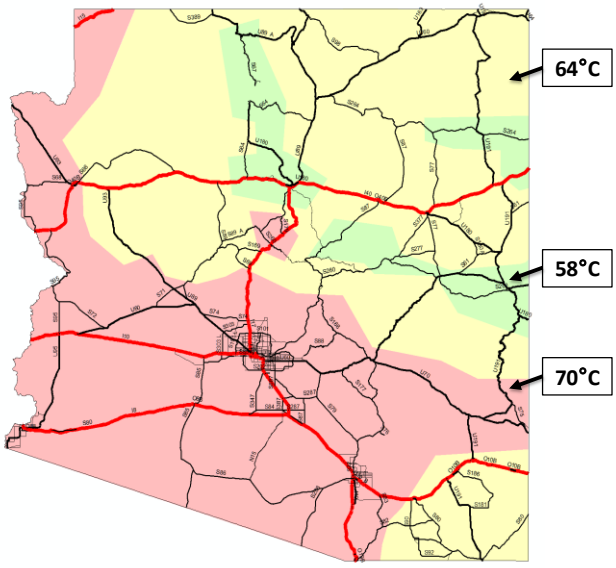

Figure 81. Recommended MSCR Testing Temperatures for AASHTO M 332 Grading in Arizona

    - ADOT may consider modifying the M 332 specification as follows:
        - Change the PAV aging temperature for PG 64H, V, and E grades to 110°C. This change will maintain consistency with current ADOT practice.
        - Eliminate the J_{nrdiff} parameter for H-, V-, and E-grade binders. No conclusive comment could be made regarding performance and, specifically, the effect of high J_{nrdiff} for S-grade binders.

- This study showed no definitive evidence that S-graded binders with J_{nrdiff} greater than 75 percent will fail in their performance. More study of S-graded binders with high J_{nrdiff} will be necessary to provide a more specific recommendation.
- Eliminate the 10°C elastic recovery and other plus-tests for polymer-modified binders and adopt the modified J_{nr} versus *%Recovery* relationship given in Equation 18. The values of $J_{nr3.2}$ and *%Recovery* can be determined at the temperatures indicated in Figure 81.

$$\%R_{3.2} = \begin{cases} 75 & J_{nr3.2} \le 0.1 \text{ kPa}^{-1} \\ 33.133\left(J_{nr3.2}\right)^{-0.35} & J_{nr3.2} > 0.1 \text{ kPa}^{-1} \end{cases} \quad \text{(Eq. 18)}$$

- Since the detailed study of the PAV issue was beyond the scope of the current study, consider investigating the issue more thoroughly in another study.

- Since developing guidelines for using the AASHTO M 332 specification to specify binders for mixtures containing RAP was beyond the scope of the current study, ADOT may consider additional research to investigate this issue.

REFERENCES

American Association of State Highway and Transportation Officials (AASHTO). 2010. *Standard Specification for Performance-Graded Asphalt Binder.* AASHTO M 320. Washington, D.C.: American Association of State Highway and Transportation Officials.

American Association of State Highway and Transportation Officials (AASHTO). 2012a. *Standard Method of Test for Determining the Flexural Creep Stiffness of Asphalt Binder Using the Bending Beam Rheometer (BBR)*. AASHTO T 313. Washington, D.C.: American Association of State Highway and Transportation Officials.

American Association of State Highway and Transportation Officials (AASHTO). 2012b. *Standard Method of Test for Determining the Rheological Properties of Asphalt Binder Using a Dynamic Shear Rheometer (DSR)*. AASHTO T 315. Washington, D.C.: American Association of State Highway and Transportation Officials.

American Association of State Highway and Transportation Officials (AASHTO). 2012c. *Standard Practice for Accelerated Aging of Asphalt Binder Using a Pressurized Aging Vessel (PAV)*. AASHTO R 28. Washington, D.C.: American Association of State Highway and Transportation Officials.

American Association of State Highway and Transportation Officials (AASHTO). 2013a. *Standard Method of Test for Effect of Heat and Air on a Moving Film of Asphalt Binder (Rolling Thin-Film Oven Test)*. AASHTO T 240. Washington, D.C.: American Association of State Highway and Transportation Officials.

American Association of State Highway and Transportation Officials (AASHTO). 2013b. *Standard Method of Test for Elastic Recovery Test of Asphalt Materials by Means of a Ductilometer*. AASHTO T 301. Washington, D.C.: American Association of State Highway and Transportation Officials.

American Association of State Highway and Transportation Officials (AASHTO). 2014a. *Standard Method of Test for Determining the Damage Characteristic Curve of Asphalt Mixtures from Direct Tension Cyclic Fatigue Tests*. AASHTO TP 107. Washington, D.C.: American Association of State Highway and Transportation Officials.

American Association of State Highway and Transportation Officials (AASHTO). 2014b. *Standard Method of Test for Hamburg Wheel-Track Testing of Compacted Hot Mix Asphalt (HMA)*. AASHTO T 324. Washington, D.C.: American Association of State Highway and Transportation Officials.

American Association of State Highway and Transportation Officials (AASHTO). 2014c. *Standard Method of Test for Multiple Stress Creep Recovery (MSCR) Test of Asphalt Binder Using a Dynamic Shear Rheometer (DSR)*. AASHTO T 350. Washington, D.C.: American Association of State Highway and Transportation Officials.

American Association of State Highway and Transportation Officials (AASHTO). 2014d. *Standard Specification for Performance-Graded Asphalt Binder Using Multiple Stress Creep Recovery (MSCR)*

Test. AASHTO M 332. Washington, D.C.: American Association of State Highway and Transportation Officials.

American Association of State Highway and Transportation Officials (AASHTO). 2015. *Standard Method of Test for Determining Dynamic Modulus of Hot Mix Asphalt (HMA)*. AASHTO T 342. Washington, D.C.: American Association of State Highway and Transportation Officials.

American Association of State Highway and Transportation Officials (AASHTO). 2016. "Sample Round Analysis." AASHTO re:source (formerly AASHTO Materials Reference Laboratory). Accessed in June 2016. http://aashtoresource.org/psp/sample-round-analysis.

Anderson, David A., Donald W. Christensen, Hussain U. Bahia, Raj Dongre, M. G. Sharma, Charles E. Antle, and Joe Button. 1994. *Binder Characterization and Evaluation, Volume 3: Physical Characterization*. Publication SHRP-A-369. Washington, D.C.: Strategic Highway Research Program, National Research Council.

Anderson, R. M. 2011. "Understanding the MSCR Test and Its Use in the PG Binder Specification." Webinar. Lexington, KY: Asphalt Institute.

Anderson, R. M. 2016. "Implementation of the MSCR Test and Specification." Presented at the AMAP Annual Meeting, February 10-11, 2016, Seattle, WA.

Arega, Z., N. Sakib, A. Bhasin, and J. Peterson. 2017. "An Investigation into the Continuous High-Temperature Grade and Elastic Recovery of Asphalt Binders Measured Using the Creep-Recovery Test." *Journal of Testing and Evaluation* 45: 1671–1679.

Arizona Department of Transportation (ADOT). 2013. *2013 State Highway System Log*. Phoenix: Arizona Department of Transportation.

Asphalt Institute. 2016. "US State Binder Specifications." Accessed on August 31, 2016. http://www.asphaltinstitute.org/specification-databases/us-state-binder-specification-database/

ASTM International. 2015. *Standard Test Method for Multiple Stress Creep and Recovery (MSCR) of Asphalt Binder Using a Dynamic Shear Rheometer*. ASTM D7405. West Conshohocken, PA: ASTM International.

Bahia, H. U., D. I. Hanson, M. Zeng, H. Zhai, M. A. Khatri, and R. M. Anderson. 2001. *Characterization of Modified Asphalt Binders in Superpave Mix Design*. NCHRP Report 459. Washington, D.C.: National Cooperative Highway Research Program, Transportation Research Board, National Research Council.

Basueny, A., D. Perraton, and A. Carter. 2014. "Laboratory Study of the Effect of RAP Conditioning on the Mechanical Properties of Hot Mix Asphalt Containing RAP." *Materials and Structures* 47: 1425–1450.

Bouldin, M., G. Row, J. Souse, and J. Shamrock. 1994. "Mix Rheology—A Tool for Predicting the High Temperature Performance of Hot Mix Asphalt." *Journal of the Association of Asphalt Paving Technologists* 63: 182–223.

Branthaver, J. F., J. C. Petersen, R. E. Robertson, J. J. Duvall, S. S. Kim, P. M. Harnsberger, T. Mill, E. K. Ensley, F. A. Barbour, and J. F. Scharbron. 1993. *Binder Characterization and Evaluation. Volume 2: Chemistry.* Publication SHRP-A-368. Washington, D.C.: Strategic Highway Research Program, National Research Council.

Buncher, Mark, and Carlos Rosenberger. 2005. "Understanding the True Economics of Using Polymer-Modified Asphalt Through Life Cycle Cost Analysis." *Asphalt* 20(2): 28–30.

Connecticut Department of Transportation. 2016. *The Standard Specifications for Roads, Bridges, Facilities and Incidental Construction*. Form 816. Newington: Connecticut Department of Transportation.

Copeland, Audrey. 2011. *Reclaimed Asphalt Pavement in Asphalt Mixtures: State of the Practice.* Publication FHWA-HRT-11-021. McLean, VA: Federal Highway Administration.

D'Angelo, J. 2009. "Development of a Performance Based Binder Specification for Rutting Using Creep and Recovery Testing." Ph.D. Dissertation. Calgary, Alberta: University of Calgary.

D'Angelo, J., R. Kluttz, R. Dongre, K. Stephens, and L. Zanzotto. 2007. "Revision of the Superpave High Temperature Binder Specification: The Multiple Stress Creep Recovery Test." *Journal of the Association of Asphalt Paving Technologists* 76: 123–162.

D'Angelo, John. 2010. "New High-Temperature Binder Specification Using Multistress Creep and Recovery." *Transportation Research Circular E-C147: Development in Asphalt Binder Specifications*: 1–13.

D'Angelo, John, and Raj Dongre. 2002. "Superpave Binder Specifications and Their Performance Relationship to Modified Binders." *Proceedings of the 47th Annual Conference of the Canadian Technical Asphalt Association* 47: 91–103.

Darter, Michael I., Leslie Titus-Glover, Harold Von Quintus, Biplab B. Bhattacharya, and Jagannath Mallela. 2014. *Calibration and Implementation of the AASHTO Mechanistic-Empirical Pavement Design Guide in Arizona.* FHWA-AZ-14-606. Phoenix: Arizona Department of Transportation.

Dongre, R. 2016. "Variability in J_{nr} Difference Value Obtained in AASHTO M 332 MSCR Test—Cause and Implications." Presented at *53rd Petersen Asphalt Research Conference*, Jackson, Wyoming, July 18-21, 2016.

Dongre, R., and John D'Angelo. 2003. "Refinement of Superpave High-Temperature Binder Specification Based on Pavement Performance in the Accelerated Loading Facility." *Transportation Research Record: Journal of the Transportation Research Board* 1829: 39–46.

El-Basyouny, Mohamed, and Myung Goo Jeong. 2009. "Effective Temperature for Analysis of Permanent Deformation and Fatigue Distress on Asphalt Mixtures." *Transportation Research Record: Journal of the Transportation Research Board* 2127: 155–163.

Federal Highway Administration (FHWA). 1993. *A Study of the Use of Recycled Paving Material: Report to Congress*. Publication FHWA-RD-93-147. Washington, D.C.: Federal Highway Administration.

Gundla, Akshay. 2018. "Understanding Viscoelastic Behavior of Asphalt Binders Through Molecular Structure Investigation." Ph.D. Dissertation. Tempe: Arizona State University.

Hansen, Kent R., and Audrey Copeland. 2013. *Annual Asphalt Pavement Industry Survey on Recycled Materials and Warm-Mix Asphalt Usage: 2009–2012*. Information Series 138. Lanham, MD: National Asphalt Pavement Association.

Hossain, Z., M. Zaman, and D. Ghosh. 2015. *Creep Compliance and Percent Recovery of Oklahoma Certified Binders Using the Multiple Stress Creep Recovery (MSCR) Method.* FHWA-OK-14-19. Oklahoma City: Oklahoma Department of Transportation.

Huang, S. C., A. T. Pauli, and Q. Qin. 2014. "Physicochemical Characteristics of RAP Binder Blends." In *Asphalt Pavements: Proceedings of the International Conference on Asphalt Pavements,* Y. Richard Kim (ed.). Boca Raton, FL: CRC Press.

Huang, Yang H. 2004. *Pavement Analysis and Design*. Upper Saddle River, NJ: Pearson Education Inc.

Jemison, H. B., B. L. Burr, R. R. Davison, J. A. Bullin, and C. J. Glover. 1992. "Application and Use of the ATR, FT-IR Method to Asphalt Aging Studies." *Fuel Science & Technology International* 10(4): 795–808.

Jin, X., R. Han, Y. Cui, and C. J. Glover. 2011. "Fast-Rate–Constant-Rate Oxidation Kinetics Model for Binders." *Industrial & Engineering Chemistry Research* 50(23): 13373–13379.

Laukkanen, O. V., H. Soenen, T. Pellinen, S. Heyrman, and G. Lemoine. 2015. "Creep-Recovery Behavior of Bituminous Binders and Its Relation to Asphalt Mixture Rutting." *Materials and Structures* 48(12): 4039–4053.

Leahy, R. B., E. T. Harrigan, and H. Von Quintus. 1994. *Validation of Relationships Between Specification Properties and Performance*. Publication SHRP-A-409. Washington, D.C.: Strategic Highway Research Program, National Research Council.

Li, X., and N. Gibson. 2013. "Analysis of RAP with Known Source History and Influence on Fatigue Performance." *Compendium of Papers, 92nd Annual Meeting of the Transportation Research Board*, Washington, D.C.

Loria, Luis, Elie Y. Hajj, Peter E. Sebaaly, Matt Barton, Said Kass, and Tara Liske. 2011. "Performance Evaluation of Asphalt Mixtures with High Recycled Asphalt Pavement Content." *Transportation Research Record: Journal of the Transportation Research Board* 2208: 72–81.

Maryland Department of Transportation. 2015. *Design Procedure for Asphalt Mixes Containing Reclaimed Asphalt Pavement (RAP) and/or Reclaimed Asphalt Shingles (RAS)*. MSMT 412. Hanover: Maryland Department of Transportation.

McDaniel, Rebecca S., Hamid Soleymani, R. Michael Anderson, Pamela Turner, and Robert Peterson. 2000. *Recommended Use of Reclaimed Asphalt Pavement in the Superpave Mix Design Method*. NCHRP Web Document 30. Washington, D.C.: National Cooperative Highway Research Program, Transportation Research Board, National Research Council.

McGennis, R. 2005. Discussion to "Mohseni, A., S. Carpenter, and J. D'Angelo. 2005. Development of Superpave High-Temperature Performance Grade (PG) Based on Rutting Damage." *Journal of the Association of Asphalt Paving Technologists* 74: 242–245.

Minnesota Department of Transportation. 2015. *Asphalt Binder Multiple Stress Creep Recovery (MSCR) Overview*. St. Paul: Minnesota Department of Transportation.

Mohseni, A., S. Carpenter, and J. D'Angelo. 2005. "Development of Superpave High-Temperature Performance Grade (PG) Based on Rutting Damage." *Journal of the Association of Asphalt Paving Technologists* 74: 197–253.

New York State Department of Transportation. 2012. *Hot Mix Asphalt (HMA) Mixture Design and Mixture Verification Procedures*. Materials Method MM 5.16. Albany: New York State Department of Transportation.

New York State Department of Transportation. 2014. *Comprehensive Pavement Design Manual*. Albany: New York State Department of Transportation.

North East Asphalt User/Producer Group (NEAUPG). 2011. *First Interlaboratory Study to Determine the Precision of AASHTO TP 70—the Multiple Stress Creep Recovery (MSCR) Test*. Lexington, KY: Asphalt Institute.

North East Asphalt User/Producer Group (NEAUPG). 2013. *Second Interlaboratory Study to Determine the Precision of AASHTO TP 70—the Multiple Stress Creep Recovery (MSCR) Test*. Lexington, KY: Asphalt Institute.

Pacific Coast Conference on Asphalt Specifications (PCCAS). 2013. *Interlaboratory Study to Evaluate the Precision of AASHTO TP 70—the Multiple Stress Creep Recovery (MSCR) Test and Commonly-Used PG-Plus Tests*. Lexington, KY: Asphalt Institute.

Petersen, J. Claine, and Ronald Glaser. 2011. "Asphalt Oxidation Mechanisms and the Role of Oxidation Products on Age Hardening Revisited." *Road Materials and Pavement Design* 12(4): 795–819.

Sargand, S. M., and S. S. Kim. 2001. "Performance Evaluation of Polymer-Modified and Unmodified Superpave Mixes." Presented at *Second International Symposium on Maintenance and Rehabilitation of Pavements and Technological Control*, Auburn, Alabama.

Southeastern Asphalt User/Producer Group (SEAUPG). 2012. *Interlaboratory Study to Determine the Precision of AASHTO TP 70—the Multiple Stress Creep Recovery (MSCR) Test*. Lexington, KY: Asphalt Institute.

Stempihar, Jeffrey, Akshay Gundla, and B. Shane Underwood. 2018. “Interpreting Stress Sensitivity in the Multiple Stress Creep and Recovery Test.” *Journal of Materials in Civil Engineering* 30(2).

Stevens, Ryan, Jeff Stempihar, B. Shane Underwood, and Dharminder (Paul) Pal. 2015. “Evaluation of Multiple Stress Creep and Recovery (MSCR) Data for Arizona.” *International Journal of Pavement Research and Technology* 8(5): 337–345.

Virginia Department of Transportation. 2016. *Road and Bridge Specifications*. Richmond: Virginia Department of Transportation.

Zhang, Jun, Lubinda F. Walubita, Abu N. M. Faruk, Pravat Karki, and Geoffrey S. Simate. 2015. “Use of the MSCR Test to Characterize the Asphalt Binder Properties Relative to HMA Rutting Performance—A Laboratory Study.” *Construction and Building Materials* 94: 218–227.

APPENDIX A. AASHTO PURCHASE SPECIFICATIONS

Table A-1. AASHTO M 332 Grading Table (AASHTO 2018)

Performance Grade	PG 46			PG 52							PG 58				
	34	40	46	10	16	22	28	34	40	46	16	22	28	34	40
Average 7-day max pavement design temp, °C[b]	<46			<52							<58				
Min pavement design temp, °C[b]	>–34	>–40	>–46	>–10	>–16	>–22	>–28	>–34	>–40	>–46	>–16	>–22	>–28	>–34	>–40
Original Binder															
Flash point temp, T 48, min °C	230														
Viscosity, T 316:[c] max 3 Pa•s, test temp, °C	135														
Dynamic shear, T 315:[d] G*/sinδ, min 1.00 kPa[e] test temp @ 10 rad/s, °C	46			52							58				
Rolling Thin-Film Oven Residue (T 240)															
Mass change, max, percent[f]	1.00														
MSCR, T 350: Standard Traffic "S" $J_{nr3.2}$, max 4.5 kPa^{-1} J_{nrdiff}, max 75% test temp, °C	46			52							58				
MSCR, T 350: Heavy Traffic "H" $J_{nr3.2}$, max 2.0 kPa^{-1} J_{nrdiff}, max 75% test temp, °C	46			52							58				
MSCR, T 350: Very Heavy Traffic "V" $J_{nr3.2}$, max 1.0 kPa^{-1} J_{nrdiff}, max 75% test temp, °C	46			52							58				
MSCR, T 350: Extremely Heavy Traffic "E" $J_{nr3.2}$, max 0.5 kPa^{-1} J_{nrdiff}, max 75% test temp, °C	46			52							58				
Pressurized Aging Vessel Residue (R 28)															
PAV aging temp, °C[g]	90			90							100				
Dynamic shear, T 315: "S" G* sinδ, max 5000 kPa[e] test temp @ 10 rad/s, °C	10	7	4	25	22	19	16	13	10	7	25	22	19	16	13
Dynamic shear, T 315: "H," "V," "E" G* sinδ, max 6000 kPa[e] test temp @ 10 rad/s, °C	10	7	4	25	22	19	16	13	10	7	25	22	19	16	13
Creep stiffness, T 313:[h] S, max 300 MPa m-value, min 0.300 test temp @ 60 s, °C	–24	–30	–36	0	–6	–12	–18	–24	–30	–36	–6	–12	–18	–24	–30
Direct tension, T 314:[h] Failure strain, min 1.0% test temp @ 1.0 mm/min, °C	–24	–30	–36	0	–6	–12	–18	–24	–30	–36	–6	–12	–18	–24	–30

[a] MSCR testing on RTFO residue should be performed at the PG grade based on the environmental high pavement temperature. Grade bumping is accomplished by requiring a lower J_{nr} value while testing at the environmental temperature.

[b] Pavement temperatures are estimated from air temperatures using an algorithm contained in the LTPP Bind program, may be provided by the specifying agency, or by following the procedures as outlined in M 323 and R 35, excluding the provisions for "grade bumping."

[c] This requirement may be waived at the discretion of the specifying agency if the supplier warrants that the asphalt binder can be adequately pumped and mixed at temperatures that meet all applicable safety standards.

[d] For quality control of unmodified asphalt binder production, measurement of the viscosity of the original asphalt binder may be used to supplement dynamic shear measurements of G*/sinδ at test temperatures where the asphalt is a Newtonian fluid.

[e] G*/sinδ = high temperature stiffness and G* sinδ = intermediate temperature stiffness.

[f] The mass change shall be less than 1.00 percent for either a positive (mass gain) or a negative (mass loss) change.

[g] The PAV aging temperature is based on simulated climatic conditions and is one of three temperatures, 90°C, 100°C, or 110°C. Normally the PAV aging temperature is 100°C for PG 58-xx and above. However, in desert climates, the PAV aging temperature for PG 70-xx and above may be specified as 110°C.

[h] If the creep stiffness is below 300 MPa, the direct tension test is not required. If the creep stiffness is between 300 and 600 MPa, the direct tension failure strain requirement can be used in lieu of the creep stiffness requirement. The m-value requirement must be satisfied in both cases.

Table A-1 (Continued). AASHTO M 332 Grading Table (AASHTO 2018)

Performance Grade	PG 64						PG 70					
	10	16	22	28	34	40	10	16	22	28	34	40
Average 7-day max pavement design temp, °C[b]	<64						<70					
Min pavement design temp, °C[b]	>–10	>–16	>–22	>–28	>–34	>–40	>–10	>–16	>–22	>–28	>–34	>–40
Original Binder												
Flash point temp, T 48, min °C	230											
Viscosity, T 316:[c] max 3 Pa•s, test temp, °C	135											
Dynamic shear, T 315:[d] G*/sinδ, min 1.00 kPa[e] test temp @ 10 rad/s, °C	64						70					
Rolling Thin-Film Oven Residue (T 240)												
Mass change, max, percent[f]	1.00											
MSCR, T 350: Standard Traffic "S" $J_{nr3.2}$, max 4.5 kPa^{-1} J_{nrdiff}, max 75% test temp, °C	64						70					
MSCR, T 350: Heavy Traffic "H" $J_{nr3.2}$, max 2.0 kPa^{-1} J_{nrdiff}, max 75% test temp, °C	64						70					
MSCR, T 350: Very Heavy Traffic "V" $J_{nr3.2}$, max 1.0 kPa^{-1} J_{nrdiff}, max 75% test temp, °C	64						70					
MSCR, T 350: Extremely Heavy Traffic "E" $J_{nr3.2}$, max 0.5 kPa^{-1} J_{nrdiff}, max 75% test temp, °C	64						70					
Pressurized Aging Vessel Residue (R 28)												
PAV aging temp, °C[g]	100						100 (110)					
Dynamic shear, T 315: "S" G* sinδ, max 5000 kPa[e] test temp @ 10 rad/s, °C	31	28	25	22	19	16	34	31	28	25	22	19
Dynamic shear, T 315: "H," "V," "E" G* sinδ, max 6000 kPa[e] test temp @ 10 rad/s, °C	31	28	25	22	19	16	34	31	28	25	22	19
Creep stiffness, T 313:[h] *S*, max 300 MPa *m*-value, min 0.300 test temp @ 60 s, °C	0	–6	–12	–18	–24	–30	0	–6	–12	–18	–24	–30
Direct tension, T 314:[h] Failure strain, min 1.0% test temp @ 1.0 mm/min, °C	0	–6	–12	–18	–24	–30	0	–6	–12	–18	–24	–30

[a] MSCR test on RTFO residue should be performed at the PG grade based on the environmental high pavement temperature. Grade bumping is accomplished by requiring a lower J_{nr} value while testing at the environmental temperature.

[b] Pavement temperatures are estimated from air temperatures using an algorithm contained in the LTPP Bind program, may be provided by the specifying agency, or by following the procedures as outlined in M 323 and R 35, excluding the provisions for "grade bumping."

[c] This requirement may be waived at the discretion of the specifying agency if the supplier warrants that the asphalt binder can be adequately pumped and mixed at temperatures that meet all applicable safety standards.

[d] For quality control of unmodified asphalt binder production, measurement of the viscosity of the original asphalt binder may be used to supplement dynamic shear measurements of G*/sinδ at test temperatures where the asphalt is a Newtonian fluid.

[e] G*/sinδ = high temperature stiffness and G* sinδ = intermediate temperature stiffness.

[f] The mass change shall be less than 1.00 percent for either a positive (mass gain) or a negative (mass loss) change.

[g] The PAV aging temperature is based on simulated climatic conditions and is one of three temperatures, 90°C, 100°C, or 110°C. Normally the PAV aging temperature is 100°C for PG 58-xx and above. However, in desert climates, the PAV aging temperature for PG 70-xx and above may be specified as 110°C.

[h] If the creep stiffness is below 300 MPa, the direct tension test is not required. If the creep stiffness is between 300 and 600 MPa, the direct tension failure strain requirement can be used in lieu of the creep stiffness requirement. The *m*-value requirement must be satisfied in both cases.

Table A-1 (Continued). AASHTO M 332 Grading Table (AASHTO 2018)

Performance Grade	PG 76					PG 82				
	10	16	22	28	34	10	16	22	28	34
Average 7-day max pavement design temp, °C[b]	<76					<82				
Min pavement design temp, °C[b]	>–10	>–16	>–22	>–28	>–34	>–10	>–16	>–22	>–28	>–34
Original Binder										
Flash point temp, T 48, min°C	230									
Viscosity, T 316:[c] max 3 Pa•s, test temp, °C	135									
Dynamic shear, T 315:[d] G*/sin δ, min 1.00 kPa[e] test temp @ 10 rad/s, °C	76					82				
Rolling Thin-Film Oven Residue (T 240)										
Mass change, max, percent[f]	1.00									
MSCR, T 350: Standard Traffic "S" $J_{nr3.2}$, max 4.5 kPa^{-1} J_{nrdiff}, max 75% test temp, °C	76					82				
MSCR, T 350: Heavy Traffic "H" $J_{nr3.2}$, max 2.0 kPa^{-1} J_{nrdiff}, max 75% test temp, °C	76					82				
MSCR, T 350: Very Heavy Traffic "V" $J_{nr3.2}$, max 1.0 kPa^{-1} J_{nrdiff}, max 75% test temp, °C	76					82				
MSCR, T 350: Extremely Heavy Traffic "E" $J_{nr3.2}$, max 0.5 kPa^{-1} J_{nrdiff}, max 75% test temp, °C	76					82				
Pressurized Aging Vessel Residue (R 28)										
PAV aging temp, °C[g]	100 (110)					100 (110)				
Dynamic shear, T 315: "S" G* sinδ, max 5000 kPa[e] test temp @ 10 rad/s, °C	37	34	31	28	25	40	37	34	31	28
Dynamic shear, T 315: "H," "V," "E" G* sinδ, max 6000 kPa[e] test temp @ 10 rad/s, °C	37	34	31	28	25	40	37	34	31	28
Creep stiffness, T 313:[h] S, max 300 MPa m-value, min 0.300 test temp @ 60 s, °C	0	–6	–12	–18	–24	0	–6	–12	–18	–24
Direct tension, T 314:[h] Failure strain, min 1.0% test temp @ 1.0 mm/min, °C	0	–6	–12	–18	–24	0	–6	–12	–18	–24

[a] MSCR test on RTFO residue should be performed at the PG grade based on the environmental high pavement temperature. Grade bumping is accomplished by requiring a lower J_{nr} value while testing at the environmental temperature.

[b] Pavement temperatures are estimated from air temperatures using an algorithm contained in the LTPP Bind program, may be provided by the specifying agency, or by following the procedures as outlined in M 323 and R 35, excluding the provisions for "grade bumping."

[c] This requirement may be waived at the discretion of the specifying agency if the supplier warrants that the asphalt binder can be adequately pumped and mixed at temperatures that meet all applicable safety standards.

[d] For quality control of unmodified asphalt binder production, measurement of the viscosity of the original asphalt binder may be used to supplement dynamic shear measurements of G*/sinδ at test temperatures where the asphalt is a Newtonian fluid.

[e] G*/sinδ = high temperature stiffness and G* sinδ = intermediate temperature stiffness.

[f] The mass change shall be less than 1.00 percent for either a positive (mass gain) or a negative (mass loss) change.

[g] The PAV aging temperature is based on simulated climatic conditions and is one of three temperatures, 90°C, 100°C, or 110°C. Normally the PAV aging temperature is 100°C for PG 58-xx and above. However, in desert climates, the PAV aging temperature for PG 70-xx and above may be specified as 110°C.

[h] If the creep stiffness is below 300 MPa, the direct tension test is not required. If the creep stiffness is between 300 and 600 MPa, the direct tension failure strain requirement can be used in lieu of the creep stiffness requirement. The m-value requirement must be satisfied in both cases.

Table A-2. AASHTO M 320 Grading Table (AASHTO 2010)

Performance Grade	PG 46			PG 52							PG 58					PG 64					
	34	40	46	10	16	22	28	34	40	46	16	22	28	34	40	10	16	22	28	34	40
Average 7-day max pavement design temp, °C[a]	<46			<52							<58					<64					
Min pavement design temperature, °C[a]	>–34	>–40	>–46	>–10	>–16	>–22	>–28	>–34	>–40	>–46	>–16	>–22	>–28	>–34	>–40	>–10	>–16	>–22	>–28	>–34	>–40
Original Binder																					
Flash point temp, T 48, min °C	230																				
Viscosity, T 316:[b] max 3 Pa•s, test temp, °C	135																				
Dynamic shear, T 315:[c] G*/sinδ,[d] min 1.00 kPa test temp @ 10 rad/s, °C	46			52							58					64					
Rolling Thin-Film Oven Residue (T 240)																					
Mass change,[e] max, percent	1.00																				
Dynamic shear, T 315: G*/sinδ,[d] min 2.20 kPa test temp @ 10 rad/s, °C	46			52							58					64					
Pressurized Aging Vessel Residue (R 28)																					
PAV aging temperature, °C[f]	90			90							100					100					
Dynamic shear, T 315: G* sinδ,[d] max 5000 kPa test temp @ 10 rad/s, °C	10	7	4	25	22	19	16	13	10	7	25	22	19	16	13	31	28	25	22	19	16
Creep stiffness, T 313:[g] S, max 300 MPa *m*-value, min 0.300 test temp @ 60 s, °C	–24	–30	–36	0	–6	–12	–18	–24	–30	–36	–6	–12	–18	–24	–30	0	–6	–12	–18	–24	–30
Direct tension, T 314:[g] Failure strain, min 1.0% test temp @ 1.0 mm/min, °C	–24	–30	–36	0	–6	–12	–18	–24	–30	–36	–6	–12	–18	–24	–30	0	–6	–12	–18	–24	–30

[a] Pavement temperatures are estimated from air temperatures using an algorithm contained in the LTPP Bind program, may be provided by the specifying agency, or by following the procedures as outlined in M 323 and R 35.

[b] This requirement may be waived at the discretion of the specifying agency if the supplier warrants that the asphalt binder can be adequately pumped and mixed at temperatures that meet all applicable safety standards.

[c] For quality control of unmodified asphalt binder production, measurement of the viscosity of the original asphalt binder may be used to supplement dynamic shear measurements of G*/sinδ at test temperatures where the asphalt is a Newtonian fluid.

[d] G*/sinδ = high temperature stiffness and G* sinδ = intermediate temperature stiffness.

[e] The mass change shall be less than 1.00 percent for either a positive (mass gain) or a negative (mass loss) change.

[f] The PAV aging temperature is based on simulated climatic conditions and is one of three temperatures, 90°C, 100°C, or 110°C. Normally the PAV aging temperature is 100°C for PG 58-xx and above. However, in desert climates, the PAV aging temperature for PG 70-xx and above may be specified as 110°C.

Table A-2 (Continued). AASHTO M 320 Grading Table (AASHTO 2010)

Performance Grade	PG 70						PG 76					PG 82				
	10	16	22	28	34	40	10	16	22	28	34	10	16	22	28	34
Average 7-day max pavement design temperature, °C[a]	<70						<76					<82				
Min pavement design temperature, °C[a]	>–10	>–16	>–22	>–28	>–34	>–40	>–10	>–16	>–22	>–28	>–34	>–10	>–16	>–22	>–28	>–34
Original Binder																
Flash point temp, T 48, min °C	230															
Viscosity, T 316:[b] max 3 Pa•s, test temp, °C	135															
Dynamic shear, T 315:[c] G*/sin δ,[d] min 1.00 kPa test temp @ 10 rad/s, °C	70						76					82				
Rolling Thin-Film Oven Residue (T 240)																
Mass change,[e] max, percent	1.00															
Dynamic shear, T 315: G*/sin δ,[d] min 2.20 kPa test temp @ 10 rad/s, °C	70						76					82				
Pressurized Aging Vessel Residue (R 28)																
PAV aging temperature, °C[f]	100 (110)						100 (110)					100 (110)				
Dynamic shear, T 315: G* sin δ,[d] max 5000 kPa test temp @ 10 rad/s, °C	34	31	28	25	22	19	37	34	31	28	25	40	37	34	31	28
Creep stiffness, T 313:[g] S, max 300 MPa *m*-value, min 0.300 test temp @ 60 s, °C	0	–6	–12	–18	–24	–30	0	–6	–12	–18	–24	0	–6	–12	–18	–24
Direct tension, T 314:[g] Failure strain, min 1.0% test temp @ 1.0 mm/min, °C	0	–6	–12	–18	–24	–30	0	–6	–12	–18	–24	0	–6	–12	–18	–24

[a] Pavement temperatures are estimated from air temperatures using an algorithm contained in the LTPP Bind program, may be provided by the specifying agency, or by following the procedures as outlined in M 323 and R 35.

[b] This requirement may be waived at the discretion of the specifying agency if the supplier warrants that the asphalt binder can be adequately pumped and mixed at temperatures that meet all applicable safety standards.

[c] For quality control of unmodified asphalt binder production, measurement of the viscosity of the original asphalt binder may be used to supplement dynamic shear measurements of G*/sinδ at test temperatures where the asphalt is a Newtonian fluid.

[d] G*/sinδ = high temperature stiffness and G* sinδ = intermediate temperature stiffness.

[e] The mass change shall be less than 1.00 percent for either a positive (mass gain) or a negative (mass loss) change.

[f] The PAV aging temperature is based on simulated climatic conditions and is one of three temperatures, 90°C, 100°C, or 110°C. Normally the PAV aging temperature is 100°C for PG 58-xx and above. However, in desert climates, the PAV aging temperature for PG 70-xx and above may be specified as 110°C.

APPENDIX A REFERENCES

American Association of State Highway and Transportation Officials (AASHTO). 2010. Standard Specification for Performance-Graded Asphalt Binder. AASHTO M 320. Washington, D.C.: American Association of State Highway and Transportation Officials.

American Association of State Highway and Transportation Officials (AASHTO). 2018. Standard Specification for Performance-Graded Asphalt Binder Using Multiple Stress Creep Recovery (MSCR) Test. AASHTO M 332. Washington, D.C.: American Association of State Highway and Transportation Officials.

APPENDIX B. EMAIL SURVEY

State: _____ Interviewee: _____Date of Interview: _____

Q.1 What are the asphalt binders that are being used in your state? Do you have any issues with high stiffness binders? Do you use lot of modified asphalts? How do you modify your asphalts?

A.

Q.2 Do you use 76 grade or your highest PG grade because of climate or are you bumping it due to traffic?

A.

Q.3 Has your state adopted MSCR guidelines either partially or completely or still under evaluation?

Yes

A.

Q.4 Was there a research project that has been conducted to evaluate the benefits of MSCR parameters and support the implementation process? What are the findings of the research?

A.

Q.5 If you have adopted the MSCR parameters, what are the limits on % recovery, Jnr @3.2 kPa and Jnr diff. for the different binder grades?

A.

Evaluating

No

Q.6 Is there any specific methodology you have adopted for evaluation? & Is there a timeline that you have adopted for implementation?

A.

Q.7 Are you planning to evaluate MSCR test parameters in the future to incorporate into your asphalt binder specs?

A.

Q.8 Any specific reason why there has not been any consideration towards implementation of MSCR in your state?

A.

Q.9 Did / Do you envision any concerns with adopting the MSCR parameters into spec?

A.

Q.10 What was the response from the local agencies? Did they raise any issues?

A.

Q. 11 Have you noticed any issues that would be relevant to ADOT, especially with high stiffness binders?

APPENDIX C. TESTS ON ASPHALT BINDERS AND MIXTURES

AASHTO T 240 AND R 28 FOR CONDITIONING BINDER SAMPLES

AASHTO T 240 (rolling thin film oven test) is used to replicate short-term aging of the binder, and AASHTO R 28 (aging using a pressurized aging vessel) is used to replicate long-term aging. In the AASHTO T 240 procedure, the rolling thin film oven (RTFO) is first set at 163 ± 1°C to attain thermal equilibrium (Figure C-1a and b) (AASHTO 2013). For sample preparation, 35 ± 0.5 g of the unaged binder is poured into a specially designed glass bottle (Figure C-1c). The poured binder is allowed to cool for a minimum of 1 hour and a maximum of 3 hours, after which the bottle is inserted into the rotating rack of the RTFO. A maximum of eight bottles can be inserted in one cycle. Inside the oven, the bottles rotate with a speed of 15 rotations per minute. The unaged binders are subjected to an air flow of 4 liters/min at a constant temperature of 163 ± 1°C for a period of 85 minutes. Subsequently, the aged material is scraped from inside the bottle using a specially designed tool. The material is then stored for future testing or is transferred to a pan for further conditioning via AASHTO R 28.

Figure C-1. (a) Overview of RTFO, (b) Inside the RTFO, and (c) RTFO Bottle

In AASHTO R 28, the pressurized aging vessel (PAV), illustrated in Figure C-2a, is first set to the desired testing temperature plus 5°C and allowed to equilibrate (AASHTO 2012c). For the sample preparation, 50 ± 0.5 g of the RTFO-aged material is poured onto each of the specially designed PAV pans. These pans are then stacked in a holder, shown in Figure C-2b, which is inserted into the vessel. Up to 10 pans can be stacked in the holder. However, there is no specified minimum or maximum number to use during the process. The decision is based on judgment as to how large an amount would be required for Dynamic Shear Rheometer and Bending Beam Rheometer testing. For the current project, five to six pans were used during any given test. After the pan holder is placed inside the vessel, the vessel is first allowed to heat to the required temperature. When the vessel is within 5°C of the desired aging temperature, it is pressurized in 0.2-MPa increments starting with 0.1 MPa until 2.1 MPa is reached. When both the desired aging temperature and the desired aging pressure are achieved, the binder is conditioned for 20 hours ± 10 minutes. Subsequently, the vessel is depressurized and the material is scraped from the pans and stored in tins for future testing.

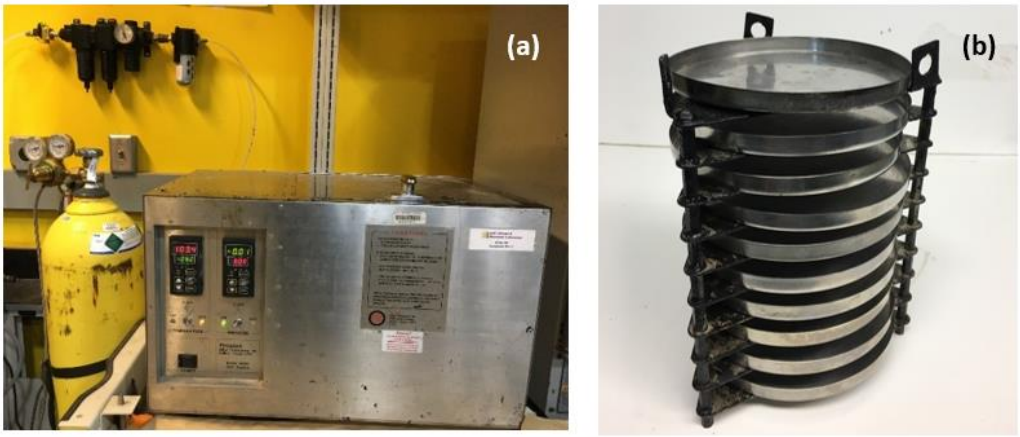

Figure C-2. (a) Overview of PAV and (b) PAV Pan and Pan Holder

AASHTO T 315—DYNAMIC SHEAR RHEOMETER

AASHTO T 315 uses a dynamic shear rheometer (DSR) to apply a sinusoidally oscillating and constant displacement angle to a binder sample (AASHTO 2012b). The testing geometry is enclosed in an environmental chamber to maintain the desired temperature during the test. The DSR used for the current project is a TA Instruments AR 2000 EX as shown in Figure C-3. The loading is applied via parallel plates either 25 mm in diameter with a 1-mm gap or 8 mm in diameter with a 2-mm gap depending on the aging level of the sample being tested. The parallel-plate geometry consists of a fixed lower plate and an upper plate that is attached to a rotating shaft/spindle. During the test, the DSR equipment tracks and records the displacement angle and applied torque. These values are used to calculate the maximum applied shear stress and shear strain according to Equations 19 and 20. Proprietary algorithms specific to the DSR equipment then apply additional corrections for machine inertia, geometry inertia,

bearing friction, and other factors. AASHTO T 315 requires calculation of the dynamic shear modulus, $|G^*|$ (reported to three significant figures); the phase angle, δ (reported to the nearest 0.1 degree); and either $|G^*|/\sin\delta$ (to the nearest 0.01 kPa) or $|G^*|\sin\delta$ (to the nearest whole number). The software that controls the DSR automatically calculates these parameters and reports them to the user.

$$\tau = \frac{2T}{\pi r^3} \quad \text{(Eq. 19)}$$

$$\gamma = \frac{\theta r}{h} \quad \text{(Eq. 20)}$$

Where τ = shear stress
T = torque
r = sample radius (25 mm or 8 mm)
γ = shear strain
θ = rotational angle
h = testing gap (1 mm or 2 mm)

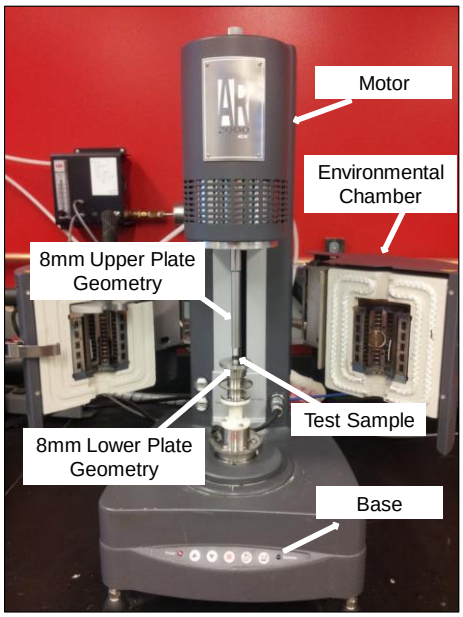

Figure C-3. Dynamic Shear Rheometer at Arizona State University

The sample preparation for the AASHTO T 315 procedure starts with pouring the binder into silicon molds, which have a designated size based on the required diameter of the sample (i.e., 8 mm or 25 mm). For testing, the parallel plates are first preheated and then the sample is detached from the molds and placed between the plates. The parallel plates are then brought within 50 µm of the final testing gap

for trimming. Once trimming is complete, the final gap is set to obtain the desired bulge in the sample. After the test gap is set, the binder samples are conditioned at the desired testing temperature so that thermal equilibrium is achieved prior to testing. During the test, the upper geometry applies a torque commensurate with the desired strain/stress and frequency values input during the test procedure.

AASHTO T 313—BENDING BEAM RHEOMETER

AASHTO T 313 evaluates the resistance of binders to low-temperature cracking by measuring the material's creep stiffness and relaxation properties at low temperatures (AASHTO 2012a). Creep stiffness, *S*, is a measure of thermal stresses in the binder, which might build up as a result of thermal contraction. If these stresses are too high, the pavement will crack. Higher values of creep stiffness are thus undesirable. Another important characteristic for binders to possess is the ability to relax the stresses quickly. When an extreme cooling event occurs, stresses build up quickly, and if they are not relaxed, they will exceed the critical point and cause cracks to occur.

During an AASHTO T 313 test, a bending beam rheometer (BBR), Figure C-4, is used to apply a constant center point load to a beam that is 6.35 ± 0.05 mm thick, 12.7 ± 0.5 mm wide, and 127 ± 2.0 mm long (see Figure C-5). In the experiments for this study, the beam is submerged in ethyl alcohol coolant, which is circulated through a chilling apparatus to maintain temperature. During the test, the load and center point deflection of the beam are monitored for 240 seconds. The resulting values are used to calculate the creep stiffness according to Equation 21. The stress relaxation properties are determined by calculating the log-log slope of the creep stiffness as a function of time, Equation 22. These values are automatically computed by the BBR software. Specification parameters from the test are the creep stiffness (reported to three significant digits) and the *m*-value (reported to the nearest 0.001) at 60 seconds. After completion of the test, AASHTO T 313 requires reporting of creep stiffness to three significant figures and the *m*-value to the nearest 0.001.

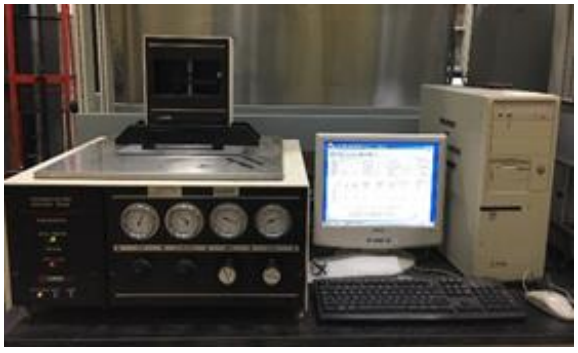

Figure C-4. Bending Beam Rheometer at Arizona State University

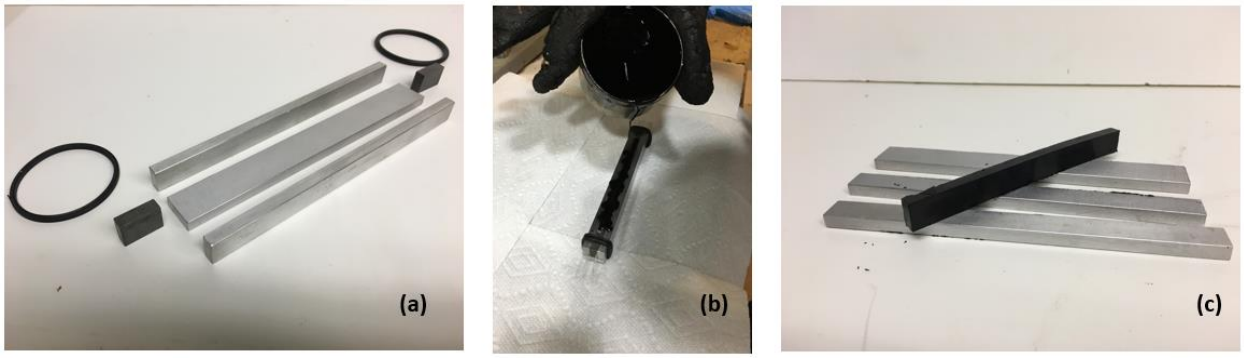

Figure C-5. (a) Disassembled BBR Mold, (b) Pouring of Asphalt into Mold, and (c) Demolded Test Specimen

$$S(t) = \frac{PL^3}{4bh^3\delta(t)} \quad \text{(Eq. 21)}$$

$$m(t) = \frac{d\log S(t)}{d\log t} \quad \text{(Eq. 22)}$$

Where S = beam stiffness
t = time
P = load
b = beam width
h = beam height
δ = beam deflection
m = logarithmic slope of beam stiffness

The AASHTO M 320 and M 332 standards call for the BBR test to be performed at a temperature 10°C lower than the ultimate low-temperature performance grade of the binder. The test is conducted on PAV-aged residue. To cast the test specimen, the material is first heated to 155° to 165°C depending on the grade of the binder, and is then poured into a mold of the appropriate dimensions, as shown in Figure C-5. After trimming and cooling, the sample is demolded and placed into the instrument for testing. For this study, the test load applied in accordance with AASHTO T 313 was 980 ± 50 mN.

AASHTO T 350—MULTIPLE STRESS CREEP AND RECOVERY

The Multiple Stress Creep and Recovery (MSCR) test is standardized by both the American Association of State Highway and Transportation Officials (in AASHTO T 350) and ASTM International (in ASTM D7405). The essential procedure in both standards is the same: A sample 25 mm in diameter and 1 mm thick is situated between two parallel plates mounted to a DSR; the sample is conditioned to a fixed specified

temperature; the sample is loaded repeatedly with a series of square-shaped stress-rest pulses (1 second loading and 9 seconds rest) at 0.1 kPa and 3.2 kPa; and the relationship between the stress input and the strain response is calculated (AASHTO 2014c, ASTM 2015). A typical strain response from the 10 3.2-kPa loading cycles used in the test is shown in Figure C-6.

AASHTO T 350 and ASTM D7405 have gone through several iterations since their first publication, but they trace their beginnings to developmental work performed through the National Cooperative Highway Research Program (Bahia et al. 2001) and the Federal Highway Administration (FHWA) (D'Angelo et al. 2007). In the case of AASHTO T 350, the method began as a provisional standard (TP 70) in 2009, was refined in 2010, 2012, and 2013, and achieved full standard status in 2014. At ASTM, the first version of D7405 appeared in 2008 and was refined in 2010 and 2015. The current versions of these two standards are identical except in one respect: The current ASTM standard provides precision and bias estimates, but the AASHTO standard does not. During the test, 20 total cycles are applied at 0.1 kPa, but only the last 10 are used for analysis. Immediately after the end of the 0.1 kPa loading, 10 creep and recovery cycles are applied at the stress level of 3.2 kPa, and all 10 are used for calculating the required test parameters.

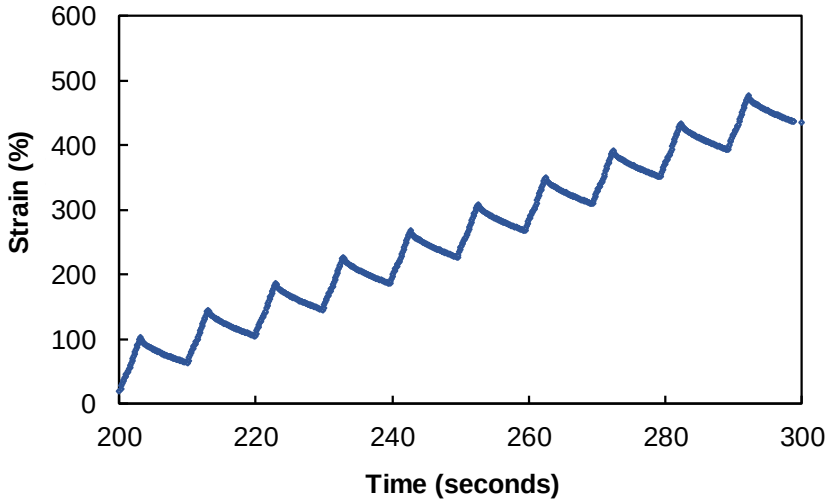

Figure C-6. Typical MSCR Strain Response During 3.2 kPa Stress Cycles

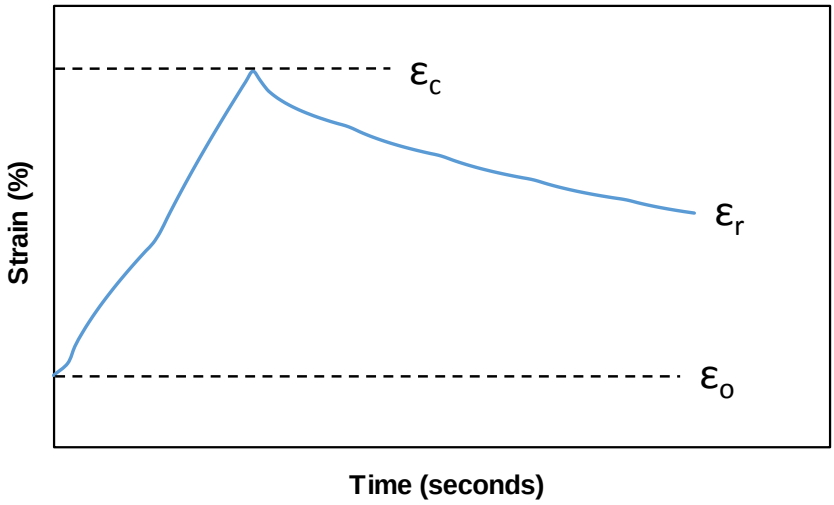

Figure C-7. Location of Strain Values During a Creep-Recovery Cycle

Figure C-7 shows the strain response for a single cycle and identifies the parameters that are extracted from each cycle. For each loading cycle, the initial strain (ε_0), maximum strain at the end of the loading (ε_c), and strain at the end of the recovery portion (ε_r) are recorded. These values are used to calculate two parameters, the nonrecoverable creep compliance at 0.1 kPa and 3.2 kPa ($J_{nr0.1}$ and $J_{nr3.2}$) and the percentage of maximum strain recovered after 3.2 kPa loading ($R_{3.2}$). The equations used to calculate these parameters and the process used for averaging are detailed in the standard and are shown below in Equations 23–33. The J_{nr} values are reported to two significant digits and the difference between the $J_{nr3.2}$ and $J_{nr0.1}$, J_{nrdiff}, is reported to the nearest 0.1 percent.

$$\varepsilon_1 = \varepsilon_c - \varepsilon_0 \quad \text{(Eq. 23)}$$

$$\varepsilon_{10} = \varepsilon_r - \varepsilon_0 \quad \text{(Eq. 24)}$$

$$\varepsilon_r(0.1, N) = \frac{(\varepsilon_1 - \varepsilon_{10}) \times 100}{\varepsilon_1} \quad \text{For cycles } N\text{=1 through } N\text{=10} \quad \text{(Eq. 25)}$$

$$\varepsilon_r(3.2, N) = \frac{(\varepsilon_1 - \varepsilon_{10}) \times 100}{\varepsilon_1} \quad \text{For cycles } N\text{=1 through } N\text{=10} \quad \text{(Eq. 26)}$$

$$R_{0.1} = \frac{SUM[\varepsilon_r(0.1, N)]}{10} \quad \text{(Eq. 27)}$$

$$R_{3.2} = \frac{SUM[\varepsilon_r(3.2, N)]}{10} \quad \text{(Eq. 28)}$$

$$J_{nr}(0.1, N) = \frac{\varepsilon_{10}}{0.1} \quad \text{(Eq. 29)}$$

$$J_{nr}(3.2,N) = \frac{\varepsilon_{10}}{3.2} \quad \text{(Eq. 30)}$$

$$J_{nr0.1} = \frac{SUM[J_{nr}(0.1,N)]}{10} \quad \text{(Eq. 31)}$$

$$J_{nr3.2} = \frac{SUM[J_{nr}(3.2,N)]}{10} \quad \text{(Eq. 32)}$$

$$J_{nrdiff} = \frac{[J_{nr3.2} - J_{nr0.1}] \times 100}{J_{nr0.1}} \quad \text{(Eq. 33)}$$

Where ε_1 = incremental strain during creep step
ε_{10} = incremental recovery strain
ε_0 = total strain at beginning of loading cycle
ε_c = total strain at end of loading portion of loading cycle
ε_r = total strain at end of recovery portion of loading cycle
$R_{0.1}$ = %Recovery at the 0.1 kPa stress level
$R_{3.2}$ = %Recovery at the 3.2 kPa stress level
J_{nr} = non-recoverable creep compliance (determined at 0.1 kPa, $J_{nr0.1}$, and 3.2 kPa, $J_{nr3.2}$, stress levels)
J_{nrdiff} = non-recoverable creep compliance difference

FOURIER TRANSFORM INFRARED SPECTROSCOPY

For many years, Fourier Transform Infrared (FT-IR) spectroscopy has been used as a tool to study the structure of materials. The application of the FT-IR technique in the field of science has been mainly for chemical characterization and for oxidation studies (Jemison et al. 1992, Petersen and Glaser 2011). The advent of attenuated total reflectance (ATR) methods has made FT-IR a rapid technique that requires minimal sample preparation and operator training. The advantages of the ATR method over conventional transmission methods are quick and easy sample preparation, natural state analysis, and clean and reproducible spectra (Jemison et al. 1992). With ATR-FT-IR, the sample is placed in contact with the sensing element, and a spectrum is recorded as a result of that contact. Unlike other sampling techniques, this one does not transmit radiation through the sample; consequently, the sample does not have to be thin enough for the radiation to be transmitted (Griffiths and de Haseth 2007). Figure C-8 shows the ATR-FT-IR instrument at Arizona State University that was used in the current study.

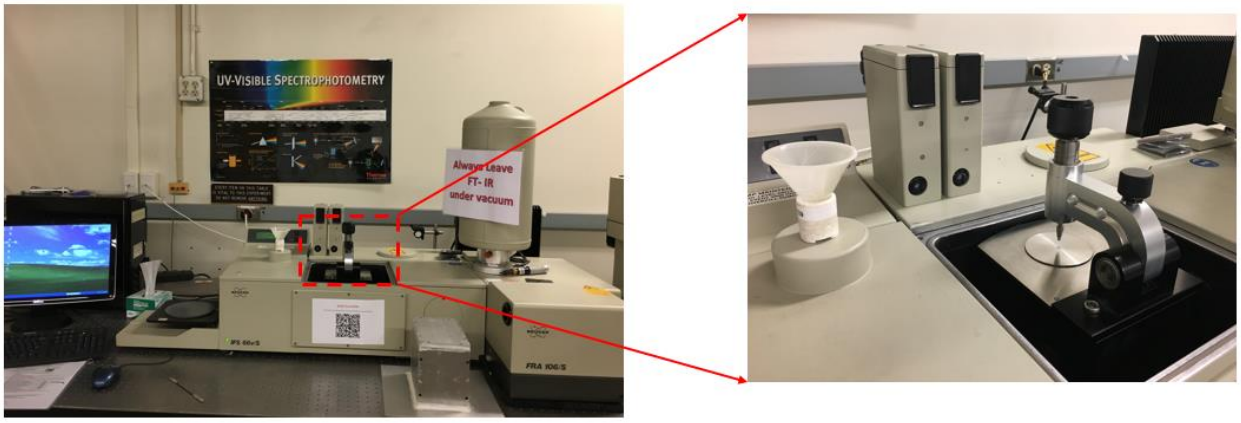

Figure C-8. Fourier Transform Infrared Spectroscopy Instrument at Arizona State University

Figure C-9 shows a typical FT-IR spectrum for binder. The figure also points out the dominant peaks in the spectrum, along with the bonds that those peaks represent. The two peaks that are of interest are the sulfoxide and carbonyl peaks. Asphalt oxidation studies (Jemison et al. 1992, Petersen and Glaser 2011) have shown that the level of oxidation can be linked directly to the area under the sulfoxide and carbonyl peaks. Figure C-10 presents a graphical representation of how the area is calculated. Also shown below is the step-by-step procedure used in the software program that was specifically developed to calculate the carbonyl and sulfoxide areas. (This program is currently being used for the NCHRP 9-54 study on long-term aging of asphalt mixtures for testing and prediction; the calculation steps were established based on discussions with and input from researchers at the Western Research Institute, which has more than 30 years of experience in analyzing FT-IR data.)

1. The data are sorted by wave number, and the user then extracts the absorbance values corresponding to the carbonyl region (1650 to 1820 cm^{-1}) and the sulfoxide region (1000 to 1050 cm^{-1}), plus the wave number used to calculate the absorbance adjustment factor (1375 cm^{-1}).
2. The user then enters in the normalization factor if known. If this value is not known, then the default of 0.1 is used. The normalization factor is the value that the absorbance should have at the wave number used for normalization. The spectrograph adjustment factor is determined by dividing the normalization factor by the measured absorbance at the normalization wave length. This adjustment process is a common technique used to correct spectrographs for known variations in FT IR scans (such as detector inconsistencies and pathway differences); it essentially involves forcing the spectrograph for a number of replicates to have a certain fixed value at a predefined wave number.
3. This adjustment factor is then multiplied by the absorbance values at all other wave numbers.
4. The normalized peak values of carbonyl and sulfoxide are extracted from the spectrograph. Depending on the data collection details, this process may require linear interpolation of the raw data at precisely 1702 cm^{-1} (carbonyl) and 1032 cm^{-1} (sulfoxide). The total

carbonyl+sulfoxide peak value is calculated by summing the individual carbonyl and sulfoxide peak values.

5. The carbonyl area (*CA*) is determined by numerical integration (trapezoidal rule) of the normalized spectrograph between wave numbers 1650 and 1820 cm^{-1}.
6. The sulfoxide area (*SA*) is determined by numerical integration (trapezoidal rule) of the normalized spectrograph between wave numbers 1000 and 1050 cm^{-1}.
7. The carbonyl+sulfoxide area (*C+SA*) is determined by adding the *CA* and *SA*.

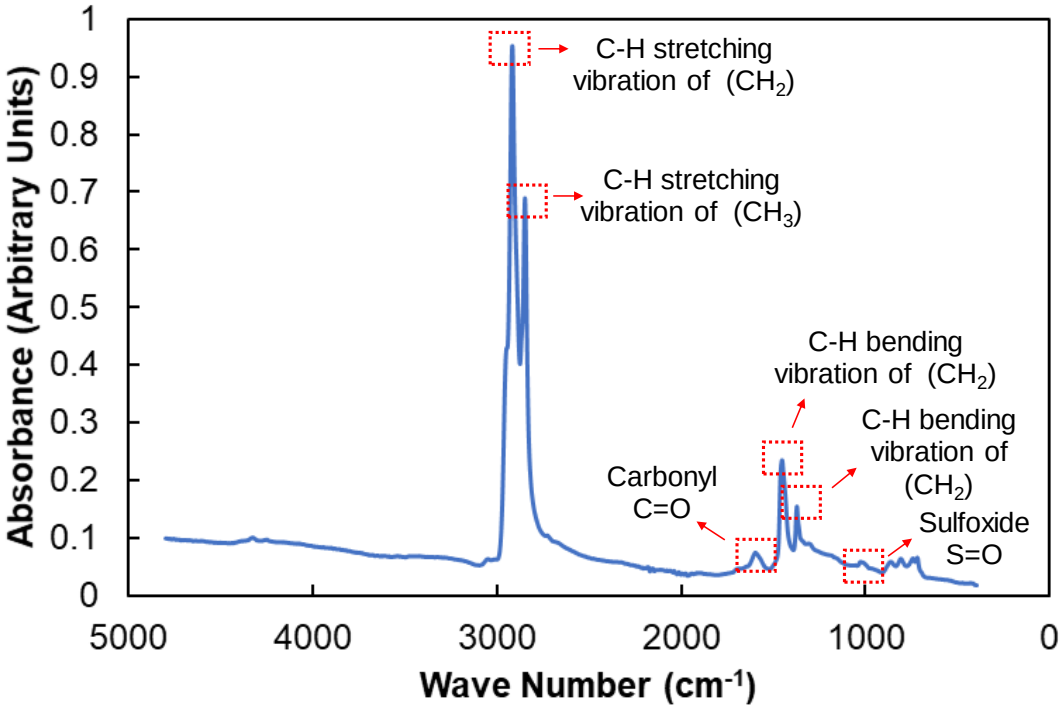

Figure C-9. Typical FT-IR Spectrum of Asphalt Binder with Dominant Peaks and the Bonds They Represent

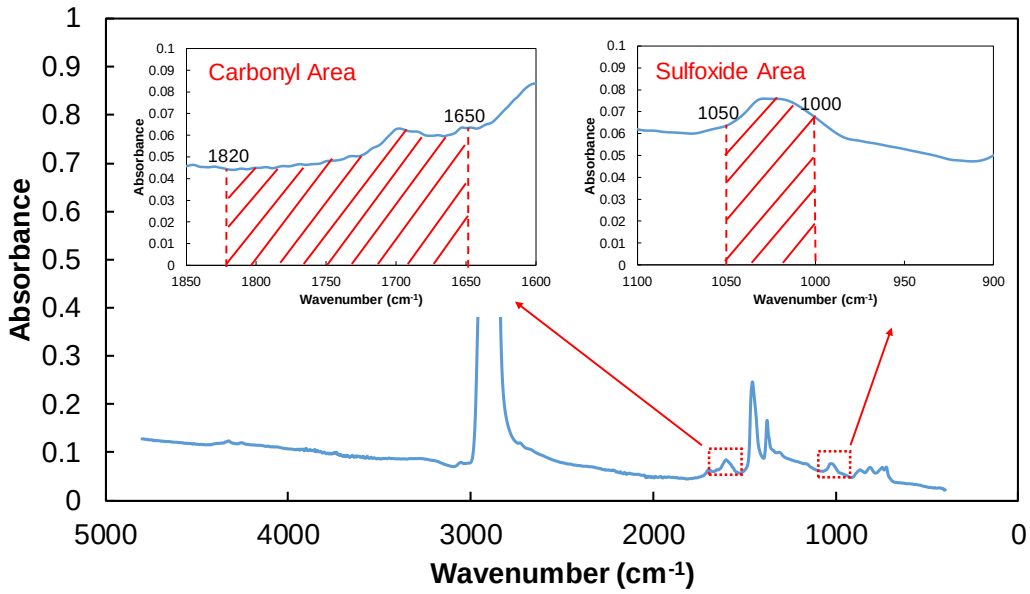

Figure C-10. Graphical Representation of Carbonyl and Sulfoxide Area Calculation

AASHTO T 342—DYNAMIC MODULUS TEST

Tests for dynamic modulus (|*E**|) are performed according to AASHTO T 342 using a servohydraulic testing machine (AASHTO 2015). There are many different manufacturers and models for this type of equipment, but the one used at Arizona State University is an Industrial Process Controls (IPC) Universal Testing Machine-25, shown in Figure C-11. The load frame capacity is 25 kN in both static and dynamic loading, and testing is conducted inside a thermally controlled chamber. The temperature control system is able to provide temperatures in the range of –15 to 60°C, and for extended periods. The loading frequencies used in this study are 25, 10, 5, 1, 0.5, and 0.1 Hz, and the test temperatures used are –10, 4.4, 21.1, 37.8, and 54°C. Tests are conducted in an increasing order of temperature and in a decreasing order of loading frequency. This temperature-frequency sequence is carried out to minimize any potential damage to the specimen before the next sequential test. The load is varied with temperature to keep the specimen response in the range of 40–80 microstrains. The number of cycles applied varies by frequency, as shown in Table C-1.

A continuous haversine wave shape, as shown in Figure C-12, is applied and measured through a load cell. Prior to testing, the sample diameter is measured and used to calculate the stresses applied to the sample from the measured forces. At the same time as the load is being monitored and controlled, the deformations are measured using three spring-loaded Linear Variable Differential Transducers (LVDTs) mounted every 120° directly on the surface of the test sample. The LVDTs are secured in place using brackets and studs glued to the specimens. The studs are glued using a specially designed apparatus to ensure proper placement and alignment. Guide rods are added to the instrumentation to ensure good alignment. Likewise, the LVDT gauge length is used to calculate the strain from the measured

displacements. Prior to the start of the test, the load cell, LVDTs, and temperature probes are calibrated and verified. The dynamic modulus test setup at Arizona State University (ASU) is shown in Figure C-11.

Table C-1. Number of Loading Cycles at Each Frequency in Dynamic Modulus Test, Following AASHTO T 342

Frequency (Hz)	Number of Cycles
25	200
10	200
5	100
1	20
0.5	15
0.1	15

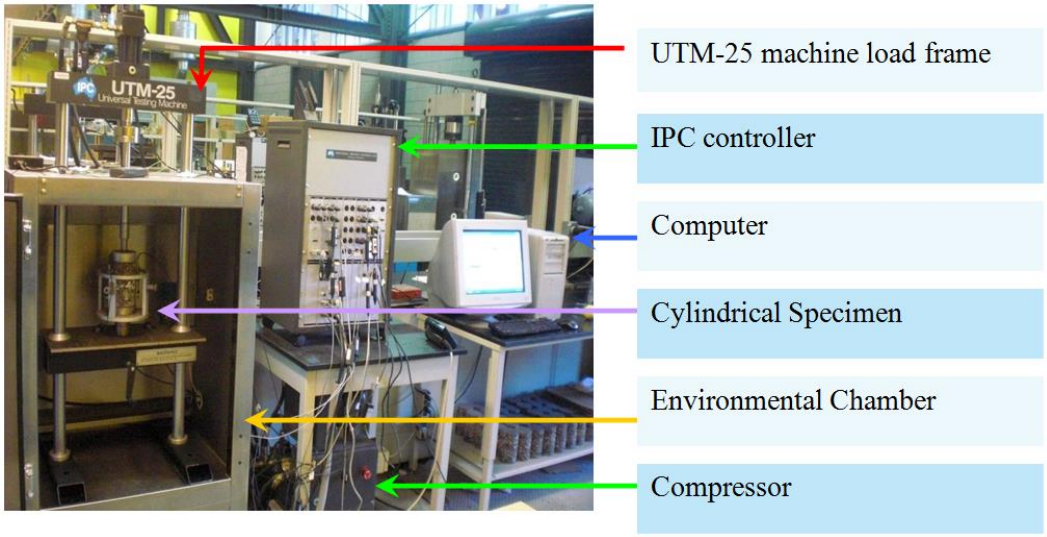

Figure C-11. Dynamic Modulus Test Setup at Arizona State University

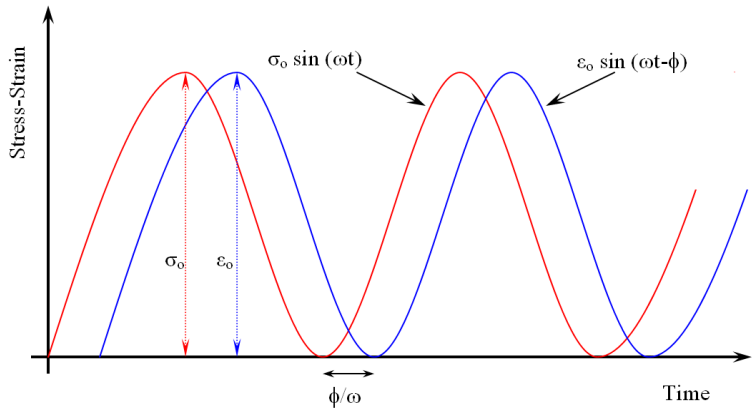

Figure C-12. Applied Stress and Strain Wave Shapes

$|E^*|$ is calculated by taking the ratio of the stress magnitude to the strain magnitude (Equation 34), while the phase angle, δ, is calculated by using the time delay (Δt) between the peak of stress and the peak of strain (Equation 35). These magnitudes and the time delay are determined by sinusoidal regression of the last five cycles of the stresses and strains at each temperature and frequency combination. The equations used for this regression are provided in AASHTO T 342 and are handled internally through the UTM-25 control software.

$$|E^*| = \frac{\sigma_0}{\varepsilon_0} \qquad \text{(Eq. 34)}$$

$$\delta = 2\pi f \Delta t \qquad \text{(Eq. 35)}$$

Where σ_0 = stress amplitude
ε_0 = strain amplitude
f = frequency
Δt = time lag
δ = phase angle

The $|E^*|$ and δ for each temperature and frequency combination (a total of 30 points) are analyzed based on the principle of time-temperature superposition to construction mastercurves. The basis of these curves is the sigmoidal function in Equation 36, the coefficients of which are identified using an optimization approach.

$$\log|E^*| = \delta + \frac{\alpha}{1 + \frac{1}{e^{\beta+\gamma(\log f_r)}}} \qquad \text{(Eq. 36)}$$

Where f_r = reduced frequency of loading (Hz)

δ = minimum logarithmic value of $|E^*|$

$\delta+\alpha$ = maximum logarithmic value of $|E^*|$

β, γ = parameters describing the shape of the sigmoidal function

The reduced frequency is the product of the test frequency and the time-temperature shift factor, a_T, which is a temperature-dependent value, T, that quantifies the amount of horizontal shift necessary to create a continuous mastercurve. T_R here is the reference temperature (21.1°C for this study). Multiple analytical representations exist for the time-temperature shift factor, and in this research the second order polynomial expression with coefficients α_1 and α_2 is adopted (Equation 37). The values of δ, α, β, γ, α_1, and α_2 are optimized to minimize the sum of the squared error between the measured and predicted dynamic modulus. Figure C-13 demonstrates the process by first showing, in C-13(a), an example of the measured data in physical frequency domain, and then showing, in C-13(b), the resultant shifted data and mastercurve function in reduced frequency domain.

$$\log(a_T) = \alpha_1 (T - T_R)^2 + \alpha_2 (T - T_R) \quad \text{(Eq. 37)}$$

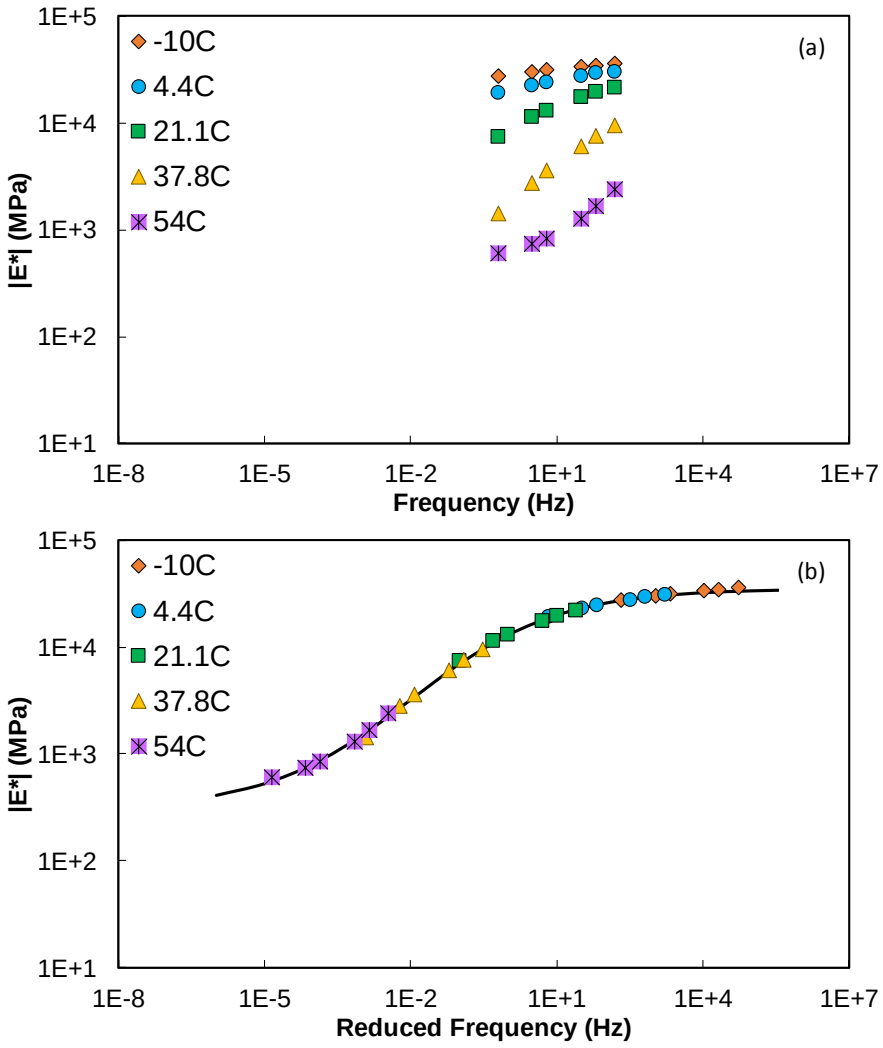

Figure C-13. (a) Measured Dynamic Modulus in Physical Frequency Domain and (b) Dynamic Modulus in Reduced Frequency Domain

AASHTO TP 107—AXIAL FATIGUE TEST

The uniaxial fatigue test applies a repeating sinusoidal load or deformation along the long axis of a cylindrical test specimen until the specimen fails (AASHTO 2014a). The test may be performed on multiple specimens and at different temperatures and deformation/load levels. The test itself is standardized in AASHTO TP 107 and uses a closed-loop servohydraulic testing machine in a temperature-controlled environment, as shown in Figure C-14. This machine applies a continuous sinusoidal loading pattern based on load, actuator displacement, or output from the on-specimen LVDTs. In this study, the actuator displacement control method is adopted as is required in AASHTO TP 107.

To obtain the appropriate test geometry, the test specimens are cored and cut from the center of gyratory-compacted plugs that are 150 mm in diameter and 180 mm in height. The ASU testing has been conducted on samples 75 mm in diameter and 150 mm in height. After the samples are cored and cut, the air voids are measured according to AASHTO T 166, and samples are glued to steel end-plates using Devcon 10240 steel putty and the jig shown in Figure C-14. This jig ensures that the sample and end-plates are axially aligned, thus eliminating loading eccentricities. Next, the samples are instrumented with four loose-core LVDTs that monitor the on-specimen deformation. The same stud and bracket system used in $|E^*|$ testing is used for this purpose. At each loading cycle, the software calculates the $|E^*|$ and δ plus the stress and strain values from the actuator and the four LVDTs. The fatigue test is run until a sudden decrease in phase angle is observed. This pattern indicates that a crack has localized and that failure has occurred.

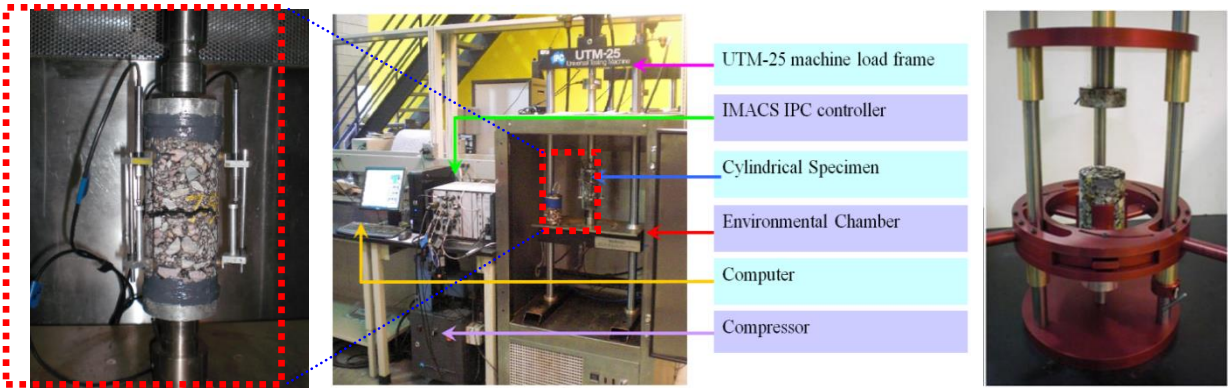

Figure C-14. Uniaxial Fatigue Test Setup and Gluing Jig

The test results are analyzed using the simplified viscoelastic continuum damage (S-VECD) approach to characterizing fatigue behavior. The first step in that approach is to establish the damage characteristic (*C*-*S*) curve. The *C*-*S* curve is a relationship unique to a given asphalt mixture that is independent of test conditions including strain levels, temperatures, mode of loading (stress-controlled or strain-controlled), and loading history. This unique function, which exists as a fundamental characteristic of the material, is characterized by employing the work potential theory as incorporated into the S-VECD formulation. It is summarized in the following equations.

$$C = \begin{cases} \dfrac{\sigma}{\varepsilon^R \times DMR} & first\ cycle \\ \dfrac{\sigma}{\varepsilon^R_{0,ta} \times DMR} & rest\ of\ cycles \end{cases} \qquad \text{(Eq. 38)}$$

$$\varepsilon^R = \frac{1}{E_R} \int_0^t E(t-\tau) \frac{d\varepsilon}{d\tau} d\tau \qquad \text{(Eq. 39)}$$

$$\left(\varepsilon_{0,ta}^{R}\right)_i = \frac{1}{E_R} \times \frac{\beta+1}{2}\left(\left(\varepsilon_{0,pp}\right)_i \times \left|E^*\right|_{LVE}\right) \quad \text{(Eq. 40)}$$

$$DMR = \frac{\left|E^*\right|_{fp}}{\left|E^*\right|_{LVE}} \quad \text{(Eq. 41)}$$

$$S_{N+1} = S_N + \left[-\frac{DMR}{2}(C_N - C_{N-1})(\varepsilon^R)^2\right]^{\frac{\alpha}{(1+\alpha)}} (\Delta\xi_i)^{\frac{1}{(1+\alpha)}} (K_1)^{\frac{1}{(1+\alpha)}} \quad \text{(Eq. 42)}$$

$$\alpha = \frac{1}{1+m} \quad \text{(Eq. 43)}$$

$$K_1 = \frac{1}{\xi_f - \xi_i}\int_{\xi_i}^{\xi_f}\left(f\left(\xi\right)\right)^{2\alpha} d\xi \quad \text{(Eq. 44)}$$

Where C = normalized pseudostiffness indicating the integrity of the material
S = internal-state variable denoting the internal damage in the material
σ = measured stress
ε^R = pseudostrain
DMR = dynamic modulus ratio
$\varepsilon^R_{0,ta}$ = tensile pseudostrain tension amplitude
E_R = reference modulus
$E(t)$ = relaxation modulus and creep compliance, respectively
t = elapsed time from specimen fabrication and time of interest
τ = time when loading began
ε = measured strain
$\varepsilon_{0,pp}$ = peak-to-peak strain amplitude
β = stress wave shape factor (1 = tension, 0 = tension-compression, and –1 = compression)
$|E^*|_{fp}$ = fingerprint dynamic modulus
$|E^*|_{LVE}$ = linear viscoelastic dynamic modulus of the material
N = number of loading cycles
$\Delta\xi_i$ = change in the average reduced time between analysis cycles
K_1 = developed functional parameter to account for the analysis of cyclic data
α = material property
m = slope in the central part of the dynamic modulus master curve for the log $E(t)$-log(t)
ξ_i = reduced starting time
ξ_f = reduced ending time

The *C*-*S* relationship generally follows an exponential or power-law decay form, as shown in Figure C-15. At small levels of damage, the material integrity is high (close to 1), but as damage increases the material integrity is lost until eventually failure will occur. Thus, from characterization of this function,

two factors emerge as important—the overall position of the *C-S* curve, and the material integrity level at which failure occurs, $C_{failure}$. All other factors being the same, materials with lower $C_{failure}$ values will exhibit superior fatigue performance. Once characterized, the *C-S* relationship can be fitted to an analytical form represented by Equation 45, where C_1 and C_2 are regression coefficients.

$$C(S) = 1 - C_1(S)^{C_2} \quad \text{(Eq. 45)}$$

To gain useful information on fatigue cracking, simulated predictions of the fatigue life under specific conditions of interest can be performed, using theoretically derived formulas for predicting the response of the material to fully reversed constant stress and constant strain loadings, as shown in the following formulations:

$$N_{failure} = \frac{\left(f_r\right)\left(2^{3\alpha}\right) S_{failure}^{\alpha-\alpha C_2+1}}{\left(\alpha-\alpha C_2+1\right)\left(C_1 C_2\right)^{\alpha}\left[\left(\varepsilon_{0.pp}\right)\left(\left|E^*\right|_{LVE}\right)\right]^{2\alpha} K_1} \quad \text{(Eq. 46)}$$

$$N_{failure} = \frac{f_r * 2^{3\alpha}\left|E^*\right|^{2\alpha}}{\left[\left(\sigma_{0,pp}\right)\right]^{2\alpha} K_1} \int_0^{\hat{S}_{failure}} \left(\frac{\left(1-\hat{C}_1\left(\hat{S}\right)^{C_2}\right)^2}{\hat{C}_1 C_2 \hat{S}^{C_2-1}} \right)^{\alpha} \left(d\hat{S}\right) \quad \text{(Eq. 47)}$$

$$\hat{S}_{failure} = \frac{S_{failure}}{\left|E^*\right|^{2\alpha/\alpha+1}} \quad \text{(Eq. 48)}$$

$$\hat{C}_{11} = C_{11}\left(\left|E^*\right|^{2\alpha/\alpha+1}\right)^{C_{12}} \quad \text{(Eq. 49)}$$

Where $N_{failure}$ = predicted cycle number of cycles to failure
f_r = reduced frequency for the condition being simulated
$|E^*|$ = dynamic modulus for the condition being simulated
$\varepsilon_{0,pp}$ = peak-to-peak strain level for simulation
$\sigma_{0,pp}$ = peak-to-peak stress level for simulation
$S_{failure}$ = damage level at failure

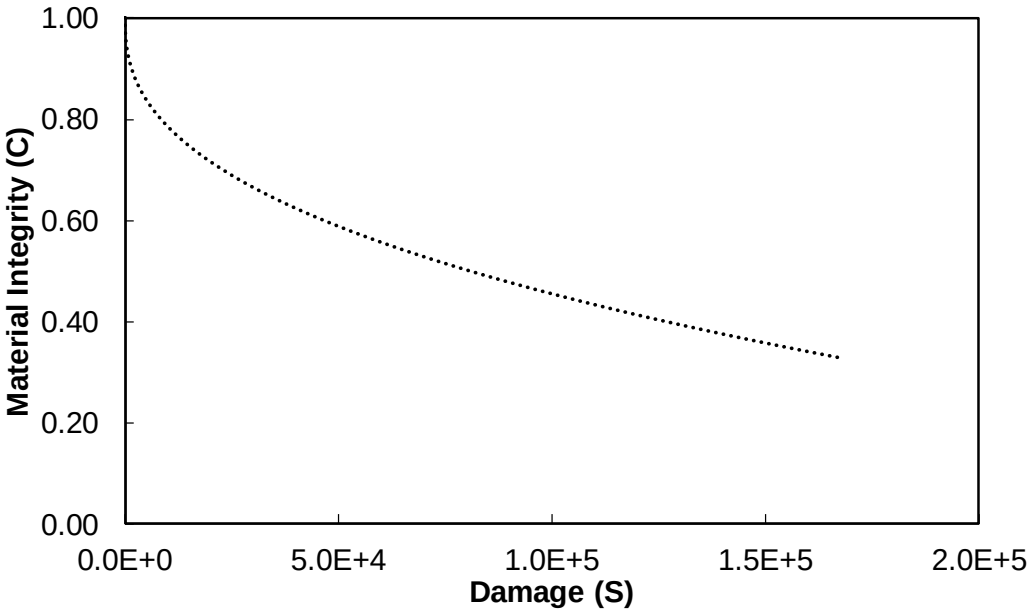

Figure C-15. Damage Characteristic Curve

AASHTO T 324—HAMBURG WHEEL TRACK TEST

The HWTT equipment, shown in Figure C-16, consists of a reciprocating wheel, which simulates a moving concentrated load. The test provides information about the rate of permanent deformation when a mixture slab or cylinder is loaded. The test uses compacted cylindrical specimens obtained from the Superpave gyratory compactor that have a diameter of 150 mm (AASHTO 2014b). The thickness of the cylinder ranges from 38 mm to 100 mm. The test requires two compacted cylinders mounted on high-density polyethylene (HDPE) molds over which the test wheel will reciprocate. Prior to mounting, the cylindrical test samples have to be cut along the secant such that when they are joined together in the molds, there is a minimal gap between the cut edges. According to AASHTO T 324, this gap should be no greater than 7.5 mm. The air void content of the cut specimens is 7 ± 1 percent. Figure C-17 shows the specimen mounting system.

Figure C-16. Hamburg Wheel Tracking Device

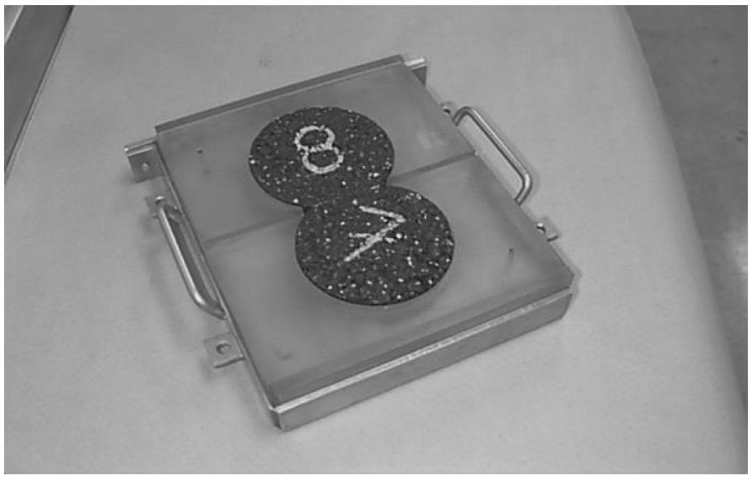

Figure C-17. Cylindrical Specimen Mounting System for the HWTT (AASHTO 2014b)

After the sample is mounted onto the equipment, rut depth is measured continuously with a series of LVDTs on the sample. HWTT results can be used to evaluate resistance to rutting and stripping. The key from the test are explained as follows (AASHTO 2014b):

1. Creep slope: The inverse of the rutting slope after postcompaction consolidation but before the stripping inflection point. Creep slope is used to evaluate rutting potential instead of rut depth because the number of load cycles at which moisture damage begins to affect rut depth varies between hot-mix asphalt (HMA) mixtures and cannot be conclusively determined from the plot.
2. Stripping inflection point: The point at which the creep slope and stripping slope intercept. This can be used to evaluate moisture damage potential. If the stripping inflection point occurs at a

low number of load cycles (e.g., less than 10,000), the HMA mixture may be susceptible to moisture damage.

3. Stripping slope: A measure of the accumulation of moisture damage. As with flow time and flow number, this portion of the plot may contain tertiary flow as well; however, it is not possible to separate out moisture damage from tertiary viscous flow.

LABORATORY PREPARATION OF POLYMER-MODIFIED ASPHALTS

A non-modified PG 58-28 binder was used in the preparation of laboratory-blended polymer-modified binders. Preparation was performed using batches of approximately 2000–2300 g and 1-gallon cans. The steps followed in preparing a batch of polymer-modified asphalt are listed below. These steps were completed using a Ross LSK high-shear mixer with a round hole disintegrating shear head, and a Glas-Col heating mantle, capable of heating 1-gallon containers. Figure C-18 shows the high-speed mixer and components.

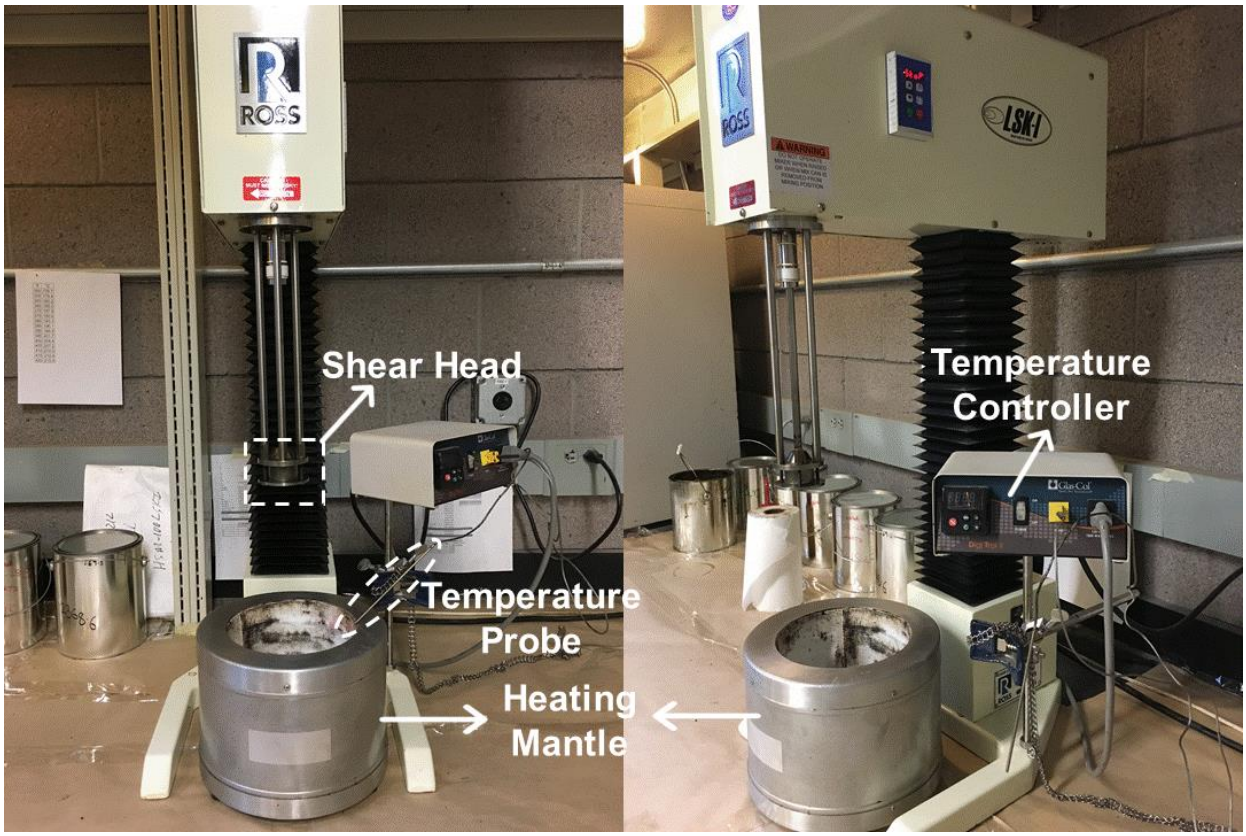

Figure C-18. High-Shear Mixer and Its Components Used for the Binder Preparation

1. If the separated binder containers have been stored at room temperature, heat the containers at 150°C for 1.5 hours.

2. Place the heated container in the heating mantle and the thermocouple into the container. Set temperature in the controller to 178°C.
3. Lower the shaft of the high-shear mixer into container and make sure that the bottom of the shearing head is within 0.5 in from the bottom of the container. This will eliminate settlement of polymer at the bottom of the container.
4. Turn on the shear mixer. The mixer will initially be at its slowest speed, 494 rpm. Gradually increase the speed to 3000 rpm over a period of one minute.
5. Once the temperature reaches 178°C (usually in 15 to 20 minutes), increase the rpm to 4500 over a period of 30 seconds. This will create just enough disturbance to avoid stagnation of polymer on the surface of the binder. Care should be taken in this step, as a larger disturbance will create a vortex which will drive oxygen into the binder, creating the possibility of oxidation.
6. Slowly add the calculated amount of polymer over a period of 5 to 10 minutes. While the polymer is being added, ensure that all polymer is being distributed into the container where the shear head is located and that none remains on the surface or adhering to the walls. If this occurs, use a popsicle stick or a coffee stirrer to push the polymer towards the center, so that it gets sucked in.
7. After all the polymer is added, the reading on the temperature controller will show that the temperature of the binder has increased about 5 to 10°C. This is due to the heat generated during the shearing mechanism in the 10-minute period.
8. Turn off the temperature controller and increase the speed to 8000 rpm. Maintain this speed for about 5 minutes. Turn on the controller to check the temperature. If the temperature of the binder is less than 197°C, keep shearing at the same speed until the temperature is between 197–200°C. The temperature increases very quickly at such high speeds, so it is recommended to check the temperature every minute after the first 5-minute period. If the temperature exceeds 200°C, but is no more than 210°C, bring the speed down to 5000 rpm and wait until the temperature comes down to 197–200°C. If the temperature exceeds 210°C, discard the batch since it is highly likely that the polymer has been damaged.
9. Once the temperature is in the range of 197–200°C, turn off the temperature controller and lower the speed to 6000–6200 rpm. It is very important that the temperature controller be turned off. This will ensure that no external heat is supplied and that the only heat generated is from the shearing action, which is sufficient to break down and disperse the polymer. At this condition, the temperature of the polymer will be maintained at 195–200°C.
10. The polymer should be sheared for 90 minutes. The countdown starts from when the speed is increased to 8000 rpm.
11. After the 90-minute shearing is completed, turn on the temperature controller. It should be remembered that the set point is still at 178°C, while the actual temperature is between 195 and 200°C. Increase the set point to 187°C and lower the speed to 3300 rpm. Leave the temperature controller on and the speed at 3300 rpm for the remainder of the preparation process. The temperature will gradually decrease to the set point (i.e., 187°C) over a period of 5–10 minutes.
12. Once the temperature reaches 187°C, add the calculated amount of sulfur and continue the shearing for 60 minutes.

13. After 60 minutes, add the calculated amount of polyphosphoric acid, and continue the shearing for an additional 30 minutes.
14. At the end of 30 minutes, turn off the temperature controller, lower the speed of the shaft to 494 rpm (default speed) over a period of 1 minute, and eventually turn off the shear controller.
15. Once the shearing stops, raise the shearing head and take the container out of the mantle. Stir the contents of the container manually using a stirring rod. Use a small cut-out portion of a screen mesh as a filter while transferring the contents into smaller containers for storage and future use. Use of a filter ensures that the polymer granules that did not break down during the shearing process can be filtered out.

The polymer-modified binders prepared for the recovery study and their respective compositions are shown in Table C-2. It should be noted that not all the polymer-modified binders blended for the study contain sulfur and PPA as cross-linking agents. For such binders, the preparation process stops at Step 10.

Table C-2. Composition of the Polymer-Modified Binders Blended for Subtask 3.4

Group	Sample	Weight Percentage (%)			
		Asphalt	SBS	Sulfur	PPA
$J_{nr3.2} < 0.5$	Y5	Provided by Supplier			
	B5	94.417	5.000	0.083	0.500
	D0.5	97.983	0.500	0.017	1.500
$0.5 < J_{nr3.2} < 1$	B2	97.433	2.000	0.067	0.500
	A3-B	96.925	3.000	0.075	0.000
	A4	96.000	4.000	0.000	0.000
$1 < J_{nr3.2} < 2$	X3	Provided by Supplier			
	A2-B	97.933	2.000	0.067	0.000
	A3	97.000	3.000	0.000	0.000

So, for the binders which have just the SBS polymer, the mixing conditions are 1.5 hours at 195°C–200°C using a shearing speed of 6000-6200 rpm. For binders which have SBS and sulfur, the mixing conditions before adding sulfur are the same as mentioned above. After addition of the sulfur, the mixing conditions are 0.5 hours at 187°C using a shearing speed of 3300 rpm. For binders which have SBS, sulfur, and PPA, the mixing conditions before adding sulfur are same as mentioned above. After addition of the sulfur, the mixing conditions are 1 hour at 187°C using a shearing speed of 3300 rpm. The same temperature and shearing speed are maintained for an additional 0.5 hour after addition of the PPA.

APPENDIX C REFERENCES

American Association of State Highway and Transportation Officials (AASHTO). 2012a. *Standard Method of Test for Determining the Flexural Creep Stiffness of Asphalt Binder Using the Bending Beam Rheometer (BBR)*. AASHTO T 313. Washington, D.C.: American Association of State Highway and Transportation Officials.

American Association of State Highway and Transportation Officials (AASHTO). 2012b. *Standard Method of Test for Determining the Rheological Properties of Asphalt Binder Using a Dynamic Shear Rheometer (DSR)*. AASHTO T 315. Washington, D.C.: American Association of State Highway and Transportation Officials.

American Association of State Highway and Transportation Officials (AASHTO). 2012c. *Standard Practice for Accelerated Aging of Asphalt Binder Using a Pressurized Aging Vessel (PAV)*. AASHTO R 28. Washington, D.C.: American Association of State Highway and Transportation Officials.

American Association of State Highway and Transportation Officials (AASHTO). 2013. *Standard Method of Test for Effect of Heat and Air on a Moving Film of Asphalt Binder (Rolling Thin-Film Oven Test)*. AASHTO T 240. Washington, D.C.: American Association of State Highway and Transportation Officials.

American Association of State Highway and Transportation Officials (AASHTO). 2014a. *Standard Method of Test for Determining the Damage Characteristic Curve of Asphalt Mixtures from Direct Tension Cyclic Fatigue Tests*. AASHTO TP 107. Washington, D.C.: American Association of State Highway and Transportation Officials.

American Association of State Highway and Transportation Officials (AASHTO). 2014b. *Standard Method of Test for Hamburg Wheel-Track Testing of Compacted Hot Mix Asphalt (HMA)*. AASHTO T 324. Washington, D.C.: American Association of State Highway and Transportation Officials.

American Association of State Highway and Transportation Officials (AASHTO). 2014c. *Standard Method of Test for Multiple Stress Creep Recovery (MSCR) Test of Asphalt Binder Using a Dynamic Shear Rheometer (DSR)*. AASHTO T 350. Washington, D.C.: American Association of State Highway and Transportation Officials.

American Association of State Highway and Transportation Officials (AASHTO). 2015. *Standard Method of Test for Determining Dynamic Modulus of Hot Mix Asphalt (HMA)*. AASHTO T 342. Washington, D.C.: American Association of State Highway and Transportation Officials.

ASTM International. 2015. *Standard Test Method for Multiple Stress Creep and Recovery (MSCR) of Asphalt Binder Using a Dynamic Shear Rheometer*. ASTM D7405. West Conshohocken, PA: ASTM International.

Bahia, H. U., D. I. Hanson, M. Zeng, H. Zhai, M. A. Khatri, and R. M. Anderson. 2001. *Characterization of Modified Asphalt Binders in Superpave Mix Design*. NCHRP Report 549. Washington, D.C.: National Cooperative Highway Research Program, Transportation Research Board, National Research Council.

D'Angelo, J., R. Kluttz, R. Dongre, K. Stephens, and L. Zanzotto. 2007. "Revision of the Superpave High Temperature Binder Specification: The Multiple Stress Creep Recovery Test." *Journal of the Association of Asphalt Paving Technologists* 76: 123–162.

Griffiths, Peter R., and James A. de Haseth. 2007. *Fourier Transform Infrared Spectrometry, Second Edition*. Hoboken, NJ: John Wiley and Sons Inc.

Jemison, H. B., B. L. Burr, R. R. Davison, J. A. Bullin, and C. J. Glover. 1992. "Application and Use of the ATR, FT-IR Method to Asphalt Aging Studies." *Fuel Science & Technology International* 10(4): 795–808.

Petersen, J. Claine, and Ronald Glaser. 2011. "Asphalt Oxidation Mechanisms and the Role of Oxidation Products on Age Hardening Revisited." *Road Materials and Pavement Design* 12(4): 795–819.

APPENDIX D. TESTS ON ASPHALT BINDERS

RESULTS FROM AASHTO T 315 EXPERIMENTS

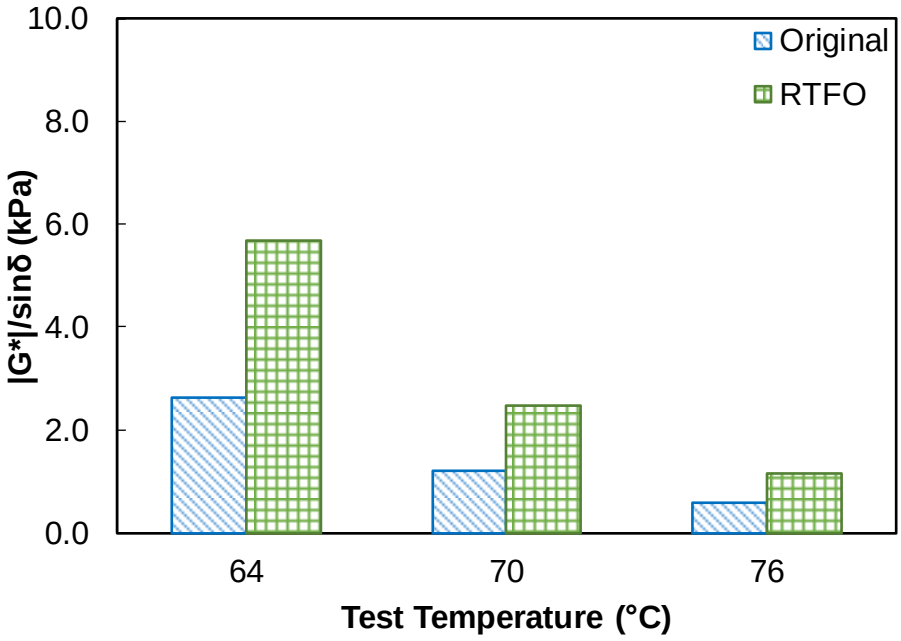

Figure D-1. Variation of $|G^*|/\sin\delta$ Parameter with Temperature and Aging Level for Binder X1

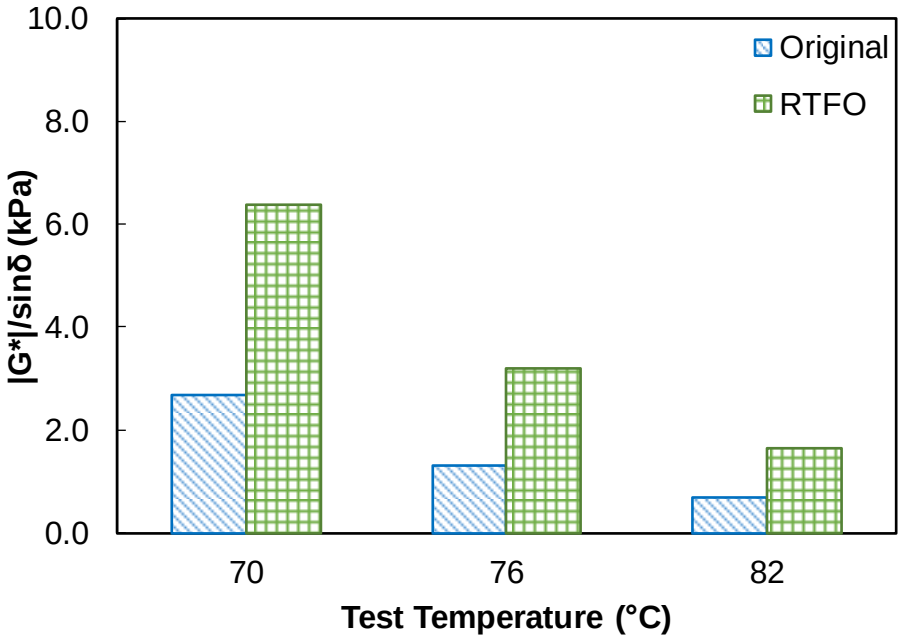

Figure D-2. Variation of $|G^*|/\sin\delta$ Parameter with Temperature and Aging Level for Binder X2

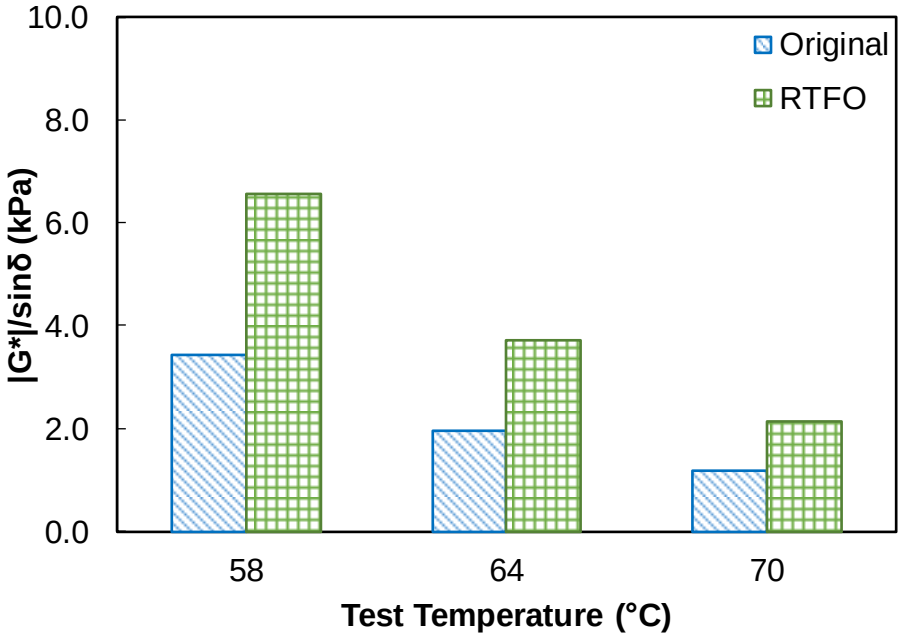

Figure D-3. Variation of $|G^*|/\sin\delta$ Parameter with Temperature and Aging Level for Binder X4

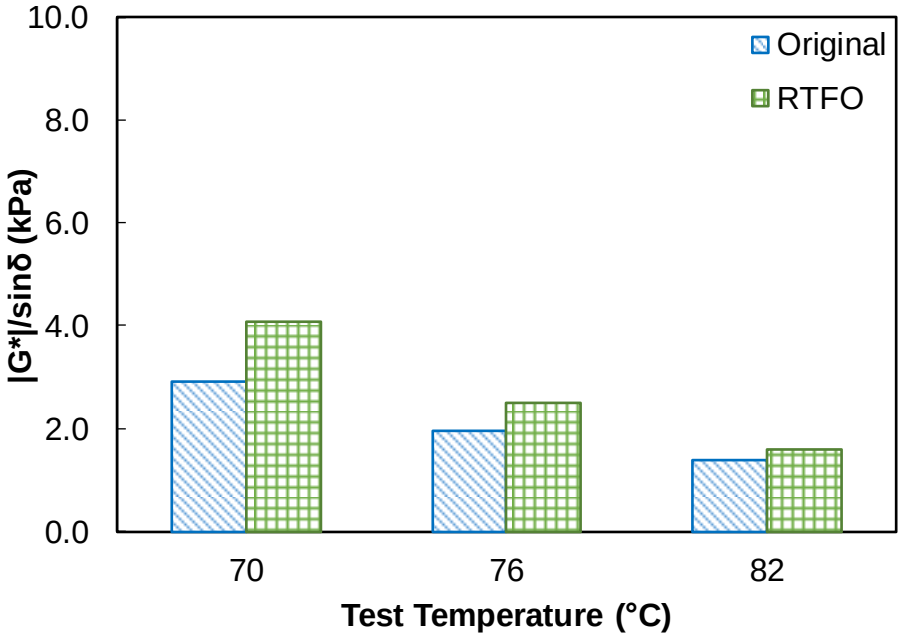

Figure D-4. Variation of $|G^*|/\sin\delta$ Parameter with Temperature and Aging Level for Binder X5

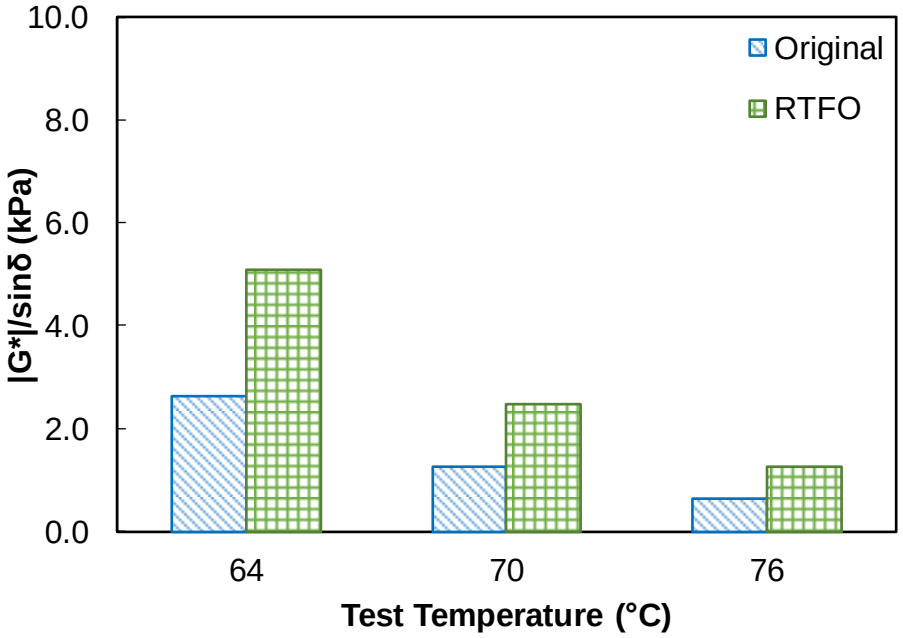

Figure D-5. Variation of $|G^*|/\sin\delta$ Parameter with Temperature and Aging Level for Binder Y2

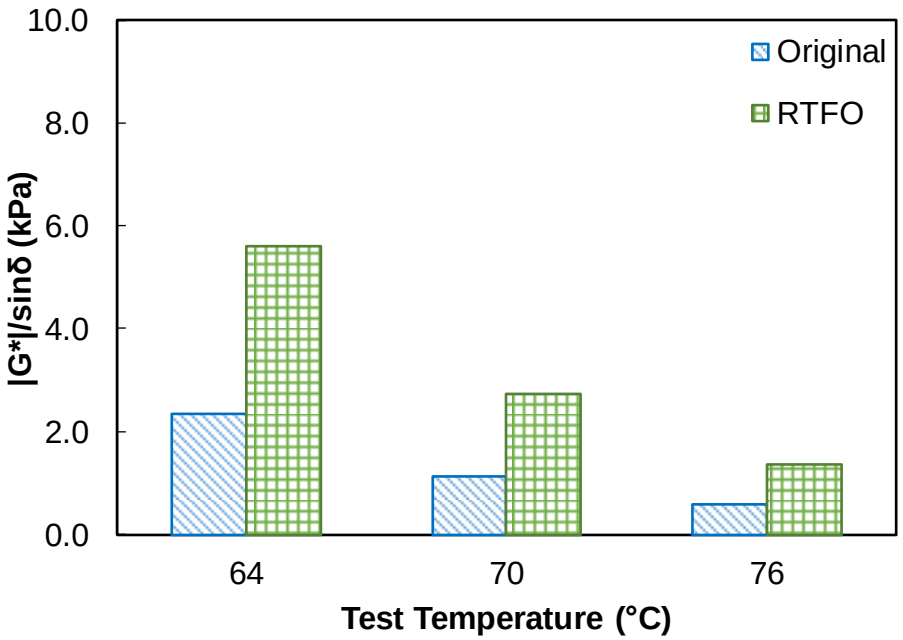

Figure D-6. Variation of $|G^*|/\sin\delta$ Parameter with Temperature and Aging Level for Binder Y3

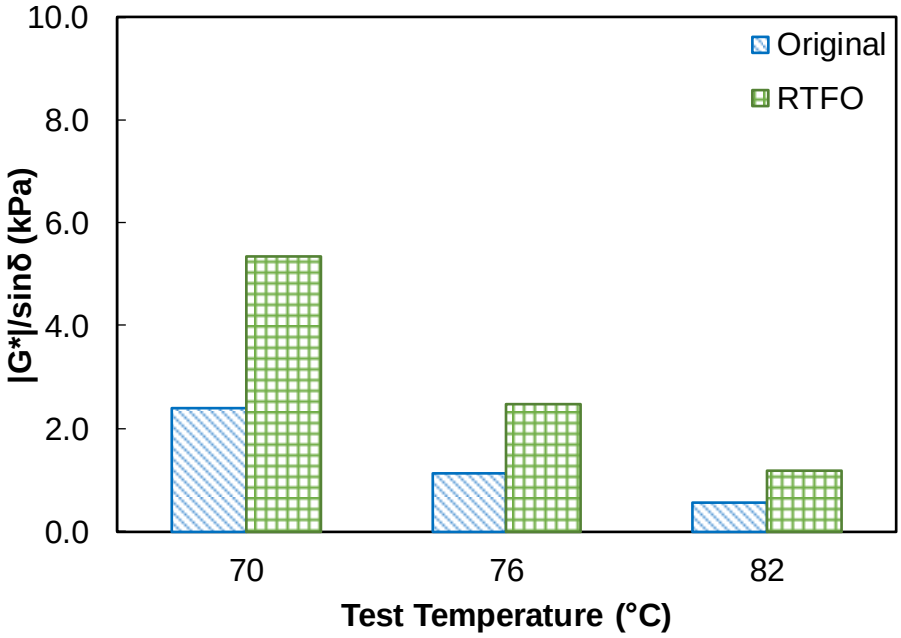

Figure D-7. Variation of $|G^*|/\sin\delta$ Parameter with Temperature and Aging Level for Binder Y4

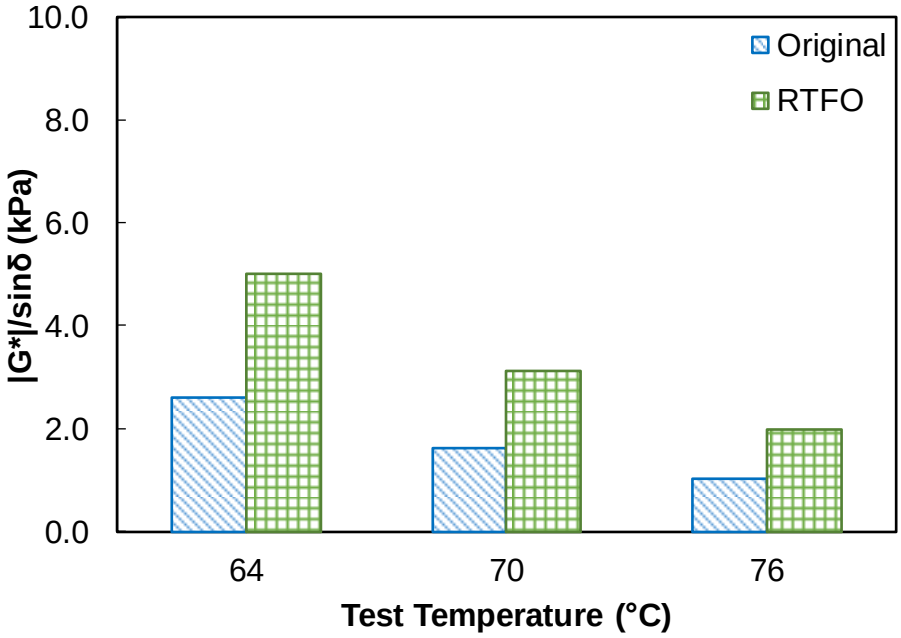

Figure D-8. Variation of $|G^*|/\sin\delta$ Parameter with Temperature and Aging Level for Binder Y5

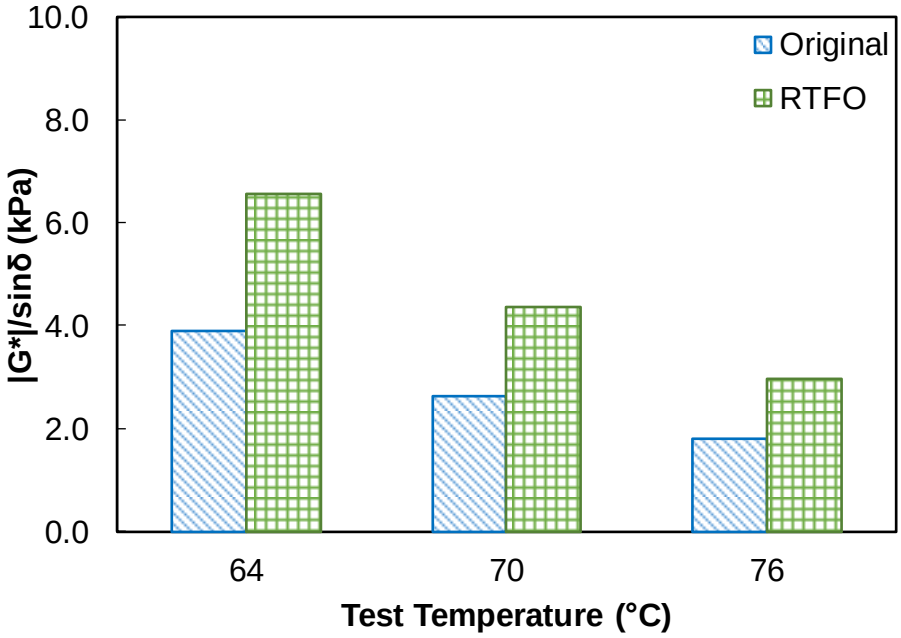

Figure D-9. Variation of $|G^*|/\sin\delta$ Parameter with Temperature and Aging Level for Binder Y6

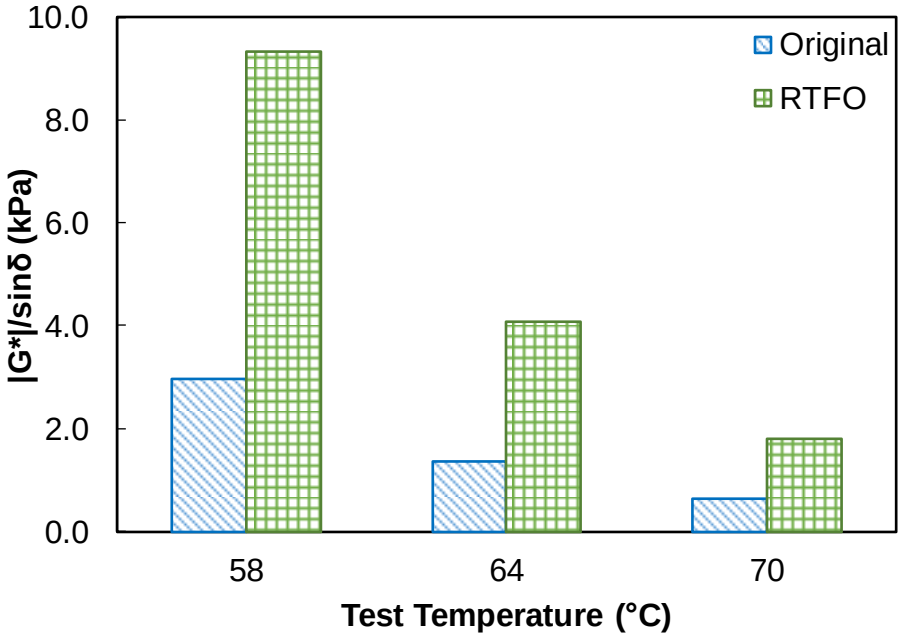

Figure D-10. Variation of $|G^*|/\sin\delta$ Parameter with Temperature and Aging Level for Binder Z1

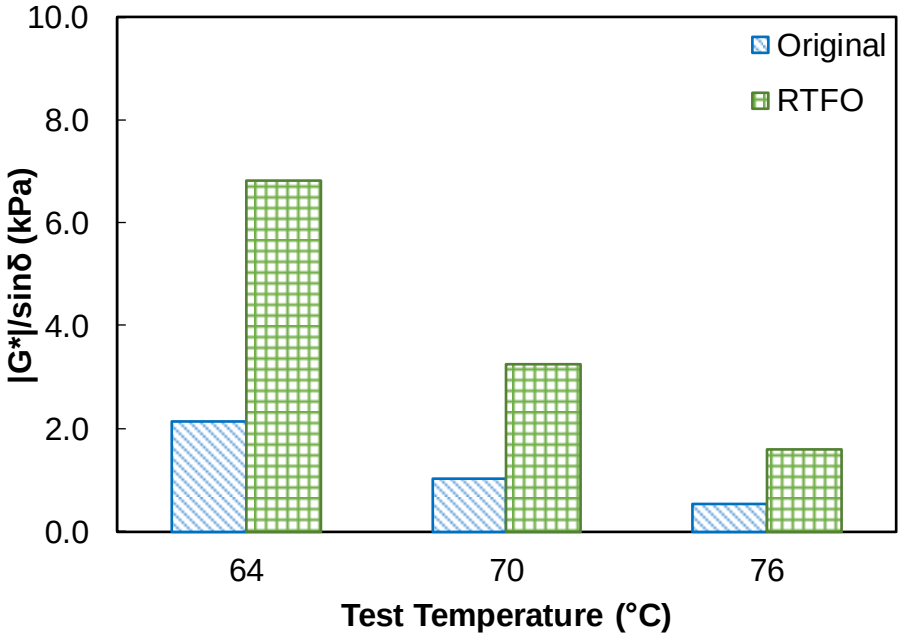

Figure D-11. Variation of $|G^*|/\sin\delta$ Parameter with Temperature and Aging Level for Binder Z2

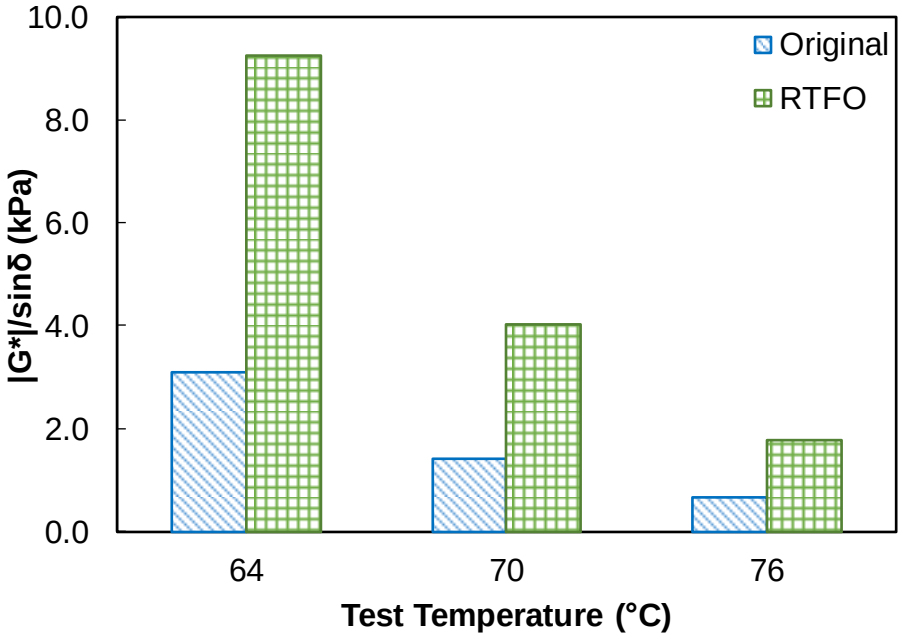

Figure D-12. Variation of $|G^*|/\sin\delta$ Parameter with Temperature and Aging Level for Binder Z3

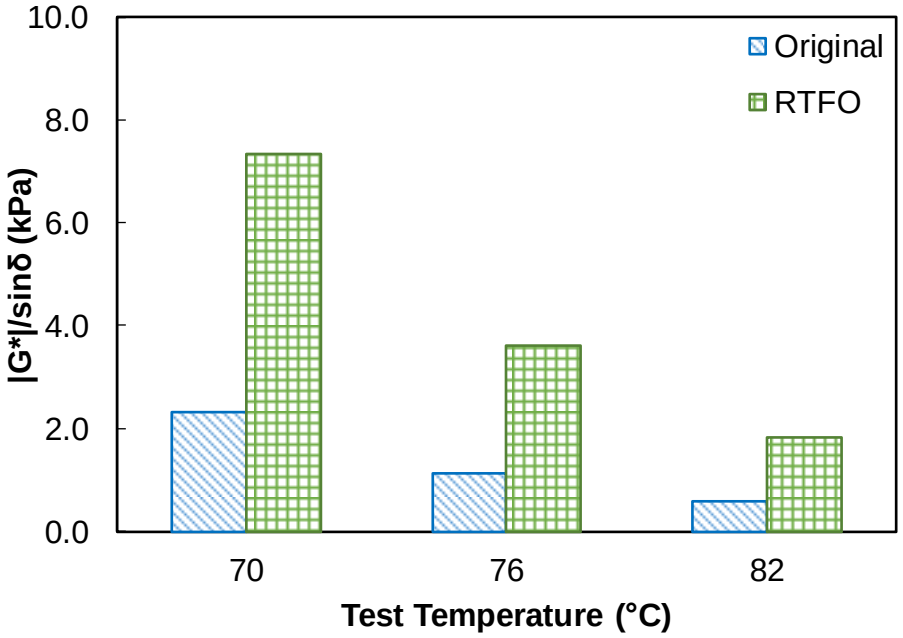

Figure D-13. Variation of $|G^*|/\sin\delta$ Parameter with Temperature and Aging Level for Binder Z4

TEST MEMORANDA

Table D-1. Asphalt Binder Test Memorandum for Binder X1

ASU Advanced Pavement Laboratory

Project Name : ADOT SPR - 742
Operator: Akshay Gundla
Binder: X1 - PG 70-10

Date	AASHTO Test Method	Aging Level	Parameter	Temperature (°C)		Result	
9/6/2016	T 315 – 25 mm	Original	|G*|/sin δ	64		2.63	kPa
				70		1.20	kPa
				76		0.59	kPa
	T 315 – 8 mm		|G*|sin δ	31		603.97	kPa
				34		361.30	kPa
				N/A		N/A	kPa
9/6/2016	T 315 – 25 mm	RTFO	|G*|/sin δ	64		5.68	kPa
				70		2.48	kPa
				76		1.15	kPa
	T 315 – 8 mm		|G*|sin δ	31		1285.44	kPa
				34		799.47	kPa
				N/A		N/A	kPa
9/6/2016	T 315 – 8 mm	PAV at 110°C	|G*|sin δ	31		4021.77	kPa
				34		2772.75	kPa
				N/A		N/A	kPa
8/28/2016	T 315 – 25 mm	PAV at 110°C	|G*|/sin δ	70		13.16	kPa
8/28/2016	T 350	Original		**64**	**70**	**76**	
			$R_{0.1}$	1.22	0.86	0.27	%
			$R_{3.2}$	0.40	0.21	0.10	%
			R_{Diff}	67.26	75.75	62.96	%
			$Jnr_{0.1}$	3.623	5.988	16.994	kPa^{-1}
			$Jnr_{3.2}$	3.765	6.244	17.732	kPa^{-1}
			Jnr_{Diff}	3.94	4.28	4.34	%
8/29/2016	T 350	RTFO		**64**	**70**	**76**	
			$R_{0.1}$	3.85	1.85	0.61	%
			$R_{3.2}$	1.81	0.54	0.18	%
			R_{Diff}	52.93	70.66	70.75	%
			$Jnr_{0.1}$	1.512	3.806	8.136	kPa^{-1}
			$Jnr_{3.2}$	1.589	4.025	8.604	kPa^{-1}
			Jnr_{Diff}	5.09	5.87	5.77	%
8/28/2016	T 313	PAV at 110°C	*m*-Value	0		0.413	
			S			76.8	MPa
8/21/2016			*m*-Value	–6		0.335	
			S			165.5	MPa
			m-Value	N/A		N/A	
			S			N/A	MPa

Table D-2. Asphalt Binder Test Memorandum for Binder X2

ASU Advanced Pavement Laboratory

Project Name : ADOT SPR - 742
Operator: Akshay Gundla
Binder: X2 - PG 76-16

Date	AASHTO Test Method	Aging Level	Parameter	Temperature (°C)		Result	
10/10/2016	T 315 – 25 mm	Original	|G*|/sin δ	70		2.68	kPa
				76		1.32	kPa
				82		0.68	kPa
	T 315 – 8 mm		|G*|sin δ	31		658.90	kPa
				34		433.42	kPa
				37		282.44	kPa
10/8/2016	T 315 – 25 mm	RTFO	|G*|/sin δ	70		6.38	kPa
				76		3.20	kPa
				82		1.64	kPa
	T 315 – 8 mm		|G*|sin δ	31		1069.83	kPa
				34		724.41	kPa
				37		487.32	kPa
10/13/2016	T 315 – 8 mm	PAV at 110° C	|G*|sin δ	31		3125.55	kPa
				34		2309.29	kPa
				37		1674.57	kPa
10/14/2016	T 315 – 25 mm	PAV at 110° C	|G*|/sin δ	76		22.38	kPa
10/11/2016	T 350	Original		**64**	**70**	**76**	
			$R_{0.1}$	16.55	10.30	5.67	%
			$R_{3.2}$	5.13	1.86	0.65	%
			R_{Diff}	68.98	82.01	88.54	%
			$Jnr_{0.1}$	1.264	3.029	6.530	kPa^{-1}
			$Jnr_{3.2}$	1.570	3.852	8.283	kPa^{-1}
			Jnr_{Diff}	24.22	27.14	26.84	%
10/8/2016	T 350	RTFO		**64**	**70**	**76**	
			$R_{0.1}$	38.61	29.10	20.54	%
			$R_{3.2}$	22.96	9.54	3.59	%
			R_{Diff}	40.56	67.21	82.56	%
			$Jnr_{0.1}$	0.340	0.845	1.993	kPa^{-1}
			$Jnr_{3.2}$	0.438	1.186	2.897	kPa^{-1}
			Jnr_{Diff}	28.82	40.40	45.44	%
10/17/2016	T 313	PAV at 110° C	*m*-Value	0		0.393	
			S			56.5	MPa
10/12/2016			*m*-Value	–6		0.3465	
			S			115.5	MPa
10/14/2016			*m*-Value	–12		0.3025	
			S			241.5	MPa

Table D-3. Asphalt Binder Test Memorandum for Binder X3

ASU Advanced Pavement Laboratory

Project Name : ADOT SPR - 742
Operator: Akshay Gundla
Binder: X3 - PG 64H-22

Date	AASHTO Test Method	Aging Level	Parameter	Temperature (°C)		Result	
10/11/2016	T 315 – 25mm	Original	|G*|/sin δ	58		3.32	kPa
				64		1.86	kPa
				70		1.08	kPa
10/13/2016	T 315 – 8mm		|G*|sin δ	22		300.62	kPa
				25		191.89	kPa
				28		122.08	kPa
10/6/2016	T 315 – 25mm	RTFO	|G*|/sin δ	58		6.37	kPa
				64		3.61	kPa
				70		2.09	kPa
10/3/2016	T 315 – 8mm		|G*|sin δ	22		586.19	kPa
				25		377.78	kPa
				28		245.24	kPa
10/6/2016	T 315 – 8mm	PAV at 100°C	|G*|sin δ	22		1582.53	kPa
				25		1107.53	kPa
				28		748.55	kPa
10/4/2016	T 315 – 25mm	PAV at 100°C	|G*|/sin δ	64		9.94	kPa
10/12/2016	T 350	Original		**58**	**64**	**70**	
			$R_{0.1}$	76.07	76.36	74.16	%
			$R_{3.2}$	29.69	19.07	9.83	%
			R_{Diff}	60.98	75.02	86.74	%
			$Jnr_{0.1}$	0.468	0.866	1.620	kPa^{-1}
			$Jnr_{3.2}$	1.569	3.587	7.621	kPa^{-1}
			Jnr_{Diff}	235.31	314.43	371.42	%
10/3/2016	T 350	RTFO		**58**	**64**	**70**	
			$R_{0.1}$	83.59	88.27	84.56	%
			$R_{3.2}$	55.01	47.25	22.87	%
			R_{Diff}	34.19	46.49	72.93	%
			$Jnr_{0.1}$	0.157	0.200	0.420	kPa^{-1}
			$Jnr_{3.2}$	0.468	1.020	2.838	kPa^{-1}
			Jnr_{Diff}	198.16	408.81	690.13	%
10/4/2016	T 313	PAV at 100°C	*m*-Value	–6		Material too soft	
			S				
10/3/2016			*m*-Value	–12		0.399	
			S			68.1	MPa
10/3/2016			*m*-Value	–18		0.337	
			S			152.5	MPa

Table D-4. Asphalt Binder Test Memorandum for Binder X4

ASU Advanced Pavement Laboratory

Project Name : ADOT SPR - 742
Operator: Akshay Gundla
Binder: X4 - PG 64V-22

Date	AASHTO Test Method	Aging Level	Parameter	Temperature (°C)		Result	
9/24/2016	T 315 – 25mm	Original	|G*|/sin δ	58		3.42	kPa
				64		1.96	kPa
				70		1.17	kPa
10/6/2016	T 315 – 8mm		|G*|sin δ	22		319.45	kPa
				25		209.26	kPa
				28		134.97	kPa
9/16/2016	T 315 – 25mm	RTFO	|G*|/sin δ	58		6.56	kPa
				64		3.71	kPa
				70		2.14	kPa
9/19/2016	T 315 – 8mm		|G*|sin δ	22		636.24	kPa
				25		411.95	kPa
				28		265.55	kPa
9/19/2016	T 315 – 8mm	PAV at 100°C	|G*|sin δ	22		1645.66	kPa
				25		1123.20	kPa
				28		755.38	kPa
9/19/2016	T 315 – 25mm	PAV at 100°C	|G*|/sin δ	64		10.01	kPa
10/6/2016	T 350	Original		**58**	**64**	**70**	
			$R_{0.1}$	87.67	88.60	89.65	%
			$R_{3.2}$	46.59	29.20	20.16	%
			R_{Diff}	46.86	67.04	77.56	%
			$Jnr_{0.1}$	0.202	0.344	0.527	kPa^{-1}
			$Jnr_{3.2}$	0.974	2.545	5.321	kPa^{-1}
			Jnr_{Diff}	382.48	642.50	952.59	%
9/17/2016	T 350	RTFO		**58**	**64**	**70**	
			$R_{0.1}$	81.99	82.73	84.15	%
			$R_{3.2}$	59.16	47.38	32.17	%
			R_{Diff}	27.90	43.43	61.80	%
			$Jnr_{0.1}$	0.167	0.281	0.478	kPa^{-1}
			$Jnr_{3.2}$	0.404	0.982	2.306	kPa^{-1}
			Jnr_{Diff}	146.75	249.48	384.55	%
9/17/2016	T 313	PAV at 100°C	*m*-Value	–6		Material too soft	
			S				
9/16/2016			*m*-Value	–12		0.406	
			S			69.85	MPa
9/17/2016			*m*-Value	–18		0.338	
			S			148	MPa

Table D-5. Asphalt Binder Test Memorandum for Binder X5

ASU Advanced Pavement Laboratory

Project Name : ADOT SPR - 742
Operator: Akshay Gundla
Binder: X5 - PG 76-22TR

Date	AASHTO Test Method	Aging Level	Parameter	Temperature (°C)		Result	
10/14/2016	T 315 – 25 mm	Original	|G*|/sin δ	70		2.91	kPa
				76		1.95	kPa
				82		1.39	kPa
10/19/2016	T 315 – 8 mm		|G*|sin δ	28		562.69	kPa
				31		351.10	kPa
				34		219.39	kPa
9/25/2016	T 315 – 25 mm	RTFO	|G*|/sin δ	70		4.07	kPa
				76		2.49	kPa
				82		1.59	kPa
9/26/2016	T 315 – 8 mm		|G*|sin δ	28		911.47	kPa
				31		566.34	kPa
				34		349.67	kPa
9/26/2016	T 315 – 8 mm	PAV at 110°C	|G*|sin δ	28		2749.40	kPa
				31		1860.54	kPa
				34		1224.36	kPa
9/28/2016	T 315 – 25 mm	PAV at 110°C	|G*|/sin δ	76		6.54	kPa
10/15/2016	T 350	Original		**64**	**70**	**76**	
			$R_{0.1}$	98.79	98.63	97.80	%
			$R_{3.2}$	95.38	93.03	72.11	%
			R_{Diff}	3.45	5.67	26.28	%
			$Jnr_{0.1}$	0.013	0.024	0.056	kPa^{-1}
			$Jnr_{3.2}$	0.050	0.113	0.763	kPa^{-1}
			Jnr_{Diff}	282.03	367.33	1270.00	%
9/25/2016	T 350	RTFO		**64**	**70**	**76**	
			$R_{0.1}$	95.66	95.65	94.98	%
			$R_{3.2}$	87.44	80.49	56.62	%
			R_{Diff}	8.60	15.85	40.39	%
			$Jnr_{0.1}$	0.036	0.064	0.118	kPa^{-1}
			$Jnr_{3.2}$	0.107	0.283	1.100	kPa^{-1}
			Jnr_{Diff}	197.43	343.70	830.04	%
9/28/2016	T 313	PAV at 110°C	*m*-Value	–6		0.383	
			S			97.25	MPa
9/25/2016			*m*-Value	–12		0.3245	
			S			195	MPa
10/6/2016			*m*-Value	–18		0.275	
			S			377.5	MPa

Table D-6. Asphalt Binder Test Memorandum for Binder Y1

ASU Advanced Pavement Laboratory

Project Name : ADOT SPR - 742
Operator: Akshay Gundla
Binder: Y1 - PG 64-22

Date	AASHTO Test Method	Aging Level	Parameter	Temperature (°C)		Result	
8/8/2016	T 315 – 25 mm	Original	|G*|/sin δ	58		2.5	kPa
				64		1.1	kPa
				70		0.6	kPa
	T 315 – 8 mm		|G*|sin δ	22		776.5	kPa
				25		489.7	kPa
				28		301.3	kPa
8/13/2016	T 315 – 25 mm	RTFO	|G*|/sin δ	58		6.9	kPa
				64		3.0	kPa
				70		1.4	kPa
	T 315 – 8 mm		|G*|sin δ	22		1538.5	kPa
				25		1027.8	kPa
				28		659.5	kPa
8/12/2016	T 315 – 8 mm	PAV at 100°C	|G*|sin δ	22		3815.5	kPa
				25		2737.7	kPa
				28		1910.2	kPa
8/12/2016	T 315 – 25 mm	PAV at 100°C	|G*|/sin δ	64		12.0	kPa
8/8/2016	T 350	Original		58	64	70	
			$R_{0.1}$	2.20	0.97	0.48	%
			$R_{3.2}$	0.68	0.20	0.12	%
			R_{Diff}	69.32	79.58	73.50	%
			$Jnr_{0.1}$	3.589	8.344	16.971	kPa^{-1}
			$Jnr_{3.2}$	3.848	8.946	18.225	kPa^{-1}
			Jnr_{Diff}	7.23	7.21	7.39	%
8/13/2016	T 350	RTFO		58	64	70	
			$R_{0.1}$	8.96	4.49	2.11	%
			$R_{3.2}$	4.14	1.32	0.42	%
			R_{Diff}	53.77	70.60	79.93	%
			$Jnr_{0.1}$	1.168	2.910	6.725	kPa^{-1}
			$Jnr_{3.2}$	1.287	3.240	7.511	kPa^{-1}
			Jnr_{Diff}	10.14	11.35	11.69	%
8/8/2016	T 313	PAV at 100°C	*m*-Value	–6		0.3965	
			S			66	MPa
8/8/2016			*m*-Value	–12		0.3265	
			S			154	MPa
8/9/2016			*m*-Value	–18		0.284	
			S			315.5	MPa

Table D-7. Asphalt Binder Test Memorandum for Binder Y2

ASU Advanced Pavement Laboratory

Project Name : ADOT SPR - 742
Operator: Akshay Gundla
Binder: Y2 - PG 70-22

Date	AASHTO Test Method	Aging Level	Parameter	Temperature (°C)		Result	
8/16/2016	T 315 – 25 mm	Original	|G*|/sin δ	64		2.62	kPa
				70		1.26	kPa
				76		0.64	kPa
8/19/2016	T 315 – 8 mm		|G*|sin δ	25		676.07	kPa
				28		435.69	kPa
				31		280.08	kPa
8/27/2016	T 315 – 25 mm	RTFO	|G*|/sin δ	64		5.09	kPa
				70		2.48	kPa
				76		1.25	kPa
	T 315 – 8 mm		|G*|sin δ	25		994.07	kPa
				28		656.77	kPa
				31		436.50	kPa
8/19/2016	T 315 – 8 mm	PAV at 110°C	|G*|sin δ	25		2957.26	kPa
				28		2156.55	kPa
				31		1560.16	kPa
8/18/2016	T 315 – 25 mm	PAV at 110°C	|G*|/sin δ	70		22.33	kPa
8/17/2016	T 350	Original		**64**	**70**	**76**	
			$R_{0.1}$	13.65	8.21	4.17	%
			$R_{3.2}$	2.16	0.77	0.26	%
			R_{Diff}	84.22	90.63	93.82	%
			$Jnr_{0.1}$	2.908	6.584	14.523	kPa^{-1}
			$Jnr_{3.2}$	3.886	8.837	19.728	kPa^{-1}
			Jnr_{Diff}	33.63	34.24	35.84	%
8/22/2016	T 350	RTFO		**64**	**70**	**76**	
			$R_{0.1}$	30.83	22.18	14.63	%
			$R_{3.2}$	7.64	2.85	1.01	%
			R_{Diff}	75.23	87.17	93.11	%
			$Jnr_{0.1}$	1.043	2.523	5.755	kPa^{-1}
			$Jnr_{3.2}$	1.573	3.947	9.120	kPa^{-1}
			Jnr_{Diff}	50.82	56.46	58.48	%
8/23/2016	T 313	PAV at 110°C	*m*-Value	–6		0.398	
			S			63.3	MPa
8/23/2016			*m*-Value	–12		0.341	
			S			135.5	MPa
8/17/2016			*m*-Value	–18		0.293	
			S			309.5	MPa

Table D-8. Asphalt Binder Test Memorandum for Binder Y3

ASU Advanced Pavement Laboratory

Project Name : ADOT SPR - 742
Operator: Akshay Gundla
Binder: Y3 - PG 70-16

Date	AASHTO Test Method	Aging Level	Parameter	Temperature (°C)		Result	
9/15/2016	T 315 – 25mm	Original	|G*|/sin δ	64		2.34	kPa
				70		1.14	kPa
				76		0.58	kPa
	T 315 – 8mm		|G*|sin δ	28		466.87	kPa
				31		299.11	kPa
				34		190.98	kPa
9/16/2016	T 315 – 25mm	RTFO	|G*|/sin δ	64		5.61	kPa
				70		2.74	kPa
				76		1.37	kPa
9/15/2016	T 315 – 8mm		|G*|sin δ	28		798.98	kPa
				31		529.50	kPa
				34		386.25	kPa
9/13/2016	T 315 – 8mm	PAV at 110°C	|G*|sin δ	28		2824.22	kPa
				31		2087.40	kPa
				34		1517.88	0.25
9/13/2016	T 315 – 25mm	PAV at 110°C	|G*|/sin δ	70		28.06	kPa
9/14/2016	T 350	Original		**64**	**70**	**76**	
			$R_{0.1}$	7.44	4.58	1.85	%
			$R_{3.2}$	1.46	0.50	0.19	%
			R_{Diff}	80.35	88.72	89.66	%
			$Jnr_{0.1}$	3.523	7.791	16.092	kPa^{-1}
			$Jnr_{3.2}$	4.289	9.618	19.655	kPa^{-1}
			Jnr_{Diff}	21.74	23.48	22.14	%
9/16/2016	T 350	RTFO		**64**	**70**	**76**	
			$R_{0.1}$	25.21	16.60	10.16	%
			$R_{3.2}$	8.40	2.92	1.03	%
			R_{Diff}	66.67	82.40	89.88	%
			$Jnr_{0.1}$	1.011	2.528	5.656	kPa^{-1}
			$Jnr_{3.2}$	1.362	3.528	7.965	kPa^{-1}
			Jnr_{Diff}	34.72	39.57	40.84	%
9/12/2016	T 313	PAV at 110°C	*m*-Value	0		0.405	
			S			0.3575	MPa
9/10/2016			*m*-Value	–6		0.3515	
			S			70.65	MPa
9/11/2016			*m*-Value	–12		0.3115	
			S			153.5	MPa

Table D-9. Asphalt Binder Test Memorandum for Binder Y4

ASU Advanced Pavement Laboratory

Project Name : ADOT SPR - 742
Operator: Akshay Gundla
Binder: Y4 - PG 76-16

Date	AASHTO Test Method	Aging Level	Parameter	Temperature (°C)		Result	
9/6/2016	T 315 – 25mm	Original	|G*|/sin δ	70		2.40	kPa
				76		1.13	kPa
				82		0.56	kPa
9/13/2016	T 315 – 8mm		|G*|sin δ	31		1378.63	kPa
				34		864.44	kPa
				37		535.98	kPa
9/7/2016	T 315 – 25mm	RTFO	|G*|/sin δ	70		5.34	kPa
				76		2.46	kPa
				82		1.19	kPa
9/13/2016	T 315 – 8mm		|G*|sin δ	31		2342.39	kPa
				34		1534.88	kPa
				37		987.32	kPa
9/13/2016	T 315 – 8mm	PAV at 110°C	|G*|sin δ	31		5867.02	kPa
				34		4286.27	kPa
				37		3097.36	kPa
9/6/2016	T 315 – 25 mm	PAV at 110°C	|G*|/sin δ	76		18.89	kPa
9/6/2016	T 350	Original		**64**	**70**	**76**	
			$R_{0.1}$	7.10	3.84	1.81	%
			$R_{3.2}$	2.37	0.79	0.26	%
			R_{Diff}	66.63	79.48	85.92	%
			$Jnr_{0.1}$	1.571	3.815	8.421	kPa^{-1}
			$Jnr_{3.2}$	1.738	4.257	9.392	kPa^{-1}
			Jnr_{Diff}	10.60	11.58	11.53	%
9/8/2016	T 350	RTFO		**64**	**70**	**76**	
			$R_{0.1}$	17.64	11.24	6.58	%
			$R_{3.2}$	10.29	3.36	1.18	%
			R_{Diff}	41.66	70.12	82.05	%
			$Jnr_{0.1}$	0.573	1.492	3.533	kPa^{-1}
			$Jnr_{3.2}$	0.641	1.730	4.167	kPa^{-1}
			Jnr_{Diff}	11.75	16.03	17.96	%
9/5/2016	T 313	PAV at 110°C	*m*-Value	0		0.372	
			S			94.8	MPa
9/4/2016			*m*-Value	–6		0.3145	
			S			181.5	MPa
9/4/2016			*m*-Value	–12		0.263	
			S			348	MPa

Table D-10. Asphalt Binder Test Memorandum for Binder Y5

ASU Advanced Pavement Laboratory

Project Name : ADOT SPR - 742
Operator: Akshay Gundla
Binder: Y5 - PG 70H-16

Date	AASHTO Test Method	Aging Level	Parameter	Temperature (°C)		Result	
9/27/2016	T 315 – 25mm	Original	|G*|/sin δ	64		2.59	kPa
				70		1.62	kPa
				76		1.02	kPa
10/21/2016	T 315 – 8mm		|G*|sin δ	28		242.53	kPa
				31		153.54	kPa
				34		97.97	kPa
9/25/2016	T 315 – 25mm	RTFO	|G*|/sin δ	64		5.02	kPa
				70		3.13	kPa
				76		1.97	kPa
	T 315 – 8mm		|G*|sin δ	28		451.25	kPa
				31		286.53	kPa
				34		181.50	kPa
9/23/2016	T 315 – 8mm	PAV at 110°C	|G*|sin δ	28		1694.80	kPa
				31		1210.50	kPa
				34		847.87	kPa
9/19/2016	T 315 – 25mm	PAV at 110°C	|G*|/sin δ	70		20.18	kPa
10/17/2016	T 350	Original		**64**	**70**	**76**	
			$R_{0.1}$	94.16	92.29	89.65	%
			$R_{3.2}$	87.67	71.55	35.21	%
			R_{Diff}	6.90	22.47	60.73	%
			$Jnr_{0.1}$	0.116	0.249	0.521	kPa^{-1}
			$Jnr_{3.2}$	0.186	0.753	3.639	kPa^{-1}
			Jnr_{Diff}	60.83	202.48	598.44	%
9/19/2016	T 350	RTFO		**64**	**70**	**76**	
			$R_{0.1}$	96.11	95.07	93.40	%
			$R_{3.2}$	92.46	90.10	80.22	%
			R_{Diff}	3.80	5.22	14.12	%
			$Jnr_{0.1}$	0.039	0.082	0.174	kPa^{-1}
			$Jnr_{3.2}$	0.061	0.119	0.386	kPa^{-1}
			Jnr_{Diff}	54.01	45.19	122.38	%
9/14/2016	T 313	PAV at 110°C	*m*-Value	0		Material too soft	
			S				
9/21/2016			*m*-Value	–6		0.36	
			S			54	MPa
9/21/2016			*m*-Value	–12		0.3065	
			S			115	MPa

Table D-11. Asphalt Binder Test Memorandum for Binder Y6

ASU Advanced Pavement Laboratory

Project Name : ADOT SPR - 742
Operator: Akshay Gundla
Binder: Y6 - PG 70V-16

Date	AASHTO Test Method	Aging Level	Parameter	Temperature (°C)		Result	
9/29/2016	T 315 – 25 mm	Original	|G*|/sin δ	64		3.89	kPa
				70		2.62	kPa
				76		1.81	kPa
	T 315 – 8 mm		|G*|sin δ	28		187.95	kPa
				31		122.11	kPa
				34		80.13	kPa
10/6/2016	T 315 – 25 mm	RTFO	|G*|/sin δ	64		6.56	kPa
				70		4.36	kPa
				76		2.96	kPa
9/30/2016	T 315 – 8 mm		|G*|sin δ	28		350.78	kPa
				31		227.42	kPa
				34		147.63	kPa
9/30/2016	T 315 – 8 mm	PAV at 110°C	|G*|sin δ	28		1548.71	kPa
				31		1131.56	kPa
				34		771.01	kPa
10/2/2016	T 315 – 25 mm	PAV at 110°C	|G*|/sin δ	70		17.43	kPa
9/28/2016	T 350	Original		**64**	**70**	**76**	
			$R_{0.1}$	98.95	98.58	97.26	%
			$R_{3.2}$	97.35	97.37	94.65	%
			R_{Diff}	1.62	1.74	2.68	%
			$Jnr_{0.1}$	0.012	0.025	0.069	kPa^{-1}
			$Jnr_{3.2}$	0.029	0.048	0.107	kPa^{-1}
			Jnr_{Diff}	140.67	90.18	54.98	%
10/1/2016	T 350	RTFO		**64**	**70**	**76**	
			$R_{0.1}$	98.57	98.26	97.25	%
			$R_{3.2}$	96.62	96.25	94.86	%
			R_{Diff}	1.98	2.05	2.46	%
			$Jnr_{0.1}$	0.010	0.019	0.044	kPa^{-1}
			$Jnr_{3.2}$	0.024	0.036	0.069	kPa^{-1}
			Jnr_{Diff}	130.93	97.14	57.92	%
	T 313	PAV at 110°C	*m*-Value	0		Material too soft	
			S				
9/29/2016			*m*-Value	–6		0.382	
			S			48.4	MPa
9/30/2016			*m*-Value	–12		0.3315	
			S			109	MPa

Table D-12. Asphalt Binder Test Memorandum for Binder Z1

ASU Advanced Pavement Laboratory

Project Name : ADOT SPR - 742
Operator: Akshay Gundla
Binder: Z1 - PG 64-22

Date	AASHTO Test Method	Aging Level	Parameter	Temperature (°C)		Result	
8/15/2016	T 315 – 25 mm	Original	|G*|/sin δ	58		2.97	kPa
				64		1.35	kPa
				70		0.64	kPa
	T 315 – 8 mm		|G*|sin δ	22		880.71	kPa
				25		568.04	kPa
				28		355.54	kPa
8/24/2016	T 315 – 25 mm	RTFO	|G*|/sin δ	58		9.33	kPa
				64		4.06	kPa
				70		1.79	kPa
8/15/2016	T 315 – 8 mm		|G*|sin δ	22		2095.56	kPa
				25		1434.30	kPa
				28		952.53	kPa
8/15/2016	T 315 – 8 mm	PAV at 100°C	|G*|sin δ	22		4518.05	kPa
				25		3394.81	kPa
				28		2437.55	kPa
8/16/2016	T 315 – 25 mm	PAV at 100°C	|G*|/sin δ	64		16.88	kPa
8/14/2016	T 350	Original		**58**	**64**	**70**	
			$R_{0.1}$	2.84	1.13	0.46	%
			$R_{3.2}$	0.90	0.27	0.12	%
			R_{Diff}	68.30	76.33	74.79	%
			$Jnr_{0.1}$	3.028	7.133	15.339	kPa^{-1}
			$Jnr_{3.2}$	3.263	7.653	16.447	kPa^{-1}
			Jnr_{Diff}	7.76	7.29	7.22	%
8/15/2016	T 350	RTFO		**58**	**64**	**70**	
			$R_{0.1}$	10.29	5.49	2.95	%
			$R_{3.2}$	5.86	1.80	0.55	%
			R_{Diff}	43.03	67.16	81.36	%
			$Jnr_{0.1}$	0.837	2.172	5.231	kPa^{-1}
			$Jnr_{3.2}$	0.902	2.401	5.846	kPa^{-1}
			Jnr_{Diff}	7.83	10.54	11.77	%
8/11/2016	T 313	PAV at 100°C	*m*-Value	–6		0.365	
			S			78.1	MPa
8/10/2016			*m*-Value	–12		0.3115	
			S			167.5	MPa
8/10/2016			*m*-Value	–18		0.263	
			S			343.5	MPa

Table D-13. Asphalt Binder Test Memorandum for Binder Z2

ASU Advanced Pavement Laboratory

Project Name : ADOT SPR - 742
Operator: Akshay Gundla
Binder: Z2 - PG 70-22

Date	AASHTO Test Method	Aging Level	Parameter	Temperature (°C)		Result	
8/27/2016	T 315 – 25 mm	Original	|G*|/sin δ	64		2.13	kPa
				70		1.03	kPa
				76		0.52	kPa
	T 315 – 8 mm		|G*|sin δ	25		675.44	kPa
				28		437.19	kPa
				31		281.08	kPa
8/19/2016	T 315 – 25 mm	RTFO	|G*|/sin δ	64		6.83	kPa
				70		3.26	kPa
				76		1.59	kPa
8/22/2016	T 315 – 8 mm		|G*|sin δ	25		1427.55	kPa
				28		958.50	kPa
				31		642.78	kPa
8/22/2016	T 315 – 8 mm	PAV at 110°C	|G*|sin δ	25		3999.39	kPa
				28		2998.78	kPa
				31		2221.71	kPa
8/25/2016	T315 – 25 mm	PAV at 110°C	|G*|/sin δ	70		30.30	kPa
8/25/2016	T 350	Original		**64**	**70**	**76**	
			$R_{0.1}$	7.50	4.04	1.73	%
			$R_{3.2}$	1.21	0.40	0.18	%
			R_{Diff}	83.92	90.13	89.37	%
			$Jnr_{0.1}$	3.823	8.598	18.073	kPa^{-1}
			$Jnr_{3.2}$	4.608	10.423	21.961	kPa^{-1}
			Jnr_{Diff}	20.56	21.23	21.51	%
8/20/2016	T 350	RTFO		**64**	**70**	**76**	
			$R_{0.1}$	25.83	17.38	10.41	%
			$R_{3.2}$	8.97	3.08	1.08	%
			R_{Diff}	65.28	82.27	89.63	%
			$Jnr_{0.1}$	0.862	2.145	5.075	kPa^{-1}
			$Jnr_{3.2}$	1.130	2.895	6.824	kPa^{-1}
			Jnr_{Diff}	31.20	34.92	34.47	%
8/20/2016	T 313	PAV at 110°C	*m*-Value	–6		0.348	
			S			81.6	MPa
8/22/2016			*m*-Value	–12		0.304	
			S			169.5	MPa
8/18/2016			*m*-Value	–18		0.2595	
			S			344.5	MPa

Table D-14. Asphalt Binder Test Memorandum for Binder Z3

ASU Advanced Pavement Laboratory

Project Name : ADOT SPR - 742
Operator: Akshay Gundla
Binder: Z3 - PG 70-10

Date	AASHTO Test Method	Aging Level	Parameter	Temperature (°C)		Result	
9/11/2016	T 315 – 25 mm	Original	|G*|/sin δ	64		3.10	kPa
				70		1.41	kPa
				76		0.67	kPa
9/13/2016	T 315 – 8 mm		|G*|sin δ	28		1062.63	kPa
				31		678.75	kPa
				34		426.13	kPa
9/10/2016	T 315 – 25 mm	RTFO	|G*|/sin δ	64		9.24	kPa
				70		4.02	kPa
				76		1.78	kPa
9/13/2016	T 315 – 8 mm		|G*|sin δ	28		2071.43	kPa
				31		1415.46	kPa
				34		941.01	kPa
9/13/2016	T 315 – 8 mm	PAV at 110°C	|G*|sin δ	28		5554.24	kPa
				31		4242.63	kPa
				34		3183.17	kPa
9/9/2016	T 315 – 25 mm	PAV at 110°C	|G*|/sin δ	70		39.22	kPa
9/12/2016	T 350	Original		**64**	**70**	**76**	
			$R_{0.1}$	3.89	2.84	0.77	%
			$R_{3.2}$	1.08	0.32	0.12	%
			R_{Diff}	71.79	87.25	83.54	%
			$Jnr_{0.1}$	2.771	6.519	14.557	kPa^{-1}
			$Jnr_{3.2}$	3.016	7.218	15.730	kPa^{-1}
			Jnr_{Diff}	8.86	10.74	8.06	%
9/11/2016	T 350	RTFO		**64**	**70**	**76**	
			$R_{0.1}$	11.21	5.96	2.75	%
			$R_{3.2}$	6.03	1.84	0.57	%
			R_{Diff}	46.15	69.09	79.04	%
			$Jnr_{0.1}$	0.818	2.174	5.152	kPa^{-1}
			$Jnr_{3.2}$	0.888	2.408	5.725	kPa^{-1}
			Jnr_{Diff}	8.32	10.76	11.12	%
9/6/2016	T 313	PAV at 110°C	*m*-	0		0.327	
			S			68.05	MPa
9/7/2016			*m*-Value	–6		0.2845	
			S			133	MPa
			m-Value	N/A		N/A	
			S			N/A	MPa

Table D-15. Asphalt Binder Test Memorandum for Binder Z4

ASU Advanced Pavement Laboratory

Project Name : ADOT SPR - 742
Operator: Akshay Gundla
Binder: Z4 - PG 76-16

Date	AASHTO Test Method	Aging Level	Parameter	Temperature (°C)		Result	
9/6/2016	T 315 – 25 mm	Original	|G*|/sin δ	70		2.31	kPa
				76		1.14	kPa
				82		0.59	kPa
	T 315 – 8 mm		|G*|sin δ	31		628.97	kPa
				34		412.12	kPa
				37		266.85	kPa
9/6/2016	T 315 – 25 mm	RTFO	|G*|/sin δ	70		7.33	kPa
				76		3.61	kPa
				82		1.81	kPa
	T 315 – 8 mm		|G*|sin δ	31		1308.82	kPa
				34		887.23	kPa
				37		597.12	kPa
9/25/2016	T 315 – 8 mm	PAV at 110°C	|G*|sin δ	31		3645.98	kPa
				34		2725.50	kPa
				37		2004.72	kPa
9/25/2016	T 315 – 25 mm	PAV at 110°C	|G*|/sin δ	76		28.14	kPa
8/31/2016	T 350	Original		**64**	**70**	**76**	
			$R_{0.1}$	13.43	7.62	4.01	%
			$R_{3.2}$	4.08	1.41	0.48	%
			R_{Diff}	69.64	81.54	88.17	%
			$Jnr_{0.1}$	1.440	3.536	7.876	kPa^{-1}
			$Jnr_{3.2}$	1.740	4.319	9.655	kPa^{-1}
			Jnr_{Diff}	20.86	22.11	22.55	%
9/4/2016	T 350	RTFO		**64**	**70**	**76**	
			$R_{0.1}$	35.69	26.28	17.73	%
			$R_{3.2}$	23.98	10.66	3.73	%
			R_{Diff}	32.82	59.46	78.98	%
			$Jnr_{0.1}$	0.312	0.786	1.866	kPa^{-1}
			$Jnr_{3.2}$	0.376	1.029	2.544	kPa^{-1}
			Jnr_{Diff}	20.67	30.98	36.35	%
8/28/2016	T 313	PAV at 110°C	*m*-Value	0		0.384	
			S			55.5	MPa
8/29/2016			*m*-Value	–6		0.3295	
			S			116.5	MPa
9/19/2016			*m*-Value	–12		0.286	
			S			232	MPa

REPLICATE DATA FOR THE TESTS CONDUCTED ON ASPHALT BINDERS

Table D-16. High-Temperature AASHTO T 315 Data for the Study Asphalt Binders at Original Condition

Binder	Replicate	58°C			64°C			70°C			76°C			82°C		
		$\|G^*\|_{orig.}$	$\delta_{orig.}$	$(G^*/\sin\delta)_{orig.}$	$\|G^*\|_{orig.}$	$\delta_{orig.}$	$(G^*/\sin\delta)_{orig.}$	$\|G^*\|_{orig.}$	$\delta_{orig.}$	$(G^*/\sin\delta)_{orig.}$	$\|G^*\|_{orig.}$	$\delta_{orig.}$	$(G^*/\sin\delta)_{orig.}$	$\|G^*\|_{orig.}$	$\delta_{orig.}$	$(G^*/\sin\delta)_{orig.}$
X1	S-1	-	-	-	2.61	87.21	2.61	1.19	88.23	1.19	0.58	88.96	0.58	-	-	-
	S-2	-	-	-	2.64	87.16	2.65	1.21	88.21	1.21	0.59	88.96	0.59	-	-	-
X2	S-1	-	-	-	5.87	77.83	6.00	2.66	80.03	2.70	1.31	81.99	1.33	0.68	83.73	0.68
	S-2	-	-	-	5.84	77.81	5.97	2.63	80.10	2.67	1.29	82.05	1.31	0.67	83.79	0.67
X3	S-1	3.07	69.40	3.28	1.74	71.03	1.84	1.02	72.04	1.07	-	-	-	-	-	-
	S-2	3.14	69.40	3.35	1.77	71.02	1.87	1.03	72.04	1.08	-	-	-	-	-	-
X4	S-1	3.16	68.03	3.40	1.81	68.90	1.94	1.08	69.27	1.15	-	-	-	-	-	-
	S-2	3.18	67.33	3.45	1.84	67.83	1.99	1.10	67.89	1.19	-	-	-	-	-	-
X5	S-1	-	-	-	5.37	63.47	6.00	2.52	61.56	2.87	1.65	59.13	1.93	1.14	55.98	1.38
	S-2	-	-	-	5.35	63.36	5.98	2.59	61.43	2.95	1.69	59.09	1.97	1.16	56.01	1.40
Y1	S-1	2.47	85.62	2.48	1.14	87.06	1.14	0.56	88.19	0.56	-	-	-	-	-	-
	S-2	2.48	85.66	2.49	1.15	87.07	1.15	0.56	88.18	0.56	-	-	-	-	-	-
Y2	S-1	-	-	-	2.57	78.79	2.62	1.25	80.74	1.27	0.64	82.56	0.64	-	-	-
	S-2	-	-	-	2.56	78.79	2.61	1.24	80.71	1.26	0.63	82.54	0.64	-	-	-
Y3	S-1	-	-	-	2.30	81.21	2.32	1.12	83.22	1.12	0.57	85.00	0.57	-	-	-
	S-2	-	-	-	2.34	81.09	2.37	1.14	83.13	1.15	0.58	84.93	0.59	-	-	-
Y4	S-1	-	-	-	5.87	82.56	5.92	2.39	84.54	2.40	1.13	85.96	1.13	0.56	87.15	0.57
	S-2	-	-	-	5.83	82.58	5.88	2.39	84.53	2.40	1.13	85.96	1.13	0.56	87.15	0.56
Y5	S-1	-	-	-	2.19	61.20	2.50	1.37	60.93	1.56	0.86	61.18	0.99	-	-	-
	S-2	-	-	-	2.35	61.03	2.69	1.47	60.75	1.68	0.92	60.97	1.06	-	-	-
Y6	S-1	-	-	-	3.10	53.39	3.86	2.06	52.30	2.61	1.41	51.70	1.80	-	-	-
	S-2	-	-	-	3.13	53.31	3.91	2.09	52.27	2.64	1.43	51.66	1.82	-	-	-
Z1	S-1	2.95	85.22	2.96	1.34	86.73	1.35	0.64	87.93	0.64	-	-	-	-	-	-
	S-2	2.98	85.24	2.99	1.35	86.75	1.36	0.64	87.96	0.64	-	-	-	-	-	-
Z2	S-1	-	-	-	2.11	82.16	2.13	1.02	83.92	1.03	0.52	85.43	0.52	-	-	-
	S-2	-	-	-	2.12	82.11	2.14	1.03	83.91	1.04	0.52	85.46	0.52	-	-	-
Z3	S-1	-	-	-	3.08	84.72	3.09	1.41	86.38	1.41	0.66	87.67	0.66	-	-	-
	S-2	-	-	-	3.09	84.68	3.10	1.41	86.35	1.41	0.67	87.65	0.67	-	-	-
Z4	S-1	-	-	-	5.63	78.46	5.74	2.29	81.26	2.31	1.13	83.22	1.14	0.59	84.89	0.59
	S-2	-	-	-	5.62	78.34	5.74	2.29	81.29	2.31	1.13	83.25	1.13	0.58	84.95	0.59

Table D-17. High-Temperature AASHTO T 315 Data for the Study Asphalt Binders at RTFO Condition

Binder	Replicate	58°C			64°C			70°C			76°C			82°C		
		$\|G^*\|_{RTFO}$	δ_{RTFO}	$(G^*/\sin\delta)_{RTFO}$	$\|G^*\|_{RTFO}$	δ_{RTFO}	$(G^*/\sin\delta)_{RTFO}$	$\|G^*\|_{RTFO}$	δ_{RTFO}	$(G^*/\sin\delta)_{RTFO}$	$\|G^*\|_{RTFO}$	δ_{RTFO}	$(G^*/\sin\delta)_{RTFO}$	$\|G^*\|_{RTFO}$	δ_{RTFO}	$(G^*/\sin\delta)_{RTFO}$
X1	S-1	-	-	-	5.65	84.35	5.67	2.48	86.07	2.48	1.15	87.43	1.15	-	-	-
	S-2	-	-	-	5.66	84.35	5.68	2.48	86.08	2.48	1.15	87.46	1.15	-	-	-
X2	S-1	-	-	-	13.32	70.84	14.10	6.11	73.07	6.39	3.11	75.32	3.21	1.61	77.63	1.65
	S-2	-	-	-	13.21	70.75	13.99	6.09	73.15	6.36	3.09	75.39	3.19	1.60	77.71	1.64
X3	S-1	5.71	64.55	6.30	3.26	65.38	3.58	1.90	66.61	2.07	-	-	-	-	-	-
	S-2	5.81	64.55	6.44	3.32	65.41	3.65	1.94	66.66	2.12	-	-	-	-	-	-
X4	S-1	5.89	64.39	6.53	3.36	65.19	3.70	1.96	66.31	2.14	-	-	-	-	-	-
	S-2	5.95	64.54	6.59	3.39	65.59	3.72	1.97	66.99	2.14	-	-	-	-	-	-
X5	S-1	-	-	-	6.91	64.11	7.68	3.62	64.11	4.02	2.20	63.35	2.46	1.39	61.93	1.57
	S-2	-	-	-	6.81	64.12	7.57	3.70	63.87	4.12	2.24	63.04	2.51	1.42	61.51	1.62
Y1	S-1	6.85	80.73	6.94	3.02	83.11	3.04	1.39	85.14	1.39	-	-	-	-	-	-
	S-2	6.85	80.70	6.94	3.03	83.10	3.05	1.40	85.11	1.40	-	-	-	-	-	-
Y2	S-1	-	-	-	4.91	73.42	5.13	2.42	75.48	2.50	1.22	77.60	1.25	-	-	-
	S-2	-	-	-	4.85	73.52	5.06	2.39	75.59	2.47	1.21	77.73	1.24	-	-	-
Y3	S-1	-	-	-	5.38	73.87	5.60	2.66	76.41	2.73	1.39	78.92	1.36	-	-	-
	S-2	-	-	-	5.40	73.85	5.62	2.67	76.37	2.75	1.35	78.91	1.37	-	-	-
Y4	S-1	-	-	-	12.91	78.05	13.20	5.34	80.61	5.41	2.47	82.54	2.49	1.20	84.23	1.20
	S-2	-	-	-	12.54	78.16	12.81	5.20	80.63	5.27	2.41	82.57	2.43	1.17	84.28	1.17
Y5	S-1	-	-	-	4.23	56.85	5.06	2.62	56.15	3.15	1.64	55.91	1.99	-	-	-
	S-2	-	-	-	4.19	57.05	4.99	2.58	56.36	3.10	1.62	56.14	1.95	-	-	-
Y6	S-1	-	-	-	5.12	50.83	6.60	3.34	49.74	4.38	2.26	49.16	2.98	-	-	-
	S-2	-	-	-	5.07	51.11	6.52	3.33	50.01	4.34	2.24	49.37	2.95	-	-	-
Z1	S-1	9.17	79.83	9.32	4.04	82.49	4.07	1.79	84.72	1.80	-	-	-	-	-	-
	S-2	9.19	79.92	9.33	4.03	82.55	4.06	1.78	84.73	1.79	-	-	-	-	-	-
Z2	S-1	-	-	-	6.60	74.71	6.84	3.16	77.20	3.24	1.56	79.61	1.59	-	-	-
	S-2	-	-	-	6.58	74.70	6.82	3.19	77.18	3.27	1.57	79.61	1.59	-	-	-
Z3	S-1	-	-	-	9.10	79.39	9.26	4.00	82.25	4.03	1.77	84.58	1.78	-	-	-
	S-2	-	-	-	9.07	79.38	9.22	3.97	82.24	4.01	1.77	84.56	1.77	-	-	-
Z4	S-1	-	-	-	17.48	69.90	18.62	7.01	73.41	7.32	3.51	75.98	3.61	1.78	78.51	1.82
	S-2	-	-	-	17.45	69.92	18.58	7.04	73.30	7.35	3.51	75.91	3.62	1.77	78.47	1.81

Table D-18. High-Temperature AASHTO T 315 Data for the Study Asphalt Binders at PAV Condition

Binder	Replicate	58°C			64°C			70°C			76°C		
		$\|G^*\|_{PAV}$	δ_{PAV}	$(G^*/\sin\delta)_{PAV}$	$\|G^*\|_{PAV}$	δ_{PAV}	$(G^*/\sin\delta)_{PAV}$	$\|G^*\|_{PAV}$	δ_{PAV}	$(G^*/\sin\delta)_{PAV}$	$\|G^*\|_{PAV}$	δ_{PAV}	$(G^*/\sin\delta)_{PAV}$
X1	S-1	-	-	-	-	-	-	12.93	78.91	13.17	-	-	-
	S-2	-	-	-	-	-	-	12.90	78.96	13.14	-	-	-
X2	S-1	-	-	-	-	-	-	-	-	-	19.89	62.62	22.39
	S-2	-	-	-	-	-	-	-	-	-	19.89	62.60	22.36
X3	S-1	-	-	-	8.74	61.95	9.90	-	-	-	-	-	-
	S-2	-	-	-	8.81	61.98	9.98	-	-	-	-	-	-
X4	S-1	-	-	-	8.79	61.51	10.00	-	-	-	-	-	-
	S-2	-	-	-	8.81	61.59	10.02	-	-	-	-	-	-
X5	S-1	-	-	-	-	-	-	-	-	-	5.95	65.24	6.55
	S-2	-	-	-	-	-	-	-	-	-	5.94	65.21	6.54
Y1	S-1	-	-	-	11.67	75.44	12.06	-	-	-	-	-	-
	S-2	-	-	-	11.56	75.43	11.95	-	-	-	-	-	-
Y2	S-1	-	-	-	-	-	-	19.17	58.96	22.38	-	-	-
	S-2	-	-	-	-	-	-	19.13	59.18	22.28	-	-	-
Y3	S-1	-	-	-	-	-	-	24.15	59.43	28.04	-	-	-
	S-2	-	-	-	-	-	-	24.17	59.42	28.07	-	-	-
Y4	S-1	-	-	-	-	-	-	-	-	-	17.92	71.13	18.93
	S-2	-	-	-	-	-	-	-	-	-	17.83	71.01	18.85
Y5	S-1	-	-	-	-	-	-	15.07	48.34	20.17	-	-	-
	S-2	-	-	-	-	-	-	15.12	48.50	20.18	-	-	-
Y6	S-1	-	-	-	-	-	-	13.18	48.67	17.55	-	-	-
	S-2	-	-	-	-	-	-	13.01	48.72	17.31	-	-	-
Z1	S-1	-	-	-	16.23	74.71	16.83	-	-	-	-	-	-
	S-2	-	-	-	16.32	74.63	16.93	-	-	-	-	-	-
Z2	S-1	-	-	-	-	-	-	26.48	60.92	30.30	-	-	-
	S-2	-	-	-	-	-	-	26.48	60.92	30.31	-	-	-
Z3	S-1	-	-	-	-	-	-	35.95	67.64	38.87	-	-	-
	S-2	-	-	-	-	-	-	36.61	67.64	39.58	-	-	-
Z4	S-1	-	-	-	-	-	-	-	-	-	24.49	61.28	27.92
	S-2	-	-	-	-	-	-	-	-	-	24.85	61.17	28.36

Table D-19. Intermediate-Temperature AASHTO T 315 Data for the Study Asphalt Binders at Original Condition

Binder	Replicate	22°C			25°C			28°C			31°C			34°C			37°C		
		|G*|	δ	|G*|sin δ	|G*|	$\delta_{orig.}$	|G*|sin δ	|G*|	δ	|G*|sin δ	|G*|	δ	|G*|sin δ	|G*|	δ	|G*|sin δ	|G*|	δ	|G*|sin δ
X1	S-1	-	-	-	-	-	-	-	-	-	637.17	72.39	607.30	376.66	74.48	362.93	-	-	-
	S-2	-	-	-	-	-	-	-	-	-	630.32	72.34	600.64	373.39	74.42	359.66	-	-	-
X2	S-1	-	-	-	-	-	-	-	-	-	747.84	63.10	666.94	485.63	64.59	438.64	312.41	65.98	285.38
	S-2	-	-	-	-	-	-	-	-	-	729.92	63.08	650.87	474.09	64.58	428.20	306.02	65.96	279.50
X3	S-1	325.16	67.70	300.84	210.45	68.11	195.29	133.78	68.12	124.15	-	-	-	-	-	-	-	-	-
	S-2	324.68	67.02	300.39	203.07	68.16	188.49	129.28	68.17	120.02	-	-	-	-	-	-	-	-	-
X4	S-1	342.03	66.96	314.77	222.55	67.48	205.58	142.76	67.61	132.00	-	-	-	-	-	-	-	-	-
	S-2	352.42	66.88	324.14	230.65	67.39	212.93	149.29	67.52	137.95	-	-	-	-	-	-	-	-	-
X5	S-1	-	-	-	-	-	-	624.38	67.59	577.22	386.84	68.43	359.74	240.57	68.71	224.16	-	-	-
	S-2	-	-	-	-	-	-	593.01	67.58	548.17	368.36	68.39	342.47	230.41	68.67	214.62	-	-	-
Y1	S-1	816.65	68.09	757.66	518.59	70.04	487.45	313.24	71.99	297.89	-	-	-	-	-	-	-	-	-
	S-2	858.58	67.88	795.39	523.46	70.05	492.05	320.53	71.93	304.73	-	-	-	-	-	-	-	-	-
Y2	S-1	-	-	-	721.94	63.98	648.74	462.28	65.43	420.41	295.13	66.74	271.14	-	-	-	-	-	-
	S-2	-	-	-	783.74	63.83	703.39	496.36	65.31	450.97	314.79	66.65	289.01	-	-	-	-	-	-
Y3	S-1	-	-	-	-	-	-	519.30	64.99	470.62	330.11	66.37	302.44	209.17	67.65	193.46	-	-	-
	S-2	-	-	-	-	-	-	511.17	64.96	463.13	322.91	66.35	295.79	203.83	67.63	188.50	-	-	-
Y4	S-1	-	-	-	-	-	-				1547.86	63.99	1391.14	950.76	66.45	871.59	581.66	68.67	541.81
	S-2	-	-	-	-	-	-				1519.25	64.05	1366.12	935.09	66.46	857.29	569.02	68.69	530.14
Y5	S-1	-	-	-	-	-	-	268.65	65.73	244.91	169.49	65.97	154.80	108.24	65.82	98.75	-	-	-
	S-2	-	-	-	-	-	-	263.30	65.80	240.16	166.66	66.03	152.29	106.48	65.88	97.19	-	-	-
Y6	S-1	-	-	-	-	-	-	202.01	66.39	185.10	131.78	65.71	120.12	87.09	64.70	78.74	-	-	-
	S-2	-	-	-	-	-	-	208.26	66.37	190.80	136.12	65.75	124.11	90.12	64.77	81.52	-	-	-
Z1	S-1	960.15	64.87	869.28	617.10	67.12	568.56	381.88	69.34	357.31	-	-	-	-	-	-	-	-	-
	S-2	987.01	64.67	892.15	616.19	67.07	567.51	378.07	69.35	353.78	-	-	-	-	-	-	-	-	-
Z2	S-1	-	-	-	763.49	62.62	677.94	487.38	64.42	439.61	310.17	66.11	283.60	-	-	-	-	-	-
	S-2	-	-	-	756.48	62.82	672.94	481.22	64.62	434.78	304.20	66.31	278.57	-	-	-	-	-	-
Z3	S-1	-	-	-	-	-	-	1237.27	60.30	1074.70	769.43	62.97	685.37	471.79	65.55	429.49	-	-	-
	S-2	-	-	-	-	-	-	1209.97	60.25	1050.55	754.94	62.91	672.12	464.70	65.47	422.77	-	-	-
Z4	S-1	-	-	-	-	-	-	-	-	-	697.74	62.74	620.25	451.01	64.26	406.27	288.26	65.73	262.78
	S-2	-	-	-	-	-	-	-	-	-	718.44	62.57	637.69	464.68	64.09	417.98	297.62	65.54	270.92

Table D-20. Intermediate-Temperature AASHTO T 315 Data for the Study Asphalt Binders at RTFO Condition

Binder	Replicate	22°C			25°C			28°C			31°C			34°C			37°C		
		|G*|	δ	G*sin δ	|G*|	δ	|G*|sin δ	|G*|	δ	|G*|sin δ	|G*|	δ	|G*|sin δ	|G*|	δ	|G*|sin δ	|G*|	δ	|G*|sin δ
X1	S-1	-	-	-	-	-	-	-	-	-	1404.10	64.66	1268.95	854.97	67.12	787.71			
	S-2	-	-	-	-	-	-	-	-	-	1440.96	64.62	1301.92	880.84	67.07	811.22			
X2	S-1	-	-	-	-	-	-	-	-	-	1252.51	56.94	1049.82	837.88	58.38	713.51	558.13	59.74	482.07
	S-2	-	-	-	-	-	-	-	-	-	1303.77	56.71	1089.84	865.00	58.21	735.31	570.97	59.62	492.57
X3	S-1	677.66	62.28	599.89	432.33	63.47	386.81	277.41	64.28	249.93	-	-	-	-	-	-	-	-	-
	S-2	646.39	62.33	572.49	411.99	63.51	368.74	266.92	64.31	240.55	-	-	-	-	-	-	-	-	-
X4	S-1	734.75	62.22	650.09	467.65	63.40	418.16	297.13	64.23	267.59	-	-	-	-	-	-	-	-	-
	S-2	703.17	62.27	622.40	453.80	63.39	405.74	292.70	64.19	263.51	-	-	-	-	-	-	-	-	-
X5	S-1	-	-	-	-	-	-	998.23	64.29	899.44	612.94	65.72	558.73	376.15	66.63	345.31			
	S-2	-	-	-	-	-	-	1024.88	64.30	923.50	629.48	65.75	573.96	385.43	66.71	354.02			
Y1	S-1	1772.93	59.12	1521.58	1175.44	61.30	1031.06	743.44	63.53	665.53	-	-	-	-	-	-	-	-	-
	S-2	1810.76	59.20	1555.32	1165.92	61.50	1024.62	728.68	63.74	653.45	-	-	-	-	-	-	-	-	-
Y2	S-1	-	-	-	1147.12	59.07	984.01	754.80	60.52	657.07	498.00	61.84	439.06	-	-	-	-	-	-
	S-2	-	-	-	1172.89	58.88	1004.13	754.65	60.45	656.47	492.42	61.79	433.94	-	-	-	-	-	-
Y3	S-1	-	-	-	-	-	-	939.88	58.34	800.00	610.03	59.78	527.12	436.69	59.84	377.58	-	-	-
	S-2	-	-	-	-	-	-	937.27	58.36	797.95	616.01	59.70	531.88	455.86	60.03	394.91	-	-	-
Y4	S-1	-	-	-	-	-	-	-	-	-	2771.89	57.05	2326.22	1769.90	59.59	1526.35	1114.49	61.96	983.68
	S-2	-	-	-	-	-	-	-	-	-	2814.59	56.93	2358.55	1791.94	59.46	1543.41	1123.91	61.85	990.95
Y5	S-1	-	-	-	-	-	-	512.10	60.52	445.79	322.85	61.33	283.28	203.70	61.73	179.42	-	-	-
	S-2	-	-	-	-	-	-	525.31	60.39	456.71	330.67	61.20	289.78	208.61	61.64	183.58	-	-	-
Y6	S-1	-	-	-	-	-	-	381.68	62.71	339.20	248.96	62.72	221.28	163.18	62.35	144.54	-	-	-
	S-2	-	-	-	-	-	-	408.01	62.64	362.37	262.89	62.68	233.57	170.23	62.29	150.71	-	-	-
Z1	S-1	2517.33	54.74	2055.59	1652.42	57.28	1390.26	1066.32	59.75	921.10	-	-	-	-	-	-	-	-	-
	S-2	2615.97	54.72	2135.52	1760.25	57.12	1478.33	1141.11	59.58	983.97	-	-	-	-	-	-	-	-	-
Z2	S-1	-	-	-	1709.98	54.74	1396.25	1136.43	56.49	947.52	751.78	58.18	638.77	-	-	-	-	-	-
	S-2	-	-	-	1791.33	54.53	1458.85	1163.81	56.41	969.47	761.33	58.16	646.78	-	-	-	-	-	-
Z3	S-1	-	-	-	-	-	-	2542.75	51.36	1986.09	1678.46	53.91	1356.30	1080.27	56.51	900.97	-	-	-
	S-2	-	-	-	-	-	-	2773.35	51.05	2156.77	1831.98	53.60	1474.62	1180.46	56.20	981.05	-	-	-
Z4	S-1	-	-	-	-	-	-				1606.44	54.74	1311.72	1068.85	56.32	889.52	708.82	57.83	600.02
	S-2	-	-	-	-	-	-				1598.54	54.78	1305.92	1063.32	56.33	884.93	702.02	57.83	594.23

Table D-21. Intermediate-Temperature AASHTO T 315 Data for the Study Asphalt Binders at PAV Condition

Binder	Replicate	22°C			25°C			28°C			31°C			34°C			37°C		
		|G*|	δ	|G*|sin δ	|G*|	δ	|G*|sin δ	|G*|	δ	|G*|sin δ	|G*|	δ	|G*|sin δ	|G*|	δ	|G*|sin δ	|G*|	δ	|G*|sin δ
X1	S-1	-	-	-	-	-	-	-	-	-	5234.54	49.89	4003.70	3479.15	52.54	2761.85	-	-	-
	S-2	-	-	-	-	-	-	-	-	-	5285.25	49.85	4039.83	3507.89	52.51	2783.65	-	-	-
X2	S-1	-	-	-	-	-	-	-	-	-	4615.80	42.63	3126.37	3307.71	44.00	2297.87	2342.10	45.43	1668.39
	S-2	-	-	-	-	-	-	-	-	-	4640.27	42.33	3124.72	3342.59	43.69	2309.29	2373.13	45.09	1680.74
X3	S-1	1961.17	51.69	1538.95	1352.28	53.40	1085.58	903.81	55.07	741.01	-	-	-	-	-	-	-	-	-
	S-2	2073.00	51.66	1626.10	1377.98	53.48	1107.53	921.89	55.09	756.08	-	-	-	-	-	-	-	-	-
X4	S-1	2150.83	51.94	1693.41	1418.87	53.77	1144.36	933.87	55.36	768.33	-	-	-	-	-	-	-	-	-
	S-2	2021.19	52.24	1597.90	1363.72	53.91	1102.03	901.15	55.47	742.43	-	-	-	-	-	-	-	-	-
X5	S-1	-	-	-	-	-	-	3482.01	51.93	2741.40	2299.00	54.17	1864.08	1477.28	56.29	1228.90	-	-	-
	S-2	-	-	-	-	-	-	3509.80	51.78	2757.40	2292.16	54.11	1857.00	1467.20	56.24	1219.82	-	-	-
Y1	S-1	5442.24	45.70	3894.95	3746.62	48.06	2787.11	2528.42	50.51	1951.28	-	-	-	-	-	-	-	-	-
	S-2	5218.90	45.72	3736.13	3612.59	48.08	2688.22	2420.53	50.55	1869.19	-	-	-	-	-	-	-	-	-
Y2	S-1	-	-	-	4313.40	42.46	2911.63	3042.73	43.76	2104.37	2139.04	45.03	1513.32	-	-	-	-	-	-
	S-2	-	-	-	4449.57	42.44	3002.88	3198.72	43.66	2208.72	2276.62	44.89	1606.99	-	-	-	-	-	-
Y3	S-1	-	-	-	-	-	-	4360.07	40.24	2816.80	3143.65	41.50	2082.92	2226.41	42.89	1515.22	-	-	-
	S-2	-	-	-	-	-	-	4381.86	40.26	2831.64	3154.57	41.54	2091.87	2231.80	42.95	1520.53	-	-	-
Y4	S-1	-	-	-	-	-	-	-	-	-	8884.55	41.57	5894.80	6263.35	43.64	4322.42	4340.55	45.76	3109.69
	S-2	-	-	-	-	-	-	-	-	-	8787.62	41.64	5839.24	6200.52	43.73	4286.27	4298.31	45.87	3085.02
Y5	S-1	-	-	-	-	-	-	2547.84	42.08	1707.55	1772.59	43.56	1221.66	1210.79	45.05	856.95	-	-	-
	S-2	-	-	-	-	-	-	2509.50	42.09	1682.05	1738.89	43.61	1199.34	1183.43	45.14	838.80	-	-	-
Y6	S-1	-	-	-	-	-	-	2155.24	44.38	1507.40	1496.25	45.74	1071.64	1022.91	47.08	749.11	-	-	-
	S-2	-	-	-	-	-	-	2282.37	44.16	1590.01	1584.73	45.56	1131.56	1085.40	46.93	792.91	-	-	-
Z1	S-1	6450.24	42.88	4389.28	4658.35	45.02	3295.28	3207.90	47.45	2363.09	-	-	-	-	-	-	-	-	-
	S-2	6858.53	42.65	4646.82	4958.60	44.81	3494.34	3421.22	47.24	2512.00	-	-	-	-	-	-	-	-	-
Z2	S-1	-	-	-	6480.45	38.61	4044.08	4734.00	40.07	3047.41	3411.52	41.49	2260.25	-	-	-	-	-	-
	S-2	-	-	-	6347.35	38.54	3954.70	4589.03	40.00	2950.14	3293.58	41.52	2183.16	-	-	-	-	-	-
Z3	S-1	-	-	-	-	-	-	9717.42	34.69	5531.12	7063.15	36.70	4221.56	5060.67	38.79	3170.44	-	-	-
	S-2	-	-	-	-	-	-	9811.04	34.64	5577.36	7141.43	36.66	4263.70	5098.41	38.82	3195.90	-	-	-
Z4	S-1	-	-	-	-	-	-	-	-	-	5612.14	40.03	3610.30	4083.13	41.37	2699.15	2921.25	42.81	1985.14
	S-2	-	-	-	-	-	-	-	-	-	5720.95	40.06	3681.66	4162.06	41.39	2751.85	2976.68	42.85	2024.30

Table D-22. AASHTO T 350 (MSCR) Test Data for the Study Asphalt Binders at Original Condition

Binder	Replicate	58°C						64°C					
		$R_{0.1}$ (%)	$R_{3.2}$ (%)	R_{Diff} (%)	$Jnr_{0.1}$ (kPa^{-1})	$Jnr_{3.2}$ (kPa^{-1})	Jnr_{Diff} (%)	$R_{0.1}$ (%)	$R_{3.2}$ (%)	R_{Diff} (%)	$Jnr_{0.1}$ (kPa^{-1})	$Jnr_{3.2}$ (kPa^{-1})	Jnr_{Diff} (%)
X1	S-1	-	-	-	-	-	-	1.286	0.395	69.324	3.621	3.766	4.011
	S-2	-	-	-	-	-	-	1.154	0.402	65.190	3.624	3.763	3.860
X2	S-1	-	-	-	-	-	-	16.690	5.100	69.440	1.267	1.580	24.632
	S-2	-	-	-	-	-	-	16.400	5.163	68.520	1.260	1.560	23.800
X3	S-1	76.241	30.882	59.494	0.453	1.514	234.289	76.116	18.749	75.368	0.878	3.612	311.510
	S-2	75.897	28.493	62.459	0.483	1.623	236.329	76.598	19.395	74.680	0.853	3.561	317.350
X4	S-1	88.310	47.445	46.272	0.189	0.947	399.890	88.004	27.780	68.430	0.362	2.621	624.158
	S-2	87.035	45.735	47.450	0.215	1.000	365.061	89.186	30.627	65.659	0.325	2.469	660.846
X5	S-1	-	-	-	-	-	-	98.800	95.320	3.520	0.013	0.051	289.685
	S-2	-	-	-	-	-	-	98.770	95.430	3.380	0.013	0.049	274.378
Y1	S-1	2.240	0.660	70.750	3.646	3.908	7.200	1.000	0.190	80.250	8.332	8.940	7.297
	S-2	2.160	0.700	67.880	3.531	3.787	7.260	0.940	0.200	78.900	8.356	8.951	7.127
Y2	S-1	-	-	-	-	-	-	13.690	2.180	84.110	2.885	3.853	33.540
	S-2	-	-	-	-	-	-	13.600	2.130	84.330	2.931	3.919	33.710
Y3	S-1	-	-	-	-	-	-	7.450	1.460	80.340	3.527	4.289	21.610
	S-2	-	-	-	-	-	-	7.420	1.460	80.360	3.519	4.288	21.860
Y4	S-1	-	-	-	-	-	-	7.168	2.396	66.576	1.554	1.717	10.470
	S-2	-	-	-	-	-	-	7.034	2.340	66.680	1.588	1.759	10.733
Y5	S-1	-	-	-	-	-	-	94.168	87.621	6.952	0.116	0.187	61.620
	S-2	-	-	-	-	-	-	94.160	87.710	6.851	0.115	0.185	60.047
Y6	S-1	-	-	-	-	-	-	98.970	97.410	1.576	0.012	0.028	141.049
	S-2	-	-	-	-	-	-	98.933	97.295	1.655	0.012	0.029	140.299
Z1	S-1	2.740	0.900	67.230	3.028	3.255	7.477	1.230	0.260	78.690	7.131	7.656	7.362
	S-2	2.930	0.900	69.370	3.027	3.271	8.044	1.020	0.270	73.960	7.134	7.649	7.210
Z2	S-1	-	-	-	-	-	-	7.390	1.210	83.660	3.836	4.611	20.218
	S-2	-	-	-	-	-	-	7.610	1.210	84.170	3.809	4.605	20.900
Z3	S-1	-	-	-	-	-	-	4.430	1.100	75.150	2.742	3.005	9.600
	S-2	-	-	-	-	-	-	3.340	1.060	68.430	2.800	3.027	8.120
Z4	S-1	-	-	-	-	-	-	13.260	4.050	69.470	1.447	1.748	20.821
	S-2	-	-	-	-	-	-	13.590	4.110	69.800	1.432	1.731	20.900

Table D-22 (Continued). AASHTO T 350 (MSCR) Test Data for the Study Asphalt Binders at Original Condition

Binder	Replicate	70°C						76°C					
		$R_{0.1}$ (%)	$R_{3.2}$ (%)	R_{Diff} (%)	$Jnr_{0.1}$ (kPa^{-1})	$Jnr_{3.2}$ (kPa^{-1})	Jnr_{Diff} (%)	$R_{0.1}$ (%)	$R_{3.2}$ (%)	R_{Diff} (%)	$Jnr_{0.1}$ (kPa^{-1})	$Jnr_{3.2}$ (kPa^{-1})	Jnr_{Diff} (%)
X1	S-1	0.852	0.218	74.485	5.84	6.088	4.247	0.229	0.094	58.850	17.167	17.877	4.138
	S-2	0.864	0.198	77.019	6.135	6.399	4.305	0.317	0.104	67.067	16.820	17.586	4.550
X2	S-1	10.300	1.870	81.890	3.018	3.833	26.992	5.670	0.650	88.460	6.509	8.245	26.672
	S-2	10.300	1.842	82.120	3.040	3.870	27.283	5.660	0.640	88.610	6.550	8.320	27.000
X3	S-1	75.216	10.031	86.660	1.551	7.648	393.000	-	-	-	-	-	-
	S-2	73.103	9.636	86.820	1.688	7.594	349.830	-	-	-	-	-	-
X4	S-1	91.971	22.312	75.740	0.416	5.221	1155.500	-	-	-	-	-	-
	S-2	87.338	18.010	79.379	0.638	5.420	749.686	-	-	-	-	-	-
X5	S-1	98.620	93.036	5.664	0.024	0.113	364.400	97.790	72.130	26.240	0.056	0.759	1261.900
	S-2	98.640	93.030	5.680	0.024	0.113	370.260	97.810	72.080	26.310	0.056	0.767	1278.100
Y1	S-1	0.368	0.118	67.810	16.936	18.126	7.026	-	-	-	-	-	-
	S-2	0.595	0.124	79.184	17.005	18.323	7.748	-	-	-	-	-	-
Y2	S-1	8.440	0.790	90.610	6.446	8.662	34.390	4.230	0.260	93.950	14.548	19.716	35.530
	S-2	7.980	0.750	90.650	6.721	9.012	34.094	4.110	0.260	93.690	14.498	19.739	36.150
Y3	S-1	3.698	0.494	86.640	7.922	9.626	21.507	1.810	0.189	89.550	16.121	19.654	21.916
	S-2	5.468	0.504	90.790	7.660	9.610	25.450	1.880	0.190	89.770	16.063	19.656	22.370
Y4	S-1	3.810	0.780	79.400	3.825	4.255	11.243	1.810	0.250	86.030	8.430	9.400	11.490
	S-2	3.860	0.790	79.550	3.805	4.258	11.914	1.800	0.260	85.810	8.411	9.383	11.560
Y5	S-1	92.240	71.030	22.990	0.253	0.775	206.480	89.720	34.180	61.900	0.525	3.806	624.884
	S-2	92.337	72.076	21.943	0.245	0.730	198.480	89.570	36.230	59.550	0.517	3.471	572.000
Y6	S-1	98.580	96.860	1.749	0.025	0.048	90.610	97.290	94.650	2.716	0.069	0.108	57.092
	S-2	98.580	97.870	1.728	0.025	0.047	89.758	97.220	94.650	2.640	0.069	0.106	52.871
Z1	S-1	0.490	0.110	77.060	15.379	16.515	7.387	-	-	-	-	-	-
	S-2	0.420	0.120	72.510	15.299	16.379	7.062	-	-	-	-	-	-
Z2	S-1	4.230	0.400	90.490	8.560	10.388	21.356	1.820	0.180	89.950	17.976	21.838	21.488
	S-2	3.850	0.390	89.760	8.636	10.458	21.097	1.640	0.180	88.790	18.170	22.083	21.533
Z3	S-1	3.800	0.328	91.370	6.436	7.261	12.810	0.880	0.120	85.880	14.481	15.674	8.240
	S-2	1.877	0.317	83.130	6.602	7.175	8.670	0.660	0.120	81.200	14.633	15.786	7.877
Z4	S-1	7.600	1.410	81.450	3.534	4.321	22.230	4.010	0.470	88.300	7.920	9.730	22.750
	S-2	7.630	1.400	81.630	3.538	4.316	21.982	4.010	0.480	88.030	7.831	9.580	22.340

Table D-23. AASHTO T 350 (MSCR) Test Data for the Study Asphalt Binders at RTFO Condition

Binder	Replicate	58°C						64°C					
		$R_{0.1}$ (%)	$R_{3.2}$ (%)	R_{Diff} (%)	$Jnr_{0.1}$ (kPa^{-1})	$Jnr_{3.2}$ (kPa^{-1})	Jnr_{Diff} (%)	$R_{0.1}$ (%)	$R_{3.2}$ (%)	R_{Diff} (%)	$Jnr_{0.1}$ (kPa^{-1})	$Jnr_{3.2}$ (kPa^{-1})	Jnr_{Diff} (%)
X1	S-1	-	-	-	-	-	-	3.641	1.787	50.924	1.517	1.592	4.930
	S-2	-	-	-	-	-	-	4.050	1.825	54.937	1.507	1.586	5.248
X2	S-1	-	-	-	-	-	-	38.650	22.980	40.550	0.339	0.437	28.957
	S-2	-	-	-	-	-	-	38.570	22.930	40.560	0.340	0.438	28.680
X3	S-1	83.965	54.798	34.737	0.150	0.460	206.624	89.120	49.496	44.460	0.187	0.965	416.455
	S-2	83.213	55.213	33.648	0.164	0.475	189.689	87.423	44.998	48.528	0.214	1.074	401.156
X4	S-1	78.710	55.830	29.070	0.199	0.443	122.330	84.650	49.190	41.890	0.268	0.954	255.790
	S-2	85.270	62.490	26.720	0.134	0.364	171.170	80.800	45.570	44.970	0.294	1.009	243.160
X5	S-1	-	-	-	-	-	-	95.846	88.046	8.139	0.035	0.104	195.045
	S-2	-	-	-	-	-	-	95.482	86.836	9.056	0.037	0.110	199.820
Y1	S-1	8.970	4.120	54.040	1.172	1.292	10.186	4.390	1.320	70.010	2.910	3.239	11.300
	S-2	8.950	4.160	53.500	1.164	1.281	10.090	4.590	1.320	71.190	2.909	3.241	11.400
Y2	S-1	-	-	-	-	-	-	30.940	7.650	75.270	1.041	1.572	51.030
	S-2	-	-	-	-	-	-	30.720	7.620	75.190	1.045	1.574	50.610
Y3	S-1	-	-	-	-	-	-	24.850	8.271	66.720	1.026	1.376	34.110
	S-2	-	-	-	-	-	-	25.560	8.530	66.610	0.996	1.348	35.320
Y4	S-1	-	-	-	-	-	-	17.880	10.430	41.650	0.563	0.630	11.855
	S-2	-	-	-	-	-	-	17.390	10.140	41.660	0.583	0.651	11.640
Y5	S-1	-	-	-	-	-	-	96.180	92.680	3.640	0.039	0.060	51.030
	S-2	-	-	-	-	-	-	96.036	92.230	3.960	0.039	0.062	56.980
Y6	S-1	-	-	-	-	-	-	98.526	96.580	1.980	0.010	0.024	127.002
	S-2	-	-	-	-	-	-	98.608	96.662	1.972	0.010	0.023	134.850
Z1	S-1	10.410	5.870	43.630	0.834	0.903	8.236	5.430	1.800	66.798	2.172	2.396	10.301
	S-2	10.170	5.850	42.430	0.839	0.901	7.428	5.540	1.800	67.530	2.172	2.405	10.773
Z2	S-1	-	-	-	-	-	-	25.930	8.950	65.480	0.859	1.128	31.400
	S-2	-	-	-	-	-	-	25.730	8.990	65.080	0.864	1.132	30.990
Z3	S-1	-	-	-	-	-	-	10.870	6.070	44.140	0.816	0.880	7.780
	S-2	-	-	-	-	-	-	11.540	5.980	48.150	0.820	0.895	8.860
Z4	S-1	-	-	-	-	-	-	35.390	23.910	32.440	0.313	0.376	20.290
	S-2	-	-	-	-	-	-	35.990	24.040	33.200	0.310	0.375	21.050

Table D-23 (Continued). AASHTO T 350 (MSCR) Test Data for the Study Asphalt Binders at RTFO Condition

Binder	Replicate	70°C						76°C					
		$R_{0.1}$ (%)	$R_{3.2}$ (%)	R_{Diff} (%)	$Jnr_{0.1}$ (kPa^{-1})	$Jnr_{3.2}$ (kPa^{-1})	Jnr_{Diff} (%)	$R_{0.1}$ (%)	$R_{3.2}$ (%)	R_{Diff} (%)	$Jnr_{0.1}$ (kPa^{-1})	$Jnr_{3.2}$ (kPa^{-1})	Jnr_{Diff} (%)
X1	S-1	1.850	0.536	71.030	3.820	4.050	6.046	0.629	0.179	71.560	8.051	8.526	5.910
	S-2	1.850	0.550	70.290	3.791	4.000	5.699	0.588	0.177	69.930	8.220	8.682	5.620
X2	S-1	28.820	9.560	66.820	0.847	1.182	39.508	20.650	3.600	82.580	1.985	2.890	45.630
	S-2	29.381	9.518	67.606	0.842	1.190	41.300	20.420	3.570	82.539	2.000	2.904	45.240
X3	S-1	88.070	23.427	73.399	0.252	2.719	977.143	-	-	-	-	-	-
	S-2	81.048	22.315	72.467	0.587	2.956	403.110	-	-	-	-	-	-
X4	S-1	85.381	33.997	60.180	0.438	2.216	406.170	-	-	-	-	-	-
	S-2	82.923	30.340	63.410	0.517	2.395	362.920	-	-	-	-	-	-
X5	S-1	95.660	80.690	15.650	0.065	0.283	339.054	95.020	56.480	40.560	0.120	1.132	840.066
	S-2	95.640	80.290	16.053	0.063	0.282	348.350	94.940	56.750	40.220	0.116	1.067	820.010
Y1	S-1	2.160	0.424	80.340	6.751	7.541	11.698	-	-	-	-	-	-
	S-2	2.060	0.420	79.510	6.699	7.481	11.678	-	-	-	-	-	-
Y2	S-1	22.110	2.830	87.190	2.526	3.956	56.650	14.640	1.010	93.100	5.724	9.066	58.380
	S-2	22.240	2.860	87.150	2.520	3.938	56.270	14.620	1.010	93.110	5.785	9.173	58.572
Y3	S-1	16.436	2.905	82.320	2.541	3.537	39.190	9.965	1.020	89.760	5.711	8.020	40.460
	S-2	16.770	2.937	82.480	2.514	3.519	39.949	10.350	1.034	90.000	5.600	7.910	41.220
Y4	S-1	11.250	3.390	69.850	1.476	1.709	15.799	6.680	1.200	82.100	3.508	4.142	18.087
	S-2	11.220	3.320	70.380	1.507	1.751	16.270	6.482	1.167	81.990	3.558	4.192	17.830
Y5	S-1	95.020	89.900	5.389	0.084	0.123	47.110	93.320	79.760	14.530	0.177	0.399	125.750
	S-2	95.110	90.300	5.056	0.081	0.115	43.260	93.480	80.680	13.700	0.170	0.372	119.010
Y6	S-1	98.270	96.280	2.030	0.018	0.036	97.541	97.220	94.820	2.470	0.044	0.069	57.443
	S-2	98.240	96.210	2.066	0.019	0.036	96.741	97.280	94.890	2.450	0.043	0.068	58.405
Z1	S-1	2.890	0.550	81.070	5.212	5.808	11.427	-	-	-	-	-	-
	S-2	3.010	0.550	81.640	5.249	5.884	12.110	-	-	-	-	-	-
Z2	S-1	17.580	3.040	82.680	2.155	2.914	35.195	10.510	1.080	89.680	5.049	6.798	34.640
	S-2	17.170	3.120	81.860	2.135	2.875	34.640	10.310	1.080	89.570	5.100	6.849	34.300
Z3	S-1	5.770	1.840	68.160	2.175	2.399	10.300	2.910	0.575	80.200	5.123	5.703	11.310
	S-2	6.140	1.840	70.020	2.173	2.417	11.210	2.580	0.570	77.870	5.181	5.747	10.930
Z4	S-1	26.260	10.770	59.000	0.782	1.021	30.580	17.660	3.734	78.850	1.861	2.534	36.110
	S-2	26.290	10.540	59.910	0.789	1.036	31.386	17.800	3.720	79.100	1.870	2.553	36.580

Table D-24. Bending Beam Rheometer (AASHTO T 313) Data for Study Binders

Binder	Replicate	0°C		–6°C		–12°C		–18°C	
		m-Value	S (MPa)	m- Value	S (MPa)	m-Value	S (MPa)	m-Value	S (MPa)
X1	S-1	0.415	77.7	0.333	167	-	-	-	-
	S-2	0.411	75.9	0.337	164	-	-	-	-
X2	S-1	0.393	55.7	0.347	114	0.303	238	-	-
	S-2	0.392	57.3	0.346	117	0.302	245	-	-
X3	S-1	-	-	Material too soft		0.4	68.1	0.34	150
	S-2	-	-			0.398	68.1	0.334	155
X4	S-1	-	-	Material too soft		0.407	70.3	0.34	149
	S-2	-	-			0.405	69.4	0.336	147
X5	S-1	-	-	0.382	98	0.328	192	0.275	369
	S-2	-	-	0.383	96.5	0.321	198	0.275	386
Y1	S-1	-	-	0.397	66.5	0.329	155	0.285	312
	S-2	-	-	0.396	65.5	0.324	153	0.283	319
Y2	S-1	-	-	0.4	63.6	0.342	136	0.293	311
	S-2	-	-	0.395	62.9	0.339	135	0.292	308
Y3	S-1	0.405	34.3	0.354	70.2	0.313	153	-	-
	S-2	0.404	34.2	0.349	71.1	0.31	154	-	-
Y4	S-1	0.372	94.3	0.313	182	0.264	348	-	-
	S-2	0.371	95.3	0.316	181	0.262	348	-	-
Y5	S-1	Material too soft		0.361	55	0.308	114	-	-
	S-2			0.359	53	0.305	116	-	-
Y6	S-1	Material too soft		0.38	48.6	0.331	110	-	-
	S-2			0.384	48.2	0.332	108	-	-
Z1	S-1	-	-	0.363	76.8	0.312	165	0.263	331
	S-2	-	-	0.367	79.4	0.311	170	0.263	356
Z2	S-1	-	-	0.35	79.8	0.305	171	0.26	340
	S-2	-	-	0.345	83.4	0.303	168	0.259	349
Z3	S-1	0.328	68	0.285	131	-	-	-	-
	S-2	0.326	68.1	0.284	135	-	-	-	-
Z4	S-1	0.384	55.1	0.33	117	0.287	231	-	-
	S-2	0.383	55.9	0.329	116	0.285	233	-	-

CORRELATION BETWEEN FT-IR AND RHEOLOGY-BASED AGING RATIOS

The researchers sought to explore if any correlations could be made between rheology-based and FT-IR–based oxidative properties. In this regard, the aging ratio (*AR*) for FT-IR, which was calculated using Equation 50, was compared with the aging ratio obtained from rheological assessment. The relationship is shown in Figure D-14 for RTFO-aged binders and in Figure D-15 for PAV-aged binders. The study binders in Figure D-14 and Figure D-15 are divided into three groups, depending on their PG high temperature. While it would have been ideal to compare all the study binders at the same temperature, that was not possible since the PAV-aged binders were tested for their high-temperature properties only at the PG high temperature and not at ±6°C.

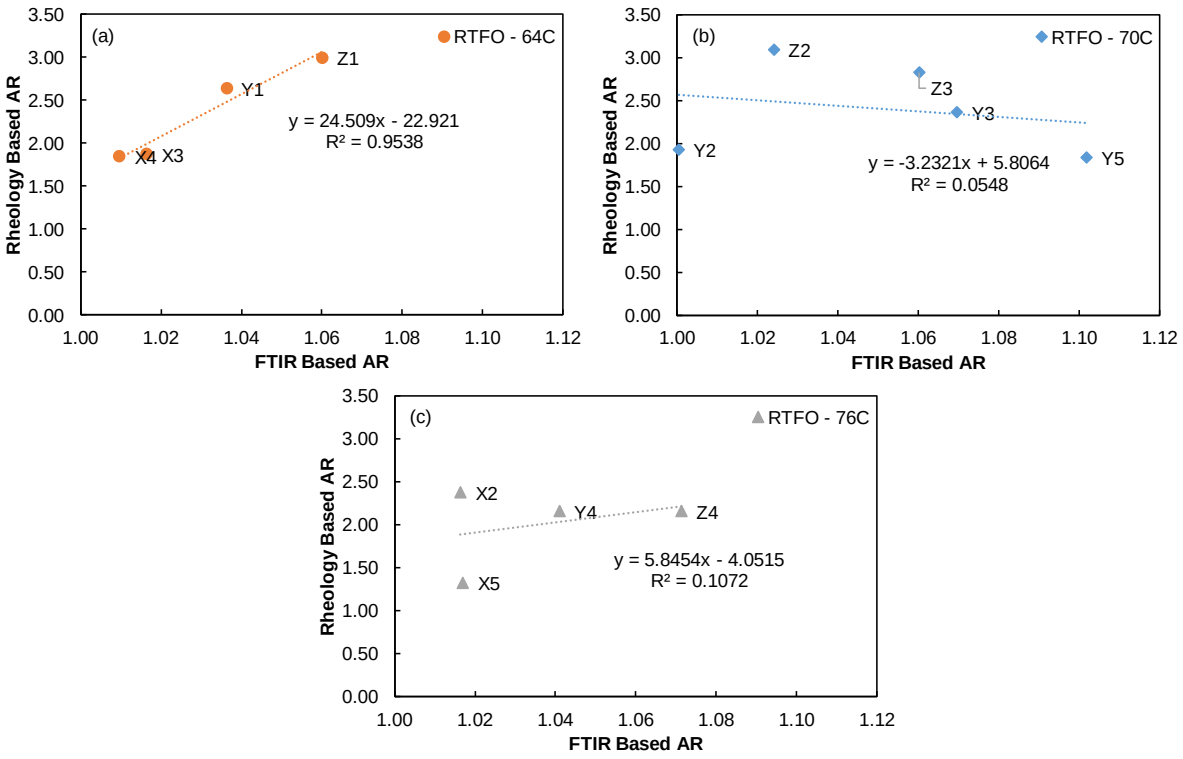

Figure D-14. Relationship Between Rheology-Based *AR* and FT-IR–Based *AR* for RTFO-Aged Binders with PG High Temperatures of (a) 64°C, (b) 70 C, and (c) 76°C

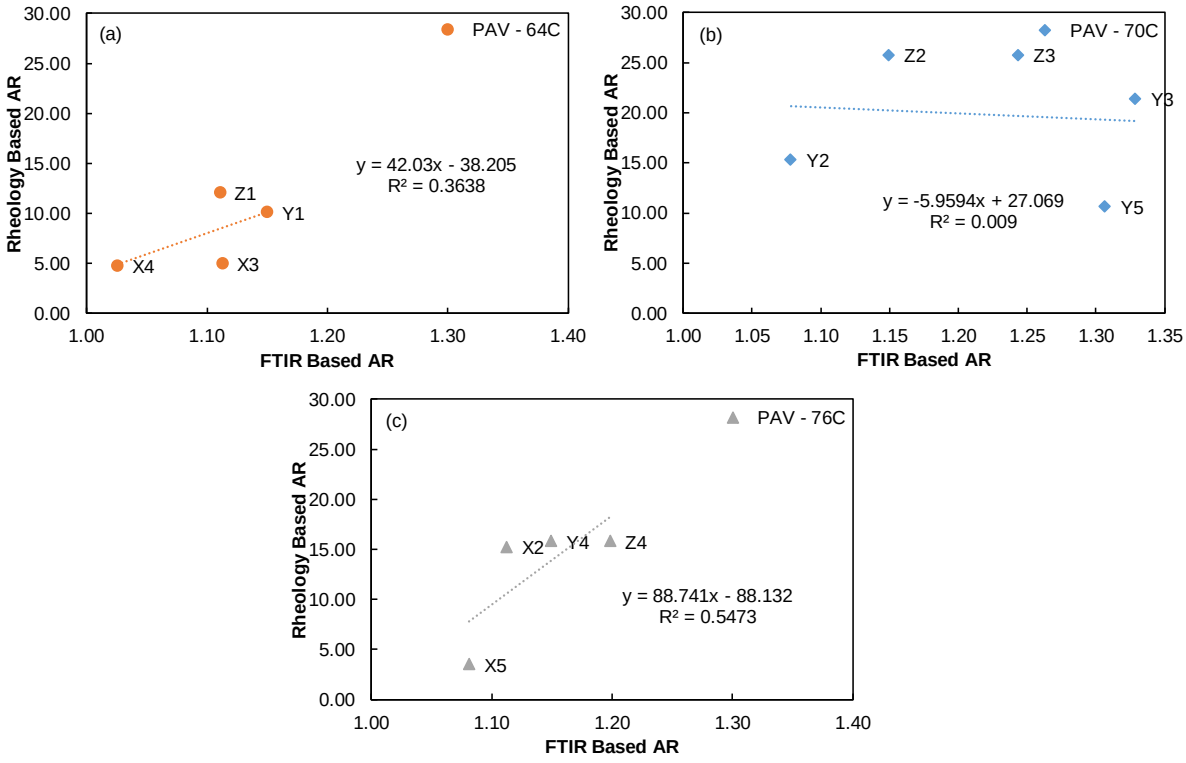

Figure D-15. Relationship Between Rheology-Based AR and FT-IR–Based AR for PAV-Aged Binders with PG High Temperatures of (a) 64°C, (b) 70°C, and (c) 76°C

The relationship between the two *AR*s is expected to be positive and linear. However, as evidenced by the R^2 values in the plots, there appears to be little or no correlation between the two *AR*s, except in Figure D-14(a).

$$AR_{FTIR} = \frac{(CA + SA)_{Aged}}{(CA + SA)_{Original}} \quad \text{(Eq. 50)}$$

Where CA = carbonyl area from FT-IR spectra
SA = sulfoxide area from FT-IR spectra
$Aged$ = refers to the summation of CA and SA after aging
$Original$ = refers to the summation of CA and SA before aging
AR_{FTIR} = aging ratio from FT-IR

APPENDIX E: MECHANICAL TESTING OF ARIZONA MIXTURES

DYNAMIC MODULUS DATA

Presented below are the dynamic modulus data for all 12 mixtures used in the study. Figure E-1 through Figure E-12 provide a graphical representation of the replicate data and the mastercurve, computed using the average of the replicates. Table E-1 through Table E-12 present in tabular form the dynamic modulus and phase angle data for all mixtures and their corresponding replicates.

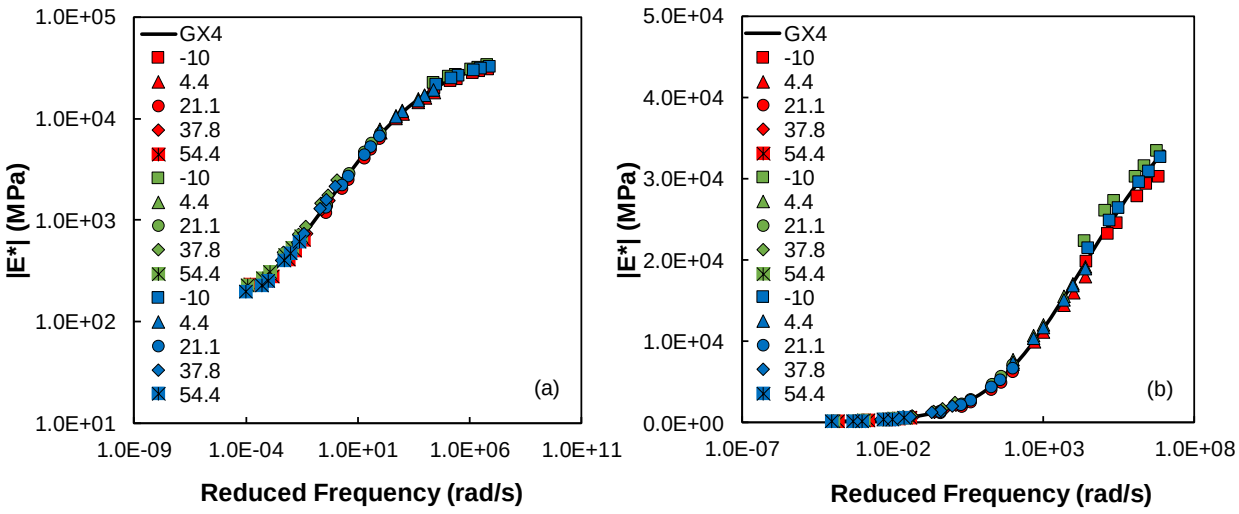

Figure E-1. Dynamic Modulus Replicate Data and Mastercurve for Mixture GX4 in (a) Log-Log Space and (b) Semilog Space

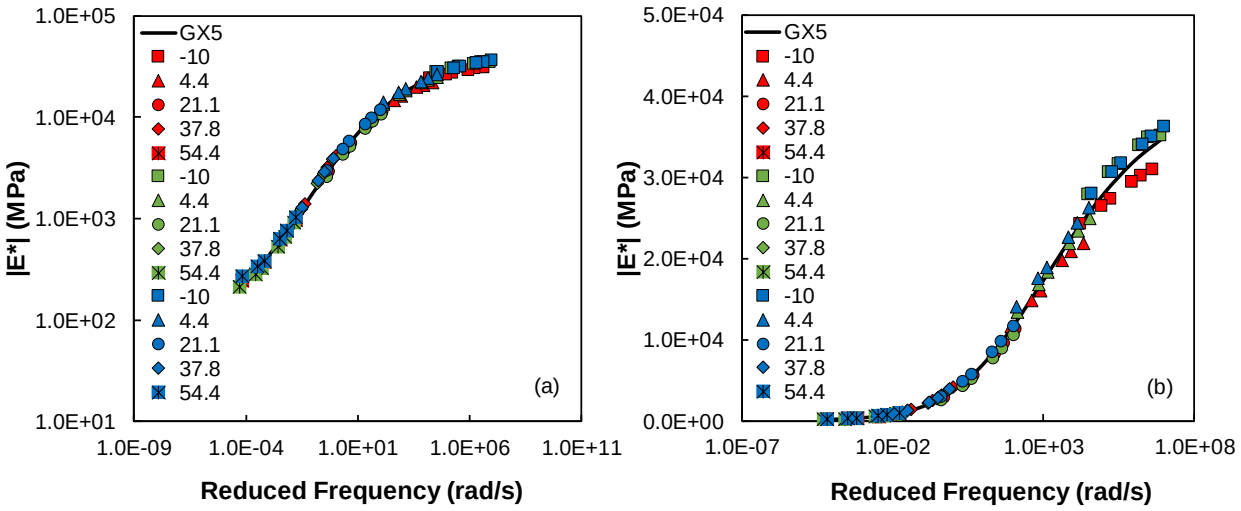

Figure E-2. Dynamic Modulus Replicate Data and Mastercurve for Mixture GX5 in (a) Log-Log Space and (b) Semilog Space

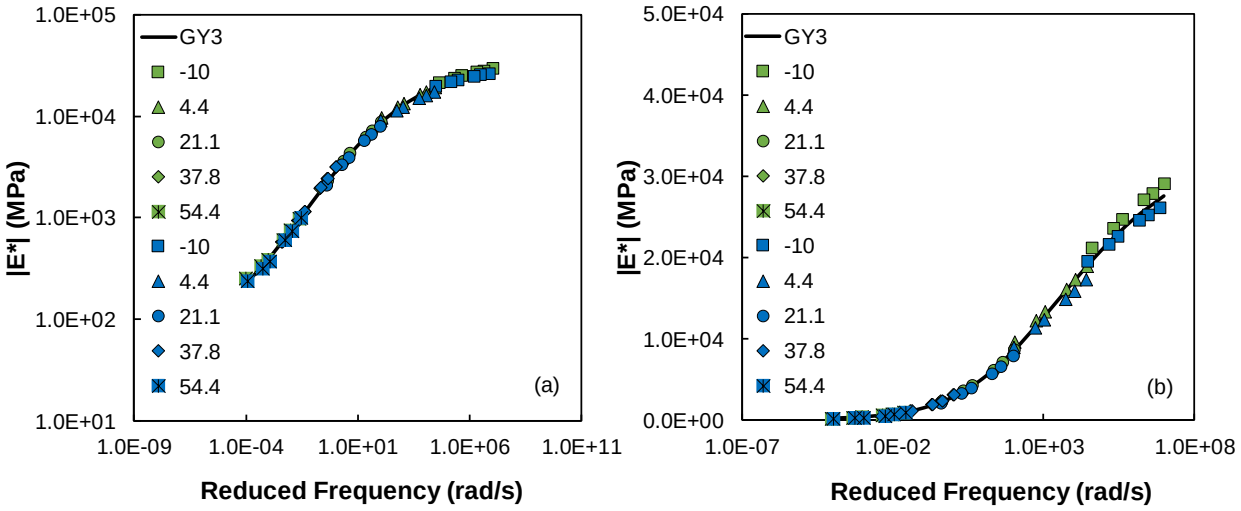

Figure E-3. Dynamic Modulus Replicate Data and Mastercurve for Mixture GY3 in (a) Log-Log Space and (b) Semilog Space

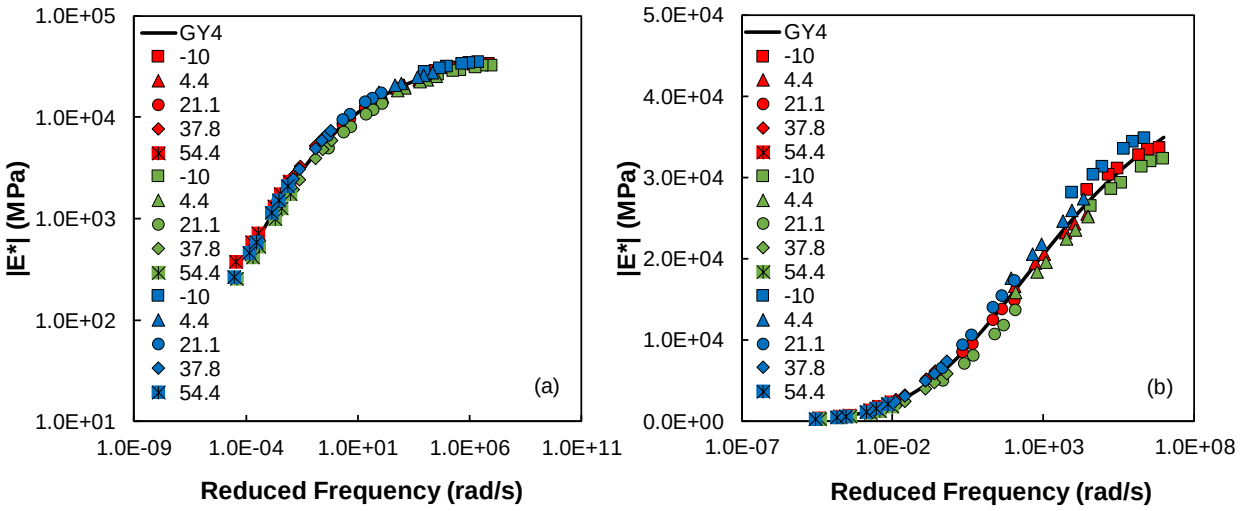

Figure E-4. Dynamic Modulus Replicate Data and Mastercurve for Mixture GY4 in (a) Log-Log Space and (b) Semilog Space

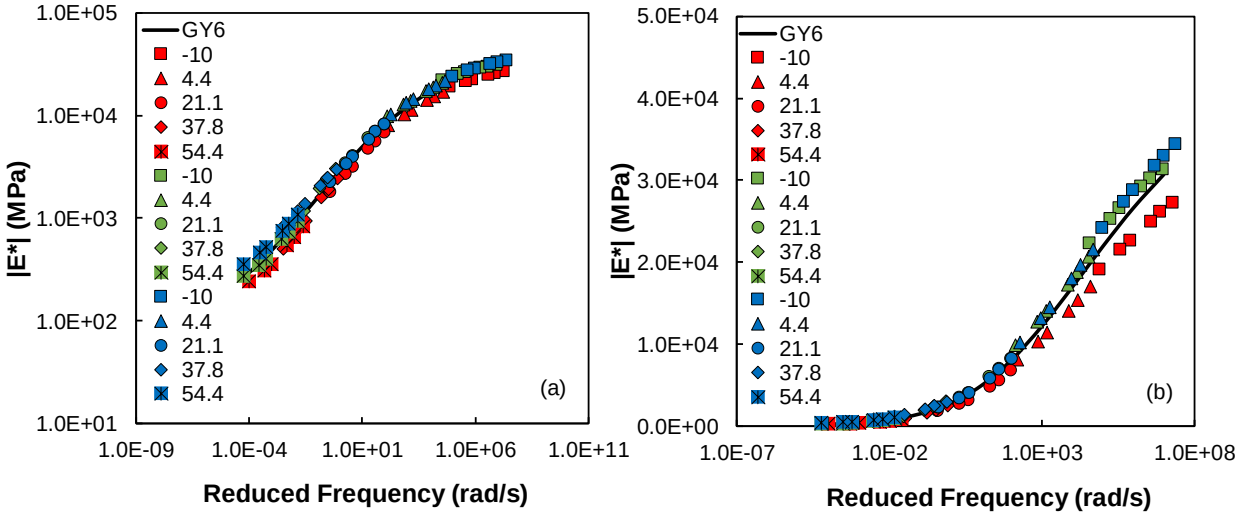

Figure E-5. Dynamic Modulus Replicate Data and Mastercurve for Mixture GY6 in (a) Log-Log Space and (b) Semilog Space

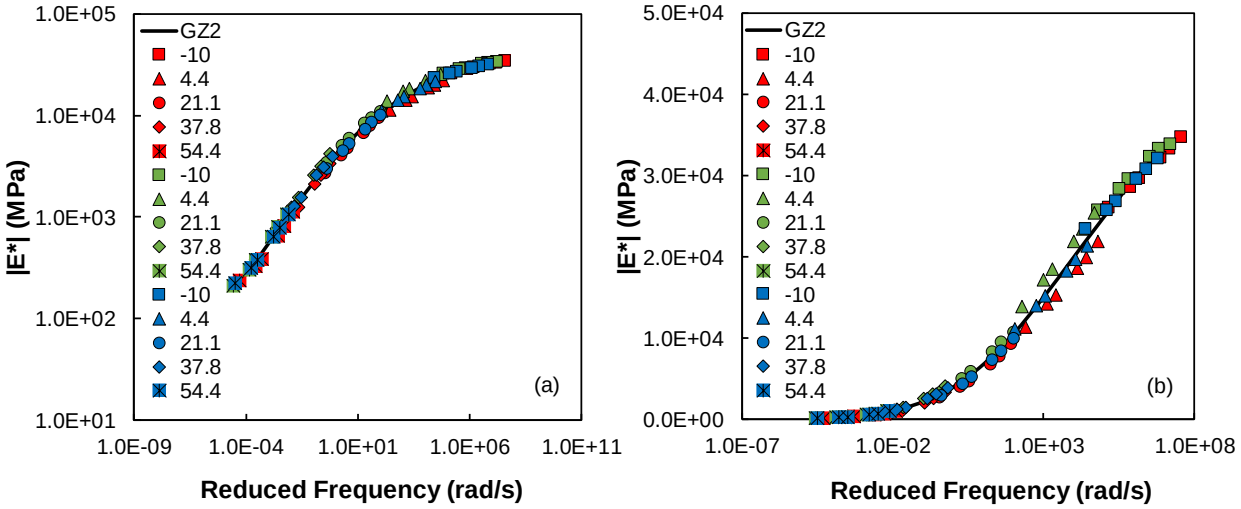

Figure E-6. Dynamic Modulus Replicate Data and Mastercurve for Mixture GZ2 in (a) Log-Log Space and (b) Semilog Space

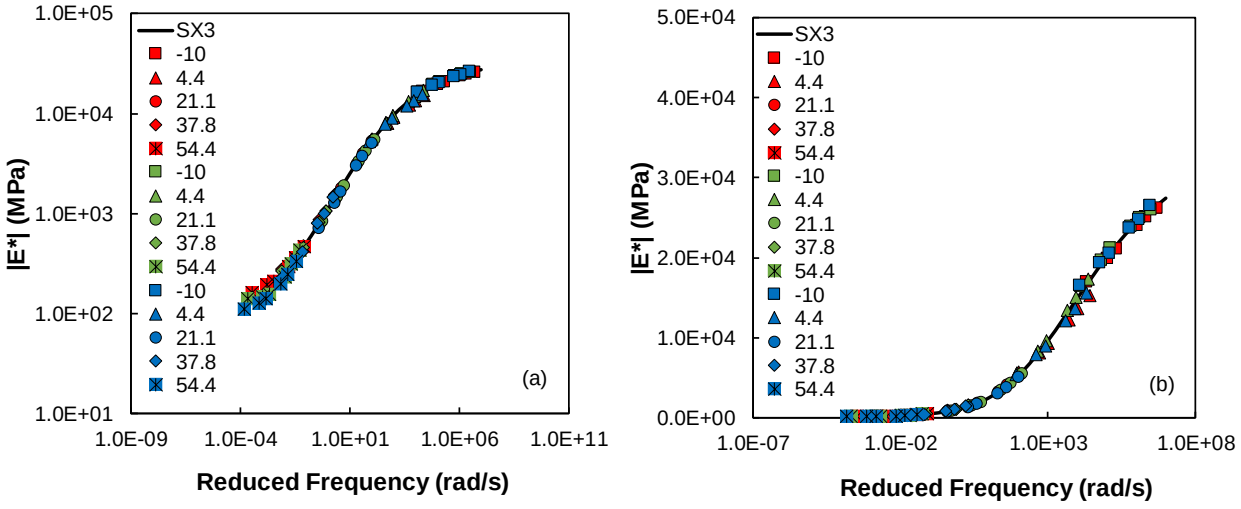

Figure E-7. Dynamic Modulus Replicate Data and Mastercurve for Mixture SX3 in (a) Log-Log Space and (b) Semilog Space

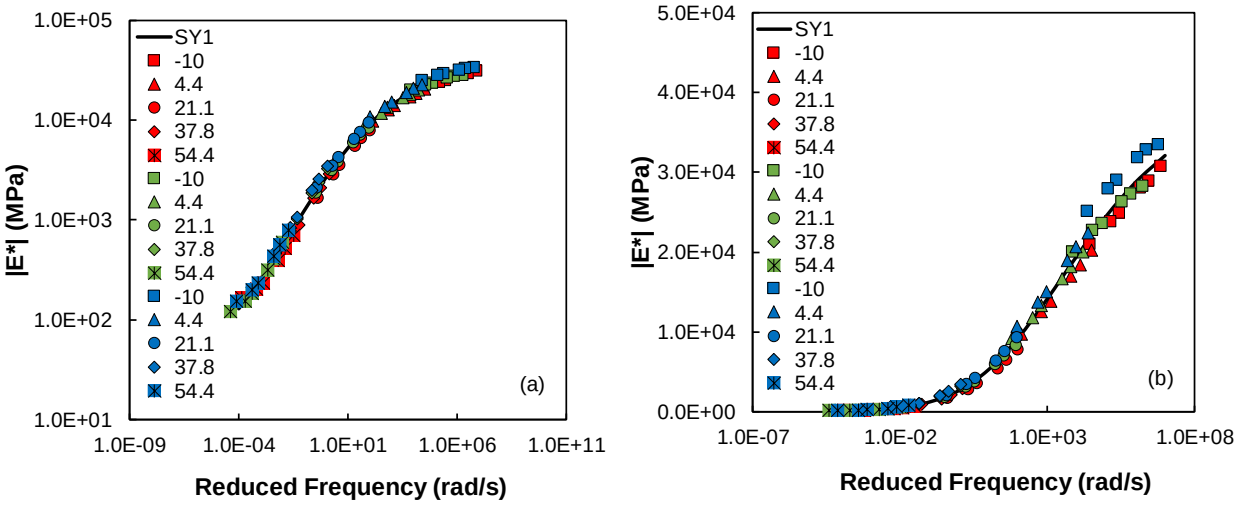

Figure E-8. Dynamic Modulus Replicate Data and Mastercurve for Mixture SY1 in (a) Log-Log Space and (b) Semilog Space

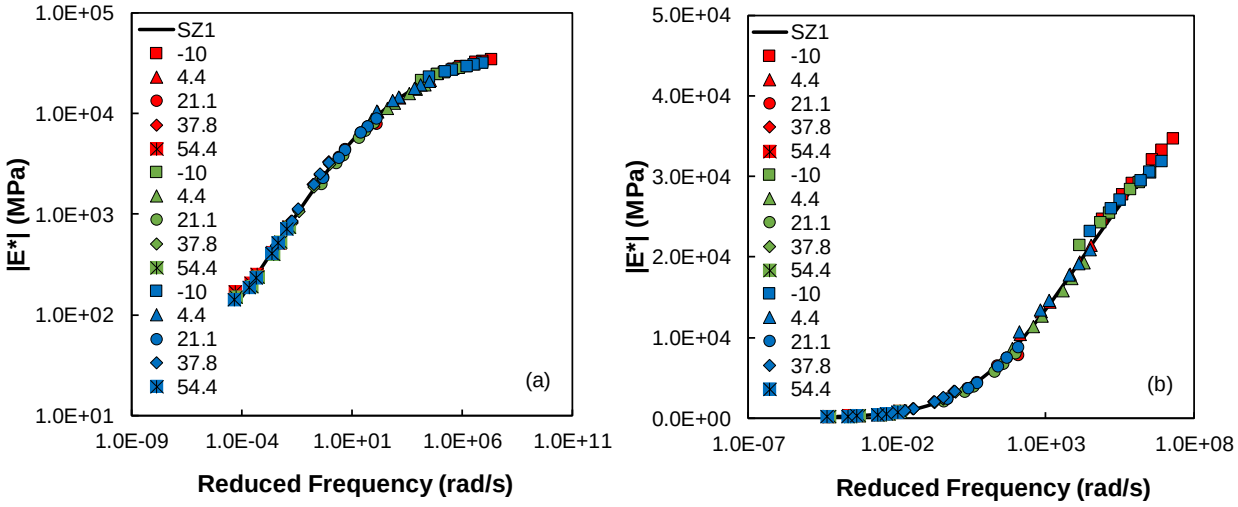

Figure E-9. Dynamic Modulus Replicate Data and Mastercurve for Mixture SZ1 in (a) Log-Log Space and (b) Semilog Space

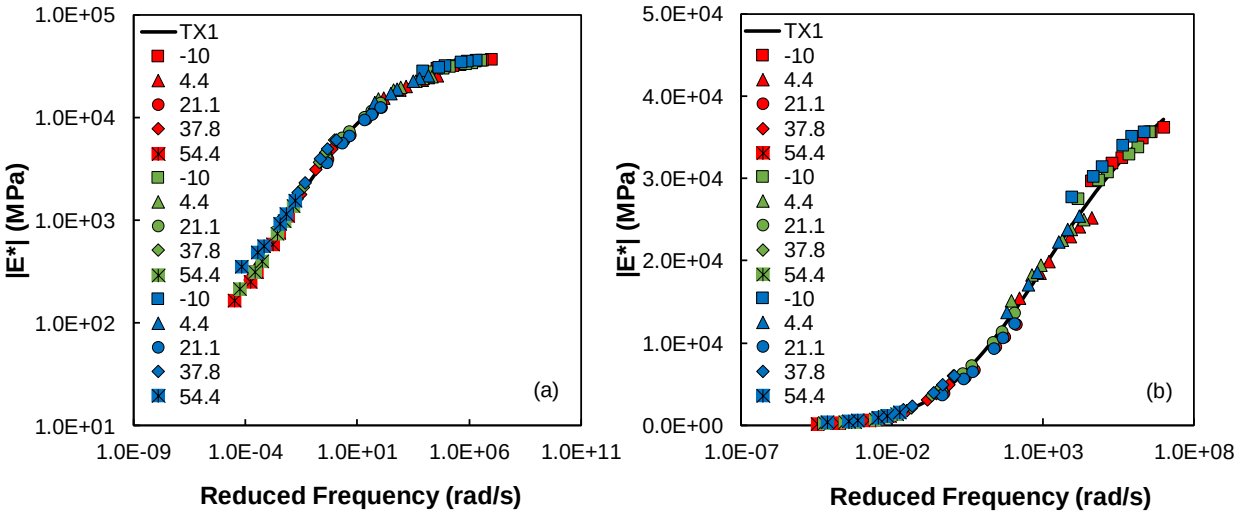

Figure E-10. Dynamic Modulus Replicate Data and Mastercurve for Mixture TX1 in (a) Log-Log Space and (b) Semilog Space

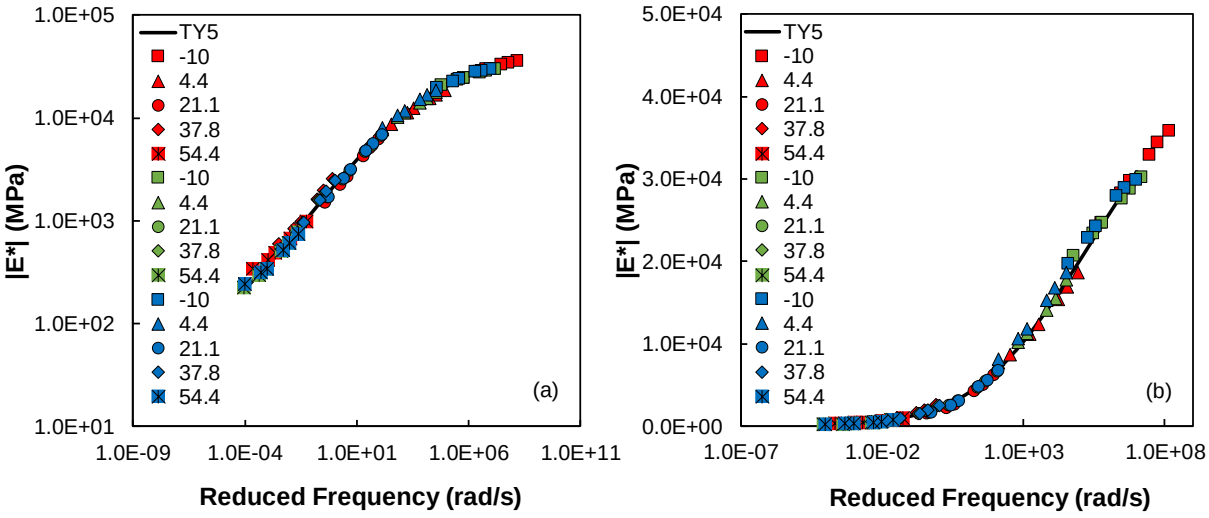

Figure E-11. Dynamic Modulus Replicate Data and Mastercurve for Mixture TY5 in (a) Log-Log Space and (b) Semilog Space

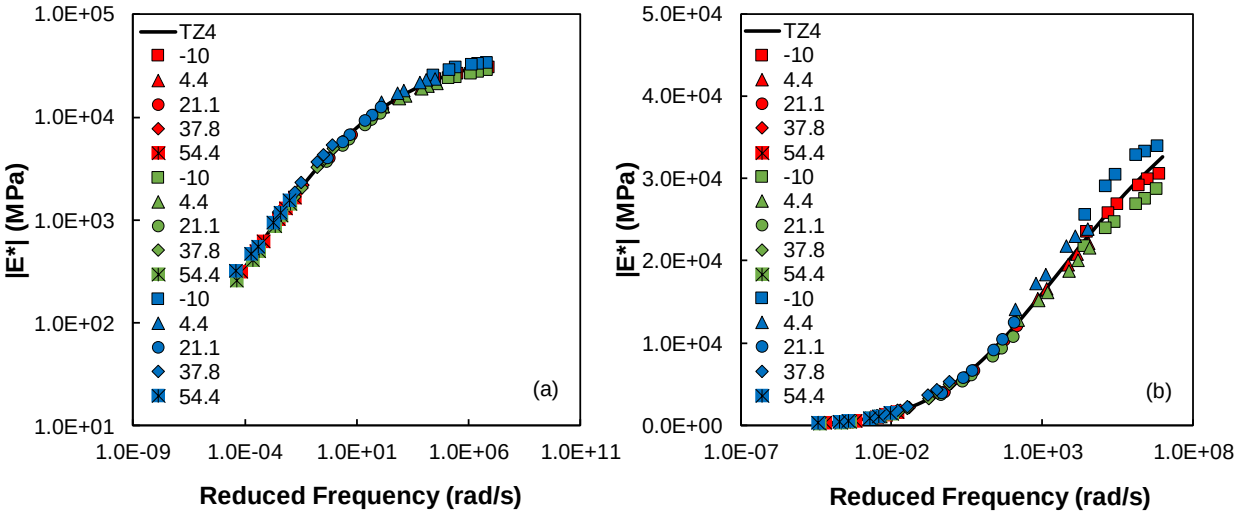

Figure E-12. Dynamic Modulus Replicate Data and Mastercurve for Mixture TZ4 in (a) Log-Log Space and (b) Semilog Space

Table E-1. Dynamic Modulus and Phase Angle Replicate Data for Mixture GX4

Temp. (°C)	Freq. (Hz)	Dynamic Modulus, |E*|			Phase Angle, δ		
		Repl. 1 (MPa)	Repl. 2 (MPa)	Repl. 3 (MPa)	Repl. 1 (Deg.)	Repl. 2 (Deg.)	Repl. 3 (Deg.)
–10.0	25	30348	33477	32761	4.8	4.9	5.8
	10	29374	31603	30910	7.2	6.3	7.4
	5	27900	30336	29644	8.3	8.6	7.8
	1	24620	27288	26407	9.9	9.6	9.7
	0.5	23302	26080	24978	10.3	10.1	10.0
	0.1	19823	22378	21487	12.3	12.1	12.5
4.4	25	18024	19163	19039	10.4	10.0	13.3
	10	16002	17138	16936	14.0	13.2	15.0
	5	14503	15586	15156	16.0	15.6	16.9
	1	11168	12125	11796	19.0	19.0	20.2
	0.5	9965	10746	10418	21.7	20.4	22.4
	0.1	7200	7847	7518	25.7	24.6	26.2
21.1	25	6311	7104	6659	22.4	21.5	21.5
	10	4901	5712	5229	27.6	26.3	26.6
	5	4014	4687	4381	28.5	28.8	28.7
	1	2495	2866	2709	33.9	32.7	33.3
	0.5	2009	2305	2208	34.5	34.0	34.5
	0.1	1185	1386	1324	33.1	32.9	32.8
37.8	25	2183	2492	2135	33.4	32.5	33.3
	10	1571	1772	1576	36.5	36.2	35.5
	5	1279	1466	1299	36.7	36.1	37.7
	1	745	864	743	36.6	33.2	35.1
	0.5	619	717	605	36.0	33.9	34.1
	0.1	410	483	399	32.4	31.0	30.1
54.4	25	634	699	611	37.6	35.5	39.6
	10	499	531	473	36.3	34.8	41.0
	5	409	456	402	35.4	32.2	38.8
	1	277	306	254	31.7	29.9	31.5
	0.5	253	269	229	29.4	27.4	28.8
	0.1	231	226	200	28.3	25.9	27.7

Table E-2. Dynamic Modulus and Phase Angle Replicate Data for Mixture GX5

Temp. (°C)	Freq. (Hz)	Dynamic Modulus, |E*|			Phase Angle, δ		
		Repl. 1 (MPa)	Repl. 2 (MPa)	Repl. 3 (MPa)	Repl. 1 (Deg.)	Repl. 2 (Deg.)	Repl. 3 (Deg.)
–10.0	25	31032	35245	36280	2.0	2.1	3.2
	10	30301	35001	35159	5.8	4.3	5.3
	5	29535	34042	34171	6.2	5.5	5.6
	1	27425	31658	31827	7.9	6.6	7.0
	0.5	26514	30715	30662	7.9	6.9	6.9
	0.1	24313	27999	28033	8.7	7.8	8.2
4.4	25	21941	24950	26260	6.6	7.0	7.6
	10	20870	23461	24448	11.3	8.9	9.9
	5	19817	21950	22675	12.1	10.0	11.2
	1	16131	18373	18989	15.9	14.1	13.9
	0.5	14824	16887	17667	16.8	14.3	14.6
	0.1	11675	13451	14084	20.6	18.3	18.9
21.1	25	11372	10565	11709	17.2	16.9	16.4
	10	9569	8970	9777	20.7	21.0	20.2
	5	8271	7677	8439	23.4	23.7	22.3
	1	5593	5140	5779	30.8	29.9	29.2
	0.5	4683	4254	4816	32.6	32.4	30.8
	0.1	2892	2556	2940	36.0	34.3	33.9
37.8	25	4146	3819	3927	26.0	27.6	26.3
	10	3179	2809	2930	30.5	32.6	30.6
	5	2526	2225	2359	33.6	34.6	34.1
	1	1394	1246	1290	35.5	35.1	35.4
	0.5	1112	984	1017	34.6	34.9	35.0
	0.1	663	589	606	30.1	30.2	30.7
54.4	25	969	908	1042	33.2	36.7	34.8
	10	756	663	769	31.7	36.4	37.6
	5	622	533	633	30.6	32.4	35.4
	1	374	325	385	27.2	28.1	27.6
	0.5	324	282	336	24.0	26.1	25.1
	0.1	245	211	272	19.8	21.5	22.6

Table E-3. Dynamic Modulus and Phase Angle Replicate Data for Mixture GY3

Temp. (°C)	Freq. (Hz)	Dynamic Modulus, |E*|			Phase Angle, δ		
		Repl. 1 (MPa)	Repl. 2 (MPa)	Repl. 3 (MPa)	Repl. 1 (Deg.)	Repl. 2 (Deg.)	Repl. 3 (Deg.)
–10.0	25	39794	29128	26125	2.3	3.2	1.6
	10	38031	27883	25293	4.1	5.0	3.3
	5	37097	27149	24547	5.6	5.6	4.7
	1	34059	24718	22565	6.4	6.7	6.0
	0.5	32891	23641	21643	6.3	6.9	6.1
	0.1	29478	21210	19594	7.5	7.8	7.0
4.4	25	26667	19040	17386	5.8	7.2	7.3
	10	24570	17390	15950	8.9	10.6	9.8
	5	22810	16155	14940	10.3	11.8	10.8
	1	19358	13428	12404	12.8	13.5	13.4
	0.5	17956	12283	11396	13.8	15.0	13.6
	0.1	14564	9619	8987	16.2	17.4	17.2
21.1	25	11787	8701	7853	16.4	15.7	16.5
	10	9980	7142	6617	21.3	20.3	19.8
	5	8717	6179	5720	22.0	22.5	22.7
	1	6017	4262	3906	27.2	27.2	27.2
	0.5	5098	3578	3282	28.0	29.6	29.2
	0.1	3379	2296	2078	30.1	32.4	30.2
37.8	25	4849	3161	3171	23.5	25.7	24.7
	10	3676	2425	2430	26.3	28.7	27.7
	5	2973	1956	1969	29.8	31.6	29.5
	1	1770	1156	1153	32.7	33.7	32.7
	0.5	1438	933	940	33.4	33.2	32.7
	0.1	883	578	573	31.4	31.2	30.5
54.4	25	1372	982	992	32.8	35.7	33.5
	10	976	747	743	34.9	37.6	34.7
	5	787	608	601	35.4	36.1	34.0
	1	487	389	369	32.8	33.2	29.1
	0.5	406	334	318	30.0	31.6	26.0
	0.1	274	255	238	26.5	26.4	22.4

Table E-4. Dynamic Modulus and Phase Angle Replicate Data for Mixture GY4

Temp. (°C)	Freq. (Hz)	Dynamic Modulus, |E*|			Phase Angle, δ		
		Repl. 1 (MPa)	Repl. 2 (MPa)	Repl. 3 (MPa)	Repl. 1 (Deg.)	Repl. 2 (Deg.)	Repl. 3 (Deg.)
–10.0	25	33626	32309	34884	1.4	3.8	2.1
	10	33473	32056	34439	3.0	5.1	2.7
	5	32843	31372	33524	3.7	5.9	3.4
	1	31137	29427	31406	5.0	6.6	4.6
	0.5	30376	28596	30374	5.3	6.6	5.0
	0.1	28543	26581	28199	6.2	7.5	5.2
4.4	25	25549	25155	27459	2.6	5.3	3.0
	10	24365	23532	25939	5.4	7.7	6.3
	5	23201	22416	24704	6.7	8.5	7.5
	1	20585	19642	21785	9.0	9.9	9.5
	0.5	19518	18402	20536	10.3	10.4	10.6
	0.1	16647	15810	17577	11.5	12.3	12.2
21.1	25	14914	13648	17329	12.5	11.8	11.7
	10	13769	11838	15379	16.3	15.2	14.8
	5	12413	10693	14005	17.8	17.2	16.7
	1	9512	8006	10627	22.7	21.5	21.5
	0.5	8469	7024	9347	25.1	23.8	24.3
	0.1	6098	4964	6489	30.1	28.3	29.1
37.8	25	7276	5855	7343	20.9	21.5	22.3
	10	6159	4768	5898	25.1	25.3	26.2
	5	5173	3956	4958	28.7	28.1	29.4
	1	3245	2412	3102	34.1	34.2	35.2
	0.5	2625	1930	2482	36.1	36.3	36.6
	0.1	1562	1095	1430	36.4	35.7	36.6
54.4	25	2332	1753	2105	33.1	33.5	32.5
	10	1733	1270	1510	37.1	37.1	36.6
	5	1314	987	1141	38.6	39.4	40.1
	1	720	525	582	37.8	37.1	39.0
	0.5	581	416	455	36.2	36.1	37.4
	0.1	373	255	268	31.1	31.5	31.3

Table E-5. Dynamic Modulus and Phase Angle Replicate Data for Mixture GY6

Temp. (°C)	Freq. (Hz)	Dynamic Modulus, |E*|			Phase Angle, δ		
		Repl. 1 (MPa)	Repl. 2 (MPa)	Repl. 3 (MPa)	Repl. 1 (Deg.)	Repl. 2 (Deg.)	Repl. 3 (Deg.)
–10.0	25	27242	31263	34425	3.4	2.3	5.6
	10	26120	30184	32960	6.9	5.2	7.7
	5	24986	29172	31804	8.0	7.4	9.4
	1	22664	26564	28833	9.7	8.5	10.3
	0.5	21552	25231	27361	9.6	8.5	11.4
	0.1	19112	22275	24201	10.6	9.7	12.7
4.4	25	17042	20626	21545	9.9	7.4	10.3
	10	15412	18814	19660	12.0	11.0	13.4
	5	14082	17232	18022	13.6	12.4	15.1
	1	11391	14002	14507	15.8	14.6	20.1
	0.5	10344	12723	13202	16.3	15.5	20.0
	0.1	8115	9907	10187	18.9	18.3	24.0
21.1	25	6786	8220	8252	19.4	18.2	24.7
	10	5601	6976	6905	23.2	23.5	27.8
	5	4781	6016	5845	24.3	25.8	29.3
	1	3188	4030	3983	28.2	29.4	31.9
	0.5	2695	3429	3345	29.6	30.4	33.0
	0.1	1791	2285	2258	30.6	31.4	31.8
37.8	25	2449	3071	2987	29.1	25.3	27.9
	10	1901	2411	2477	31.4	29.0	29.6
	5	1580	1967	2069	31.5	31.1	31.3
	1	943	1175	1386	32.2	32.8	30.4
	0.5	777	953	1167	31.9	32.6	28.6
	0.1	507	629	820	30.4	30.3	26.2
54.4	25	836	933	1092	31.4	32.6	30.7
	10	658	733	882	32.5	33.4	29.4
	5	545	624	759	30.2	31.5	28.9
	1	353	404	526	28.3	28.1	22.5
	0.5	312	348	463	28.5	26.3	24.2
	0.1	244	272	359	26.1	23.2	22.6

Table E-6. Dynamic Modulus and Phase Angle Replicate Data for Mixture GZ2

Temp. (°C)	Freq. (Hz)	Dynamic Modulus, |E*|			Phase Angle, δ		
		Repl. 1 (MPa)	Repl. 2 (MPa)	Repl. 3 (MPa)	Repl. 1 (Deg.)	Repl. 2 (Deg.)	Repl. 3 (Deg.)
–10.0	25	34778	33952	32123	3.4	2.0	5.0
	10	33416	33381	30848	5.6	3.1	6.9
	5	32284	32341	29624	6.0	4.2	7.2
	1	29794	29598	26923	7.4	5.7	8.2
	0.5	28617	28488	25853	8.4	5.7	8.7
	0.1	26086	25780	23452	8.3	6.0	9.2
4.4	25	21996	25457	21446	8.0	6.6	5.4
	10	19991	23519	19793	9.8	7.5	8.4
	5	18684	21995	18372	11.0	9.6	9.5
	1	15394	18519	15251	14.0	12.0	12.6
	0.5	14232	17241	14041	15.3	12.8	12.8
	0.1	11444	13955	11202	17.7	14.2	15.2
21.1	25	9384	10784	9968	17.7	17.1	15.3
	10	7801	9504	8463	21.1	19.1	19.1
	5	6763	8296	7326	22.5	21.4	21.9
	1	4755	5939	5219	27.5	25.6	26.9
	0.5	4053	5095	4427	29.2	27.5	28.7
	0.1	2721	3438	2964	32.4	29.7	31.8
37.8	25	3385	4186	3962	24.3	24.2	23.1
	10	2586	3187	3133	26.7	28.1	27.0
	5	2098	2599	2583	30.4	31.0	29.6
	1	1258	1558	1557	32.5	34.5	33.8
	0.5	1069	1256	1274	32.1	34.2	35.1
	0.1	670	771	787	31.1	32.1	33.1
54.4	25	1127	1067	1071	37.8	34.8	33.5
	10	820	808	778	39.7	33.7	35.6
	5	647	645	641	38.5	35.9	37.2
	1	384	380	380	33.4	33.2	34.3
	0.5	329	304	316	30.0	31.2	33.2
	0.1	238	212	224	27.6	26.8	29.5

Table E-7. Dynamic Modulus and Phase Angle Replicate Data for Mixture SX3

Temp. (°C)	Freq. (Hz)	Dynamic Modulus, |E*|			Phase Angle, δ		
		Repl. 1 (MPa)	Repl. 2 (MPa)	Repl. 3 (MPa)	Repl. 1 (Deg.)	Repl. 2 (Deg.)	Repl. 3 (Deg.)
–10.0	25	26195	26008	26457	3.0	4.1	5.9
	10	25129	24988	24810	7.0	7.6	8.4
	5	23970	23944	23713	8.0	10.0	8.1
	1	21034	21195	20524	9.3	10.9	10.3
	0.5	19875	19690	19392	9.8	11.5	9.8
	0.1	17003	16452	16530	12.4	12.9	11.8
4.4	25	15262	17278	15585	12.1	13.5	12.2
	10	13574	15044	13623	16.2	16.9	16.2
	5	12155	13393	12110	17.5	18.6	18.2
	1	9226	9608	8992	21.3	25.2	22.5
	0.5	8107	8272	7812	23.4	26.8	24.5
	0.1	5642	5551	5338	27.6	30.6	29.2
21.1	25	5262	5521	5053	25.2	25.3	25.4
	10	4027	4248	3793	28.8	28.7	30.6
	5	3174	3371	3031	32.1	31.4	33.5
	1	1806	1910	1672	35.5	36.1	35.9
	0.5	1381	1465	1269	37.0	35.9	36.0
	0.1	775	837	714	33.8	33.1	33.9
37.8	25	1561	1531	1477	34.8	36.7	36.3
	10	1080	1071	1016	35.1	38.9	39.4
	5	877	822	801	35.3	39.9	38.1
	1	479	460	418	31.4	34.6	33.2
	0.5	387	384	333	30.1	32.2	30.4
	0.1	279	269	226	25.6	25.7	24.6
54.4	25	474	435	337	36.7	45.9	32.0
	10	365	316	250	32.3	43.1	30.2
	5	300	233	200	29.3	41.1	27.7
	1	214	156	143	20.8	34.0	23.0
	0.5	194	147	128	19.5	32.6	20.2
	0.1	163	141	111	17.9	33.3	17.0

Table E-8. Dynamic Modulus and Phase Angle Replicate Data for Mixture SY1

Temp. (°C)	Freq. (Hz)	Dynamic Modulus, |E*|			Phase Angle, δ		
		Repl. 1 (MPa)	Repl. 2 (MPa)	Repl. 3 (MPa)	Repl. 1 (Deg.)	Repl. 2 (Deg.)	Repl. 3 (Deg.)
–10.0	25	30739	28283	33489	3.2	4.8	4.2
	10	28944	27273	32809	5.6	6.8	5.8
	5	27999	26281	31868	6.2	7.8	6.6
	1	24905	23645	29038	7.7	8.6	8.0
	0.5	23815	22725	27927	8.0	8.6	8.2
	0.1	20937	20063	25057	9.3	9.4	9.0
4.4	25	20202	20007	22385	7.9	7.0	7.8
	10	18434	18200	20631	10.9	11.0	10.7
	5	17021	16665	18899	12.5	12.7	12.0
	1	13816	13316	15035	15.2	17.4	16.2
	0.5	12562	11744	13747	16.6	17.5	16.5
	0.1	9693	9121	10702	19.1	20.4	19.5
21.1	25	7728	8298	9301	20.2	21.9	19.6
	10	6462	6992	7529	23.9	27.3	23.3
	5	5414	5916	6392	26.5	29.9	26.1
	1	3483	3801	4209	32.3	34.2	31.5
	0.5	2812	3133	3439	32.8	35.9	34.6
	0.1	1640	1835	2068	34.8	36.3	36.5
37.8	25	2867	3255	3406	29.7	30.6	29.3
	10	2095	2376	2526	31.5	33.3	32.8
	5	1633	1863	1979	35.8	38.0	34.7
	1	883	1023	1059	36.5	38.8	38.7
	0.5	689	768	825	36.3	38.6	38.9
	0.1	387	459	475	32.5	33.6	36.6
54.4	25	695	593	790	38.4	40.9	39.4
	10	512	405	559	37.4	41.2	40.2
	5	387	312	427	33.5	37.6	36.6
	1	231	183	230	29.9	31.2	30.7
	0.5	201	151	198	27.5	27.8	28.0
	0.1	165	120	152	23.7	23.4	21.3

Table E-9. Dynamic Modulus and Phase Angle Replicate Data for Mixture SZ1

Temp. (°C)	Freq. (Hz)	Dynamic Modulus, |E*|			Phase Angle, δ		
		Repl. 1 (MPa)	Repl. 2 (MPa)	Repl. 3 (MPa)	Repl. 1 (Deg.)	Repl. 2 (Deg.)	Repl. 3 (Deg.)
–10.0	25	34628	30388	31804	4.3	4.7	3.3
	10	33181	29246	30459	4.4	7.2	5.2
	5	32063	28286	29468	6.2	8.0	6.2
	1	29073	25390	26986	6.3	9.1	7.6
	0.5	27643	24223	25898	7.5	9.0	8.2
	0.1	24667	21398	23153	8.4	10.3	9.0
4.4	25	21386	19198	20847	8.8	8.2	7.2
	10	19342	17290	19155	10.9	10.4	10.4
	5	17871	15799	17746	12.2	12.6	11.6
	1	14366	12623	14549	15.3	15.2	14.0
	0.5	13117	11296	13362	16.1	17.1	15.3
	0.1	10301	8572	10621	19.1	19.2	18.1
21.1	25	7757	7931	8740	18.2	18.3	17.4
	10	7434	6673	7391	23.4	22.4	21.7
	5	6411	5699	6346	25.2	24.2	24.0
	1	4345	3821	4309	30.3	29.8	28.6
	0.5	3642	3188	3616	31.8	31.1	30.1
	0.1	2312	1988	2281	34.8	32.9	32.3
37.8	25	3289	3146	3265	30.0	27.3	26.8
	10	2453	2326	2503	32.6	29.3	30.6
	5	1988	1843	1990	35.0	32.0	33.2
	1	1108	1069	1119	35.5	35.0	34.9
	0.5	844	820	857	35.8	35.2	35.7
	0.1	469	479	489	32.5	32.6	33.8
54.4	25	746	745	707	37.6	36.6	37.8
	10	516	523	516	39.8	38.3	42.4
	5	414	400	409	38.4	37.4	40.6
	1	250	238	231	30.5	31.2	33.6
	0.5	207	192	187	28.1	29.0	28.5
	0.1	168	151	140	21.0	23.0	24.1

Table E-10. Dynamic Modulus and Phase Angle Replicate Data for Mixture TX1

Temp. (°C)	Freq. (Hz)	Dynamic Modulus, |E*|			Phase Angle, δ		
		Repl. 1 (MPa)	Repl. 2 (MPa)	Repl. 3 (MPa)	Repl. 1 (Deg.)	Repl. 2 (Deg.)	Repl. 3 (Deg.)
–10.0	25	36115	35609	35612	4.8	5.6	3.6
	10	35666	33732	35124	6.6	3.2	5.5
	5	34860	32899	33964	7.3	3.4	5.6
	1	32450	30770	31426	9.0	4.5	6.5
	0.5	31777	29752	30223	8.5	5.1	7.3
	0.1	29691	27463	27727	9.2	5.7	8.3
4.4	25	25217	24956	25473	6.6	8.2	6.5
	10	24088	23808	23819	9.5	6.0	8.4
	5	22880	22514	22284	10.1	8.2	10.3
	1	19869	19475	18599	12.5	10.7	12.8
	0.5	18524	18211	17099	12.6	11.2	13.4
	0.1	15435	15109	13760	15.0	14.7	16.7
21.1	25	12237	13606	12325	14.6	15.5	15.7
	10	10707	11295	10556	18.0	18.5	20.7
	5	9459	9969	9255	19.8	20.9	22.5
	1	6616	7156	6442	26.2	26.8	27.7
	0.5	5829	6189	5553	29.4	30.1	31.0
	0.1	3839	3999	3589	34.3	35.7	36.2
37.8	25	4950	5966	5975	23.9	26.3	26.8
	10	3862	4540	4877	29.0	30.9	30.0
	5	3077	3619	3932	32.4	33.5	32.8
	1	1777	2080	2286	35.9	38.6	37.6
	0.5	1378	1612	1826	36.4	39.0	38.4
	0.1	749	869	1053	34.1	36.8	34.7
54.4	25	1102	1377	1539	37.7	38.1	37.4
	10	756	976	1136	38.6	39.8	37.0
	5	576	732	908	37.2	39.8	37.1
	1	308	393	561	32.5	35.0	32.1
	0.5	248	314	486	30.3	32.3	26.9
	0.1	164	212	348	24.5	26.8	19.9

Table E-11. Dynamic Modulus and Phase Angle Replicate Data for Mixture TY5

Temp. (°C)	Freq. (Hz)	Dynamic Modulus, |E*|			Phase Angle, δ		
		Repl. 1 (MPa)	Repl. 2 (MPa)	Repl. 3 (MPa)	Repl. 1 (Deg.)	Repl. 2 (Deg.)	Repl. 3 (Deg.)
–10.0	25	35933	30233	29948	4.3	5.8	6.0
	10	34450	28883	29004	7.1	5.6	7.2
	5	32937	27721	28010	8.0	7.6	7.9
	1	29870	24725	24335	9.4	8.0	9.9
	0.5	28282	23483	22869	9.9	8.8	11.3
	0.1	24702	20761	19757	11.6	10.0	12.8
4.4	25	18624	17826	18622	11.9	9.3	8.5
	10	16899	15563	16828	14.8	11.3	13.3
	5	15399	14167	15334	15.5	13.0	14.1
	1	12372	11293	11813	18.0	15.7	17.4
	0.5	11201	10175	10630	18.4	16.5	18.5
	0.1	8745	7744	8113	21.4	18.8	20.5
21.1	25	6206	6657	6783	22.8	18.9	20.0
	10	5050	5400	5589	27.7	22.7	24.3
	5	4242	4690	4794	29.5	23.7	25.2
	1	2669	3078	3117	33.8	27.0	30.4
	0.5	2246	2542	2570	34.1	28.0	31.7
	0.1	1499	1686	1693	31.7	28.2	32.3
37.8	25	2596	2493	2478	28.8	26.9	29.1
	10	1976	1910	1961	29.0	31.2	30.4
	5	1613	1588	1601	31.8	30.4	32.1
	1	982	970	962	33.0	30.4	33.2
	0.5	833	794	781	32.9	29.6	32.5
	0.1	599	537	527	27.5	26.7	30.7
54.4	25	992	774	744	28.7	30.6	33.7
	10	799	608	615	28.1	31.6	31.3
	5	681	514	517	26.2	28.4	26.3
	1	492	340	344	24.5	25.6	28.5
	0.5	420	297	314	22.5	25.3	27.6
	0.1	340	226	243	19.6	21.7	23.3

Table E-12. Dynamic Modulus and Phase Angle Replicate Data for Mixture TZ4

Temp (°C)	Freq. (Hz)	Dynamic Modulus, |E*|			Phase Angle, δ		
		Repl. 1 (MPa)	Repl. 2 (MPa)	Repl. 3 (MPa)	Repl. 1 (Deg.)	Repl. 2 (Deg.)	Repl. 3 (Deg.)
–10.0	25	30600	28795	34004	2.2	5.0	3.8
	10	29977	27555	33284	4.5	4.1	5.3
	5	29189	26875	32847	5.1	4.6	5.8
	1	26882	24756	30486	6.1	5.6	6.5
	0.5	25851	24008	29051	6.4	5.4	7.0
	0.1	23511	21853	25583	7.0	6.5	8.0
4.4	25	22149	21606	23861	5.7	4.8	6.6
	10	20834	20118	23026	7.3	7.9	8.3
	5	19543	18813	21804	8.5	9.0	10.0
	1	16669	16218	18348	10.6	10.1	12.2
	0.5	15476	15251	17234	11.1	10.9	12.5
	0.1	12762	12794	14138	13.3	12.4	14.9
21.1	25	12022	10778	12526	12.9	13.3	16.5
	10	10356	9377	10473	16.8	17.0	19.4
	5	9103	8419	9193	18.1	17.9	21.5
	1	6703	6145	6696	22.0	22.7	25.4
	0.5	5829	5330	5783	24.1	24.5	27.9
	0.1	4036	3707	3979	27.7	28.0	31.1
37.8	25	5119	4971	5362	20.9	19.9	22.5
	10	4132	3940	4349	25.7	25.6	27.9
	5	3462	3298	3689	27.5	26.9	29.5
	1	2199	2081	2311	31.5	29.9	33.5
	0.5	1828	1711	1888	32.4	32.1	34.2
	0.1	1167	1070	1197	32.2	31.7	34.2
54.4	25	1674	1457	1570	30.4	30.6	31.3
	10	1302	1111	1176	31.2	31.7	32.0
	5	1038	873	947	31.8	32.7	33.6
	1	621	498	551	30.2	29.9	32.4
	0.5	497	409	471	29.5	28.2	30.9
	0.1	318	257	324	26.8	25.7	26.8

Table E-13. |E*| Mastercurve and Shift Function Parameters for All Mixtures

Mixture	Mastercurve Parameters				Shift Function Parameters	
	δ	α	β	γ	α_1	α_2
GX4	1.8914	2.7410	0.2631	0.4573	0.0007	-0.1643
GX5	1.9242	2.6815	0.7195	0.5037	0.0005	-0.1541
GY3	1.0199	3.5228	1.0236	0.3623	0.0012	-0.1918
GY4	0.8919	3.7134	1.5965	0.3883	0.0004	-0.1533
GY6	1.8959	2.7211	0.4927	0.3987	0.0008	-0.1753
GZ2	1.2393	3.4195	0.9980	0.3506	0.0006	-0.1720
SX3	1.8369	2.6816	0.0854	0.5422	0.0007	-0.1554
SY1	1.5662	3.0118	0.7301	0.4744	0.0004	-0.1469
SZ1	1.3402	3.3071	0.7849	0.3919	0.0005	-0.1609
TX1	1.5794	3.0499	1.0571	0.4509	0.0005	-0.1492
TY5	1.8840	2.7595	0.3076	0.3958	0.0011	-0.1888
TZ4	1.1664	3.4635	1.1735	0.3581	0.0006	-0.1605

HAMBURG WHEEL TRACKING TEST DATA

The rut depths reported in Chapter 5 are consistent with current ADOT practice and the methodology proposed in AASHTO T 324, which calls for only the maximum rut depth across all sensors to be reported. The same methodology is currently followed in six other states: California, Colorado, Massachusetts, Utah, Washington, and Wisconsin. However, many other states, such as Texas, Oklahoma, Illinois, Louisiana, Montana, and Iowa, have adopted different methodologies for calculating the rut depth after it is obtained from the Hamburg Wheel Tracking Test. During the research phase of this study, these methods were investigated to avoid potential unintended bias that might occur because of the method chosen. Presented below are the different methods used by the above-named states to calculate rut depths. Also presented is another method, developed by ASU researchers, which is called the 1.5 IQR method. The 1.5 IQR method presents a robust technique for identifying outlier data and creates a statistical basis for accepting or rejecting data for consideration in rut depth calculation. This detailed, filtering-based approach is absent from the methods adopted by the above states.

Texas/Oklahoma

These states use the average of the middle three sensors to calculate rut depths. The rationale is similar to the one underlying the 1.5 IQR method: It supposes that any single measurement can be affected by localized rutting and not representative of the material.

Illinois

Illinois uses the average of three sensor readings, which include the sensor at which the maximum rut depth is measured and the two sensor readings beside it. Generally, these sensors will be the center three sensors, and in this case the Illinois method and the Texas/Oklahoma method are identical.

Louisiana

Louisiana reports rut depth as the average of the middle five sensors.

Montana

Montana reports the average of the middle seven sensors.

Iowa

Iowa also uses an averaging method, but it is somewhat more sophisticated than those just described. In Iowa, if the average rut depth at the final pass is larger than 12 mm, then the average of five middle sensors is reported. On the other hand, if the average rut depth at the final pass is less than 12 mm, then the average of 10 sensors is reported, with the first and the last sensor being excluded.

In the current study, all the above-mentioned methods except for Iowa's have been implemented, and the corresponding rut depths have been calculated. These results are compared in Figure E-13 through Figure E-16 and in Table E-14. Note that the graphs show the average rut depths, and the error bars show the range of values from the left- and right-side specimens.

1.5 IQR Method

In this method, the first and last sensors are ignored because they often are inconsistent with the other sensors. The data from the remaining 10 sensors are divided into quartiles based on their magnitude (i.e., sensors in the 25th percentile are considered to be in Q1, those in the 50th percentile are in Q2, and those in the 75th percentile are in Q3). Subsequently, the interquartile range (IQR) is calculated by subtracting Q1 from Q3 (IQR = Q3–Q1). Outlying measurements are computed using the 1.5 x IQR rule, which identifies outlying data if they are greater than IQR by a factor of 1.5 than Q3 or less than Q1. The data from sensors between these bounds are deemed suitable, and those outside these bounds are termed as outliers and ignored in the rut depth calculation. The purpose of this filtering is to eliminate data that are grossly different from the central tendency of the sensors collectively, and to avoid situations where the test results are influenced by very localized defects and thus not representative of the whole. Once all the suitable sensors are compiled, they are averaged to find the rut depth. The same process is used for both the left and the right wheel.

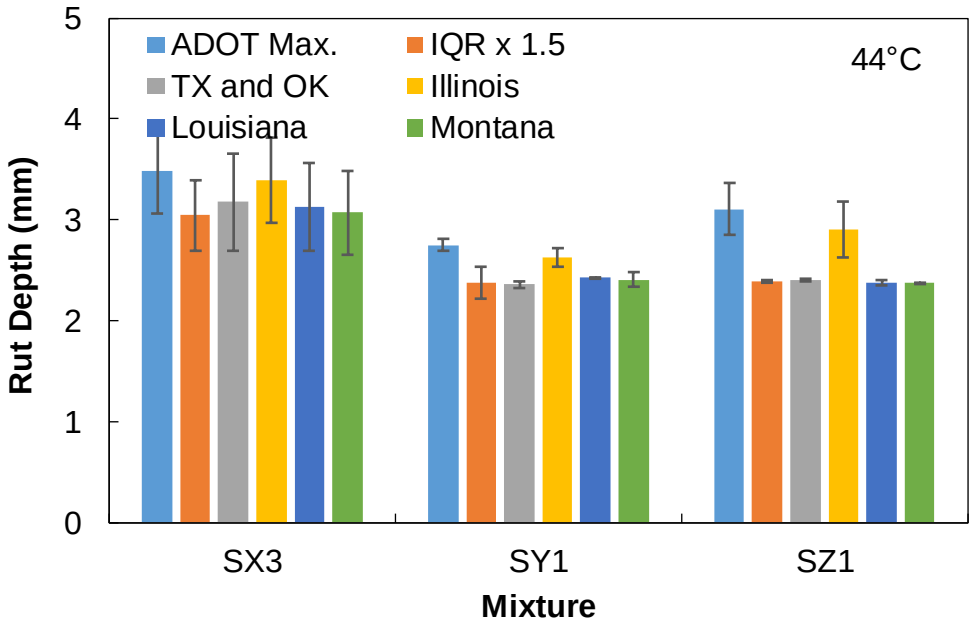

Figure E-13. Rut Depths at 44°C Calculated Using Different Methods

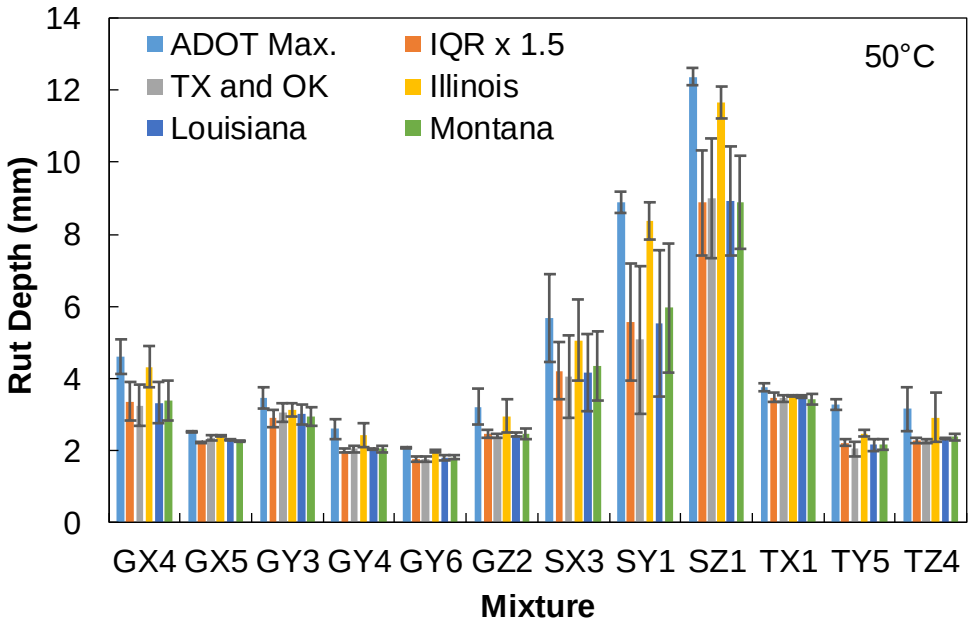

Figure E-14. Rut Depths at 50°C Calculated Using Different Methods

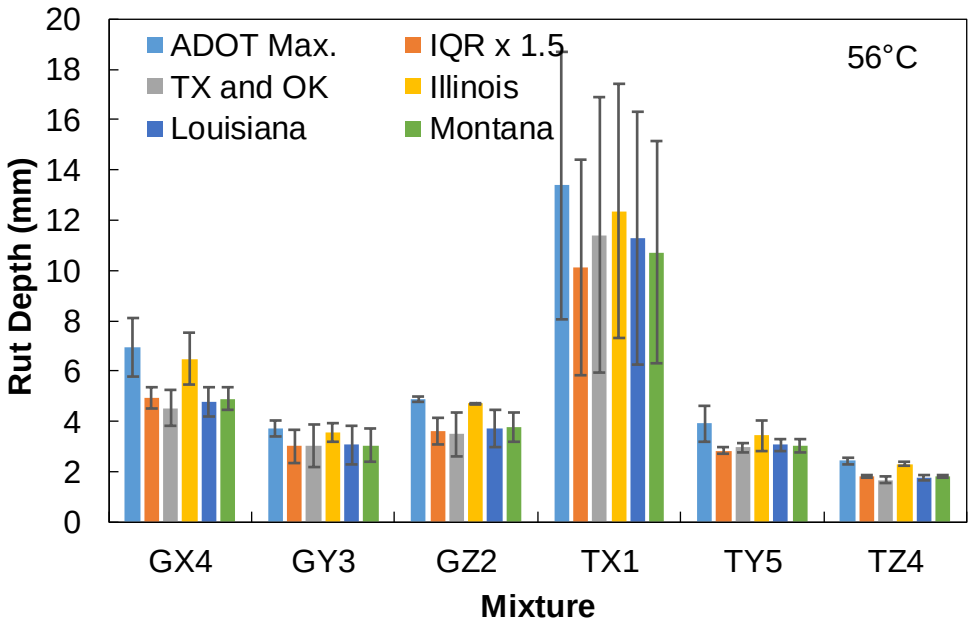

Figure E-15. Rut Depths at 56°C Calculated Using Different Methods

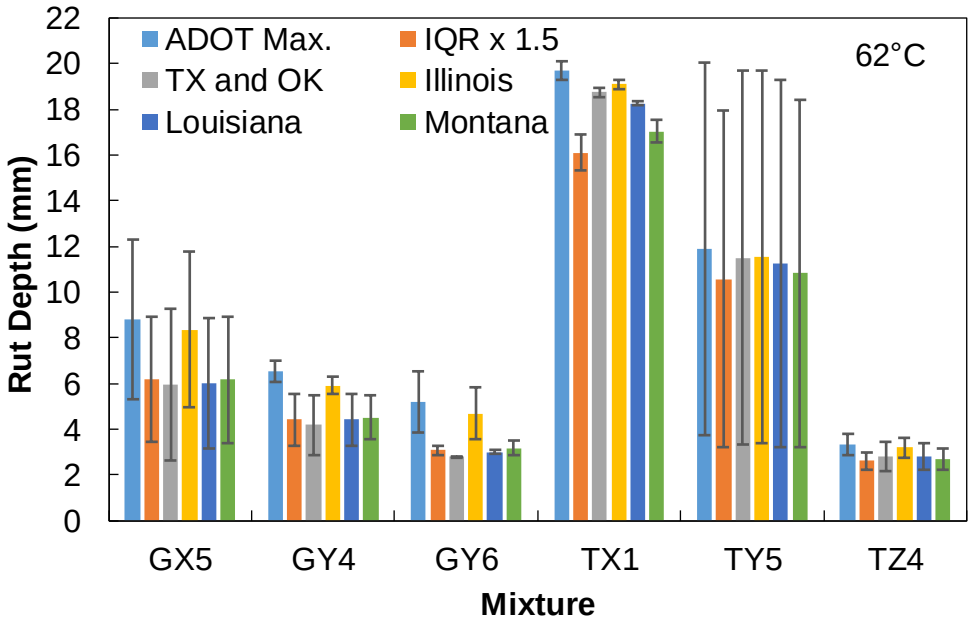

Figure E-16. Rut Depths at 62°C Calculated Using Different Methods

It can be seen from the above figures and from Table E-14 that the method currently employed by ADOT gives the highest rut depth, followed by the method adopted in Illinois. The remaining four methods yield very similar rut depths.

It is worth noting from Figure E-13 through Figure E-16 that for most of the mixtures, the methods that use averaging are seen have less apparent specimen-to-specimen variability. These methods include 1.5 IQR and the approaches used by Texas, Oklahoma, Louisiana, and Montana. The analysis excludes Illinois because even though that state employs averaging of sensors, the sensors to be averaged depend on the one that gives the maximum rut depth. That is possibly one of the reasons why the methods used by ADOT and Illinois show similar variability.

Table E-14. Rut Depths of 12 Asphalt Mixtures Calculated Using Different Analysis Methods

Mixture	Temperature (°C)	Average Rut Depth (mm)					
		ADOT Max.	IQR x 1.5	TX and OK	Illinois	Louisiana	Montana
GX4	50	4.6	3.4	3.3	4.3	3.3	3.4
	56	6.9	4.9	4.5	6.5	4.8	4.9
GX5	50	2.5	2.2	2.3	2.4	2.3	2.3
	62	8.8	6.2	5.9	8.4	6.0	6.2
GY3	50	3.4	2.9	3.1	3.1	3.0	2.9
	56	3.7	3.0	3.0	3.5	3.1	3.0
GY4	50	2.6	2.0	2.0	2.4	2.1	2.0
	62	6.5	4.4	4.2	5.9	4.4	4.5
GY6	50	2.1	1.8	1.8	2.0	1.8	1.8
	62	5.2	3.1	2.8	4.7	3.0	3.2
GZ2	50	3.2	2.4	2.4	3.0	2.4	2.5
	56	4.9	3.6	3.5	4.7	3.7	3.8
SX3	44	3.5	3.0	3.2	3.4	3.1	3.1
	50	5.7	4.2	4.0	5.1	4.2	4.3
SY1	44	2.8	2.4	2.4	2.6	2.4	2.4
	50	8.9	5.6	5.1	8.4	5.5	6.0
SZ1	44	3.1	2.4	2.4	2.9	2.4	2.4
	50	12.4	8.9	9.0	11.7	8.9	8.9
TX1	50	3.8	3.5	3.5	3.5	3.5	3.4
	56	13.4	10.1	11.4	12.4	11.3	10.7
	62	19.7	16.1	18.8	19.1	18.3	17.0
TY5	50	3.3	2.2	2.0	2.5	2.2	2.2
	56	3.9	2.8	3.0	3.4	3.1	3.0
	62	11.9	10.6	11.5	11.5	11.3	10.8
TZ4	50	3.2	2.3	2.3	2.9	2.3	2.4
	56	2.4	1.8	1.7	2.3	1.8	1.8
	62	3.3	2.6	2.8	3.2	2.8	2.7

The purpose of comparing various rutting calculation methodologies with ADOT's current practice was to evaluate the similarities or differences among these methods. Visual observations of the same are provided in the paragraphs above, and the statistical observations are provided in the following paragraphs. Under current ADOT practice, the acceptance criterion for rutting is 20 mm. If ADOT plans

to adopt any of the other techniques, the new method would be less conservative, and there is a chance that mixtures that previously failed to pass the 20-mm criterion would now pass under the new methodology. This is, however, based on the assumption that the acceptance criterion will remain set at 20 mm.

A two-tail t-test at 95 percent confidence interval was used to test the similarity/dissimilarity in rutting obtained using the different analysis methods. Each analysis method was compared with one of the others, and while most of them seemed to suggest that there was no significant difference between the analysis techniques, a few rut depths at specific conditions for five mixtures suggested otherwise. These mixtures, and the conditions at which a statistical difference was observed, are tabulated in Table E-15. It can be inferred that for the mixtures at the conditions shown in Table E-15, the analysis-method pairs being compared will yield statistically different rut depths. This can be a critical issue especially when either of the analysis methods is used for the calculation of rut depths and subsequently in the decision-making process of accepting or rejecting a mixture. In such a scenario, it is possible that the rut depth based on one analysis method would result in acceptance of a mixture while the rut depth resulting from the other method would result in rejection of that mixture.

Table E-15. Asphalt Mixtures, Rutting Conditions, and Pairs of Analysis Methods for Which a Statistically Significant Difference Was Observed

Mixture	44°C	50°C	56°C	62°C
GX5	-	ADOT vs. IQR x 1.5	-	-
	-	ADOT vs. Illinois	-	-
	-	ADOT vs. Louisiana	-	-
	-	ADOT vs. Montana	-	-
	-	IQR x 1.5 vs. Illinois	-	-
	-	IQR x 1.5 vs. Louisiana	-	-
GY6	-	ADOT vs. Montana	-	-
SY1	ADOT vs. TX&OK	-	-	-
	ADOT vs. Louisiana	-	-	-
TY5	-	ADOT vs. IQR x 1.5	-	-
	-	ADOT vs. TX&OK	-	-
	-	ADOT vs. Illinois	-	-
	-	ADOT vs. Louisiana	-	-
	-	ADOT vs. Montana	-	-
TZ4	-	-	ADOT vs. IQR x 1.5	-
	-	-	IQR x 1.5 vs. Illinois	-
	-	-	Illinois vs. Montana	-

It is worth noting here that among all the conditions at which statistical significant differences were seen and presented in Table E-15, none of them were at the effective temperature that corresponds to the

given mixture. This suggests that for the Arizona mixtures tested in this study, if the HWTT is performed at the effective temperature of that corresponding mixture, the type of analysis method chosen will not have any bearing on any comparative outcomes.

AXIAL FATIGUE TEST DATA

As mentioned in Chapter 5, the axial fatigue test was performed at four strain levels for each mixture, and the data were analyzed using the viscoelastic continuum damage theory (S-VECD) formulation as explained in Appendix C. The actual number of cycles to failure and the on-specimen strain for the sample is tabulated in Table E-16. The result of the S-VECD model is the damage characteristic, or *C vs*. *S,* curve. In Chapter 5, only the fitted *C vs. S* curve was shown. In the figures below, the *C vs. S* data at all four strain levels along with the fit function are shown for each of the 12 mixtures.

Table E-16. Actual Number of Cycles to Failure and Input Machine Strain on the Sample

Mixture	Input Machine Strain	No. of Cycles to Failure (N_f)	Actual Strain @ 80th Cycle (με)	Mixture	Input Machine Strain	No. of Cycles to Failure (N_f)	Actual Strain @ 80th Cycle (με)
GX4	250 με	122151	218	SX3	300 με	285605	224
	300 με	67931	229		500 με	57165	412
	350 με	16307	259		600 με	19730	429
	400 με	34823	314		650 με	11710	552
GX5	300 με	127534	236	SY1	200 με	203622	165
	400 με	36115	252		300 με	57002	202
	450 με	13506	323		400 με	33733	241
	480 με	7702	282		450 με	3234	400
GY3	200 με	490553	127	SZ1	250 με	83005	191
	250 με	48516	196		300 με	35569	204
	300 με	13706	223		400 με	16355	256
	350 με	8899	248		430 με	3697	371
GY4	250 με	131361	163	TX1	200 με	535573	112
	275 με	47531	151		300 με	122474	184
	300 με	16700	206		350 με	45029	220
	325 με	2698	287		400 με	8502	259
GY6	300 με	142351	238	TY5	250 με	57878	256
	350 με	37103	241		300 με	57355	243
	400 με	15909	343		350 με	18811	319
	450 με	10307	400		400 με	9534	364
GZ2	250 με	20516	164	TZ4	250 με	76507	179
	300 με	43319	192		300 με	42919	215
	350 με	16298	230		400 με	19927	272
	400 με	4898	302		450 με	3713	321

Table E-17. Regression Coefficients C_1 and C_2 for *C vs. S* Relationship

Mixture	Coefficients	
	C_1	C_2
GX4	0.0065	0.4051
GX5	0.0007	0.5456
GY3	0.0008	0.5789
GY4	0.0002	0.6465
GY6	0.0031	0.4510
GZ2	0.0007	0.5749
SX3	0.0145	0.3403
SY1	0.0017	0.5101
SZ1	0.0033	0.4443
TX1	0.0001	0.6806
TY5	0.0058	0.4104
TZ4	0.0004	0.5991

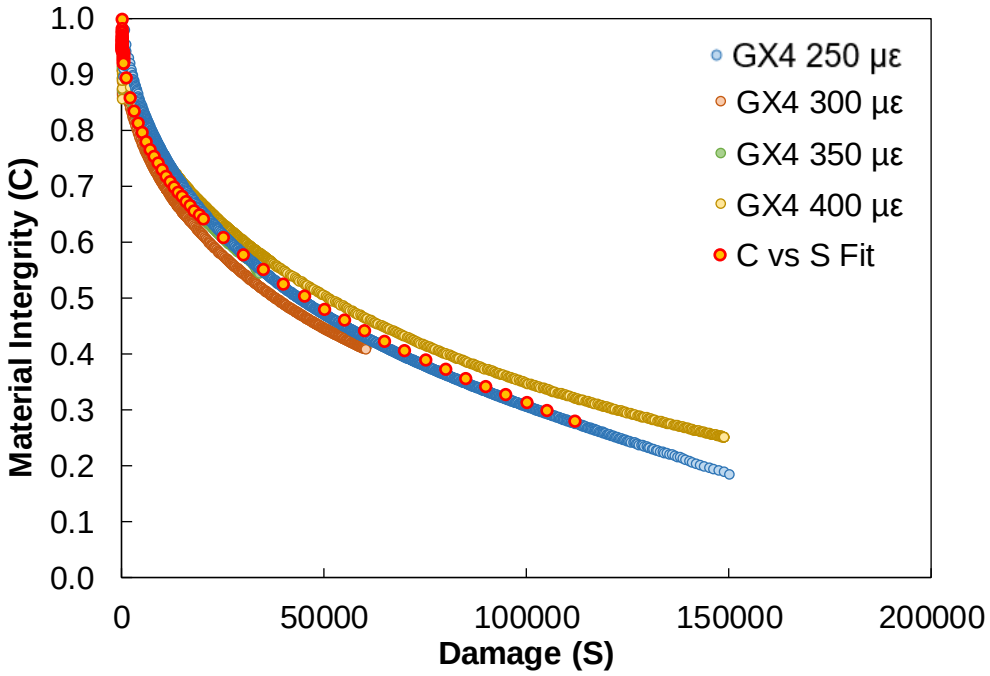

Figure E-17. *C vs. S* Curve for GX4 with Data at All Strain Levels

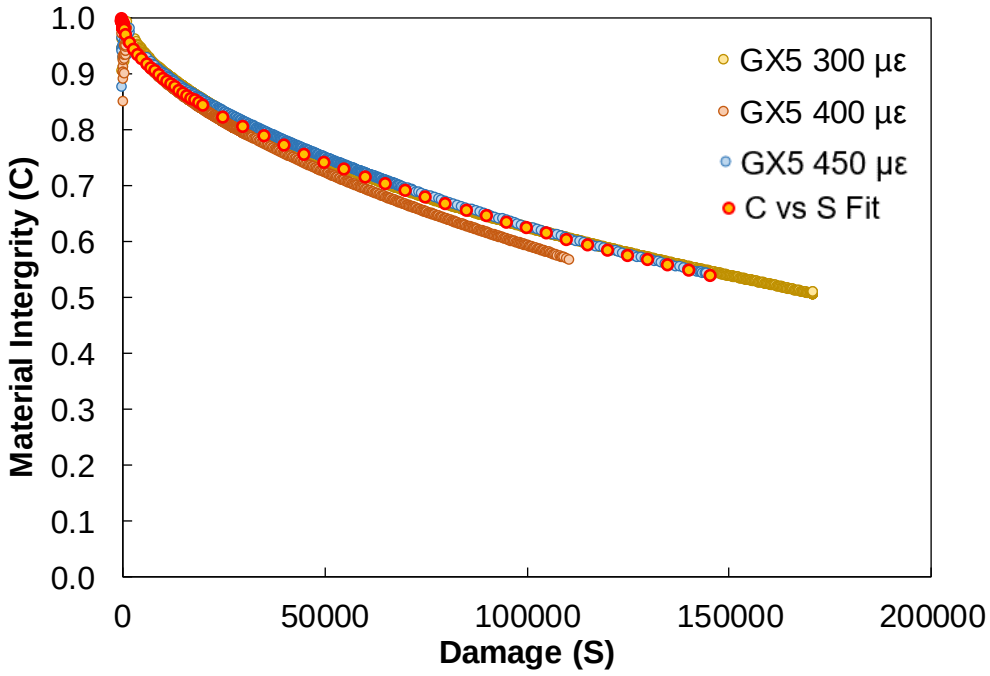

Figure E-18. *C vs. S* Curve for GX5 with Data at All Strain Levels

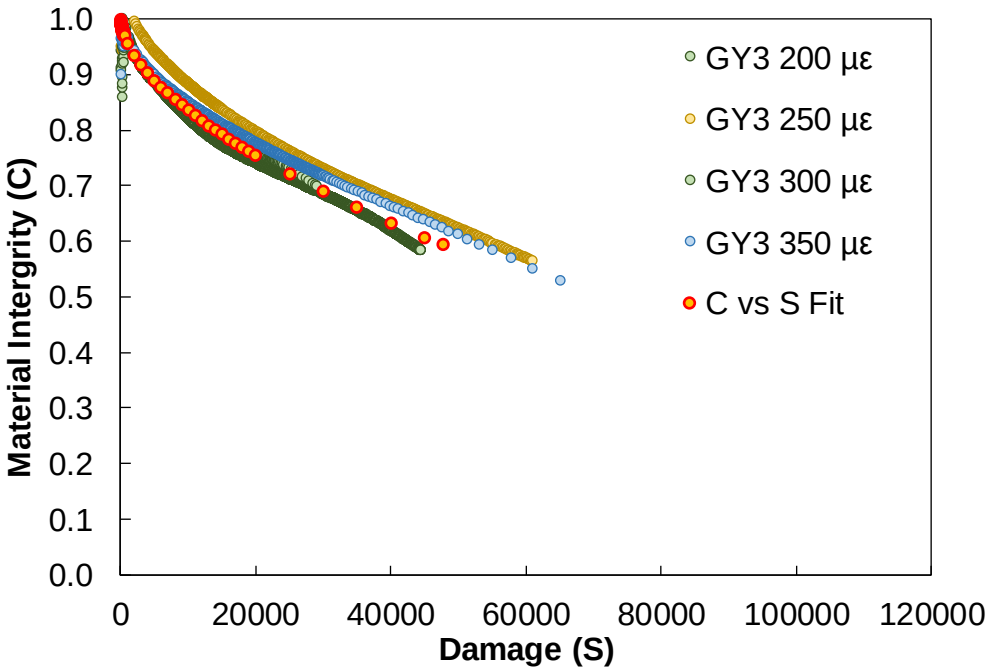

Figure E-19. *C vs. S* Curve for GY3 with Data at All Strain Levels

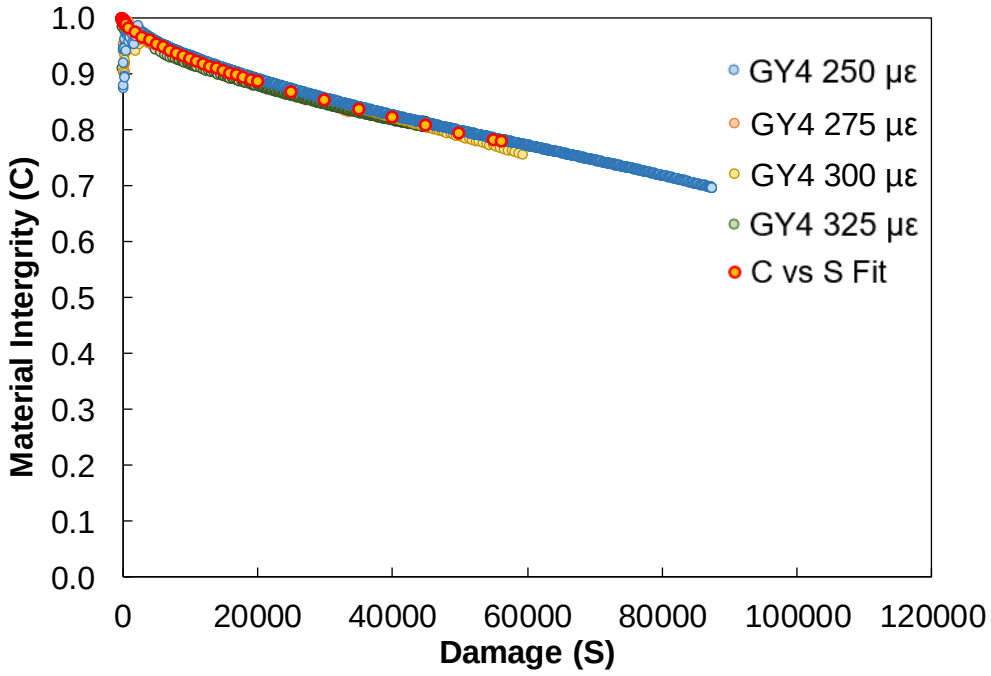

Figure E-20. *C vs. S* Curve for GY4 with Data at All Strain Levels

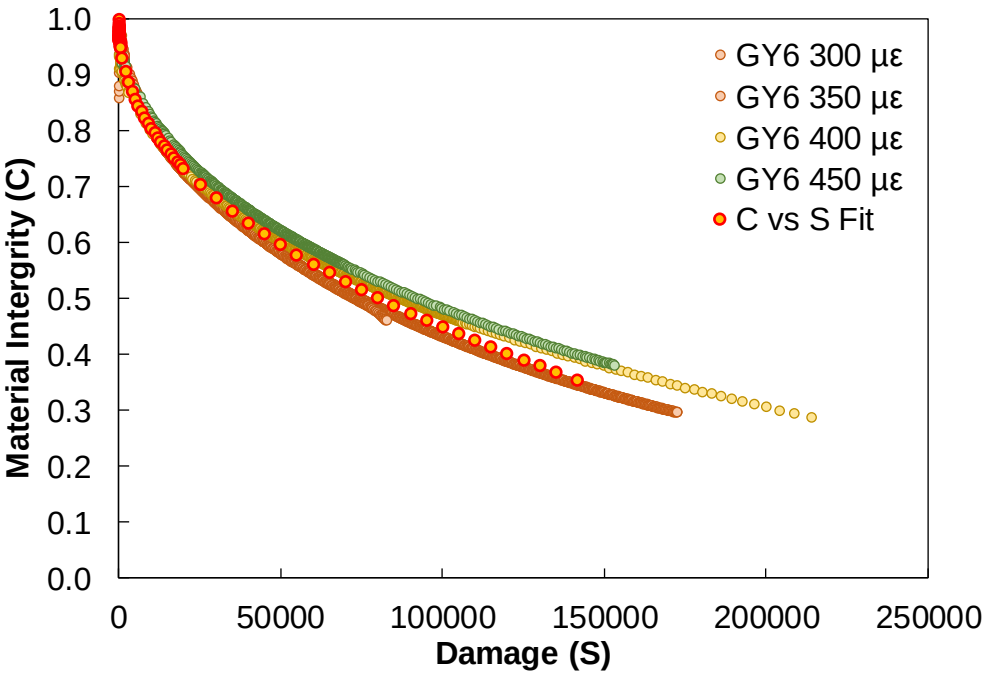

Figure E-21. *C vs. S* Curve for GY6 with Data at All Strain Levels

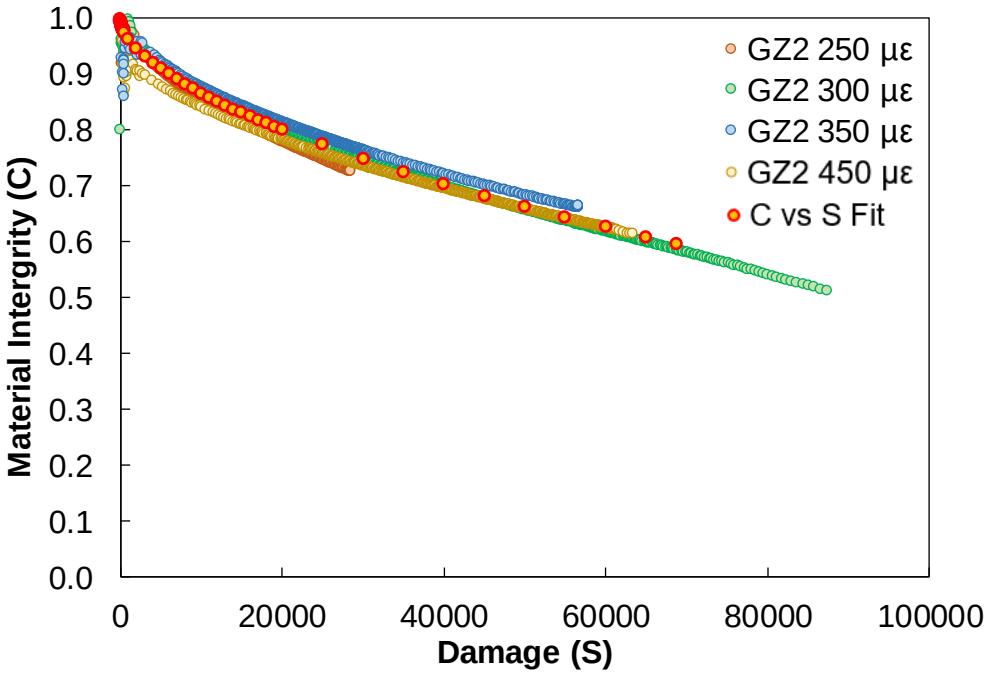

Figure E-22. *C vs. S* Curve for GZ2 with Data at All Strain Levels

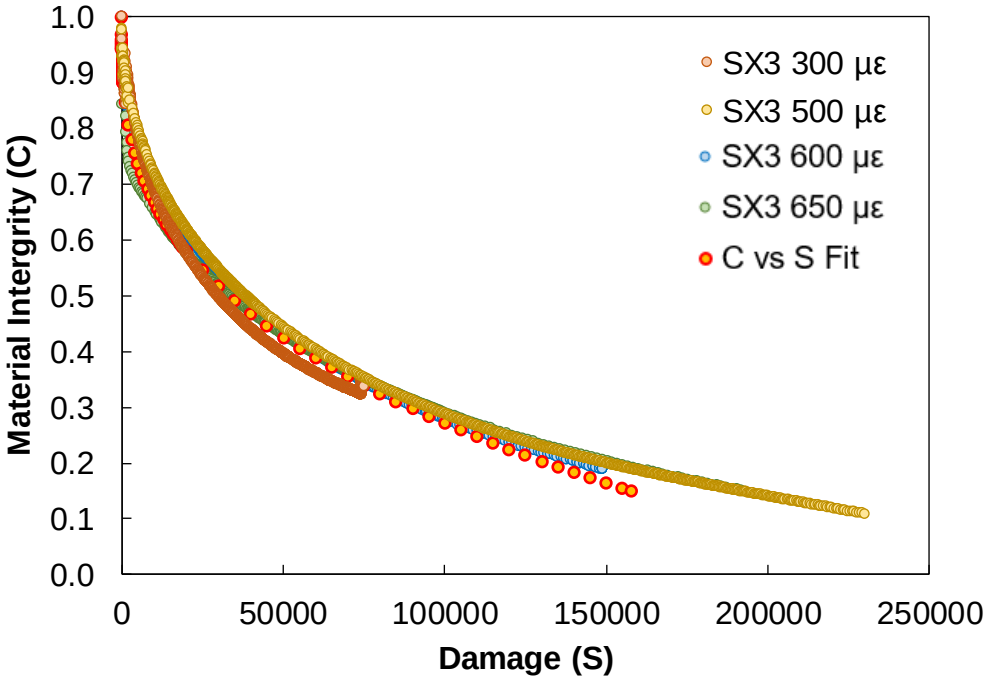

Figure E-23. *C vs. S* Curve for SX3 with Data at All Strain Levels

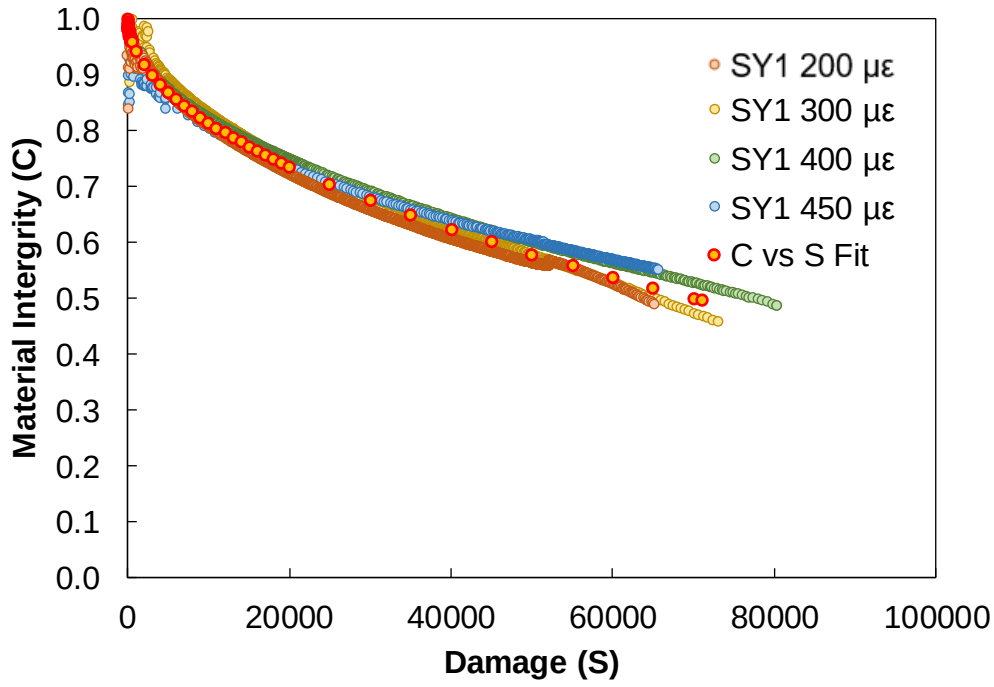

Figure E-24. *C vs. S* Curve for SY1 with Data at All Strain Levels

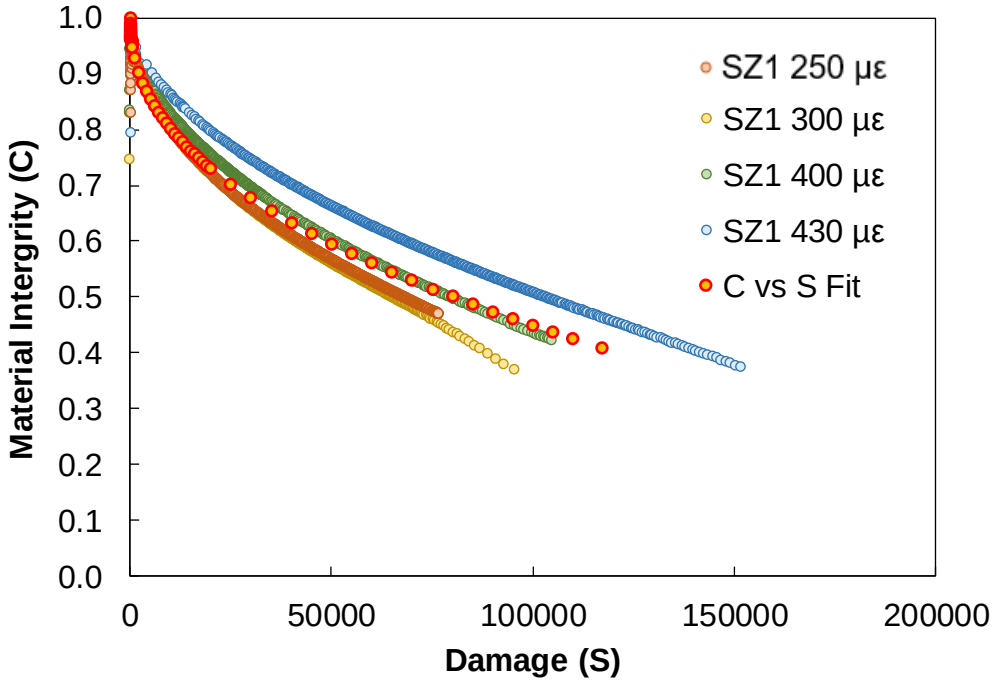

Figure E-25. *C vs. S* Curve for SZ1 with Data at All Strain Levels

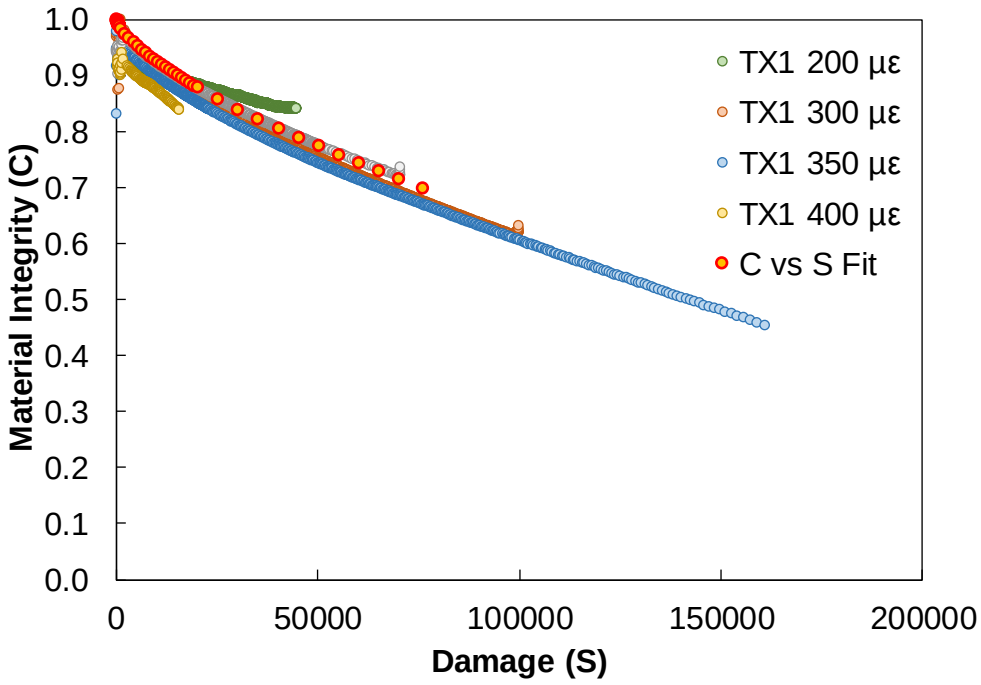

Figure E-26. *C vs. S* Curve for TX1 with Data at All Strain Levels

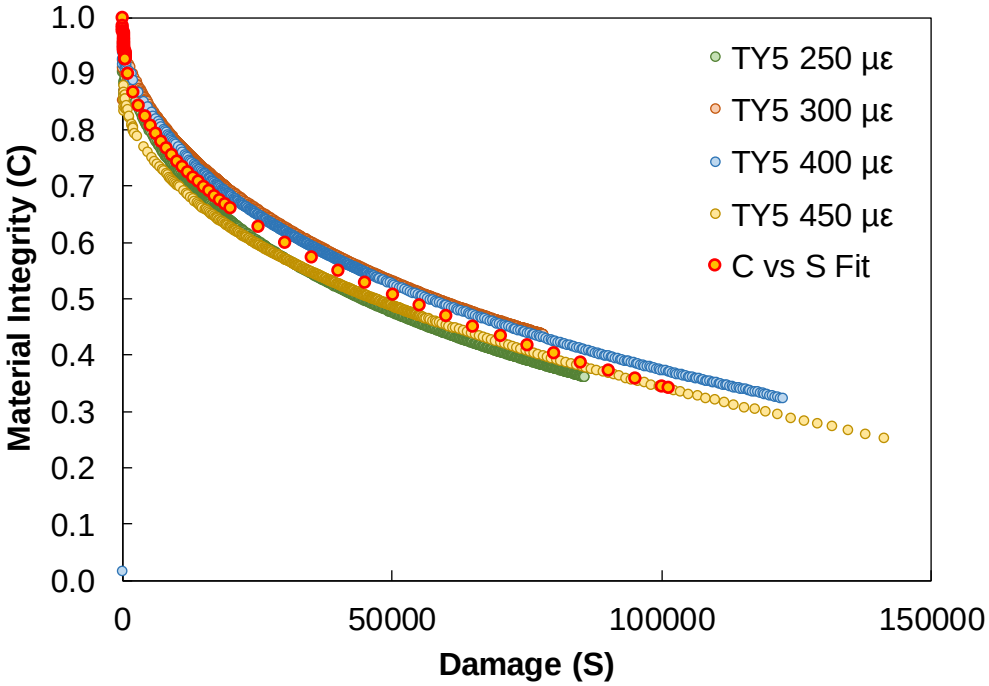

Figure E-27. *C vs. S* Curve for TY5 with Data at All Strain Levels

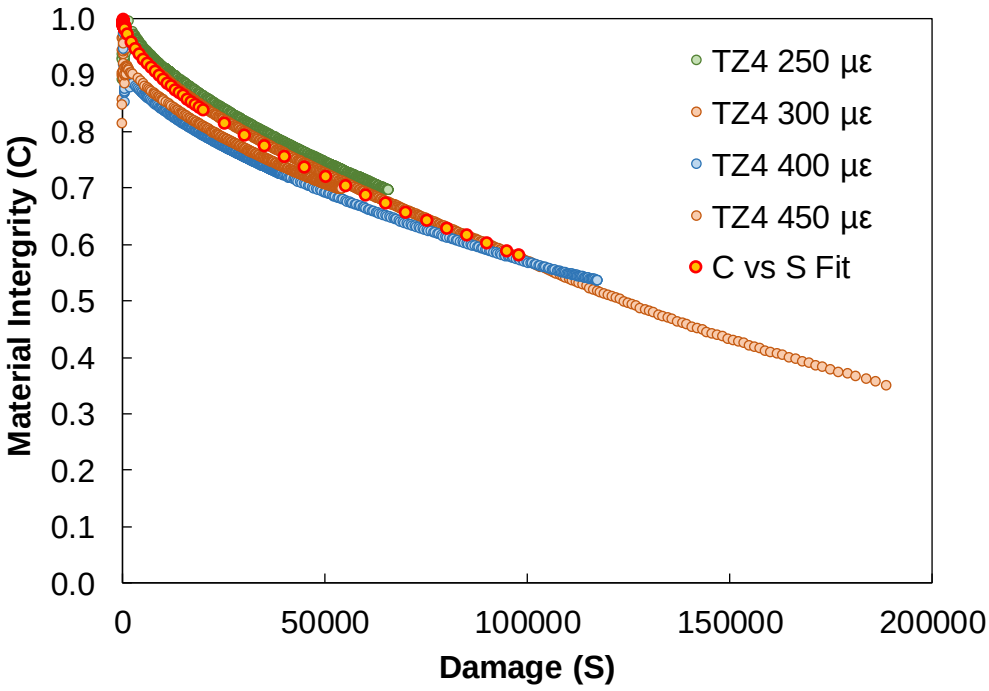

Figure E-28. *C vs. S* Curve for TZ4 with Data at All Strain Levels

APPENDIX F: EVALUATION OF EFFECT OF MSCR RECOVERY

TEST MEMORANDA

Table F-1. Asphalt Binder Test Memorandum for Binder Y5

ASU Advanced Pavement Laboratory

Project Name : ADOT SPR - 742
Operator: Akshay Gundla
Binder: Y5 - PG 70H-16

Date	AASHTO Test Method	Aging Level	Parameter	Temperature (°C)		Result	
9/27/2016	T 315 – 25 mm	Original	|G*|/sin δ	64		2.59	kPa
				70		1.62	kPa
				76		1.02	kPa
10/21/2016	T 315 – 8 mm		|G*|sin δ	28		242.53	kPa
				31		153.54	kPa
				34		97.97	kPa
9/25/2016	T 315 – 25 mm	RTFO	|G*|/sin δ	64		5.02	kPa
				70		3.13	kPa
				76		1.97	kPa
	T 315 – 8 mm		|G*|sin δ	28		451.25	kPa
				31		286.53	kPa
				34		181.50	kPa
9/23/2016	T 315 – 8 mm	PAV at 110°C	|G*|sin δ	28		1694.80	kPa
				31		1210.50	kPa
				34		847.87	kPa
9/19/2016	T 315 – 25 mm	PAV at 110°C	|G*|/sin δ	70		20.18	kPa
10/17/2016	T 350	Original		**64**	**70**	**76**	
			$R_{0.1}$	94.16	92.29	89.65	%
			$R_{3.2}$	87.67	71.55	35.21	%
			R_{Diff}	6.90	22.47	60.73	%
			$Jnr_{0.1}$	0.116	0.249	0.521	kPa^{-1}
			$Jnr_{3.2}$	0.186	0.753	3.639	kPa^{-1}
			Jnr_{Diff}	60.83	202.48	598.44	%
9/19/2016	T 350	RTFO		**64**	**70**	**76**	
			$R_{0.1}$	96.11	95.07	93.40	%
			$R_{3.2}$	92.46	90.10	80.22	%
			R_{Diff}	3.80	5.22	14.12	%
			$Jnr_{0.1}$	0.039	0.082	0.174	kPa^{-1}
			$Jnr_{3.2}$	0.061	0.119	0.386	kPa^{-1}
			Jnr_{Diff}	54.01	45.19	122.38	%
9/14/2016	T 313	PAV at 110°C	*m*-Value	0		Material too soft	
			S				
9/21/2016			*m*-Value	–6		0.36	
			S			54	MPa
9/21/2016			*m*-Value	–12		0.3065	
			S			115	MPa

Table F-2. Asphalt Binder Test Memorandum for Binder B5

ASU Advanced Pavement Laboratory

Project Name : ADOT SPR - 742
Operator: Akshay Gundla
Binder: B5

Date	AASHTO Test Method	Aging Level	Parameter	Temperature (°C)		Result	
6/20/2017	T 315 – 25mm	Original	|G*|/sin δ	64		8.26	kPa
				70		4.73	kPa
				76		2.78	kPa
				82		1.70	kPa
6/18/2017	T 315 – 25mm	RTFO	|G*|/sin δ	64		18.11	kPa
				70		10.71	kPa
				76		6.33	kPa
				82		3.779	kPa
6/30/2017	T 315 – 8mm	PAV at 110°C	|G*|sin δ	28		977.45	kPa
				31		721.32	kPa
				34		533.46	kPa
6/20/2017	T 350	RTFO		**64**	**70**	**76**	
			$R_{0.1}$	82.21	-	67.47	%
			$R_{3.2}$	73.83	-	40.91	%
			R_{Diff}	10.20	-	39.40	%
			$Jnr_{0.1}$	0.053	-	0.304	kPa^{-1}
			$Jnr_{3.2}$	0.080	-	0.665	kPa^{-1}
			Jnr_{Diff}	51.10	-	120.23	%
6/27/2017	T 313	PAV at 110°C	*m*-Value	–18		0.324	
			S			156.5	MPa

Table F-3. Asphalt Binder Test Memorandum for Binder B2

ASU Advanced Pavement Laboratory

Project Name : ADOT SPR - 742
Operator: Akshay Gundla
Binder: B2

Date	AASHTO Test Method	Aging Level	Parameter	Temperature (°C)		Result	
9/1/2017	T 315 – 25 mm	Original	|G*|/sin δ	64		2.76	kPa
				70		1.47	kPa
				76		0.79	kPa
9/5/2017	T 315 – 25 mm	RTFO	|G*|/sin δ	64		6.93	kPa
				70		3.75	kPa
				76		2.03	kPa
9/7/2017	T 315 – 8 mm	PAV at 110° C	|G*|sin δ	22		3539.72	kPa
				19		4972.26	kPa
				16		6926.60	kPa
9/6/2017	T 350	RTFO		**64**	**70**	**76**	
			$R_{0.1}$	64.78	51.54	-	%
			$R_{3.2}$	50.50	28.19	-	%
			R_{Diff}	22.04	45.31	-	%
			$Jnr_{0.1}$	0.316	0.856	-	kPa^{-1}
			$Jnr_{3.2}$	0.479	1.486	-	kPa^{-1}
			Jnr_{Diff}	51.37	73.68	-	%
9/7/2017	T 313	PAV at 110° C	*m*-Value	–18		0.303	
			S			209	MPa

Table F-4. Asphalt Binder Test Memorandum for Binder D0.5

ASU Advanced Pavement Laboratory

Project Name : ADOT SPR - 742
Operator: Akshay Gundla
Binder: D0.5

Date	AASHTO Test Method	Aging Level	Parameter	Temperature (°C)		Result	
9/13/2017	T 315 – 25mm	Original	|G*|/sin δ	64		3.52	kPa
				70		1.78	kPa
				76		0.92	kPa
9/13/2017	T 315 – 25mm	RTFO	|G*|/sin δ	64		9.39	kPa
				70		5.06	kPa
				76		2.74	kPa
9/14/2017	T 315 – 8 mm	PAV at 110°C	|G*|sin δ	22		3606.58	kPa
				19		4925.95	kPa
				16		6712.60	kPa
9/14/2017	T 350	RTFO		**64**	**70**	**76**	
			$R_{0.1}$	63.03	51.55	-	%
			$R_{3.2}$	41.14	19.54	-	%
			R_{Diff}	34.74	62.10	-	%
			$Jnr_{0.1}$	0.243	0.627	-	kPa^{-1}
			$Jnr_{3.2}$	0.410	1.256	-	kPa^{-1}
			Jnr_{Diff}	68.67	100.27	-	%
9/14/2017	T 313	PAV at 110°C	*m*-Value	–18		0.3025	
			S			202.5	MPa

Table F-5. Asphalt Binder Test Memorandum for Binder X3

ASU Advanced Pavement Laboratory

Project Name : ADOT SPR - 742
Operator: Akshay Gundla
Binder: X3 - PG 64H-22

Date	AASHTO Test Method	Aging Level	Parameter	Temperature (°C)		Result	
10/11/2016	T 315 – 25mm	Original	|G*|/sin δ	58		3.32	kPa
				64		1.86	kPa
				70		1.08	kPa
10/13/2016	T 315 – 8mm		|G*|sin δ	22		300.62	kPa
				25		191.89	kPa
				28		122.08	kPa
10/6/2016	T 315 – 25mm	RTFO	|G*|/sin δ	58		6.37	kPa
				64		3.61	kPa
				70		2.09	kPa
10/3/2016	T 315 – 8mm		|G*|sin δ	22		586.19	kPa
				25		377.78	kPa
				28		245.24	kPa
10/6/2016	T 315 – 8mm	PAV at 100°C	|G*|sin δ	22		1582.53	kPa
				25		1107.53	kPa
				28		748.55	kPa
10/4/2016	T 315 – 25mm	PAV at 100°C	|G*|/sin δ	64		9.94	kPa
10/12/2016	T 350	Original		**58**	**64**	**70**	
			$R_{0.1}$	76.07	76.36	74.16	%
			$R_{3.2}$	29.69	19.07	9.83	%
			R_{Diff}	60.98	75.02	86.74	%
			$Jnr_{0.1}$	0.468	0.866	1.620	kPa^{-1}
			$Jnr_{3.2}$	1.569	3.587	7.621	kPa^{-1}
			Jnr_{Diff}	235.31	314.43	371.42	%
10/3/2016	T 350	RTFO		**58**	**64**	**70**	
			$R_{0.1}$	83.59	88.27	84.56	%
			$R_{3.2}$	55.01	47.25	22.87	%
			R_{Diff}	34.19	46.49	72.93	%
			$Jnr_{0.1}$	0.157	0.200	0.420	kPa^{-1}
			$Jnr_{3.2}$	0.468	1.020	2.838	kPa^{-1}
			Jnr_{Diff}	198.16	408.81	690.13	%
10/4/2016	T 313	PAV at 100° C	*m*-Value	–6		Material too soft	
			S				
10/3/2016			*m*-Value	–12		0.399	
			S			68.1	MPa
10/3/2016			*m*-Value	–18		0.337	
			S			152.5	MPa

Table F-6. Asphalt Binder Test Memorandum for Binder A3-B

ASU Advanced Pavement Laboratory

Project Name : ADOT SPR - 742
Operator: Akshay Gundla
Binder: A3-B

Date	AASHTO Test Method	Aging Level	Parameter	Temperature (°C)		Result	
8/18/2017	T 315 – 25mm	Original	|G*|/sin δ	64		2.35	kPa
				70		1.30	kPa
				76		0.76	kPa
8/25/2017	T 315 – 25mm	RTFO	|G*|/sin δ	64		5.50	kPa
				70		2.93	kPa
				76		1.59	kPa
8/30/2017	T 315 – 8mm	PAV at 110°C	|G*|sin δ	25		2445.08	kPa
				22		3523.08	kPa
				19		5003.13	kPa
8/28/2017 and 11/29/17	T 350	RTFO		**58**	**64**	**70**	
			$R_{0.1}$	61.39	54.10	47.76	%
			$R_{3.2}$	52.80	34.88	15.61	%
			R_{Diff}	13.99	35.54	67.32	%
			$Jnr_{0.1}$	0.235	0.564	1.266	kPa^{-1}
			$Jnr_{3.2}$	0.299	0.882	2.511	kPa^{-1}
			Jnr_{Diff}	27.47	56.47	98.32	%
9/23/2017	T 313	PAV at 110°C	*m*-Value	–18		0.305	
			S			209	MPa

Table F-7. Asphalt Binder Test Memorandum for Binder A4

ASU Advanced Pavement Laboratory

Project Name : ADOT SPR - 742
Operator: Akshay Gundla
Binder: A4

Date	AASHTO Test Method	Aging Level	Parameter	Temperature (°C)		Result	
6/28/2017	T 315 – 25mm	Original	|G*|/sin δ	64		2.72	kPa
				70		1.45	kPa
				76		0.82	kPa
6/28/2017	T 315 – 25mm	RTFO	|G*|/sin δ	64		7.07	kPa
				70		3.57	kPa
				76		1.84	kPa
8/2/2017	T 315 – 8mm	PAV at 110°C	|G*|sin δ	25		3224.58	kPa
				22		4460.56	kPa
				19		6118.06	kPa
6/28/17 and 11/29/17	T 350	RTFO		**64**	**70**	**76**	
			$R_{0.1}$	37.02	33.32	-	%
			$R_{3.2}$	19.84	10.47	-	%
			R_{Diff}	46.42	68.72	-	%
			$Jnr_{0.1}$	0.677	1.442	-	kPa^{-1}
			$Jnr_{3.2}$	0.946	2.294	-	kPa^{-1}
			Jnr_{Diff}	39.72	59.10	-	%
7/24/2017	T 313	PAV at 110°C	*m*-Value	–12		0.3075	
			S			129.5	MPa

Table F-8. Asphalt Binder Test Memorandum for Binder A2-B

ASU Advanced Pavement Laboratory

Project Name : ADOT SPR - 742
Operator: Akshay Gundla
Binder: A2-B

Date	AASHTO Test Method	Aging Level	Parameter	Temperature (°C)		Result	
8/2/2017	T 315 – 25mm	Original	|G*|/sin δ	58		3.28	kPa
				64		1.66	kPa
				70		0.88	kPa
8/4/2017	T 315 – 25mm	RTFO	|G*|/sin δ	58		7.42	kPa
				64		3.69	kPa
				70		1.88	kPa
8/9/2017	T 315 – 8mm	PAV at 100° C	|G*|sin δ	22		2731.05	kPa
				19		4067.63	kPa
				16		5946.00	kPa
8/4/2017 and 11/29/17	T 350	RTFO		**58**	**64**	**70**	
			$R_{0.1}$	49.03	42.98	-	%
			$R_{3.2}$	37.98	20.90	-	%
			R_{Diff}	22.57	51.38	-	%
			$Jnr_{0.1}$	0.469	1.188	-	kPa^{-1}
			$Jnr_{3.2}$	0.604	1.866	-	kPa^{-1}
			Jnr_{Diff}	28.72	56.99	-	%
8/9/2017	T 313	PAV at 100° C	*m*-Value	–18		0.317	
			S			208	MPa

Table F-9. Asphalt Binder Test Memorandum for Binder A3

ASU Advanced Pavement Laboratory

Project Name : ADOT SPR - 742
Operator: Akshay Gundla
Binder: A3

Date	AASHTO Test Method	Aging Level	Parameter	Temperature (°C)		Result	
7/26/2017	T 315 – 25mm	Original	|G*|/sin δ	64		1.84	kPa
				70		0.94	kPa
				76		0.50	kPa
7/26/2017	T 315 – 25mm	RTFO	|G*|/sin δ	64		4.55	kPa
				70		2.22	kPa
				76		1.12	kPa
8/2/2017	T 315 – 8mm	PAV at 100°C	|G*|sin δ	22		3189.12	kPa
				19		4656.75	kPa
				16		6691.20	kPa
7/26/2017	T 350	RTFO		**64**	**70**	**76**	
			$R_{0.1}$	21.63	-	-	%
			$R_{3.2}$	9.19	-	-	%
			R_{Diff}	57.81	-	-	%
			$Jnr_{0.1}$	1.416	-	-	kPa^{-1}
			$Jnr_{3.2}$	1.829	-	-	kPa^{-1}
			Jnr_{Diff}	29.30	-	-	%
8/1/2017	T 313	PAV at 100°C	*m*-Value	–12		0.354	
			S			106.5	MPa

REPLICATE DATA FOR THE TESTS CONDUCTED ON ASPHALT BINDERS

Table F-10. High-Temperature AASHTO T 315 Data for the Study Asphalt Binders at Original Condition

Binder	Replicate	58°C			64°C			70°C			76°C			82°C		
		$\|G^*\|_{orig.}$	$\delta_{orig.}$	$(G^*/\sin\delta)_{orig.}$	$\|G^*\|_{orig.}$	$\delta_{orig.}$	$(G^*/\sin\delta)_{orig.}$	$\|G^*\|_{orig.}$	$\delta_{orig.}$	$(G^*/\sin\delta)_{orig.}$	$\|G^*\|_{orig.}$	$\delta_{orig.}$	$(G^*/\sin\delta)_{orig.}$	$\|G^*\|_{orig.}$	$\delta_{orig.}$	$(G^*/\sin\delta)_{orig.}$
Y5	S-1	-	-	-	2.19	61.20	2.50	1.37	60.93	1.56	0.86	61.18	0.99	-	-	-
	S-2	-	-	-	2.35	61.03	2.69	1.47	60.75	1.68	0.92	60.97	1.06	-	-	-
B5	S-1	-	-	-	6.85	58.97	7.99	4.03	61.95	4.57	2.44	64.37	2.701	1.51	66.36	1.65
	S-2	-	-	-	7.23	58	8.53	4.28	61.22	4.88	2.57	63.9	2.86	1.59	66.07	1.74
B2	S-1	-	-	-	2.589	70.70	2.74	1.40	73.10	1.46	0.76	76.20	1.89	-	-	-
	S-2	-	-	-	2.61	70.60	2.77	1.41	72.90	1.47	0.77	76.20	1.88	-	-	-
D0.5	S-1	-	-	-	3.34	71.05	3.53	1.73	74.02	1.79	0.90	77.20	0.92	-	-	-
	S-2	-	-	-	3.32	71.10	3.50	1.70	74.10	1.77	0.89	77.30	0.91	-	-	-
X3	S-1	3.07	69.40	3.28	1.74	71.03	1.84	1.02	72.04	1.07	-	-	-	-	-	-
	S-2	3.14	69.40	3.35	1.77	71.02	1.87	1.03	72.04	1.08	-	-	-	-	-	-
A3-B	S-1	-	-	-	2.24	73.20	2.34	1.24	73.2	1.29	0.72	71.80	0.76	-	-	-
	S-2	-	-	-	2.25	73.00	2.35	1.24	72.9	1.30	0.73	71.10	0.77	-	-	-
A4	S-1	-	-	-	2.52	75.16	2.61	1.36	76.10	1.40	0.77	75.30	0.80	-	-	-
	S-2	-	-	-	2.73	73.83	2.84	1.46	75.60	1.51	0.82	75.85	0.84	-	-	-
A2-B	S-1	3.16	75.50	3.26	1.61	76.70	1.66	0.85	77.30	0.87	-	-	-	-	-	-
	S-2	3.19	75.29	3.30	1.62	76.70	1.67	0.86	77.30	0.88	-	-	-	-	-	-
A3	S-1	-	-	-	1.78	81.06	1.78	0.91	82.91	0.92	0.49	84.10	0.49	-	-	-
	S-2	-	-	-	1.85	80.90	1.87	0.95	82.85	0.95	0.50	84.18	0.50	-	-	-

Table F-11. High-Temperature AASHTO T 315 Data for the Study Asphalt Binders at RTFO Condition

Binder	Replicate	58°C			64°C			70°C			76°C			82°C		
		$\|G^*\|_{RTFO}$	δ_{RTFO}	$(G^*/\sin\delta)_{RTFO}$	$\|G^*\|_{RTFO}$	δ_{RTFO}	$(G^*/\sin\delta)_{RTFO}$	$\|G^*\|_{RTFO}$	δ_{RTFO}	$(G^*/\sin\delta)_{RTFO}$	$\|G^*\|_{RTFO}$	δ_{RTFO}	$(G^*/\sin\delta)_{RTFO}$	$\|G^*\|_{RTFO}$	δ_{RTFO}	$(G^*/\sin\delta)_{RTFO}$
Y5	S-1	-	-	-	4.23	56.85	5.06	2.62	56.15	3.15	1.64	55.91	1.99	-	-	-
	S-2	-	-	-	4.19	57.05	4.99	2.58	56.36	3.10	1.62	56.14	1.95	-	-	-
B5	S-1				13.79	50.49	17.88	8.51	53.55	10.58	5.22	56.8	6.25	3.227	59.92	3.73
	S-2				14.10	50.26	18.33	8.69	53.24	10.84	5.34	56.4	6.41	3.301	59.52	3.83
B2	S-1				6.21	63.16	6.96	3.42	65.10	3.77	1.89	68.04	2.04	-	-	-
	S-2				6.15	63.20	6.89	3.39	65.10	3.73	1.88	68.10	2.02	-	-	-
D0.5	S-1				8.24	61.10	9.41	4.55	63.10	5.10	2.52	65.90	2.76	-	-	-
	S-2				8.19	61.10	9.36	4.49	63.20	5.03	2.49	66.00	2.72	-	-	-
X3	S-1	5.71	64.55	6.30	3.26	65.38	3.58	1.90	66.61	2.07	-	-	-	-	-	-
	S-2	5.81	64.55	6.44	3.32	65.41	3.65	1.94	66.66	2.12	-	-	-	-	-	-
A3-B	S-1	-	-	-	5.04	66.3	5.50	2.72	68.50	2.93	1.50	70.80	1.59	-	-	-
	S-2	-	-	-	5.05	66.4	5.51	2.73	68.60	2.93	1.50	71.00	1.59	-	-	-
A4	S-1	-	-	-	6.55	70.30	6.95	3.38	74.25	3.51	1.77	77.20	1.82	-	-	-
	S-2	-	-	-	6.72	69.10	7.19	3.48	73.60	3.63	1.81	76.80	1.86	-	-	-
A2-B	S-1	6.97	70.41	7.40	3.51	72.30	3.68	1.81	74.60	1.88	-	-	-	-	-	-
	S-2	7.00	70.40	7.43	3.52	72.20	3.69	1.81	74.60	1.88	-	-	-	-	-	-
A3	S-1	-	-	-	4.37	75.60	4.51	2.17	79.13	2.21	1.105	81.83	1.12	-	-	-
	S-2	-	-	-	4.43	75.45	4.58	2.19	79.13	2.23	1.112	81.97	1.12	-	-	-

Table F-12. Intermediate-Temperature AASHTO T 315 Data for the Study Asphalt Binders at PAV Condition

Binder	Replicate	16°C			19°C			22°C			25°C			28°C			31°C		
		|G*|	δ	|G*|sin δ	|G*|	δ	|G*|sin δ	|G*|	δ	|G*|sin δ	|G*|	δ	|G*|sin δ	|G*|	δ	|G*|sin δ	|G*|	δ	|G*|sin δ
Y5	S-1	-	-	-	-	-	-	-	-	-	-	-	-	2547.84	42.08	1707.55	1772.59	43.56	1221.66
	S-2	-	-	-	-	-	-	-	-	-	-	-	-	2509.50	42.09	1682.05	1738.89	43.61	1199.34
B5	S-1	-	-	-	-	-	-	-	-	-	-	-	-	1489.96	41.48	986.92	1093.63	41.74	728.16
	S-2	-	-	-	-	-	-	-	-	-	-	-	-	1471.94	41.11	967.99	1080.26	41.41	714.49
B2	S-1	11157.92	39.96	6911.42	7730.79	39.96	4964.99	5324.96	41.62	3536.57	-	-	-	-	-	-	-	-	-
	S-2	11215.76	39.93	6941.79	7758.16	39.93	4979.52	5336.4	41.60	3542.87	-	-	-	-	-	-	-	-	-
D0.5	S-1	11718.57	35.34	6779.11	8403.5	36.31	4976.64	6023.03	37.26	3646.29	-	-	-	-	-	-	-	-	-
	S-2	11411.29	35.62	6646.08	8171.3	36.63	4875.25	5843.72	37.62	3566.87	-	-	-	-	-	-	-	-	-
X3	S-1	-	-	-	-	-	-	1961.17	51.69	1538.95	1352.28	53.40	1085.58	903.81	55.07	741.01	-	-	-
	S-2	-	-	-	-	-	-	2073.00	51.66	1626.10	1377.98	53.48	1107.53	921.89	55.09	756.08	-	-	-
A3-B	S-1	-	-	-	7598.57	41.43	5027.96	5161.70	43.42	3547.60	3470.91	45.41	2471.80	-	-	-	-	-	-
	S-2	-	-	-	7524.28	41.42	4978.3	5088.94	43.43	3498.57	3392.01	45.48	2418.36	-	-	-	-	-	-
A4	S-1	-	-	-	9913.01	37.72	6065.22	6934.02	39.63	4422.74	4840.52	41.49	3207.14	-	-	-	-	-	-
	S-2	-	-	-	10135.95	37.50	6170.90	7077.94	39.46	4498.37	4899.31	41.43	3243.02	-	-	-	-	-	-
A2-B	S-1	8728.39	43.54	6012.74	5722.94	45.98	4115.24	3707.22	48.39	2771.72	-	-	-	-	-	-	-	-	-
	S-2	8539.56	43.51	5879.26	5589.45	45.99	4020.03	3582.18	48.50	2690.38	-	-	-	-	-	-	-	-	-
A3	S-1	10004.72	41.77	6664.90	6638.82	44.25	4632.87	4351.98	46.70	3167.37	-	-	-	-	-	-	-	-	-
	S-2	10103.01	41.68	6717.49	6721.97	44.13	4680.62	4422.15	46.56	3210.88	-	-	-	-	-	-	-	-	-

Table F-13. AASHTO T 350 (MSCR) Test Data for the Study Asphalt Binders at RTFO Condition

Binder	Replicate	58°C						64°C						70°C					
		$R_{0.1}$ (%)	$R_{3.2}$ (%)	R_{Diff} (%)	$Jnr_{0.1}$ (kPa^{-1})	$Jnr_{3.2}$ (kPa^{-1})	Jnr_{Diff} (%)	$R_{0.1}$ (%)	$R_{3.2}$ (%)	R_{Diff} (%)	$Jnr_{0.1}$ (kPa^{-1})	$Jnr_{3.2}$ (kPa^{-1})	Jnr_{Diff} (%)	$R_{0.1}$ (%)	$R_{3.2}$ (%)	R_{Diff} (%)	$Jnr_{0.1}$ (kPa^{-1})	$Jnr_{3.2}$ (kPa^{-1})	Jnr_{Diff} (%)
Y5	S-1	-	-	-	-	-	-	96.180	92.680	3.640	0.039	0.060	51.030	95.020	89.900	5.389	0.084	0.123	47.110
	S-2	-	-	-	-	-	-	96.036	92.230	3.960	0.039	0.062	56.980	95.110	90.300	5.056	0.081	0.115	43.260
B5	S-1	-	-	-	-	-	-	82.048	73.548	10.36	0.054	0.081	51.114	-	-	-	-	-	-
	S-2	-	-	-	-	-	-	82.376	74.104	10.042	0.052	0.079	51.083	-	-	-	-	-	-
B2	S-1	-	-	-	-	-	-	64.950	50.670	21.985	0.315	0.478	51.595	51.582	28.324	45.090	0.854	1.478	73.110
	S-2	-	-	-	-	-	-	64.614	50.339	22.092	0.317	0.479	51.140	51.494	28.051	45.525	0.857	1.494	74.250
D0.5	S-1	-	-	-	-	-	-	63.15	41.21	34.76	0.242	0.409	68.99	51.2	19.33	62.25	0.636	1.266	99.18
	S-2	-	-	-	-	-	-	62.91	41.06	34.72	0.243	0.410	68.35	51.89	19.75	61.94	0.618	1.245	101.35
X3	S-1	83.965	54.798	34.737	0.150	0.460	206.624	89.120	49.496	44.460	0.187	0.965	416.455	88.070	23.427	73.399	0.252	2.719	977.143
	S-2	83.213	55.213	33.648	0.164	0.475	189.689	87.423	44.998	48.528	0.214	1.074	401.156	81.048	22.315	72.467	0.587	2.956	403.110
A3-B	S-1	61.252	52.669	14.011	0.235	0.299	27.315	54.405	35.192	35.315	0.563	0.881	56.432	47.759	15.784	66.951	1.263	2.494	97.43
	S-2	61.527	52.927	13.977	0.234	0.298	27.632	53.800	34.558	35.767	0.564	0.883	56.503	47.756	15.429	67.69	1.269	2.528	99.202
A4	S-1	-	-	-	-	-	-	34.159	18.206	46.700	0.692	0.942	36.040	35.215	11.828	66.413	1.385	2.229	60.885
	S-2	-	-	-	-	-	-	59.890	21.480	46.140	0.662	0.949	43.390	31.421	9.107	71.017	1.499	2.358	57.307
A2-B	S-1	50.135	39.530	21.152	0.460	0.590	28.213	42.076	20.449	51.40	1.208	1.877	55.302	-	-	-	-	-	-
	S-2	47.928	36.431	23.989	0.478	0.617	29.219	43.884	21.346	51.36	1.168	1.854	58.685	-	-	-	-	-	-
A3	S-1	-	-	-	-	-	-	18.749	7.509	59.952	1.478	1.870	26.472	-	-	-	-	-	-
	S-2	-	-	-	-	-	-	24.507	10.867	55.658	1.353	1.788	32.123	-	-	-	-	-	-

Table F-13. (Continued). AASHTO T 350 (MSCR) Test Data for the Study Asphalt Binders at RTFO Condition

Binder	Replicate	76°C					
		$R_{0.1}$ (%)	$R_{3.2}$ (%)	R_{Diff} (%)	$Jnr_{0.1}$ (kPa^{-1})	$Jnr_{3.2}$ (kPa^{-1})	Jnr_{Diff} (%)
Y5	S-1	93.320	79.760	14.530	0.177	0.399	125.750
	S-2	93.480	80.680	13.700	0.170	0.372	119.010
B5	S-1	65.033	38.83	40.29	0.339	0.707	108.620
	S-2	69.902	42.99	38.5	0.268	0.622	131.846
B2	S-1	-	-	-	-	-	-
	S-2	-	-	-	-	-	-
D0.5	S-1	-	-	-	-	-	-
	S-2	-	-	-	-	-	-
X3	S-1	-	-	-	-	-	-
	S-2	-	-	-	-	-	-
A3-B	S-1	-	-	-	-	-	-
	S-2	-	-	-	-	-	-
A4	S-1	-	-	-	-	-	-
	S-2	-	-	-	-	-	-
A2-B	S-1	-	-	-	-	-	-
	S-2	-	-	-	-	-	-
A3	S-1	-	-	-	-	-	-
	S-2	-	-	-	-	-	-

Table F-14. Bending Beam Rheometer (AASHTO T 313) Data for Study Binders

Binder	Replicate	0°C		–6°C		–12°C		–18°C	
		m-Value	-*S* (MPa)	*m*-Value	*S* (MPa)	*m*-Value	*S* (MPa)	*m*-Value	-*S* (MPa)
Y5	S-1	Material too soft		0.361	55	0.308	114	-	-
	S-2			0.359	53	0.305	116	-	-
B5	S-1	-	-	-	-	-	-	0.323	156
	S-2	-	-	-	-	-	-	0.325	157
B2	S-1	-	-	-	-	-	-	0.304	207
	S-2	-	-	-	-	-	-	0.302	211
D0.5	S-1	-	-	-	-	-	-	0.302	200
	S-2	-	-	-	-	-	-	0.303	205
X3	S-1	-	-	Material too soft		0.4	68.1	0.340	150
	S-2	-	-			0.398	68.1	0.334	155
A3-B	S-1	-	-	-	-	-	-	0.303	210
	S-2	-	-	-	-	-	-	0.306	208
A4	S-1	-	-	-	-	0.306	126	-	-
	S-2	-	-	-	-	0.309	133	-	-
A2-B	S-1	-	-	-	-	-	-	0.319	213
	S-2	-	-	-	-	-	-	0.314	203
A3	S-1	-	-	-	-	-	-	0.357	106
	S-2	-	-	-	-	-	-	0.351	107

DYNAMIC MODULUS DATA

Presented below are the dynamic modulus data for all nine binders used to study the effect of recovery on the performance of asphalt concrete. Each mixture has three replicates. The figures below present the replicate data and the mastercurve, computed using the average of the three replicates.

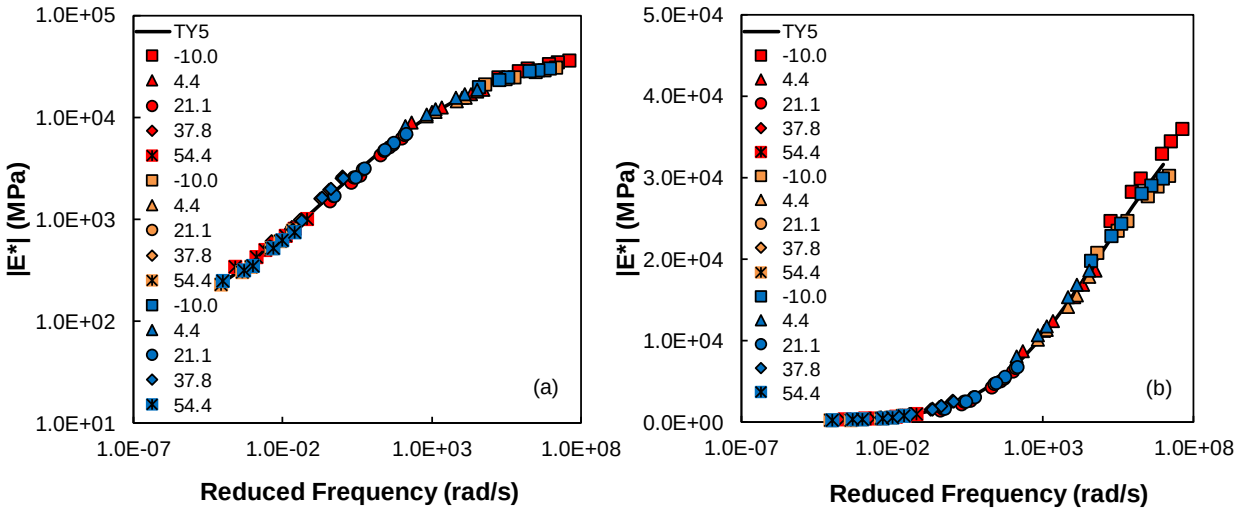

Figure F-1. Dynamic Modulus Replicate Data for Mixture TY5 in (a) Log-Log Space and (b) Semilog Space

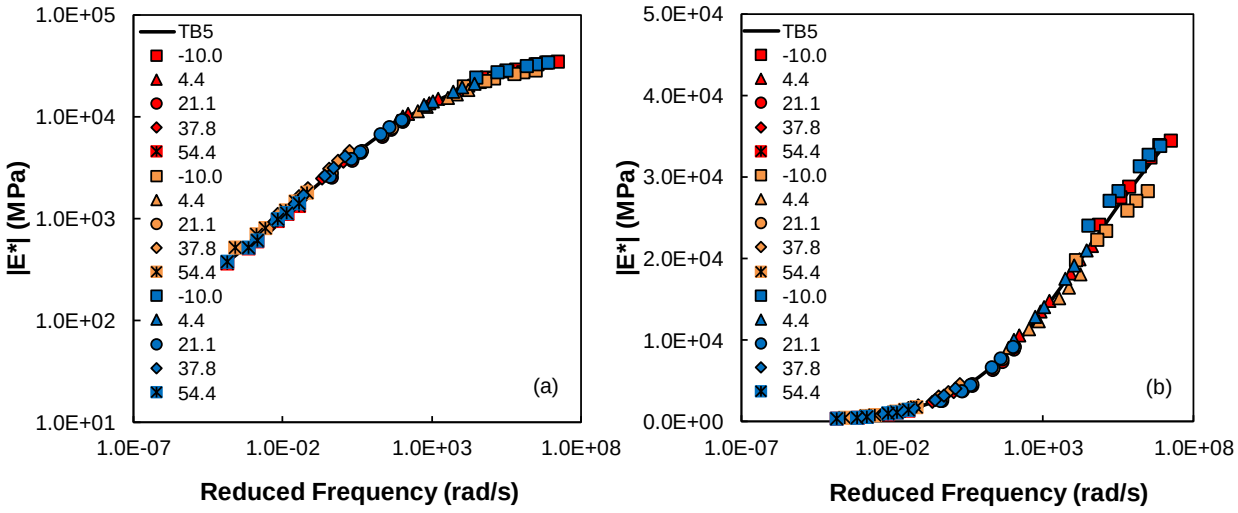

Figure F-2. Dynamic Modulus Replicate Data for Mixture TB5 in (a) Log-Log Space and (b) Semilog Space

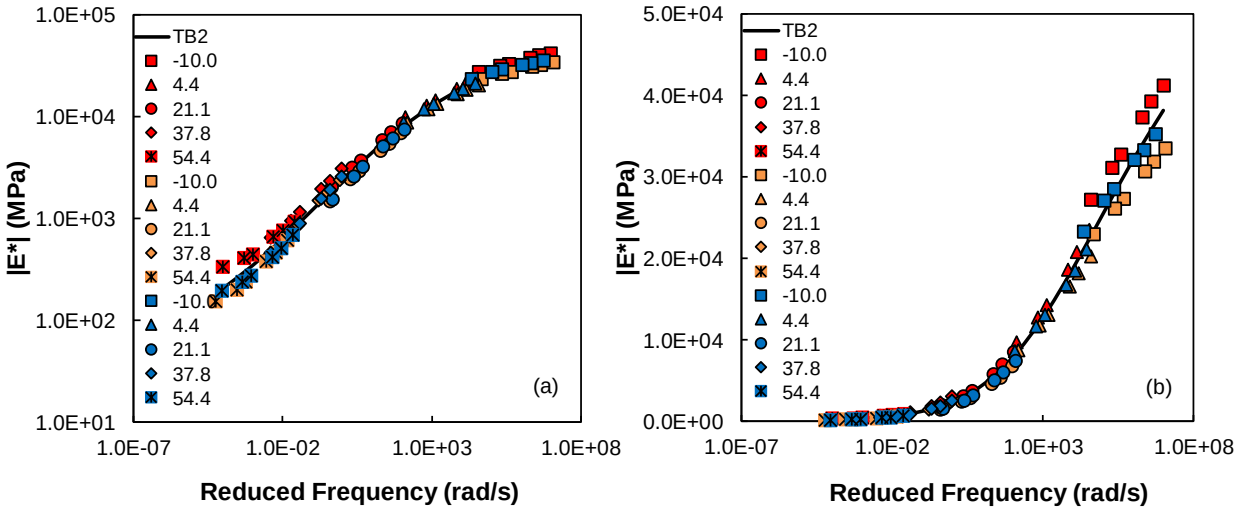

Figure F-3. Dynamic Modulus Replicate Data for Mixture TB2 in (a) Log-Log Space and (b) Semilog Space

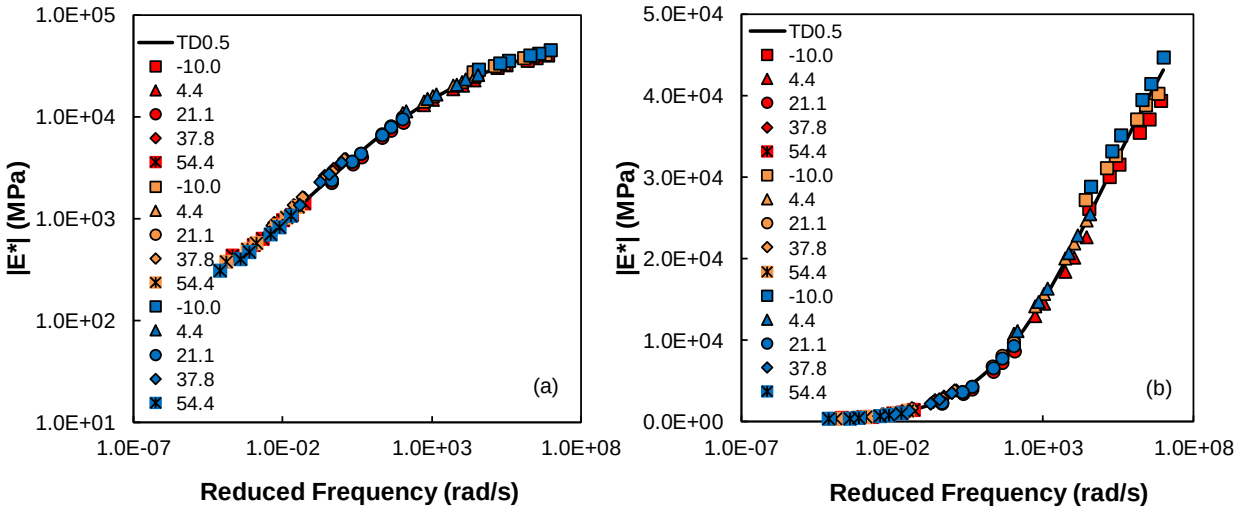

Figure F-4. Dynamic Modulus Replicate Data for Mixture TD0.5 in (a) Log-Log Space and (b) Semilog Space

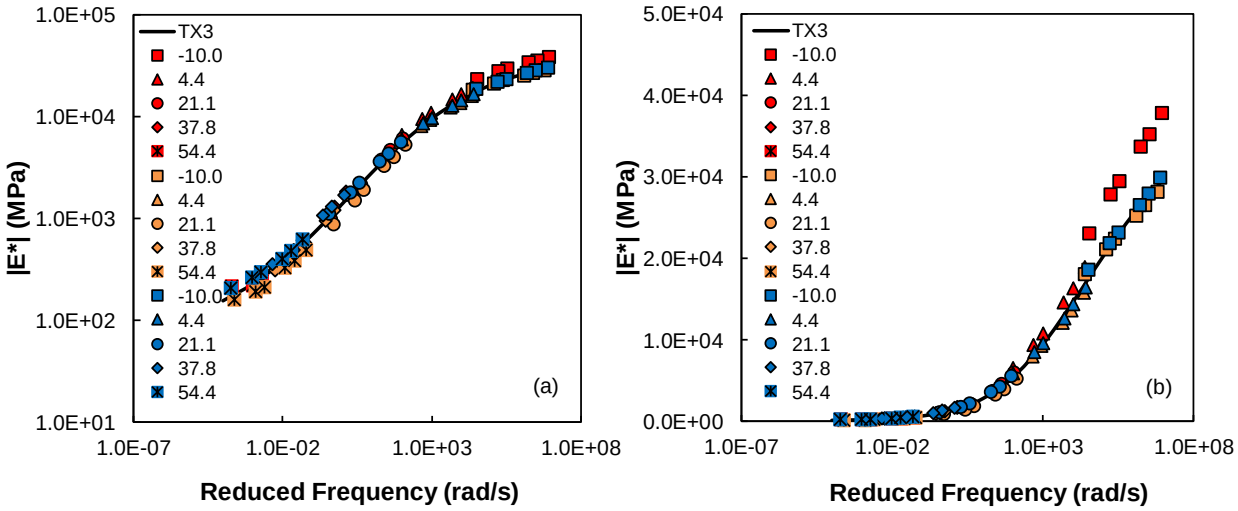

Figure F-5. Dynamic Modulus Replicate Data for Mixture TX3 in (a) Log-Log Space and (b) Semilog Space

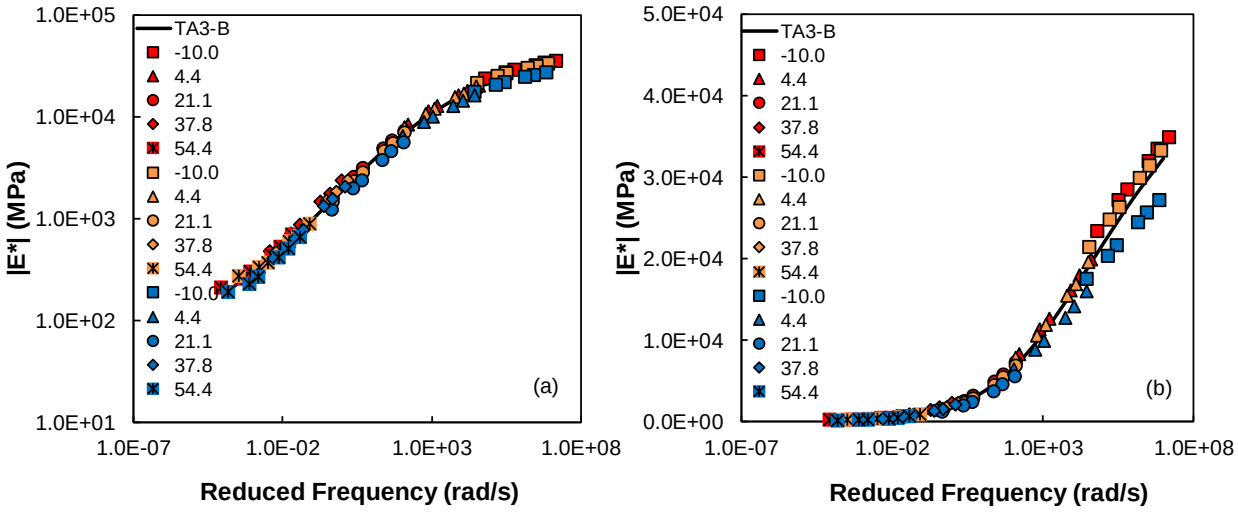

Figure F-6. Dynamic Modulus Replicate Data for Mixture TA3-B in (a) Log-Log Space and (b) Semilog Space

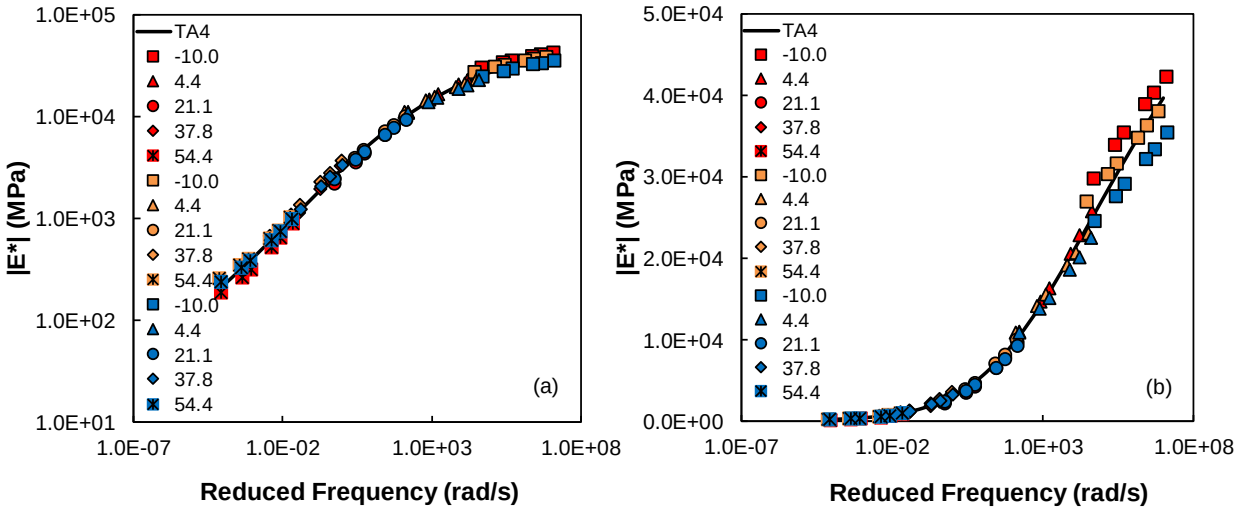

Figure F-7. Dynamic Modulus Replicate Data for Mixture TA4 in (a) Log-Log Space and (b) Semilog Space

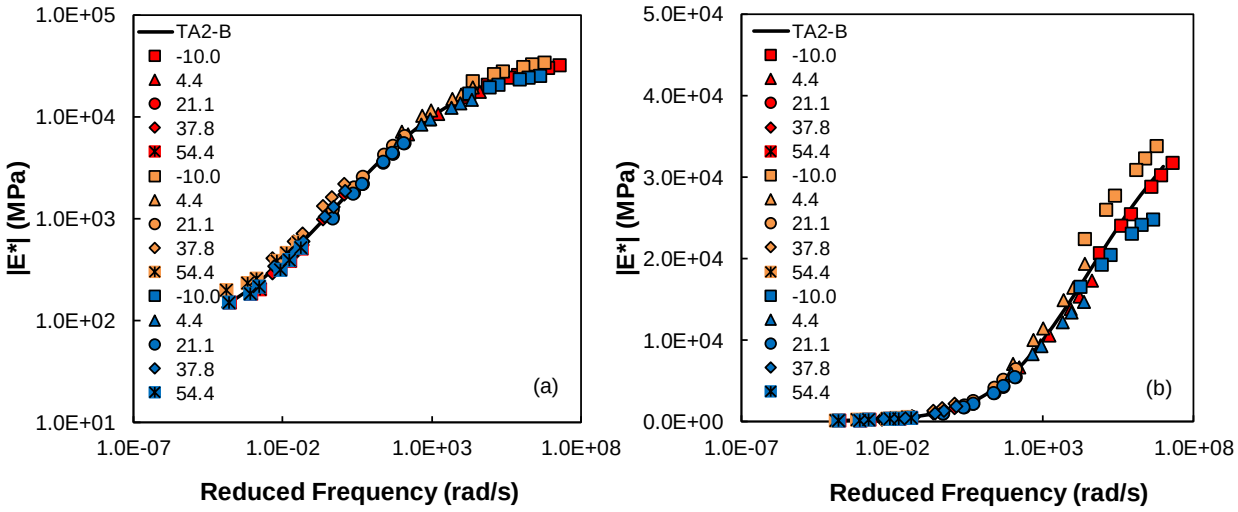

Figure F-8. Dynamic Modulus Replicate Data for Mixture TA2-B in (a) Log-Log Space and (b) Semilog Space

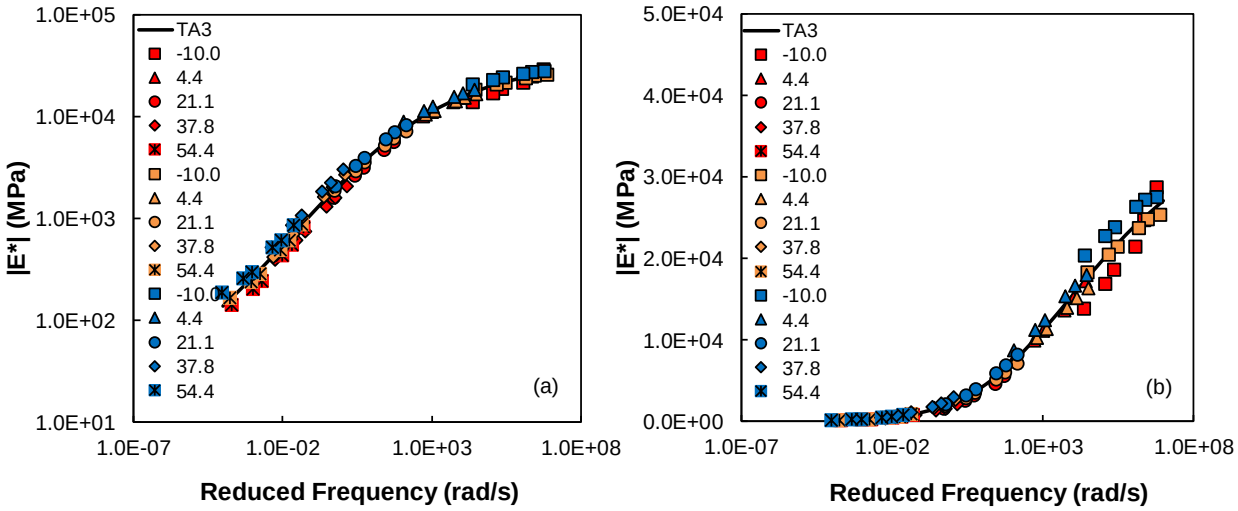

Figure F-9. Dynamic Modulus Replicate Data for Mixture TA3 in (a) Log-Log Space and (b) Semilog Space

Table F-15. Dynamic Modulus and Phase Angle Replicate Data for Mixture TY5

Temp. (°C)	Freq. (Hz)	Dynamic Modulus, |E*|			Phase Angle, δ		
		Repl. 1 (MPa)	Repl. 2 (MPa)	Repl. 3 (MPa)	Repl. 1 (Deg.)	Repl. 2 (Deg.)	Repl. 3 (Deg.)
–10.0	25	35933	30233	29948	4.3	5.8	6.0
	10	34450	28883	29004	7.1	5.6	7.2
	5	32937	27721	28010	8.0	7.6	7.9
	1	29870	24725	24335	9.4	8.0	9.9
	0.5	28282	23483	22869	9.9	8.8	11.3
	0.1	24702	20761	19757	11.6	10.0	12.8
4.4	25	18624	17826	18622	11.9	9.3	8.5
	10	16899	15563	16828	14.8	11.3	13.3
	5	15399	14167	15334	15.5	13.0	14.1
	1	12372	11293	11813	18.0	15.7	17.4
	0.5	11201	10175	10630	18.4	16.5	18.5
	0.1	8745	7744	8113	21.4	18.8	20.5
21.1	25	6206	6657	6783	22.8	18.9	20.0
	10	5050	5400	5589	27.7	22.7	24.3
	5	4242	4690	4794	29.5	23.7	25.2
	1	2669	3078	3117	33.8	27.0	30.4
	0.5	2246	2542	2570	34.1	28.0	31.7
	0.1	1499	1686	1693	31.7	28.2	32.3
37.8	25	2596	2493	2478	28.8	26.9	29.1
	10	1976	1910	1961	29.0	31.2	30.4
	5	1613	1588	1601	31.8	30.4	32.1
	1	982	970	962	33.0	30.4	33.2
	0.5	833	794	781	32.9	29.6	32.5
	0.1	599	537	527	27.5	26.7	30.7
54.4	25	992	774	744	28.7	30.6	33.7
	10	799	608	615	28.1	31.6	31.3
	5	681	514	517	26.2	28.4	26.3
	1	492	340	344	24.5	25.6	28.5
	0.5	420	297	314	22.5	25.3	27.6
	0.1	340	226	243	19.6	21.7	23.3

Table F-16. Dynamic Modulus and Phase Angle Replicate Data for Mixture TB5

Temp. (°C)	Freq. (Hz)	Dynamic Modulus, |E*|			Phase Angle, δ		
		Repl. 1 (MPa)	Repl. 2 (MPa)	Repl. 3 (MPa)	Repl. 1 (Deg.)	Repl. 2 (Deg.)	Repl. 3 (Deg.)
–10.0	25	34488	28245	33791	4.8	4.1	3.5
	10	33937	27115	32697	7.8	6.5	7.2
	5	32370	25926	31331	8.3	7.1	7.5
	1	28838	23337	28295	9.8	7.8	8.3
	0.5	27515	22267	27082	10.1	8.2	8.6
	0.1	24185	19844	24030	11.1	9.1	10.2
4.4	25	21543	18032	20957	9.2	9.7	9.1
	10	19900	16429	19104	11.5	12.3	11.6
	5	18188	15136	17508	12.7	13.6	13.3
	1	14795	12345	14030	16.2	15.2	15.8
	0.5	13503	11329	12827	16.7	15.7	16.8
	0.1	10566	9017	10038	19.0	18.4	19.3
21.1	25	8784	9113	9131	18.0	17.1	17.0
	10	7317	7622	7760	24.3	20.8	23.2
	5	6320	6580	6628	25.0	21.6	23.2
	1	4356	4598	4464	28.9	26.0	28.0
	0.5	3677	3941	3779	30.1	27.0	29.5
	0.1	2485	2748	2561	31.2	27.6	29.6
37.8	25	3577	4556	4046	25.0	22.7	22.9
	10	2909	3637	3137	28.0	24.7	25.0
	5	2464	3041	2624	32.0	26.3	27.4
	1	1536	1975	1675	34.2	29.6	30.3
	0.5	1270	1650	1367	34.9	29.3	30.3
	0.1	841	1107	911	33.9	28.6	28.8
54.4	25	1329	1776	1403	30.0	26.7	29.9
	10	1091	1453	1115	27.9	26.4	28.9
	5	933	1205	969	34.3	29.5	30.3
	1	587	805	600	32.3	27.8	28.4
	0.5	500	689	518	30.9	27.5	27.4
	0.1	361	513	372	28.4	25.3	25.0

Table F-17. Dynamic Modulus and Phase Angle Replicate Data for Mixture TD0.5

Temp. (°C)	Freq. (Hz)	Dynamic Modulus, |E*|			Phase Angle, δ		
		Repl. 1 (MPa)	Repl. 2 (MPa)	Repl. 3 (MPa)	Repl. 1 (Deg.)	Repl. 2 (Deg.)	Repl. 3 (Deg.)
–10.0	25	39332	40245	44702	2.5	4.8	5.3
	10	37018	38755	41363	5.9	6.6	7.0
	5	35474	37093	39505	7.3	8.1	8.6
	1	31583	32649	35126	8.2	9.0	9.6
	0.5	30029	31122	33138	8.7	9.7	10.2
	0.1	26055	27165	28824	10.1	11.0	11.7
4.4	25	22617	24649	25395	12.6	11.1	9.9
	10	20082	21899	22863	13.6	13.6	12.6
	5	18417	20012	20618	15.0	15.5	14.5
	1	14532	15668	16289	18.0	18.4	17.3
	0.5	13012	14129	14717	19.0	19.8	18.4
	0.1	9819	10789	11165	22.1	22.7	21.3
21.1	25	8584	9750	9285	20.5	19.9	19.7
	10	7184	8033	7795	24.0	25.7	23.4
	5	6105	6718	6568	25.3	27.4	25.1
	1	3941	4317	4267	29.8	32.6	30.0
	0.5	3349	3573	3569	30.9	34.3	30.2
	0.1	2211	2349	2361	31.4	33.8	30.9
37.8	25	3784	3821	3502	27.7	26.5	25.2
	10	3066	2885	2733	30.3	27.6	27.4
	5	2604	2424	2244	32.4	30.0	29.3
	1	1591	1616	1357	32.4	28.6	31.1
	0.5	1311	1347	1092	32.5	27.0	30.2
	0.1	906	852	718	29.0	24.2	27.7
54.4	25	1410	1305	1051	31.6	28.5	32.2
	10	1088	1018	814	33.3	24.8	31.4
	5	957	846	699	33.2	25.2	29.2
	1	625	568	464	30.6	21.6	25.3
	0.5	549	498	394	28.4	20.5	23.8
	0.1	426	374	307	24.6	16.8	20.9

Table F-18. Dynamic Modulus and Phase Angle Replicate Data for Mixture TA4

Temp. (°C)	Freq. (Hz)	Dynamic Modulus, |E*|			Phase Angle, δ		
		Repl. 1 (MPa)	Repl. 2 (MPa)	Repl. 3 (MPa)	Repl. 1 (Deg.)	Repl. 2 (Deg.)	Repl. 3 (Deg.)
–10.0	25	28687	25354	27491	3.3	4.6	2.5
	10	24664	24752	27151	4.7	6.2	4.9
	5	21474	23738	26276	5.1	6.2	6.3
	1	18629	21426	23815	6.8	8.0	7.3
	0.5	16906	20478	22756	7.2	8.5	7.6
	0.1	13790	18261	20392	8.1	9.4	8.5
4.4	25	17193	16361	17968	7.8	8.7	6.9
	10	15160	15090	16623	10.4	11.4	10.7
	5	13613	13982	15359	12.1	12.0	12.3
	1	11074	11310	12375	14.7	14.7	14.7
	0.5	9956	10267	11219	16.7	16.2	16.1
	0.1	7449	7972	8763	20.3	19.6	19.2
21.1	25	7194	7104	8125	19.1	18.0	16.2
	10	5571	6036	6907	23.0	21.7	21.0
	5	4649	5135	5899	24.4	25.3	24.2
	1	3133	3502	3906	31.9	31.6	29.7
	0.5	2582	2883	3235	33.6	32.8	31.6
	0.1	1587	1844	2052	35.9	35.9	33.3
37.8	25	2061	2655	2982	27.6	28.2	26.6
	10	1577	2004	2223	29.8	32.8	29.3
	5	1299	1609	1818	32.2	33.8	32.0
	1	740	903	1066	32.7	35.5	31.6
	0.5	604	698	844	31.9	35.5	31.0
	0.1	389	416	514	28.0	30.9	28.2
54.4	25	814	858	841	35.4	37.1	31.4
	10	550	609	610	37.6	39.3	32.6
	5	434	486	510	33.8	35.4	29.2
	1	240	281	296	31.0	32.7	28.0
	0.5	202	237	255	29.2	30.1	25.6
	0.1	140	165	187	26.3	25.1	20.0

Table F-19. Dynamic Modulus and Phase Angle Replicate Data for Mixture TA3-B

Temp. (°C)	Freq. (Hz)	Dynamic Modulus, |E*|			Phase Angle, δ		
		Repl. 1 (MPa)	Repl. 2 (MPa)	Repl. 3 (MPa)	Repl. 1 (Deg.)	Repl. 2 (Deg.)	Repl. 3 (Deg.)
–10.0	25	34843	33279	27191	4.4	5.0	3.9
	10	33458	31388	25646	5.5	7.2	6.4
	5	31985	29908	24433	7.2	7.7	7.5
	1	28493	26296	21606	8.8	9.8	8.8
	0.5	27183	24848	20387	8.6	10.4	9.6
	0.1	23366	21412	17507	9.8	11.8	10.9
4.4	25	19912	19563	15964	10.2	12.6	9.3
	10	17924	16900	14177	12.7	14.2	13.1
	5	16159	15413	12769	14.6	15.8	14.6
	1	12675	11907	9935	17.6	18.8	17.6
	0.5	11323	10606	8816	19.2	20.5	19.8
	0.1	8257	7818	6415	22.5	24.2	22.7
21.1	25	7261	6881	5564	21.4	21.4	21.2
	10	5812	5472	4550	24.4	25.6	25.7
	5	4882	4535	3744	26.1	28.8	28.2
	1	3130	2834	2375	30.4	33.5	31.1
	0.5	2573	2307	1969	31.7	35.0	32.0
	0.1	1596	1460	1214	31.8	34.6	32.1
37.8	25	2353	2366	2064	30.5	32.4	28.3
	10	1734	1804	1543	33.9	35.8	32.4
	5	1457	1482	1306	32.0	35.1	31.3
	1	858	845	762	31.9	35.7	30.5
	0.5	709	693	626	30.1	33.9	28.3
	0.1	471	464	408	26.8	29.4	24.5
54.4	25	691	888	652	31.8	32.9	33.5
	10	522	663	502	32.1	33.3	33.4
	5	442	589	412	28.4	31.5	31.4
	1	300	368	268	24.8	28.1	27.4
	0.5	255	329	228	22.1	26.3	25.8
	0.1	210	270	189	18.9	22.8	23.3

Table F-20. Dynamic Modulus and Phase Angle Replicate Data for Mixture TB2

Temp. (°C)	Freq. (Hz)	Dynamic Modulus, |E*|			Phase Angle, δ		
		Repl. 1 (MPa)	Repl. 2 (MPa)	Repl. 3 (MPa)	Repl. 1 (Deg.)	Repl. 2 (Deg.)	Repl. 3 (Deg.)
–10.0	25	41207	33460	35230	4.5	3.9	4.1
	10	39228	31874	33239	6.6	6.2	5.7
	5	37284	30652	32057	7.5	6.8	7.3
	1	32699	27331	28512	10.1	8.5	8.7
	0.5	31118	26071	27131	10.0	8.5	9.6
	0.1	27156	22916	23269	11.9	9.9	10.7
4.4	25	23452	20216	21051	11.9	8.9	13.5
	10	20807	18196	18520	15.0	11.6	14.9
	5	18612	16548	16772	17.4	12.9	17.3
	1	14274	13102	13076	21.0	15.7	19.3
	0.5	12772	11761	11656	22.3	17.5	20.9
	0.1	9752	8682	8638	25.8	21.4	24.5
21.1	25	8466	6803	7435	22.3	18.9	20.9
	10	6963	5351	6024	27.7	24.8	25.1
	5	5828	4549	5077	29.1	25.8	26.9
	1	3677	2891	3163	34.4	30.6	30.7
	0.5	3095	2388	2552	34.9	30.7	32.0
	0.1	2017	1464	1525	34.0	30.6	31.6
37.8	25	3041	2344	2551	29.2	29.0	32.3
	10	2301	1774	1893	30.9	32.5	36.5
	5	1913	1487	1542	33.6	31.8	36.1
	1	1136	846	877	33.6	30.7	35.7
	0.5	932	674	715	33.8	29.1	34.3
	0.1	641	424	457	30.1	25.0	30.4
54.4	25	915	600	680	35.1	33.3	34.8
	10	748	453	508	34.7	28.9	33.1
	5	656	373	414	32.1	29.1	30.1
	1	438	234	269	30.2	24.9	26.9
	0.5	405	197	234	26.8	23.5	24.0
	0.1	334	153	192	20.2	18.3	23.5

Table F-21. Dynamic Modulus and Phase Angle Replicate Data for Mixture TA2-B

Temp. (°C)	Freq. (Hz)	Dynamic Modulus, |E*|			Phase Angle, δ		
		Repl. 1 (MPa)	Repl. 2 (MPa)	Repl. 3 (MPa)	Repl. 1 (Deg.)	Repl. 2 (Deg.)	Repl. 3 (Deg.)
–10.0	25	31727	33818	24797	3.6	3.4	4.3
	10	30187	32290	24110	6.2	4.8	6.3
	5	28859	30839	23018	7.0	6.7	7.0
	1	25432	27701	20416	9.1	8.4	8.3
	0.5	24004	26017	19289	9.8	9.2	9.2
	0.1	20645	22364	16596	11.5	10.7	10.8
4.4	25	17305	19374	14643	10.7	12.5	11.8
	10	15390	16461	13408	15.1	14.4	14.4
	5	13811	14920	12178	16.2	16.6	16.9
	1	10571	11408	9291	20.2	20.3	20.4
	0.5	9367	10073	8237	22.2	22.2	22.2
	0.1	6627	7062	5850	26.0	27.4	25.9
21.1	25	5453	6455	5506	21.4	23.4	23.6
	10	4323	5146	4377	26.5	27.8	28.4
	5	3546	4196	3559	29.2	30.1	29.4
	1	2183	2528	2160	32.3	35.7	35.1
	0.5	1768	2010	1733	33.8	36.7	35.9
	0.1	1044	1221	1005	32.7	35.6	34.9
37.8	25	1702	2194	1865	31.3	34.8	33.7
	10	1215	1611	1284	35.6	37.5	37.3
	5	972	1313	1040	33.6	36.4	35.7
	1	548	713	591	32.4	34.8	34.3
	0.5	437	587	465	30.8	31.1	31.6
	0.1	288	407	337	26.6	26.3	27.5
54.4	25	506	580	518	32.6	34.8	35.5
	10	383	452	389	33.8	34.8	34.2
	5	317	378	314	31.6	31.7	30.5
	1	202	255	212	27.6	28.9	26.8
	0.5	180	233	182	25.7	26.9	24.3
	0.1	149	195	148	20.2	23.4	20.9

Table F-22. Dynamic Modulus and Phase Angle Replicate Data for Mixture TA3

Temp. (°C)	Freq. (Hz)	Dynamic Modulus, |E*|			Phase Angle, δ		
		Repl. 1 (MPa)	Repl. 2 (MPa)	Repl. 3 (MPa)	Repl. 1 (Deg.)	Repl. 2 (Deg.)	Repl. 3 (Deg.)
–10.0	25	42302	38053	35462	2.4	3.9	5.2
	10	40361	36296	33406	4.9	5.2	6.2
	5	38958	34815	32179	5.7	5.9	7.0
	1	35439	31620	29137	7.3	7.9	8.4
	0.5	33923	30317	27639	7.4	8.0	8.8
	0.1	29753	27005	24594	10.2	9.6	9.7
4.4	25	25815	23009	22543	9.8	8.1	9.0
	10	22818	20695	20145	13.7	11.6	10.7
	5	20609	19120	18564	14.8	12.9	12.2
	1	16348	15527	15102	17.9	15.7	14.9
	0.5	14676	14144	13779	18.7	17.1	16.2
	0.1	11029	10926	10843	22.3	20.8	18.4
21.1	25	9704	9993	9268	20.5	18.4	17.9
	10	7892	8217	7634	26.5	22.4	22.6
	5	6602	7067	6599	26.7	24.8	23.5
	1	4285	4672	4504	33.8	29.4	28.3
	0.5	3528	3916	3754	35.4	31.3	29.6
	0.1	2184	2466	2419	36.3	32.2	32.2
37.8	25	3248	3664	3306	29.0	26.8	26.5
	10	2424	2783	2537	30.6	29.3	28.1
	5	1932	2243	2046	34.2	31.0	30.7
	1	1123	1341	1223	33.4	31.2	30.9
	0.5	895	1073	983	31.7	29.5	30.9
	0.1	556	672	609	28.7	25.7	27.1
54.4	25	888	1014	980	35.0	31.2	32.0
	10	646	749	734	36.6	32.3	32.9
	5	518	628	600	33.2	29.7	30.5
	1	311	393	378	29.4	23.6	26.5
	0.5	262	347	322	26.5	21.6	24.3
	0.1	187	257	235	22.9	16.7	24.4

Table F-23. Dynamic Modulus and Phase Angle Replicate Data for Mixture TX3

Temp. (°C)	Freq. (Hz)	Dynamic Modulus, |E*|			Phase Angle, δ		
		Repl. 1 (MPa)	Repl. 2 (MPa)	Repl. 3 (MPa)	Repl. 1 (Deg.)	Repl. 2 (Deg.)	Repl. 3 (Deg.)
–10.0	25	37779	28212	29917	4.0	4.3	5.8
	10	35246	26533	27971	7.4	5.8	8.3
	5	33651	25212	26500	8.5	7.3	9.9
	1	29480	22432	23201	10.0	8.5	11.4
	0.5	27858	21076	21854	11.2	9.5	11.8
	0.1	23094	18020	18622	13.9	11.6	13.7
4.4	25	18920	15757	16421	14.4	12.5	13.4
	10	16284	13576	14388	17.1	14.4	16.7
	5	14568	12124	12644	19.6	17.0	17.8
	1	10755	9214	9597	23.9	21.9	22.8
	0.5	9384	8012	8511	26.4	23.0	24.8
	0.1	6503	5584	5897	28.3	28.0	29.5
21.1	25	6060	5238	5521	25.3	24.8	25.4
	10	4627	3983	4285	29.4	29.3	30.0
	5	3702	3244	3572	31.9	31.0	31.3
	1	2111	1873	2228	35.6	35.1	35.4
	0.5	1669	1491	1767	36.1	35.2	36.0
	0.1	984	869	1095	33.7	33.6	34.1
37.8	25	1814	1671	1661	35.3	34.7	35.6
	10	1282	1200	1283	38.5	37.5	38.2
	5	1041	939	1049	37.9	35.2	36.7
	1	573	565	609	35.0	33.7	34.1
	0.5	470	445	485	32.2	31.1	31.8
	0.1	314	306	351	27.6	27.2	27.2
54.4	25	518	481	618	36.4	36.0	32.8
	10	399	383	471	32.7	33.7	29.8
	5	334	323	399	28.9	31.5	26.9
	1	239	211	292	26.5	27.5	23.4
	0.5	219	188	260	24.4	24.0	20.1
	0.1	212	158	205	18.6	19.4	19.0

Table F-24. |E*| Mastercurve and Shift Function Parameters for All Mixtures

Mixture	Mastercurve Parameters				Shift Function Parameters	
	δ	α	β	γ	α_1	α_2
TY5	1.8840	2.7595	0.3076	0.3958	0.0011	–0.1888
TB5	1.6807	2.9880	0.6877	0.3556	0.0010	–0.1723
TB2	1.8339	2.8929	0.3246	0.4185	0.0007	–0.1640
TD0.5	1.8616	2.9464	0.4175	0.3683	0.0009	–0.1700
TX3	1.8967	2.6886	0.0876	0.4643	0.0009	–0.1724
TA3-B	1.8241	2.8259	0.2803	0.4206	0.0009	–0.1693
TA4	1.4741	3.0641	0.6799	0.4273	0.0007	–0.1544
TA2-B	1.7836	2.8404	0.1962	0.4590	0.0007	–0.1590
TA3	1.6797	3.0655	0.5470	0.3981	0.0007	–0.1616

HAMBURG WHEEL TRACKING TEST DATA

The rut depths reported in Chapter 6 are consistent with current ADOT practice and the methodology proposed in AASHTO T 324, which calls for only the maximum rut depth across all sensors to be reported. However, rut depths consistent with those seen using the other methods identified in Appendix E were also compiled for the mixtures used in Chapter 6. The results from this analysis appear in Figure F-10 through Figure F-13.

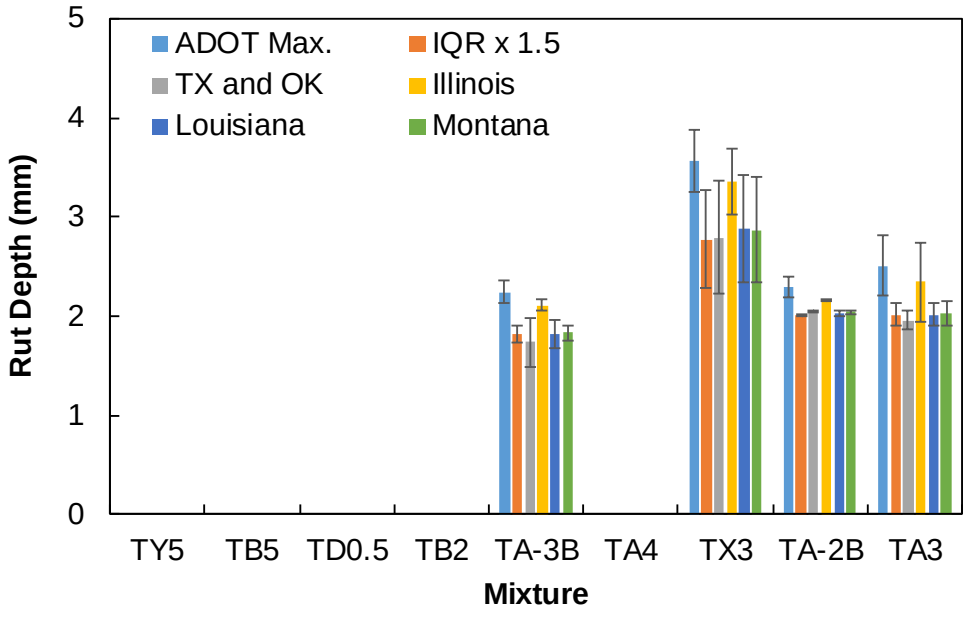

Figure F-10. Comparison of Rut Depths at 44°C Calculated Using Different Methods

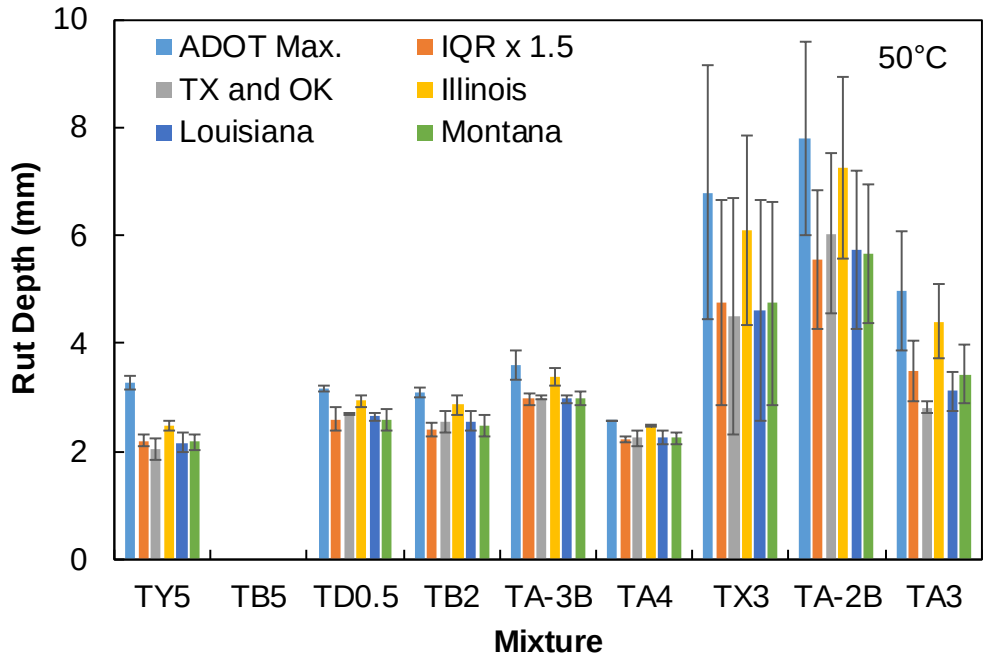

Figure F-11. Comparison of Rut Depths at 50°C Calculated Using Different Methods

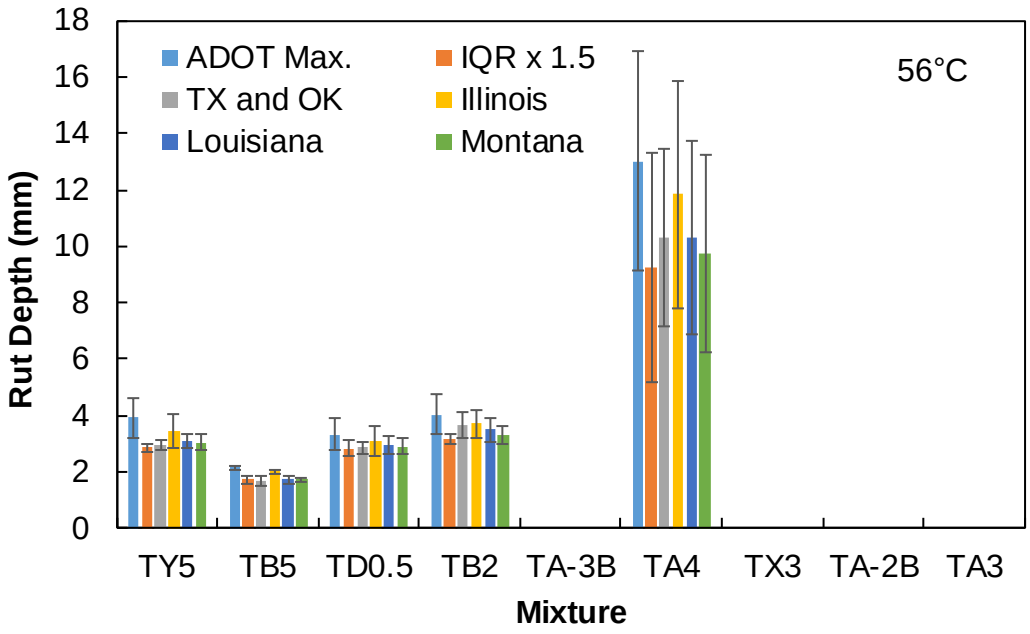

Figure F-12. Comparison of Rut Depths at 56°C Calculated Using Different Methods

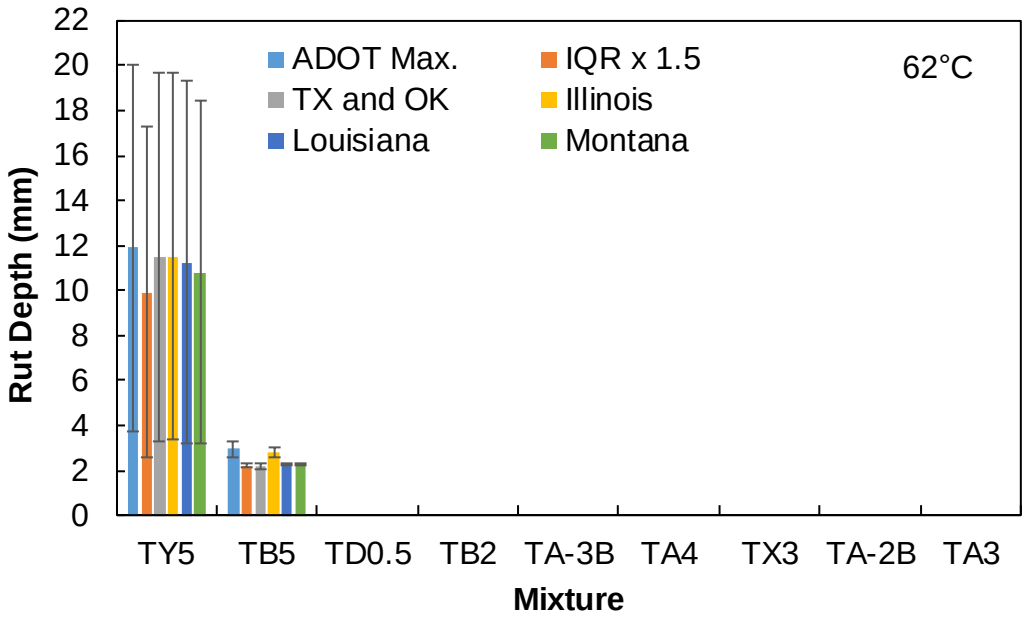

Figure F-13. Comparison of Rut Depths at 62°C Calculated Using Different Methods

It can be seen from the above figures and Table F-25 that the method currently employed by ADOT gives the highest rut depth, followed by the method adopted by Illinois. The remaining four methods report very similar rut depths.

Table F-25. Rut Depths of 12 Asphalt Mixtures Calculated Using Different Analysis Methods

Mixture	Temperature (°C)	Average Rut Depth (mm)					
		ADOT Max.	1.5 IQR	TX and OK	Illinois	Louisiana	Montana
TY5	50	3.3	2.2	2.0	2.5	2.2	2.2
	56	3.9	2.9	3.0	3.4	3.1	3.0
	62	11.9	9.9	11.5	11.5	11.3	10.8
TB5	56	2.2	1.7	1.7	2.0	1.7	1.7
	62	3.0	2.2	2.2	2.8	2.3	2.3
TD0.5	50	3.2	2.6	2.7	2.9	2.7	2.6
	56	3.3	2.8	2.8	3.1	2.9	2.9
TB2	50	3.1	2.4	2.6	2.9	2.6	2.5
	56	4.0	3.1	3.6	3.7	3.5	3.3
TA-3B	44	2.2	1.8	1.7	2.1	1.8	1.8
	50	3.6	3.0	3.0	3.4	3.0	3.0
TA4	50	2.6	2.2	2.2	2.5	2.2	2.2
	56	13.0	9.3	10.3	11.9	10.3	9.7
TX3	44	3.6	2.8	2.8	3.4	2.9	2.9
	50	6.8	4.7	4.5	6.1	4.6	4.8
TA-2B	44	2.3	2.0	2.1	2.2	2.0	2.0
	50	7.8	5.6	6.0	7.3	5.7	5.7
TA3	44	2.5	2.0	2.0	2.3	2.0	2.0
	50	5.0	3.5	2.8	4.4	3.1	3.4

AXIAL FATIGUE TEST DATA

As mentioned in Chapter 6, the axial fatigue test was performed at four strain levels for each mixture, and the data were analyzed using the viscoelastic continuum damage theory (S-VECD) formulation as explained in Appendix C. The result of the S-VECD model is the damage characteristic, or *C vs. S,* curve. In Chapter 6, only the fitted *C vs. S* curve was shown. In Table F-26 and the figures below, the *C vs. S* data at all four strain levels along with the fit function are shown for each of the nine mixtures. Also, the regression coefficients C_1 and C_2 for the *C* vs. *S* relationship are provided in Table F-27.

Table F-26. Actual Number of Cycles to Failure and Input Machine Strain on the Sample

Mixture	Input Machine Strain	No. of Cycles to Failure (N_f)	Actual Strain @ 80th Cycle (με)	Mixture	Input Machine Strain	No. of Cycles to Failure (N_f)	Actual Strain @ 80th Cycle (με)
TY5	250	57878	256	TX3	500	3090	422
	300	57355	243		600	2290	529
	350	18811	319	TA3-B	400	163495	259
	400	9534	364		450	78943	335
TB5	250	528634	151		500	9908	383
	300	44959	264		480	3387	432
	400	13911	278	TA4	300	68940	212
	450	9506	341		350	7330	235
TB2	300	812306	201		400	1420	330
	400	144355	281		450	1897	310
	500	33739	355	TA2-B	300	273929	224
	600	11901	454		350	92582	272
TD0.5	300	123594	202		400	19679	363
	400	41677	281		450	12919	338
	450	23705	309	TA3	300	60620	221
	500	298	381		350	52818	236
TX3	300	288673	219		400	1699	310
	400	35326	273		450	13309	305

Table F-27. Best Fit Coefficients C_1 and C_2 for C vs. S Relationship

Mixture	Coefficients	
	C_1	C_2
TY5	0.0058	0.4104
TB5	0.0028	0.4615
TD0.5	0.0021	0.4801
TA4	0.0012	0.5401
TA3-B	0.0064	0.3982
TB2	0.0041	0.4272
TA2-B	0.0039	0.4471
TA3	0.0014	0.5246
TX3	0.0047	0.4459

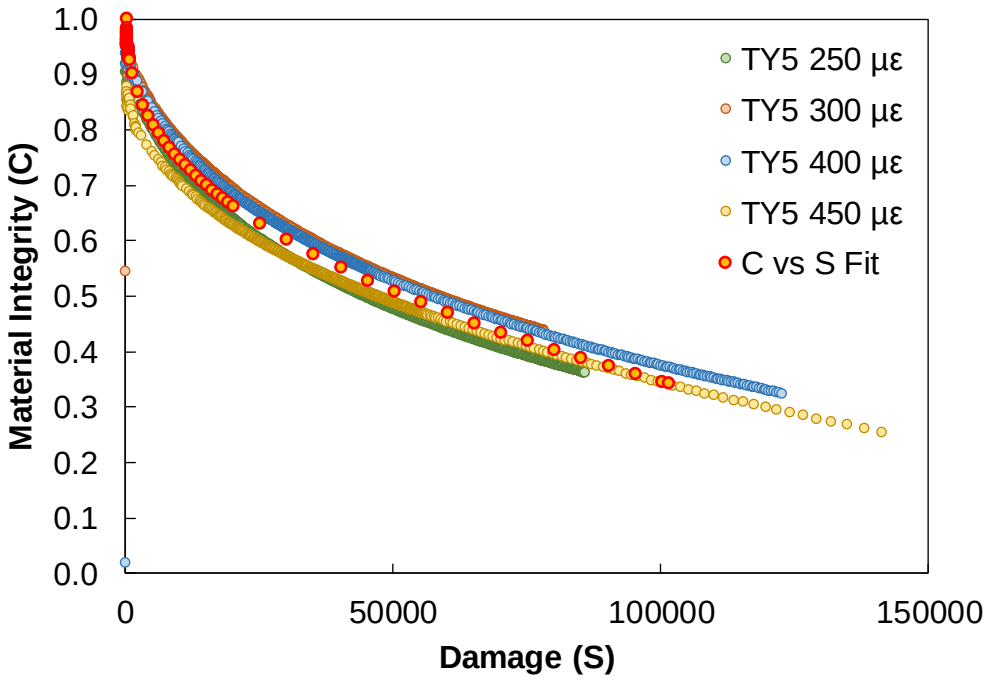

Figure F-14. *C vs. S* Curve for TY5 with Data at All Strain Levels

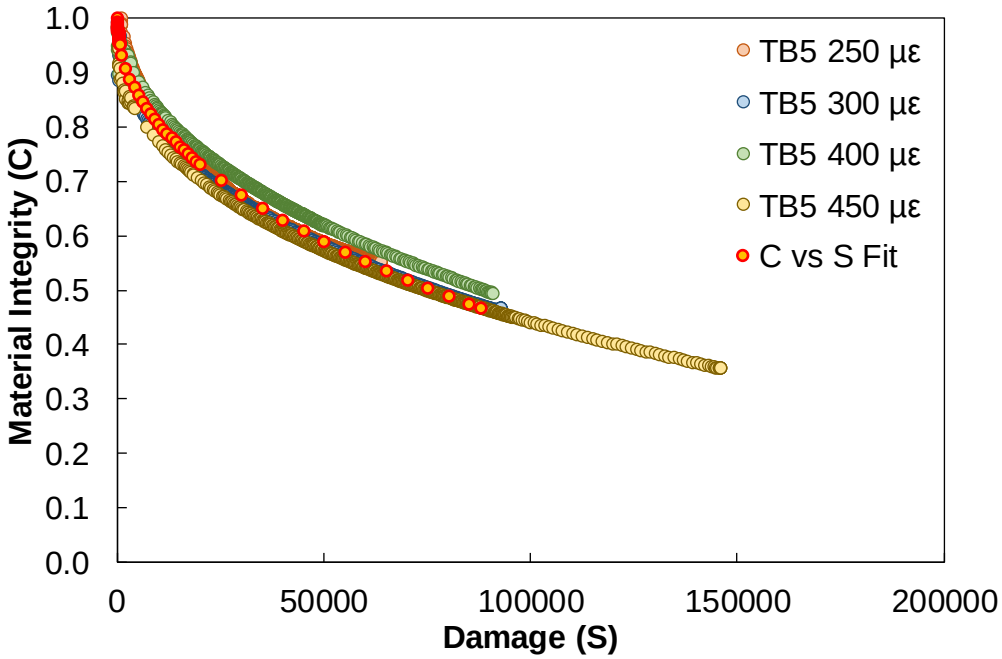

Figure F-15. *C vs. S* Curve for TB5 with Data at All Strain Levels

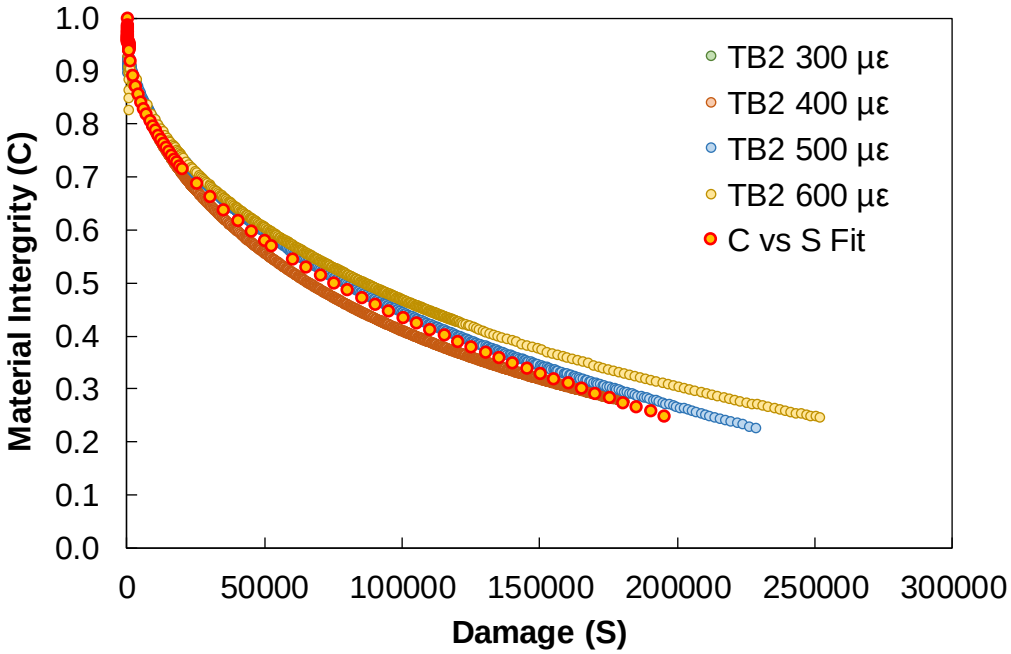

Figure F-16. *C vs. S* Curve for TB2 with Data at All Strain Levels

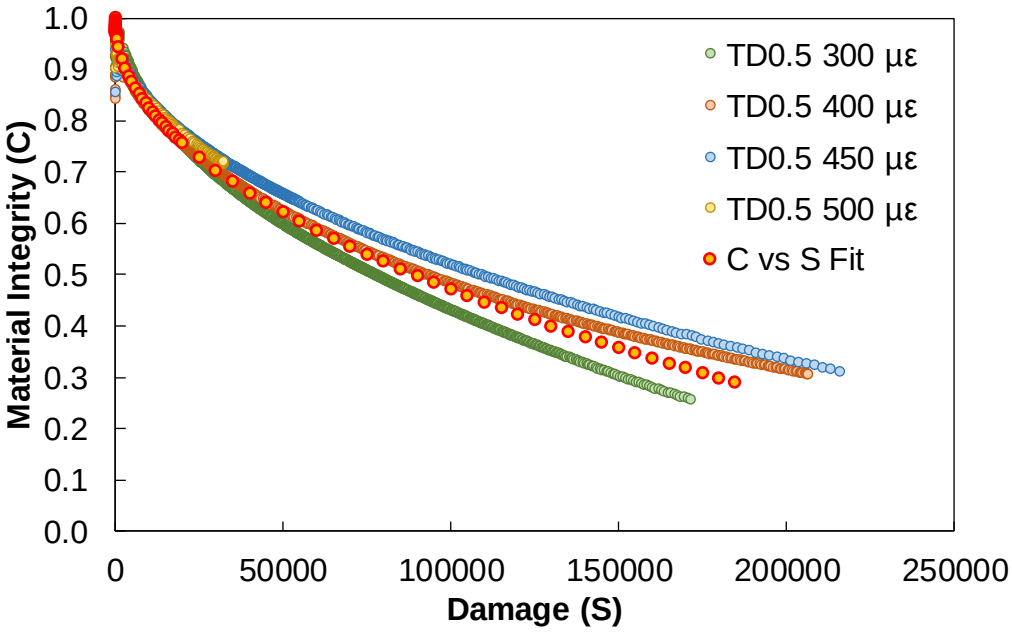

Figure F-17. *C vs. S* Curve for TD0.5 with Data at All Strain Levels

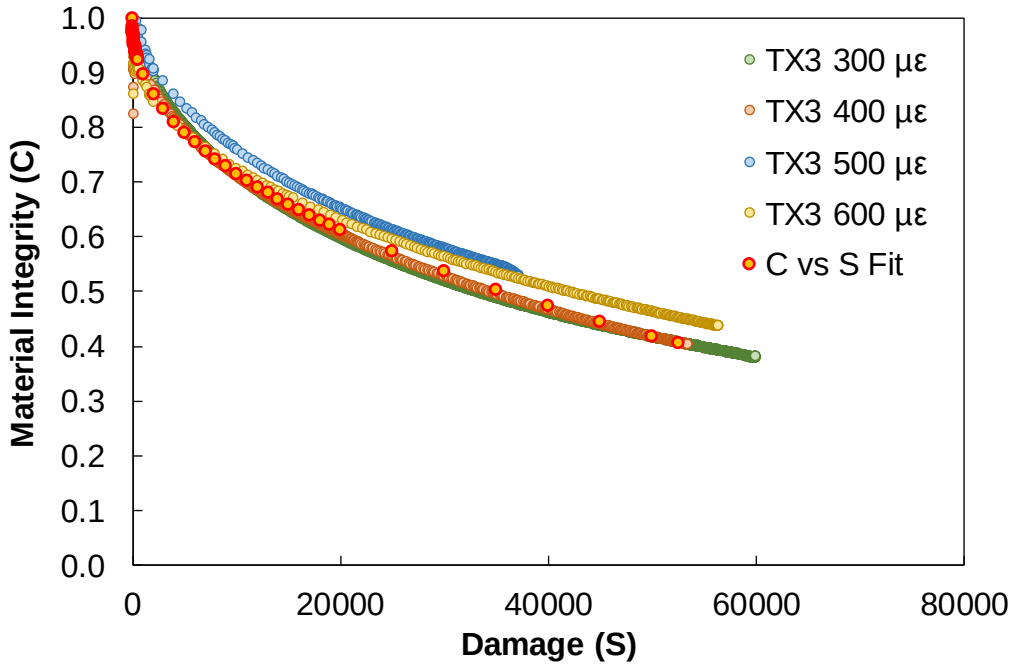

Figure F-18. *C vs. S* Curve for TX3 with Data at All Strain Levels

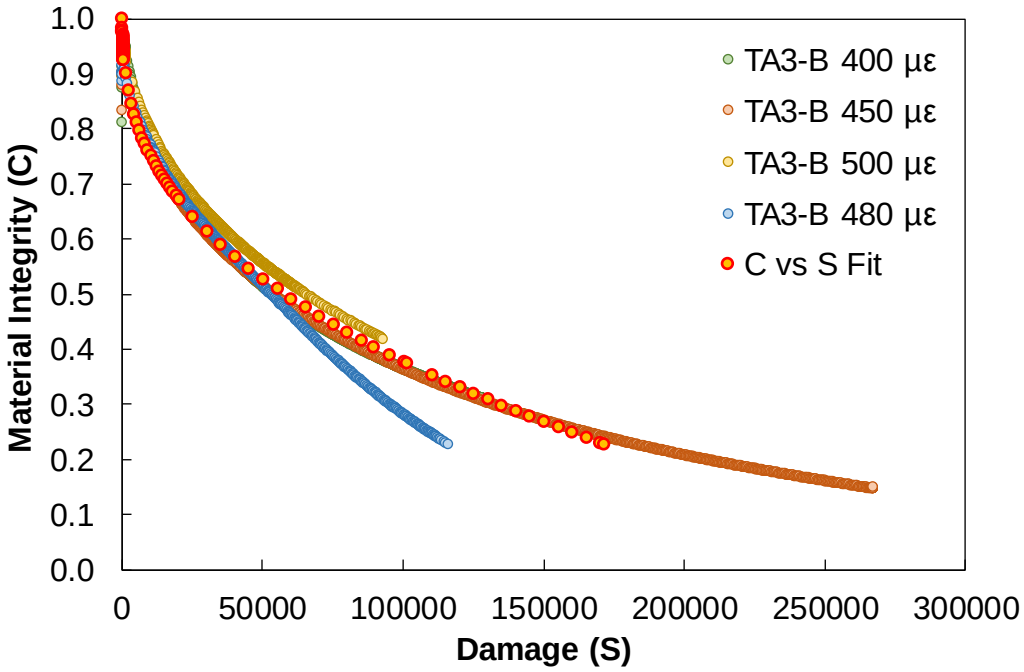

Figure F-19. *C vs. S* Curve for TA3-B with Data at All Strain Levels

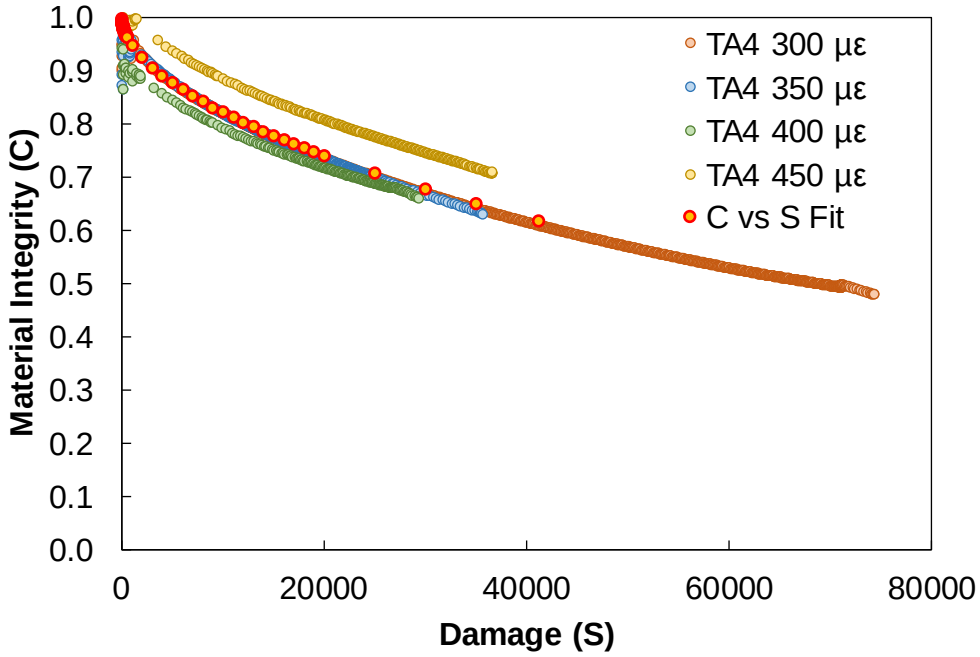

Figure F-20. *C vs. S* Curve for TA4 with Data at All Strain Levels

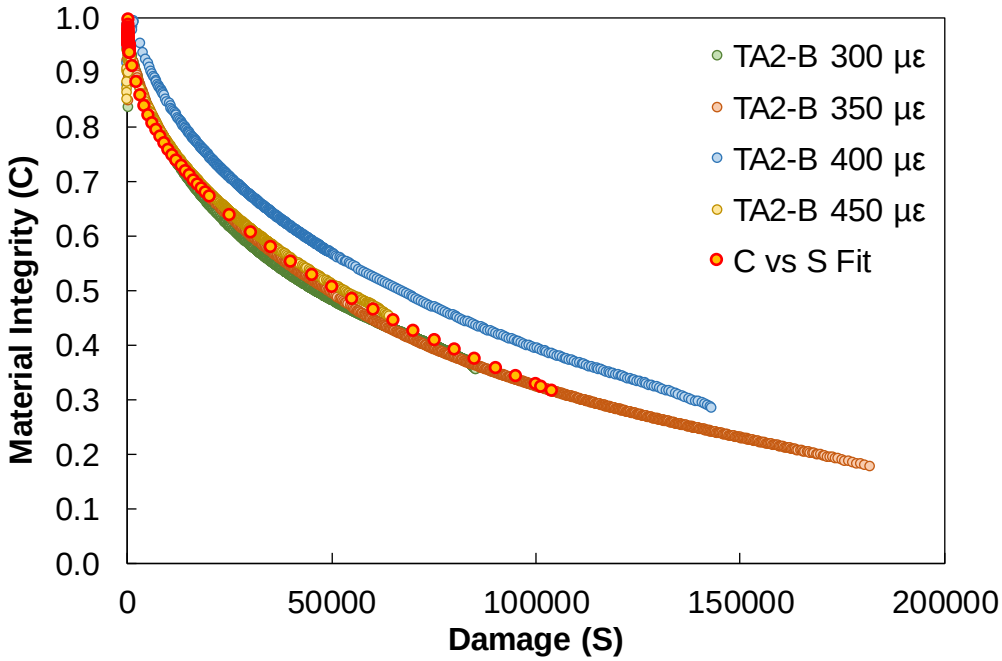

Figure F-21. *C vs. S* Curve for TA2-B with Data at All Strain Levels

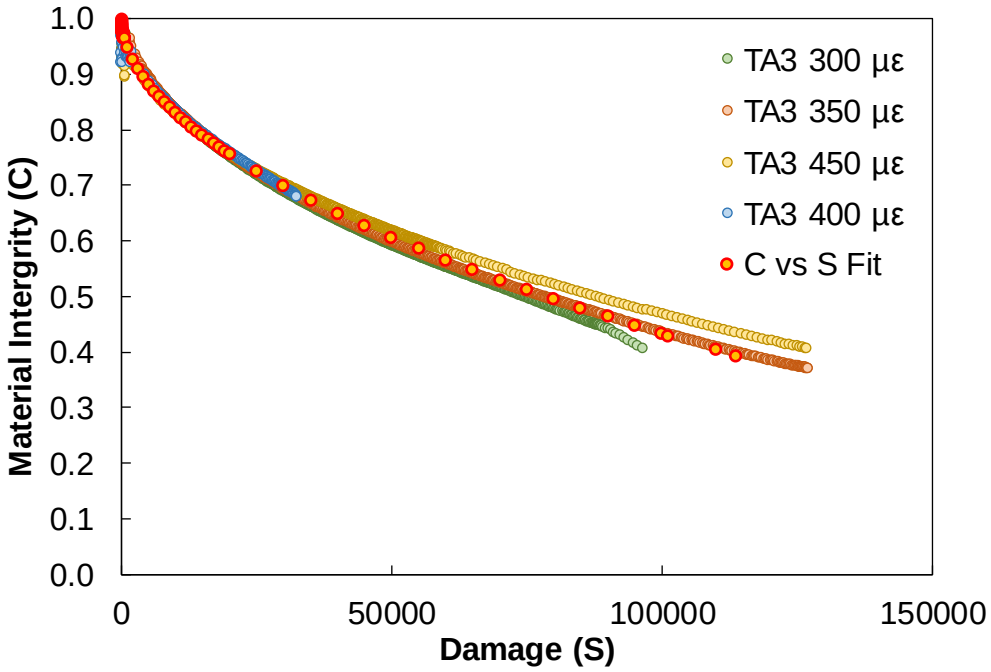

Figure F-22. *C vs. S* Curve for TA3 with Data at All Strain Levels

APPENDIX G: ANTICIPATED IMPACTS OF A CHANGE TO AASHTO M 332

MULTIPLE AASHTO M 332 GRADES BASED ON PAV AGING SCENARIOS

Table G-1. Different AASHTO M 332 Grades for Binders from Supplier Y for Four Different PAV Aging Temperature Scenarios

Scenario 1					Scenario 2				
Binder	**S Grades**	**H Grades**	**V Grades**	**E Grades**	**Binder**	**S Grades**	**H Grades**	**V Grades**	**E Grades**
Y1	64S-16	58H-16	-	-	**Y1**	64S-16	58H-16	-	-
	64S-22	58H-22	-	-		64S-22	58H-22	-	-
Y2	70S-16	64H-16	-	-	**Y2**	70S-16	64H-16	-	-
	70S-22	64H-22	-	-		70S-22	64H-22	-	-
Y3	70S-16	64H-16	-	-	**Y3**	70S-16	64H-16	-	-
	70S-22	64H-22	-	-		70S-22	64H-22	-	-
Y4	76S-10	70H-10	64V-10	-	**Y4**	76S-10	70H-10	64V-10	-
	76S-16	70H-16	-	-		76S-16	70H-16	-	-
Y5	70E-22	64E-16	-	-	**Y5**	70E-22	64E-16	-	-
	76E-22	64E-22	-	-		76E-22	64E-22	-	-
Y6	70E-22	64E-16	-	-	**Y6**	70E-22	64E-16	-	-
	76E-22	64E-22	-	-		76E-22	64E-22	-	-
Scenario 3					**Scenario 4**				
Binder	**S Grades**	**H Grades**	**V Grades**	**E Grades**	**Binder**	**S Grades**	**H Grades**	**V Grades**	**E Grades**
Y1	64S-16	58H-16	-	-	**Y1**	64S-16	58H-16	-	-
	64S-22	58H-22	-	-		64S-22	58H-22	-	-
Y2	70S-16	64H-16	-	-	**Y2**	70S-16	64H-16	-	-
	70S-22	64H-22	-	-		70S-22	64H-22	-	-
	-	**64H-28**	-	-		-	**64H-28**	-	-
Y3	70S-16	64H-16	-	-	**Y3**	70S-16	64H-16	-	-
	70S-22	64H-22	-	-		70S-22	64H-22	-	-
	70S-28	**64H-28**	-	-		**70S-28**	**64H-28**	-	-
Y4	76S-10	70H-10	64V-10	-	**Y4**	76S-10	70H-10	64V-10	-
	76S-16	70H-16	-	-		76S-16	70H-16	-	-
Y5	70E-22	64E-16	-	-	**Y5**	70E-22	64E-16	-	-
	76E-22	64E-22	-	-		76E-22	64E-22	-	-
	-	**64E-28**	-	-		-	**64E-28**	-	-
Y6	70E-22	64E-22	-	-	**Y6**	70E-22	64E-22	-	-
	76E-22	**64E-28**	-	-		76E-22	**64E-28**	-	-
XX	Acceptable grade and experimental data exist				XX	Experimental data do not exist; grade is estimated to be acceptable			
XX	Unacceptable grade and experimental data exist				XX	Experimental data do not exist; grade is estimated to be unacceptable			
XX	Additional grades added				-				

Table G-2. Different AASHTO M 332 Grades for Binders from Supplier Z for Four Different PAV Aging Temperature Scenarios

Scenario 1					Scenario 2				
Binder	S Grades	H Grades	V Grades	E Grades	Binder	S Grades	H Grades	V Grades	E Grades
Z1	64S-16	-	58V-16	-	Z1	64S-16	-	58V-16	-
	64S-22	-	58V-22	-		64S-22	-	58V-22	-
Z2	70S-16	64H-16	-	-	Z2	70S-16	64H-16	-	-
	70S-22	64H-22	-	-		70S-22	64H-22	-	-
Z3	70S-10	-	64V-10	-	Z3	70S-10	-	64V-10	-
Z4	76S-10	70H-10	-	64E-10	Z4	76S-10	70H-10	-	64E-10
	76S-16	70H-16	-	64E-16		76S-16	70H-16	-	64E-16
Scenario 3					**Scenario 4**				
Binder	S Grades	H Grades	V Grades	E Grades	Binder	S Grades	H Grades	V Grades	E Grades
Z1	64S-16	-	58V-16	-	Z1	64S-16	-	58V-16	-
	64S-22	-	58V-22	-		64S-22	-	58V-22	-
Z2	70S-16	64H-16	-	-	Z2	70S-16	64H-16	-	-
	70S-22	64H-22	-	-		70S-22	64H-22	-	-
	-	**64H-28**	-	-		-	**64H-28**	-	-
Z3	70S-10	-	64V-10	-	Z3	70S-10	-	64V-10	-
	-	-	**64V-16**	-		-	-	**64V-16**	-
Z4	76S-10	70H-10	-	64E-10	Z4	76S-10	70H-10	-	64E-10
	76S-16	70H-16	-	64E-16		76S-16	70H-16	-	64E-16
XX	Acceptable grade and experimental data exist				XX	Experimental data do not exist; grade is estimated to be acceptable			
XX	Unacceptable grade and experimental data exist				XX	Experimental data does not exist; grade is estimated to be unacceptable			
XX	Additional grades added				-				

QUESTIONNAIRE TO SUPPLIERS

Production

Question 1: What is your current production (tonnage) by each grade and operating facility?

Question 2: Do you have an estimate of the percentage (by grade) that you provide to cities/counties within Arizona?

Question 3: Do any of your Arizona facilities provide binder for out-of-state use?

Question 4: Do any of your out-of-state facilities provide binder for use in Arizona?

Storage

Question 5: What is the current storage capacity in whole and by grade?

Question 6: What is the cost estimate to you for adding additional tank storage?

Question 7: Are you willing to add additional tanks?

Question 8: If you do not use dedicated tank(s), what are the issues (e.g., cleaning and disposal costs)? Will there be costs associated with end of season at any locations?

Operations

Question 9: What is the current operational terminal area in acres? Area wise, do you have any constraints?

Question 10: Would the operational terminal area need to be expanded in order to increase tank storage? And have you looked (recently or in the past) at acquisition costs?

Question 11: Are there any delivery issues currently?

Open Discussion

Question 12: Are there any challenges to the new spec being implemented?